Some Opportunities for International Scientific Collaboration in the Japan-Kamchatka-Alaska Region

John Eichelberger, Volcano Hazard Program, U.S. Geological Survey (jeichelberger@usgs.gov)
Evgeny Gordeev, Institute of Volcanology and Seismology, FEB RAS (gordeev@kscnet.ru)
Pavel Izbekov, Geophysical Institute, University of Alaska Fairbanks (pavel@gi.alaska.edu)

The Great Tohoku Earthquake of 2011 brings to five the number of M9 earthquakes that have occurred on Earth since instrumental records have been kept. Three of these, or one each, have occurred in Japan, Kamchatka, and Alaska. All produced far-reaching tsunamis. The record of volcanic eruptions is no less impressive, including Katmai 1912, Bezymianny 1956, Shiveluch 1964, Tolbachik 1975, Ksudach 1907, and Usu 1663. More remote, but disruptive to air traffic while lacking ground monitoring networks, are volcanoes like Sarychev (2009) in the Kuriles and Kasatochi (2008) in the Aleutians. At the center of this region the Aleutian and Kurile-Kamchatka arcs and Hawaiian hotspot trace collide, while rollback of the unsupported, torn Pacific plate slab rifts Kamchatka above it[1]. Three Kamchatka volcanoes near this cusp, one basaltic, one andesitic, and one dacitic, are in almost continuous eruption.

Despite the fact that this region lies within or near the territories of three technologically adept countries, segments of it, especially the Kurile and western Aleutian arcs, are among the least studied and most poorly monitored in the world. This is because the resident population is relatively small and the environment harsh. Nevertheless, people do live here, there are resources vital to all three countries, and the importance of the area will further increase as the Arctic opens to shipping. From an American perspective, attention to Alaska by new US scientific initiatives of the U.S. National Science Foundation (NSF) like Geodynamic Processes at Subducting and Rifting Margins (GeoPRISMs), Earthscope, and Creating a More Disaster Resilient America (CaMRA), longstanding partnerships such as the Global Seismic Network (GSN, with USGS, NSF, and Russia's MES and RAS) and the Russian Far East and Alaska volcano observatories (RAS and USGS), together with bilateral discussions among government agencies of the US and Russia, raise the hope of invigorated research into Japan-Kamchatka-Alaska subduction processes. That this is not an idle hope is demonstrated support from NSF and RAS of a large project, within Partners in International Research and Education (PIRE), centered on Bezymianny volcano, involving numerous graduate students, faculty members, and government scientists from Russia and the US. Additionally, ongoing deliberations within the International Civil Aviation Organization (ICAO), following international-scale disruption of aviation by ash eruptions, may eventually provide a path for expansion of ground-based monitoring networks on the region's remote volcanoes. Such networks provide warning in advance of explosive ash eruptions rather than eruption detection only, as is the case for satellite remote sensing, when ash clouds may already block flight routes.

We note two of many possibilities for bilateral or trilateral collaboration here. One would be a region-wide effort to improve and interlink geophysical monitoring, specifically seismic and geodetic networks, and to improve rapidity and accuracy of detection of earthquakes, volcanic unrest and eruption, and tsunamis. This could be accompanied by state-of-the-art seismic and volcano hazard assessments with development of risk mitigation strategies for important communities at risk, such as Petropavlovsk-Kamchatsky and Dutch Harbor/Unalaska, Alaska, bringing together the best methodologies of all three countries. In addition, marine surveys are needed to understand the complex structure of the western portion of the Aleutian arc, including within-arc rifting, block rotation, and submarine volcanism, as coupling of the arc transitions westward from the North American plate to the Pacific plate, and as plate motion transitions from oblique subduction to strike-slip faulting[1]. Without a complementary effort in the Russian Aleutians to extend the reach of GeoPRISMs, the chance to develop a comprehensive whole-arc view will be lost. More broadly, subduction beneath the Kurile-Kamchatka and Aleutian arcs cannot be well

understood without knowing the dynamics of the Okhotsk and Bering microplates on which these arcs are built. Years of collaboration between Japanese universities and Russian Far East institutes have brought considerable detail about Okhotsk plate motion and coupling with the Kurile-Kamchatka arc, but data concerning Bering plate dynamics remains sparse.

A second possibility lies in the area of scientific drilling. Already, significant ocean drilling efforts have been conducted by Japan, Russia, and the US, some as part of the Deep Sea Drilling Program (DSDP), Ocean Drilling Program (ODP), and Integrated Ocean Drilling Program (IODP). Complementary efforts on land have been lacking. In 2006, the International Continental Scientific Drilling Program (ICDP) funded a workshop to develop a proposal for drilling Mutnovsky Volcano's magma-hydrothermal system[2]. A proposal submitted to NSF for pre-drilling geophysical work was not funded, but a drilling project at Mutnovsky remains an attractive possibility that ICDP would consider. In 2008 and 2009, ICDP drilled a young meteor impact crater in Chukotka, El'gygytgyn, for its 3-million-year climate record and to explore the impact structure. The drill rig used was subsequently transferred to Magadan, and remains available for future scientific drilling projects until 2014. This development substantially lowers the logistical costs of scientific drilling at Mutnovsky, or at other targets in Kamchatka. The equipment is capable of continuously coring at HQ size (63.5 mm core, 96.0 mm hole) to 800 m and then NQ size (47.6 mm core, 75.7 mm hole) to 1200 m. Besides Mutnovsky, other attractive targets include the intracaldera stratigraphy of Gorely Caldera and the hydrothermal system, stratigraphy and structure of the flanks of Avachinsky Volcano. Where temperatures are not high, the boreholes could be used to emplace seismometers, tiltmeters, and/or strainmeters in a low-noise environment, thereby enhancing detection and interpretation of volcano unrest.

References cited

1. Eichelberger, J.C., D.W. Scholl, and E.I. Gordeev, 2009a, Aleutian subduction: A scientific opportunity whose time has returned, *Margins Newsletter*, 22, 11-14.

2. Eichelberger, J., A. Kiryukhin, and A. Simon, 2009b, The magma-hydrothermal system at Mutnovsky Volcano, Kamchatka Peninsula, Russia, *Scientific Drilling*, 7, 54-50.

THE 1955-2010 PERIOD OF ERUPTIVE ACTIVITY AT BEZYMIANNY VOLCANO, KAMCHATKA: STORY IN ROCKS

Pavel Izbekov[1] and PIRE team[2]

[1] Alaska Volcano Observatory, Geophysical Institute, University of Alaska Fairbanks
[2] http://gps.alaska.edu/PIRE/index.html

Bezymianny volcano in Kamchatka has been in a state of nearly continuous eruptive activity for more than five decades. It started in late 1955 after ca. 1000 years of quiescence. A moderate explosive and extrusive eruption from the central vent of the volcano abruptly escalated on March 30, 1956, when a sudden collapse of the eastern flank of the volcano triggered an energetic directed blast followed by four hours of paroxysmal explosive eruption. The eruption destroyed summit of the volcano and formed a 1.3-km-wide horseshoe crater breached to the east. Within weeks the volcano started rebuilding its edifice through extrusion of the dome in the middle of the crater, intermittent dome collapses, and associated block-and-ash flows. By mid 70s, as the volume of the dome increased, the dome-building extrusive activity became complemented by short explosive events with pyroclastic flows and surges followed by effusions of lava flows. In late 90s the explosive eruptions became remarkably regular with 1-2 events per year.

The erupted Bezymianny magmas were remarkably homogeneous both texturally and compositionally. Their composition changed gradually from 60.9 wt. % SiO_2 in 1956 to 56.8 wt. % SiO_2 in 2010 (figure 1). The composition of exceptionally rare mafic enclaves from the products of the 1997 and 2007 eruptions overlapped with the composition of recent Kliuchevskoy magmas (figure 2, Kliuchevskoy data from Almeev, 2005). The MgO-SiO_2 binary diagram shows that MgO content increased linearly from 1956 to ca. 1973 along the mixing line connecting points corresponding to the 1956 andesite and the high-Mg, Kliuchevskoy-type basalt. In ca. 1973 the linear trend changed the slope and followed a mixing line between 1973 magma and low-Mg Kliuchevskoy-type basalt. The same kink in trend is observed in a variety of other elements (Turner et al., this volume). The 2009 and 2010 magmas of Bezymianny contained light-colored enclaves of vesicular amphibole-bearing andesites, which composition mimicked the composition of magmas erupted in 1989 and during 1997-2003.

The change in whole-rock composition correlated with changes in magma temperature and mineral assemblage. Based on ilmenite-magnetite and two-pyroxene geothermometry the pre-eruptive temperature of Bezymianny magmas increased from 950°C in 1956 to 1050°C in 2006 (Shipman et al., this volume). Amphibole, abundant in 1956 magma, gradually disappeared by mid 60s and most recently occurred only as resorbed cores in OPx-CPx-Pl aggregates. Its composition changed from 8-10 wt. % Al_2O_3 in 1956 to 13-15 wt. % Al_2O_3 in 2010 (figure 4). The modal proportion and size of clinopyroxene crystals gradually increased; its composition became more Mg-rich (figure 6). This correlated with increase of Mg content in orthopyroxenes (figure 5). Despite conspicuous changes in whole rock composition and temperature, the range of compositional variations of plagioclase remained nearly the same. It is remarkable that plagioclase composition returned repeatedly to 48-50 mol. % An throughout the entire period of eruptive activity. The compositional plateaus in the oscillatory zoned plagioclases preceding the outermost dissolution boundaries in the 1956 magma compositionally resembled those in the most recent eruptive products (figure 3).

Although the new data from a trace element study of plagioclases, ion microprobe study of melt inclusions, and phase equilibria experiments may slightly modify our interpretation, the observed compositional trends are generally consistent with continuous input(s) of Kliuchevskoy-like basalts to the magma system of Bezymianny volcano.

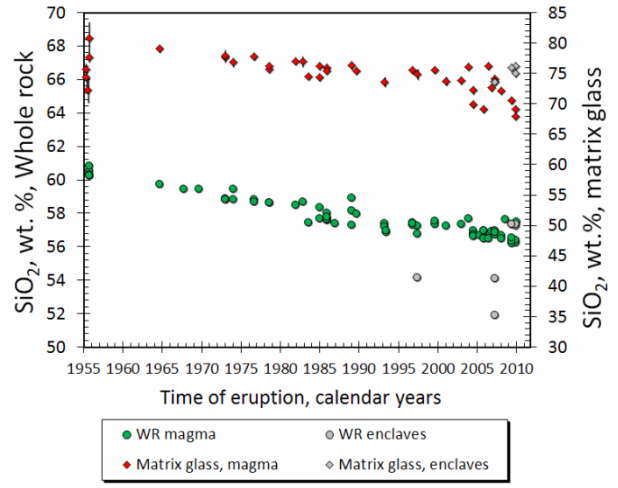


Figure 1: Whole rock and matrix glass compositions

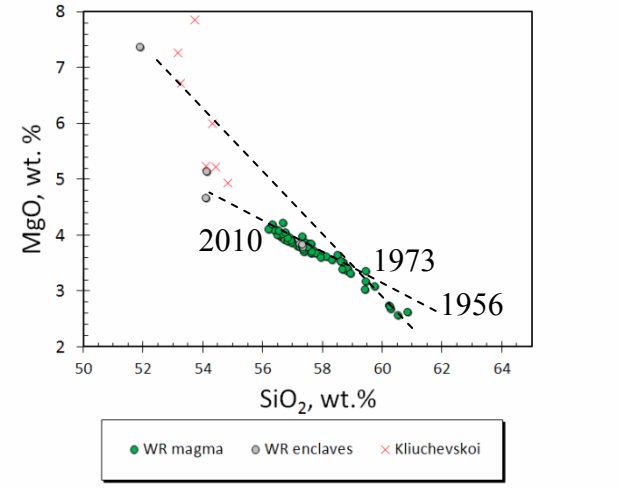


Figure 2: Whole rock composition

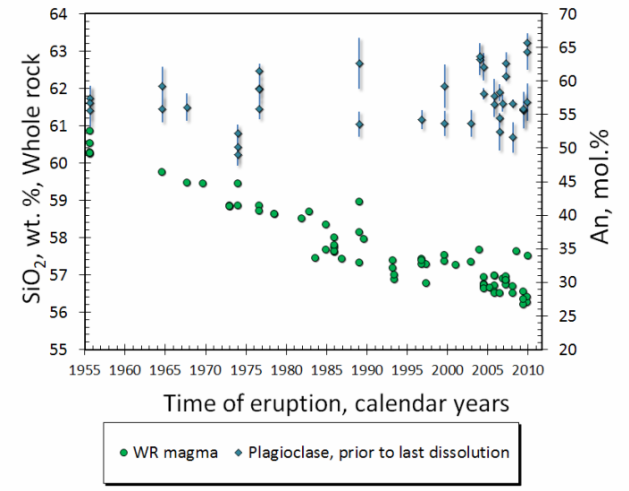


Figure 3: Composition of plagioclase phenocrysts immediately prior to the last dissolution event

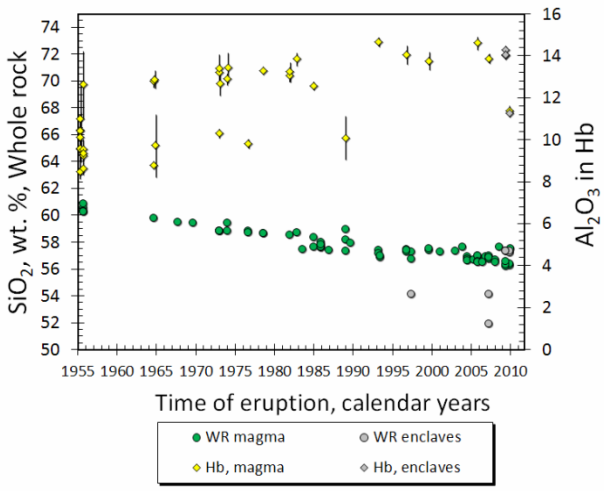


Figure 4: Composition of amphibole phenocrysts

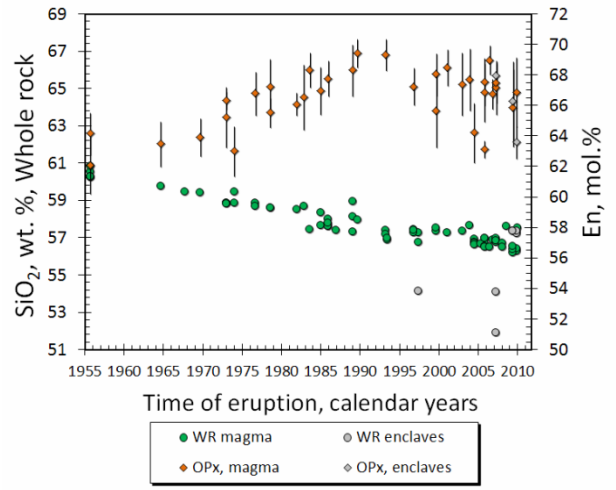


Figure 5: Composition of orthopyroxene phenocrysts

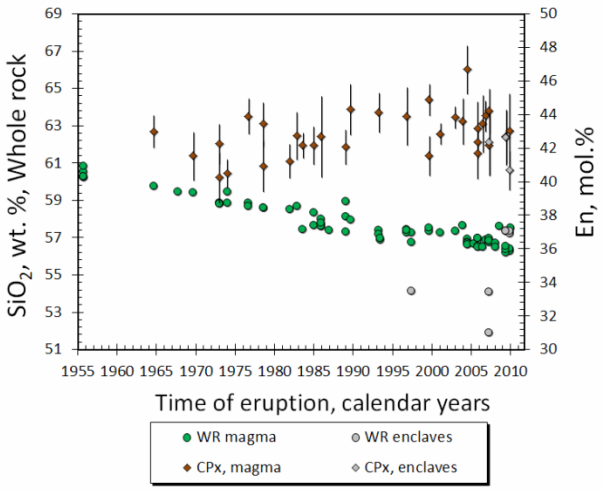


Figure 6: Composition of clinopyroxene phenocrysts

RESULTS OF WORK OF THE REGIONAL PERMANENT GNSS NETWORK "KAMNET"

Titkov N.N., Bahtiarov V. F.

Kamchatka Branch Geophysical Service, Petropavlovsk-Kamchatsky, Russia

(nik@emsd.ru)

In the end of 1997, for the purpose of studying of geodynamic processes on Kamchatka and Komandor Islands, the regional permanent GNSS network «KAMNET» has been created. The network contained 7 stations since its inception with 30 second of record rate interval. Now the network consists of 19 stations. The data from 16 stations is transferred daily. 10 stations works in 1 second of record rate interval.

The territory covered by a network is located in the area of interaction of three largest plates: Eurasia, North American and Pacific and two plates of the average size: Okhotia and Beringia.

Long-term GNSS observation have allowed to define model parameters of lithospheric plates motions and deformation of southern Kamchatka. At the same time the network density is extremely insufficient for such difficult region in the deformation plan as Kamchatka. The small number of stations does not allow to build deformation model and to define kinematic parameters of plates movement on borders between Okhotian, Beringian and North American plates and also to build fuller inhomogeneous deformation model of southern Kamchatka.

By the network has been registered co-seismic displacement from three large earthquakes: : the Kronotskii earthquake of December 5, 1997, MW = 7.8; the Bering I. earthquake of December 5, 2003, MW = 6.6; the Olyutorskii earthquake of April 20, 2006, MW = 7.6. High-frequency 1 second interval record rate GNSS observations, and development of methods of kinematic processing has allowed to investigate in more details dynamic processes accompanying strong earthquakes.

РЕЗУЛЬТАТЫ РАБОТЫ РЕГИОНАЛЬНОЙ СЕТИ ПОСТОЯННЫХ GNSS НАБЛЮДЕНИЙ KAMNET

Титков Н.Н., Бахтиаров В.Ф.

Камчатский филиал Геофизической службы РАН, г. Петропавловск-Камчатский
(*nik@emsd.ru***)**

В конце 1997 года, с целью изучения геодинамических процессов на Камчатке и Командорских островов, была создана региональная сеть постоянных GPS наблюдений KAMNET. Первоначально в составе сети было 7 станций с 30 секундной регистрацией. В настоящее время в составе сети 19 станций. Данные с 16 станций передаются ежедневно.10 станций работают в 1 секундном режиме наблюдений.

Территория, охватываемая сетью, располагается в области конвергентного сочленения трех крупнейших плит: Евразийской, Северо-Американской и Тихоокеанской. В окрестности их тройного сочленения обособились две плиты среднего размера: Охотия и Беринги, а также ряд более мелких блоков. Многолетние GPS наблюдения позволили определить параметры перемещений литосферных плит, и построить модель деформации южной Камчатки, находящейся под воздействием процесса субдукции Тихоокеанской плиты под Охотскую. В то же время плотность сети крайне недостаточна для такого сложного в деформационном плане региона как Камчатка. Малое количество станций не позволяет определить параметры деформаций и перемещений блоков на границах между Охотской, Берингийской и Североамериканской плитами, а также построить более полную модель деформации, учитывающую неоднородный ее характер.

За время работы сети были зарегистрированы косейсмические процессы от трех крупных землетрясений: Кроноцкое землетрясение 05.12.1997, Mw=7.8, землетрясение в районе острова Беринга 05.12.2003, Mw=6.6 и Олюторское землетрясение 20.04.2006, Mw=7.6. Высокочастотная 1 секундная регистрация GNSS наблюдений, а также развитие методов кинематической обработки позволило более детально исследовать динамические процессы, сопровождающие сильные землетрясения.

SYSTEM OF SEISMIC OBSERVATIONS IN THE TSUNAMI WARNING SURVEY ON THE FAR EAST RUSSIA

V.N. Chebrov[1], A.A. Gusev[1,2], D.V. Droznin[1], V.N. Mishatkin[3], V.A. Sergeev[1], Y.V. Shevchenko[1], D.V. Chebrov[1]

[1] *Kamchatkan branch of Geophysical Survey of RAS, Petropavlovsk-Kamchatsky, Russia*
[2] *Institute of volcanology and seismology of RAS, Petropavlovsk-Kamchatsky, Russia*
[3] *Geophysical survey of RAS, Obninsk, Russia*

In 2006–2010 on the Far East Russia, seismological system was modernized by the Geophysical Survey of Russian Academy of Science (GS RAS). For the tsunami warning purposes Seismic Subsystem of Tsunami Warning System (SS TWS) was created. The new generation Seismic Subsystem includes:

- seismic network, consisting of five base specialized digital seismic stations, six auxiliary ones and sixteen strong motion observe points. Base stations represent seismic groups, and located near the towns on the coast.
- three regional informational-processing centers (RIPC) of GS RAS, equipped with satellite communication system. RIPC'es are located in Petropavlovsk-Kamchatsky, Yuzhno-Sahalinsk and Vladivostok.

In addition, for the more accurate estimations of tsunami possibility, Global Seismographic Network data and regional GS stations data are involved in processing.
Strong motion observe points, operated in automatic mode, equipped with the accelerometers and deployed as close to source areas of Kuril-Kamchatka large earthquakes as possible. Maximal ground acceleration in these points may reach *g*.
All seismic stations are equipped with devices of the same type (velosimeters Güralp CMG-3ESP and CMG-6TD, accelerometers Güralp CMG-5 and CMG-5TD) and software for the digital registration and processing of seismic data in automatic and interactive modes.
Frequency and dynamic ranges of seismometric channels of specialized stations of SS TWS are presented on Fig.1.

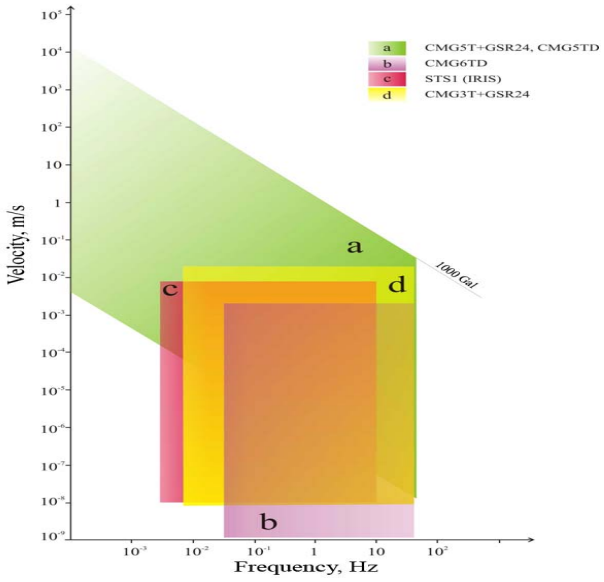


Fig. 1. Seismic channels of SS TWS and their frequency and dynamic ranges

Data collection network is realized on the satellite communication channels (VSAT), on the allocated Internet resources, special radio-Ethernet networks (5.3 GHz) (Fig. 2). Seismic data from

the stations, that involved in SS TWS, are transferred in real time mode to RIPC'es of GS RAS. Software provides visualization of seismic data streams on the monitors and data processing in automatic and interactive modes on the RIPC level.

RIPC'es in Petropavlovsk-Kamchatsky, Yuzhno-Sahalinsk and Vladivostok estimate earthquake parameters at the same time (in parallel). Joint parallel job of RIPC'es is provided by their equal and full access to the all data of all seismic stations of SS TWS. So, this way the RIPC functions reservation is ensured.

The problem of the fastest tsunami warning in the near field is solved based on macroseismic intensity estimations. This estimations are obtained from the data of base stations. Also, knowledge about special distribution of earthquakes in the Kuril-Kamchatka seismic region are used.

New generation Seismic Subsystem of TWS was in experimental operation mode during 2008–2010, and in November 2010, after test-period, was released.

In the zone of responsibility, depending of seismic network coverage, new generation SS TWS allows to realize three levels of tsunami warning. There are different temporal limits for every warning level:

- up to 4 minutes for settlements and coasts equipped with the base station. This warning type implies alarm message only on the local level, for the limited area.
- up to 7 minutes for potential tsunamigenic earthquakes with epicentral distances to any specialized SS TWS station within 200 km. It is supposed to estimate tsunami potential of event according to magnitude-geographic criterion.
- up to 20 minutes for the all zone of responsibility. Tsunami potential for such events is estimated according to magnitude-geographic criterion.

Operating experience of SS TWS, including processing results of March, 11, 2011 Japan earthquake, has allowed us to verify adequacy and reliable of all elements of SS TWS and effectiveness of developed and implemented software and algorithms for seismic data processing in operational mode according to regulations of TWS.

Currently in force TWS regulations do not take into account the real potential of new seismic subsystem. In particular, the technological capabilities of new generation SS TWS provide parallel seismic network data processing on the RIPC'es. Thus, any of ones can monitor all zone of responsibility. Big Japan earthquake (March, 11, 2011) processing results confirm this point of view.

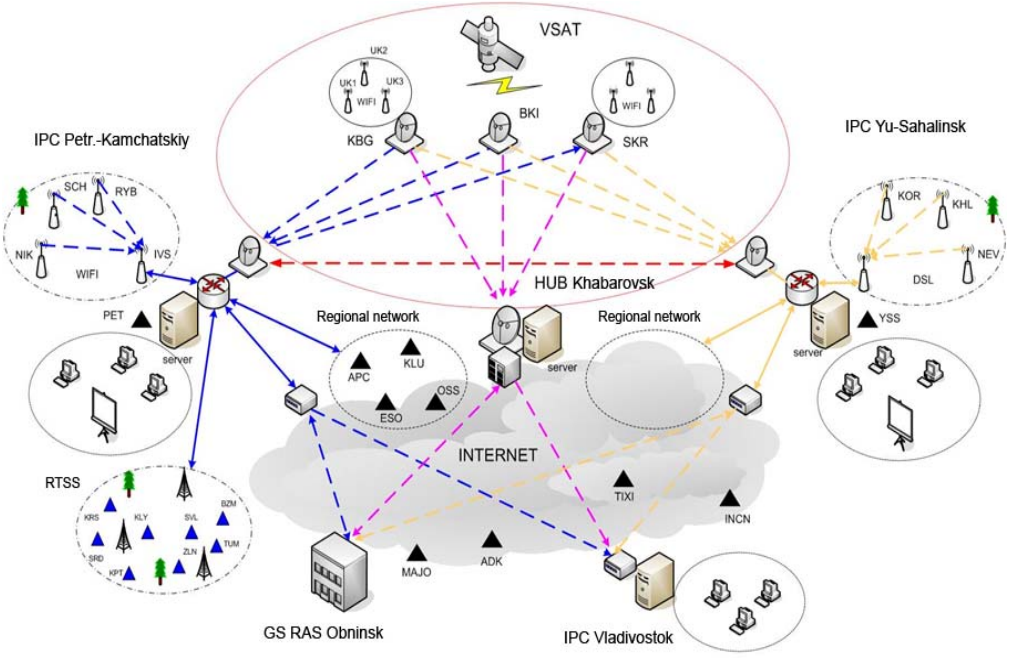


Fig. 2. Structure of distributed informational system of SS TWS

СИСТЕМА СЕЙСМОЛОГИЧЕСКИХ НАБЛЮДЕНИЙ В СЛУЖБЕ ПРЕДУПРЕЖДЕНИЯ О ЦУНАМИ НА ДАЛЬНЕМ ВОСТОКЕ РОССИИ

В.Н. Чебров[1], А.А. Гусев[1,2], Д.В. Дрознин[1], В.Н. Мишаткин[3], В.А. Сергеев[1], Ю.В. Шевченко[1], Д.В. Чебров[1]

[1]*Камчатский филиал Геофизической службы РАН, Петропавловск-Камчатский,* chebr@emsd.ru
[2] *Институт вулканологии и сейсмологии ДВО РАН, Петропавловск-Камчатский,* gusev@emsd.ru
[3] *Геофизическая служба РАН, Обнинск,* vmish@gsras.ru

В 2006–2010 гг. на Дальнем Востоке России Геофизической службой РАН была проведена модернизация системы сейсмологических наблюдений. В целях предупреждения о цунами была разработана и создана сейсмическая подсистема СПЦ нового поколения, которая включает в себя:

- -сейсмологическую сеть, состоящую из пяти опорных (ОЦС) и шести вспомогательных (ВЦС) специализированных цифровых сейсмических станций, а также 16 пунктов регистрации сильных движений (ПР СД). Опорные станции представляют собой сейсмические группы, расположенные в районах крупных населенных пунктов.
- -три региональных информационно-обрабатывающих центра (РИОЦ) Геофизической службы РАН, оснащенные спутниковой коммуникационной системой. РИОЦ располагаются в Петропавловске-Камчатском, Южно-Сахалинске и Владивостоке.

Кроме того, для уточнения решения о возможности цунами привлекаются данные станций Мировой сейсмической сети (GSN) и станций региональных сетей ГС РАН.
Пункты регистрации сильных движений, работающие в автономном автоматическом режиме, оснащены акселерометрами и установлены максимально близко к очаговым зонам возможных сильных землетрясений в Курило-Камчатском регионе. Максимально возможные ускорения в этих пунктах могут достигать g.
Все сейсмические станции и пункты регистрации сильных движений СП СПЦ оснащены отнотипным оборудованием (велосиметрами Güralp CMG-3ESP и CMG-6TD, акселерометрами Güralp CMG-5 и CMG-5TD), однотипными алгоритмами и программным обеспечением цифровой регистрации и обработки сейсмических данных в автоматическом и автоматизированном режиме.
Частотный и динамический диапазоны сейсмометрических каналов специализированных станций СП СПЦ и сети GSN представлены на рис. 1.

Сеть сбора данных реализована на спутниковых (VSAT) каналах связи, на выделенных ресурсах Internet, специализированных радио Ethernet сетях технологической связи диапазона 5.3ГГц, рис. 2. Данные сейсмостанций, вовлеченных в сейсмическую подсистему СПЦ, передаются в реальном масштабе времени в информационно-обрабатывающие центры Геофизической службы РАН. Программное обеспечение СП СПЦ обеспечивает отображение потоков сейсмических данных в реальном времени на мониторах, автоматическую и автоматизированную оценку параметров сильного землетрясения на уровне ИОЦ.
Региональные ИОЦ ГС РАН в городах Петропавловск-Камчатский, Южно-Сахалинск и Владивосток одновременно (параллельно) решают задачу определения параметров сильных землетрясений. Параллельная работа региональных ИОЦ обеспечивается созданием их равного и полного доступа к данным всех сейсмических станций, вовлеченных в службу предупреждения о цунами. Это обеспечивает резервирование выполнения функций каждого ИОЦ.

Задача максимально быстрого предупреждения о цунами в ближней зоне решается в автоматическом режиме по данным опорной специализированной сейсмической станции на основе оценки макросейсмической интенсивности (балльности) с использованием знаний о пространственно-временных закономерностях распределения очагов сильных землетрясений в Курило-Камчатской сейсмофокальной зоне.

Сейсмическая подсистема СПЦ нового поколения в 2008–2010 гг. прошла апробацию и в ноябре 2010 г. по результатам испытаний была принята в эксплуатацию.

В зоне ответственности, в зависимости от обеспеченности сейсмологическими наблюдениями, СП СПЦ нового поколения позволяет реализовать три уровня тревоги цунами с различными временными ограничениями:

- до 4 минут для населенных пунктов или участков побережья, где установлены опорные станции. Сообщение о возможности цунами в этом случае передается только на локальном уровне, то есть для конкретных населенных пунктов или участков побережья.
- до 7 минут – для потенциально цунамигенных землетрясений с очагами до 200 км от любой специализированной станции СП СПЦ с оценкой цунамигенности события по магнитудно-географическому критерию.
- до 20 минут – по всей зоне ответственности СПЦ в соответствие с магнитудно-географическим критерием.

Опыт эксплуатации СП СПЦ, в том числе результаты обработки землетрясения 11 марта 2011 г. в Японии, позволили проверить адекватность и надежность всех элементов сейсмической подсистемы СПЦ и эффективность разработанных и внедренных алгоритмов и ПО обработки сейсмологических данных в оперативном режиме по регламентам СПЦ.

Действующие сегодня в СПЦ на Дальнем Востоке регламенты не учитывают всех возможностей новой сейсмической подсистемы. В частности, технологические возможности СП СПЦ нового поколения обеспечивают параллельную обработку данных по полной сети станций всеми РИОЦ. Таким образом, все РИОЦ в дублирующем режиме способны контролировать зону ответственности СПЦ в целом. Результаты обработки землетрясения 11 марта 2011 г. и его афтершоков это подтверждают.

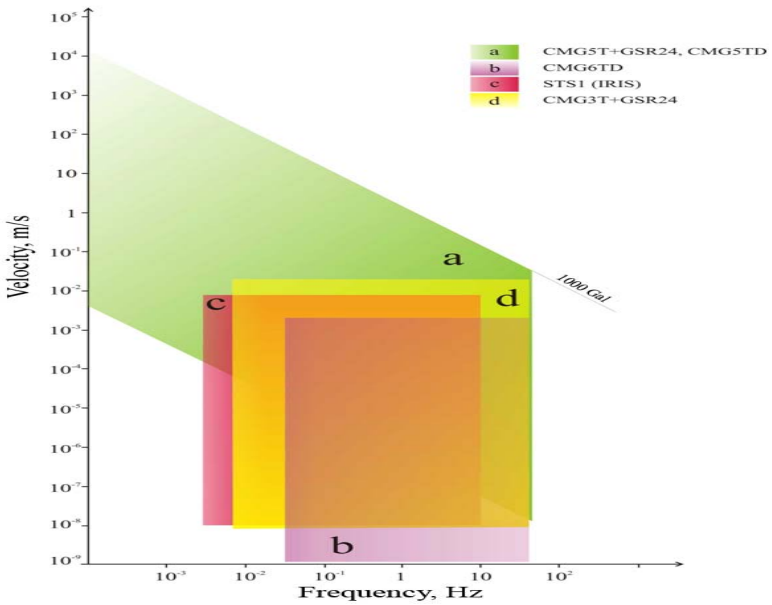


Рис. 1. Диапазоны сигналов, регистрируемые каналами сейсмической подсистемы СПЦ

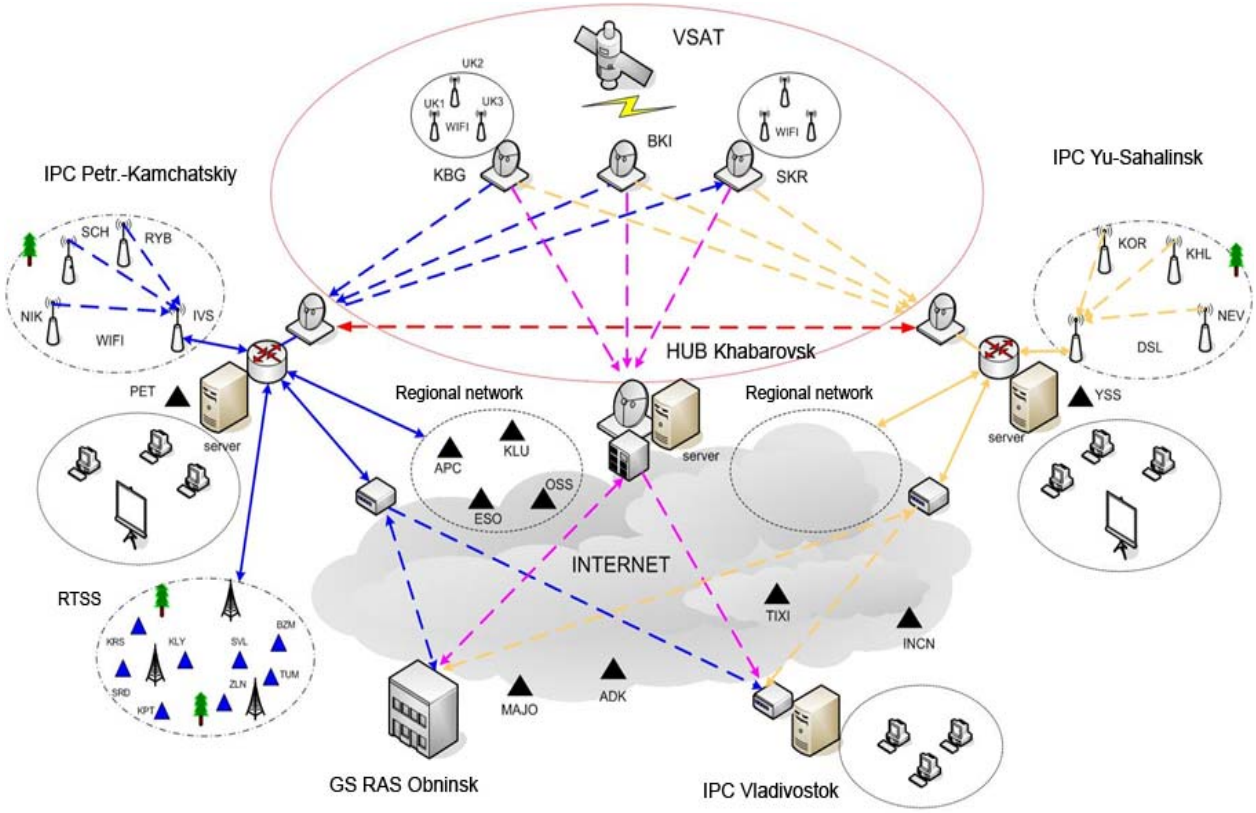


Рис. 2. Структура распределенной информационной системы сейсмической подсистемы СПЦ

Numerical modeling of the natural state of the Geysers Valley hydrothermal system (Kronotsky Nature Reserve, Kamchatka) preceding of the Giant Landslide

A.V. Kiryukhin, T.V. Rychkova, I.K. Dubrovskaya
Institute of Volcanology and Seismology FEB RAS
AVKiryukhin2@mail.ru; *Avk2@kscnet.ru*

Introduction. The Geysers Valley is located in the Kronotsky State Reserve of the Kamchatka Peninsula, Russia. It has the largest natural discharge rate of the twelve high-temperature hydrothermal systems in the Kamchatka. On June 3, 2007, a catastrophic Giant landslide took place in the Geysers Valley, Kamchatka. It occurred synchronously with a steam explosion and was then transformed into a debris mudflow. Within a few minutes, 20 x 10^6 m^3 of rocks were shifted 2 km downstream the Geysernaya river, which created a dam with Podprudnoe lake behind, and buried more than 23 geysers, including 5 famous geysers (Pervenetz, Troinoy, Conus, Maly and Bolshoy). The 20-30 m deep Podprudnoe lake started to inject cold water into the remaining part of the Geysers Valley hydrothermal system.

Landslides with hydrothermal explosions are a challenge to safety conditions for visitors to Geysers Valley, which amounts to 3000 people annually. Hence it is important to understand what hydrothermal system parameters are responsible for landslides/hydrothermal eruptions to set up proper monitoring and recognize precursors of such events. Geysers Valley geothermal reservoir conditions and processes are also may learn as analog for places of potential nuclear waste storage (like Yucca Mountain, Nevada, USA) and heat driven gas pressure buildup (like Fukusima nuclear power plant accident).

The objectives of the present study are to integrate available hydrogeological data (Kiryukhin et al, 2010, 2011) to develop 3D thermal hydrodynamic (chemical) models to deduce a mechanism for the formation hydrothermal system and its response to changing recharge/discharge conditions after the Giant landslide of June 3, 2007, and to understand triggers of such catastrophic events to be able to forecast future ones.

Model set up. TOUGH2-EOS3 software and PetraSim pre- postprocessor were used. EOS3 (equation of state 3) module is capable of describing two-phase (liquid+gas) two-component (water+air) unsaturated zone conditions prevalent in the elevated parts of the Geysers Valley. The model boundary was defined so as include the main thermal features: Lower Geysers Field and Upper Geysers Field, where most of the deep component thermal discharge of 260-300 kg/s occur, and follows the main structural/hydrodynamic boundaries along Uzon-Geysernaya caldera rim, the Geyseranaya and Shumnaya rivers basins. The top of the model coincides with the topographic elevations and the bottom is at -2000 m.a.s.l. The two main geological units (layers) defined in the model are: (1) Pliocene-Quaternary volcanogenic reservoir, (2) Tertiary sedimentary basement. The bottom of the reservoir (top of basement) is defined at -150 m.a.s.l. The polygonal Voronoi mesh generation processing was applied to the model, and the upper layer was divided into 10-mesh sub layers, while the lower layer was divided into 5-mesh sub layers. The total number of grid elements is 10,500. Model zonation includes the following domains with different material properties: caprock units, composed of caldera lake tuffs; host reservoir; fractured reservoir (two permeable fault zones); more permeable lateral contact zone in reservoir (contact between caldera lake tuffs and pre-caldera volcanic units); host basement; fractured basement (two permeable fault zones); reservoir earth surface - top mesh sub layer used to assign atmospheric conditions (pressure of 1 bar and gas saturation of 0.9). This automatically allows discharge at lowlands. Discharge conditions were assigned to 59 hot springs and fumaroles known before the Giant landslide of June 3, 2007. All thermal discharge features were assigned as wells on deliverability. Initial conditions were deduced corresponding to conductive heat flow of 60 mW/m^2 at the bottom of the model and hydrostatic pressure distribution. Heat and mass sources (high temperature upflow recharge) were distributed in the elements at the bottom of the model basement layer along permeable fault zones

within the area above of the suggested magma body (a total injected mass flowrate of 250 kg/s, with an enthalpy of 900 kJ/kg).

Modeling results. Modeling runs were completed with outputs at 1000 - 100,000 years, in order to explore the possible timing of the Geysers Valley formation. Inverse modeling capabilities of iTOUGH2-EOS3 were used to calibrate reservoir permeability and productivity indexes of 39 most significant springs based on their flowrates data. Based on modeling different scenarios, it was found that the formation of Geysers Valley hydrothermal system took from 20,000 to 30,000 years in terms of temperature distributions and discharge flowrates. By then most of the modeled springs became boiling with enthalpies of 500-700 kJ/kg and quasi-stable flowrates, while higher thermal features came into two-phase conditions. The shape of the temperature anomaly covers the known thermal features distributions and most of the permeable reservoir maintains a temperature of around 210°C, which corresponds to geothermometry estimates. It was found in the model, that meteoric recharge took place on the outcrops of Mt. Geysernaya rhyolite extrusion $\alpha\xi Q_3^4$ on the right bank of Geysernaya river. Model analysis shows that steam pressure in the wide two-phase zone reaches 7.0-8.5 bars at a depth of 150-250 m between steam vent, backing Giant landslide of June 3, 2007 and geyser Velikan, which are conditions of potential steam explosion, if steam pressure transmits to shallower levels.

Conclusions. The Geysers Valley hydrothermal system is hosted within a system of two permeable faults (confirmed by mapping thermal features), adjacent to suggested partially melted magmatic body and recharged by meteoric water along outcrops of rhyolite-dacite extrusions (ξQ_3^4). Natural state thermal hydrodynamic iTOUGH2-EOS3 modeling shows that 20,000-30,000 years with a high temperature upflow of 250 kg/s and enthalpy of 900 kJ/kg is can build up a hydrothermal system in the Geysers Valley basin with observed output discharge. Modeling also shows that high temperature upflow include two roots (below Lower Geysers and Upper Geysers Fields), meteoric recharge occurs mainly through outcrops of Mt. Geysernaya rhyolite-dacite extrusion (ξQ_3^4) and that steam accumulating below the inclined caprock (southeast from Lower Geysers Field) may have hydrothermal eruption potential. Model parameters are verified by hot springs flowrates, the isotopic composition of thermal fluids (δD, δ^{18}O) and silica geothermometry.

References.

Kiryukhin, A.V., Rychkova, T.V., Droznin, V.A., Chernykh, E.V., Puzankov, M.Y., Vergasova, L.P., 2010. Geysers Valley hydrothermal system (Kamchatka): Recent changes related to landslide of June 3, 2007. Proc. WGC- 2010 Bali, Indonesia, 25-29 April 2010, 6 p.

Kiryukhin, A.V., Rychkova, T.V., 2010. Hydrothermal system in Geysers Valley (Kamchatka) and triggers of the Giant landslide. Proc. 13-th Int. Conf. Water-Rock Interaction, Guanajuato, Mexico, 16-20 Aug. 2010, p. 917-920.

Kiryukhin, A.V., Rychkova T.V., 2011. Conditions of Formation and State of the Geysers Hydrothermal System (Kronotsky Zapovednik, Kamchatka). Geoecology. Engineering Ecology. Hydrogeology. Geocriology. #3, 114-129. (in Russian).

Vadim SALTYKOV, Nadezhda KRAVCHENKO

A STATISTICAL ESTIMATION OF SEISMICITY LEVEL: THE METHOD AND RESULTS OF APPLICATION TO ALASKA AND ALEUTIAN ISLANDS

Kamchatka Branch, Geophysical Survey, Russian Academy of Sciences
Petropavlovsk_Kamchatsky, 683006 Russia
e-mail: salt@emsd.ru

Information on the current seismicity of a region is rather widely required. The persons who are interested include not only members of the seismological community, but also organizations that are professionally involved in the monitoring of the natural environment (in particular, the Ministry of Emergencies and administrative units). A separate problem apart is that of providing earthquake information to residents of seismic regions.

In view of the wide range of potential users, the characteristics used must be, on the one hand, intuitively understandable and, on the other, their definition must be based on quantitative seismicity parameters. Traditionally the solution is to make scales that convert numerical values to qualitative characteristics.

A formalized scale of the seismicity level makes for greater terminological definiteness in descriptions of the state of the seismicity in a region and avoids several ambiguities in assessment and comparisons between seismicities in different space–time volumes. In particular, the concept of "seismic background" is formalized thereby.

There is description of the scale for seismicity level that relies on the statistical distribution function of seismic moment M_0 as a parameter that characterizes the seismicity level in a specified space object during a specified time interval. Considering that the basic parameter is statistical in character, the procedure proposed was called *Statistical Estimate of Seismicity Level*, or *SESL*.

The technique has been introduced into the practice of the Kamchatka Branch of the Geophysical Survey RAS [*Saltykov*, 2011]. Estimates of the current seismicity level on Kamchatka are reported on a weekly note to the Kamchatka Branch of the Russian Expert Council for Earthquake Prediction, Assessment of Volcanic Hazards, and Risk and can be found in the Council's conclusions about the seismic situation in the region.

A scale of seismicity levels.

The concept of "background" is associated with the notions of "usual, widely prevalent, and of the most frequent occurrence," in contrast to the notion of an "anomaly," which is observed rather rarely. Bearing this in mind, we propose to define the threshold values of the distribution function F as follows: $F = 0.005$, 0.025, 0.15, 0.85, 0.975, and 0.995. The intervals between these values make a scale that contains five seismicity levels:

extremely high,	$0.995 \le F$,
high,	$0.975 \le F < 0.995$,
background,	$0.025 < F < 0.975$,
low,	$0.005 < F \le 0.025$,
extremely low,	$F \le 0.005$.

According to this scale, seismicity is 95% of the time at the background level, with 2% occurring at high and low levels and 0.5% at extremely high/low levels, which may be defined as seismicity anomalies. To make the division more detailed, the background level can be subdivided into three further sublevels:

lower background,	$0.025 < F \le 0.15$,
intermediate background,	$0.15 < F < 0.85$,
higher background,	$0.85 \le F < 0.975$.

With this refinement, the intermediate background level will occur 70% of the monitoring time, while 12.5% are for the higher/lower background levels.

Conclusions

The *SESL* technique in order to estimate the seismicity level in a specified space–time region in qualitative terms based on a quantitative parameter, viz., the distribution function of seismic moment M_0 was developted.

Suggested scale for estimating seismicity levels contains five basic grades and three additional ones.

The main features of this technique and demonstrated certain restrictions on its uses were outlined.

An example of using the technique for one of the most seismically active regions of the world – Alaska and Aleutian Isl. was demonstrated.

References

Saltykov V.A. A statistical estimate of seismicity level: the method and results of application to Kamchatka // Journal of Volcanology and Seismology, 2011, Vol. 5, No. 2, pp. 123–128. (*Original Russian Text: V.A. Saltykov, 2011, published in Vulkanologiya i Seismologiya, 2011, No. 2, pp. 53–59*). DOI: 10.1134/S0742046311020060

Studying volcanoes and faults based on correlations of ambient seismic noise

Nikolai Shapiro
Institut de Physique du Globe de Paris, France

Traditional observational methods in seismology are based on earthquake records. It results in two main shortcomings. First, most techniques are based on waves emitted by earthquakes that occurred only in geologically active areas, mainly plate boundaries. This results in a limited resolution in all other areas where earthquakes are not present. Second, the repetition of earthquakes is rare, preventing the study continuous changes within active structures such as volcanoes or faults.

Nowadays, the seismic networks are producing continuous recordings of the ground motion. These huge amounts of data consist mostly of so called seismic noise, a permanent vibration of the Earth due to natural or industrial sources. As described in many studies where noise has been used to obtain the Green's function between receivers, coherent waves are extracted from noise signals even if, at first sight, this coherent signal appears deeply buried in the local incoherent seismic noise. Recent studies on passive seismic processing have focused on two applications, the noise-extracted Green's functions associated to surface waves leads to subsurface imaging on scales ranging from thousands of kilometres to very short distances; on the other hand, even when the Green's function is not satisfactorily reconstructed from seismic ambient noise, it has been shown that seismic monitoring is feasible using the scattered waves of the noise-correlation function.

One of the advantages of using continuous noise records to characterize the earth materials is that a measurement can easily be repeated. This led recently to the idea of a continuous monitoring of the crust based on the measurements of wave speed variations. The principle is to apply a differential measurement to correlation functions, considered as virtual seismograms. The technique developed for repeated earthquakes (doublets), proposed by Poupinet et al., 1984, can be used with correlation functions. In a seismogram, or a correlation function, the delay accumulates linearly with the lapse time when the medium undergoes a homogeneous wave speed change and a slight change can be detected more easily when considering late arrivals. It was therefore reasonable, and often necessary, to use coda waves for the measurements of temporal changes. Noise based monitoring relies on the autocorrelation or cross-correlation of seismic noise records (Sens-Schönfelder and Wegler, 2006, Brenguier et al., 2008a,b). When data from a network is available, using cross-correlation take advantage of the number of pairs with respect to the number of stations.

SEMIAUTOMATIC MOMENT TENSOR INVERSION USING REGIONAL BROADBAND SEISMOGRAMS

Victor Pavlov, Iskander Abubakirov

Kamchatkan Branch of Geophysical Survey of RAS, Petropavlovsk-Kamchatsky, Russia

The seismic moment tensor (SMT) contains information on the mechanism and the moment magnitude Mw of an earthquake source. The reliable and quick estimates of SMT as well as the estimates of the depth and the duration of the source process of earthquakes are very important for the assessment of potential damage and tsunami forecast.

In earlier studies (Abubakirov, Pavlov, 2010; Pavlov, Abubakirov, 2009) an interactive algorithm was developed for simultaneous assessment of SMT, depth and source duration by complete regional broadband seismograms. The algorithm testing for 5 strong earthquakes (Mw 7.6-8.3) was successful but revealed that surface waves were sometime distorted by instrument errors at periods more than 120 seconds. For correct estimation of magnitude M_w of large earthquakes the longer periods are required.

In this paper a modified version of the algorithm is proposed that can be applied to body waves only. Both algorithms share the following points. The radiation of an extended source at low frequencies is approximated by radiation of a point source with symmetric-triangular source time function (STF) of adjustable duration τ. For fixed point source depth h and duration τ, SMT (having null trace) is calculated by linear inversion. The best estimate of SMT is seeking by systematic search over h and τ. The modified algorithm differs from the previous one by the features: (1) deconvolution in time domain; (2) automatic procedure of selecting intervals for fitting; (3) using of a Green's functions library. (Green's functions were calculated by the technique developed in (Pavlov, 2009)). The algorithm is semiautomatic; the only manual operation to automate is the data collection.

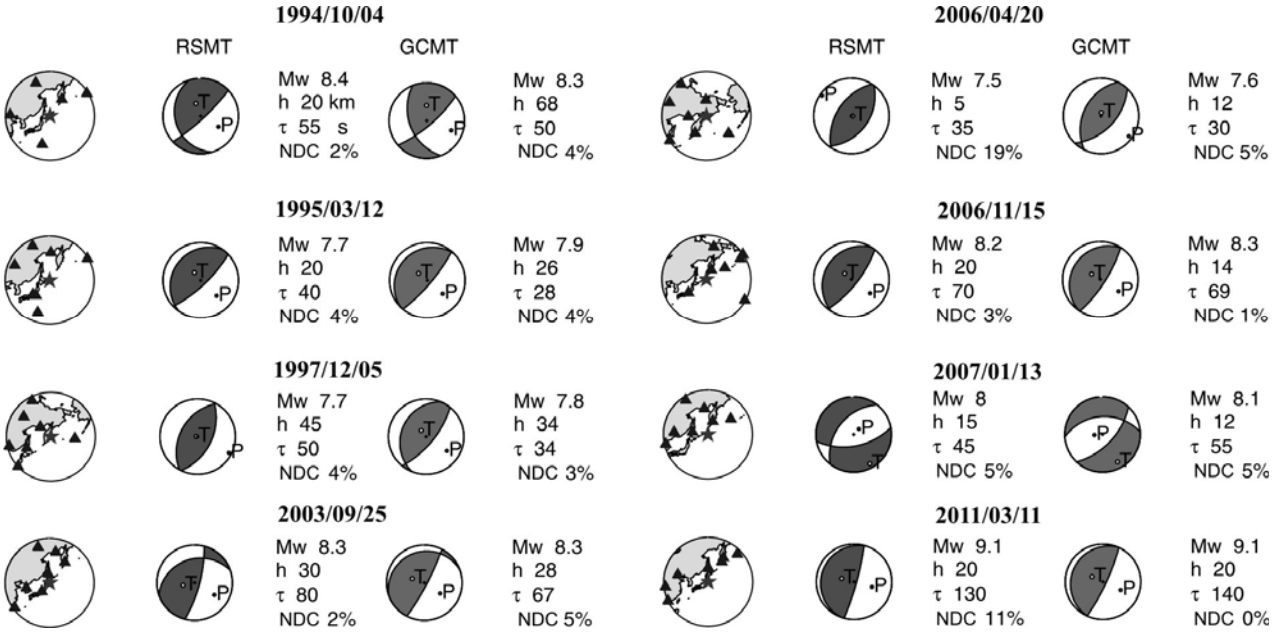


Fig. 1. Summary of results of this study (RSMT) and those of CMT estimations (GCMT, http://www.globalcmt.org). Epicenter and station locations are shown. NDC is the percentage of non double part of the SMT.

Practical estimation of SMT was performed for 8 largest earthquakes occurred in the Far East of Russia and Japan (Mw 7.6-9.1) (fig. 1). In figures 2, 3 details are shown for the largest (Mw 9.1) Tohoku earthquake 2011/3/11.

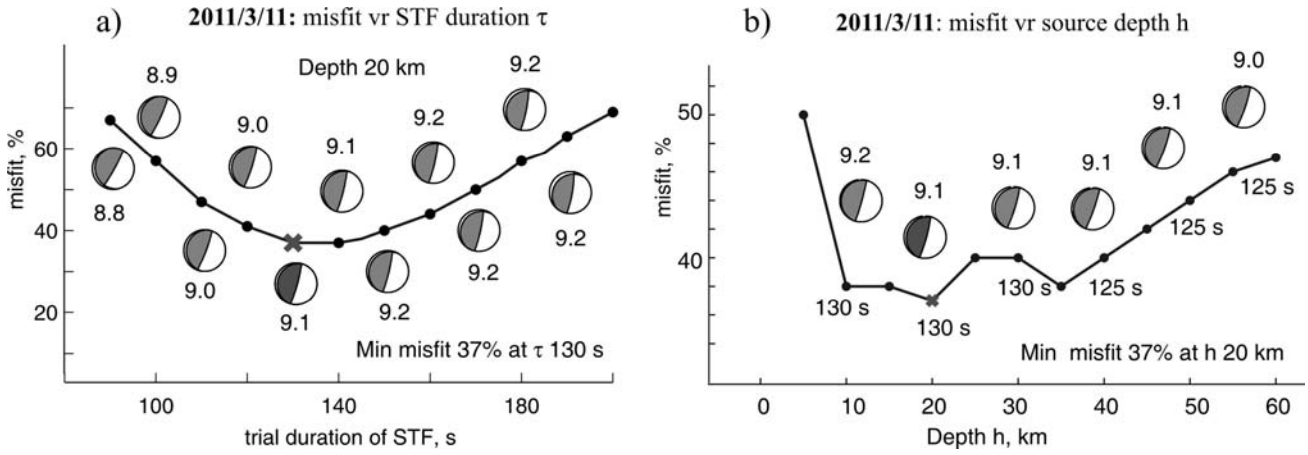


Fig. 2. Dependence of misfit on duration (a) and depth (b).

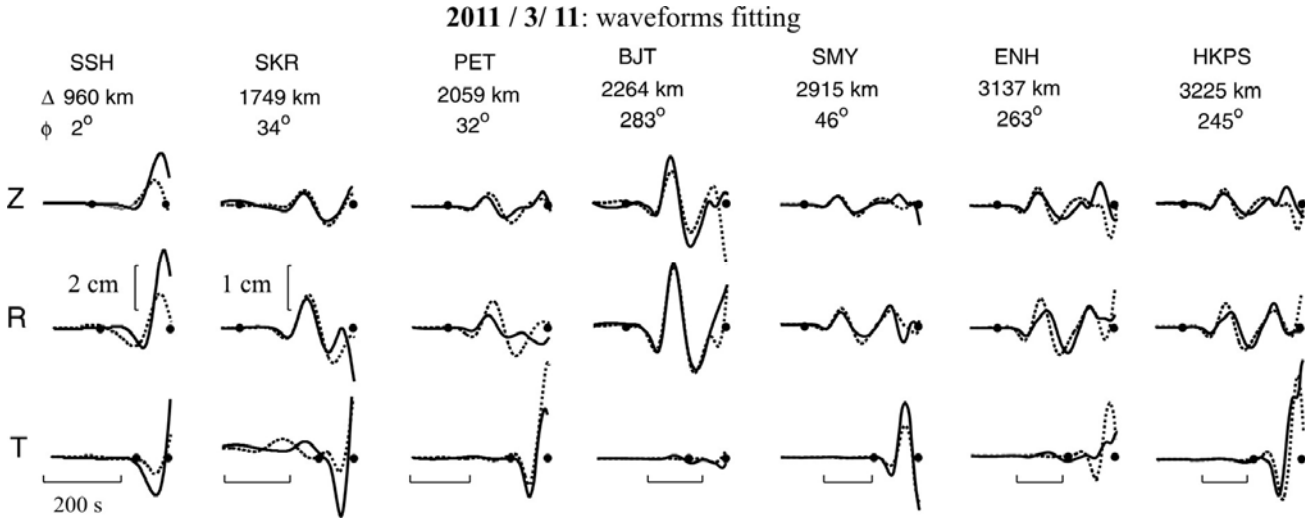


Fig. 3. Observed (solid lines) and calculated (dashed lines) displacements for 2011/3/11 event (Mw 9.1). The points mark the fitting intervals. Epicentral distances and azimuths of the used stations are shown. The period band is 100-300 seconds.

References

Abubakirov I.R., Pavlov V. A moment tensor estimation algorithm for regional earthquakes // Problems of seismicity and recent geodynamics of the Far East and Eastern Siberia: June 1-4, 2010, Khabarovsk, Eds. V.G. Bykov, A.N. Didenko. P. 235-338 (in Russian).

Pavlov V.M. Matrix impedance in the problem of the calculation of synthetic seismograms for a layered-homogeneous isotropic elastic medium // Izvestiya, Physics of the Solid Earth, 2009. V. 45. No. 10. P. 848–858.

Pavlov V.M., Abubakirov I.R.. A moment tensor estimation algorithm based on a new method of synthetic seismogram calculation // JKASP-2009. June 22-26, 2009. Abstracts. Geophysical Institute, University of Alaska. Fairbanks, Alaska. P. 155-156.

ПОЛУАВТОМАТИЧЕСКИЙ РАСЧЕТ ТЕНЗОРА МОМЕНТА ПО РЕГИОНАЛЬНЫМ ШИРОКОПОЛОСНЫМ СЕЙСМОГРАММАМ

Павлов В.М., Абубакиров И.Р.

Камчатский филиал Геофизической службы РАН, Петропавловск-Камчатский, Россия

Тензор сейсмического момента (ТСМ) содержит информацию о механизме и моментной магнитуде Mw очага землетрясения. Надежные и быстрые оценки ТСМ, а также оценки глубины и очаговой длительности землетрясений имеют первостепенное значение для оценки потенциального ущерба и прогноза цунами.

Ранее в работах авторов [1, 3] был разработан интерактивный алгоритм одновременной оценки ТСМ, глубины и очаговой длительности по полным региональным широкополосным сейсмограммам. Опробование алгоритма для 5 сильных (M_w=7.6-8.3) землетрясений было успешным. Вместе с тем было обнаружено, что поверхностные волны зачастую искажены помехами на периодах больших 120 секунд, что приводит к занижению оценки Mw сильных землетрясений.

В данной работе предлагается модифицированная версия алгоритма, которая может использовать только объемные волны. Оба алгоритма сходны в следующем. Излучение протяженного очага на низких частотах апроксимируется излучением точечного источника с треугольной временной функцией (ВФИ) длительности τ. При фиксированных глубине источника h и продолжительности ВФИ τ, ТСМ (с нулевым следом) вычисляется при помощи линейной инверсии. Наилучшая оценка ТСМ ищется перебором по значениям h и τ. Новый алгоритм отличается от предыдущего тем, что: (1) деконволюция проводится во временной области; (2) процедура выбора сегментов для подгонки автоматизирована; (3) используется библиотека функций Грина (рассчи-тывались по алгоритму работы [2]). В результате алгоритм становится полуавтомати-ческим – не автоматизирована лишь процедура отбора исходных сейсмограмм.

Алгоритм был применен к 8 наиболее сильным землетрясениям Дальнего Востока России и Японии (Mw 7.6-9.1) (рис. 1). На рис. 2, 3 приведены подробности для крупнейшего (Mw 9.1) землетрясения Тохоку 2011/3/11.

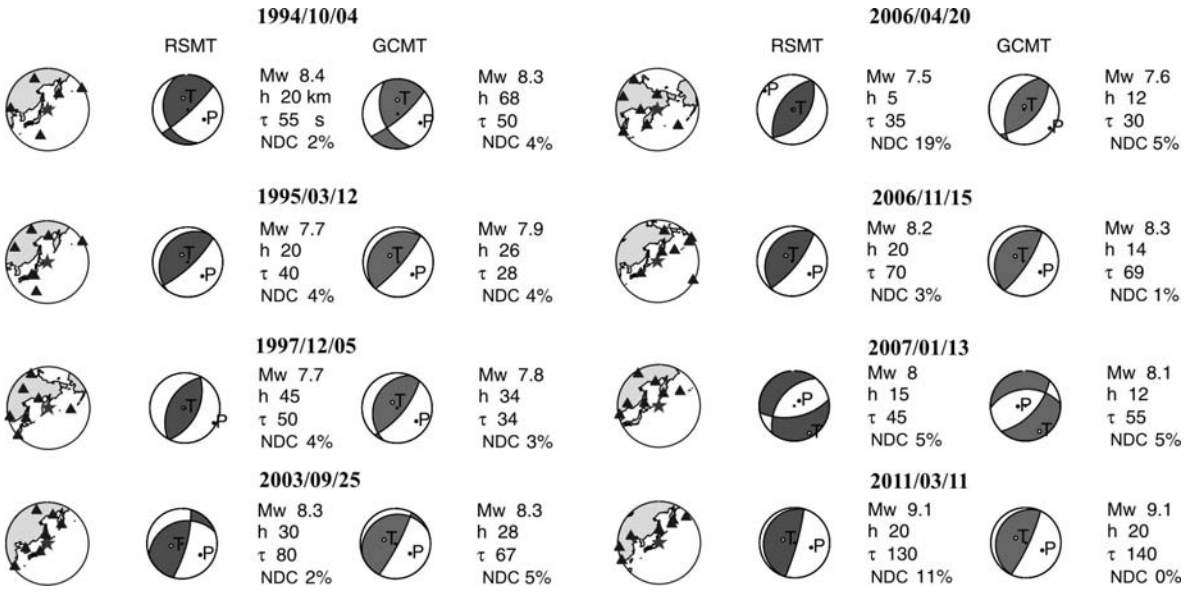


Рис. 1. Сводка результатов данной работы (RSMT) и CMT оценок (GCMT, http://www.globalcmt.org). Показано положение эпицентров и станций. NDC – коэффициент отклонения от двойного диполя без момента.

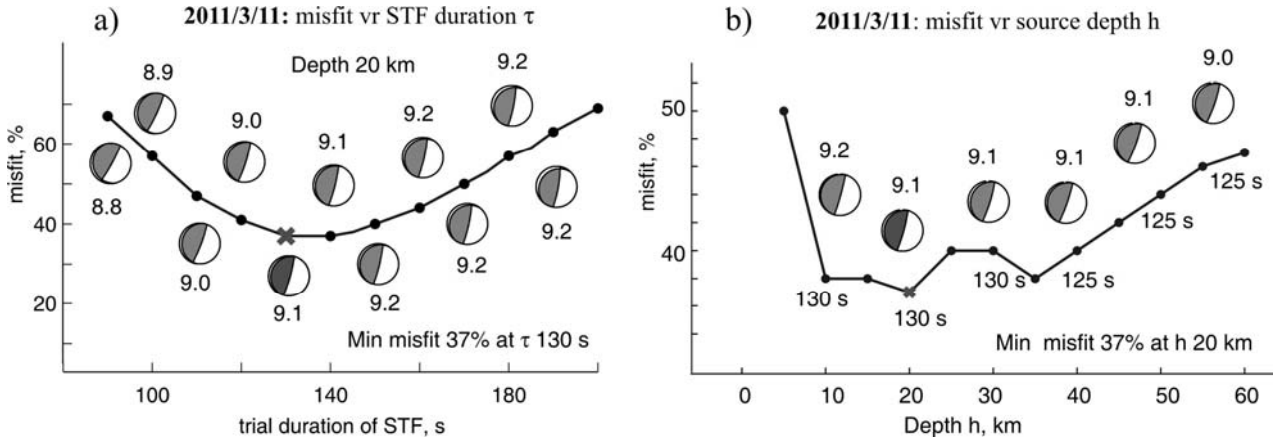


Рис. 2. Зависимость невязки от длительности ВФИ (a) и глубины (b).

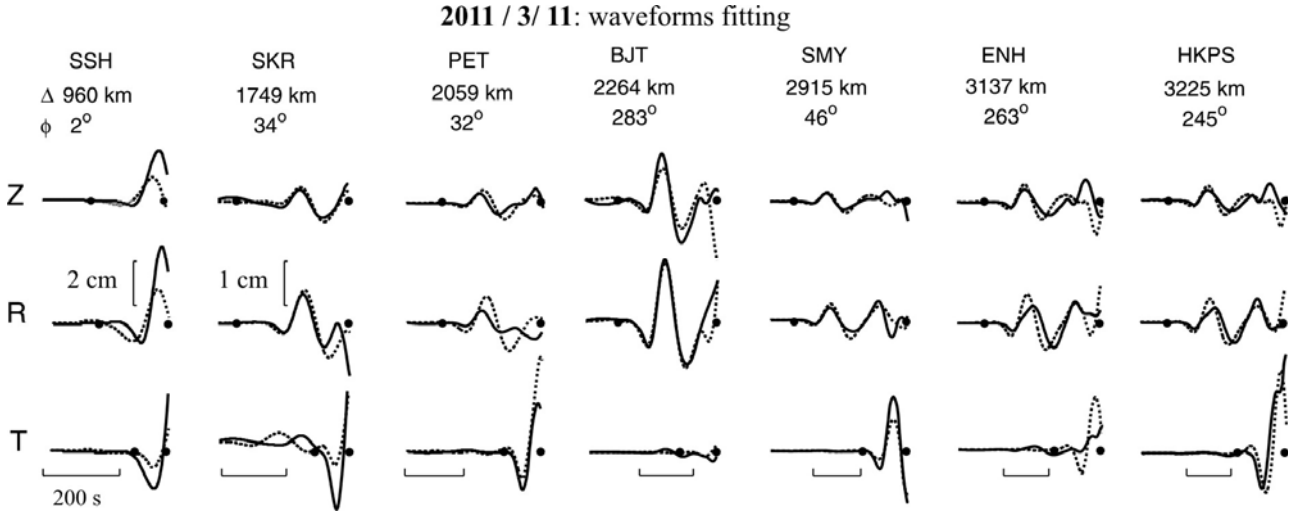


Рис. 3. Наблюденные (сплошные) и рассчитанные (пунктирные) смещения для землетрясения 2011/3/11 (Mw 9.1). Точки отмечают интервал подгонки. Приведены значения эпицентральных расстояний и азимутов использованных станций. Полоса периодов 100-300 секунд.

Список литературы

1. Абубакиров И.Р., Павлов В.М. Алгоритм расчета тензора сейсмического момента для региональных землетрясений // Проблемы сейсмичности и современной геодинамики Дальнего Востока и Восточной Сибири: 1–4 июня 2010, Хабаровск / ред. В.Г. Быков, А.Н. Диденко. С. 235-238.
2. Павлов В.М. Матричный импеданс в задаче расчета синтетических сейсмограмм в слоисто-однородной изотропной упругой среде //Физика Земли. 2009. № 10. С. 14-24.
3. Pavlov V.M., Abubakirov I.R.. A moment tensor estimation algorithm based on a new method of synthetic seismogram calculation // JKASP-2009. June 22-26, 2009. Abstracts. Geophysical Institute, University of Alaska. Fairbanks, Alaska. P. 155-156.

Determination of space–time characteristics of sources of large earthquakes from teleseismic high-frequency records

Alexander A. Gusev, Evgenia M. Guseva

Institute of Volcanology and Seismology, Russ.Ac.Sci. Petropavlovsk-Kamchatsky,Russia
Kamchatka Branch, Geophysical Service, Russ.Ac.Sci. Petropavlovsk-Kamchatsky,Russia

For large earthquakes, high-frequency (HF) source size and duration can be recovered using time histories of the instant power (squared amplitudes, high frequency power signals, HFPS) of radiated HF waves, in particular teleseismic *P* waves. The technique for such an inversion was developed by A.A.Gusev and V.M.Pavlov in 1990ies. It is based on two original procedures: (1) to apply inverse filtering to observed HFPS using an aftershock records to determine empirical Green function representing HFPS propagated along a certain ray path and (2) to reconstruct, by linear inversion, power moments of the radiator and use them to deduce gross space-time properties of a source.

Recently this approach was applied to two interesting earthquakes. The first is the great Sumatra-Andaman islands earthquake of 2004 December 26 (*M*w = 9.1–9.3) We processed teleseismic *P* waves at 36 BB stations, using, in sequence: (1) bandpass filtering (four bands: 0.4–1.2, 1.2–2, 2–3 and 3–4 Hz); (2) squaring wave amplitudes, producing four HFPS per trace and (3) stripping the propagation-related distortion (*P* coda, etc.) from the recorded HFPS, thus recovering radiated source HFPS. For each ray we thus obtain signals with relatively well-defined end and no coda. From these signals we extract: total duration (joint estimate for all four bands) and temporal centroid of signal power for each band. Through linear inversion, the set of duration values for a set of rays delivers estimates of the rupture stopping point and stopping time. Similarly, the set of temporal centroids can be inverted to obtain the position of the space– time centroid of HF energy radiator. For the source length and duration the following estimates were obtained: 1241±224 km, 550±10 s. The estimated stopping point position corresponds to the northern extremity of the aftershock zone. Spatial HF radiation centroids are located at distances 350–700 km from the epicentre, in a systematic way: the higher is the frequency, the farther is the centroid from the epicentre. Average rupture propagation velocity is estimated as 2.25 km/s.

Similar technique was applied to records of 2006 April 20 (Mw=7.6) Olyutorskii earthquake, a unique crustal event in Koryakia whose rupture delineated a 150-km stretch of arguable Beringia-North America plate boundary. This is a smaller-scale event, making data processing more difficult; in addition, its bilateral mode of rupturing prevented simple determination of fault size from the position of a single rupture stopping point. Still, using 57 stations and two frequency bands (0.7–1.7 and 1.5–2.5 Hz), we have determined the parameters of the HF radiator for this event. To overcome problems with bilateral rupture, we assumed the source to consist of two linked linear segments ruptured bilaterally from the hypocenter at a constant velocity. The estimates of space-time parameters are as follows: total length 128 ± 52 km, the strike of the longer arm of the rupture 225° ± 19° SW, the distance from the epicenter to the centroid 23 ± 9 km, and rupture velocity 2.5 ± 0.8 km/s. The rupture was bilateral with a moderate asymmetry. The rupture duration was 35.0 ± 1.6 s for the southwestern arm and about 23 s for the northeastern arm. Estimated spatial parameters match fault rupturing observed at the day surface by T.K.Pinegina, and agree with the geometry of the aftershock cloud.

Detection of Strombolian Activity in Satellite Data

Anna Worden, *Alaska Volcano Observatory, Geophysical Institute, University of Alaska Fairbanks,903 Koyukuk Drive, Fairbanks, AK, 99709, (akworden@gi.alaska.edu)*
Jonathan Dehn, *Alaska Volcano Observatory, Geophysical Institute, University of Alaska Fairbanks,903 Koyukuk Drive, Fairbanks, AK, 99709, (jdehn@gi.alaska.edu)*
Maurizio Ripepe, *Dipartimento Scienze della Terra, Università di Firenze, via LaPira 4, 50121 Firenze, Italy (maurizio.ripepe@unifi.it)*
Andrew Harris, *Laboratoire Magmas et Volcans, Université Blaise Pascal, 5 Rue Kessler, 63038 Clermont Ferrand, France (A.Harris@opgc.univ-bpclermont.fr)*

Strombolian activity across the remote volcanoes of the Aleutian Islands and Kamchatka Peninsula cannot be monitored easily or safely by direct methods. Satellite remote sensing offers a useful means to routinely monitor these volcanoes.

In order to model the expected time-dependent thermal signal recorded by the satellite/sensors, we carried out laboratory-based experiments and collected field data for cooling spatter and bomb fields. Preliminary laboratory work was focused on finding an acceptable lava analog, as well as appropriately scaled pressures and vent sizes. Honey emitted from 0.5-3.8 cm diameter vents by explosions with pressures of around 0.05 MPa seemed to work the best. Scaled explosions were recorded with a FLIR thermal camera and a digital video camera. Explosions at Stromboli Volcano in Italy were also recorded with the same thermal camera over a period of days in May and June, 2010, and were compared to the scaled explosions. In both the modeled and actual explosions, vent diameter directly dictates the type of explosion and deposit distribution ranging from intense jetting from small vents to diffuse spattering from larger vents. The style of emission controls the area of, and distribution of bombs within, the resulting bomb field. This, in turn, influences the cooling rate of the bomb field.

The cooling rate of spatter and bomb fields (most likely the source of thermal anomalies in satellite data) for both modeled and actual explosions compared well, and is on the order of seconds to minutes. For a single explosion of average size, the thermal signal is detectable by satellite for a time period in terms of tens of seconds. Thus, in order to see a thermal signature related to a strombolian explosion, a satellite must pass over the volcano (with acceptable geometries) within about a minute of an explosion. A volcano with 70 explosions per day would produce roughly an hour of detectable thermal anomalies. With about a dozen possible NOAA and NASA satellite overpasses daily, dependent on weather and viewing geometry, an anomaly would be seen every couple of days and almost certainly once a week. Satellite images from Stromboli volcano in Italy, Mt. Chuginadak (Cleveland) and Shishaldin volcanoes in Alaska, and Karymsky volcano in Kamchatka are analyzed to detect thermal anomalies likely associated with strombolian explosions and determine the relative frequency of activity. By calibrating events observed by satellite with events recorded in infrasonic, seismic, and FLIR data a tool can be developed to gauge increasing or decreasing strombolian activity at remote volcanoes.

Using Local and Remote Infrasound Recordings to Detect and Characterize Explosive Volcanic Activity

David Fee, Stephen R. McNutt, Taryn M. Lopez, Kenneth M. Arnoult, Curt A. L. Szuberla, John V. Olson, Michael West

Geophysical Institute, University of Alaska Fairbanks

Remote infrasound arrays have become increasingly useful in detecting and characterizing explosive volcanic activity. The explosive phase of the 2009 Redoubt Volcano eruption produced predominantly short duration, high amplitude infrasound signals recorded up to 4500 km away. All 19 numbered explosive events were recorded at a local microphone (DFR, 12 km), as well as at an infrasound array in Fairbanks, Alaska (I53US, 547 km), most with high signal to noise ratios. The local microphone provides an estimate of the source parameters, and comparison between the two datasets allows the unique opportunity to evaluate acoustic source term estimation at a remote array. High waveform similarity between DFR and I53US occurs during much of the explosive phase due to strong stratospheric ducting, permitting accurate source constraints inferred from I53US data. Cross-correlation analysis after applying a Hilbert transform to the I53US data shows how the acoustic energy has passed through a single caustic, as predicted by ray theory. Similar to previous studies, significant low frequency infrasound from Redoubt recorded at I53US is coincident with high altitude ash emissions. The largest events also produced considerable energy at greater than 50 s periods, likely related to the initial oscillations of the volcanic plume or jet. Many of the explosive events have emergent onsets, somewhat unusual for explosive, short-duration eruptions. Comparison of the satellite-derived SO_2 emissions with the relative amount of acoustic energy at I53US shows a very high, statistically significant correlation. We also present volcano infrasound recordings from the I44RU (Petropavlovsk-Kamchatsky, Russia) infrasound array, and discuss future infrasound monitoring in Kamchatka and the North Pacific region. This study reiterates the utility of using remote infrasound arrays for detection of hazardous emissions and characterization of large volcanic eruptions, and demonstrates how, under typical meteorological conditions, remote infrasound arrays can provide an accurate representation of the acoustic source.

Yan Y. Kagan

Department Earth and Space Sciences (ESS), UCLA, Los Angeles, CA 90095-1567, USA

GLOBAL HIGH-RESOLUTION EARTHQUAKE FORECASTS AND THEIR TESTING

Since 1977 we have developed statistical short- and long-term earthquake forecasts to predict earthquake rate per unit area, time, and magnitude. The forecasts are based on smoothed maps of past seismicity and assume spatial and temporal clustering.

Our recent program forecasts earthquakes on a 0.1 degree grid for a global region 90N--90S latitude. We use the PDE catalog that reports many smaller quakes (M>=5.0). For the long-term forecast we test two types of smoothing kernels based on power-law and on the spherical Fisher distribution. We employ adaptive kernel smoothing which improves our forecast in seismically quiet areas.

Our forecasts can be tested within a relatively short time period since smaller events occur with greater frequency. The forecast efficiency can be measured by likelihood scores expressed as the average probability gains per earthquake compared to spatially or temporally uniform Poisson distribution. The other method uses the error diagram to display the forecasted point density and the point events.

As an illustration, we display several short-term forecasts, made before and after the M9.1 Japanese Tohoku earthquake of 2011/3/11. A M7.5 foreshock occurred two days before the mainshock. Due to this, the short-term rate immediately preceding the Tohoku event was about 100 times higher than the long-term rates. After the Tohoku earthquake the rate increased by a factor of 1000. One month later, the rate remained about 100 times higher than the long-term rate.

The major issue for the long-term seismicity forecast in the Tohoku area was the maximum earthquake size. Whereas 2009 Japan's seismic hazard map predicted the maximum magnitude of 8.0 or less, the estimate based on seismic moment conservation principle anticipated the maximum magnitude of the order M8.6--9.6.

Is the focal area of the Tohoku earthquake "destressed", making the probability of a new large event lower in this area, though it can increase in nearby zones? Our results suggest that this may not be the case. We find that earthquakes as large as M>=7.5 often occur in practically the same area as previous large events.

THE LONG-TERM EARTHQUAKE FORECAST FOR THE KURIL-KAMCHATKA ARC FOR 2011 - 2016

Sergei A. Fedotov, Alexey V. Solomatin, Sergey D. Chernyshev
Institute of Volcanology and Seismology, Petropavlovsk-Kamchatskiy, Russia
karetn@list.ru, fedotov@kscnet.ru, alf55@mail.ru, chernsd@gmail.com

More 40 years ago a number of essential regularities has been noted by S.A. Fedotov at research of the Kuril-Kamchatka seismogenic region seismicity. Major of them are «seismic gaps» and «seismic cycle» of the strongest earthquakes. In 1965-1968 the method of the long-term earthquake forecast for the Kuril-Kamchatka region and Northeast Japan on the basis these and some other regularities has been proposed by S.A. Fedotov [1]. This method is successfully applied till now. The values of the seismic process parameters for previous 5 years in the most seismically active strip of the Kuril-Kamchatka seismogenic region (total length of 2100 km, width 100 km and depths of the hypocenters of 0-80 km) are the initial basis for the specified method long-term earthquake forecasts [1-3]. Now a number of values for 20 areas, comparable on the size with the strongest earthquakes areas, for the following fifth years is predicted [2-3]:

- the seismic cycle phase (I - the previous strongest earthquake aftershock period, II - the long stable seismic energy accumulation phase, III – the seismic activation before the following strongest earthquake);
- the seismic gaps locations - areas in which a last strongest earthquake was more than 80 years ago;
- the expected seismic activity A_{10} (the rationed number of the weak, Ks=10 or M=3.6, earthquakes);
- the magnitude of the average magnitude earthquakes, which are expected with the probability equal to 0.8, 0.5, and 0.15;
- the magnitude of the expected strongest earthquakes and the probability of the $M \geq 7.7$ earthquakes.

The D parameter (a released seismic energy rationed value) and A_{11} (a seismic activity defined on the basis of the average earthquakes with Ks=11 or M=4.3) are used together with the A_{10} parameter.

The seismic process has the complex, unstable character at the III phase. It is accompanied by the short-term quiescence periods. Nevertheless, the received for the extensive time and area intervals data show, that within the last 5-10 years of the seismic cycle the essential seismic process activation is observed. This fact is the basis for the seismic gaps danger definition. The III seismic cycle phase probability for the seismic gaps is proportional to $1\text{-}B = 1\text{-}P(A_{10})*P(D)*P(A_{11})$, where $P(A_{10})$, P(D), and $P(A_{11})$ are the accidental appearance probabilities for the observable values A_{10}, D, and A_{11} at the II (quiet) seismic cycle phase.

The earthquake forecasts are updated twice a year or more often. Their results are compared to the other methods forecasts data [2, 3].

For the more than 40-year-old period of the method application the following strongest earthquakes have been successfully predicted: on Kuril islands (1969, 1973, 1978, 1994 and 2006), on Kamchatka (1971 and 1997). All these earthquakes filled the seismic gaps among the 2-3 most dangerous ones [2, 3, etc.].

The last published forecast has been given in October, 2010. It has confirmed the earlier conclusions concerning the extremely high seismic danger for the Petropavlovsk-Kamchatskiy city [3].

From the method initial time it was applied also to the strongest earthquakes forecast in the Northeast Japan region. The place of the strongest earthquake 1968 near the island Honshu forecast was the first success of the method.

Afterwards the method was successfully used in 2004 at the retrospective Hokkaido 15.XI 2003, M=8.1 earthquake forecast, and in 2005 at construction of the long-term earthquake forecast for

2005-2010, when the extensive seismic gap near Honshu island has been detected (this gap was filled 11.III 2011 by the M = 9 catastrophic earthquake).
In connection with the earthquake 11.III 2011 ecological aftermath, when the atomic power station blocks in a province Fukushima (Japan) were damaged, it is necessary to notice, that in 1975-1976 under the director of Institute of Volcanology of S.A. Fedotov insisting the inadmissible dangerous building of an atomic power station near to Petropavlovsk-Kamchatskiy has been stopped. The correctness of this decision is confirmed by the last long-term earthquake forecast.
The important part of the long-term earthquake forecast method, concerning the probability of the strongest earthquakes foreshocks and aftershocks estimation - «the foreshocks and aftershocks scenario», was offered in 1994, and justified in practice. These estimations can be used at planning of the activity, concerning the seismic safety as directly ahead of the strongest earthquake - in the form of its short-term forecast, and after it - for the danger aftershock estimation at the rescue and restorative works.
This long-term earthquake forecast method can be used in other, similar on seismotectonic conditions, regions, and also for the long-term tsunami forecast.
The long-term earthquake forecasts data have been important as arguing for taking advance measures for seismic safety, seismic protection, and retrofitting. On their basis in 1986-2001 it were issued 6 of the USSR, RSFSR, and the Russian Federation Governmental Decisions and Orders. In 2006-2008 a number of the Commissions has been given by the Presidents of the Russian Federation V.V. Putin and D.A. Medvedev for purpose of enhancing the earthquake resistance of residential buildings, major facilities, life-support systems of the Kamchatskiy Kray (Kamchatka area) and the Sakhalin area in 2009-2013. This works have begun in Petropavlovsk-Kamchatskiy since October, 2010.

References:

1. Fedotov S.A. On Patterns Observed in the Locations of Large Earthquakes in Kamchatka, the Kuril Islands, and Northeastern Japan. Trudy IFZ AN SSSR, 1965, no. 36, pp. 66□93 (in Russian).
2. Fedotov S.A. Long-term Earthquake Prediction for the Kuril-Kamchatka Arc. Moscow: Nauka, 2005. 302 p. (in Russian).
3. Fedotov S.A., Solomatin A.V., Chernyshev S.D. A Long-Term Earthquake Forecast for the Kuril-Kamchatka Arc for the Period from September 2010 to August 2015 and the Reliability of Previous Forecasts, as well as their Applications // Journal of Volcanology and Seismology. 2011. Vol. 5, No 2. P. 75 – 99.

ДОЛГОСРОЧНЫЙ СЕЙСМИЧЕСКИЙ ПРОГНОЗ ДЛЯ КУРИЛО-КАМЧАТСКОЙ ДУГИ НА 2011 – 2016 гг.

С.А. Федотов, А.В. Соломатин, С.Д. Чернышев
Институт вулканологии и сейсмологии ДВО РАН, Петропавловск-Камчатский,
karetn@list.ru, fedotov@kscnet.ru, alf55@mail.ru, chernsd@gmail.com

Более 40 лет назад при исследовании сейсмичности Курило-Камчатской сейсмогенной зоны С.А. Федотовым был выделен ряд пространственно-временных закономерностей, важнейшими из которых являются «сейсмические бреши» и «сейсмический цикл» сильнейших землетрясений. В 1965-1968 гг. на основе этих и некоторых других закономерностей С.А. Федотовым был предложен метод долгосрочного сейсмического прогноза для Курило-Камчатского региона и Северо-Восточной Японии [1-3], успешно применяемый до настоящего времени.

Исходной основой для составления долгосрочных сейсмических прогнозов на основе указанного метода являются данные о параметрах сейсмического процесса за предшествующие 5 лет в наиболее сейсмически активной полосе Курило-Камчатской сейсмогенной зоны общей длиной 2100 км, шириной 100 км и с глубинами очагов 0-80 км [1-3].

В настоящее время для 20 участков, сравнимых по размеру с очагами сильнейших землетрясений, на следующее пятилетие прогнозируется ряд величин [2-3]:

- стадии сейсмического цикла (I - афтершоковый период сильнейшего землетрясения, II - длительная стабильная стадия накопления сейсмической энергии, III - сейсмическая активизация перед следующим сильнейшим землетрясением);
- положение сейсмических брешей - участков, в которых последнее сильнейшее землетрясение было более чем 80 лет назад;
- ожидаемая сейсмическая активность A_{10} (нормированное количество слабых, Ks=10 или M=3.6, землетрясений);
- величины магнитуд землетрясений средней силы, ожидающиеся с вероятностью 0.8, 0.5 и 0.15;
- максимальные магнитуды ожидаемых сильнейших землетрясений и вероятности землетрясений с $M \geq 7.7$.

К используемым в методе сейсмическим параметрам вместе с A_{10} относятся также D - относительная величина сброшенной сейсмической энергии и A_{11} - сейсмическая активность, определяемая на основе землетрясений средней силы (Ks=11 или M=4.3).

Сейсмический процесс на заключительной III стадии носит сложный, нестабильный характер, сопровождается возникновением кратковременных периодов затиший. Тем не менее, данные, полученные для больших пространственно-временных интервалов, показывают, что в течение последних 5-10 лет сейсмического цикла наблюдается его существенная активизация. Этот факт является основой для определения опасности сейсмических брешей. Вероятность наступления III стадии сейсмического цикла в наиболее сейсмически опасных участках - сейсмических брешах - пропорциональна величине $1\text{-}B = 1\text{-}P(A_{10})*P(D)*P(A_{11})$, где $P(A_{10})$, $P(D)$ и $P(A_{11})$ – вероятности случайного появления наблюдаемых значений A_{10}, D и A_{11} на II (спокойной) стадии сейсмического цикла [2, 3] и др.

Сейсмические прогнозы обновляются дважды в год или чаще. Их результаты сравниваются с данными прогнозов, полученными на основе других методов [2, 3].

За более чем 40-летний период применения метода были успешно предсказаны следующие сильнейшие землетрясения: на Курильских о-вах (1969, 1973, 1978, 1994 и 2006 гг.), на Камчатке (1971 и 1997 гг.). Все эти землетрясения заполняли те сейсмические бреши, которые относились к числу 2-3 наиболее опасных [2, 3] и др.

Последний опубликованный прогноз был дан в октябре 2010 г. Он подтвердил сделанные ранее выводы о чрезвычайно высокой сейсмической опасности в районе г. Петропавловск-Камчатский [3].

С самого начала метод применялся также для прогноза сильнейших землетрясений Северо-Восточной Японии, где первым успехом был прогноз места сильнейшего землетрясения возле о-ва Хонсю, оправдавшийся в 1968 г. [2]. Впоследствии метод успешно оправдался в 2004 г. при построении ретроспективного прогноза сильнейшего землетрясения возле о. Хоккайдо 15.XI 2003 г., M=8.1 и в 2005 г., когда при построении пробного сейсмического прогноза для Северо-Восточной Японии на 2005-2010 гг. была указана протяженная сейсмическая брешь возле о. Хонсю, заполнившаяся 11.III 2011 г. в результате катастрофического землетрясения с M = 9.

В связи с экологическими последствиями землетрясения 11.III 2011 г., повредившего блоки атомной электростанции в провинции Фукусима (Япония), необходимо отметить, что в 1975-1976 гг. по настоянию директора Института вулканологии С.А. Федотова было остановлено недопустимо опасное строительство атомной электростанции вблизи Петропавловска-Камчатского. Правильность такого решения подтверждают последние долгосрочные сейсмические прогнозы.

Важной частью метода долгосрочного сейсмического прогноза является предложенный в 1994 г., и оправдавший себя на практике метод оценки вероятности сильных ($M \geq 6.0$) форшоков и афтершоков сильнейших землетрясений – «сценарий форшоков и афтершоков». Эти оценки могут быть использованы при планировании действий по обеспечению сейсмической безопасности как непосредственно перед сильнейшим землетрясением – в виде его краткосрочного прогноза, так и после него – для оценки опасности афтершоков в период спасательно-восстановительных работ.

Метод долгосрочного сейсмического прогноза С.А. Федотова может быть использован и для других, сходных по сейсмотектоническим условиям регионов, а также для долгосрочного прогноза цунами.

Данные долгосрочных сейсмических прогнозов по методу С.А. Федотова явились обоснованием для принятия государственных заблаговременных мер по сейсмобезопасности, сейсмозащите и сейсмоусилению. На их основе в 1986-2001 гг. было принято 6 соответствующих Решений и Постановлений Правительства СССР, РСФСР и РФ. В 2006-2008 гг. был дан ряд Поручений президентов РФ В.В. Путина и Д.А. Медведева по обеспечению сейсмобезопасности, проведению сейсмоусиления жилого фонда и объектов социальной сферы в Камчатском крае, а также по выделению средств на эти цели из федерального бюджета. В 2009 г. правительство РФ выделило такие средства Камчатскому краю и Сахалинской области, и с октября 2010 г. в г. Петропавловск-Камчатский ведутся интенсивные работы по сейсмоусилению.

Литература:

1. Федотов С.А. О закономерностях распределения сильных землетрясений Камчатки, Курильских островов и северо-восточной Японии // Тр. ИФЗАН СССР. 1965. № 36. С. 66-93.
2. Федотов С.А. Долгосрочный сейсмический прогноз для Курило-Камчатской дуги. М.: Наука, 2005. 302 с.
3. Федотов С.А., Соломатин А.В., Чернышев С.Д. Долгосрочный сейсмический прогноз для Курило-Камчатской дуги IX 2010 – VIII 2015 гг., достоверность предыдущих прогнозов и их применение. // Вулканология и сейсмология. 2011. № 2. С. 3-27.

Renat Shakirov
Russian Academy of Sciences
V.I. Il'ichev Pacific Oceanological Institute
43 Baltiyskaya Str., Vladivostok, 690041, RUSSIAN FEDERATION
ren@poi.dvo.ru

Western an eastern margins of Pacific Ocean presents numerous gashydrates sites, distributed as Gashydrates Provinces (referred to the sea's title) which can be combined to Circum Pacific Gashydrate Belt. Gas (mainly methane) hydrates accumulation induced by varies active geological features determined by geodynamic and tectonic type and seismic state's of Pacific and adjoining lithosphere plate's borders. Bering Sea, Okhotsk Sea, Japan Sea, East-China Sea, Sea of Vietnam, Celebes and Sulu Seas and southward to New Zealand offshore presents Western Pacific Gas Hydrate Belt and exposed methane hydrates distribution in sediments. Hydroacoustic, seismics, coring were a prime methods applied to gashydrate searching and exploration. Methane hydrates was explored since 88-th (Okhotsk Sea). Gas hydrates supplying fluid within the thick Cenozoic sediment basins (up to 10 km thickness) are linked to multiple hydrocarbon accumulations: mainly oil and gas deposits, and gas (methane) hydrates – proved for the Bering, Okhotsk and Japan Seas. Submarine gas seepage usually accompanied by contrast seismic and acoustic anomalies in the sediments and water column (e.x. up to 700 gas "flares" prior to 2010 indicates gas hydrate fracture type accumulation in western Okhotsk Sea). High hydrocarbons were found as well, but methane is dominated everywhere. Methane sources discussed as mixture of thermogenic and biogenic origin. Gas hydrate occupies mainly 20-45% of pore volume. BSR was found globally, but this border means not gas hydrate stability zone only. Methane resources trapped in Western Pacific gas hydrates estimated based on latest investigations at least for $5\times10^{*13}$ cubic meters.

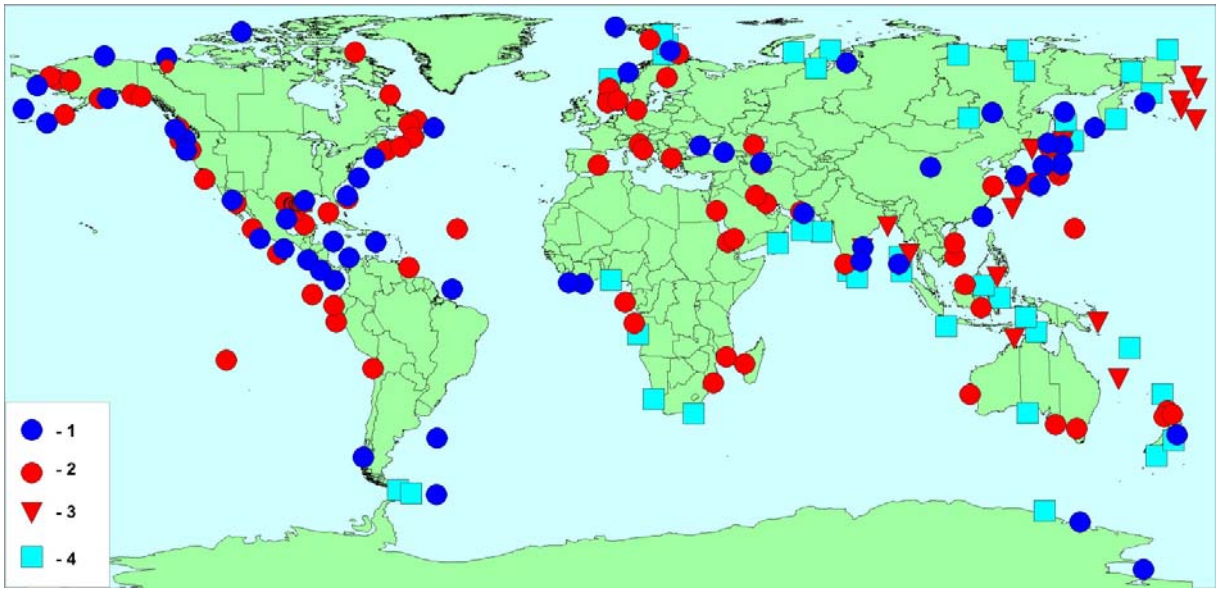


Fig. 1. Worldwide gas hydrate occurrence. 1 – recovered; 2 – hydrate sediment signs with methane leakages; 3 – inferred; 4 – potential (by BSR and geochemical anomalies).

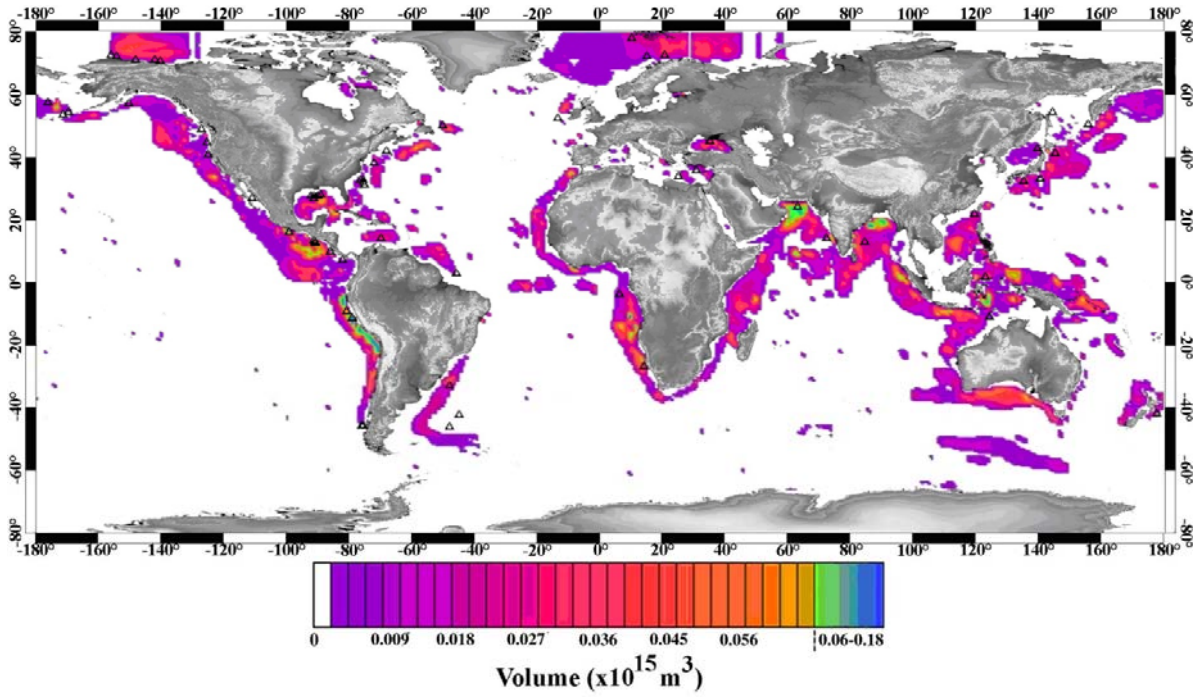


Fig. 2. Modeled gas hydrates distribution in World Ocean (Klauda J.B., 2011).

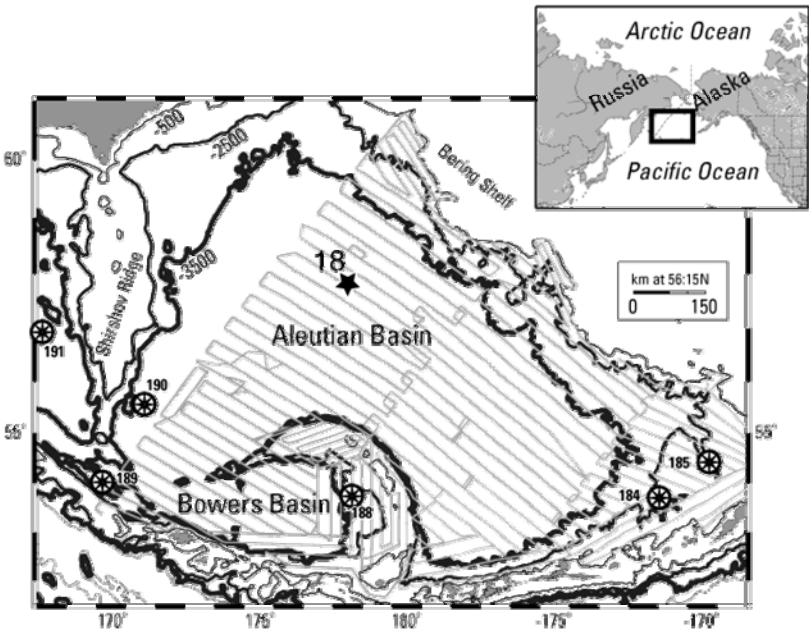


Fig. 3. Bering Sea, North Pacific Ocean. Bathymetric contour lines are in meters, with the darkest line representing 3,500-m water depth. Star, location of VAMP example; circled stars, nearest drilled wells, from Deep-Sea Drilling Program (DSDP) leg 19. Track lines (gray) represent approximately 24,000 km of digitally recorded USGS single-channel seismic data. After Scholl et al., 2007.

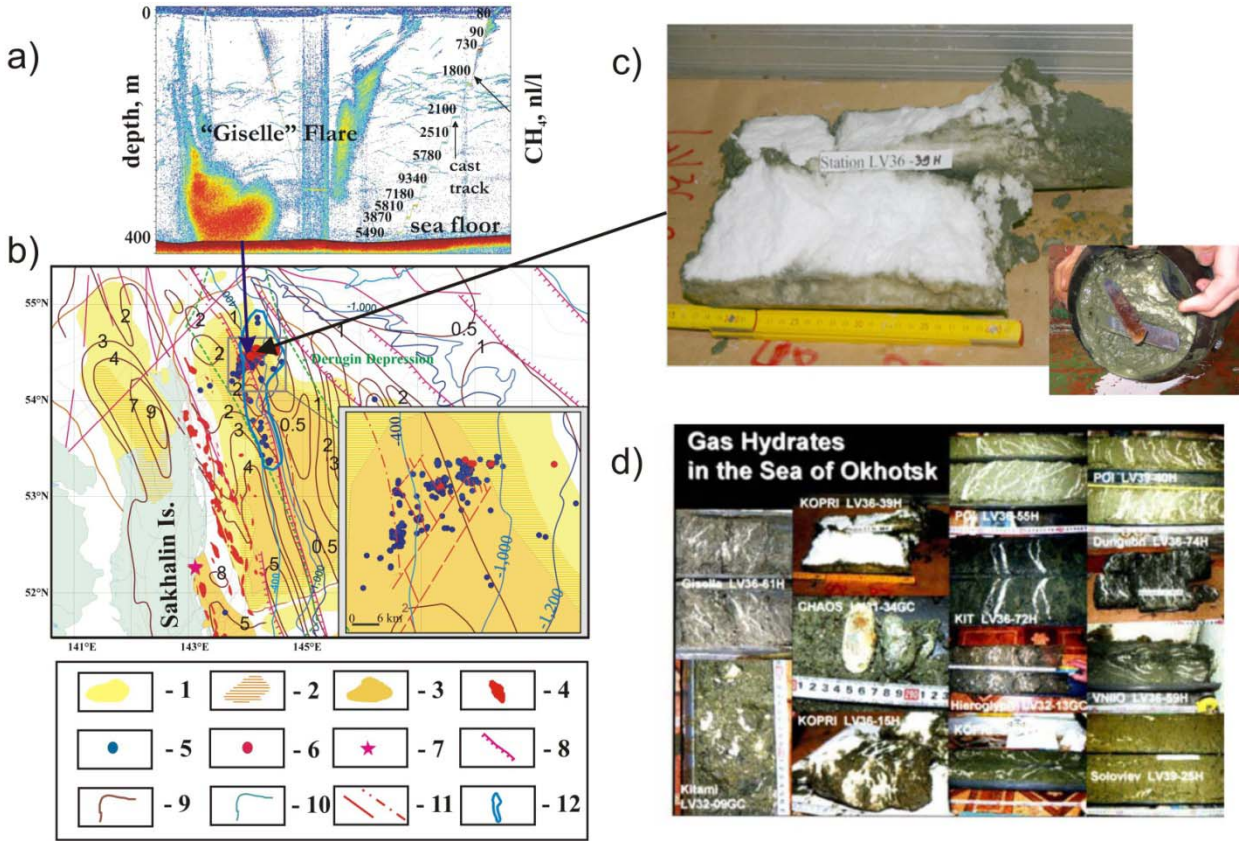


Fig. 4. Geological state of the North East Sakhalin Slope. Legend: 1,2,3 – density of the hydrocarbon generation (see Fig. 5); 4 – oil-gas deposits; 5 – methane vent/flares; 6 – methane hydrate findings; 7 – mud volcano; 8 – rift zones; 9 – isopachits; 10 – isobaths; 11 – tectonic faults; 12 – methane hydrate province proposed in 2005 and confirmed in southern part in 2009-2010.



Fig. 5. Gas hydrate from Ulleung Basin (Chun et al., 2011).

REFERENCES

Baranov BV, Karp BYa and Wong HK. Areas of gas seepage. GEOMAR Report 82 INESSA. RV Professor Gagarinsky, Cruise 22. Kiel, 1999. P. 45-52.

Bogdanov NA and Khain VE. (eds) Explanation report for the tectonic map of the Okhotsk sea region, VE scale 1:250,000. Institute of Lithosphere of Border and Internal Sea RAS, Moscow. 2000.

Chi Wu-Cheng, Reed DL and Tsai Chin-Chin. Gas Hydrate Stability Zone in Offshore Southern Taiwan. Terr. Atmos. Ocean. Sci., Vol. 17, No. 4. P. 829-843, 2006.

Chun J.-Hwa, Ryu Byong-Jae, Lee Sung-Rock. Korea Gas Hydrate R&D Program. Report of the PETRAD-CCOP-PETROVIETNAM-VASI Workshop on Gashydrates. 1-3 March 2011. HaLong, Viet Nam. 44 p.

Gretskaya EV, Ilyov AYa and Gnibidenko HS. Hydrocarbon potential of the sediment-rock basins of the Okhotsk Sea. Institute of Marine Geology and Geophysics. Yuzhno-Sakhalinsk, 1992. 51 p.

IEO2010 Reference case. Chapter 3. Natural Gas. 2010. P. 41-60.

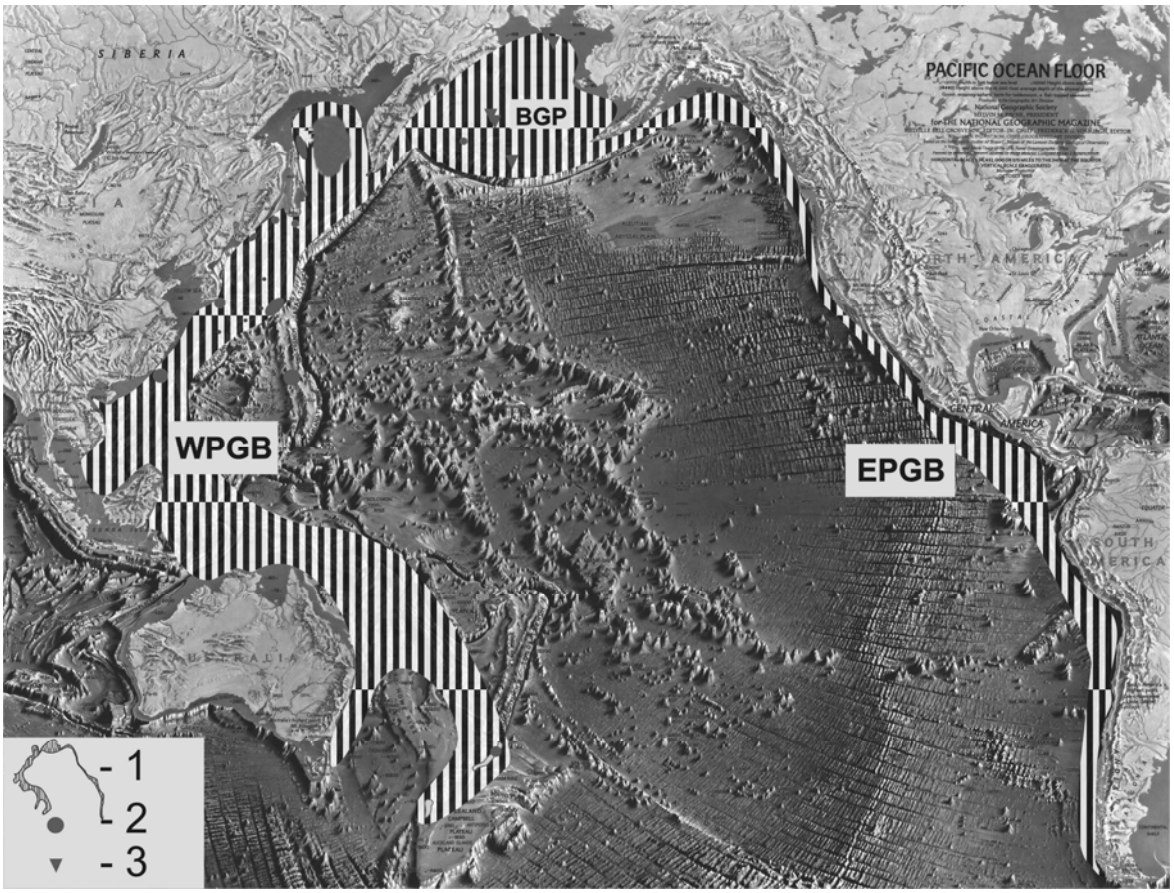


Fig. 6. Circum Pacific Gas Hydrate Belt. WPGHB – Western Pacific Gas Hydrate Belt; EPGHB – Eastern Pacific Gas Hydrate Belt; BSGHP – Bering Sea Gas Hydrate Province . 1 - Circum Pacific Gas Hydrate Belt.; 2 – inferred hydrates (examples); 3 – potential GH sites (examples).

Klauda J.B. Gas Hydrates: Natural Energy Source and Storage for CO2 and Hydrogen. University of Maryland. 2011. http://terpconnect.umd.edu/~jbklauda/research/projects.html.

Kharakhinov, V.V. (1998): Tectonics of the Sea of Okhotsk oil-gas province. Sakhalin NIPI Morneft, Okha-na-Sakhaline, 77 p. (In Russian)

Ludmann T and Wong HK. Characteristics of gas hydrate occurrences associated with mud diapirism and gas escape structures in the northwestern Sea of Okhotsk. Marine Geology, 201. 2003. P. 269–286.

Matsumoto, R. (2001): Methane hydrates. Academic Press, University of Tokyo, Tokyo, Japan. doi:10.1006/rwos.2001.0042. 1745–1756.

Max, M.D. (ed) (2000): Natural gas hydrate in oceanic and permafrost environments. Kluwer Academic Publishers. P.O. Box 332, 3300 AH Dordrecht, the Netherlands, 410 p.

Pecher I.A., Fohrmann M. Natural Gas Hydrates as an Energy Resource and New Developments in Gas Hydrate Exploration. PETRAD-CCOP-PETROVIETNAM-VASI Workshop on Gashydrates. 1-3 March 2011. HaLong, Viet Nam. 44 p.

Proceedings of the Ocean Drilling Program. Volume 190. Initial Reports Deformation and Fluid Flow Processes in the Nankai Trough Accretionary Prism. Covering Leg 190 of the cruises of the Drilling Vessel JOIDES Resolution. Sites 1173–1178. 2000. P. 25-32.

Scholl D., Barth G., Childs J., and Gibbons H. Bering Sea likely rich in hydrates. Vol. 12, No. 3. Week of January 21, 2007. Reported by Bailey A. http://www.petroleumnews.com/pntruncate/286678373.shtml.

Sloan E.D., Dendy J.E., Koh C. Clathrate hydrates of natural gases. New York. Basel. 2007. 856 p.

Smith E.M. Clathrate to Production. 2010. http://chiefio.wordpress.com/2010/11/30/clathrate-to-production.

Suess, E., Torres, M.E., Bohrmann, G., Collier, R.W., Greinert, J., Linke, P., Rehder, G., Trehu, A., Wallmann, K., Winckler, G. and Zuleger, E. (1999): Gas hydrate destabilization: enhanced dewatering, benthic material turnover and large methane plumes at the Cascadia convergent margin. Earth and Planetary Science Letters, 170, 1–15.

Tanahashi M. Present status of Japanese methane gas hydrate research and development program. PETRAD-CCOP-PETROVIETNAM-VASI Workshop on Gashydrates. 1-3 March 2011. HaLong, Viet Nam. 44 p.

Wang Xiaoxue. Oil/Gas Accumulative Structures Discovered in the Yellow Sea. China Chemical Reporter Publish. March 26, 2001. China National Chemical Information Center. 2009.

Wilde P., Quinby-Hunt M.S. Methane clathrate outgassing and anoxic expansion in South-East Asian deeps due to global warming. ENVIRONMENTAL MONITORING AND ASSESSMENT V. 44, P. 149-153. 1997.

Wu N., Yang Sh., Zhang H., Su Zh., Zhang K., Mordis G.J. Gas Hydrate System in Northern South China Sea and Numerical Investigation of Gas Production Strategy in Shenhu Area. PETRAD-CCOP-PETROVIETNAM-VASI Workshop on Gashydrates. 1-3 March 2011. HaLong, Viet Nam. 44 p.

Content of microelements in hydrothermal and lake waters of Ksudach Volcano Caldera (South Kamchatka)

A.G. Nikolayeva[1], A.Yu. Bychkov[2]
[1] Institute of Volcanology and Seismology FEB RAS, Petropavlovsk-Kamchatsky, ocean@kscnet.ru
[2] M.V. Lomonosov Moscow State University, Moscow, andrewbychkov@rambler.ru

Ksudach Volcano is a caldera-type volcano (Fig. 1). This type of volcanoes is characterized by intensive and continuous volcanic activity accompanied by intensive degassing (Selyangin, 1987). The last caldera eruption occurred in 1907. It was a directed blast eruption (similar to the eruption of Bezymianny Volcano) that partially destroyed the basement of Shtyubel Cone. Nowadays the crater is field by a lake. The volcano erupted a large amount of volcanogenic material (Dubik, 1971; Melekestsev, 1987). The erupted material and modern gas-hydrothermal activity in the caldera are of special interest. Low temperature low-alkaline thermal sources discharge pressure waters from the hydrothermal system of the caldera (Pilipenko, 2001). These thermal sources discharge in the north-west part of Klyuchevoye Lake, in so called Goryachy Plyazh (Hot Beach), in the area of the intrusion Nezametnaya (Shtyubelevsky thermal springs). The Crater Lake Shtyubel still manifests signs of activity. Echolocation investigations (Nikolaev, 1995) evidence for gas effluxes rising from the bottom of the lake (*Fig. 1*). We revealed high concentrations of N_2, CO_2, He, CH_4, and hydrocarbons (Pilipenko, 2001). We revealed that in surface waters of the Crater Lake Shtyubel the concentration of SO_4^{2-} is threefold and the concentration of Ca is tenfold compared to Dubik, 1971. These elements concentrations also agree with the data on S/Cl ratio in the same water (Nikolatyeva, 2007). Fluid flows rising from the bottom of this Crater Lake resulted in these anomalies.

Microelements composition in natural waters of this caldera is understudied. Pilipenko, 2001, was the first who has mentioned high concentrations of Fe, Mn and Zn in the layer of water and Fe, As and Hg in bottom sediments of Shtyubel Lake. To defined chemical composition we collected water samples from Ksudach Volcano Caldera. ICP-MS method allowed determining microelements concentrations in thermal sources and crater lakes of the caldera. These data analysis evidences that Goryachy Plyazh (Hot Beach) and Shtyubelevsky thermal springs supply lakes of the caldera with mineral elements. Atmospheric precipitations reduce microelements concentration in Sulphatny sources and surface waters of Shtyubel and Klyuchevoye Lakes. These thermal sources transport 200-300 times bigger Mn and Li, 30 times bigger Al, Sr, Zn and Sc, 10 times bigger Ge and Rb compared to the background values. Fe, Cr, Sr and Ti are maximally transported from Sulphaty Sources; As and Zr from Shtyubelevsky Springs and Shtyubel Lake; V from Pemzovy brook. Besides we reveal small amounts of Re and In in the Crater Lake Shtyubel and in the head of Tyoplaya River.

Figure 2 shows content of rare earth elements (REE) in volcanogenic hydrothermal sources and lake waters of Ksudach Caldera normalized to REE composition in chondrites. We used also the data on REE composition in ocean fluid (Dubinin, 2006) and the data on thermal sources in Uzon and Akademiya Nauk Calderas. It is evident, that ocean fluid is characterized by insignificant Eu maximum (?), whereas other types of hydrothermal sources are characterized by negative Eu anomaly and less evident decrease of heavy REE content. High content of Li, Fe, As, Sr, Zn, Re and other microelements in thermal sources and Shtyubel Lake evidences for transportation of these elements by fluid flows from the upper crust magma chambers beneath the caldera. The transportation of REE in the form of chloride complexes is probably carried out by deep high-temperature thermal sources of Cl-Na type. All other types of hydrothermal sources make up the above mentioned sources in the near-surface conditions. We can not exclude that dissolution from wall-rocks influences on the concentration of REE in carter lakes. In the nearest future we are going to study wall-rocks microelements content. The ore formation processes are characteristic for calderas of this type. Ore is formed here simultaneously with volcanic processes in caldera lakes, where solutions are boiling in the area of hydro-chemical barriers and unloading ore at the bottom of the lake.

The research was supported by the Russian Basic Research Foundation grant № 11-05-00572a.

References:

1. Dubik, Yu.M., Menyaylov I.A., 1971. Ksudach Caldera gas-hydrothermal activity. Bull. Volcanol. (Stancii) 47, 40-43.
2. Dubinin, A.V., 2006. The geochemistry of the rare earth elements (REE) in an ocean. Nauka, Moscow, p. 360.
3. Melekestsev, I. V., Sulerzhitsky L.D., 1987. Ksudach Volcano (Kamchatka) over the last 10 000 years. Volcanol. Seismol. 4, pp. 28-39.
4. Nikolaev A.S., 1995. The list of echolocation records for waters biophysical heterogeneities in Kamchatka lakes. Investigations of biology and dynamics of population for commercial fishes in Kamchatka Shelf. Vol., 4, pp. 12-15.
5. Nikolaeva A.G., 2007. Results of hydro-geochemical observations of thermal manifestations in Ksudach Volcano Caldera, South Kamchatka, (on data of 1937-2006). Volcanism and related processes. Proceedings of the scientific conference dedicated to the 100th anniversary of March 28-29, 1907 Ksudach Volcano eruption, Petropavlovsk-Kamchatsky. pp. 18-36.
6. Pilipenko G.F., Razina A.A., Fazlullin S. M., 2001. Hydrothermal sources of Ksudach Volcano Caldera. Volcanol. Seismol. 6, pp. 43-57.
7. Selyangin O.B., 1987. Geological structure and evolution of the caldera complex of Ksudach Volcano. Volcanol. Seismol. 5, pp. 16-27.

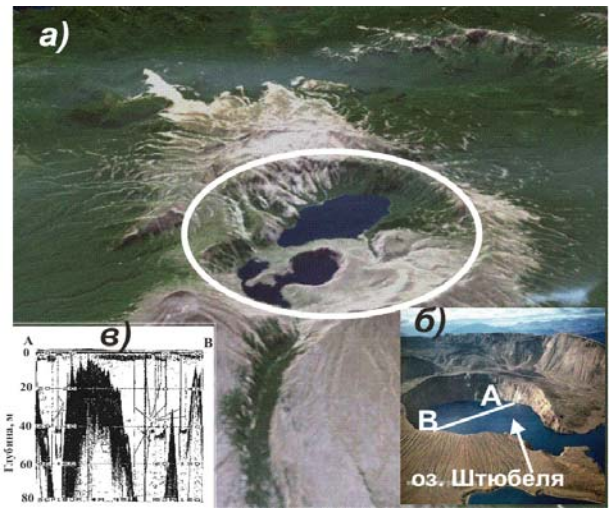


Fig. 1. Ksudach Volcano Caldera from the west-north (a), Shtyubel Crater is in the right bottom corner of the figure (b), lateral hydroacoustic profile A-B with effluxes plumes (c) (1991).

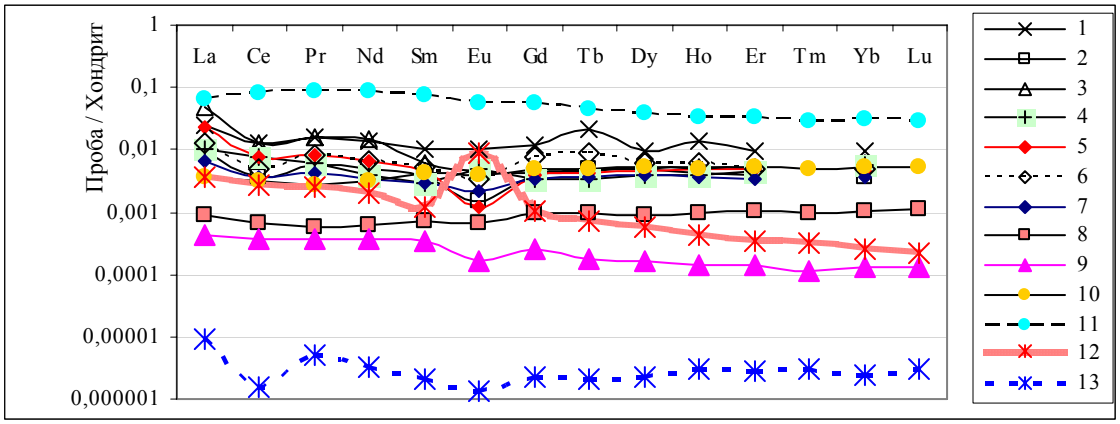


Fig. 2. The graphic of REE content in hydrothermal sources and lake waters of Ksudach Caldera (mcg/l). 1 –Goryachy Plyazh (Hot Beach) sources; 2 – the central part of the lake Klyuchevoye; 3 – Shtyubelevsky thermal springs; 4 – the central part of the lake Shtyubel; 5 – the central part of the lake Maloye; 6 – Pemzovy brook; 7 –Sulphatny sources; 8 – Antimonitovye sources; 9 – Piipovsky (Akademiya Nauk Caldera); 10 – Banny Brook (Caldera Uzon); 11 – Troitskogo Lake (Maly Semiatchik Volcano); 12 – underwater hydrothermal fluid (13º East-Pacific Raising); 13 – sea water.

The harmonic and spectral analysis of the geomagnetic field and correlation of its components with earthquake sources in the Northern Tien Shan

Vorontsova E.V.,

E-mail: vorontsova@gdirc.ru

RS RAS, Bishkek-49, Kyrgyzstan

A lot of scientific articles study correlation of seismic activity with variations of different components of the Earth's magnetic field. More often this is correlation with a single factor, such as secular variations, Sq-variations, Wolf's numbers, Kp- and Ap- indices, as well as with the frequency and origin times of geomagnetic storms, etc. However, a complete analysis requires different Earth's field components taken together. Only then, it will allow comparing planetary and local field variations and calculating a ratio of the external (ionospheric) field T_e to the induced (lithospheric) variations δT_i.

The magnetic field T_T observed on the Earth's surface is the superposition of several fields: $T_{T=} T_0 + T_a + T_e + \delta T_i$ [1], where

1. T_0 is the main field of Earth's core produced by processes deep in the Earth's interior;
2. T_a is the main local field due to the magnetization of rocks and processes in the upper crust;
3. T_e is the field produced and modulated in the ionosphere by external sources from the Sun (S) and the Moon (L), the solar wind and the interplanetary field (T_{st}), and geomagnetic pulsations (P): $T_e = S+L+T_{st}+P$;
4. δT_i are the variations induced by T_e in the lithosphere, in the upper mantle, and in the ocean.

The total Earth's field T_T is a sum of the global (T_{glob}) and local (T_{loc}) components, where $T_{glob} = T_0 + \delta T_{glob}$ and $T_{loc} = T_a + \delta T_{loc}$. The component T_{glob} bears signature of planetary processes: the long-term variation of the main field T_0, the solar and lunar variations, and the global geomagnetic storms. T_{loc} is a sum of the main local field T_a and the field δT_{loc}, which results from local magnetic disturbances and induced variations in lithospheric conductors, including fault zones.

The two components δT_{glob} and δT_{loc} are inferred from data of remote and local stations, respectively.

In this work, we analyzed the hourly means of H, D, Z components of the geomagnetic field from fifteen magnetic stations (18.62°-55.47° N, 0.5°-144.19° E) and the total field T at the station Ak-Suu (42.6° N, 74° E), for the observation period of 1980 through 2009. The data processing included spectral analysis and calculation of the following components: secular variations T_0+T_a, Sq- and L- variations, and variations $T_{st}+P$ of the geomagnetic storms and pulsations.

The spectral analysis of geomagnetic field has shown the solar periods of 6; 8; 12; 24 hours, 13.8; 27.8; 93; 128; 195; 350 days and 11 years; and the lunar periods of 6.103; 8.185; 12.421; 25.744 hours, and the period 29.53 days which is equal to the lunar month. The observed periods agree better with the commonly known periods (annular, seasonal, daily, and the ~27-day period of solar activity). The amplitudes and phases of the diurnal and semidiurnal variations of the total magnetic field have an annular period. The amplitude maximum is at the solstices and the minimum is at the equinoxes.

According to the high-resolution spectral analysis, the solar and lunar harmonics split as a result of annular and ~27-day modulations associated with solar activity. The spectrum contains the

sidebands S_n and L_n at the frequencies $f_n \pm k/365.25$ and R_n at $f_n \pm k/27.5$ (n=1,2, …; f_n is the main frequency of the n-th harmonic in cpd, k=±1, ±2, ±3,…).

The Sq- and L- variations are commonly calculated with the Chapman-Miller harmonic analysis. In this work, however, we applied three different methods (Chapman-Miller harmonic analysis [2], Fourier filtering and inversion, and SSA) and compared the results. Each method has its advantages and drawbacks. The Chapman-Miller analysis allows using data with time gaps, but it is very sensitive to pulse noise and the error increases considerably as the time window decreases. The two other methods are free from these problems but require long continuous time series. The SSA method is more accurate than the Fourier one and allows working with individual (diurnal, semidiurnal, etc.) components but it takes much time and computing resources.

After the secular trend T_0+T_a, Sq- and the L- variations has been removed, the residual component $T_{st}+P$ characterizes disturbance from storms and pulsations. The inter-hourly differences IHV_T (Inter-Hourly Value [3]) of the total field T and the H, D, Z components were calculated for data from each magnetic station. The comparison of geomagnetic data and the patterns of calculated IHV_T for different stations allows one to determine the origin time of geomagnetic storms, as well as to find and separate the global and local storms. This analysis provides a more precise characteristic of local geomagnetic disturbances than the use of the Kp- and Dst- indices.

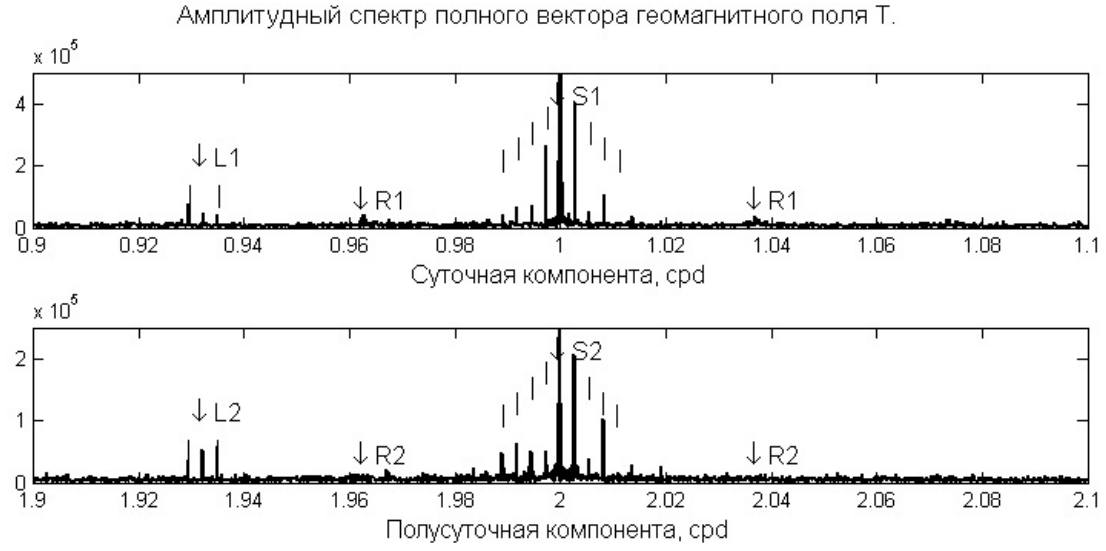
The variations of geomagnetic magnetic field were correlated with seismic data from the KNET-catalog of earthquakes for the Northern Tien Shan region (40.5°-44.5° N, 71.5°-78.5° E), which includes 6475 seismic events within the period 1994-2009.

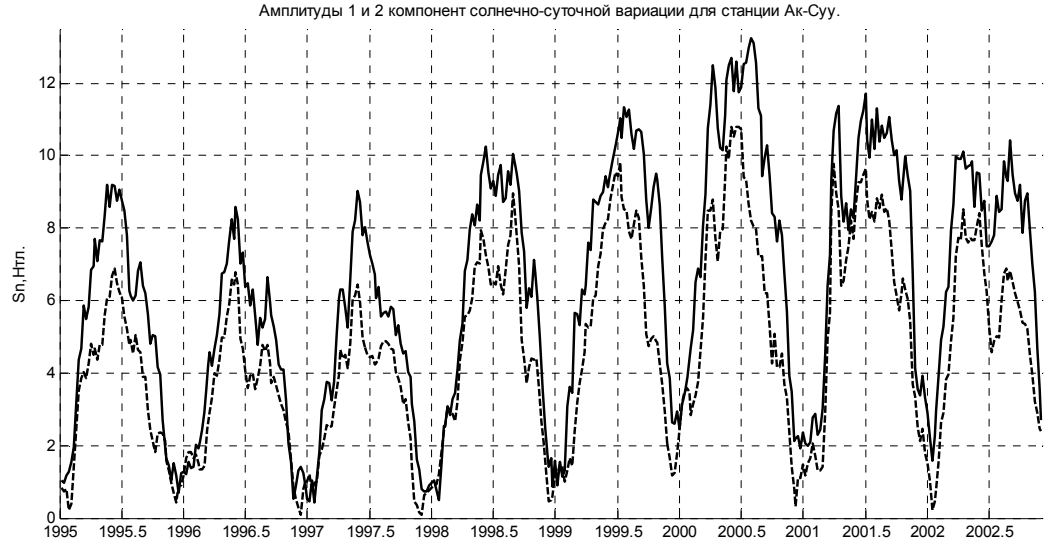
Various statistical and spectral analyses of the seismic activity time series have yielded long and short periods of 12, 14, 18, 27.3, 120, 360 days and 8; 12; 14.5; 24 hours, respectively.

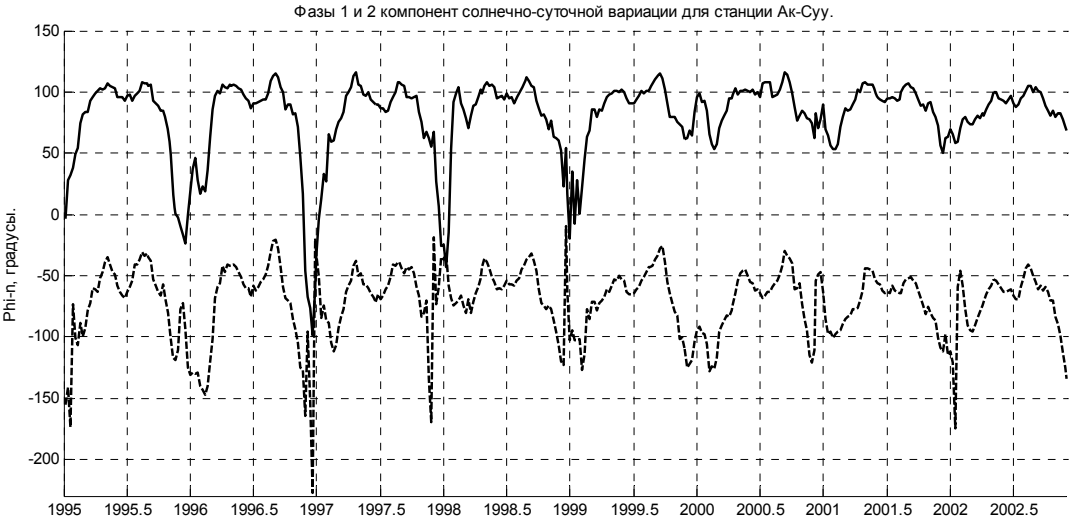
The reported study has revealed a number of common periods (8, 12, 24 hours, 13.8; ~27.8; 120; 360 days) in the geomagnetic field and seismic activity variations, possibly indicating a correlation between the two.

References

1. Yanovskiy: Earth's magnetism. 1978.
2. Chapman, Lindzen: Atmostheric tides. 1969.
3. Svalgaard: IHV - a new long-term geomagnetic index. 2000.
4.




Амплитуды 1 и 2 компонент солнечно-суточной вариации для станции Ак-Суу.
Sn,Htn.
0
2
4
6
8
10
12
1995
1995.5
1996
1996.5
1997
1997.5
1998
1998.5
1999
1999.5
2000
2000.5
2001
2001.5
2002
2002.5


Фазы 1 и 2 компонент солнечно-суточной вариации для станции Ак-Суу.
Phi-n, градусы.
150
100
50
0
-50
-100
-150
-200
1995
1995.5
1996
1996.5
1997
1997.5
1998
1998.5
1999
1999.5
2000
2000.5
2001
2001.5
2002
2002.5

Гармонический анализ вариаций полного вектора T геомагнитного поля, и связь компонент с сейсмической активностью Северного Тянь-Шаня

Е.В. Воронцова, e-mail: vorontsova@gdirc.ru
Научная станция РАН, Бишкек-49, Кыргызстан

Большое количество научных работ, опубликованных в периодических изданиях, посвящено исследованиям связи сейсмической активности Земли с вариациями компонент магнитного поля и солнечной активностью. При этом исследуются корреляции сейсмической активности Земли с вариациями векового тренда магнитного поля, S_q-вариацией, с числами Вольфа W, с индексами геомагнитной активности Kp, Ap, с количеством и моментами возникновения геомагнитных бурь, и другими геофизическими факторами. Но только исследование всех возможных компонент магнитного поля совместно позволяет провести комплексный анализ, выделить (оценить) вклад общепланетарных геомагнитных процессов и локальных откликов, т.е. рассчитать соотношение внешнего поля T_e и индуцированных вариаций δT_i (ионосферной и литосферных частей наблюдаемого магнитного поля).

Наблюдаемое на поверхности Земли магнитное поле T_T является суперпозицией нескольких полей $T_{T=} T_0+ T_a +T_e+ \delta T_i$ [1]:

1) главного поля T_0, создаваемого ядром Земли и процессами, протекающими в глубинных горизонтах земного шара,
2) локального поля T_a, обусловленного намагниченностью и процессами верхних частей земной коры.
3) магнитного поля T_e, вызываемого и модулируемого влиянием внешних источников: Солнца, Луны, потоков солнечного ветра (T_{st}), и пульсаций: $T_e=S+L+T_{st}+P$,
4) поля вариаций, индуцированных в земной коре, верхней мантии и в океанической среде – δT_i, причины генерации которых связываются с источниками, расположенными вне земного шара.

Полный вектор магнитного поля T_T, наблюдаемый на земной поверхности, является суммой глобальной компоненты T_{glob} и локальной компоненты T_{loc}, где $T_{glob}= T_0 + \delta T_{glob}$, $T_{loc}= T_a + \delta T_{loc}$. T_{glob} несет информацию об общепланетарных процессах: долгопериодных вариациях главного поля T_0, вариациях S, L, и общепланетарных магнитных возмущениях. T_{loc} представляет собой сумму локального поля T_a, и поля δT_{loc}, связанного с локальными магнитными возмущениями и локальным откликом в проводящих слоях литосферы и в разломных зонах. Для определения δT_{glob} необходимо исследовать магнитограммы с различных географически удаленных друг от друга станций. Для определения δT_{loc} следует использовать магнитограммы близко расположенных станций.

В работе использовались среднечасовые значения компонент H, D, Z для 15 магнитных станций, расположенных в северном полушарии (18.62°-55.47°N, 0.5°-144.19°E) и значения полного вектора магнитного поля T для станции Ак-Суу (42.6°N, 74°E) за период 1980-2009 годы. Для используемых данных был проведен спектральный анализ и рассчитаны следующие компоненты: вековой тренд T_0+T_a, Sq- и L-вариации, остаточная $T_{st}+P$ вариация магнитных бурь и пульсаций.

При спектральном анализе геомагнитного поля Земли, выделяются «солнечные» периоды: 6; 8; 12; 24; часа, 13.8; 27.8; 93; 128; 195; 350 дней, 11 лет и «лунные» периоды: 6.103; 8.185; 12.421; 25.744 часа и период 29.53 суток, равный лунному месяцу. Полученные периоды хорошо согласуются с общеизвестными периодами (годовые, сезонные, суточные и 27-дневным квазипериодом солнечной активности). Амплитуды и фазы гармоник имеют выраженную годовую периодичность. В дни зимнего солнцестояния амплитуда наименьшая.

Более детальный спектральный анализ полного вектора T с высоким разрешением по частотам показывает расщепление солнечных S и лунных L гармоник из-за годовой модуляции и квазимодуляции периодом ~27-28 дней. На спектре видны серии боковых пиков

S_n и L_n с периодами $f_n \pm k/365.25$ и серии R_n с частотами $f_n \pm k/27.5$, где n - номер компоненты, f_n - соответсвующая ей частота в циклах в день (cpd).

Для выделения суточных магнитных вариаций S_q- и L-вариаций классическим методом является гармонический анализ Чепмена-Миллера. В данной работе параметры S_q- и L-вариация определялись 3-мя способами (что позволило сравнить эффективность использования данных методов): методом Чепмена-Миллера (гармонический анализ) [2], фильтрацией и восстановлением по Фурье-спектру, методом SSA-анализа.

Каждый из перечисленных методов имеет свои достоинства и недостатки. Метод Чепмена-Миллера позволяет работать с временными рядами даже при отсутствии некоторых значений («разорванные ряды»). Однако, этот метод наиболее чувствителен к выбросам и импульсным помехам, и при уменьшении длины временного окна значительно возрастает ошибка вычислений. Второй и третий методы лишены перечисленных недостатков, но требуют длинных непрерывных рядов. Метод SSA-анализа в сравнении с восстановлением по Фурье-спектру более точен и позволяет работать с отдельными компонентами (суточными, полусуточными и т.д.), но требует больших временных и аппаратных ресурсов.

После удаления векового тренда T_0+T_a и S_q- и L-вариаций, остаточная компонента $T_{st}+P$ характеризует вариацию магнитных бурь и пульсаций. Для каждой станции вычислялась межчасовая разница IHV_T (Inter-Hourly Value [3]) значений полного вектора T, для станций с данными для трех компонент также вычислялась межчасовая разница значений H, D, Z. Сравнение геомагнитных данных и распределений полученных межчасовых разниц для большого числа станций позволяет определить время начала магнитных бурь и выделить глобальные и локальные бури. Такой анализ позволяет более точно характеризовать локальную геомагнитную возмущенность по сравнению с использованием Kp- и Dst-индексов.

Для анализа возможного влияния геомагнитного поля Земли на сейсмическую активность использовался каталог землетрясений сети KNET, включающий 6475 событий за 1994-2009 гг. В работе проведены различные статистические и спектральные анализы каталога сейсмической активности. Для выбранного региона были выделены характерные периоды сейсмической активности. Длинные периоды 12, 14, 18, 27.3, 120, 360 суток и короткие периоды 8; 12; 14.5; 24 часов.

В результате работы показано наличие общих периодов 8, 12, 24 часа, 13.8; ~27.8; 120; 360 суток для вариаций геомагнитного поля Земли и сейсмической активности, что указывает на взаимосвязь этих процессов.

Литература.

5. Яновский Б.М. Земной магнетизм. 1978.
6. Chapman, Lindzen. Atmostheric tides. 1969.
7. Svalgaard. IHV - a new long-term geomagnetic index. 2000.

GEOMAGNETIC AND NUCLEAR-GEOPHYSICAL INVESTIGATIONS OF THERMAL TRAVERTINE AREAS IN THE NALYCHEVO HYDROTHERMAL SYSTEM, KAMCHATKA

P.P. Firstov[1], V.A. Rashidov[2], A.V. Melnikova[3], V.N. Shulzhenkova[3]

[1] Kamchatkan Branch of Geophysical Survey RAS, Petropavlovsk-Kamchatsky, Russia 683006
[2] Institute of Volcanology and Seismology FEB RAS, Petropavlovsk-Kamchatsky, Russia 683006
[3] Kamchatka Bering State University, Petropavlovsk-Kamchatsky, Russia 683032

In July 2010 the scientists from Kamchatkan Branch of Geophysical Survey RAS, Institute of Volcanology and Seismology FEB RAS and students from Kamchatka Bering State University carried out geomagnetic and nuclear-geophysical investigations at two thermal travertine areas: young – «Kotel» [1, 2] and modern anthropogenic – «Grifon Ivanova» [3, 4]. The thermal areas are located in the valley of the Goryachaya River being the part of the 15-20 thousand years old Nalychevo hydrothermal system. The thermal waters of Nalychevo hydrothermal system are carbonaceous sodium-chloride with high concentration of arsenic and boron [5].

The thermal travertine area «Kotel» was named for travertine dome, and thermal area «Grifon Ivanova» was given that name because of an anthropogenic grifon, named after the soviet hydrogeologist V.V. Ivanov.

The thermal area «Kotel» is ~ 180×200 m, and the thermal area «Grifon Ivanova» is 90×100 m. In each of 501 observation points the vector magnitude of magnetic inductance, magnetic susceptibility and the dose rate of γ-radiation were sequentially measured. Volumetric activity of Rn in subsoil air was measured in 73 bore holes.

Geomagnetic research revealed that travertine dome «Kotel» is located within the zone of negative magnetic field (ΔT)a. The map of magnetic susceptibility shows zonal distribution of various types of sediments. The maximum value of magnetic susceptibility in the south-western and east-southeastern parts of the travertine area «Kotel» coincide with those from the anomalous magnetic field.

Laboratory analysis of sampled rocks revealed that travertines are almost non-magnetic rocks.

2.5D magnetic modeling showed that within the thermal area «Kotel» that cause anomalies are located at the depth of 15-25 m in argillic and detritus-pebbly sediments [6].

Research revealed that local anomalies of γ-radiation with values 20-30 mR/hr were caused by high radium concentration which deposited in travertine cover in zones of unloading of thermal waters. The authors also detected volumetric activity of Rn that reached 78.6 kBq/m^3 in the subsoil air. High values were caused by both emanating collectors with high concentration of Ra and fracture zones.

Numerous travertine formations, as cup-shaped so dome-shaped, revealed within the thermal area «Kotel» are located along radiating cracks observed both in relief and in geophysical fields.

We didn`t reveal significant anomalies of magnetic field (ΔT)a produced by natural source within the thermal area «Grifon Ivanova». Anomaly, observed on Grifon Ivanova, is caused by casing tube and with iron-rich rocks modified by hydrothermal influence developed in zone of the bore-hole.

Anomalies with γ-radiation at the thermal area «Grifon Ivanova» stretch northeastward. There are two local anomalies with values 8-10 mR/hr: the first is located within the Grifon`s zone; another is about 90 m away from it. We suppose that this is a zone where radium-bearing minerals deposit into evolving modern travertine cover.

Studied thermal areas are ideal natural laboratory for various 4D surveys which are currently developing at the hydrothermal regions [7, 8].

References

1. Novograblenov P.T. Nalychevskie i Kraevedcheskie goryachie klyuchi na Kamchatke // Izvestiya russkogo geograficheskogo obshestva, 1929. P. 285-297.
2. Piyp B.I. Termalnye klyuchi Kamchatki. M.-L.: Izdatelstvo Academii nauk SSSR, 1937. 268 p.
3. Rashidov V.A., Melinikova A.V. Geomagnitnye issledovaniya termalnoy ploshadki "Kotel" (Nalychevskaya gidrotermalnaya sistema, Kamchatka) // Voprosy teorii i praktiki geologicheskoy interpretacii geofizicheskix poley: Materialy 38-y sessii Mezhdynarodnogo nauchnogo seminara imeni D.G.USPENSKOGO, Perm, 24-28 yanvarya 2011: GI YrO RAN, 2011. P. 254-256.
4. Firstov P.P., Rashidov V.A., Melinikova A.V. i drugie. Compleksnye geofizicheskie issledovaniya v prirodnom parke "Nalychevo" (Kamchatka) v 2010 // Vulkanizm i svyazannye s nim processy tradicionnaya regionalnaya nauchnaya conferenciya, posvyashennaya Dnyu Vulkanologa. Tezisy dokladov. Petropavlovsk-Kamchatskiy. 30 Marta - 1 Aprelya 2011 Petropavlovsk-Kamchatskiy: IVIS DVO RAN, 2011. P. 86. (http://www.ivs.kscnet.ru/ivs/conferences/documents/tezis_2011.pdf).
5. Masurenkov YU.P., Komkova L.A. Geodinamika i rudoobrazovanie v kupolno-kolcevoy strukture vulkanicheskogo poyasa. M.: Nayka, 1978. 274 p.
6. Naboko S.I. Gidrotermalnyy metamorfizm porod v vulkanicheskix oblastyax. M.: Izdatelstvo Academii nauk, 1963. 172 p.
7. Glyn W.-J., Rymer H., Mauri G. et al. Toward continuous 4D microgravity monitoring of volcanoes // Geophysics. 2008. V. 73. № 6. P. WA19–WA28.
8. Sugihara M., Ishido T. Geothermal reservoir monitoring with a combination of absolute and relative gravimetry // Geophysics. 2008. V. 73. № 6. P. WA37–WA47.

ГЕОМАГНИНЫЕ И ЯДЕРНО-ГЕОФИЗИЧЕСКИЕ ИССЛЕДОВАНИЯ ТЕРМАЛЬНЫХ ТРАВЕРТИНОВЫХ ПЛОЩАДОК НАЛЫЧЕВСКОЙ ГИДРОТЕРМАЛЬНОЙ СИСТЕМЫ (КАМЧАТКА)

П.П. Фирстов[1], В.А. Рашидов[2], А.В. Мельникова[3], В.Н. Шульженкова[3]

[1]Камчатский филиал Геофизической службы РАН, г. Петропавловск-Камчатский, Россия;
[2]Институт вулканологии и сейсмологии ДВО РАН, г. Петропавловск-Камчатский, Россия;
[3]Камчатский государственный университет им. Витуса Беринга, г. Петропавловск-Камчатский, Россия

В июле 2010 г. сотрудниками Камчатского филиала ГС РАН, Института вулканологии и сейсмологии ДВО РАН и студентами Камчатского государственного университета им. Витуса Беринга на двух термальных травертиновых площадках: молодой – «Котел» [1, 2] и современной техногенной – «Грифон Иванова» были выполнены геомагнитные и ядерно-геофизические исследования [3, 4]. Термальные площадки расположены в долине реки Горячей в нескольких сотнях метров от ее русла и являются частью Налычевской гидротермальной системы, существующей около 15-20 тыс. лет. Термальные воды Налычевской системы относятся к углекислым натриево-хлоридным с повышенным содержанием мышьяка и бора [5].

Травертиновая термальная площадка «Котел» получила название по травертиновому куполу, а термальная площадка «Грифон Иванова» – по одноименному техногенному грифону, названному в честь известного советского гидрогеолога В.В. Иванова.

Термальная площадка «Котел» имеет размер ~ 180×200 м, а термальная площадка «Грифон Иванова» – 90×100 м. В каждой из 501 точек наблюдения последовательно измерялись модуль вектора магнитной индукции, магнитная восприимчивость и мощность дозы γ-излучения. На профиле, пересекающем обе термальные площадки, в 73 шпурах выполнены измерения объемной активности Rn в подпочвенном воздухе.

Геомагнитные исследования показали, что травертиновый купол «Котел» располагается в области развития отрицательного магнитного поля (ΔT)а. Зональность осадков различного типа находит свое отражение на карте магнитной восприимчивости. При этом максимальные значения магнитной восприимчивости в юго-западной и восток-юго-восточной частях на травертиновой площадке «Котел» совпадают с максимальными значениями аномального магнитного поля.

Лабораторные исследования отобранных горных пород показали, что травертины являются практически немагнитными.

2.5D магнитное моделирование показало, что в пределах термальной площадки «Котел» аномалеобразующие тела расположены на глубинах 15-25 м в развитых здесь глинистых и валунно-галечных отложениях [6].

В результате проведенных исследований установлено, что локальные аномалии γ-излучения со значением 20-30 мкР/ч обусловлены повышенным содержанием радия, который откладывался в травертиновом покрове в местах разгрузки термальных вод. Здесь зарегистрированы значения объемной активности Rn в подпочвенном воздухе достигающие 78.6 кБк/м^3. Такие высокие значения обусловлены эманирующими коллекторами с повышенным содержанием Ra и зонами дизъюнктивных нарушений.

Многочисленные травертиновые чаши и купола, выявленные в пределах термальной площадки «Котел», развиты вдоль радиальных трещин, что находит свое отражение, как в рельефе, так и геофизических полях.

Существенных аномалий магнитного поля (ΔT)а, связанных с естественными источниками, на термальной площадке «Грифон Иванова» не выявлено. Аномалия,

наблюдаемая над грифоном Иванова, связана с обсадной трубой и с ожелезненными гидротермально-измененными породами, развитыми в районе скважины.

На термальной площадке «Грифон Иванова» аномалии γ-излучения имеют четко выраженное северо-восточное простирание. Выявлены две локальные аномалии величиной 8-10 мкР/ч: непосредственно в районе грифона и на расстоянии около 90 м от него. По-видимому, здесь, в основном, происходит осаждение радийсодержащих минералов в формирующемся современном травертиновом покрове.

Исследованные термальные площадки представляют собой легкодоступную идеальную природную лабораторию для различных 4D съемок, которые интенсивно развиваются в настоящее время в гидротермальных районах [7, 8].

Список литературы

1. Новограбленов П.Т. Налычевские и Краеведческие горячие ключи на Камчатке // Изв. русск. геогр. общ-ва, 1929. С. 285-297.
2. Пийп Б.И. Термальные ключи Камчатки. М.-Л.: Издательство Академии наук СССР, 1937. 268 с.
3. Рашидов В.А., Мельникова А.В. Геомагнитные исследования термальной площадки «Котел» (Налычевская гидротермальная система, Камчатка) // Вопросы теории и практики геологической интерпретации геофизических полей: Материалы 38-й сессии Международного научного семинара имени Д.Г.Успенского, Пермь,24-28 января 2011 г. Пермь: ГИ УрО РАН, 2011. С. 254-256.
4. Фирстов П.П., Рашидов В.А., Мельникова А.В. и др. Комплексные геофизические исследования в природном парке «Налычево» (Камчатка) в 2010 году // Вулканизм и связанные с ним процессы традиционная региональная научная конференция, посвященная Дню Вулканолога. Тезисы докладов. Петропавловск-Камчатский. 30 марта – 1 апреля 2011 г. Петропавловск-Камчатский: ИВиС ДВО РАН, 2011. С. 86 (http://www.ivs.kscnet.ru/ivs/conferences/documents/tezis_2011.pdf).
5. Масуренков Ю.П., Комкова Л. А. Геодинамика и рудообразование в купольно-кольцевой структуре вулканического пояса. М.: Наука, 1978. 274 с.
6. Набоко С.И. Гидротермальный метаморфизм пород в вулканических областях. М.: Изд-во Академии Наук, 1963. 172 с.
7. Glyn W.-J., Rymer H., Mauri G. et al. Toward continuous 4D microgravity monitoring of volcanoes // Geophysics. 2008. V. 73. № 6. P. WA19–WA28.
8. Sugihara M., Ishido T. Geothermal reservoir monitoring with a combination of absolute and relative gravimetry // Geophysics. 2008. V. 73. № 6. P. WA37–WA47.

Changing the composition, structure and properties of andesite Koshelev volcano and tuffs geothermal field Pauzhetka in the surface zone of modern hydrothermal systems

Shanina V.V., Nuzhdaev A.A.

Modern hydrothermal systems are confined to areas of volcanic activity. The study of hydrothermal systems in practical applications associated with the electricity and heat, is conducted in many countries. Hydrothermal system at depth together as a united front of the thermal power, forming a "geothermal areas". In the south of Kamchatka is located Pauzhetsko-Kambalno-Koshelevo area, which is particularly active research in recent years it Southkamchatsko-Kuril expedition of the Institute of Volcanology and Seismology, headed by Prof. S.N. Rychagov. In 2005, 2007-2010, staff and students of the Engineering and Ecological Geology, Geological Faculty of Lomonosov Moscow State University as part of expeditionary force was a collection of volcanic rocks, in varying degrees of recycled of the thermal waters, which served as the basis for writing many term papers, bachelor's and master's works.

The purpose of this study - to identify patterns of changes in the composition, structure and properties of andesite of Koshelevo volcanic massif and tuffs of Pauzhetka geothermal field under the influence of thermal waters in real time, compare the transformation of rocks at different thermal fields and to see how fit obtained regularities in the trends identified by other researchers for these rocks in their transformations in the geological time.

Field experiments on the Lower-Koshelevo thermal field and Pauzhetskaya field were initiated in summer 2009, and in 2010 was an increase in the number of experimental points (boiling water and mud pots, sinks from the wells) and laid the first samples in the Upper-Koshelevo thermal field. The samples of rocks were characteristic of the thermal field , studied composition and properties, cut into cubes, placed in natural boilers and plums from the wells in a specially prepared wooden cups with holes drilled to ensure maximum contact of the solution with the experimental samples.

In the area of Lower-Koshelevo thermal fields studied unaltered volcanics, confined to the West-Koshelevo volcano composed almost horizontal lava flows of two-pyroxene andesites, andesite-basalt, andesite-dacite (Bliumkina, Cherebatov, 2011). The density of rocks 2,45-2,51 g/cm^3, the density of the solid component (mineral density) 2,68-2,76 g/cm^3. Under the action of water neutral bicarbonate composition (pH 6-8, T = 95 ° C) andesite gradually transformed into montmorillonite clay (Luchko et al, 2009). It all begins with reducing the density of rocks to 2.05 g/cm^3, with a slight decrease in the density of solid particles (up to 2.65 g/cm^3), increases the porosity of up to 23% and hygroscopic moisture of up to 1%.

The main process in the Upper-Koshelevo field is a sulfuric acid leaching, which occurs under the action of acid sulfate waters and leads to the formation of light, porous opalitov (Luchko et al, 2009). The magnetic susceptibility decreases by three orders of magnitude because of the destruction of ore and mafic minerals containing iron in its composition and with ferromagnetic and paramagnetic properties (Frolova et al, 2010).

Differences in the transformation of rocks Koshelev volcano, originally having andesitic composition, primarily attributed to the predominance of hydrogen sulphide or methane in the gas composition of the thermal fields (Zuhubaya, Lucko, 2009).

Unaltered tuffs of verhnepauzhetskoy subsuite of the size of the fragments are divided into psefitic, psammitic, pelitic (Zharenova, Sulimova, 2006; Sulimova, 2006). On the geothermal field under the hot water primary minerals are destroyed and replaced by secondary, which noticeably affects the properties of tuffs. Depending on the composition and temperature of thermal waters marked silicification, chloritization and calcitezation (with epidote, prehnite) zeolitization rocks (Zharenova, 2006; Zharenova, Sulimova, 2006).

The first conclusions of the experiments. Tuffs: increasing the density of rocks, hydroscopic moisture 2-4 times, while reducing the density of the solid component, porosity, water saturation, velocity of longitudinal waves does not change, significantly increases the magnetic susceptibility,

changing the properties of tuffs in good agreement with the increasing content of clay minerals, which replace the primary and heal the pores, and silica minerals (primarily on the open surface of the samples). Andesites: for three weeks significantly increases magnetic susceptibility (redistribution of Fe and modified minerals with ferromagnetic properties) and decreases the open porosity; year trends in the properties of similar of tuffs besides increasing porosity (the formation of secondary porosity due to leaching and removal of the primary components) and reduction of the magnetic susceptibility (the destruction of ore and mafic minerals).

Literature

1. Bliumkina M.E., Cherebatov D.A. Petrophysical properties of andesite West-Koshelev volcano (Southern Kamchatka). Proceedings of the International Youth Science Forum "Lomonosov-2011". [Electronic resource] - M.: MAKS Press, 2011.

2. Zharenova M. Yu. Effect of hydrothermal transformations on the properties of tuffs Pauzhetka hydrothermal deposits (Southern Kamchatka) / / Materials of scientific-practical conference of young specialists. M. 2006. Pp. 145-148.

3. Zharenova M. Yu., Sulimova A. Yu. Effect of hydrothermal processing on the properties of the tuffs (Pauzhetka geothermal field, Southern Kamchatka) / / Proceedings of the XIII International Conference of Students and Young Scientists "Lomonosov-2006". M.: Moscow State Univ. Pp. 60-61.

4. Zuhubaya D.Z., Luchko M.V. Differences in the hydrothermal transformation of andesites in the Upper and Lower-Koshelevo thermal fields (South Kamchatka). Proceedings of the XVI International Conference of Students and Young Scientists "Lomonosov". [Electronic resource] - M.: MAKS Press, 2009.

5. Luchko M.V., Zuhubaya D.Z., Frolova J.V. Petrophysical transform andesites on Koshelevo thermal fields (Southern Kamchatka). Proceedings of X International Conference "Physical-chemical and petrophysical studies in earth sciences." M. 2009. Pp. 250-254.

6. Sulimova A. Yu. Effect of structure and composition of the tuffs on their properties (Pauzhetka region, South Kamchatka) / / Engineering survey for construction. Proceedings of the scientific-practical conference of young specialists. M. 2006. Pp. 152-156.

7. Frolova J.V., Ladygin V.M., Luchko M.V., Zuhubaya D.Z. Transformation of volcanic rocks under the action of sulfuric acid leaching into surface zone of modern hydrothermal systems. Proceedings of the International conference “Actual problems of engineering geology and ecological geology”. M.: MGU, 2010. Pp. 29-30.

Изменение состава, строения и свойств андезитов Кошелевского вулкана и туфов Паужетского геотермального месторождения в приповерхностной зоне современных гидротермальных систем

Шанина В.В., Нуждаев А.А.

Современные гидротермальные системы приурочены к областям развития активной вулканической деятельности. Изучение гидротермальных систем в практических целях, связанное с электро- и теплофикацией, ведется во многих странах мира. Гидротермальные системы на глубине объединяются единым фронтом теплового питания, образуя «геотермальные районы». На юге Камчатки расположен Паужетско-Камбально-Кошелевский район, активное изучение которого особенно в последние годы ведется Южнокамчатско-Курильской экспедицией Института вулканологии и сейсмологии ДВО РАН, возглавляемой д.г.-м.н. С.Н. Рычаговым. В 2005, 2007-2010 годах сотрудниками и студентами кафедры инженерной и экологической геологии геологического факультета МГУ им. М.В.Ломоносова в составе экспедиционной группы была собрана коллекция образов вулканогенных пород, в различной степени переработанных термальными водами, послужившая основой для написания многочисленных курсовых, бакалаврских и магистерских работ.

Цель настоящей работы - выявить закономерности изменения состава, строения и свойств андезитов Кошелевского вулканического массива и туфов Паужетского геотермального месторождения под воздействием термальных вод в режиме реального времени, сравнить преобразования пород на разных термальных полях и посмотреть как укладываются полученные закономерности в тенденции, выявленные другими исследователями для данных пород при их преобразованиях в течение геологического времени.

Натурные эксперименты на Нижне-Кошелевском термальном поле и Паужетском месторождении были начаты летом 2009 года, в 2010 году произошло увеличение количества экспериментальных точек (кипящие водные и грязевые котлы, сливы со скважин) и заложены первые образцы на Верхне-Кошелевском термальном поле. Образцы характерных для данного термального поля пород, изученного состава и свойств, нарезанные в виде кубиков, помещались природные котлы и сливы со скважин в специально приготовленных деревянных стаканчиках с высверленными отверстиями для обеспечения максимального контакта раствора с экспериментальными образцами.

В районе Нижне-Кошелевского термального поля изучены неизмененные эффузивы, приуроченные к Западно-Кошелевскому вулкану, сложенному почти горизонтальными лавовыми потоками средне-верхнечетвертичных двупироксеновых андезитов, андези-базальтов, андези-дацитов (Блюмкина, Черебатов, 2011). Плотность пород 2,45-2,51 г/см^3, плотность твердой компоненты (минеральная плотность) 2,68-2,76 г/см^3. Под действием субнейтральных вод гидрокарбонатного состава (pH 6-8, T~95 °C) андезиты постепенно преобразуются в монтмориллонитовые глины (Лучко и др., 2009). Все начинается с уменьшения плотности пород до 2,05 г/см^3, при незначительном снижении плотности твердых частиц (до 2,65 г/см^3), увеличивается пористость до 23%, а гигроскопическая влажность до 1%.

Основным процессом на Верхне-Кошелевском поле является сернокислотное выщелачивание, происходящее под действием кислых сульфатных вод и приводящее к образованию легких, пористых опалитов (Лучко и др., 2009). Магнитная восприимчивость уменьшается на три порядка из-за разрушения рудных и темноцветных минералов, содержащих в своем составе железо и обладающих ферромагнитными и парамагнитными свойствами (Фролова и др., 2010).

Различия в преобразовании пород Кошелевского вулкана, изначально имеющих андезитовый состав, в первую очередь связывают с преобладанием сероводорода или метана в газовом составе термальных полей (Зухубая, Лучко, 2009).

Неизмененные туфы верхнепаужетской подсвиты по размеру обломков делятся на псефитовые, псаммитовые, алевритовые, пелитовые (Жаренова, Сулимова, 2006; Сулимова, 2006). На геотермальном месторождении под действием горячих вод первичные минералы разрушаются и замещаются вторичными, что заметно отражается на свойствах туфов. В зависимости от состава и температуры термальных вод отмечается окварцевание, хлоритизация и кальцитизация (с эпидотом, пренитом), цеолитизация, агриллитизация пород (Жаренова, 2006; Жаренова, Сулимова, 2006).

Первые выводы по проведенным экспериментам. Туфы: увеличение плотности пород, гигроскопической влажности в 2-4 раза, при снижении плотности твердой компоненты, пористости, водонасыщения; скорость распространения продольных волн не изменяется, незначительно увеличивается магнитная восприимчивость, изменение свойств туфов хорошо согласуется с увеличением содержания глинистых минералов, которые замещают первичные и залечивают поры, и минералов кремнезема (в первую очередь на открытой поверхности образцов). Андезиты: за три недели незначительно увеличивается магнитная восприимчивость (перераспределение Fe и изменение минералов, обладающих ферромагнитными свойствами) и уменьшается открытая пористость пород; за год тенденции изменения свойств аналогичные туфам, кроме увеличения пористости пород (формированием вторичной пористости вследствие выщелачивания и выноса первичных компонентов) и снижения магнитной восприимчивости (разрушение рудных и темноцветных минералов).

Литература

1. Блюмкина М.Е., Черебатов Д.А. Петрофизические свойства андезитов Западно-Кошелевского вулкана (Южная Камчатка). Материалы Международного молодежного научного форума «Ломоносов-2011». [Электронный ресурс] — М.: МАКС Пресс, 2011.

2. Жарёнова М. Ю. Влияние гидротермальных преобразований на свойства туфов Паужетского гидротермального месторождения (Южная Камчатка) // Материалы научно-практической конференции молодых специалистов. М. 2006. С. 145-148.

3. Жаренова М. Ю., Сулимова А. Ю. Влияние гидротермальной переработки на свойства туфов (Паужетское геотермальное месторождение, Южная Камчатка) // Материалы XIII Международной конференции студентов, аспирантов и молодых ученых «Ломоносов-2006». М. Изд-во МГУ. С. 60-61.

4. Зухубая Д. З., Лучко М. В. Различия в гидротермальных преобразованиях андезитов в районе Верхне- и Нижне-Кошелевских термальных полей (Южная Камчатка). Материалы XVI Международной конференции студентов, аспирантов и молодых ученых «Ломоносов». Электронный ресурс. М.: МАКС Пресс, 2009.

5. Лучко М.В., Зухубая Д.З., Фролова Ю.В. Петрофизические преобразования андезитов на Кошелевских термальных полях (Южная Камчатка). Материалы X международной конференции «Физико-химические и петрофизические исследования в науках о Земле». М. 2009. С. 250-254.

6. Сулимова А. Ю. Влияние состава и строения туфов на их свойства (Паужетский район, Южная Камчатка) // Инженерные изыскания в строительстве. Материалы научно-практической конференции молодых специалистов. М. 2006. С. 152-156.

7. Фролова Ю.В., Ладыгин В.М., Лучко М.В., Зухубая Д.З. Преобразование вулканогенных пород под действием сернокислотного выщелачивания в приповерхностной зоне современных гидротермальных систем // Труды Международной конференции «Актуальные вопросы инженерной геологии и экологической геологии». М.: Изд-во МГУ, 2010. С. 29–30.

Deep Structure of the Region of the Uzon-Geyser Volcanic-tectonic Depression (Kamchatka) by Low-Frequency Microseismic Sounding

Yu. A. Kugaenko[1], V. A. Saltykov[1], A. V. Gorbatikov[2], and M. Yu. Stepanova[2]
1 Kamchatka Branch of the Geophysical Survey, RAS, Petropavlovsk-Kamchatsky, Russia e-mail: ku@emsd.ru
2 Schmidt Joint Institute of Physics of the Earth, RAS, Moscow, Russia

The the Uzon-Geyser Volcanic-tectonic Depression (Kamchatka) is volcanic structure of oval shape elongated in the latitudinal direction with a size of 9×18 km. It is related to the Eastern Kamchatka volcanic belt and includes two world-renown unique natural sites: the Valley of the Geysers and Uzon Caldera [4]. The depression is related to the cross-section node of large regional fractures: magmatic and fluid conducting volcanic gaping fault of the northeastern extension and sublatitudinal Uzon-Valaginskii strike strip fault.

On base of new passive seismic technique the deep structure of the Uzon-Geyser Volcanic-tectonic Depression was investigated. In September 2009, special geophysical observations were performed for the first time to reconstruct the deep structure and the medium in the depression region.

In order to reconstruct the deep structure, we have chosen the method of microseismic sounding [1, 2] in which surface Rayleigh waves of different frequencies play the role of sounding signals. The Rayleigh waves determine the main contribution to the vertical component of the Earth's microseismic field. The geological structures presenting the velocity inhomogeneities interact with the incident Rayleigh waves (refraction, exchange, scattering) and distort the amplitude spectrum of the microseismic field in their vicinity. Spectral amplitudes of microseismic signals decrease at the Earth's surface over high-velocity anomalies and increase over low-velocity anomalies.

Thus, deep sections up to 30 km, which reflects the distribution of relative velocities of transversal seismic waves, were constructed for the first time in the hardly accessible conditions of Uzon-Geyser Depression zone using the method of low-frequency microseismic sounding (fig.1). Their integral interpretation using the previously known results of the geological, morphological, and petrological investigations was performed. Crystallized acid magma chamber under the caldera complex at depths of 6–10 km was identified and localized. The regions of concentration of basalt melts were distinguished and localized. We emphasize high consistency between the upper parts of the sections with the geological concepts about the peculiarities of the structure in the study region. The geometry of the revealed deep structures is in agreement with the model of the supposed magma intrusion into the upper layers of the crust based on the data of the satellite interferometry [5]. For more details see [3].

Supported by Russian Foundation for Basic Research (Grant 10-05-00139).

References

1. Gorbatikov, A. V , Stepanova, M. Yu., Korablev, G. E. (2008) Microseismic Field Affected by Local Geological Heterogeneities and Microseismic Sounding of the Medium, Izvestiya, *Physics of the Solid Earth*, Vol. 44, No. 7, pp. 577–592.
2. Gorbatikov, A. V., Tsukanov, A. A. (2011) Simulation of the Rayleigh Waves in the Proximity of the Scattering Velocity Heterogeneities. Exploring the Capabilities of the Microseismic Sounding Method Izvestiya, *Physics of the Solid Earth*, Vol. 47, No. 4, pp. 354–369.
3. Kugaenko, Yu. A., Saltykov, V. A., Gorbatikov, A. V., Stepanova, M. Yu. (2010) Deep Structure of the Region of the Uzon-Geyser Volcanic-Tectonic Depression Based on the Data of Microseismic Sounding // *Doklady Earth Sciences*, Vol. 435, Part 1, pp. 1465–1470.

4. Leonov, V.L., Grib, E.K., Karpov, G.A., Sugrobov, V.M ., Sugrobova, N.G., and Zubin, M.I. (1991) Uzon Caldera and Valley of Geysers, in *Active Volcanoes of Kamchatka*, edited by S.A. Fedotov and Y.P.Masurenkov. Vol.2. pp.92-141. Moscow: Nauka.

5. Lundgren P., Lu Zh. (2006) Inflation model of Uzon caldera, Kamchatka, constrained by satellite radar interferometry observations. *Geophysical Research Letters*. VOL. 33, L06301, doi:10.1029/2005GL025181

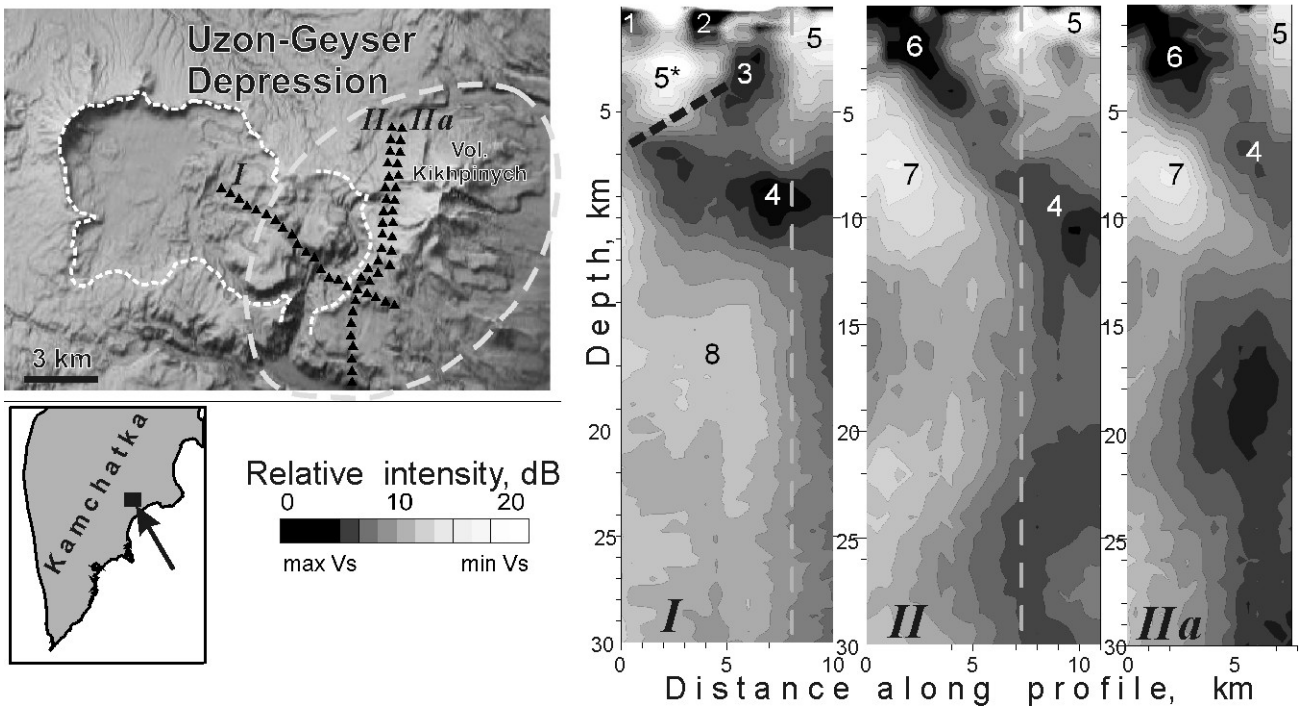


Fig.1. Normally oriented profiles of measurements and deep sections along profiles presented in the parameters of relative velocities of transversal seismic waves. The dashed line shows the cross section of sections ***I*** and ***II***. Elements of the deep structure (1-8):
1 - a hardened lava massif of dacite and rhyodacite (Belyaya Mountain) composition covered by lacustrine deposits;
2 - region of extrusive domes of Late Pleistocene age in central part of depression;
3, 4 - parts of the crystallized acid magma chamber; the depth of the location of the main part of the chamber (region 4) corresponds to the boundary of the crystal basement;
5 - zone of not-segmented deposits of the precaldera complex;
6 - the pathways of magma propagation along the system of sublatitudinal distortions controlled by the regional Uzon-Valaginsky Fracture in the Quaternary time, which manifested itself as a tension structure;
7 - region of increased concentration of basalt magma, which is a peripheral source that fed the Holocene basalt eruptions of the Kikhpinych volcanic center;
8 – possible basalt magma chamber under intrusive 4. Its formation is related with partial blocking of the free basalt spreading to the surface due to the screening effect of the crystallized acid magma chamber 4.

Hydrothermal systems of North and Central Kuril islands.

E.G.Kalacheva
Institute of volcanology and seismology FEB PAS, Petropavlovsk-Kamchatsky, keg@kscnet.ru

On the Northern and Central Kuril Islands eight of the hydrothermal systems of thermal power from 1200 to 15 000 kcal / sec were allocated. They are located in the interior of volcanoes.

The volcanoes have similar complex construction of the Somma-Vesuvius [Bogoiavlenskay, Gorshkov, 1966], similar to the material composition (two-pyroxene andesites), they are characterized by active solfataric activity in the apical part of the structure and the different types of thermal waters are unloaded on their slopes. Features of the development of volcanic activity, hydrological and geological conditions have led to several differences in the conditions of formation and discharge of the hydrothermal systems of the region.

Surface manifestations of the North Shiashkotan and Ketoy hydrothermal systems occur over 5-8 km on the slopes of the volcanoes and have the classic vertical zonation. Hydrothermal solfataras are located in the area of the main updraft in several thermal areas near the craters of volcanoes. By its chemical composition these are acidic sulfate, aluminum (calcium) waters with total mineralization to 8g / liter and a temperature of 80 ° C. Boiling chloride sodium springs with near-neutral pH values are found at the edge of the sea. Total mineralization is up to 15 g / liter. The heat source for hydrothermal systems are cooling shallow magma bodies (<2-3 km), which bring some of magmatic gases, salts and metals in the circulating hydrothermal system.

In construction of the volcano Ebeko (Paramushir Island) local hydrothermal system is formed. The main water-bearing rock is a complex of Quaternary volcanic. The source of heat supply is shallow intrusions. The dissolution of magmatic gases (mainly HCl and SO_2) in the aeration zone of the groundwater leads to the formation of reservoir of the ultra acid chloride-sulfate brine directly below the crater part of volcano. Climatic conditions in the region provide a constant replenishment of the reservoir by infiltration water. Structural, stratigraphic and topographic features of the volcano Ebeko define a limited drainage from "the lake" in the northwestern part of the volcano. A series of permeable coarse interbedded lavas, exposed in the basin form a hydraulic channel between the underground "lake" and the output of thermal waters in the basin of Yuriev River. Upper-Yurievsky springs - are highly temperature (42-90°C), highly mineralized (up to 14 g / liter), ultra acid (pH <2) waters of chloride-sulfate composition. Ions of aluminum and iron are the main amidst cations.

The problem of the presence and the role of the deep reservoir of chloride-sodium waters in the bowels of the volcano Ebeko remains obscure. The exploration well in the neighbour of Severo-Kurilsk opened the slightly alkaline (pH7.5-8.0), chloride-bicarbonate sodium groundwater with temperatures up to 95°C and total mineralization of 9.5 g / liter. However, the sodium chloride thermal waters outlet have not been marked on surface.

Hydrothermal systems, confined to volcanoes constructions, craters of which are occupied by the calderas filled with lake or sea water (Calder Zavaritsky (Simushir) and Ushishirskaya hydrothermal system), have no opportunity of the formation of ultra-acid sulfate waters due to low hypsometric marks in the crater pert. Upstream of neutral chloride sodium waters discharged directly into the central part of the system in the area of intersection of breaking zones as at the water's surface and on the bottom. On surface areas solfataric grounds with bubbling springs and

steam jets are formed. By the chemical composition they are also chloride sodium, but with more lower pH values from 2.5 to 6. The general model of the formation of such hydrothermal systems can be represented as follows [by Taran et al, 1993]. Downdrafts reach meteoric water heated by magma nidus of zone located at a shallow depth (1-2 km) where the infiltrated water and magmatic gases or the partially neutralized by interaction the rock with the magmatic brine are mixed. Intensive additional source of gas and high temperatures lead to the formation of the steam flow in the lower parts of the reservoir, which rising to the surface is partially condensed by mixing with groundwater and surface water.

SPATIAL COMPOSITIONAL VARIATIONS IN QUATERNARY VOLCANICS FROM THE NORHERN KURIL ISLANDS, RUSSIA

O.V. Kuvikas[1,2], M.Nakagawa[2], G.P. Avdeiko[1], V.A. Rashidov[1]

[1] *Institute of Volcanology and Seismology FEB RAS, Petropavlovsk-Kamchatski, Russia.*

[2] *Department of Natural History Science, Graduate School of Science, Hokkaido Univ., Japan.*

The Northern Kuril Islands form the part of Kuril-Kamchatka volcanic arc. Approximately steady-state subduction beneath the islands occurred since the late Miocene (Avdeiko et al, 2006). We newly determined major and trace element compositions of number Quaternary rocks from 7 subarial and 3 submarine volcanoes (Fig. 1) - to demonstrate systematic changes in magma genesis across arc. Peculiarities of whole-rock chemistry, and petrography of these rocks enable us to divide of all volcanoes into five main groups. These volcanic groups have good correlation with geological data. Each unit of the volcanic group is characterized by narrow range of chemical variations (Fig. 2). These five groups are as follows.

Chikurachki, Tatarinov, Lomonosov, 1.3 volcanic group:-

These volcanoes locate at the front zone. The lowest contents of incompatible elements (e.g. Rb, Ba, K) are typical. Rocks are Ol-Cpx bearing Opx basaltic andesite.

Fuss, Antsiferov volcanic group:-

It locates at the intermediate zone. The rocks show higher contents of incompatible elements. Hbl-Cpx-Ol-bearing Opx andesite are commonly characterized by the presence of hornblende phenocryst.

Ebeko volcanic group:-

It locates at the northern part of Paramushir island. Rocks show intermediate contents of Rb, Ba, K_2O, Rb/Zr. Compositional area vary in average data from typical front volcanoes to intermediate volcanoes. The rocks are Ol-Cpx-bearing Opx basaltic andesite.

Alaid, Grigorev volcanic group:-

These volcanoes locate at the back arc zone. The rocks show highest contents in K_2O and Rb. In addition this group is characterized by the highest contents of Nb. Compared with other volcanic groups, these group have the largest eruptive volume (150 km^3). The rocks are Ol-bearing Cpx basalt.

1.4 volcanic group:-

This volcano is situated at the distance of more than 250 km from the trench. Two types of rock occur in this volcanic group: Cpx-bearing Hbl andesite and Cpx-basalt. The basalt is characterized by low contents of Rb, Ba, K_2O, whereas the andesite show highest contents of incompatible elements.

These results and previous data (Bindeman and Bailey, 1999: Churikova et al, 2001) generally show that regular enrichment of LILE (e.g. Rb, K, Ba) and depletion HFSE (e.g. Nb, Zr, Y) in volcanic rocks depend from the slab depth. However, there exist several anomalies, such as in Alaid and 1.4 groups, which would not be explained by a simple subduction model. In order to discuss in detail, we are now determining REE and Sr-Nd isotopes.

Reference

Avdeiko et al., 2006: Petrologiya 14 (3): 248-265.

Bindeman, Bailey, 1999. EPSL 169: 209-226.

Churikova et al., 2001: Journal of petrology 42(8): 1567-1593.

Martynov et al, 2009: Science about Earth. Letters of FEB RAS 4: 17-23.

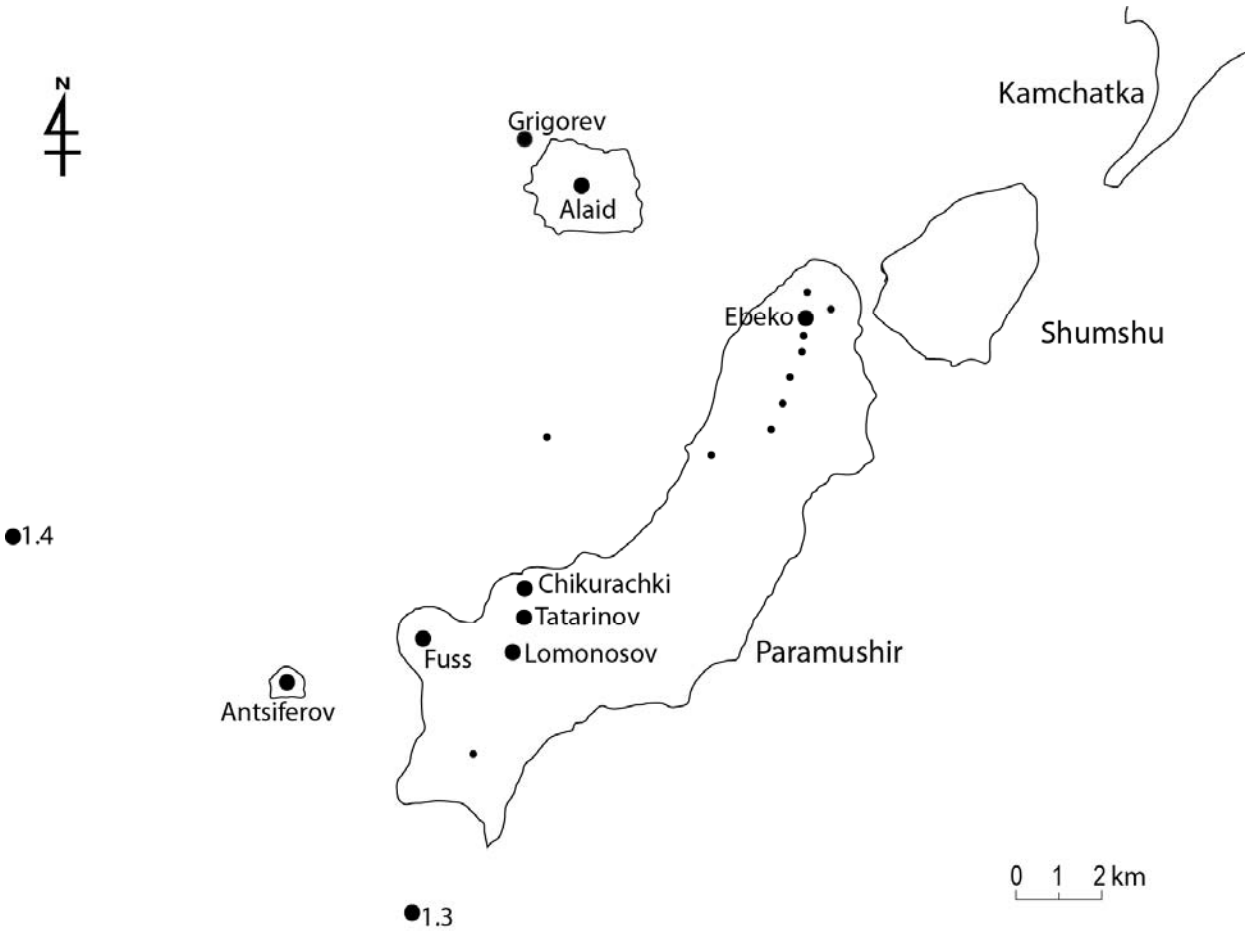


Figure 1. Schematic map of the Northern Kuril Islands.

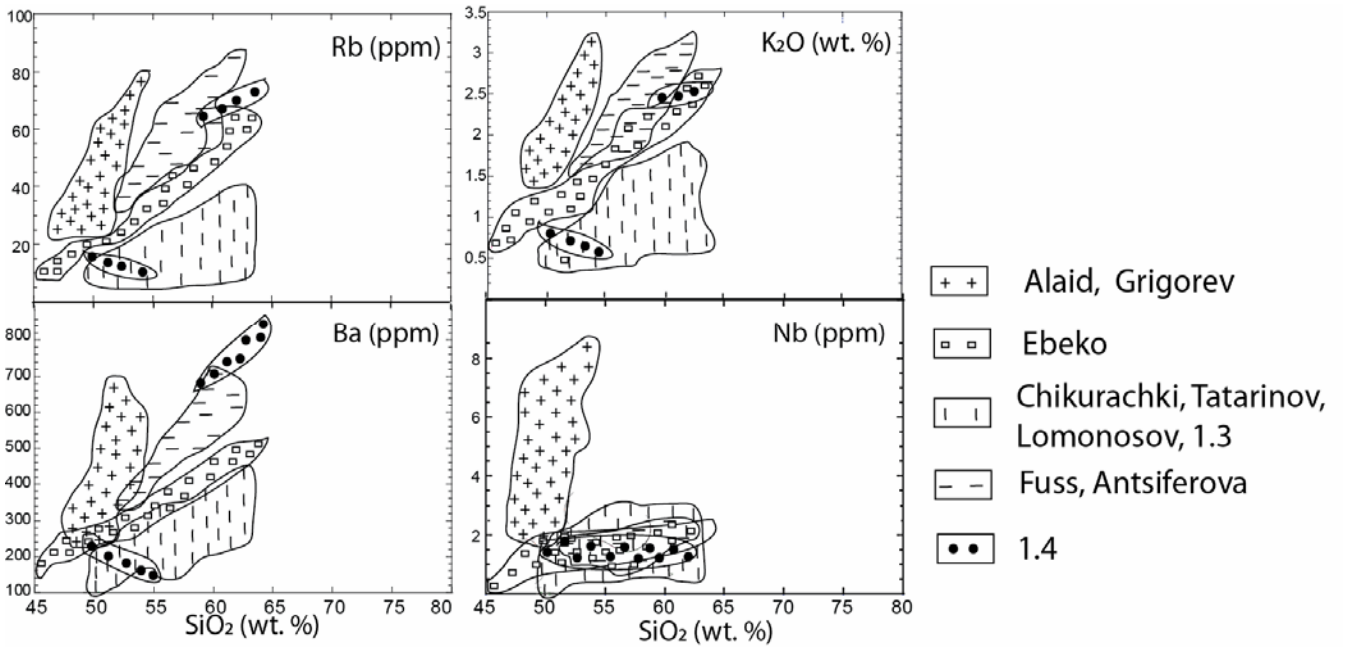


Figure 2. Harker's diagrams. Variations of major and trace elements in the volcanic rocks from the Northern Kuril Islands.

MODERN TECHNIQUES FOR INTERDISCIPLINARY INVESTIGATION OF SUBMARINE VOLCANOES IN THE KURILE ISLAND ARC

Yu.I. Blokh[1], V.I. Bondarenko[2], A.S. Dolgal[3], P.N. Novikova[3], V.A. Rashidov[4], A.A. Trusov[5]

[1] Moscow, Russia;
[2] Nekrasov State University of Kostroma, 15600, Russia;
[3]Mining Institute of the Ural Branch of the RAS, Perm, 614007, Russia;
[4] Institute of Volcanology and Seismology, FEB RAS, 683006, Russia;
[5]ZAO « GNPP Aerogeofizika», Moscow, 107140, Russia

The Kuril Island Arc with submarine volcanoes on the side of Okhotskoye Sea slope is a key element of a transit zone between Asia continent and the Pacific Ocean. Scientists carried out 11 systematic and multidisciplinary investigations of submarine volcanic activity within the Kuril Islands Arc onboard R/V «Vulkanolog» [7].

The volcanologic investigation included echo-sounding survey, continuous seismoacoustic profiling, hydromagnetic survey, and geologic sampling, and consisted of two phases. In the first phase we carried out profiling and areal survey. During the second phase we carried out draging within zones determined from results of geophysical survey. Geophysical research at the monitored area was carried out using profile network which were chosen according to goals of volcanological investigation. The authors used various profile networks extending the monitored area during following cruises. Unfortunately, profiles were irregular and their density was low.

In order to process the data from irregular networks, we created a high-performance technology for quantitative interpretation of data from hydromagnetic survey using continuous seismoacoustic profiling, echo-sounding survey, and analysis of remanent magnetization and chemical composition of dredged rocks. This technology allows interpretation using benchmark data and avoids gridding [2, 4].

The technology consists of a method of singularity using SINGULAR software [3], 2.5D modeling [6] on single profiles, followed by 3D modeling for all profiles using SIGMA-3D [1] software. This technology uses a model of sub-horizontal layer which suffers fluctuation of magnetization along lateral.

In order to correct vector direction of magnetization of a volcanic edifice we use IGLA software [5] which uses initial magnetic field.

For modeling the authors used a true relief of volcanic edifices determined by echo-sounding survey and continuous seismoacoustic profiling.

In order to locate attitude position of submarine volcanoes conduits an assembly method was used [2, 8].

Modern techniques allowed distinguishing single lava flows, summit calderas, lateral volcanic cones, active volcanic centers, peripheral magmatic chambers, conduits and estimating magnetic properties of rocks in natural deposits within large volcanic edifices of the Kuril Islands Arc.

Multidisciplinary method allows creating the most accurate geomagnetic model.

New submarine volcanoes, calderas and zones of mud volcanic and hydrothermal activity were revealed within the Kuril Islands Arc. The authors traced evolution of certain isolated volcanoes and volcanic massifs as well as estimated zones, types and, in some cases, duration of submarine volcanic activity.

Investigation was sponsored by the Far Eastern Branch of the Russian Academy of Sciences, the project № 09-3-A-08-427.

References

1. Babayants P.S., Bloch Yu.I., Bondarenko V.I., Rashidov V.A., Trusov A.A. Primeneniye Paketa programm strukturnoy interpretatsiyi SiGMA-3D pri izucheniyi podvodnih vulkanov Kuril'skoy ostrovnoy dugi. Vestnik KRAUNTS. Nauki o Zemle. 2005. № 2. V. 6. P. 67-76.
2. Blokh Yu.I., Bondarenko V.I., Dolgal A.S., Novikova P.N., Rashidov V.A., Trusov A.A. Geophisicheskiye issledovaniya podvodnogo vulkana 6.1 (Kurilskaya ostrovnaya duga). Voprosy teorii i praktiki geologicheskoy interpretatsii geophisicheskikh poley. Materialy tridtsat vosmoy sessii Mezhdunarodnogo nauchnogo seminara imeni D.G. Uspenskogo, Perm, 24-28 yanvarya 2011 goda. Perm, GI UrO RAN, 2011. P. 32-35.
3. Blokh Yu.I., Bondarenko V.I., Rashidov V.A., Trusov A.A. Primeneniye integrirovannoy sistemy SINGULYAR dlya izucheniya glubinnogo stroeniya podvodnikh vulkanov Kurilskoy ostrovnoy dugi. Voprosy teorii i praktiki geologicheskoy interprettatsii gravitatsionnikh, magnitnikh i elektricheskikh poley. Materialy tridtsat vosmoy sessii Mezhdunarodnogo nauchnogo seminara imeni D.G. Uspenskogo, Moskva, 25-29 yanvarya 2010 goda. M: IPhZ RAN, 2010. P. 62-65.
4. Blokh Yu.I., Bondarenko V.I., Rashidov V.A., Trusov A.A. Istoriya geomagnitnikh issledovaniy podvodnikh vulkanov Kurilskoy ostrovnoy dugi. Materialy Vserossiyskoy konferintsii, posvyashonnoy semidesyatipyatiletiyu Kamchatskoy vulkanologicheskoy stantsii. Otv. red. akademik E.I. Gordeev. Petropavlovsk-Kamchatskiy. Izdatelstvo IViS DVO RAN, 2010. P. 6-10 (http://www.kscnet.ru/ivs/slsecret/75-KVS/Material_conferenc/art2.pdf)
5. Blokh Yu.I., Trusov A.A. Programma IGLA dlya interaktivnoy ekspress-interpretatsii lokalnikh gravitatsionnikh i magnitnikh anomaliy. Voprosy teorii i praktiki geologicheskoy interpretatsii gravitatsionnikh, magnitnikh i elektricheskikh poley: materialy tridtsatchetvyortoy sessii mezhdunarodnogo seminara imeni D.G. Uspenskogo. M: IPhZ RAN, 2007. P. 36-38.
6. Rashidov V.A., Bondarenko V.I. Geofizicheskiye issledovaniya podvodnogo vulkana Krylatka (Kurilskaya ostrovnaya duga). Vulkanologiya i seysmologiya. 2004. № 4. P. 65-76.
7. Podvodniy vulkanizm i zonalnost Kurilskoy ostrovnoy dugi. Otv. red. Yu. M. Pusharovskiy. M: Nauka, 1992. 528 p.
8. V.N. Strakhov, M.I. Lapina. Montazhniy metod resheniya obratnoy zadachi fravimetrii. DAN. 1976. V. 227. № 2. P. 344-347.

СОВРЕМЕННЫЕ ТЕХНОЛОГИИ ПРИ КОМПЛЕКСНОМ ИЗУЧЕНИИ ПОДВОДНЫХ ВУЛКАНОВ КУРИЛЬСКОЙ ОСТРОВНОЙ ДУГИ

Ю.И. Блох[1], В.И. Бондаренко[2], А.С. Долгаль[3], П.Н. Новикова[3], В.А. Рашидов[4], А.А. Трусов[5]

[1]Москва, Россия;
[2]Костромской государственный университет им. Н.А. Некрасова, Кострома, Россия;
[3]Горный институт УрО РАН, Пермь, Россия ;
[4]Институт вулканологии и сейсмологии ДВО РАН, Петропавловск-Камчатский, Россия;
[5]ЗАО «ГНПП Аэрогеофизика», *Москва, Россия*

Курильская островная дуга (КОД), на Охотоморском склоне которой расположены подводные вулканы, – важный элемент зоны перехода от Азиатского материка к Тихому океану**.** Планомерное комплексное изучение подводного вулканизма КОД было проведено в 11-ти рейсах НИС «Вулканолог» [7].

В комплекс вулканологических исследований входили эхолотный промер, непрерывное сейсмоакустическое профилирование (НСП), модульная гидромагнитная съемка (ГМС) и геологическое опробование. Исследования проводились в два этапа: на первом выполнялись профильные и площадные геофизические исследования, а на втором отрабатывались станции геологического опробования в точках, выбранных по результатам геофизических работ. Полигонные геофизические исследования проводились по сетям профилей, выбранных с учетом задач комплексных вулканологических исследований. Применялись различные системы профилей, а сети наращивались при последующих работах на объектах. К большому сожалению, часто сети съемочных профилей оказывались нерегулярными, а их плотность невысокой.

Для обработки данных, полученных на нерегулярных редких сетях наблюдений, была разработана эффективная технология количественной интерпретации материалов ГМС в комплексе с эхолотным промером, НСП и анализом естественной остаточной намагниченности и химического состава драгированных горных пород, позволяющая проводить интерпретацию непосредственно по исходным данным, не прибегая к некорректной процедуре их предварительного восстановления в узлах регулярной сети [2, 4].

Технология состоит в применении методов особых точек с помощью интегрированной системы СИНГУЛЯР [3] и 2.5D моделирования [6] на отдельных галсах и последующего 3D моделирования с помощью программ пакета структурной интерпретации СИГМА-3D [1] по всему массиву исходных данных на базе модели субгоризонтального слоя с латерально изменяющейся намагниченностью.

Уточнение основного направления вектора суммарной намагниченности вулканической постройки осуществляется непосредственно по исходному аномальному полю программой ИГЛА [5].

При моделировании всегда используется истинный рельеф вулканических построек с учетом погребенного под осадками основания, полученный по данным эхолотного промера и НСП.

Для уточнения пространственного положения подводящих каналов подводных вулканов КОД применяется монтажный метод решения обратной задачи магнитометрии по аномальным значениям поля [2, 8].

Применение современных технологий позволило выделить в пределах вулканических построек КОД отдельные лавовые потоки, вершинные кальдеры, побочные вулканические конусы, активные вулканические центры, периферические магматические очаги, подводящие каналы и оценить магнитные свойства горных пород в естественном залегании.

Комплексирование геолого-геофизических методов позволило уменьшить неоднозначность решения обратной задачи и построить наиболее реалистичные геомагнитные модели.

В пределах КОД идентифицированы новые подводные вулканы и кальдеры, выявлены зоны проявления грязевого вулканизма и гидротермальной активности. Прослежена эволюция ряда изолированных вулканов и вулканических массивов, оценены масштабы, форма и, в ряде случаев, продолжительность проявления подводной вулканической деятельности.

Работа выполнена при финансовой поддержке ДВО РАН (проект 09-3-А-08-427).

Список литературы

1. Бабаянц П.С., Блох Ю.И., Бондаренко В.И., Рашидов В.А., Трусов А.А. Применение пакета программ структурной интерпретации СИГМА-3D при изучении подводных вулканов Курильской островной дуги // Вестник КРАУНЦ. Науки о Земле. 2005. № 2. Вып. 6. С. 67-76.
2. Блох Ю.И., Бондаренко В.И., Долгаль А.С., Новикова П.Н., Рашидов В.А., Трусов А.А. Геофизические исследования подводного вулкана 6.1 (Курильская островная дуга) // Вопросы теории и практики геологической интерпретации геофизических полей: Материалы 38-й сессии Международного научного семинара имени Д.Г. Успенского, Пермь, 24-28 января 2011 г. Пермь: ГИ УрО РАН, 2011. С. 32-35.
3. Блох Ю.И., Бондаренко В.И., Рашидов В.А., Трусов А.А. Применение интегрированной системы «СИНГУЛЯР» для изучения глубинного строения подводных вулканов Курильской островной дуги // Вопросы теории и практики геологической интерпретации гравитационных, магнитных и электрических полей**:** Материалы 37-й сессии Международного семинара им. Д.Г. Успенского, Москва, 25-29 января 2010 г. М.: ИФЗ РАН, 2010. С. 62-65.
4. Блох Ю.И., Бондаренко В.И., Рашидов В.А., Трусов А.А. История геомагнитных исследований подводных вулканов Курильской островной дуги // Материалы Всероссийской конференции, посвященной 75-летию Камчатской вулканологической станции / Отв. ред. академик Е.И. Гордеев. Петропавловск-Камчатский: Изд-во ИВиС ДВО РАН, 2010. С. 6-10 (http://www.kscnet.ru/ivs/slsecret/75-KVS/Material_conferenc/art2.pdf).
5. Блох Ю.И., Трусов А.А. Программа «IGLA» для интерактивной экспресс-интерпретации локальных гравитационных и магнитных аномалий // Вопросы теории и практики геологической интерпретации гравитационных, магнитных и электрических полей: материалы 34-й сессии международного семинара им. Д.Г.Успенского. М: ИФЗ РАН, 2007. С. 36-38.
6. Рашидов В.А., Бондаренко В.И. Геофизические исследования подводного вулкана Крылатка (Курильская островная дуга) // Вулканология и сейсмология. 2004. № 4. С. 65-76.
7. Подводный вулканизм и зональность Курильской островной дуги / Отв. ред. Пущаровский Ю.М. М.: Наука, 1992. 528 с.
8. Страхов В. Н., Лапина М. И. Монтажный метод решения обратной задачи гравиметрии // ДАН. 1976. Т. 227. № 2. С. 344-347.

Along-arc variations of K-Ar ages for the submarine volcanic rocks in the Kurile Islands

Yoshihiro Ishizuka[a], Mitsuhiro Nakagawa[b], Akira Baba[b], Takeshi Hasegawa[c], Ayumi Kosugi[b], Shimpei Uesawa[b], Akikazu Matsumoto[a] and Alexander Rybin[d]

[a] *Geological Survey of Japan, AIST, 1-1-1 Higashi, Tsukuba, Ibaraki 305-8567, Japan*
[b] *Hokkaido University, N10 W8 Kita-ku, Sapporo, 060-0810, Japan*
[c] *Ibaraki University, 2-1-1 Bunkyo, Mito, Ibaraki 310-8512, Japan*
[d] *Institute of Marine Geology and Geophysics, 5 Nauka Street, Yuzhno-Sakhalinsk, 693022, Russia*

Seventeen K-Ar ages of submarine volcanic rocks from Urup to Paramushir Islands, south to north Kurile Islands, are measured in order to reveal the evolution of the Kurile arc. These islands construct a volcanic active arc (Greater Kurile Ridge) that formed from vigorous submarine volcanic activity beginning in the Miocene (Nemoto and Sasa, 1960; Gorshkov, 1970; Sergeyev and Krasny, 1987). We described submarine volcanic rocks consisting of hyaloclastites and dykes with minor amount of pillow lavas at the coastal cliffs at each islands.

Sampled hyaloclastites are meter-sized breccias that have polyhedron with radial cooling joints and matrix of very fine to fine sand size's ash. Dykes have cooling joints with several centimeters. They are composed of basalt to andesite having 49-59% SiO_2 in whole-rock chemistries. K-Ar ages of selected unalternated to weekly alternated rocks are measured in Geological Survey of Japan, AIST, by isotope dilution method. The ages of the islands based on K-Ar ages as follows.

(a) South Kurile: 8.36 Ma, 5.82 Ma and 4.21 Ma (Urup Island)
(b) Central Kurile: 3.13 Ma, 2.13 Ma, 1.78 Ma and 1.45 Ma (Simushir Island),
1.17 Ma (Ushishir Island)
1.15 Ma, 1.06 Ma and 0.79 Ma (Rasshua Island)
1.61 Ma (Matua Island.)
0.97 Ma, 0.62 Ma (Shiashkotan Island)
(c) North Kuril: 1.29 Ma (Makanrushi Island)
7.04 Ma and 3.49 Ma (Paramushir Island)

These results show that the submarine volcanic rocks on Urup and Paramushir Islands are old in Late Miocene to Early Pliocene. On the contrast, the rocks on Ushishir, Rasshua, Matua, Shiashkotan, and Makanrushi Islands are young in Quaternary. This shows that the ages of submarine volcanic rocks shift from old in the south, young in the central to old in the north. In addition, the ages of submarine volcanic rocks have the gap between Urup and Simushir Islands that are separated by the deepest strait (Boussole Strait) in the Kurile arc. This gap of ages for submarine volcanic rocks might be harmonized with the tectonic setting and crustal thickness beneath the Kurile arc.

THE ORIGIN OF MIOCENE ALKALINE BASALTS OF THE KRONOTSKY ISTHMUS

Savelyev D.P., Kartasheva E.V., Savelyeva O.L.

Institute of Volcanology and Seismology FEB RAS, Petropavlovsk-Kamchatsky, Russia

E-mail savelyev@kscnet.ru

The origin of Neogene alkaline rocks with an "intraplate" geochemical signature is one of disputable questions of the geological history of Kamchatka. Their formation preceded the Pliocene-Quaternary stage of the Eastern Kamchatka volcanism. The alkaline volcanism of the Eastern Kamchatka is closely related to the Miocene terrigenous sequence of the Tyushevka Trough, that is, the Schapinskaya Formation in the basin of the Left Zhupanova River [8] and on the Kronotsky Isthmus [6, 7]. Previous studies related "intraplate" geochemical characteristics of these rocks with deep fractures in the continental plate that originated in the result of the collision of the Kronotsky terrane [8] or with transversal sublatitudinal strike-slip fault zones stretched from the Pacific plate to the Kurile-Kamchatka island arc [2]. Isotope and geochemical characteristics of these rocks are unique for the Eastern Kamchatka. Some authors explain this fact by flowing of an enriched mantle from under the Meiji Seamount through a slab window at the initiation of the modern subduction zone [4].

Here we report new data on alkaline basalts from a core at the Konusnaya site drilled in the Tyushevka River basin on the Kronotsky Isthmus, that is, in the depression filled by terrigenous deposits between the Kronotsky Peninsula and Gamchen Ridge.

The basalts form two sills among the Middle Miocene tuffaceous-terrigenous rocks [6]. Their petrochemical features were studied earlier by O.I. Suprunenko and B.A. Markovskiy [6]. XRF data on major and trace elements (analytical centre of the Institute of Volcanology and Seismology FEB RAS) confirmed the high-potassium composition of the rocks and high concentrations of TiO2 and P2O5 (TiO_2=2.2-3.1 %, K_2O=1.6-6 %, P_2O_5=0.9-1 %). Judging from trace element composition (Nb= 67-92 г/т, Zr = 413-567 г/т, Zr/Y=15-19), the rocks are similar to alkaline gabbroids and trachydolerites from the Small Chazhma River Basin [7] and have even stronger "intraplate" signature expressed in higher K, Nb and Zr contents. The rocks studied are also similar to the Miocene alkaline basalts described in the Left Zhupanova River basin [8].

On the basis of the new data we propose that the Miocene alkaline basalts of the Kronotsky Isthmus were generated on the western slope of the Kronotsky paleoarc before its collision with Kamchatka (Fig. 1).

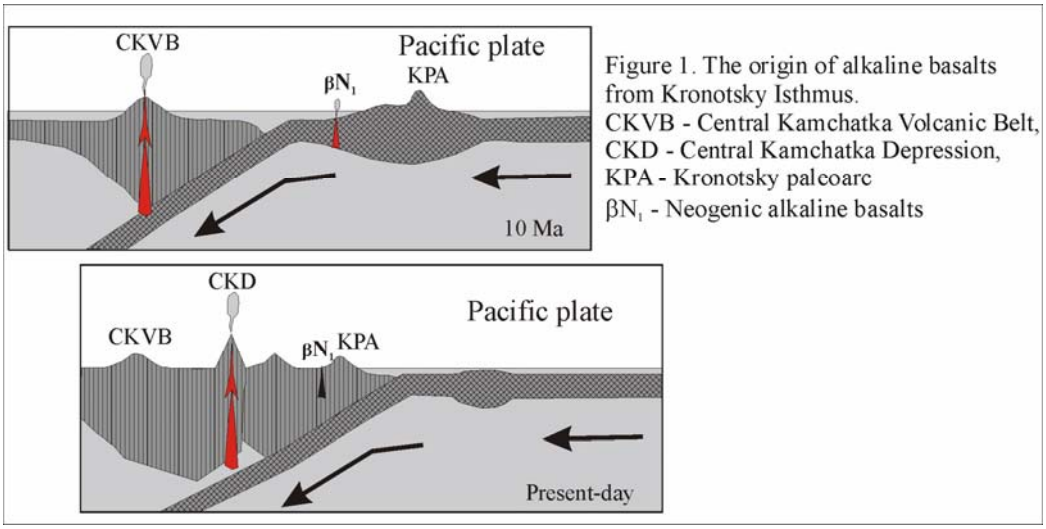


Figure 1. The origin of alkaline basalts from Kronotsky Isthmus.
CKVB - Central Kamchatka Volcanic Belt,
CKD - Central Kamchatka Depression,
KPA - Kronotsky palcoarc
βN_1 - Neogenic alkaline basalts

Recently, N. Hirano and co-authors [3] showed, that small alkaline basaltic volcanoes can be formed on an ancient (thick enough) oceanic plate near to a subduction zone on distance more than 400 km from trench. The volcanism is thought to originate due to decompression melting in the asthenosphere in response to plate flexure as it approaches trench. Similar volcanoes could be formed on the Pacific plate offshore Kamchatka, particularly, when lithosphere of increased thickness approached the zone of flexural deformations. During the Middle Miocene, the Kronotsky paleoarc had already been inactive and moved towards Kamchatka as a part of the Pacific plate [5]. When the arc terranes approached subduction zone, the plate of an increased thickness (Kronotsky paleoarc) experienced deformations at the base of the lithosphere, which could result in small degree decompression melting (according to N.Hirano's model [3]). An alkaline magmatism of small volume could also occur in such conditions 10-15 million years ago to the west of the Kronotsky paleoarc (on its submarine slope). Small submarine volcanoes and sills have been formed in association with terrigenous deposits in conditions of terrigenous sedimentation in the Tyushevka basin between Kamchatka and the Kronotsky paleoarc. When the Kronotsky paleoarc collided with Kamchatka, an eastward jump of the subduction zone to its present position took place [1].

According to our model, alkaline basalts of the Kronotsky Isthmus are not genetically related to the modern subduction zone. They were more likely formed on the Pacific plate before the Kronotsky paleoarc joined Kamchatka. Such type of volcanism can be named “precollisional” for Kamchatka. The proposed model explains the presence of alkaline basalts of intraplate geochemical type between the Kronotsky paleoarc and the front of the Eastern Kamchatka Volcanic Belt.

This work was supported by RFBR grant No. 10-05-00065a.

[1] Avdeiko G. P., Popruzhenko S. V., and Palueva A. A. (2002) *Geotectonics,* V. 36, No. 4, P. 312-327.

[2] Bakhteev M.K., Tikhomirova S.R., and Sverdlov V.S. (1995) *Otechestvennaya Geol*., 1995, No. 4, P. 37-45.

[3] Hirano N., Takahashi E., Yamamoto J. et al. Volcanism (2006) *Science*, V. 313, P. 1426-1428.

[4] Hoernle K., Portnyagin M.V., Hauff F. et al. (2009) *Goldschmidt Conference Abstracts*, A538.

[5] Lander A. V. and Shapiro M.N. (2007). *American Geophysical Union, Geophysical Monograph* 172, P. 57-64.

[6] Suprunenko O.I. and Markovskiy B.A. (1973) *Transactions (Doklady) of the Academy of Sciences USSR*, V. 211, No. 3, P. 682-685.

[7] Tikhomirova S.R. (1994*) Transactions (Doklady) of the Russian Academy of Sciences*, V. 335, No. 5, P. 626-629.

[8] Volynets O.N., Karpenko S.F., Kay R.W., Gorring M. (1997) *Geochemistry International*, V. 35, P. 884-896.

ГЕНЕЗИС МИОЦЕНОВЫХ ЩЕЛОЧНЫХ БАЗАЛЬТОВ КРОНОЦКОГО ПЕРЕШЕЙКА

Савельев Д.П., Карташева Е.В., Савельева О.Л.

Институт вулканологии и сейсмологии ДВО РАН, Петропавловск-Камчатский

E-mail savelyev@kscnet.ru

Происхождение неогеновых щелочных пород «внутриплитного» геохимического типа - один из спорных вопросов геологического строения Камчатки. Их формирование предшествовало плиоцен-четвертичному этапу восточнокамчатского вулканизма. Щелочнй вулканизм Восточной Камчатки тесно связан с миоценовыми терригенными толщами Тюшевского прогиба – щапинской свитой в бассейне р. Левой Жупановой [3] и на Кроноцком перешейке [4, 5]. «Внутриплитные» характеристики этих пород различные авторы связывают с глубокими расколами в континентальной плите, возникшими в связи с коллизией (в результате причленения Кроноцкого террейна) [3], или приуроченностью их к поперечным субширотным зонам сбросо-сдвигов, протягивающихся из Тихоокеанской плиты в пределы Курило-Камчатской островной дуги [2]. Уникальные для Восточной Камчатки изотопные и геохимические характеристики данных пород некоторые авторы объясняют поступлением обогащенной мантии из-под гайота Мейджи через slab window при заложении современной зоны субдукции [7].

Авторами получены новые данные по щелочным базальтам из керна Конусной скважины, пробуренной в бассейне р. Тюшевки в пределах Кроноцкого перешейка (понижения, выполненного преимущественно терригенными толщами, между Кроноцким п-овом и хребтом Гамчен).

Породы залегают в виде двух силлов среди туфотерригенных пород среднемиоценового возраста [4], их петрохимические особенности были изучены ранее О.И. Супруненко и Б.А. Марковским [4]. Данные рентгенофлуоресцентного анализа (аналитический центр ИВиС ДВО РАН) подтвердили высококалиевый характер пород, высокие содержания в них титана и фосфора (TiO_2=2,2-3,1%, K_2O=1,6-6%, P_2O_5=0,9-1%). По геохимическим характеристикам (содержание Nb 67-92 г/т, Zr – 413-567 г/т, отношение Zr/Y=15-19) породы сходны с щелочными габброидами и трахидолеритами бассейна р. Мал. Чажмы [5], но отличаются большей «внутриплитной» спецификой – большей калиевой щелочностью, более высокими содержаниями ниобия и циркония. Другим аналогом изученных пород являются миоценовые щелочные базальты правых притоков р. Левой Жупановой [3].

В представленном докладе предлагается модель, согласно которой миоценовые щелочные базальты Кроноцкого перешейка сформировались на западном склоне Кроноцкой палеодуги перед ее причленением к Камчатке.

Недавно Н. Хирано с соавторами [6] показал, что вблизи зоны субдукции на расстоянии более 400 км от нее на древней (достаточно мощной) океанической плите могут формироваться небольшие щелочнобазальтовые вулканы. Они образуются за счет декомпрессионного плавления в астеносфере в зоне изгиба плиты при приближении к желобу. Подобные вулканы могли формироваться на Тихоокеанской плите, движущейся к Камчатке, в те моменты, когда к зоне деформаций подходили участки с увеличенной мощностью. В среднем миоцене Кроноцкая палеодуга была уже неактивной и в составе Тихоокеанской плиты двигалась в сторону Камчатки [8]. При приближении к зоне субдукции плита испытывала деформации, и из-за увеличенной мощности (за счет Кроноцкой палеодуги) в нижней части плиты возникли расколы, что могло привести к декомпрессионному плавлению (согласно модели Н. Хирано [6]). Именно в такой

обстановке 10-15 млн. лет назад и мог проявиться щелочной магматизм небольшого объема западнее Кроноцкой палеодуги (на ее подводном склоне). Небольшие подводные вулканы и силлы образовались среди терригенных осадков в условиях терригенного осадконакопления (в Тюшевском бассейне между Камчаткой и Кроноцкой палеодугой). Затем Кроноцкая палеодуга была причленена к Камчатке, и произошел перескок зоны субдукции на восток в современное положение [1]. Т.е., в соответствии с моделью авторов данного доклада, щелочные базальты Кроноцкого перешейка не связаны с современной зоной субдукции, а сформировались на Тихоокеанской плите до причленения Кроноцкой палеодуги к Камчатке. Для Камчатки такой тип вулканизма можно назвать предколлизионным. Данная модель объясняет наличие щелочных базальтов внутриплитного геохимического типа между образованиями Кроноцкой палеодуги и фронтом Восточно-Камчатского вулканического пояса.

Работа выполнена при поддержке гранта РФФИ № 10-05-00065а.

Литература

1. Авдейко Г.П., Попруженко С.В., Палуева А.А. Тектоническое развитие и вулкано-тектоническое районирование Курило-Камчатской островодужной системы // Геотектоника, 2002, № 4, С. 64-80.

2. Бахтеев М.К., Тихомирова С.Р., Свердлов В.С. Геолого-структурная позиция позднемиоцен-плиоценового щелочного магматизма Восточной Камчатки // Отечественная геология. 1995. № 4. С. 37-44.

3. Волынец О.Н., Карпенко С.Ф., Лэй Р.У., Горринг М. Изотопный состав поздненеогеновых K-Na-Щелочных базальтоидов Восточной Камчатки: отражение гетерогенности мантийного источника магм // Геохимия. 1997. № 10. С. 1005-1018.

4. Супруненко О.И., Марковский Б.А. Щелочные вулканиты полуострова Кроноцкого (Камчатка) // ДАН СССР, 1973, Т. 211, № 3, С. 682-685.

5. Тихомирова С.Р. Позднекайнозойские тешениты Восточной Камчатки // Докл. АН, 1994, Т. 335, № 5, С. 626-629.

6. Hirano N., Takahashi E., Yamamoto J. et al. Volcanism in Response to Plate Flexure // Science, 2006, V. 313, pp. 1426-1428.

7. Hoernle K., Portnyagin M.V., Hauff F. et al. The origin EM1 of alkaline magmas during Cenozoic reorganization of subduction zone of Kamchatka // Geochim. Cosmochim. Acta. 2009. V. 73. № 13S. P. A538

8. Lander A. V. and Shapiro M.N. The Origig of the Modern Kamchatka Subduction Zone // Volcanism and Subduction: The Kamchatka Region (J. Eichelberger, E. Gordeev, P. Izbekov, J. Lees editors). Geophysical Monograph 172. American Geophysical Union, Washington, DC, 2007. P. 57-64.

VOLCANIC ASH LAYERS IN THE OKHOTSK SEA HOLOCENE-PLEISTOCENE DEPOSITS

Derkachev A.N.[1], Nikolaeva N.A.[1], Gorbarenko S.A.[1], Portnyagin M.V.[4], Ponomareva V.V.[2], Sakhno V.G.[3], Nürnberg D.[4], Sakamoto T.[5], Iijima K.[5], Lv Hua Hua[6], Wang Kunshan[6], Chen Zhihua[6]

[1] V.I. Il'ichev Pacific Oceanological Institute, FEB RAS, 43 Baltiyskaya Str., Vladivostok 690041, Russia. E-mail: derkachev@poi.dvo.ru
[2] Institute of Volcanology and Seismology, FEB RAS, 9 Piip Boulevard, Petropavlovsk-Kamchatsky, 683006, Russia
[3] Far Eastern Geological Institute, FEB RAS, 159 Pr-t 100-letiya Vladivostoka, Vladivostok, 690022
[4] IFM-GEOMAR, Leibniz Institute of Marine Sciences, Wischhofstrasse, 24148 Kiel, Germany
[5] Institute of Biogeosciences JAMSTEC, Japan Agency for Marine-Earth Science and Technology, 2-15 Natsushima-cho, Yokosuka 237-0061, Japan
[6] The First Institute of Oceanography, SOA, 6 Xianxialing Road, Qingdao 266061, P.R.China

Volcanic ash layers (tephra) are reliable indicators of the large explosive volcanic eruptions within transitional zone from continent to ocean. They occur in terrestrial outcrops as well as in sedimentary cover of the adjacent marine basins. At present such layers have estimated in many dating records of the marine and terrestrial Holocene-Pleistocene deposits within the north-eastern sector of transitional zone from the Asian continent to the Pacific Ocean. They are studied in detail within the Japan Islands, adjacent areas of the Japan Sea and the Pacific Ocean as well as on the Kamchatka Peninsula. The Okhotsk Sea Quaternary deposits remained insufficiently studied until recently.

Some multidisciplinary marine expeditions were carried out by the Russian, German, and Japanese scientists in the Okhotsk Sea during the last 15 years. Volcanic ash layers were estimated in more than 40 sediment cores. On the basis of their complex investigations (including morphology of glass shards, chemical composition of shards and minerals, study of rare earth elements, determination of refractive indices for the shards, mineralogy etc.), 20 ash layers of different composition and age were identified (KO, TR(Zv), K2, K3, K4, K5, K6, Mr1, Mr2(AL7.2a), Kc2-3, AL7.2b, AL7.4, Mr3(AL9.22), Mr4(AL9.24), AL10, T, Aso4, Md1, Md2, Md3). Results on generalization of data (both published and own researches of authors) on composition of ash from the Okhotsk Sea are quoted in the given study.

Figure 1 shows the characteristic features of chemical composition for the shards from the Okhotsk Sea ash layers (on the basis of 1300 chemical analyses). The received results have allowed add essentially the data on composition of shards from the Okhotsk Sea region, to estimate their age, to identify some of them with known ash falls of an adjoining land. Ash layers (KO, TR(Zv), K2, Aso4, Kc2-3) for which sources of a pyroclastic material are established, were most confidently identified. These sources are volcanoes of Kurile Lake (Kamchatka), Zavaritsky (Simushir Island), Nemo III (Onekotan Island), Aso (Kyushu Island), Kutcharo (Hokkaido Island) accordingly. The assumption about influence of the Sredinny Ridge (Kamchatka) volcanic explosions on the formation of AL7.4, AL7.2b, Md2 ash layers is made. Ash fall areas of some large explosive volcanic eruptions from Kamchatka and Kurile Islands are specified and established. As an example, scheme of layer K2 distribution is constructed (Fig. 2), and the volume of explosive material (nearby 9 km^3) from Nemo III eruption is estimated on the basis of it.

This work was conducted under financial support of the Russian-German KOMEX and KALMAR Projects, Russian-Japanese (№ 06-05-91576 JP, JSPS) and Russian-Chinese (№ 40710069004, № 41076038 NNSF of China, SOA) grants as well as grants of Russian Fund of Fundamental Investigations (№ 10-05-00160a and № 11-05-00506a).

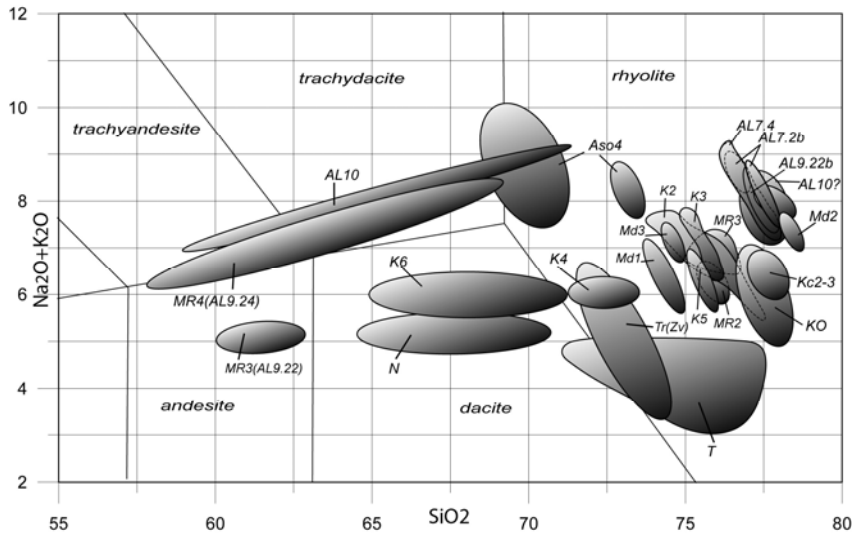


Fig. 1. Discriminant diagram (SiO_2–Na_2O+K_2O) of chemical composition for the glass shards from the Okhotsk Sea ash layers.

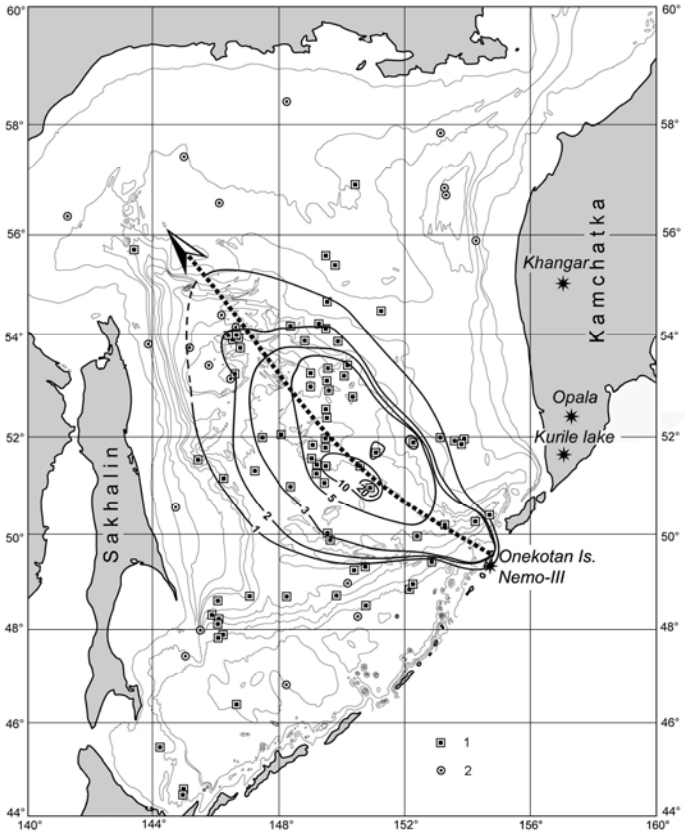


Fig. 2. Scheme of distribution and thickness (cm) of the K2 ash layer in the Okhotsk Sea deposits

1 – sediment cores recovered ash layers of different age, 2 - sediment cores without ash layers.

ПРОСЛОИ ВУЛКАНИЧЕСКИХ ПЕПЛОВ В ГОЛОЦЕН-ПЛЕЙСТОЦЕНОВЫХ ОТЛОЖЕНИЯХ ОХОТСКОГО МОРЯ

Деркачев А.Н.[1], Николаева Н.А.[1], Горбаренко С.А.[1], Портнягин М.В.[4], Пономарева В.В.[2], Сахно В.Г.[3], Нюрнберг Д.[4], Сакамото Т.[5], Ииджима К.[5], Лив Хуахуа [6], Вонг Куншан [6], Чен Жихуа [6]

[1] ТОИ ДВО РАН, Тихоокеанский океанологический институт им. В.И. Ильичева ДВО РАН,
Владивосток, ул. Радио, 43, 690041, Россия. E-mail: derkachev@poi.dvo.ru
[2] ИВиС ДВО РАН, Институт вулканологии и сейсмологии ДВО РАН, Петропавловск-Камчатский,
бульвар Пийпа, 9, 683006, Россия
[3] ДВГИ ДВО РАН, Дальневосточный геологический институт ДВО РАН, пр. 100-лет Владивостоку,
159, 690022, Россия
[4] IFM-GEOMAR, Leibniz Institute of Marine Sciences, Wischhofstrasse, 24148 Kiel, Germany
[5] Biogeos, JAMSTEC , Institute of Biogeosciences, Japan Agency for Marine-Earth Science and Technology, 2-15 Natsushima-cho, Yokosuka 237-0061, Japan
[6] the First Institute of Oceanography, SOA, Xian-Xia-Ling Road, 6, Qingdao, 266061, China

Одним из надежных индикаторов проявления крупных эксплозивных извержений вулканов в пределах зоны перехода континент-океан являются прослои вулканического пепла (тефры), встречаемые как в отложениях суши, так и в осадочном чехле прилегающих морских бассейнов. В настоящее время прослои тефры установлены во многих датированных записях морских и континентальных отложений позднего плейстоцена - голоцена в пределах северо-западного сектора зоны перехода от Азиатского континента к Тихому океану. Достаточно детально они изучены в пределах Японских островов и прилегающих районах Японского моря и Тихого океана, а также на полуострове Камчатка. Четвертичные отложения Охотского моря в этом отношении до последнего времени оставались слабо изученными.

За последние пятнадцать лет в ходе проведения нескольких комплексных экспедиций российскими, немецкими, японскими учеными в Охотском море прослои тефры были выявлены в более чем 40 колонках. На основе комплексных исследований пеплов (морфологии частиц, химического состава вулканических стекол и минералов, изучения редкоземельных элементов, определения показателя преломления вулканических стекол, минералогии и др.) было выделено 20 прослоев тефры разного состава и возраста (КО, TR(Zv), K2, K3, K4, K5, K6, Mr1, Mr2(AL7.2a), Kc2-3, AL7.2b, AL7.4, Mr3(AL9.22), Mr4(AL9.24), AL10, T, Aso4, Md1, Md2, Md3). В данном сообщении приводятся результаты обобщения сведений (как опубликованных, так и собственных исследований авторов) по составу тефры Охотского моря. На рис. 1 показаны характерные признаки химического состава (на основе 1300 химических анализов) вулканических стекол из прослоев тефры Охотского моря. Полученные результаты позволили существенно дополнить данные по составу тефры Охотоморского региона, определить их возраст, провести для некоторых из них идентификацию с известными пеплопадами прилегающей суши. Наиболее уверенно идентифицируются прослои пепла (КО, TR(Zv), K2, Aso4, Kc2-3), для которых установлены источники пирокластического материала, которыми являются соответственно вулканы Курильского озера (Камчатка), Заварицкого (о. Симушир), Немо III (о. Онекотан), Aco (о. Кюсю), Кутчаро (о. Хоккайдо). Сделано предположение о влиянии эксплозий вулканов Срединного хребта Камчатки на формирование прослоев тефры AL7.4, AL7.2b, Md2. Уточнены и установлены ареалы пеплопадов ряда крупных эксплозивных извержений

вулканов Камчатки и Курильских островов. Для примера на рис. 2 приведена схема распределения тефры К2, на основании чего проведена оценка объема (около 9 км^3) эксплозивного материала извержения вулкана Немо-III.

Работа выполнена при финансовой поддержке российско-германских проектов KOMEX и KALMAR, российско-японского (грант № 06-05-91576 JP, JSPS и РФФИ) и российско-китайского грантов (грант № 40710069004, № 41076038 NNSF of China, SOA), а также грантов РФФИ (№ 10-05-00160а и № 11-05-00506а).

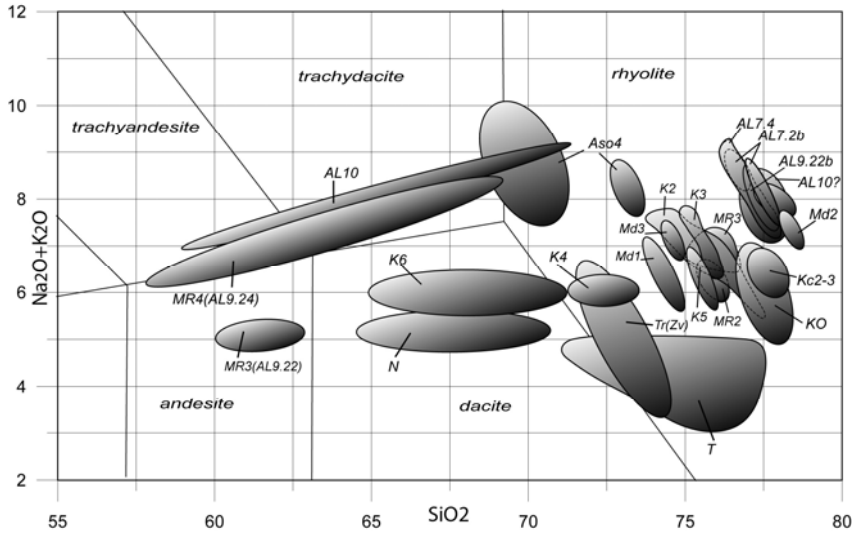


Рис.1. Дискриминантная диаграмма SiO_2 – Na_2O+K_2O химического состава вулканических стекол прослоев тефры Охотского моря

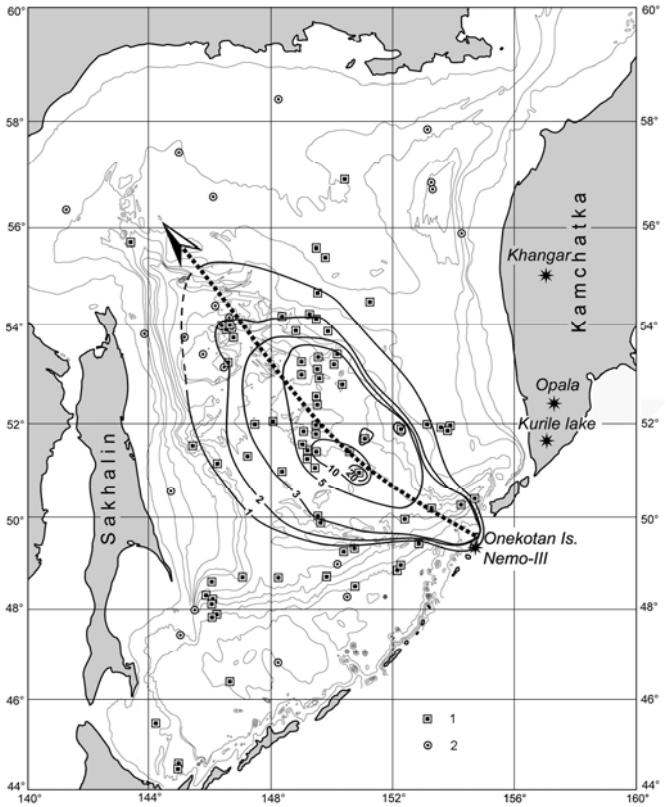


Рис. 2. Схема распределения и мощность (в см) прослоя тефры К2 в отложениях Охотского моря
1 – колонки, в которых обнаружены прослои тефры разного возраста. 2 – колонки без прослоев тефры.

Physical and chemical properties of volcanic ashes of different ages (Kamchatka)

Kuznetsova E.[1], Muravyev Ya.[2], Motenko R.[1]

[1]Geological faculty, Lomonosov Moscow State University, Moscow, geotap@gmail.com
[2]Institute of Volcanology and Seismology FEB RAS, Petropavlovsk-Kamchatsky,

Soil-pyroclastic cover that spreads on the most part of the territory of Kamchatka Peninsula consists of tephra horizonts and buried soils. Ashes of the greatest eruptions form clear marker layer that can be observed within large areas. The strata between ash marker layers are also generated from pyroclastic materials and include both the products from less great or remote eruptions and secondary redeposited ashes [1]. This paper presents the results of the study of physical and chemical properties of volcanic ashes, which are both markers and unidentified tephra.
The following methods were applied within our research:

- granulometric composition was carried out using the pipette method [2];
- mineral composition of ashes was determined using infrared absorption spectroscopy with FSM-1201 IR-spectrometer (LOMO, Russia) over the range from 400 to 4000 cm^{-1} at room temperature [11];
- chemical analysis of volcanic glasses was carried out with Jeol JSM-6480LV microprobe complex (All laboratory analyses were carried out by V.O. Yapaskurt and E.V. Guseva, faculty of Geology, Moscow State University);
- phase composition of moisture and freezing temperature were determined by contact and cryoscopic methods combination [4];
- thermal conductivity was determined using I type regular method (α-calorimeter) [4].

The analyzed ash samples were collected in the Kluchevskaya volcano group and in Kamchatka river valley, the sampling places are situated at the attitudes from 190 to 1630 m a.s.l. Most of the ashes are Holocene, except the sample collected from lake diatom clay sediments of steep bank “Polovinka” whose age is determined as second half of early Pleistocene (Q^2_1). The sample is a white vitroclastic ash with acid composition.

Volcanic ashes are referred to very fine sands by granulometric composition [3]. According to silicon dioxide the volcanic glass of our samples belongs to three types: andesite, basaltic and rhyolite. IR-spectra data indicates that in Kamchatka amorphous allophane is associated with andesitic and basaltic glass whereas opal with rhyolitic glass (allophane is hydrous aluminium silicate clay mineral, opal is hydrated silicon dioxide) [10].

The following experimental results were obtained.

Phase composition of water. For the first time there were obtained the experimental data concerning phase composition of water (the content of ice, unfrozen water and steam) in frozen volcanic ashes [5]. The main characteristic of phase composition of water is the dependence of unfrozen water content on temperature which was carried out for the range of temperature from 0 to -15°C; the changes in unfrozen water content at the temperature below -3°C are insignificant. It was established that unfrozen water content in the frozen volcanic ashes is changed from 0 to 11% under the temperature of thermal conductivity determination (-10 °C). The presence of unfrozen water content is presumably connected with volcanic glass transformation and clay minerals (allophane etc) occurrence that have large surface area [6, 9].

Thermal conductivity. The thermal conductivities of volcanic ashes for thawed and frozen states were obtained in the wide range of humidity and density. While density (ρ_d) and humidity (W) are changing from 0.7 to 1.65 g/sm^3 and from 10 to 80 % respectively the thermal conductivity (λ) increases from 0.37 to 1.0 W/(m·K) in a thawed state and from 0.41 to 1.27 W/(m·K) in a frozen state [7, 8]. In spite of the fact that volcanic ashes are very close to sedimentary fine sands, they have completely different thermal properties. The thermal conductivity for sedimentary rocks is higher than for volcanic deposits in both frozen and thawed states. This discrepancy might be explained by different reasons, for example, distinctions between thermal

conductivities of mineral skeleton (thermal conductivity of quartz and amorphous glass are distinguished in 3-4 times) or the particle shapes. The ash particles have compound and polyhedral shape. Most of particles, especially volcanic glasses are defined as fragments of complex overlapping of gas bubbles. That's why the conductivity process becomes more complicated in volcanic deposits.

Salinity. The analysis of salinity showed that according to GOST 25100-95 [3] all investigated ashes, excepting the sample from steep bank "Polovinka", are unsalted, their the total soluble salt content is about 0.02-0.03%. The ash sample from steep bank is highly salted. The chemical analysis of aqueous extract shows that the amount of salt is 1.815% by substance weight and the main component of chemical composition is sulfate (SO_4^{2-} content is 1.242% by substance weight). Also very low pH = 3.4 was observed.

1. Bazanova L.I., Brayceva L.I., Diksen O.V., Sulzhenicky L.D., Danhara T. Ash falls of the largest Holocene eruptions on the traverse of Ust-Bolsheretsk - Petropavlovsk-Kamchatsky: sources, chronology, frequency // Volcanology and seismology. 2005. № 6. P. 30-46.
2. GOST (State Standard) 12536-79: Soils. Methods of Laboratory Determination of Granulometric and Microaggregate Distribution, 1979.
3. GOST (State Standard) 25100-95: Soils. Classification, 1996.
4. Methods of geocryological studies, edited by E.D. Ershov. Mosk. Gos. Univ., 2004. 512 p.
5. Kuznetsova E.P., Motenko R.G., Vigasina L.V., Melchakova L.V. The Study of Unfrozen Water in Volcanic Ashes (Kamchatka) // Moscow University Geology Bulletin, 2011, Vol. 66, No. 1, pp. 65–71.
6. Kuznetsova E.P., Motenko R.G., Vigasina L.V., Melchakova L.V Connection between mineral composition and volcanic glass alteration // First Russian meeting "Clays-2011", 2011, pp.75-76.
7. Kuznetsova E., Motenko R. Thermal properties of volcanic ashes (Kamchatka) // 4th conference of geocryologists of Russia, vol. 1, pp. 91-97.
8. Motenko R.G., Kuznetsova E.P. The role of ice and unfrozen water content on estimation of thermal conductivity of frozen volcanic ashes (Kamchatka) // Ice and snow. No. 2, 2011, pp. 99-103.
9. Motenko R.G., Kuznetsova E.P., Vigasina L.V., Melchakova L.V. The influence of allophane and palagonite appearance on the unfrozen water content in the frozen volcanic ashes // ACTA Mineralogica-Petrographica, abstract series, IMA2010 and MECC2010 conferences, volume 6 (edited by L. Zaharia, A. Kis, B. Topa, C. Papp, T. G. Weiszburg). Budapest, Hungary, 2010, p. 625.
10. Peng Wenshi, *IR Spectra of Minerals,* Beijing, Science, 1982.
11. Plyusnina, I.I. Infrared Spectra of Minerals, Moscow: Mosk. Gos. Univ.,1977.

GEOCHEMICAL CHARACTERISTICS OF YOTEI VOLCANO AND SHIRIBETSU VOLCANO, SOUTHWESTERN HOKKAIDO, JAPAN

Akane Umetsu[1], Mitsuhiro Nakagawa[1] and Shimpei Uesawa [1]

[1]Department of Natural History Sci., Graduate School of Sci., Hokkaido University.

Yotei Volcano locates at the arc-arc junction of Kuril and Northeast Japan arcs (Fig. 1) and shows local anomaly in regional spatial compositional variations of volcanic rocks from Hokkaido and NE Japan volcanoes (Nakagawa, 1992). However, there has existed no systematic petrological geochemical study of the volcano. Recently, the structure of Yotei Volcano has been revealed (Uesawa et al., in prep.). Based on the stratigraphic relations, we carry out petrological and geochemical study of Yotai and adjacent volcanoes, Shiribetsu (Sh) and Kimobetsu pfl (K-pfl) (Fig. 1). The activity of Yotei volcano can be divided into two major stages, Old (Y-1) and Young Yotei (Y-2). The latter stage can also be divided into two sub-stages, early (Y-2-1) and late (Y-2-2). In this study, we show analytical data of major and trace elements, REE, and Sr-Nd isotopes to reveal the temporal and spatial change of magma and the plumbing systems beneath the volcanic field.

The rocks of Yotei and Shiribetsu volcanoes are andesite and dacite and their whole-rock SiO_2 contents are 55 - 70 wt% in Y-1, 55 - 68 in Y-2-1, 55 - 65 in Y-2-2, 59 – 66 in Sh, and 65 – 69 in K-pfl, respectively. These are classified as medium-K series on the K_2O-SiO_2 diagram. Phenocryst contents and assemblages of these rocks from Sh, K-pfl and Y-1 are similar and are distinct from those of Y-2-1 and Y-2-2. The rocks of Y-2-1 and Y-2-2 are nearly aphyric (<15 vol.%) and contain plagioclase, orthopyroxene,clinopyroxene and Fe-Ti oxides phenocryst often associated with olivine. On the other hand, the rocks of Y-1, Sh and K-pfl are porphyritic (6 – 47 %) and are characterized by the presence of hornblende and quartz phenocrysts, in addition to plagioclase, pyroxenes and Fe-Ti oxides phenocrysts. Olivine phenocrysts are often recognized in some rocks of Y-1. On the basis of the FeO/MgO-SiO_2 diagram, the rocks of Y-2-1 and Y-2-2 are classified into tholeiitic series, whereas those of Y-1, Sh and K-pfl show variations of calk-alkaline series.

Whole-rock chemistry of the rocks from two adjacent volcanoes, Yotei (Y-1 and Y-2) and Shiribetsu (Sh and K-pfl), are distinct on many SiO_2 variation diagrams (Fig. 3). On the SiO_2 –Rb, Ba, Nb, Pb, Zr and Y diagrams, although mafic rocks of the both volcanoes have similar contents, the silicic rocks are distinct on these diagrams. In contrast, although MgO contents of the silicic rocks of both volcanoes are similar, those of the mafic rocks are largely different. P_2O_5 contents of the rocks of Sh and K-pfl decrease simply with increasing of SiO_2 content, whereas the rocks of Yotei volcano have maximum P_2O_5 contents in silicic andesite (SiO_2~62 %). Comparing with the rocks of each stage of Yotei volcano, it seems that systematic, temporal changes of whole-rock chemistry are recognized. Rb, Ba, Nb, Zr, Y and Na_2O contents of the rocks increase from Y-1 to Y-2-1. The rocks of Yotei volcano show systematic, temporal increase of contents of incompatible elements, such as Zr and Ba, from Y-1 to Y-2-1 (Fig. 3). These chemical differences among geological stage suggest that magma generation and/or magma

differentiation processes have changed temporally in the volcanic field. Now, we are analyzing REE and Sr-Nd isotopes of the representative rocks from the volcanoes to discuss temporal and spatial evolution of magma source region and structures of magma plumbing systems.

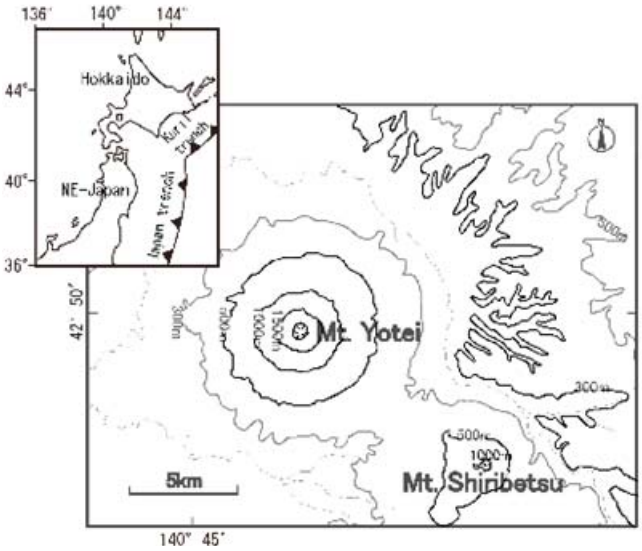


Fig. 1 Locality of Mt. Yotei volcano and Shiribetsu volcano.

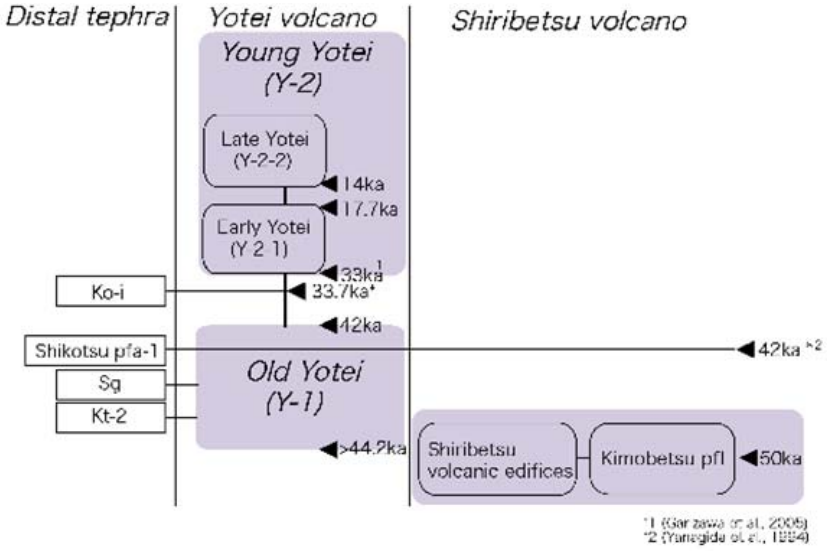


Fig. 2 Block diagram showing the relationships between Yotei and Shiribetsu volcano and four distal tephras.

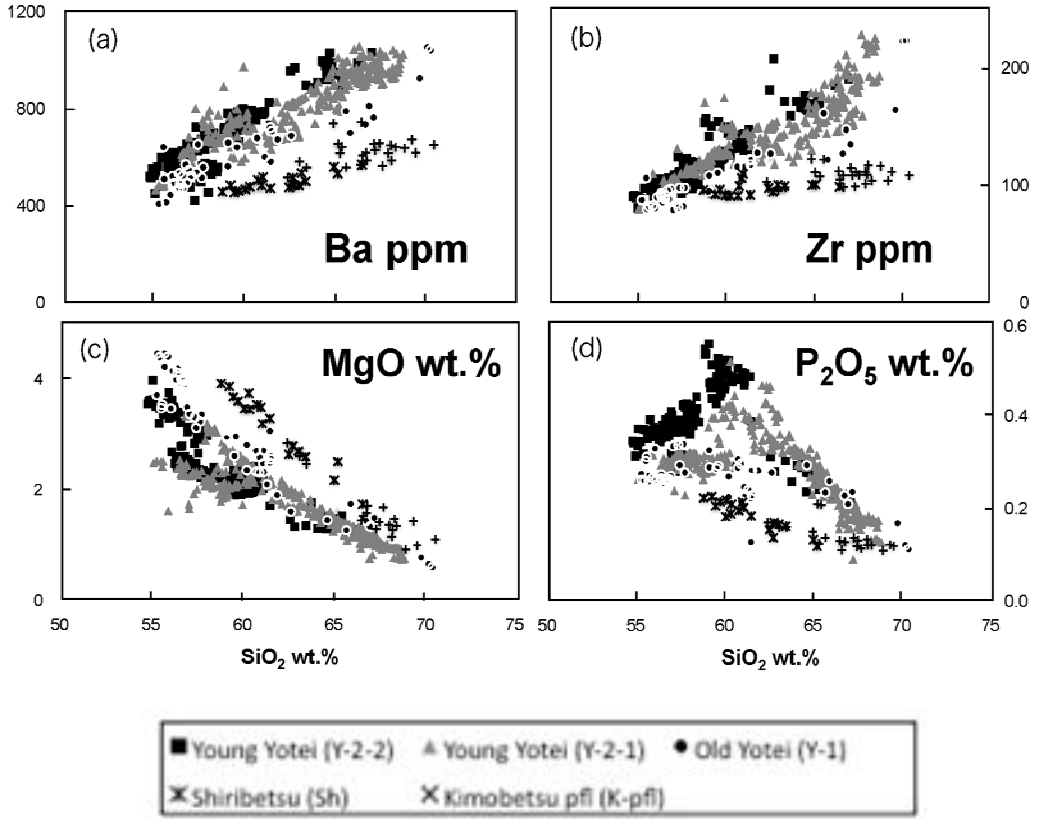


Fig. 3 (a, b, d) incompatible elements and (c) major of whole rock chemistry, respectively.

Petrochemical characteristics of volcanic rocks of Anaun area

Rodin Vladimir (GIN RAS, Geological faculty of MSU; rodinwork@gmail.com)

The Anaun area is located in the central part of the Middle Ridge to the north of Anavgai. It is a gentle-hill volcanic plateau in which 14 volcanoes and about 100 of monogenetic cones are located [1]. The largest volcanic building is stratovolcano Anaun. The other volcanoes belong to a shield type.

During field research in southern part of Anaun area in 2010 were sampled Anaun, Buduli and Geodesistov and some others volcanoes and several monogenetic cones.

The researched rocks of volcanoes are porphyritic and have high degree of cristallization. The most spread mineral is plagioclase, also include piroxene and olivine. The monogenetic cones are characterized by porfiritic and subafiric structure. Among the phenocristes mafic minerals (piroxene and olivine) play the mane role, there may be no plagioclase at all.

All the researched rocks are represented by basaltes and andesibasaltes of calc-alkaline series. The most basic rocks are the rocks of the Encavtenup cone and from the right bank of Balygingan river (48-48,5 % SiO2 (weight percentes are used in the whole text)). They differ from the other rocks of the Anaun area by a higher contents of K_2O (2,1-2,5 vs. 0,8-1,5%) and Rb (34-38 vs.10-18 ppm). This rocks differ from each other by contents of MgO and Cr. The rocks of monogenetic cone are enriched by these components (11 % and 517 ppm).

Anaun area's andesibasaltes are the products of volcanoes and monogenetic cones. These rocks have quite similar compositions (52-56 % SiO_2, 3-6 % MgO, 2,8-3,7 % Na2O). The concentrations of main petrogenic oxides of the rocks don't show no significant variations. Microelement compositions of the rocks vary over a wider range.

The rocks of Anaun stratovolcano are characterized by high contents of Sr (about 900 ppm). Monogenetic cones are characterized by low content of this element (500-600 ppm). Products of some of the cones are enriched by Zr and Y, which agrees well with the concept of Late Quaternary areal volcanism of Middle Ridge of Kamchatka[2].

At the initial stage of its activity Anaun represented the shield volcano, which currently is the basis of a later stratovolcano. In this case, the composition of lavas of the volcano has not changed significantly – the melt has become slightly more silicic (from 52 to 55% SiO_2). But the degree of crystallization increases significantly.

This can be attributed with a long stop of magma in the intermediate chamber, during which the melt temperature decreased. At this time, substantially increased the number of phenocrysts. This led to an increase in the viscosity of the lava and forming of stratovolcano.

This study was financially supported by program 4 of the Presidium of RAS, Program 8 Department of Earth Sciences, and RFFI (project no. 10-05-01122).

References

1. *Ogorodov N., Kozhemyaka N., Vazheevskaya A., Ogorodova A.* Volcanoes and Quaternary Volcanism of the Middle Ridge of Kamchatka. - Part 2. Catalog Middle Ridge volcanoes. - Moscow: Nauka, 1972. - 192.

2. Volynets A., Churikova T., Woerner G., Gordeychik B., Layer P. Mafic Late Miocene - Quaternary volcanic rocks in the Kamchatka back arc region: implications for subduction geometry and slab history at the Pacific-Aleutian junction // Contributions to Mineralogy and Petrology. 2010. V. 159. Issue 5. P. 659-687.

Петрохимические характеристики пород Анаунского дола

Родин В.С. (ГИН РАН, Геологический ф-т МГУ; rodinwork@gmail.com)

Анаунский дол расположен в центральной части Срединного хребта к северу от пос. Анавгай. Это пологохолмистое вулканическое нагорье, на территории которого расположены 14 вулканов и около 100 моногенных конусов [1]. Наиболее крупной вулканической постройкой дола является стратовулкан Анаун, остальные вулканы принадлежат к щитовому типу.

В ходе полевых работ в южной части Анаунского дола в 2010 г. были опробованы вулканы Анаун, Будули и Геодезистов, несколько моногенных конусов, а также породы, принадлежащие, скорее всего, морфологически не выраженным в настоящее время вулканам.

Породы вулканов характеризуются порфировой структурой и высокой степенью раскристаллизованности, среди вкрапленников наиболее распространен плагиоклаз, также присутствует клинопироксен и оливин (редко). Для пород моногенных конусов характерны порфировая или субафировая структуры, среди вкрапленников ведущее положение занимают цветные минералы (оливин и пироксен), плагиоклаз может совсем отсутствовать.

Все изученные породы представлены базальтами и андезибазальтами нормального щелочного ряда известково-щелочной серии. Наиболее основными являются породы конуса Енкавтенуп и вулканиты, отобранные в обрыве правого берега р. Балыгинган (48-48,5 % SiO_2 (здесь и далее все проценты весовые)). Они же отличаются от прочих пород Анаунского дола повышенными содержаниями K_2O (2,1-2,5 против 0,8-1,5 %) и Rb (34-38 против 10-18 ppm). Между собой эти породы разделяются по MgO и Cr – породы моногенного конуса значительно обогащены и тем и другим (11 % и 517 ppm соответственно).

Андезибазальты Анаунского дола, представленные продуктами как вулканов, так и моногенных конусов, имеют довольно схожие составы (52-56 % SiO_2, 3-6 % MgO, 2,8-3,7 % Na_2O) и по петрогенным элементам практически не различаются. Некоторые особенности составов отдельных объектов заметны при рассмотрении микроэлементов. Так, породы вулкана Анаун отличаются повышенными содержаниями Sr (около 900 ppm), а моногенных конусов – пониженными (500-600 ppm). Кроме этого, продукты некоторых конусов характеризуются обогащением по Zr и Y, что хорошо согласуется с представлениями о позднечетвертичном ареальном вулканизме Срединного хребта [2].

На начальном этапе своей деятельности Анаун представлял из себя щитовой вулкан, который в настоящее время служит основанием более позднего стратовулкана. При этом, состав лав вулкана существенным образом не изменился – произошло незначительное подкисление расплава – с 52 до 55 % SiO_2, но довольно сильно увеличилась степень раскристаллизованности пород. Это можно связать с длительным нахождением магмы в промежуточном очаге, во время которого температура расплава снижалась и происходил активный рост минералов-вкрапленников, что привело к увеличению вязкости изливающейся лавы и формированию стратовулкана.

Работа выполнена при поддержке Программы 4 Президиума РАН, Программы 8 ОНЗ РАН и гранта РФФИ 10-05-01122.

Список литературы:

1. *Огородов Н. В., Кожемяка Н. Н., Важеевская А. А., Огородова А. С.* Вулканы и четвертичный вулканизм Срединного хребта Камчатки. — Ч. 2. Каталог вулканов Срединного хребта. — М. : Наука, 1972. — 192 с.

2. *Volynets A., Churikova T., Woerner G., Gordeychik B., Layer P.* Mafic Late Miocene - Quaternary volcanic rocks in the Kamchatka back arc region: implications for subduction geometry and slab history at the Pacific-Aleutian junction // Contributions to Mineralogy and Petrology. 2010. V. 159. Issue 5. P. 659-687.

On Some Results of the Middle East and Kamchatka EQs Catalogues Analysis

Vladimir Prelov

Mechanical Engineering Research Institute of the Russian Academy of Sciences RUSSIA 101990 Moscow, M.Kharitonievskiy per.,4

The industry of IT opens a wide spectrum of new opportunities and states the set of new requirements for an efficiency at the both forecasting and risk-management problems for the fatal nature events. We discuss the problem and present some methods to estimate a set of seismic risks. By crossdisciplinary paradigm in solving a complex scientific problem, we take a chance in using of some statistical forecasting methods to detect the ongoing fatal events with EQs catalogues processing.

First, we suppose that all geoactivity signals at the stations reflect the processes of the fatal-oriented open dynamical, chaotic at both time and space, system. Then, we state that for every natural catastrophe has to have a set of precursors – by means of relationships at both space and time scales while the self-organization. The problem is, by means of that, to create the logical chain to burning and realizing of such precursors and mainshocks theirselves as well as to develop the tool to filter the false events.

It was shown that opportunities to collect the geoinfo and to analyze the datum flows let us rely on solving the problems such as crucial events forecasting, as well as the problem of short-term seismic control in a real-time mode. The problem to control the geoinformation datum streams, the reasons for so-called “system-time” to be introduced, as well as the seismic shocks forecasting opportunities by means of so-called “reversal time” tools are the subjects of our approach.

It was realized that restricted series like Kamchatka’s EQs Catalogue of about 50000 records since 01.01.1962 and, for example, Iranian EQs Catalogue of about 17000 records since 01.01.1900 provide us with some statistical results on probabilities and periods for the EQs given magnitude to be realized.

The most effective way to increase the reliability of the EQs forecasting systems is a strong collaboration between long-, medium- and short-term techniques of forecasting and, as well, an interdisciplinarity of research methods. It is extremely difficult to guess the location and magnitude of coming EQ with precursors recorded at only one seismic station, so we take a chance in using standard EQs catalogues for the whole region given to solve a problem.

We consider both general practical and theoretical results obtained with analytical processing of catalogues. For example, we found out that Entropy method could be applied to reduce a complexity of medium term EQs forecasting problem. We discuss over our recent

HYPOTHESIS

EQs forecasting uncertainty with Entropy methods is E □ 37 ,8167 %.

ACKNOWLEDGMENTS

Author thanks Dr. Nikolay Makhutov, the Correspondent Member of RAS, and Dr. Victor Chebrov, the Chief of the Kamchatka Branch of RAS Geophysical Service, for their non-stop attention, fruitful discussions and consulting on the problem and results obtained.

Basaltic activity episode at 4600-3100 ^{14}C years BP (3370-1400 calBC) at andesitic Shiveluch volcano, Kamchatka

M.M. Pevzner[1], A.D. Babansky[2]

[1]*Geological Institute RAS, Moscow, Russia*

[2]*IGEM RAS, Moscow, Russia*

Shiveluch is one of the most active volcanoes of Kamchatka. It is situated nearby the northern edge of the Pacific plate. Holocene deposits of this volcano are represented essentially by the andesitic pyroclastic rocks [*Ponomareva et al., 2007*]. Only two horizons of the basaltic pyroclastic rocks have been distinguished yet; they were formed at 7600 and 3600 ^{14}C yrs BP [*Volynets et al., 1997*].

We have found an episode in Holocene eruptive history of this volcano, which continued about 2 thousand years long. During this episode a lateral basaltic vent has been working parallel to the main crater, which erupted andesites. The products of the lateral eruption are represented by tephra: coarse sands with brittle lapilli of scoria up to 3 cm in diameter. Chemical and mineralogical composition of tephra (high-K Mg-basalts containing Ol and Phl) is similar to the previously known eruption at 3600 BP. Totally, there are 5 eruptions with the same composition of products. The eruptive center is not found; most likely it might have been situated at the near-apical part of the western sector of the volcano.

The earliest eruption of the discussed composition has happened about 4600 BP; its deposits are represented only by juvenile material. The eruption at 3600 BP has been previously described as the horizon of compact and low-porous chips. We have found that juvenile basalts are present in the top part of this horizon. Probably the cinder cone, formed during the eruption at 4600 BP, was destroyed by the explosion at 3600 BP, after which the eruption of the juvenile material started. The youngest eruption of the basalts took place 3100 BP. In the SE part of the volcano it is represented by the 4 meters-thick pyroclastic flow. Sandy joining material is rich by basaltic scoria lapilli and large lapilli of the compact andesitic pumice, which may result from the simultaneous work of the main crater and lateral vent.

The andesites of the main crater, erupted during the interval between 4500 and 3000 BP, are characterized by high Cr content (250-450 ppm; during the other intervals of the Holocene history of Shiveluch volcano activity the Cr content in andesites is not higher than 180 ppm); at the same time there are no substantial variations of K_2O content and Mg# in these rocks.

The work is supported by the financial support of Program 4 of the Presidium of RAS, Program 8 of the Departament of Earth Sciences of RAS and RFBR grants № 08-05-00092, 10-05-01122.

1. Ponomareva V.V., Kyle P.R., Pevzner M.M., Sulerzhitsky L.D., Hartman M. Holocene eruptive history of Shiveluch volcano, Kamchatka Peninsula. In: Eichelberger J., Gordeev E., Kasahara M., Izbekov P., Lees J. (Eds) "Volcanism and Tectonics of the Kamchatka Peninsula and Adjacent Arcs", Geophysical Monograph Series. 2007. V. 172. P. 263-282.

2. Volynets O.N., Ponomareva V.V., Babansky A.D. Magnesian basalts of the andesitic Shiveluch volcano, Kamcahtka // Petrology. 1997. V. 5. № 2. P. 206-221.

Эпизод 4600-3100 ^{14}C л.н. (3370-1400 гг. до н.э.) базальтовой активности на андезитовом вулкане Шивелуч, Камчатка

М.М. Певзнер[1], А.Д. Бабанский[2]

[1]*Геологический институт РАН, Москва*

[2]*ИГЕМ РАН, Москва*

Шивелуч – один из наиболее активных вулканов Камчатки – расположен вблизи северной границы Тихоокеанской плиты. Голоценовые отложения вулкана представлены преимущественно пирокластикой андезитового состава [*Ponomareva et al., 2007*]. Было известно только два горизонта пирокластики основного состава, которые образовались 7600 и 3600 ^{14}C л.н. [*Волынец и др.,* 1997].

В голоценовой эруптивной истории вулкана нами обнаружен эпизод продолжительностью около 2 тысяч лет, когда, параллельно с главным жерлом, поставлявшим андезиты, работал побочный конус основного состава. Материал извержений представлен главным образом тефрой: грубыми песками с хрупкими лапилли шлака до 3 см в поперечнике. Химический и минералогический состав тефр (высоко-К Mg-базальт, содержащий оливин и флогопит) аналогичен составу ранее известного извержения 3600 ^{14}C л.н. Всего установлено 5 извержений такого состава. Эруптивный центр не обнаружен; предположительно он может находиться в привершинной части западного склона вулкана.

Наиболее раннее извержение обсуждаемого состава произошло около 4600 ^{14}C л.н. и его отложения представлены только ювенильным материалом. Извержение 3600 ^{14}C л.н. ранее было описано как горизонт плотных и слабопористых обломков. Мы обнаружили, что в его кровле также присутствуют ювенильные базальты. Возможно, шлаковый конус, образовавшийся во время извержения 4600 ^{14}C л.н., был разрушен взрывом 3600 ^{14}C л.н., после чего началось извержение ювенильного материала. Наиболее молодое извержение базальтов произошло около 3100 ^{14}C л.н. В ЮВ секторе вулкана оно представлено пирокластическим потоком до 4 м мощностью. Песчанистый заполнитель исключительно богат как лапилли шлаков базальтового состава, так и крупными лапилли плотной пемзы андезитового состава, что, по-видимому, свидетельствует об одновременной работе главного жерла и побочного конуса.

Андезиты главного жерла, извергавшиеся в интервале 4500-3000 ^{14}C л.н., характеризуются содержанием Cr 250-450 ppm (в другие интервалы голоценовой истории Шивелуча содержание Cr в андезитах не превышает 180 ppm), при этом заметных вариаций в количестве K_2O и величине #Mg не отмечается.

Работа выполнена при финансовой поддержке Программы 4 Президиума РАН, Программы 8 ОНЗ РАН и РФФИ (№ 08-05-00092, 10-05-01122).

1. Волынец О.Н., Пономарева В.В., Бабанский А.Д. Магнезиальные базальты андезитового вулкана Шивелуч, Камчатка // Петрология. 1997. Том 5. № 2. С. 206-221.

2. Ponomareva V.V., Kyle P.R., Pevzner M.M., Sulerzhitsky L.D., Hartman M. Holocene eruptive history of Shiveluch volcano, Kamchatka Peninsula. In: Eichelberger J., Gordeev E., Kasahara M., Izbekov P., Lees J. (Eds) "Volcanism and Tectonics of the Kamchatka Peninsula and Adjacent Arcs", Geophysical Monograph Series. 2007. V. 172. P. 263-282.

GEOCHEMISTRY AND MINERALOGY OF THE LATE PLEISTOCENE OLD SHIVELUCH VOLCANO, KAMCHATKA

Natalia Gorbach[1], Maxim Portnyagin[2]

[1] Institute of Volcanology and Seismology FEB RAS, Piip Blvd. 9, Petropavlovsk-Kamchatsky, 683006, Russia; email: n_gorbach@mail.ru
[2] Leibniz Institute of Marine Sciences, IFM-GEOMAR, Wischhofstrasse 1-3, 24148, Kiel, Germany

Shiveluch is one of the largest and most active volcanic centers in Kamchatka, located at the Kurile–Kamchatka and Aleutian arc junction. This complex volcanic massif includes the Late Pleistocene partially destroyed by a sector collapse Old Shiveluch stratovolcano and Young Shiveluch eruptive center, which has been active through the Holocene (Melekestsev et al., 1991). Due to the unique geodynamic setting and the occurrence of magnesian andesites among erupted products (Volynets, 1997; Ponomareva et al., 2007), the origin and evolution of Shiveluch Volcano is of high importance for the modern models of magma generation in Kamchatka. Petrological and geochemical studies (Volynets et al., 1997; Ponomareva et al., 2007; Portnyagin et al., 2007; Gorbach Portnyagin, 2011) has mainly focused on the products of the Young Shiveluch. A few attempts only (Menyailov, 1955; Melekestsev et al., 1991; Ferlito, 2011) have been made to obtain information about the Late Pleistocene geochemical evolution of the volcano. Here we report results of a detailed field geological study of the Old Shiveluch volcanic edifice and geochemical and mineralogical investigation of the volcanic rocks .

At the base of the Old Shiveluch we mapped a thick sequence of andesitic agglomerate and psephitic tuffs related to the initial extrusive and explosive Shiveluch activity. Stratigraphically younger Old Shiveluch lava complex is related to four distinct eruptive centers, which produced mainly andesitic and basaltic andesitic lava flows and minor pyroclastics. Three main type of rock were distinguished in the Old Shiveluch volcanic edifice: volumetrically dominant magnesian andesites (SiO_2=57.3-63.8, Al_2O_3=16.5-17.6, MgO=2.8-4.8, K_2O=1.2-1.7 (wt.%), Mg#=52.5-57.0 mol. %.), high-Al basaltic andesites (SiO_2=53.5-55.7, Al_2O_3=16.6-17.5, MgO=4.4-5.9, K_2O=0.9-1.2 (wt. %), Mg#=52.1-56.1 mol%) and small volume high-Mg basaltic andesites (SiO_2=53.9-55.0, Al_2O_3=15.1-16.5, MgO=6.1-7.5, K_2O=1.2-1.3 (wt.%), Mg#=58.8-63.7 mol.%). All studied rocks belong to the medium-K calc-alkaline series and exhibit strong enrichment in incompatible elements (Cs, Rb, Ba, K, Pb, Sr, U and Th) and depletion in HREE (e.g., Portnyagin et al., 2007).

Major and trace elements concentrations in the Old Shiveluch rock series correlate well and indicate that all Old Shiveluch rocks are likely genetically related to each other. With decreasing MgO content, concentrations of incompatible lithophile elements (e.g., Ba, K, Th) increase and concentrations of compatible trace elements (e.g., Cr, Ni) decrease in the rock series. This suggests the dominant role of fractional crystallization at creating the diversity of the Old Shiveluch rocks. At given Mg#, the high-Al basaltic andesites have higher Al_2O_3 and lower SiO_2 than typical Old Shiveluch andesites. Incompatible trace element concentrations and their ratios are, however, similar in both rock types and imply the existence of a common parental melts for the Old Shiveluch. The observed diversity of the evolved rocks can be related to variable conditions of crustal evolution of mantle-derived magmas beneath Shiveluch. Similar REE patterns and incompatible trace elements ratios (e.g. Zr/Y, La/Yb, Ba/Th, Ba/La, Th/La, Th/Yb) of high-Mg and high-Al basaltic andesites also indicate their origin from a common parental melts.

Petrographic and mineralogical data for different Old Shiveluch rock types indicate long and multi-stage crystallization history of the magmas at the different crustal levels. Compositions of olivine in high-Mg basaltic andesites are bimodal with the majority of compositions falling at Fo_{90-92} and Fo_{86-88}. The composition of rare olivine in high-Al basaltic andesites is similar to phenocrysts rims (Fo_{82-84}) of high-Mg rocks. The compositions of clinopyroxene phenocrysts are very similar

(Mg# =74-88) in all rocks types. Some samples of the Old Shiveluch magnesian andesites contains Al-rich high-pressure amphiboles which coexist with Al-poor, low-pressure hornblendes in the same samples.

Both mineralogical and whole-rock geochemical data suggest that the occurrence of high-Mg and high-Al basaltic andesites in the Old Shiveluch volcano is most likely related to different pressure conditions of magma evolution rather than to different and spatially separated deep magma sources in the mantle and subducting slab, which have been proposed for Shiveluch volcanic massif in some recent models (e.g., Ferlito, 2011).

This research was supported by the KALMAR project, which funded geochemical and mineralogical investigations and the Grants of the Far East Division Russian Academy of Sciences (##07-III-D-08-095 and 09-III-A-08-422).

References

Ferlito C (2011) Bimodal geochemical evolution at Sheveluch stratovolcano, Kamchatka, Russia: Consequence of a complex subduction at the junction of the Kuril Kamchatka and Aleutian island arcs. Earth-Science Reviews 105(1-2): 49-69

Gorbach NV, Portnyagin MV (2011) Geology and petrology of the lava complex of Young Shiveluch volcano, Kamchatka. Petrology (Engl. Transl.) 19/2: 140–172.

Melekestsev I. V., Volynets O. N., Ermakov V. A., Kirsanova T. P., and Yu. P. Masurenkov (1991), Shiveluch volcano. In: Fedotov S. A., Masurenkov Yu. P. (Eds.) Active volcanoes of Kamchatka. 1, Nauka Press, Moscow: 84-92

Menyailov A.A. (1955) Sheveluch Volcano, its geologic structure, composition and eruptions. Trudi Laboratorii Vulkanologii, 9, 264 pp (in Russian).

Ponomareva V.V., Kyle P., Pevzner M. M., Sulerzhitsky L.D., and Hartman M. (2007). Holocene Eruptive History of Shiveluch Volcano, Kamchatka Peninsula, Russia. In: Volcanism and Subduction: The Kamchatka region. Eichelberger J., Gordeev E., Izbekov P., Lees J. (Eds), AGU Geophysical Monograph, 172: 263-282.

Portnyagin M.V., Bindeman I.N., Hoernle K., and Hauff F. Geochemistry of primitive lavas of the Central Kamchatka Depression: magma genesis at the edge of the Pasific Plate // Volcanism and Subduction: The Kamchatka region. Eichelberger J., Gordeev E., Izbekov P., Lees J.(Eds). AGU Geophysical Monograph 172: 203-244.

Volynets, O.N., Ponomareva, V.V, and Babanskii, A.D., Magnesian Basalts of Shiveluch Andesite Volcano, Kamchatka, Petrology (Engl. Transl.) 5/2: 183–196.

Evolution of a Zoned Magma Chamber during the Historic Eruptions of Hokkaido–Komagatake Volcano, Northern Japan

Ryo TAKAHASHI[1] and Mitsuhiro NAKAGAWA[2]
1: Geological Survey of Hokkaido, Hokkaido Research Organization
2: Department of Natural History Sciences, Faculty of Science, Hokkaido University

Hokkaido–Komagatake volcano is one of the most active volcanoes in Japan, and began eruptive activities (the historic eruptions) in 17th century after about 5000 years' dormancy. Plinian eruption occurred in 1640, 1694, 1856 and 1929, and phreatomagmatic eruption in 1942. The juvenile ejecta can be classified into four types, white pumice (SiO_2=59.8–62.4 wt.%), gray pumice (SiO_2=58.2–60.5 wt.%), scoria (SiO_2=57.4–58.9 wt.%) and banded pumice. Gray pumice did not erupt in the 1640 eruption, and scoria has not since the 1929 eruption. In all plinian eruptions, more mafic ejecta erupted prior to felsic one. Whole rock and glass compositions form a linear trend, implying a binary mixing relationship. White pumice showing highly porphyritic feature (24.9–51.5 vol.%) has no evidences for magma mixing, hence it derived from the mushy felsic end–member magma (WP magma). Scoria shows nearly aphyric feature (less than 7 vol.%), and phenocrysts originated from the felsic magma. It indicates that the mafic end–member magma (S magma) was aphyric.
The 1640 banded pumice shows a linear chemical trend connecting white pumice and scoria, suggesting that magma mingling occurred between two end–members. In the 1640 eruption, the injected S magma ascended in the WP chamber while mingling and erupted first. After the eruption, these magmas formed a zoned chamber. Because the density of the S magma (2.52±0.02 g/cm^3) was lighter than that of the WP magma (>2.55 g/cm^3), the S magma was located above the WP magma. The hybrid magma had been formed by mixing until the 1694 eruption. Since the 1694 eruption, the magmas have ejected sequentially from the upper part of the chamber without the S magma injection. As a result, the mafic ejecta erupted prior to the felsic one. Homogeneous mixing could occur during the eruption because of the existence of the hybrid magma showing the intermediate viscosity between two end–members. Consequently, gray pumice has erupted since the 1694 eruption. The residual volume of the S magma had decreased by repeated eruptions, and most of the magma had been spent until the 1929 eruption. As a result, scoria has not erupted since the 1929 eruption. Moreover, the 1942 ejecta are mostly composed by white pumice. Thus we can determine that the present chamber mostly consists of the WP magma. The viscosity of the magma ranges from $10^{6.3}$ to $10^{7.5}$ Pa s. Such highly viscous magma can hardly erupt, and the total volume of erupted magma in 1640–1942 has already reached nearly the same order of magnitude as the previous eruption period (6.0–5.5 ka). These might indicate that large–scale eruption hardly occurs in the near future and the volcano is in several thousand years' dormancy.

PETROLOGICAL CONSTRAINTS ON THE MECHANISMS OF CATASTROPHIC EXPLOSIVE ERUPTIONS OF ANDESITIC AND ACID MAGMAS

A P. Maximov

Institute of Volcanology and Seismology FED RAS (Petropavlovsk-Kamchatsky)

maximov@kscnet.ru

There were about ten catastrophic explosive eruptions of andesitic and acid magmas during 20th century. These eruptions are characterized by large volumes of juvenile material (about 1 km^3 and more) and their high intensivity withdrawing (n $\times 10^5$ m^3/s) at paroxysmal phase. We can recognize two main types among these eruptions: I – eruptions with unimodal rock composition (Santa-Maria, Bezymianny, Shiveluch, Sent-Helens) and II – with contrast rock compositions (Ksudach - Stubel, Katmai - Novarupta, Quizapu - Cerro-Azul, Pinatubo, Hadson). Eruptions of the first type just produce single-composition magma which undergoes slow composition evolution in time. Second type is characterized by simultaneous eruption of juvenile products with different compositions (two or three in the case of Katmai) with evident signs of mingling. These types are clearly distinguished by character of volcanic activity.

Formation of large-scale volcanic dome with following prolonged (years – many tens of years) extrusive activity is inherent for eruptions of the first group. Eruptions with contrast compositions of the products continue several hours or days. These eruptions cause no exrusive domes or they are very small.

We suppose that the above mentioned relationships result from different structures of the feeding zone of these volcanoes. Eruptions of the first group are caused by retrograde boiling of magma in a single chamber. Energy of the future eruption accumulates during cooling of magma and when volatile pressure in the chamber exceeds a particular critical pressure, it causes a paroxismal explosion. Thereafter the velocity of ascending watersaturated magma gradually decreases resulting in large dome formations. Hornblende rocks are very inherent for given types of eruption, which indicates sufficiently deep position of magma chambers.

Eruptions of the second type are consequences of influx of volatile saturated acid magma in a shallow chamber of more basic magma. In this case all the volume of very viscous acid magma pass rapidly through liquid basic chamber, reaches surfaces, violently degases there, and eruption finishes. This type is characterized by considerably large volumes of the products erupted at paroxysmal stage. Acid (or andesite) rocks play main role, and may comprise up to 95% and even more among eruption products. Hornblende rocks are also usual, but not ubiquitous.

We think that these constraints give direction for following study of mechanisms of catastrophic explosive eruptions and feeding systems of andesitic volcanoes. Presented scheme provides possibility for forecasting of temporal course of considered eruptions. So, the activity at Chaiten Volcano, that started in 2008, will apparently continue for many years.

ПЕТРОЛОГИЧЕСКИЕ МОДЕЛИ КАТАСТРОФИЧЕСКИХ ЭКСПЛОЗИВНЫХ ИЗВЕРЖЕНИЙ АНДЕЗИТОВЫХ И КИСЛЫХ МАГМ

А.П. Максимов

Институт вулканологии и сейсмологии ДВО РАН,

Петропавловск-Камчатский, 683006; e-mail: maximov@kscnet.ru

В XX столетии произошло около десяти катастрофических эксплозивных извержений андезитовых и более кислых магм. Эти извержения отличаются большими объемами ювенильного материала (около 1 км^3 и более) и высокой интенсивностью выноса вещества в пароксизмальную фазу (десятки-сотни тыс. м^3/с). Среди них можно выделить два основных типа: I - с одномодальным составом пород (Санта-Мария, Безымянный, Шивелуч, Сент-Хеленс) и II - с контрастными составами продуктов (Ксудач-Штюбель, Катмай-Новарупта, Квицапу-Сьерра-Ассуль, Пинатубо, Хадсон). При извержениях первого типа происходит поступление одной медленно эволюционирующей магмы. Второму типу свойственно сопряженное извержение ювенильных продуктов разного состава (двух или трех, в случае Катмая-Новарупты), с явными признаками смешения. Эти группы отчетливо различаются по характеру протекания вулканической активности.

Извержениям первой группы свойственно образование крупных вулканических куполов и последующая длительная экструзивная активность (годы-десятилетия). Извержения с контрастным составом продуктов длятся часы – дни. Экструзивные купола при этом либо не образуются, либо слабо выражены.

Объяснение указанных закономерностей видится в различном строении зон питания вулканов. Извержения первой группы вызываются поступлением магмы из одного очага. В очаге магма накапливает энергию для извержения за счет ретроградного кипения. При достижении давления выше критического наступает пароксизмальный взрыв с последующим снижением скорости поступления магмы. Медленное продвижение к поверхности водонасыщенной магмы и вызывает развитие мощных куполов. Для данных извержений весьма характерны роговообманковые породы, что указывает на достаточно глубокое положение очагов в коре.

Извержения второго типа вызваны внедрением насыщенной кислой магмы в вышерасположенный очаг более основного состава. В этом случае, порция вязкой кислой насыщенной летучими магмы быстро полностью проходит через жидкую основную, и извержение заканчивается. Для второго типа характерны значительно большие объемы продуктов, изверженных в пароксизмальную фазу. Главную роль среди них играют кислые составы, доля которых может превышать 95%. Роговообманковые породы также характерны, но не для всех извержений.

Представляется, что данная схема дает направление для дальнейшего анализа механизма катастрофических эксплозивных извержений и строения систем питания андезитовых вулканов. Она позволяет прогнозировать развитие рассмотренных типов извержений во времени. Так, начавшаяся в 2008 г. активность вулкана Чайтен, извергающего только риолиты, вероятно, будет продолжаться многие годы.

Petrology of the KIWIKIWI Formation – Mt Ruapehu

A. Auer*
J.D.L. White
Mike Palin

Department of Geology,
University of Otago,
PO Box 56, Dunedin
[*corresponding author: auean368@student.otago.ac.nz]

Mt Ruapehu is a large composite cone on the central plateau of New Zealand's North Island, and a source of multiple volcanic hazards.

Young explosive activity took place during the Taurewa episode ca. 10.000 years ago producing widely dispersed plinian fall deposits as well as small pyroclastic flows. Within the last 2000 years Ruapehu has produced frequent, but much smaller eruptions, which formed the TufaTrig formation characterized by a distinctive pyroclast petrography. Its youngest member was formed in1995 / 1996.

Until recently the time in-between these eruptive episodes was believed to represent a period of relative quiescence. A newly identified and voluminous deposit of reworked-pyroclastic rocks – the Kiwikiwi Formation (about 4600 years old), may, however, be the missing link in the series, andprovide insight into the reasons for the change in eruptive style and pyroclast composition and petrography. Such an investigation has to consider physical controls on eruption (e.g. the presence or absence of a crater lake, activity through different summit vents) as well as deep and shallow magma genesis and evolution as reflected in the geochemical data. In this study we present some preliminary data from the study of melt inclusions from the Kiwikiwi Formation and compare our results with those for the preceding and following eruptive episodes.

Sr and Nd isotopic composition of ~1.7Ma volcanic rocks in Hokkaido, Japan: Implication for magma source at the arc-arc junction

Ayumi KOSUGI and Mitsuhiro NAKAGAWA
Department of Natural History Sciences, Graduate School of Science,
Hokkaido University, Sapporo, Japan

Hokkaido Island is located at the arc-arc junction of two active island arcs, Northeast (NE) Japan and Kurile. Many authors discussed lateral geochemical variation of volcanic rocks from NE Japan arc using abundant major, trace and isotopic data (e.g. Shibata and Nakamura, 1997; Kimura and Yoshida, 2006). Recently, general features of isotopic compositions of the rocks from Kurile Islands are also revealed (Martynov et al., 2007). However, the data on isotopic composition of volcanic rocks from Hokkaido are scanty. In this study, we newly present Sr and Nd isotopic composition of volcanic rocks from ~1.7Ma volcanoes in Hokkaido. We focus on the basaltic rocks (SiO_2 <54wt.%) and compare these with northern NE Japan and Kurile Islands to clarify isotopic feature of arc-arc junction.

The ~1.7Ma volcanoes are distributed in three volcanic fields, southwestern Hokkaido (SWH), Taisetsu-Tokachi-Shikaribetsu (TTS) and Akan-Shiretoko (AKS) volcanic fields (Figure 1). In each field, the volcanic rocks range from basalt to rhyolite. The rocks from SWH and AKS clearly show across-arc compositional variations, whereas those from TTS do not show spatial variations (Nakagawa, 1999). The basaltic rocks from each field are clearly distinguishable on $^{87}Sr/^{86}Sr - ^{143}Nd/^{144}Nd$ diagram (Figure 2). The rocks from SWH show largest variation among three fields and are divided into two compositional clusters, the frontal and the rear-arc region. The rear-arc volcanoes of SWH have clearly lower $^{87}Sr/^{86}Sr$ than the frontal volcanoes with distinct compositional gap. Although the rocks from TTS and AKS also have lower $^{87}Sr/^{86}Sr$ composition in the rear-arc volcanoes than in the frontal volcanoes, they show continuous and narrower variations than those from SWH. The rocks from TTS have similar $^{143}Nd/^{144}Nd$ to those from SWH, and medium $^{87}Sr/^{86}Sr$ between the rear-arc and the frontal volcanoes of SWH. The rocks from AKS clearly show higher $^{143}Nd/^{144}Nd$ than those from TTS and SWH.

Comparing with the basaltic rocks from northern NE Japan and Kurile Islands, the rocks from northern NE Japan show large $^{87}Sr/^{86}Sr$ variation similar to those from SWH. In the Kurile Islands, the rocks from central and northern islands show higher $^{143}Nd/^{144}Nd$ than those from southern Islands, as the longitudinal along-arc chemical variation (Ishikawa and Tera, 1997; Martynov et al., 2007). The rocks from southern Kurile Islands (Kunashir and Itrup) show comparable composition to those from AKS. Although the rocks from TTS are plotted on the more fertile field than those from Kurile Islands, these compositions are consistent with along-arc variations in Kurile Islands.

Based on the spatial isotopic variations of the basaltic rocks, SWH can be considered as the northern end of the NE Japan arc, whereas AKS and TTS as the southern end of Kurile arc. The presence of rear-arc volcanoes of NE Japan is the distinct characteristic of NE Japan arc. In contrast, Kurile arc shows clear along-arc variation from TTS to Kurile Islands. These characteristics must reflect regional difference not only in magma generation processes but also in specific tectonic history of each arc.

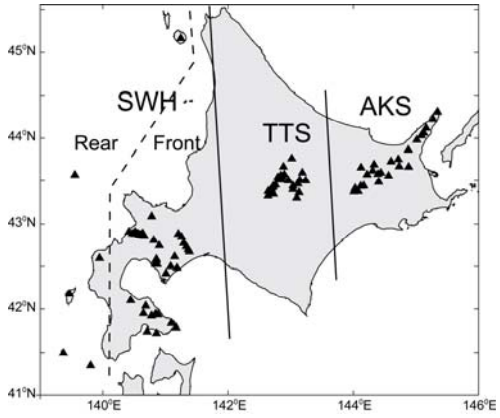


Figure 1
Distribution of ~1.7Ma volcanoes in Hokkaido.

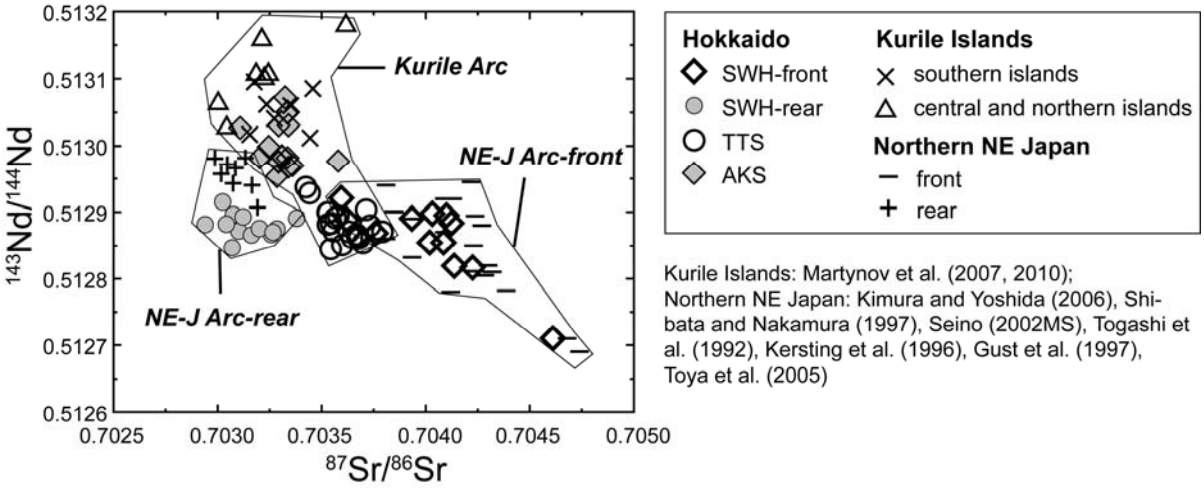


Figure 2
$^{87}Sr/^{86}Sr - ^{143}Nd/^{144}Nd$ diagram of the basaltic rocks (SiO_2 <54wt.%) from Hokkaido and neighbors

References

Gust, D. et al. (1997) Canad. Mineral., 35, 347-365
Ishikawa, T. and Tera, F. (1997) Earth Planet. Sci. Lett., 152, 123-138
Kersting, A. et al. (1996) Science, 272, 1464-1468
Kimura, J. and Yoshida, T. (2006) Jour. Petrol., 47, 2185-2232
Martynov, Y. et al. (2007) Doklady Earth Sciences, 417, 1206-1211
Martynov, Y. et al. (2010) Island Arc, 19, 86-104
Nakagawa, M. (1999) Resource geology special issue, 20, 161-176
Shibata, T. and Nakamura, E. (1997) Jour. Geophys. Res., 102, 8051-8064
Togashi, S. et al. (1992) Geochem. Jour., 26, 261-277
Toya, N. et al. (2005) Contrib. Mineral. Petrol., 148, 566-581

THE STRUCTURAL EQUILIBRIA IN SILICATE MELTS: APPLICATION TO PETROLOGICAL ESSENTIAL HETEROGENEOUS REACTIONS

O. A. Khleborodova

Institute of Volcanology & Seismology, Petropavlovsk-Kamchatskiy, Russia,
e-mail: khleborodova@kscnet.ru

The simulation of igneous processes in the natural magmatic systems often requires a recognizing of a mechanism of reactions between solid phases and melt components. Especially it is important for processes occurring in open systems with varying conditions. But identification of melt species involving in heterogeneous reactions is generally uncertain. Theory of the atomic structure of silicate melts are based on laboratory studies using nuclear magnetic resonance (NMR), vibrational spectroscopy and Raman scattering spectroscopy (e. g. Mysen, 1990). It is known that the melts (glass materials) are characterized by absent of long-range ordering. But the net structure of silicate melt consists of structural units resembling of unit cells of main silicate minerals – Q^4, Q^3, Q^2, Q^1, Q^0 (index means the number of bridging oxygen in the structural unit) The above structural units have a short live time (~1 μs), and they always exchange for bridging $[BO]^0$ and non-bridging oxygen $[NBO]^-$ with each other. It is supposed that such permanent reconstruction of melt structure is the main mechanism of a viscous melt flow (Liu et al., 1988).

The structural disproportionation equilibra $2Q^n=Q^{n-1}+Q^{n+1}$ with n = 1, 2, 3, are described for modeling of liquid silicates in homogeneous silicate systems – glasses. But similar structural equilibria have not been used for characterization of heterogeneous chemical reactions and phase equilibria in multi-component silicate systems until now. Insufficient resolution of spectroscopic and scattering methods does not allow the direct determination of structural complexes in multi-component systems. The NMR spectroscopy technique is more sensitive for analysis of composed system, but such type of NMR-data are not sufficient still. Usually the melt species composition is guessed on the basis of all compounds, occurring in studied systems.

The simulating of liquidus phase equilibria in heterogeneous silicate systems based on principle about equality in chemical potentials for liquid and solid phases on the liquidus. The calculations are reduced to determination of melt species distribution on the basis of the mixing Gibbs free energy minimization for the whole melt species combination (e. g. Ghiorso, 1985). However, if a chemical reaction runs in the system, the Gibbs free energy change of the reaction has to take into account in that causes.

The main idea promoted here consists in that the “chemical-structural” equilibria (reactions) could occur in multi-component silicate melts. Thermodynamic effect of such reactions may be more considerable then the mixing effect only. The first attempt to construct some structural equilibria in heterogeneous multi-component silicate systems having a petrological interest is made (Khleborodova, 2010), that included 1) the estimation of relative chemical affinity of network modifying cations to some structural units, deriving from the structural unite distribution in the simple silicate systems studied earlier and available from literature (e. g. Mysen, 1990; Maekawa et al. 1997; Neuville et al., 2008) 2) simulation of structural equilibria of An-Fo-melt and Ab-An-Di-melt reactions, using the new structural equilibria $Q^0+Q^4=2Q^2$ and known structural equilibrium $2Q^3=Q^2+Q^4$ 3) the calculation of the enthalpy change ΔrH, Gibbs function change ΔrG and constants K of these equilibriums using thermodynamic data (Holland&Powell, 1998**),** 3) the analyses of these equilibria behavior in heterogeneous aphlobasaltic systems undergoing varying conditions.

The simulated heterogeneous reactions were examined in aspect of theirs application to some petrological processes, running at nonequilibrium conditions, specifically the melt-wall rock and melt-fluid interaction under pressure and temperature gradients. The some geochemical trends of magmatic differentiation of high magnesia rocks of North Kamchatka group volcanoes are shown in this respect.

References

Ghiorso M.S. Chemical transfer in magmatic processes. Thermodynamic relations and numerical algorithms //Contrib. Mineral. Petrol., 1985, v.90:107-120.

Khleborodova O.A. “The structural equilibria in heterogeneous silicate systems: on the hypothesis to practice” in Goldschmidt 2010: Earth, Energy, and the Environment, June 2010 //Geochimica et Cosmochimica Acta, 2010, v.74, Iss.12, p.A512., http://dx.doi.org/10.1016/j.gca.2010.04.036
Maekawa H., Maekawa T., Kawamura K., and Yokokawa T. The structural groups of alkali silicate glasses determined from 29Si MAS-NMR. // J. Non-Cryst. Solids, 1991, N127 (1), pp.53–64.
Mysen, B. O. Relationships between silicate melt structure and petrologic processes //Earth Sci. Rev., 1990, v.27, pp. 281-365.
Neuville D.R., Cormier L., Montouillout V., Florian P., Millot F., Rifflet J.-C., Massiot D. Structure of Mg- and Mg/Ca aluminosilicate glasses: 27Al NMR and Raman spectroscopy Investigations //American Mineralogist, 2008, v. 93, pp.1721–1731.

This work was supported by the grant: RFBR 11-05-98555-р_восток_а.

Estimation of subsurface structure using microtremor H/V spectral ratio around Unzen volcano

Natsumi ITOYA and Takeshi MATSUSHIMA*
(Institute of Seismology and Volcanology, Kyushu University, JAPAN)

The Shimabara peninsula where Unzen volcano was erupted, located on the west edge of the Beppu-Shimabara grabenwhich crosses the center part in Kyushu island from east to west. Seventy percent of the peninsula is composed by volcanic product fromthe volcano. Using strong motion H/V spectral ratio, the Central Disaster Prevention Council (2008) pointed out that the long-period strong ground motions in the Shimabara peninsula are amplified so much like the Quaternary plains though the sedimentary layer of Quaternary Era is not thick in the peninsula. Especially, in the Yadake region (center part of the peninsula), the long-period ground motions amplify to the same extent as Tokyo area in the Kanto plains. In order to estimate a ground structure in the Shimabara peninsula by using microtremor H/V (horizontal-to-vertical) spectral ratio as an evaluation method of the ground structure, we carried out microtremor observations at 60 points in the whole area of Shimabara peninsula.

The microtremor observations using a three-components wideband portable seismometer of characteristic period 120 second were carried out at each observation site. The data of microtremor were recorded by a portable data-logger with 100Hz sampling.Power spectrum of UD, NS, and EW were calculated and smoothed by using the ensemble average of thirty times, and power ratio of H/V spectra was estimated.

By using data from 60 observation sites, we traced a contour map of primary natural peak period (the longest peak period that exists from 1 to 10 seconds). Peak period of 5-6 s in H/V spectra was obtained at a lot of observation sites at east side of the Shimabara peninsula, where volcanic sediments are thickly distributed. It is thought that the thick volcanic sediment layer is a cause of such longer peak period in H/V spectra.

In the central western area of the Shimabara Peninsula, there are no remarkable peaks in the observed H/V spectra. According to explosion seismic research (Explosion seismic research group of Unzen Volcano, 1995), this area corresponds to rock layer having Vp=3.5km/s, which distributed in shallow to ground surface as a solid lava layer. This structure is reflected in shape of H/V spectra; the value of H/V spectra in this area is nearly constant in the frequency of microtremor.

Next, we are going to estimate subsurface structures in the peninsula using the observed H/V spectra. Using P wave velocity that had been obtained by the explosion seismic research, S wave velocity and density were calculated by relation estimated by Ludwig et al. (1970). During a trial-and-error estimation process, S wave velocity, P wave velocity and density were fixed, and we adjusted the thickness of the sedimentary layers to find a reasonable fit of primary natural peak period of the calculated H/V spectra and the observed H/V spectra to determine the ground structure. Then, the depth to Vs=600m/s layer is estimated as 1.2km at the boring site USDP2 in east side of Shimabara peninsula. Our result is consisting with boring-core sampling data from the borehole.

The horizontal component of long-period microtremor, locally exceed in Yadake site of the center part of Shimabara peninsula. If the ground structure is determined by using the same parameter as surrounding sites, the depth to the basement in the site should be estimated as about 1000 m. However, nearby tectonic map and the result of explosion seismic research do not showsuch a steep basin structure under the site. Thus, we changed S wave velocity of shallow part of the underground structure,and we found that the very low-velocity layer exists beneath surrounding of Yadake site. Because the rich hot-spring resourcesexist in around the site, it is thought enough that existence of the low-velocity layer, which causes the increase of thelong-period strong ground motions.

"Dry" rivers hydrology on the territory of active volcanism in Kamchatka

Ludmila Kuksina[1]

[1] Lomonosov Moscow State University, Moscow, Russian Federation

(ludmilakuksina@gmail.com)

Territories of modern volcanic activity are specific regions including hydrology. The largest volcanic regions on the Russian territory are Avachinskaya and Kliuchevskaya volcano groups.

Special characteristics have rivers flowing down the active volcanoes. Friable volcanic deposits on the slopes and foots of volcanoes determine peculiar features of rivers' hydrological regime, sediment inflow and transport, channel morphology. Rivers carry out large quantity of sediment into the ocean in these conditions.

Upstream of volcanic territories rivers is characterized by maximum slopes; rivers mainly have mountain channel. River sources are at the height of 2000 – 2500 m for Kliuchevskaya volcano group; length of upstream river reach is about 5 km. The similar characteristics for Avachinskaya volcano group are 1400 – 1600 m and 4 km accordingly. Fluctuations of water level and turbidity are anisochronous here (fig. 1).

At the height 1000 – 1500 m rivers flow within lahar valleys. Characteristic is heightened turbidity of the flow here which is determined by maximum rate of suspended sediment runoff. Turbidity and water level fluctuations are synchronous here (fig. 2). Erosion of friable volcanic deposits and steep slopes (about 25 – 60 ‰) contribute capability of "dry" rivers to transport significant amount of suspended sediment even for small water discharges.

Downstream of "dry" rivers is characterized by heightened turbidity as the result of material receipt from upstream feeders. Flowing into rivers forming outside of volcanic slopes "dry" rivers bring a lot of suspended sediment; turbidity trail spreads to deltas.

Characteristic features of volcanic rivers hydrological regime are shown in daily, annual and long-term flow fluctuations. Daily flow fluctuations of volcanic rivers depend on ice and snow melting and transform at the expense of filtration. Water content and sediment flow changes are accompanied with riverbed transformations which rate is the highest one. Within-year variability is also very irregular. During the law-water season most part of volcanic rivers doesn't reach their receiving basins because of high infiltration. The main sediment removal occurs during the flood time; its duration is 3 months for this territory. Fluctuations of high-water, low-water and water-average periods are determined by climatic factors and internal causes. High-water periods are often coincided with volcanic eruptions in winter when huge amount of ice and snow melts. Considerable eruptions are reasons of law-water periods whereas the source of water feeding could be diminished or destroyed.

Temporal averaging of flow fluctuations allows us to estimate sediment yield of "dry" rivers on the basis of regression model taking into account unit discharge of water M_Q, l/sec·km^2; catchment area F, km^2; coefficient of friable volcanic rocks availability $\frac{F_{\text{vol}}}{F}$ on catchment basin.

Estimation is made for 62 basins of Kliuchevskaya and Avachinskaya volcano groups. The total sediment flow with the expense of "dry" rivers into Pacific Ocean from the eastern

coast of Kamchatka is 10.2 mil t/year; sediment inflow from “dry” rivers basins (its area is 5620 km^2 and about 3% of eastern part of the peninsula area) is 3.5 mil t/year or 35 % of the total sediment flow.

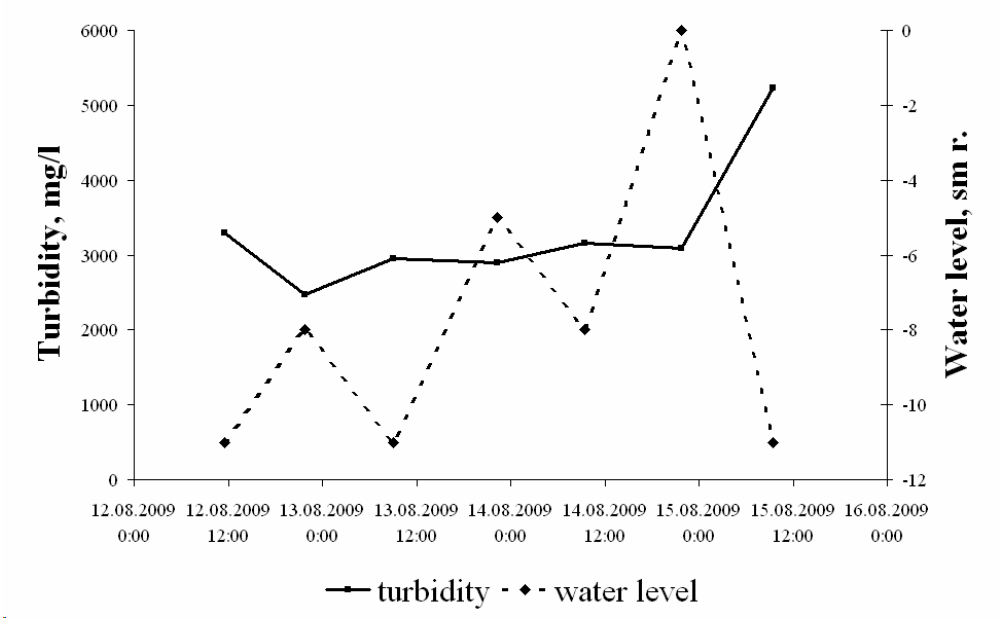


Fig. 1. Diurnal variation of turbidity and water level in the Bilchenok river (Ushkovskiy volcano)

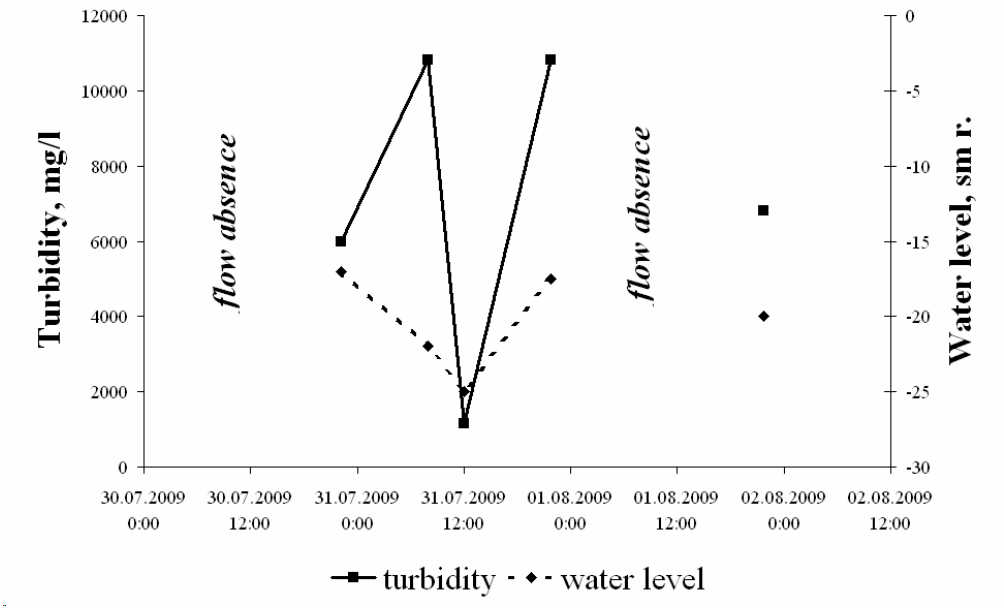


Fig.2. Diurnal variation of turbidity and water level in the Lavoviy river (Kliuchevskoy volcano)

Mechanisms of lahar formation in Kamchatka

Chernomorets S.S.[1], Seynova I.B.[2], Tutubalina O.V.[1], Brichevsky A.S.[1]

[1]M.V.Lomonosov Moscow State University, Faculty of Geography, Moscow, Russia
[2]University Centre for Engineering Geodynamics and Monitoring, Moscow, Russia

We considered features of the formation of volcanic debris flows (lahars), on the basis of our field research in 2008, interpretation of satellite images, and analysis of literature on volcanic eruptions of Klyuchevskoy and Shiveluch volcanoes in Kamchatka Peninsula, Russia. We reconstructed the chronology of volcano-induced debris flows at these volcanoes over the last decades and have compiled a map of debris flow formation conditions for the eastern sector of the Klyuchevskoy Volcano. We focused particular attention on the formation of the water component of volcano-induced debris flows. Mechanisms of lahar initiation as a result of glacial processes and of snow melting on volcanoes have been highlighted. We interpreted satellite images and made 19 sketch maps and database on lahars in Kamchatka. Also we analysed granulometric composition of lahar deposits.

Механизмы формирования лахаров на Камчатке

Черноморец С.С.[1], Сейнова И.Б.[2], Тутубалина О.В.[1], Бричевский А.С.[1]

[1]Московский государственный университет имени М.В.Ломоносова, географический факультет, Москва, Россия
[2]Университетский центр инженерной геодинамики и мониторинга, Москва, Россия

В результате полевых исследований 2008 г., анализа космических снимков и литературных материалов были изучены особенности и механизмы формирования вулканогенных селей (лахаров) при извержениях вулканов Ключевской и Шивелуч на Камчатке. Реконструирована хронология вулканогенных селей на этих вулканах за последние десятилетия. Составлена карта условий формирования селей восточного сектора Ключевского вулкана. Особое внимание уделено формированию водной составляющей селевых потоков на вулканах. Выявлены особенности механизмов зарождения лахаров гляциально-вулканического и нивально-вулканического генезиса. Созданы 19 схем дешифрирования и база данных по лахарам Камчатки. Проведен детальный анализ мелких фракций отложений лахаров.

Scanning UV Gas Imaging System (SUGIS) for remote measurements of volcanic gas emissions

Olga Neussypina, Hendrik Fischer, Arne Krueger, Peter Rusch, Roland Harig
Institute of Measurement Technology, Hamburg University of Technology, Hamburg, Germany

The passive DOAS technique can be used for remote measurements of volcanic gas emissions. This work describes the construction of a scanning imaging DOAS system that can measure gases with spectral signatures in the range between 290-385 nm. The device is based on a combination of a UV-spectrometer USB2000+ and an azimuth-elevation scanning mirror system. In addition it includes a telescope, a video camera, a GPS receiver and a notebook. Cloud imaging is accomplished by scanning the field of view with the moving mirror. For each pixel a spectrum is recorded. The slant column densities for each pixel are retrieved using a non-linear radiative transfer model in combination with the Levenberg-Marquard algorithm. The results are visualized in a false color image, which is overlayed on the video image. This allows identification, imaging and tracking of the cloud. Two devices have been built for simultaneous measurement of the cloud from different directions. In this case a developed 3D Tomography algorithm and the generation of a 3D cloud model are possible. The paper describes the system and presents some test measurements.

Formation of parasitic cones on polygenetic volcanoes

by I. Yokoyama, The Japan Academy, No. 7, Ueno Park, Taito-Ward, Tokyo 110-0007 Japan

Formation of parasitic volcanoes at different distances from the central vent of a polygenetic volcano may be understood from the standpoint of material mechanics. The theory of maximum shearing stress is applied to interpret the formation of parasitic vents on the flanks of volcanoes in terms of crustal strength. Whether the new magma erupts at the main crater or at a new parasitic crater depends on conditions of the main crater and on the relative strengths of both the sites. Distributions of parasitic vents are closely related to movement of magma beneath central volcanoes. The radial distribution of parasitic vents is characterized in terms of the number of parasitic vents per unit area with distance from the central vent. The distributions are exemplified on some volcanoes in Japan; Comparatively high concentration of parasitic vents at a certain distance from the central crater can be interpreted to reflect the shallow magma plumbing system. That is, ascending magmas branch from a central conduit at different depths and hence reach the surface at different distances from the central crater. Parasitic volcanoes are usually monogenetic; its reason may be explained by their formation mechanisms.

Evidences of magma mixing event under Unzen Volcano (Japan) during 1991-1995 eruption

Ilya S. Fomin, Pavel Yu. Plechov, Alexandra E. Tsay
Petrology department, Lomonosov Moscow State University, Russia
Corresponding author: fomin@web.ru

Recent eruption of Unzen Volcano in 1991-1995 has caught attention of scientists all over the world because of disastrous character of previous one in 1792. Intrusion of andesitic magma to the chamber with rhyolitic magma is proposed as a trigger for this eruption. Parameters of two end-member magmas has been estimated several times, but usually estimations are based on phenocrysts assemblages. Origin of these phenocrysts is unclear: usually only mineral composition and reaction rims are used to prove their source. So it is possible to propose another explanation of phenocrysts formation instead of magma mixing.

In our work we selected several mafic enclaves from 1995 lava dome and proved a magma mixing origin only by petrographic features. Our arguments are:

- Smooth edges of enclaves have “chilled margins” structures. Major axis of microlithes in margin is usually between 0.4-0.9 from the size of the major axis of microlithes inside enclave, which is a general feature for quenching process. An X-Ray microtomography has been applied to estimate it (Skyscan 1172).
- “Chilled margin” near cusps (angular in form edges) is absent. It can be interpreted as a result of enclave fragmentation process after quenching and host magma heating.
- In some places chilled margin is found broken and host rock groundmass with small phenocrysts can be found in cracks. According to these observations, chilled magrin’s microlithes formed after the enclave formation and before crack formation. It give us direct prove for magma-in-magma heterogeniety.
- Large plagioclase phenocrysts can be observed in enclaves. They are the same to phenocrysts from host rock, so they could be rapidly captured from it before quenching.
- In addition, such features as opacitization of hornblend and biotite in host rock, pyroxene rims around quartz phenocrysts, as well as two glasses inside mafic enclaves also can be used to estimate magma mixing exent. Absence of quartz microlithes is another argument for this theory.

Therefore it is possible to use these mafic enclaves instead of phenocrysts for estimation of thermodynamic parameters. Also it confirms the possibility of capturing of the phenocrysts from intruded magma.

Previous investigations provided us with the following thermodynamic conditions:

- For host rhyolitic magma: 100÷300MPa, 775÷875 C, 4±1 wt. % H_2O, f_{O2} = NNO [Holtz et al., 2005]; 790±20 C, 160 MPa [Venezky, Rutherford, 1999]; 770 C, 300-400 MPa, 7÷8 wt. % H_2O [Cichy et al., 2009].
- For intruded andesitic magma: 1050±75 C, up to 8 wt. % H_2O [Holtz et al., 2005]; 1030÷1130 C [Venezky, Rutherford, 1999]; 1050 C [Cichy et al., 2009].

- For magma after mixing: 870÷900 C, 6±1 wt. % H_2O [Holtz et al., 2005]; 850÷930 C [Venezky, Rutherford, 1999], 930 C [Cichy et al., 2009].

Our thermometry data (two pyroxenes, hornblende and plagioclase, oxides) gave 750÷850 C for host magma, 1050÷1100 C for intruded one and 850÷950 C for magma after mixing.

This data provided the possibility to calculate the volume per cent of intruded magma in a part of magmatic chamber, that was involved both to the magma mixing and extrusive processes. Our estimation is 16 vol.%.

Maximum observed size of the enclaves is 20 cm. We assume, that thermal equillibration time was not exceeded 32 hours [Plechov et al., 2008]. That means, that chilled magrins formed quickly enough to prevent any effective assimilition of enclaves and this fact can be used to estimate mafic end member of the mixing process.

The presence of altered phenocrysts could be a result of principally another mechanism of intruding. We suppose, that the first portion of andesitic magma formed enclaves and only heated magmatic chamber, while the further magma could be efficiently mixed with the host one before crystallisation.

Literature:

- Cichy S.B., Holtz F., Botcharnikov R.E., Behrens H., Vetere F., Sato H. Preeruptive conditions and dynamic processes in magmatic systems: the example of Unzen 1991-1995 eruption // Geochimica et Cosmochimica Acta Supplement, Volume 73, p.A225
- Holtz F., Sato H., Lewis J., Behrens H., Nakada S. Experimental Petrology of the 1991–1995 Unzen Dacite, Japan. Part I: Phase Relations, Phase Composition and Pre-eruptive Conditions // Journal of petrology, 2005, vol. 46, No 2, pp. 319-337
- Plechov P., Fomin I., Melnik O., Gorokhova N. Melt evolution during intruding basalts into acid magmatic chamber // Moscow University Geology Bulletin, 2008, Vol. 63, No. 4, pp. 247-257.
- Venezky D.Y., Rutherford M.J. Petrology and Fe–Ti oxide reequilibration of the 1991 Mount Unzen mixed magma // Journal of Volcanology and Geothermal Research, 1991, vol. 89, pp. 213–230.

Доказательства смешения магм в течение извержения вулкана Унзен (Япония) в 1991-1995 гг.

Илья С. Фомин, Павел Ю. Плечов, Александра Е. Цай
Кафедра петрологии, Московский Государственный Университет им. М.В.Ломоносова, Россия
Контактный e-mail: fomin@web.ru

Недавнее извержение вулкана Унзен в 1991-1995 гг. Привлекло внимание учёных всего мира вследствие катастрофических последствий, вызванных предыдущим извержением в 1792 г. В качестве причины извержения предполагается внедрение в кислый вулканический очаг порции андезитовой магмы. Работы по установлению термодинамических параметров конечных членов смешения были сделаны несколько раз, но обычно они основаны на изучении гломеропорфировых сростков и фенокристов. Источник этих вкрапленников неоднозначен, так как обычно доказательство базируется исключительно на минеральном составе и реакционных каймах. Однако для объяснения их происхождения можно предположить и иную по сравнению со смешением магм модель.

В нашей работе мы выбрали несколько темноцветных включений (анклавов) из экструзивного купола 1995 года и доказали их происхождение в результате смешения магм, используя только петрографические критерии. Этими критериями являются:

- Скруглённые границы включений имеют структуры закалочного типа (“chilled margins”). Длинная ось микролитов в кайме обычно составляет около 0.4-0.9 от размера соответствующей оси микролитов внутри включения. Это было подтверждено рентгеновской микротомографией (Skyscan 1172).
- Вблизи угловатых границ включений границы закалочного типа отсутствуют. Это может быть интерпретировано как результат фрагментации внедрившейся магмы после закалки и прогрева вмещающей магмы.
- В некоторых местах закалочная кайма разбита трещинами, в которые проникает вещество (расплав и микролиты) вмещающей магмы. Поэтому закалочные каймы образовались после образования включений и до образования трещин. Это является прямым доказательством наличия глобул одной магмы в другой.
- Наличие во включениях крупных вкрапленников плагиоклаза, аналогичных таковым во вмещающих породах, может быть объяснено их захватом до закалки анлавов.
- Такие особенности, как опацитизация роговой обманки и биотита, пироксеновые каймы вокруг кварца, два стекла внутри темноцветных включений также могут свидетельствовать в пользу смешения магм. Присутствие кварца только в фенокристах также свидетельствует в пользу данного предположения.

Таким образом, эти включения могут быть использованы вместо фенокристов для установления термодинамических параметров. Следует отметить, что проведённое доказательство подтверждает возможность захвата фенокристов из внедрившейся магмы.

В предыдущих исследованиях получены следующие значения термодинамических параметров:

- Для вмещающей риолитовой магмы: 100÷300MPa, 775÷875 C, 4±1 wt. % H_2O, f_{O2} = NNO [Holtz et al., 2005]; 790±20 C, 160 MPa [Venezky, Rutherford, 1999]; 770 C, 300-400 MPa, 7÷8 wt. % H_2O [Cichy et al., 2009].
- Для внедрившейся андезитовой магмы: 1050±75 C, up to 8 wt. % H_2O [Holtz et al., 2005]; 1030÷1130 C [Venezky, Rutherford, 1999]; 1050 C [Cichy et al., 2009].
- Для магмы после смешения: 870÷900 C, 6±1 wt. % H_2O [Holtz et al., 2005]; 850÷930 C [Venezky, Rutherford, 1999], 930 C [Cichy et al., 2009].

Наши данные по термометрии следующие (по двум пироксенам, роговой обманке и плагиоклазу, оксидам): 750÷850 C для магмы очага до смешения, 1050÷1100 C для внедрившейся и 850÷950 C для магмы после смешения.

Эти данные позволяют рассчитать объёмную долю внедрившейся магмы в части магматического очага, непосредственно вовлечённой и в процессы смешения, и экструзии на поверхности. Наша оценка - 16 об.%.

Максимальный наблюдаемый размер включений – 20 см. Время температурного уравновешивания (по [Plechov et al., 2008]) не превышало 32 часов. Это означает, что закалочные каймы формировались достаточно быстро для предотвращения значительной ассимиляции вещества анклавов. Это означает, что они подходят для изучения внедрившейся магмы.

Наличие изменённых фенокристов является, скорее всего, следствием принципиально другого режима внедрения. Мы предполагаем, что первая порция андезитовой магмы образовала анклавы и прогрела магматическую камеру, в то время как последующие порции магмы могли быть эффективно ассимилированы веществом очага до кристаллизации.

Литература:

- Cichy S.B., Holtz F., Botcharnikov R.E., Behrens H., Vetere F., Sato H. Preeruptive conditions and dynamic processes in magmatic systems: the example of Unzen 1991-1995 eruption // Geochimica et Cosmochimica Acta Supplement, Volume 73, p.A225
- Holtz F., Sato H., Lewis J., Behrens H., Nakada S. Experimental Petrology of the 1991–1995 Unzen Dacite, Japan. Part I: Phase Relations, Phase Composition and Pre-eruptive Conditions // Journal of petrology, 2005, vol. 46, No 2, pp. 319-337
- Plechov P., Fomin I., Melnik O., Gorokhova N. Melt evolution during intruding basalts into acid magmatic chamber // Moscow University Geology Bulletin, 2008, Vol. 63, No. 4, pp. 247-257.
- Venezky D.Y., Rutherford M.J. Petrology and Fe–Ti oxide reequilibration of the 1991 Mount Unzen mixed magma // Journal of Volcanology and Geothermal Research, 1991, vol. 89, pp. 213–230.

Oxygen isotopes and U-Th-Pb dating of zircons from post-Cougar Point Tuff lavas of the Bruneau-Jarbidge eruptive center of the Yellowstone hotspot

Angela Seligman[1], Barbara Nash[1], Henrietta Cathey[1], John Valley[2], Jorge Vazquez[3], Joe Wooden[4].

[1]Department of Geology and Geophysics, University of Utah. Salt Lake City, UT, 84112, USA.
[2]Department of Geology and Geophysics, University of Wisconsin, Madison, WI, 53706, USA.
[3] USGS-Stanford Ion Microprobe Laboratory, U.S. Geological Survey, Menlo Park, CA 942025, USA.
[4]USGS-Stanford Ion Microprobe Laboratory, Stanford University, Stanford, CA 94305, USA.

The Yellowstone hotspot is characterized by magmas with both normal and light $^{16}O/^{18}O$ ratios. The production of isotopically light magmas at the Heise volcanic center and on the Yellowstone volcanic plateau appears to be associated with cycles of multiple caldera-forming eruptions that lead to deep burial and remelting of hydrothermally altered rhyolites. In the central Snake River Plain, all of the eruptive products are isotopically light, and there is no evident cyclical behavior. Low $\delta^{18}O$ magmas have also been discovered at Kamchatka, Iceland, China, and the Karelian rift, suggesting that this is not a localized occurrence. Determining the cause of this occurrence is important, as it could reveal processes that ultimately lead to volcanic eruptions. We report here the results of oxygen isotopic analyses and U-Th-Pb dating on single crystals of zircon from 11-8 Ma lavas from the Bruneau-Jarbidge eruptive center (BJEC) that mostly post-date the large-volume ignimbrites of the Cougar Point Tuff (12.8-10.5 Ma). Zircons were separated from thirteen lavas to analyze for $\delta^{18}O$, ages, and Ti-in-zircon thermometry. 109 zircons were analyzed with the Cameca IMS-1280 ion microprobe at the University of Wisconsin to determine $\delta^{18}O$ of cores, rims, and interiors. U-Th-Pb ages for zircon spots previously analyzed for oxygen were determined on the Stanford SHRIMP together with trace element analyses including Ti. All $\delta^{18}O$ analyzes average 1.47 $^{o}/_{oo}$, with values ranging from -3.41 $^{o}/_{oo}$ up to 8.10 $^{o}/_{oo}$. Rims of zircons have a larger range in values (1.58 standard deviation) than cores (1.39 standard deviation), opposite from explosive members of the Cougar Point Tuff (CPT). The combination of data from the CPT and the younger lavas suggest that the $\delta^{18}O$ value of the magmatic system began with an average value just over 2 $^{o}/_{oo}$ with the first eruption of CPT III; the system then dropped to an average value closer to 0 $^{o}/_{oo}$ around 11 Ma, and later recovered to an average value around 2 $^{o}/_{oo}$ at the end stages of the BJEC. This indicates that from the beginning of the development of the CPT all the way through the eruption of the lavas, the BJEC continued to produce low $\delta^{18}O$ products. Ti-in-zircon temperatures average 930 °C, with values as low as 817 °C and as high as 996 °C. These values indicate the high sustained temperature of the magma system, even following the large-volume eruptions of the ten members of the CPT. There does not appear to be any systematic correlation between temperature and time through the eruption of the rhyolite units, except for the continuation of high temperatures. Findings from this study indicate that a continually ^{18}O depleted and hot eruptive center persisted in the central Snake River Plain from 12.8 to 8 Ma.

Rapid genesis of large "supervolcanic" volumes of silicic magmas in the upper crust based on microanalytical isotope investigation of crystals in eruptive products and numerical modeling of melting and segregation processes

Быстрая генерация больших "супервулканических" объёмов кислой магмы в верхней коре на основании микроаналитического изотопного изучения кристаллов в продуктах извержений и численного моделирования процессов плавления

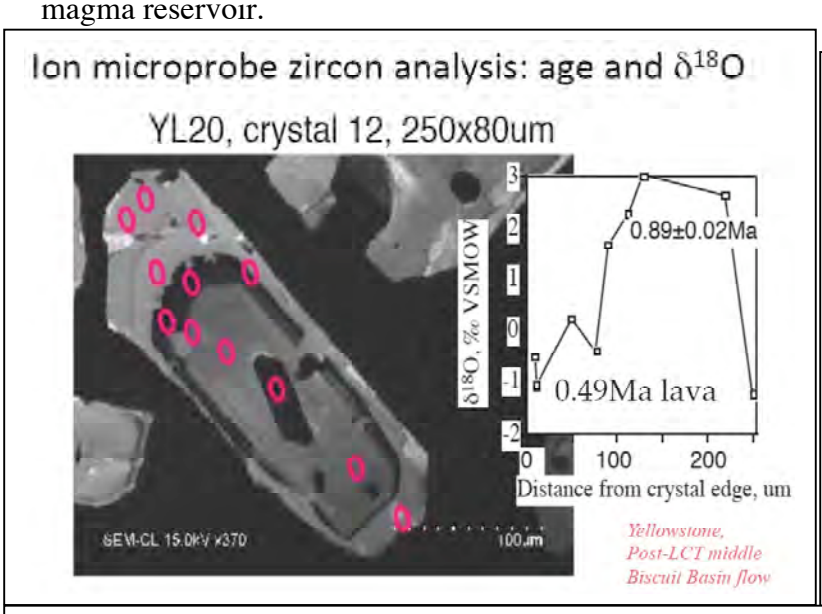
Bindeman[1] Ilya N., Watts[1] Kathryn E., Simakin[2] Alexander G.
Department of Geological Sciences, 1272 University of Oregon, Eugene OR 97403, USA, bindeman@uoregon.edu
[2]Institute of the Physics of the Earth, Russian Academy of Sciences, Moscow, Russia

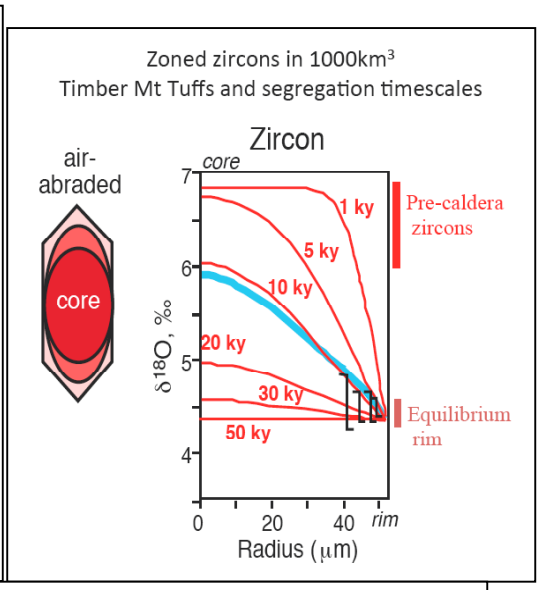
We present new results of *in-situ* geochronologic and isotopic investigation of zircons using SHRIMP and Cameca 1270-1280 large radius ion microprobes. We investigated isotopic variations of oxygen and determined U-Pb and U-Th geochronologic ages of Holocene and Pleistocene zircons from a variety of settings: intraplate high-silica rhyolites from Yellowstone, many older low and high-silica rhyolites from the Snake River Plain, dacites and rhyolites from Timber Mt Caldera, Nevada, silicic rocks from Iceland's largest silicic centers, and a silicic rocks from Kamchatka. Many of these units are additionally fingerprinted by low-$\delta^{18}O$ values, characteristic of meteoric waters. The origin of such isotopically-fingerprinted large-volume ignimbrites and smaller volume intra-caldera lavas requires shallow remelting of large volumes of variably ^{18}O-depleted volcanic and sub-volcanic rocks altered by hydrothermal activity. Zircons provide probes of these processes as they preserve older ages and inherited $\delta^{18}O$ values. In total we have a database exceeding 1000 $\delta^{18}O$ analyses of cores and rims of zircons coupled with their U-Pb and U-Th ages.

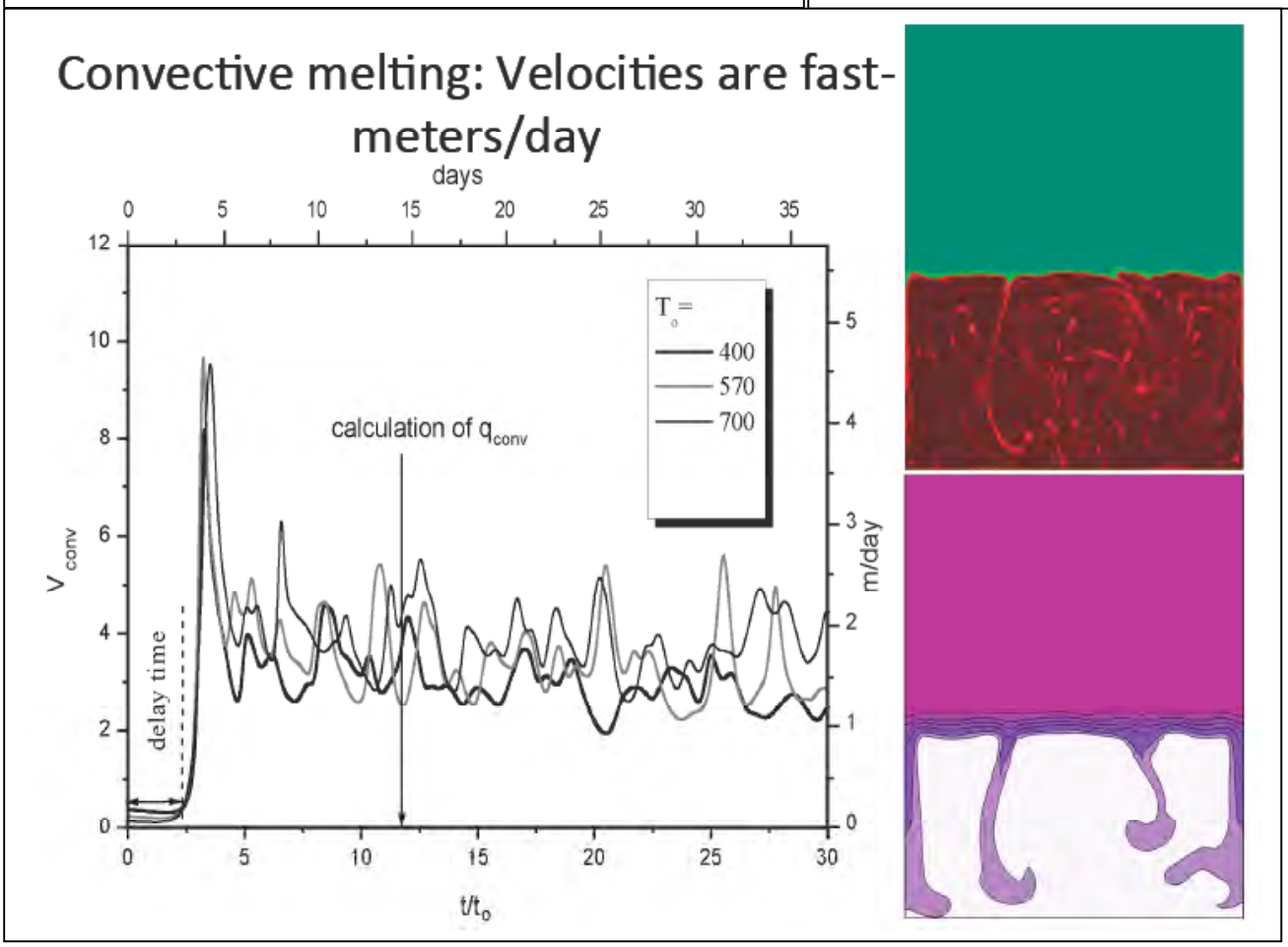
The results of this work provide the following new observations.
(1) Most zircons from post-caldera low-$\delta^{18}O$ lavas are zoned, with higher $\delta^{18}O$ values and highly variable U-Pb ages in the cores that suggest inheritance from pre-caldera rocks often exposed on the surface. (2) Many of the higher-$\delta^{18}O$ zircon cores in these lavas have U-Pb zircon crystallization ages that postdate caldera formation, but pre-date the eruption age by 10-20 kyr, and represent inheritance of unexposed post-caldera sub-volcanic units that have $\delta^{18}O$ similar to the caldera-forming tuffs. (3) intra-caldera lavas often contain zircons with both high-$\delta^{18}O$ and low $\delta^{18}O$ cores surrounded by an intermediate-$\delta^{18}O$ rim. This implies inheritance of a variety of rocks from high- $\delta^{18}O$ pre-caldera and low-$\delta^{18}O$ post-caldera units, followed by residence in a common intermediate- $\delta^{18}O$ melt prior to eruption. (4) Major ignimbrites also display significant ranges of ages and $\delta^{18}O$, but they diminish with increase in the magma residence time due to progressive annealing. (5) Mineral diffusive timescales estimates based on the initiation of melting to eruptive quench are in a few thousand years suggesting rapid silicic magma production rates of 0.1 to 0.5km^3/yr.

We also present a series of finite element numerical experiments on rhyolitic magma genesis by remelting in shallow crustal conditions using temperature ranges, appropriate phase diagram with defined dynamic eutectic zone, and physical and material parameters appropriate for these environments. The goal is to estimate conditions required and the scale of the remelting in the upper crust, describe the dynamics of the convecting melting, and compare it to the earlier

parametric and numerical attempts to model more generic silicic systems by underplating. The proposed model can explain the origin of crystal-poor "recycled" (750-850ºC) rhyolites with inherited crystal cargo. We advocate that the proposed mechanism can adequately explain rapid generation of large, supervolcanic volumes rhyolites through remelting of their erupted and subvolcanic predecessors and this process may proceed via multi-step, incremental batch assembly provided adequate magma supply rates from the mantle to the bottom of the silicic magma reservoir.







Upward Migration of Earthquake Swarms Beneath Mammoth Mountain, California -- Evidence for Movement of Magma in the Lower Crust?

David R. Shelly[1] and David P. Hill[1]
[1]*U.S. Geological Survey, Menlo Park, CA, USA*

Mammoth Mountain is a cluster of dacitic domes erupted between 100 to 50 ka standing on the southwest topographic rim of Long Valley caldera in eastern California. Among the signs of episodic unrest observed beneath the mountain since 1980 are brief swarms of lower-crustal, brittle-failure earthquakes, occurring at 20-30 km depth. Overlying these events are two distinct zones of seismicity: mid-crustal long-period earthquakes (10-20 km depth) and shallow brittle failure earthquakes (generally above 8 km). We suggest that the deep brittle-failure earthquakes are occurring within the more mafic lower crust, which can remain brittle to temperatures as high as ~700° C. The mid-crustal long-period earthquakes likely occur within the silicic crust, but below the rheological transition from brittle to plastic behavior, expected at temperatures of ~350 to 400° C. Above this transition are the shallow brittle-failure earthquakes.

Seismic waveform correlation analysis of deep swarms that occurred beneath Mammoth on June 16-17, 2006 and September 29-30, 2009 reveals that these swarms consist of hundreds of similar events, allowing us to identify and locate ~10 times the number of events in the Northern California Seismic Network (NCSN) catalog. For the 2009 episode, preliminary double-difference locations based on cross-correlation measurements suggest that the swarm occurred in a relatively small volume with dimensions of 1 km. Locations show a clear upward migration as the sequence progresses. This swarm occurred 6-8 km almost directly above the 2006 activity, suggesting a possible relationship between these swarms. We are currently exploring models that could link these patterns to stresses related to intrusion or pressurization in the lower crust.

FORMATION OF A ZONED MAGMA CHAMBER AND ITS TEMPORAL EVOLUTION DURING THE HISTORIC ERUPTIVE ACTIVITY OF TARUMAI VOLCANO, JAPAN: PETROLOGICAL IMPLICATIONS FOR A LONG-TERM FORECAST OF ERUPTIVE ACTIVITY OF AN ACTIVE VOLCANO

Mitsuhiro NAKAGAWA[1], Naoto HIRAGA[1, 2] & Ryuta FURUKAWA[3]

[1]: Division of Earth & Planetary System Science, Hokkaido University, Sapporo, Japan
[2]: Present address, Nittetsu Mining Company Ltd., Tokyo, Japan
[3]: Geological Survey of Japan/AIST, Tsukuba, Japan

Tarumai Volcano started a series of historic eruptive activity in AD 1667 after a dormancy of approximately 2000 years. The historic juvenile ejecta are mainly silicic andesite pumice associated with scoria, banded pumice and dome lava (SiO_2=55-63%), and are mixing products of two or three end-member magmas. In the initial largest plinian eruptions (AD 1667 period), simple mixing between two end-member magmas, silicic andesite (SA) and basalt, occurred. Large plinian eruptions (AD 1739 period) and the latest intermittent eruptions (AD 1804 – AD 1909: latest period) also produced mixed magmas including both the SA, intermediate-SiO_2 andesite (IA), and basalt. Magmatic temperatures of the SA and IA magmas are 900-950 ºC and approximately 1000 ºC, respectively. The rocks of each period form linear trends in oxide-oxide diagrams, suggesting that mixing of two end-member magmas occurred in each period. Thus, it can be estimated that the IA magma was formed by mixing between the basaltic and SA magmas. These relations suggest that the injection of the basaltic magma into the SA magma occurred before the AD 1667 period, resulting in the formation of a zoned magma chamber. These two magmas were then withdrawn to mingle, during the AD 1667 period. After the period, the zoned chamber was composed of an upper SA magma and a lower mixed IA magma. Chemical compositions of the basaltic magma have been slightly different in each period since AD 1667. In addition, the phenocrystic minerals of the IA magma also have changed as a consequence of re-equilibration with the more mafic IA bulk magma compositions present from AD 1739 to AD 1909. Thus, distinct basaltic magma has repeatedly injected into the zoned chamber before each eruption. Although the scale of eruptions became much smaller after the plinian eruptions of AD 1739, the ratio of IA magma in the latest eruptive materials is much larger than that in AD 1739 (Fig. 1), suggesting that a larger amount of the lower part (IA magma) of the zoned magma chamber was effectively withdrawn in the latest period. However, withdrawal depth should be much shallower in the latest activity compared with the activities in AD 1667 and AD 1739 because the tapping depth from a chamber strongly depends on eruption rate. Thus, it is hypothesized that most of the SA magma in the upper part of the zoned magma chamber was consumed in the AD 1667 and AD 1739 periods. The temporal change of the magma system suggests that a large plinian eruption similar to what occurred in AD 1667 or AD 1739 is unlikely in the near future because most of the major magma (SA magma) has already erupted. Because it took considerable time (ca. 2000 y) to accumulate a large volume of SA magma previously, we forecast that the volcano will enter a prolonged dormant period to accumulate voluminous SA magma for a next eruptive stage, or it will erupt only IA magma similar to the small eruptions that occurred during AD 1804 – 1909 (Nakagawa et al., in press).

References

Furukawa R. (1998) Ph D thesis Hokkaido University p212
Nakagawa et al. (in press) J. Volcanol. Geotherm. Res.

Local GeoInformatic Systems as a part of general project "Volcanic hazard of Kuril-Kamchatka island arc"

Klimenko E. [1], Muravyev Y. [2]

[1] Lomonosov Moscow State University, Moscow
[2] Institute of Volcanology and Seismology, Petropavlovsk-Kamchatsky

During recent years GIS-technologies were applied in many spheres. Extensive use of GIS-technologies in geosciences substantially enhanced efficiency of work and gave a possibility to solve complex problems which either demanded huge efforts or were insoluble before. On one hand modern GIS could be considered as a database of geographically referenced data that allows to store and analyze information of a study region. On the other hand it is a powerful tool for large data sets processing and deriving new information on this basis.

GIS creation for the territory of active volcanism provides a possibility to collect and classify information of past eruptive activity of studied volcanoes, perform spatial analysis on the basis of measurements in points, make models of volcanic ash distribution, formation of pyroclastic and lava flows, lahar descends etc. As a result by means of GIS-technologies natural hazard risk assessment for the territory adjacent to a volcano can be performed.

Since 2009 the complex GIS "Volcanic hazard of Kuril-Kamchatka island arc" has been created in the Institute of Volcanology and Seismology located in Petropavlovsk-Kamchatsky. It includes the following blocks:

- The first one contains a set of thematic small-scale maps presenting a general information of the physiographic conditions and volcanic activity of the research area.
- The second block consists of large-scale independent GIS projects dedicated to certain volcanoes or groups of volcanoes. They could be used as a valid basis for numerical analysis and modeling of the processes accompanying volcanic eruptions.

To date such systems have been developed for Northern group of volcanoes of Kamchatka Peninsula and for Kizimen volcano that recently resumed its eruptive activity.

The GIS of the North group of volcanoes contains data of recent eruptions of four main active volcanoes – Kluichevskoy, Bezymianniy, Shiveluch and Tolbachik. Moreover, within its bounds we have defined some thematic blocks such as glaciological block where the glaciation monitoring could be held or the block for lahar danger assessment.

Regarding Kizimen volcano GIS creation we mainly focused on its latest eruption. Using satellite images (ASTER), data of field observations, and ArcGIS tools for spatial analysis we have defined the territory exposed to ash falls, reconstructed their intensity and calculated the approximate volume of emitted material and the area of its distribution. Moreover, the data base of given GIS project also includes information of previous eruptions of Kizimen volcano.

Локальные ГИС в структуре общего проекта «Вулканоопасность Курило-Камчатской островной дуги»

Клименко Е.С.[1], Муравьев Я.Д.[2]
[1] Московский Государственный Университет им.М.В. Ломоносова, г. Москва
[2] Институт Вулканологии и Сейсмологии ДВО РАН, г. Петропавловск-Камчатский

Развитие ГИС-технологий и их последующее широкое распространение в современном мире сделало возможным решение многих проблем наук о Земле и существенно повысило оперативность работ, выполнение которых раньше казалось невозможным или же требовало больших затрат сил и времени. Современные ГИС, с одной стороны, можно рассматривать как базу географически привязанных данных, позволяющих накапливать и сопоставлять информацию о районе исследования, а с другой, как мощный инструмент обработки этих данных и получения новых сведений на их основе.

Так, создание ГИС для территорий активного вулканизма дает возможность собрать воедино весь ранее накопленный материал о прошлой эруптивной активности изучаемых вулканов, выполнить пространственный анализ данных на основе точечных измерений, создать модели распределения отложений пепла, образования пирокластических и лавовых потоков, схода лахаров и т.п. Комплексный анализ в системе базы данных ГИС позволяет перейти к оперативной оценке природного риска для территории, попадающей под влияние извержения вулкана в зависимости от сценария его развития.

С 2009 г. в Институте Вулканологии и Сейсмологии ДВО РАН, г. Петропавловск-Камчатский, началось создание комплексной ГИС «Вулканоопасность Курило-Камчатской островной дуги», которая содержит:

- Блок тематических мелкомасштабных карт, дающих общее представление о физико-географических условиях и вулканической активности исследуемой территории
- Крупномасштабные независимые ГИС отдельных вулканов или групп вулканов, представляющие собой полноценную базу для анализа и моделирования процессов, сопровождающих извержения

Сегодня ведется активная разработка локальных ГИС для Северной группы вулканов п-ова Камчатка, а также для вулкана Кизимен, возобновившего эруптивную активность в конце ноября 2010 г.

На сегодняшний момент ГИС Северной группы вулканов уже содержит информацию как об исторических, так и о недавних извержениях четырех активных вулканов – Ключевского, Безымянного, Шивелуча и Толбачика. Также в ее рамках созданы специальные тематические блоки: например, гляциологический блок, где проводится мониторинг оледенения вулканов, или блок, посвященный лахароопасности.

Основное внимание при создании ГИС вулкана Кизимен уделяется его последнему извержению. Основываясь на данных полевых исследований и материалах космической съемки (ASTER) с помощью инструментов пространственного анализа программы ArcGIS 9.3, нам удалось выделить территорию, подверженную пеплопадам, восстановить их интенсивность, рассчитать примерный объем изверженного пепла, а также площадь их распространения. Кроме того, слои базы данных ГИС вekrfyf Кизимен содержат информацию о предыдущих крупных извержениях вулкана.

Microseismic profile across Tolbachik Dol (Kamchatka)

Yu.A. Kugaenko[1], V.A. Saltykov[1], I.F. Abkadyrov[2], A.V. Gorbatikov[3], M.Yu. Stepanova[3]

1 Kamchatka Branch of the Geophysical Survey, RAS, Petropavlovsk-Kamchatsky, Russia, e-mail: ku@emsd.ru
2 Institute of Volcanology and Seismology, FEB RAS, Petropavlovsk-Kamchatsky, Russia
3 Schmidt Joint Institute of Physics of the Earth, RAS, Moscow, Russia

Deep section up to 20 km, which reflects the distribution of relative velocities of transversal seismic waves, was constructed for the profile across Tolbachik Dol using the method of low-frequency microseismic sounding (fig.1). Tolbachik Dol is the southern regional zone of cinder cones of Plosky Tolbachik volcano in the southwestern sector of the Kluchevskaya group of volcanoes (Kamchatka). Last eruption within Tolbachik Dol is the Great Tolbachik fissure eruption 1975-76, included Northern and Southern vents [4]. Microseismic profile with the length 14 km crossed Tolbachik Dol through cinder cones of Northern vent.

In order to reconstruct the deep structure, we have chosen the method of microseismic sounding [1, 2], in which surface Rayleigh waves of different frequencies play the role of sounding signals. The waves determine the main contribution to the vertical component of the Earth's microseismic field. The geological structures presenting the velocity inhomogeneities interact with the incident Rayleigh waves (refraction, exchange, scattering) and distort the amplitude spectrum of the microseismic field in their vicinity. Spectral amplitudes of specific frequency f decrease at the Earth's surface over high velocity anomalies and increase over low velocity anomalies. It was found experimentally and in the model calculations that frequency f is related to the depth of inhomogeneity H and velocity of the fundamental mode of the Rayleigh wave $V_R(f)$ according to expression $H = 0.4V_R(f)/f$. This method was successfully tested in volcanic area [3] and some other geological objects of various scales and genesis. Wide-band digital velocimeters Guralp CMG-6TD (frequency range 0.03–50 Hz) were used for recording. We note that the selection of this method was to a great extent determined by the fact of its realization in difficult landscape conditions of the studied territory taking into account the difficulties in access to it.

Detected heterogeneities of the deep structure were interpreted by using of the results of the Great Tolbachik fissure eruption study. Some new features of the deep structure of magma conduits were found.

Supported by Russian Foundation for Basic Research (Grants 10-05-100059, 10-05-00139).

References

1. Gorbatikov A. V , M. Yu. Stepanova, and G. E. Korablev (2008) Microseismic Field Affected by Local Geological Heterogeneities and Microseismic Sounding of the Medium, *Izvestiya, Physics of the Solid Earth*, Vol. 44, No. 7, pp. 577–592.

2. Gorbatikov A. V., Tsukanov A. A. (2011) Simulation of the Rayleigh Waves in the Proximity of the Scattering Velocity Heterogeneities. Exploring the Capabilities of the Microseismic Sounding Method. *Izvestiya, Physics of the Solid Earth*, Vol. 47, No. 4, pp. 354–368.

3. Gorbatikov, A.V., Kalinina, A.V., Volkov, V.A., Arnoso J., Vieira R., Velez E. (2004) Results of Analysis of Data of Microseismic Survey at Lanzarote Island, Canary, Spain // *Pure appl. Geophys*. V. 161. P. 1561–1578.

4. The 1976-1976 Large Tolbachik Fissure Eruption in Kamchatka. Moscow: Nauka, 1984. 638 p.

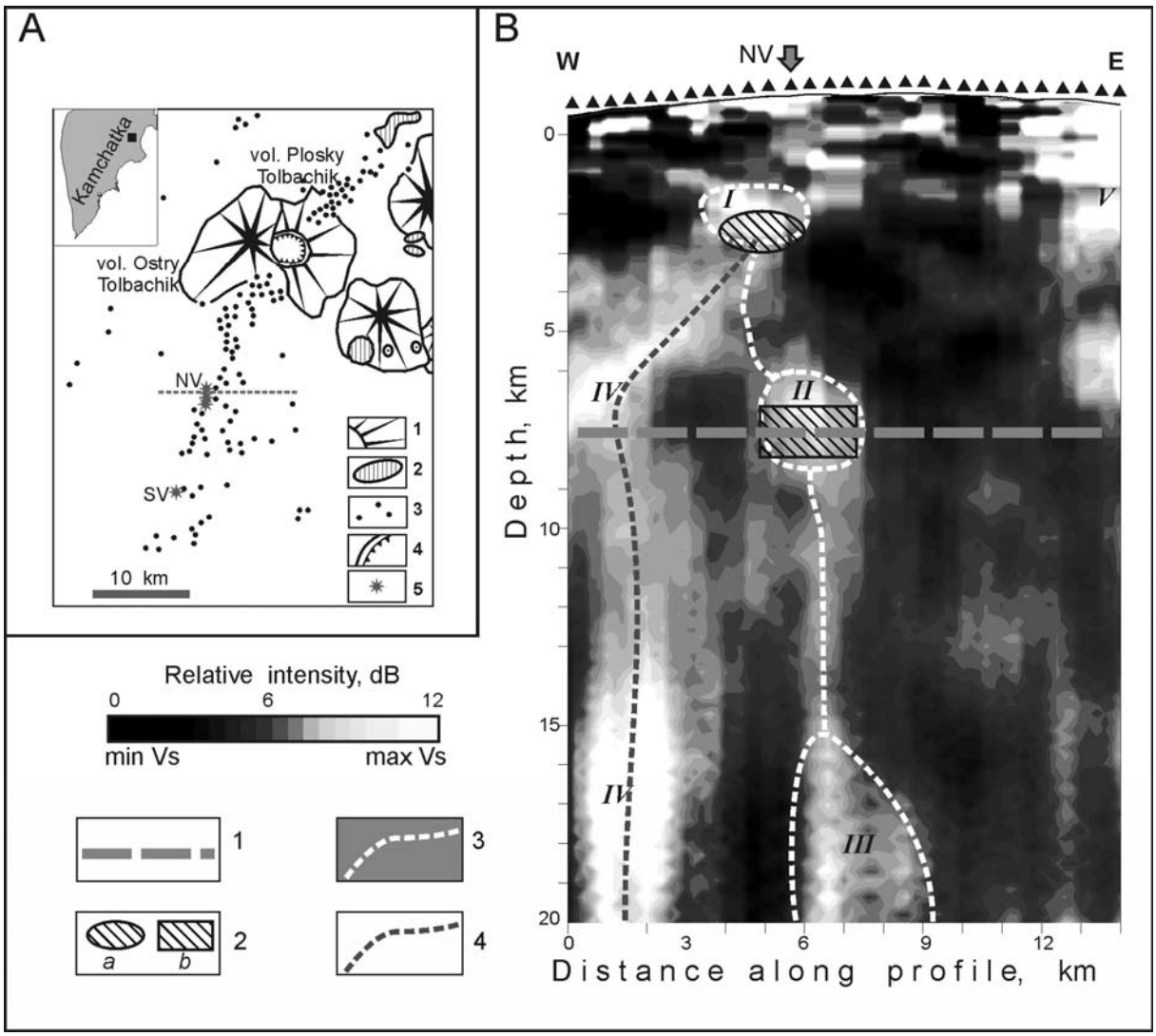


Fig.1. Investigated area and results of microseismic sounding.
A - Southwestern sector of the Kluchevskaya group of volcanoes. The dashed line - microseismic profile. 1 – cones of stratovolcanoes; 2 – exstrusions; 3 – Holocene cinder cones; 4 – calderas; 5 – New Tolbachik volcanoes of 1975-76 Great Tolbachik fissure eruption (NV - Northern vent, SV - Southern vent).
B - Deep section along microseismic profile, presented in the parameters of relative velocities of transversal seismic waves. ***I – V*** – low-velocity areas, detected by the method of microseismic sounding. 1 – the boundary of the crystal basement ; 2 – magma chambers under Northern vent on the depth 2-3 km (a) and 7-8 km (b) according to [4]; 3 – the main magma conduit of Northern vent with the proposed magma chambers ***I***, ***II*** and ***III***; 4 – possible alternative way for magma motion to the chamber ***I*** through low-velocity area ***IV***.

Special Circumstances: geophysical and geochemical evidence for an auxiliary magma source of Klyuchevskoy volcano lavas

Alex Nikulin[1], Vadim Levin[1], Michael Carr[1], Claude Herzberg[1] and Michael West[2].

1Rutgers University, Department of Earth and Planetary Sciences, 610 Taylor Rd., Piscataway, NJ 08854.
2University of Alaska, Fairbanks, Geophysical Institute, 903 Koyukuk Dr., Fairbanks, AK 99775.

Volcanoes of Central Kamchatka Depression (CKD) form the most active arc volcano system in the world, and among them the Klyuchevskoy volcanic group (KG) stands out as the single most vigorous volcanic center. Notably, the tectonic setting of the KG is far from the textbook case. Besides being close to the junction of two major plate boundaries (the Kamchatka subduction zone and the locally transcurrent Aleutian Arc), the KG has one of the largest distances (>170 km) to the top of the subducting plate where the flux feeding arc magmatism is expected to arise.

A number of geophysical observations suggest complexity of the upper mantle structure beneath the KG. Early studies of regional seismic wave attenuation, tomographic imaging, and, most recently, studies of the mode-converted body waves all point to the presence of a region of distinct seismological properties at depths ~100 km. This region may be best characterized as a planar body with lower seismic velocity that is bound by relatively sharp (~2 km) gradients in seismic properties, has a thickness of a few tens of km, and appears to dip to the north. This body is clearly separate from the subducting Pacific plate.

The geochemical signature of KG lavas has been studied extensively. Very high rate of magma production, a clear subduction signature, extremely high δ - O^{18} and H_2O content, a lack of slab-melt and sediment inputs all have been noted. On the basis of its first-order geochemistry, the KG is a quintessential island arc volcano. A well-recognized distinctive feature of the KG is the simultaneous eruption of low-Al and high-Al lavas, a fact that inspired numerous explanations. Using recently compiled databases of geochemical analyses (specifically, GEOROC) we report a previously un-noted bi-modal distribution of Zr/Nb concentration ratios in lavas of the Klyuchevskoy Group. In Central America, this ratio correlates closely with the depth to the slab, growing larger as the slab becomes less deep. We speculate that distinct values of Zr/Nb ratios derive from different depths beneath the KG as well.

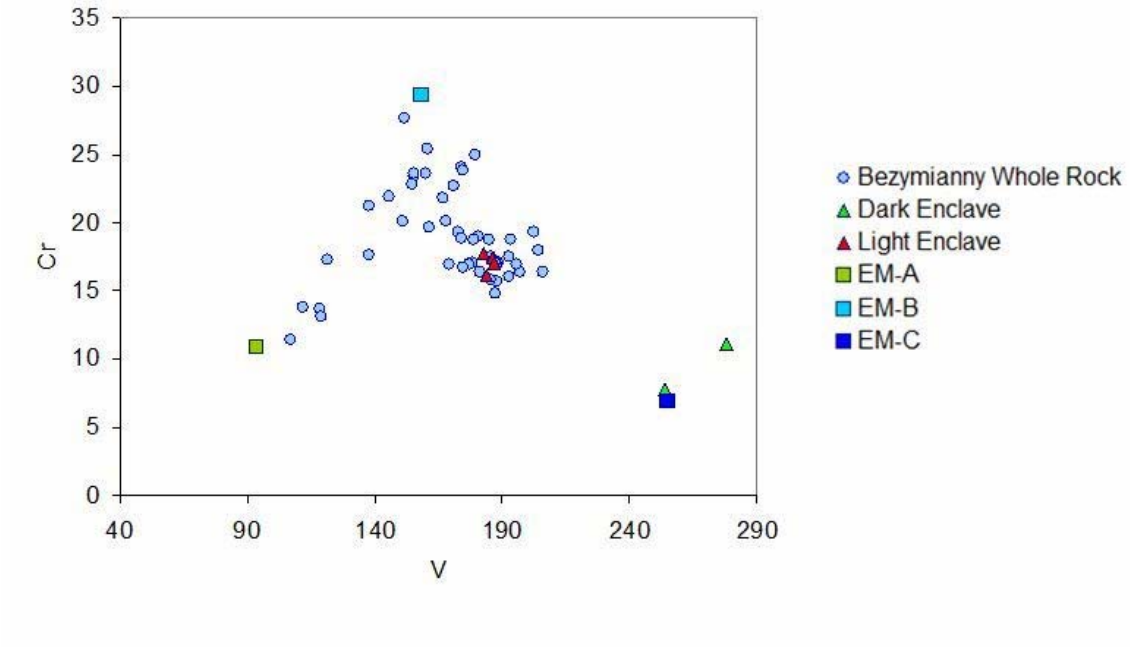
On the basis of our geophysical results combined with geochemical evidence we argue for the presence of a distinct body of rock ~100 km deep in the upper mantle beneath the KG, that contributes magmas to the volcanic center. The origin of this body is enigmatic, with possible explanations being a fragment of the previously subducted lithosphere that has been left behind due to plate boundary reorganization, or alternatively a plume of sediments originating from the subducting slab and propagating into the wedge.

Trace element constraints on the origin of magma diversity at Bezymianny volcano, Kamchatka

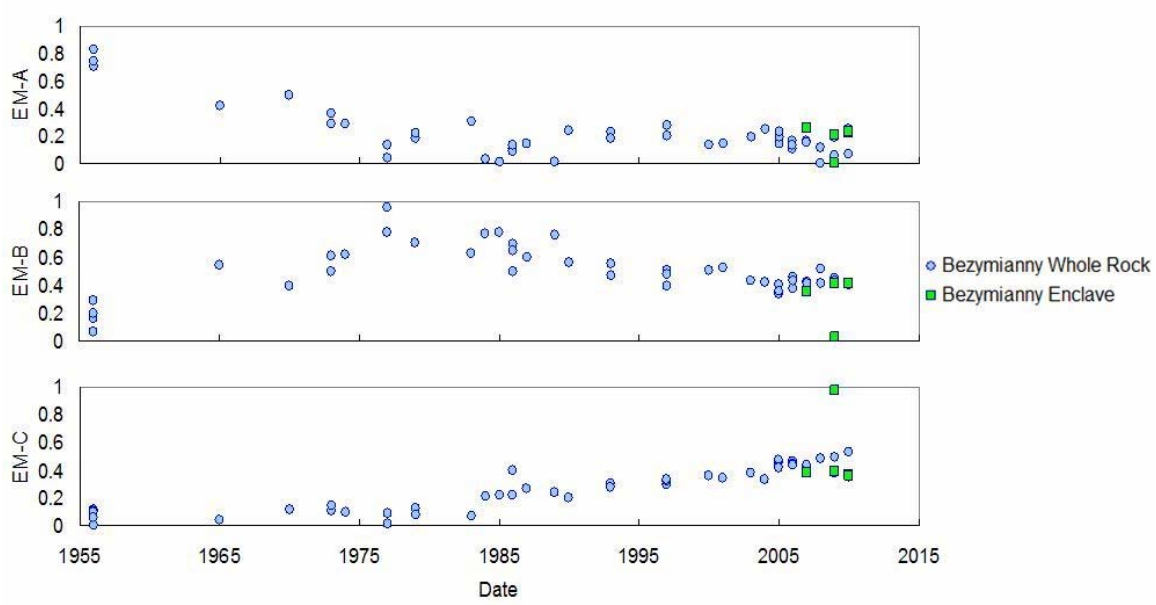
Stephen Turner[1], Jill Shipman[2], Pavel Izbekov[2], and Charles Langmuir[1]

[1]Harvard University, Cambridge, MA. USA.
[2]Geophysical Institute, Alaska Volcano Observatory, University of Alaska Fairbanks, Fairbanks, AK. USA.

Bezymianny volcano has erupted repeatedly since 1956, providing an opportunity to study real-time processes affecting the chemical evolution of an arc volcano. This work incorporates trace element analyses into the ongoing geochemical and petrological investigation of Bezymianny volcano, Kamchatka. Previous work (e.g. Shipman et al, 2006 & Izbekov et al, 2006) demonstrated a rapid change in major element compositions of the magma since 1956. This trend is characterized by a shift from more silicic magma in 1956 (~60.4% SiO2) to more mafic compositions (e.g. 56.45% SiO2 in 2007). Recent eruptive products contain both light and dark colored enclaves, which have also been analyzed for major and trace elements. Trends on element-element variation diagrams support a model in which at least three mixing end-members are combined in various proportions to produce the range of compositional variation seen in the data (figure 1).



Principal component analysis of the dataset, following Weltje (1997), shows that three end-members can reproduce analytical results to within error for 41 elements measured in 53 samples. End-member compositions were determined from the principal component vectors via a least squares fit, enabling the calculation of end-member mixing proportions for each erupted magma. The end-member mixing proportions vary systematically between 1956 and 2010, with maximums for end-members A, B and C during 1956, ~1979, and 2010, respectively (figure 2).



The light colored enclaves are easily reproduced by the calculated mixing end-members, though via different mixing proportions than their host magmas. Two of the dark colored enclaves are likely candidates for end member C.

Measured major element compositions of phenocrysts, combined with published trace element partition coefficients, are used to demonstrate that each of the three end members may have evolved from a common parental magma, provided that their liquid lines of descent differ. The compositional variation of the end members was most likely produced by storage and evolution of a parental magma at three discreet pressures, resulting in fractionation of different mineral assemblages and proportions. The bimodal distribution of amphibole compositions lends additional support to this hypothesis. Systematic variations of the end member proportions through time are consistent with a model in which three magma bodies are connected in series. End member A, presumably stored in the reservoir most directly connected to the vent, dominated the erupted magma compositions in 1956. By 1979, this first reservoir was almost entirely diluted as it drew from a second reservoir initially containing magma with the composition of end-member B. By the 1980s, erupted magmas started to contain detectable quantities of end member C, though this magma may have begun to infiltrate the lower reservoir at any point. Presently, erupted host magmas are a mixture of end members B and C.

References

1) Shipman, J. S., and PIRE team (2006) Compositional and Textural Trends at Bezymianny Volcano, Kamchatka, Russia 1956 to 2006: Implications for Magma Storage and Eruption Response at Volcanoes That Have Experienced Edifice Collapse. Eos Trans. AGU, 87(52), Fall Meet. Suppl., Abstract V24A-03.

2) Izbekov, P., Eichelberger, J., Belousova, M., Ozerov, A., and PIRE team (2006) Post-collapse trends at Bezymianny Volcano, Kamchatka, Russia and the May 6, 2006 eruption. Eos Trans. AGU, 87(52), Fall Meet. Suppl., Abstract V11B-0576.

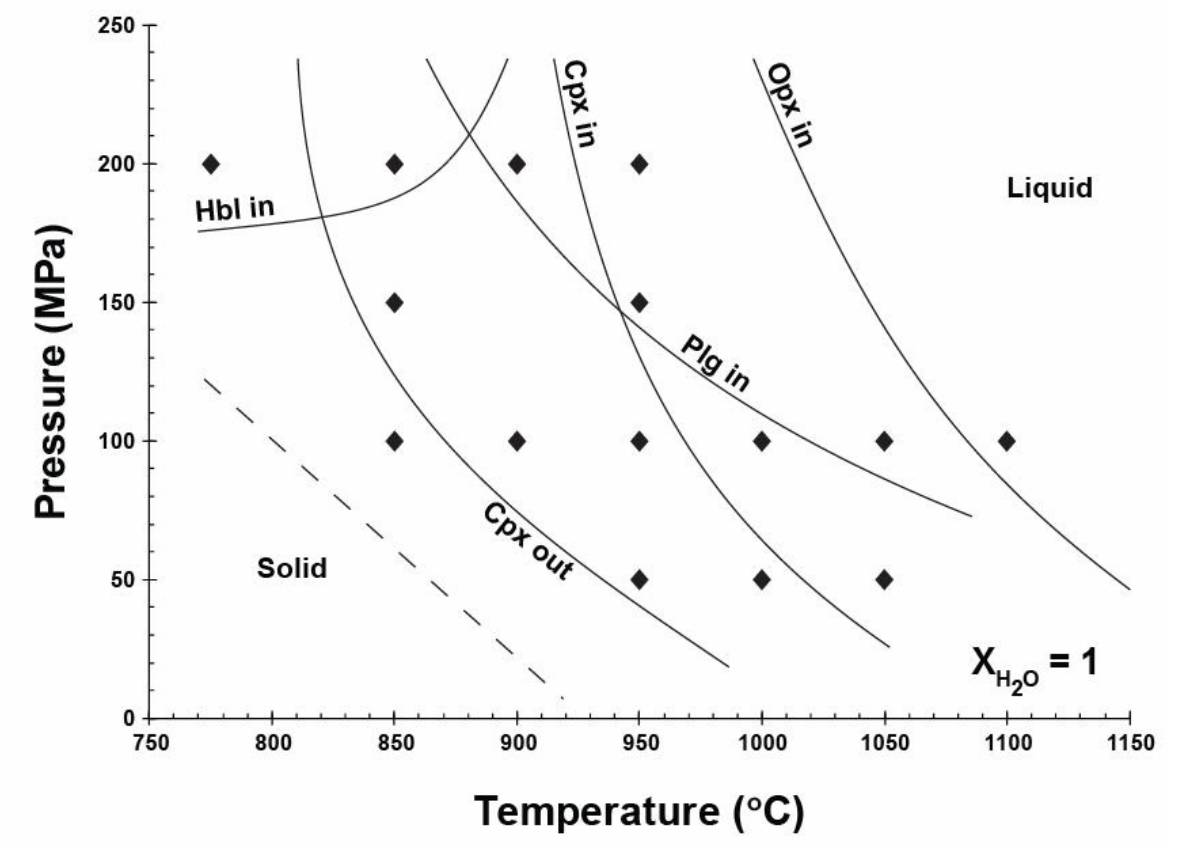
3) Weltje, G.J. (1997) End-member modelling of compositional data: Numerical-statistical algorithms for solving the explicit mixing problem. Journal of Mathematical Geology, 29, 503-549.

Phase equilibria constraints on pre-eruptive conditions of the 1956 Bezymianny magma

Vasily D. Shchebakov[1], Owen K. Neill[2], Pavel E. Izbekov[2], Pavel Yu. Plechov[1]
[1]Geological department of Lomonosov Moscow State University, Moscow, Russia
[2]Geophysical Institute, University of Alaska, Fairbanks, Alaska, USA

Phase equilibria experiments were conducted to constraint pre-eruptive conditions of 1956 magma. Experimental conditions were in range 775-1100°C and 50-200 MPa, water-saturated conditions and NNO oxygen buffer. Lightly crushed sample from 1956 pyroclastic flow was used as starting material. Experiments were conducted in TZM and Renee type pressure vessels, duration of the experiments varied from 8-12 h to 165 h at high-T and low-T conditions respectively.

Hornblende is stable at pressure above 200 MPa and temperature below 900°C (Figure 1).



Natural phenocrysts assemblage of 1956 andesite, which contains plagioclase, hornblende, orthopyroxene is reproduced at 850°C and 200 MPa, however clinopyroxene common in experimental run at those conditions is almost absent in natural assemblage.

Experimental glass compositions show clear variations of all major elements content with T-P conditions. Matrix glass composition is poor in CaO and MgO and SiO_2 and K_2O rich which indicates that magma last equilibrated at low pressures (less than 50 MPa). Melt inclusions composition show much wider variations comparing to matrix glass which probably indicates that magma experienced long crystallization history at wide T-P range.

Crystallization at wide range of pressures is also indicated by wide range of aluminum content in natural hornblende phenocrysts, which usually have high-Al core and relatively low-Al rim. Total range of Al_2O_3 variations is 8-14 wt. %.

Morphometry and dynamic of the destruction of Pleistocene-Holocene cinder cones in Kamchatka

Melnikov D[1]., Gilichinsky M[2]., Melekestsev I[1]., Inbar M. [3]

[1]Institute of volcanology and seismology FEB RAS, Petropavlovsk-Kamchatsky, Russia
[2]Department of Forest Resource Management, SLU, SE-901 83 Umea, Sweden
[3]Department of Geography and Environmental Studies, University of Haifa, Haifa, Israel

Cinder cones are the simplest and most frequently found forms of volcanic landscape. Usually they are located in the areas of monogenetic (areal) volcanism, may have different age and structure; they may be located in different climatic conditions and represent the perfect possibility to study the processes of their destruction and changes of landscape from the moment of the cinder cone formation until the current time.

Here we present the morphometric parameters of more than 200 monogenetic cinder cones in Kamchatka. The methodic of the calculations of the main morphometric characteristics is unified on a base of the digital models of landscape of the various spatial resolution; the estimates of the precision of the models are done. On a base of the satellite interferometry (ALOS PALSAR) the parameters of deformations of the contemporary cinder cones of the Big Fissure Tolbachic eruption are evaluated. The dependence of the morphometric characteristics of cinder cones and their age is determined.

Sharp tectonic and volcanic unrest at 2800-2900 ^{14}C BP – evidences from river terrace and monogenetic volcanoes dating

Oleg Dirksen[1], Christel van den Bogaard[2], Tohru Danhara[3], Bernhard Diekmann[4].
1- Institute of Volcanology and Seismology, Petropavlovsk-Kamchatsky, Russia, dirksen@kscnet.ru;
2 - Leibniz Institut fur Meereswissenschaften (IFM-GEOMAR), Kiel, Germany
3- Kyoto Fission Track Co. Ltd., Kyoto, Japan;
4- Alfred-Wegener-Institut für Polar- und Meeresforschung (AWI), Potsdam, Germany

Tephrochronological investigations conducted under the umbrella of KALMAR project have allowed us to determine the age of the lake and river terraces as well as date the paleolandslides, i.e. the events which trace the tectonic activity, at northern (Two-Yurts lake) and southern (Three sister river) parts of Kamchatka. We also correlated the results with previously obtained data on other parts of Kamchatka to get a regional time-schedule of tectonic and volcanic activity.

Detail study of distal tephras around Two-Yurts lake established the main marker ash layers at this area. These are the ashes of different Kamchatka volcanoes: Shiveluch, 900, 1400, 1750, 2800, 4700, 4800 and 8300 ^{14}C BP; Ksudach, 1800 ^{14}C BP, Avachinsky, ca 2000 ^{14}C BP, Klyuchevskoy 2850 ^{14}C BP, and Khangar, 6900 ^{14}C BP. The main ash markers for Three Sister river are the tephras of Ksudach (1000 ^{14}C BP), Khodutka (2500 ^{14}C BP), Dikii Greben (4500 ^{14}C BP) volcanoes and Kuril lake caldera (7600 ^{14}C BP). We used these local tephrastratigraphical scales to reconstruct the timing of landscape change, in particular to date the formation of lake and river terraces and the landslide events. Both features can be regarded as indicators of increased tectonic activity.

The oldest Holocene lake terrace found near Two-Yurts lake is ca. 3 m high above the present day level of the lake. The age of the terrace is about 2900-3000 ^{14}C BP. Two younger terraces of 0.5 m and 1 m height reveal an age of about 1000 and less than 900 ^{14}C BP. We also found several Holocene landslides which probably were the results of strong earthquakes which, in turn, could also testify for tectonic activity. The ages of landslides were estimated as ca. 4000, 2900 and 2000-2100 ^{14}C BP. At the southernmost tip of Kamchatka, at Three sister river valley, we found two terraces, which have ages of 8000 and 2800-2900 ^{14}C yrs, respectively.

At the junction of Levaya Avacha and Vershinskaya rivers we discovered six river terraces. They are either 1, 1.5, 2, 4, 7.5 and 11 m above the recent holm. The ages of these terraces are about 600, 2000, 2900, 7500 and 9000 ^{14}C BP, respectively. At Savan river we have dated seven terraces. The age of three older terraces range from 10000 to 8300 14C BP. The other four are 4300, 2900, 2600 and 1000 ^{14}C years old.

Thus, two main stages of tectonic activity can be distinguished for the most part of the peninsula: Early Holocene (8000 – 10000 ^{14}C BP) and Late Holocene (2900 – 600 ^{14}C BP) separated by a mid-Holocene tectonic repose period (3000 – 8000 ^{14}C BP). These periods of unrest are characterized by numerous tectonic movements that resulted in sequences of river and lake terraces and landslides. The most dramatic event was the beginning of the Late Holocene stage. According to our data, the sharp increase of tectonic activity occurred at 2800 – 2900 ^{14}C BP at southern, eastern and northern parts of Kamchatka. Tectonic movements ca 2900-3000 ^{14}C BP were detected for the Central Kamchatka Depression (Pevzner et al., 2006). It was also the time of sharp increase of volcanic activity. Several large monogenetic volcanoes erupted 2800-2900 ^{14}C BP at Tolmachev Dol, upper stream of Avacha river, Sedankinsky Dol, and probably Tolbachinsky Dol (Dirksen, Melekestsev, 1999, Dirksen et al., 2003, etc.). Strong eruptions of stratovolcanoes also occurred at that time(Bazanova et al., 2005, Ponomareva et al., 2007, etc.). Thus, we suppose, that the time of 2800-2900 ^{14}C BP could be regarded as a time of whole-Kamchatka sharp and sudden increase of tectonic and volcanic activity.

The study was supported by KALMAR project as well as DFG and RFBR grants.

References:

Bazanova, L. I., Braitseva O. A., Dirksen O.V., Sulerzhitsky L. D., and Danhara T., (2005) Ashfalls from the largest Holocene eruptions along the Ust'-Bol'sheretsk - Petropavlovsk-Kamchatsky traverse: sources, chronology, recurrence. Volcanol. and Seismol., (6), 30–46, (In Russian)

Dirksen, O. V., Melekestsev I. V., (1999), Chronology, evolution and morphology of plateau basalt eruptive centers in Avacha River area, Kamchatka, Russia, Volcanol and Seismol., 21(1), 1–28.

Dirksen, O., Bazanova L., Portnyagin M., (2003), Chronology of the volcanic activity in the northern part of Sredinny Range (Sedanka lava field) in the Holocene, in Volcanism and geodynamics, Materials of the II Russian symposium on volcanology and paleovolcanology, Ekaterinburg, 871–874.

Pevzner, M. M., Ponomareva V. V., Sulerzhitsky L. D., (2006), Holocene soil-pyroclastic successions of the Central Kamchatka depression: ages, structure, depositional features, Volcanol. and Seismol., (1), 24–38, (In Russian).

Ponomareva V.V., Kyle P.R., Pevzner M.M., Sulerzhitsky L.D., Hartman M., (2007) Holocene eruptive history of Shiveluch volcano. Kamchatka Peninsula. In: Eichelberger J., Gordeev E., Kasahara M., Izbekov P., Lees J.(Eds) "Volcanism and Subduction: The Kamchatka Region", American Geophysical Union Geophysical Monograph Series, Volume 172: 263-282.

Crustal deformation due to volcanic activity by continuous GPS observation network in Shinmoedake, Kirishima, Japan

Shigeru Nakao[1], Yuichi Morita[2], Kazuhiko Goto[1], Hiroshi Yakiwara[1], Shuichirou Hirano[1], Jun Oikawa[2], Hideki Ueda[3], Tomofumi Kozono[3], Yasuhiro Hirata[2], Hiroaki Takahashi[4], Yusaku Ohta[5], Takeshi Matsushima[6], Masato Iguchi[7]

1Kagoshima University, 2ERI, University of Tokyo, 3NIED, 4Hokkaido University, 5Tohoku Univesity, 6Kyushu University, 7DPRI, Kyoto University

Kirishima volcano is one of the active volcanoes in southern Kyushu, Japan and is categorized into a composite volcano whose active summits are Shinmoe-dake and Ohachi. It started to erupt at Shinmoe-dake on 19 January, 2011, and was followed by sub-Pulinian eruption on 27 January. Eruptive activity gradually ceased since February 2, and moved to Vulcanian activities. Recently eruptions become rare, but crustal deformation due to magma recharge at the reservoir is going on. We have deployed continuous GPS network around the volcano. The crustal deformation related to the eruption is presented in this paper.

We deployed three GPS sites, which are KVO, KRSP and YMNK on March in 2007 and added a station KKCD on October, 2010. NIED installed two stations: KRMV and KRHV in April, 2010. GSJ manages three GEONET(nation-wide GPS network) stations around the volcano. Kyoto Univ. has been installed a station YOSG northwestward of the summit. Therefore, 10 stations were in operation before the eruption within distance of 20km from the summit. Bernese GPS Software Ver. 5.0 is used for the analysis for all data. After the sub-Pulinian eruption, six GPS sites were additionally installed and we can use dense GPS network to study the ground deformation related to a series of the volcanic eruption.

Before the eruption, extension of baseline length started on December 2009. However, acceleration was not observed from October 7, 2010 to January 25, 2011, an inflation source is found at the depth of 9.7km beneath the point of about xx km WNW-ward from the summit. The volume is 6.8 million cubic meter under the assumption of Mogi's model. The total volume charged at the source is estimated 32 million cubic meters, if we can assume the accumulation rate was constant. An abrupt volume change of the source was observed during the sub-Pulinian eruption. The Volume defect reached to 24 million cubic meters, that is the almost coincide with the estimated equivalent magma volume emitted during the sub-Pulinian episode. Then, the magma began to be recharged again at the source.

Even in the recent time, the inflation of the source continues and magma may be recharged. It shows that the volcano has still potential to erupt in the following stage. We would like to reveal the relation between the process of magma charge and the following eruption.

Crustal structure around the source area of the 1952 Tokachi-oki earthquake, off Hokkaido, by an airgun-OBS seismic experiment

R. Azuma[1], Y. Murai[1], K. Mochizuki[2]
[1]ISV, Hokkaido Univ., Sapporo, Japan, [2]ERI, Univ. of Tokyo, Tokyo, Japan

We conducted an airgun-OBS (Ocean Bottom Seismometer) seismic experiment between the Tokachi-oki and the Nemuro-oki seismogenic segments in August 2010. Airgun shooting was operated along two lines; one is parallel to the Kuril Trench axis and runs ~50 km landward from the trench axis, and another crosses the trench axis at the Nemuro-oki segment. The seismic lines stride the source area of the 1952 Tokachi-oki interplate earthquake (M8.2), where the largest amount of coseismic slip of 7 m occurred at the eastern central part of the line. The corresponding area didn't slip during the 2003 Tokachi-oki earthquake (M8.0) which is thought as a repeater of the former event. This slip difference in each event can be caused by a physical condition on the plate boundary, such as the topography of the slab surface, the existence of the low velocity layer on the subducting plate. The object of this experiment is to investigate the relation between the seismic structure and the interplate rupture area.

OBSs recorded clear airgun signals and imply a structural difference bounded on the central part of the line. All OBSs observed clear fast arrivals; ~4.0 km/s within the offset 25 km, ~5.2 km/s between the offset 20 to 40 km, rapidly increase to > 7.2 km/s around the offset 40 km. The fast arrivals of most OBSs image a shadow zone around the offset 40 km, which is more definite at the western OBSs. Several later phases were observed within the offset 40 km but not so clear to pick at the western OBSs.

We run a first arrival travel time inversion method, after detecting the Vp in the sedimentary layer by a forward approach. Obtained Vp model showed the along-arc variation of Vp in the island arc crust which faces on the subducted Pacific Plate. In addition the along-arc difference in discontinuity of fast arrivals, those differences correspond to a structural difference between the 1952 rupture area and its surrounding area. We expect that further analyses using travel time and wave form data will extract lateral structural variation related to the extent of rupture area.

The spatial grouping features of the Kamchatka's earthquake hypocenters

A.N. Krolevets
Far East State Technical University in Petropavlovsk-Kamchatsky
A.M. Makeev
Vitus Bering Kamchatka State University, Petropavlovsk-Kamchatsky, an@kamgpu.ru

Algorithm and the computer program were presented in paper [1] intended to reveal spatial grouping planes of the earthquake hypocenters. At present the program is capable to find the hypocenters grouping planes on basis of formal criteria. However the problem remains open whether grouping on some of planes that has been found are casual. The purpose of the present work is dedicated to make clear the question on basis of seismic data for the Kamchatka region.

The GS RAN catalogue records of the Kamchatka's earthquakes were the raw data for analysis. The earthquakes were selected with the energy class AE 9, with date interval from 1962.01.01 to 2003.12.31, and which hit in spatial window with the borders in the latitude 51°N $\leq\varphi_0\leq$57°N, and in the longitude 156°E $\leq\lambda_0\leq$166°E. The Cartesian coordinate system was used for searching the planes [2]. The home of the system was positioned on the Earth surface point with geographical coordinates λ_0=162°E and φ_0=53.956°N. The axis Ox is directed to the orient, Oy – to the north, Oz – to zenith. Vector of normal ***n*** were determined as well as distances d from home of coordinate's system for every of the plane found. The following criteria-parameters were used for the search:

- D -is the admissible scatter interval for the d values, D/2- is the permissible distance deflections of the hypocenters from the plane found;
- M -is minimal number of the hypocenters belonged to plane;
- β – is the most possible angular sampling step in normal vectors orientation.

290 planes were found in the area which were satisfied the criteria. The output parameters of the searching planes procedure were: the vector ***n*** components, the value of d, the area S of the convex polygon to the plane, the list of the hypocenters coordinates circumscribing the plane along the perimeter, the DP and the STK angles of the plane.

There are reasons to assume that the hypocenters grouping on some of the planes found are casual. Additional selection criteria were provided for excluding such "casual" planes.

First, the search procedures were repeated but now it was based on independent sub catalogues. For this purpose the whole earthquakes catalogue was divided into two sub catalogues. The first one have got the records with uneven numbers, the other one have had the remained records. Now the parameter M was taken 2 times smaller (compare to search, based on whole catalogue), because the total amount of record were cut by half. In result of search, the lists of founded planes for each of catalogues were obtained. The results of the search in even and uneven parts of general catalogue were compared and later on we take into consideration only such planes, which had been found in each of sub catalogue. During comparison planes were believed identical, if the distance D_M between the planes were D_M <= 10 km, and the angle α_M between the normal vectors were α_M <=10°.

At second, we considered the planes, which were found with the help of catalogue records up to 2004, are really existing, if amount of hypocenters which occurred from 2004 to 2009 and hit into the unit of volume V_0 within ±100 km, are substantially smaller than corresponding amount which hit into the unit of volume V_{pl} directly adjoining to the planes within ±5 km. Ratios $P_{pl}=N_{pl}/V_{pl}$ и $P_0= N_0/V_0$ were calculated and then compared for unbiased comparison of corresponding hypocenter densities. The number of the hypocenters were calcu-

lated, which hit in the volume V_{pl} adjoining to the plane. The volume V_0 and V_{pl} shape was cylindrical. The element of cylinder was the plane perimeter. The cylinder V_0 height was equal to 200 km, the plane was in the centre of its axis. In cases when part of the cylinder lean out the earth surface, volume, which is come out, was excluded from the cylinder volume. The dimension V_{pl} was calculated by the formula $V_{pl}=D \cdot S_{pl}$. Later on the factor $k_P = P_{pl}/P_0$ was calculated, which show how many times the probability for hypocenters to hit in the unit volume of V_{pl} adjacent to the plane, greater than the probability to hit in the unit volume of 200-kilometers "cylinder". The k_P factor in the same way shows, how small the probability for plane to be "random". To bigger k_P corresponds to smaller probability. It may happen that not only single plane fall in the volume V_0, but two or more. If it is the case the k_P factors for each plane were calculated separately.

The abovementioned additional hard selection criteria allowed selecting 15 planes out of 290 which had been found on base of formal criteria only. Three of them are located beside the south seaside Kamchatka's region near the Cape Lopatka, also another three are located near the Cape Shipunskiy, 5 planes in the Kronockaya Bay and next four in the Gulf of Kamchatka nearby the Kronockiy Peninsula. In each of mentioned four areas some planes are crossing each other. Permanent seismic activity was noted on each of the plane and new seismic event registration. 3 from 15 planes are part of the subduction zone.

n_x	n_y	n_z	k_P	DP	STK	S, thousand, km^2	d, km
0,295	0,909	0,292	15,88	73	18	9	38,4
-0,494	0,411	0,766	10,64	40	310	11	9,6
0,387	-0,461	0,799	10,49	37	140	8	-54
-0,721	0,666	0,191	9,62	79	313	9,6	41,4
0,755	0	0,656	8,64	49	90	10,6	-133
-0,301	0,521	0,799	8,22	37	330	15	-0,1
-0,597	0,79	0,14	8,15	82	323	11,4	-93
-0,91	0,233	0,342	7,42	70	284	18,7	85,4
-0,994	-0,104	0,035	6,13	87	265	31,5	172
-0,25	0,397	0,883	5,83	27	328	13	17
-0,545	0,254	0,799	5	37	295	9,2	-1
-0,708	0,514	0,485	4,86	61	306	9	48,4
0,179	-0,483	0,857	4,67	31	159	11	-91
0,407	-0,881	0,242	4,24	76	155	6	181
0,429	-0,621	0,656	4,17	49	145	8,1	55,5

1. Krolevets A.N., Makeev A.M. The computer program of revealing the earthquake hypocenters spatial grouping planes // The complex problems of geophysical monitoring of the Russian Far East. Proceeding of the second regional scientific and technical conference. Petropavlovsk-Kamchatski. 11-17 October 2009 / M.e. V.N. Chebrov. Petropavlovsk-Kamchatski: GS RAN, 2010. 358-362 p.
2. Krolevets A.N. The planes rupture of the Kronotskiy earthquakes on 5 December 1997 year. // The geophysical monitoring of the Kamchatka. The science-technical materials of the conference 17-18 January 2006. Ottisk, 2006. p. 32-39.

А.Н. Кролевец
Дальневосточный государственный технический университет в г. П-Камчатском
А.М. Макеев
Камчатский государственный университет имени Витуса Беринга, кафедра прикладной математики, Петропавловск-Камчатский, an@kamgpu.ru

Особенности пространственного группирования гипоцентров Камчатских землетрясений.

В работе [1] описаны алгоритм и программа поиска плоскостей пространственного группирования гипоцентров землетрясений. Программа по формальным признакам отыскивает плоскости группирования гипоцентров, однако до последнего времени открытым оставался вопрос – не является ли группирование на некоторых из найденных плоскостей случайным. Данная работа посвящена исследованию этого вопроса с использованием сейсмических данных для Камчатского региона.

Исходными данными для анализа являлись записи каталога Камчатских землетрясений ГС РАН. Отбирались землетрясения энергетического класса не ниже 9, произошедшие с 1.01.1962 по 31.12.2003, попадающие также в пространственное окно с границами по широте 51°N $\leq\varphi_0\leq$57°N, по долготе 156°E $\leq\lambda_0\leq$166°E. Для поиска плоскостей использовались *декартовы* координаты [2]. Начало координатной системы помещалось в точку на поверхности Земли с географическими координатами λ_0=162°E и φ_0=53.956°N, ось Ox направлена на восток, Oy – на север, Oz – к зениту. Для найденных плоскостей определялись векторы нормали $\boldsymbol{n}$ и расстояния от начала координат d. Во время поиска использовались следующие критерии-параметры:

- D - допустимый разброс значений d, D/2-допустимые отклонения гипоцентров от плоскости;
- M - минимальное число гипоцентров с расстояниями d;
- β - максимально допустимый шаг угла дискретизации ориентаций векторов нормали.

В области поиска было найдено 290 плоскостей группирования. Выходными параметрами работы программы поиска плоскостей являлись: координаты вектора нормали к плоскости, расстояние от начала координат до плоскости, площадь выпуклого многогранника плоскости, список координат гипоцентров описывающих плоскость по периметру, угол падения и угол простирания плоскости.

Есть основания полагать, что на части из найденных плоскостей гипоцентры группируются случайно, для исключения таких «случайных» плоскостей были предусмотрены *дополнительные критерии отбора*.

Во-первых, плоскости заново отыскивались в независимых подкаталогах. Для их реализации отобранный каталог с гипоцентрами землетрясений был разделен на два подкаталога, в один попали записи с нечетными номерами, а в другом с четными. Поиск плоскостей осуществлялся в каждом из подкаталогов. При этом поиске параметр M принимался в 2 раза меньшим, поскольку количество гипоцентров сократилось вдвое. В результате, для каждого из каталогов были получены списки с найденными плоскостями. Результаты поиска в четном, нечетном и общем каталоге сравнивались и далее обрабатывались данные только о тех плоскостях, которые оказывались найденными в каждом из подкаталогов. Плоскости считались идентичными, если максимальное расстояние плоскостей друг от друга D_M <= 10 км, а угол между нормалями α_M <=10°.

Во-вторых, мы полагали, что плоскость, найденная по каталогам до 2004 года, действительно существует в пространстве, если количество гипоцентров N_{pl} землетря-

сений каталога с 2004 по 2009 года попадающих в единицу объема V_{pl}, в пределах ±5 км, непосредственно прилегающего к плоскости, оказывается существенно большим, чем их количество N_0, попадающее в в единицу объёма V_0 в пределах ±100 км. Для объективного сравнения соответствующих плотностей, для указанного временного промежутка, вычислялись и сравнивались отношения $P_{pl}=N_{pl}/V_{pl}$ и $P_0= N_0/V_0$. *Вычислялось количество гипоцентров, попавших в объем* V_{pl} *непосредственно прилегающий к плоскости.* Форма объёмов V_0 и V_{pl} принималась цилиндрической. Образующей цилиндра являлся периметр плоскости. Высота цилиндра принималась равной 200 км, плоскость находилась в центре. Объем части цилиндра, выступающий над земной поверхностью, из всего объема исключался. Объем V_{pl} вычислялся по формуле $V_{pl}=D\cdot S_{pl}$. Далее вычислялся коэффициент, показывающий, во сколько раз вероятность попадания гипоцентров в объём толщиной D, прилегающий к плоскости, выше вероятности попадания в 200-километровый «цилиндр»: $k_P =P_0/P_{pl}$. Данный коэффициент так же показывает, насколько мала вероятность плоскости, оказаться «случайной». При больших k_P соответствующая вероятность оказывается меньшей. В объеме плоскость может находиться не одна. В таких случаях вероятность группирования гипоцентров вблизи каждой плоскости рассчитывались по отдельности.

Дополнительные жёсткие критерии отбора позволили из 290 плоскостей, найденных ранее, оставить 15 плоскостей. Согласно расчетам 3 из них расположены у южного побережья Камчатки, в районе м. Лопатка, 3 плоскости расположены возле м. Шипунский, 5 плоскостей в Кроноцком заливе и 4 в Камчатском заливе в области Кроноцкого полуострова. В каждой из указанных областей плоскости пересекают друг друга. На каждой из них плоскостей была отмечена постоянная сейсмическая активность и регистрация новых событий. 3 из 15 плоскостей являются частью зоны субдукции.

n_x	n_y	n_z	k_P	DP	STK	S, thousand, km^2	d, km
0,295	0,909	0,292	15,88	73	18	9	38,4
-0,494	0,411	0,766	10,64	40	310	11	9,6
0,387	-0,461	0,799	10,49	37	140	8	-54
-0,721	0,666	0,191	9,62	79	313	9,6	41,4
0,755	0	0,656	8,64	49	90	10,6	-133
-0,301	0,521	0,799	8,22	37	330	15	-0,1
-0,597	0,79	0,14	8,15	82	323	11,4	-93
-0,91	0,233	0,342	7,42	70	284	18,7	85,4
-0,994	-0,104	0,035	6,13	87	265	31,5	172
-0,25	0,397	0,883	5,83	27	328	13	17
-0,545	0,254	0,799	5	37	295	9,2	-1
-0,708	0,514	0,485	4,86	61	306	9	48,4
0,179	-0,483	0,857	4,67	31	159	11	-91
0,407	-0,881	0,242	4,24	76	155	6	181
0,429	-0,621	0,656	4,17	49	145	8,1	55,5

1. *Кролевец А.Н., Макеев А.М.* Компьютерная программа поиска плоскостей группирования гипоцентров землетрясений // Проблемы комплексного геофизического мониторинга Дальнего Востока России. Труды Второй региональной научно-технической конференции. Петропавловск-Камчатский. 11-17 октября 2009 г. / Отв. ред. В.Н. Чебров. Петропавловск-Камчатский: ГС РАН, 2010. 358-362 с.
2. *Кролевец А.Н.* Плоскости разломов Кроноцкого землетрясения 5 декабря 1997 г. // Геофизический мониторинг Камчатки. Материалы научно-технической конференции 17 – 18 января 2006 г. Оттиск, 2006. С. 32– 39.

SPECTRAL COMPONENTS IN THE WAVEFORMS OF VOLCANO SEISMIC EVENTS

Kugaenko Yulia, Nuzhdina Irina

Kamchatkan Branch of Geophysical Survey, Russia, Petropavlovsk-Kamchatsky, ku@emsd.ru

There is continuous, real-time, seismic monitoring at 11 from 29 active Kamchatka's volcanoes. In active volcanoes we can observe both volcano-tectonic (VT) earthquakes and low-frequency (LF) seismic events. LF volcanic earthquakes are the indicators of magma transportation and activity within shallow conduit systems. LF earthquakes appearance in seismic flow can be a precursor of coming volcanic eruption. For example, by seismic data of Kamhatkan regional seismic network, current Kizimen activization was observed from June, 2009. All earthquakes were VT with clear P waves and S waves. Eruption began with strong explosive events on December 12, 2010. LF earthquakes appeared in seismic records in the middle of November as the main precursor of coming eruption (Fig.1). LF seismicity significantly increased on December 9-10 (two days before the strong explosive events).

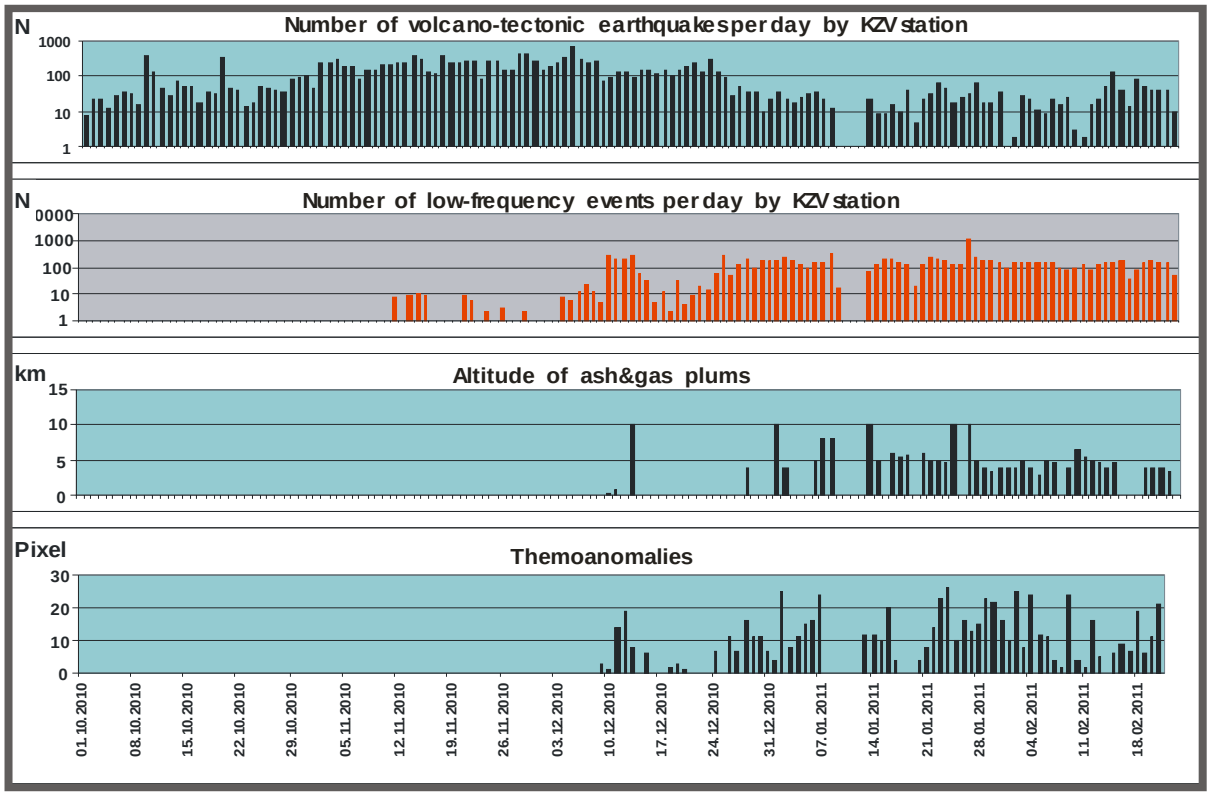


Fig. 1. The beginning of explosive eruption at Kizimen volcano in 2010.

In Kamchatka seismic monitoring survey, earthquakes processing is interactive digital signal analysis on PC screen. In the case of volcanic activization the number of earthquakes increases significantly. So signal processing and fast detection of LF earthquakes becomes difficult. Partially the problem solving is in automatic analysis of spectral amplitudes of seismic records.

We used Kamchatka regional seismic catalog and data base of earthquakes wave forms (digital records) of Geophysical Survey of Russia. Dominant frequencies of LF earthquakes are between 2-3 Hz. VT earthquakes usually have high-frequency components in spectrum. We propose to use for analysis the dispersion of seismic signal in three frequency ranges: 1.5-3.0 Hz, 3.0-6.0 Hz and 6.0-12.0 Hz. For visualization of hidden correlation in waveform spectral characteristics the triangle diagram is available.

In given report we present VT and LF earthquakes separation with the triangle diagram for 4 active volcanoes, located in the Eastern Kamchatka volcanic belt (fig.2): (1) Mutnovsky (continues intensive fumaroles and hydrothermal activity); (2) Koryaksky (2009-2010 activization, strong steam-gas and ash emission); (3) Kizimen (2010-2011 explosive eruption); (4) Gorely (2010 activization).

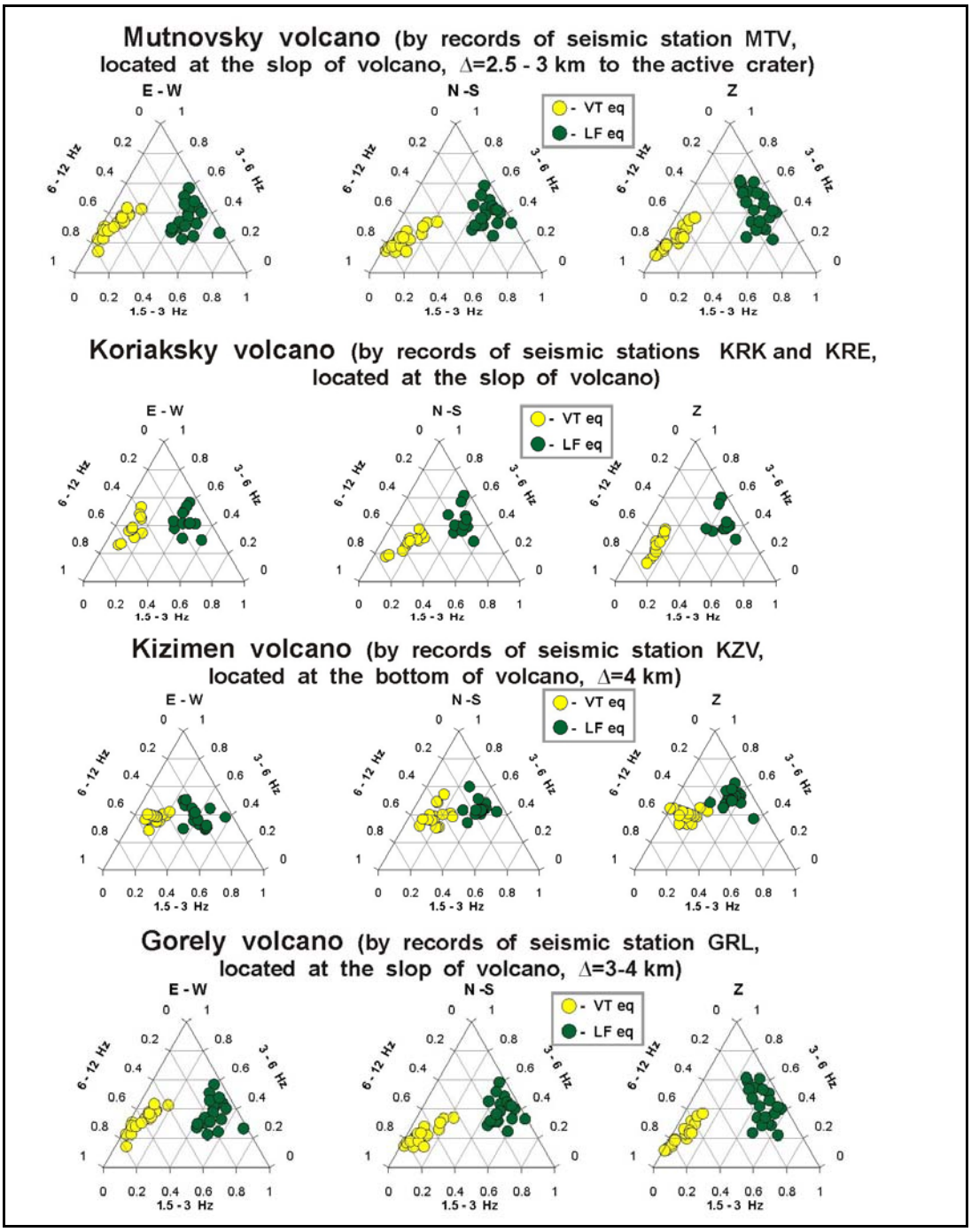


Fig.2. Relative intensity of the seismic signal in the different frequency bands for volcano-tectonic earthquakes and low-frequency events.

ON THE SHORT-TERM PREDICTABILITY OF STRONG EARTHQUAKES. NEEDED DATA VOLUME INCREASE AND SPECIFIC AND NONSPECIFIC PRECURSORS

M.V. Rodkin
IIEPT RAS, Moscow, Russia, rodkin@mitp.ru

The generalized vicinity of large earthquake (LEGV) was constructed as a combination of all events occurring in the space–time vicinities of strong (M≥7) and strongest (M≥7.5) earthquakes, and the examination of the seismicity behavior in LEGV was carried out. The inverse cascade (seismicity rate increasing toward the time of the main shock), the aftershock cascade, and the essentially lesser increase in seismic activity occurring in the larger vicinity of the main shock were found and examined. It is shown that the inverse and aftershock cascades are accompanied by several anomalies indicating the development of a set of precursory anomalies in LEGV; these anomalies consist in decrease of apparent stresses, in decrease of the b-values, in an increase of relative contribution of low frequency oscillations in the earthquake spectrum, and in an increase in correlation (homogeneity) of stress and strain. The majority of these anomalies were found to agree with the power-law character of behavior while approaching the moment of the main shock as it should be expected in the model treating the strong earthquake as an example of the critical-like phenomenon. As an example of such power-law like behavior the b-value behavior in LEGV is presented at the Figure.

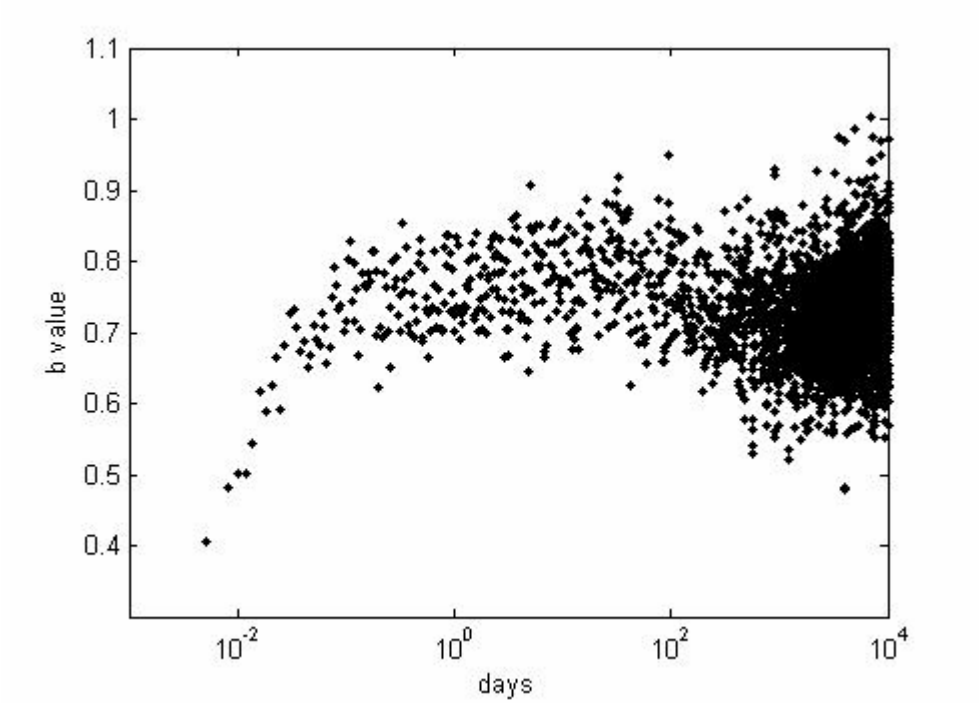
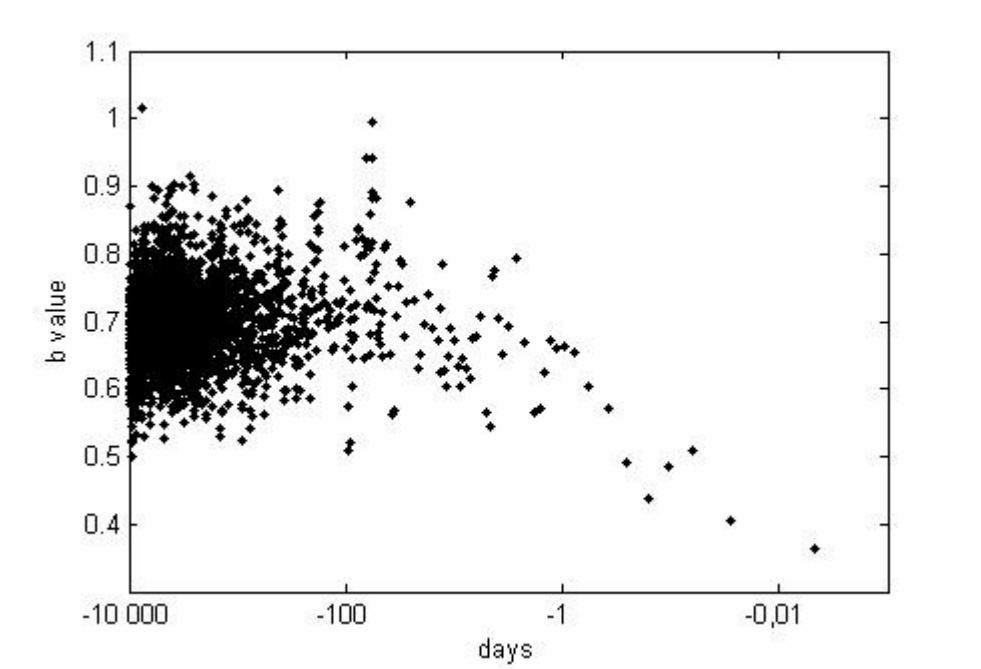


Figure. The change of the mean b-values in LEGV in the foreshock (a) and aftershock (b) areas. X-axis - the time interval of the group of earthquakes from the moment of the main shock.



The precursor anomaly in b-values as well as aftershock b-value anomaly is quite evident. The similar behavior takes place for other mentioned parameters. Thus it seems that "the strong earthquake prediction" is quite possible for the case of the "generalized strong earthquake". And this precursor behavior is similar to this one expected in the case of realization of the scenario of the critical process. The similar anomalies cannot be found however for data concerning any particular strong event because of a strong noise component in the seismic regime and the shortage of data. From here it is possible to assume that the strong earthquake prediction could be possible in the case of a considerable increase in available data, and the needed increase of available information could be evaluated to be approximately 1-2 orders.

It is emphasized also that the mentioned above prognostic features revealing the power-law behavior in the LEGV should be attributed as nonspecific precursors. These precursors correspond to the common features of instability occurrence, but they do not point out the particular physical mechanism of development of the instability. A few examples of possible specific precursors of strong earthquake are discussed also. Some of these precursors appear to be connected with the deep fluid involvement in the process of the earthquake occurrence.

AN ALGORITHM FOR CALCULATION OF SYNTHETIC SEISMOGRAMS IN A LAYERED HALF-SPACE WITH APPLYING MATRIX IMPEDANCE

Victor Pavlov

Kamchatkan Branch of Geophysical Survey of RAS, Petropavlovsk-Kamchatsky, Russia

A new semianalytic algorithm is proposed for calculating complete synthetic seismograms caused by a moment-tensor point source in a plane-parallel medium consisting of homogeneous elastic isotropic layers. Following to the idea of work [2], an artificial cylindrical boundary (ACB) is introduced, on which definite conditions are assigned. This allows to derive the representations for a displacement and the tension on a horizontal plane in frequency domain which include series over discrete wavenumbers.

Unknown coefficients of the representations depend on depth and form the stress-motion vector that satisfies a system of ordinary differential equations. The matrix impedance (see [3, 9]), i.e., the matrix function of depth, by which motion vector must be multiplied in order to obtain the stress vector, is introduced for solving this system. An independent nonlinear equation is obtained for the impedance. The propagator for the motion vector is constructed with the aid of the impedance. The closed analytical formulas, which do not contain any exponents with positive indices, are obtained both for the impedance and for the motion-vector propagator. The algorithm for the calculation of seismograms, free of limitations on the number and thickness of layers, as well as on the frequency range of interest, is constructed on the basis of these formulas. The algorithm is tested with the aid of an analytical solution (fig. 1, 2).

The proposed algorithm is a development of the Fat'yanov [4] method based on the use of the displacement potentials and the so-called auxiliary functions. In author's works [3, 9] the auxiliary functions (matrix impedance) were introduced directly for the motion–stress vectors without using of the potentials.

The algorithm differs radically from other algorithms existing at the present time (see [1, 5-8] among others).

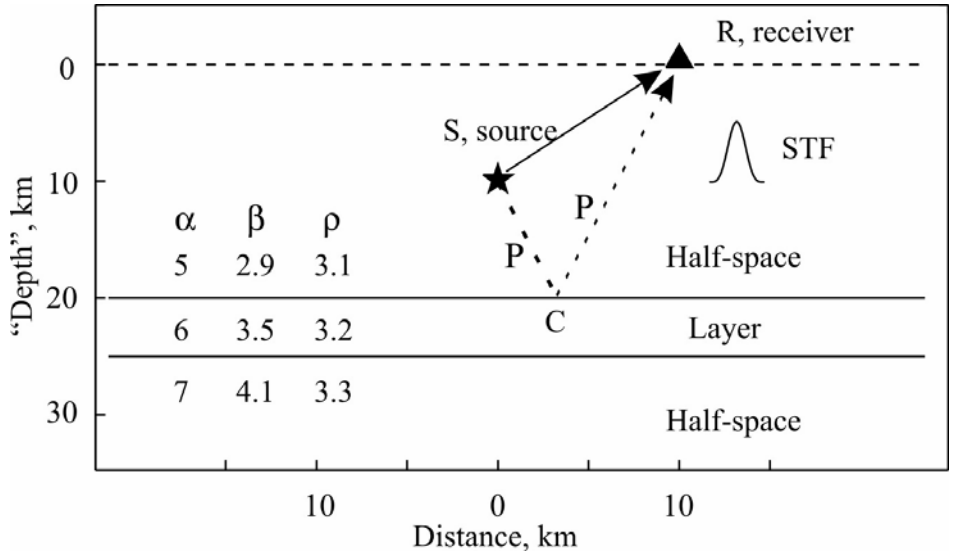


Fig.1. Two half-spaces divided by the layer of power 5 km. The source "depth" is 10 km. The receiver is located at depth 0 km and epicentral distance 10 km. The velocity and density values are shown. STF is the source time function; its duration is 0.25 s. The reflected PP wave (ray SCR) arrives at the receiver in 6.3 s. Before this time the direct waves at R are the same as in unbounded space.

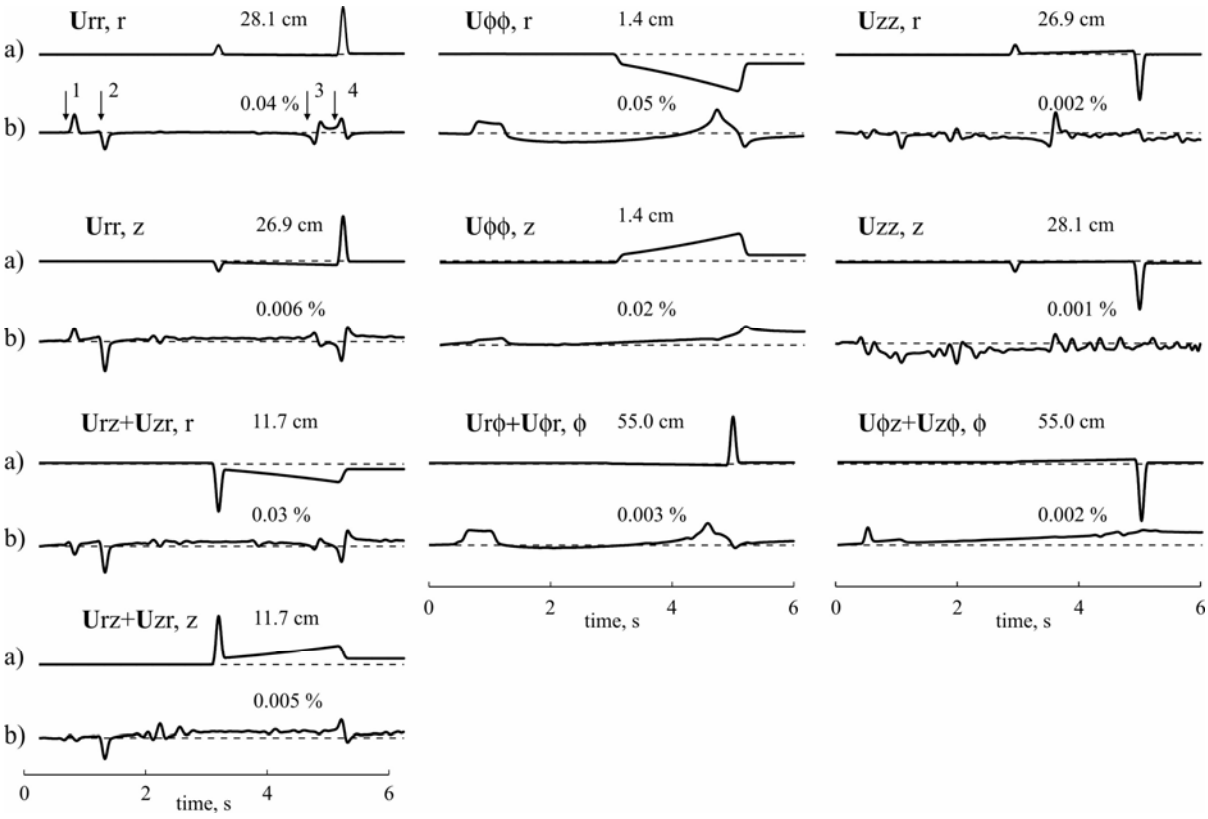


Fig. 2. Green's functions (convolved with STF) calculated by the algorithm (a) and differences between algorithm and analytical solution (b). **U***pq* (*p*,*q*=*r*,*φ*,*z*) – displacement vector caused by the moment tensor component M*pq*=M_0 (M*qp*=M*pq*, $M_0=10^{18}$ Nm). The distance to ACB is 86 km. The arrows mark the waves reflected from ACB. The waves 2 and 4 reflect firstly from the layer and then from ACB. Absolute amplitude values and percent ratio to them are shown.

References

1. Aki K., Richards P.G. Quantitative seismology. W.H. Freeman and Company. San Francisco. 1980.
2. Alekseev A.S., Mikhilenko B.G. The solution of dynamic problems of elastic wave propagation in inhomogeneous media by a computation of partial separation of variables and finite-difference methods. J. Geophys., v. 48, pp. 161-172, 1980.
3. Pavlov V.M. Matrix impedance in the problem of the calculation of synthetic seismograms for a layered-homogeneous isotropic elastic medium. Izvestiya, Physics of the Solid Earth, 2009. V. 45. No. 10. P. 848–858.
4. Fatyanov A.G. A semianalitical method for solution of direct dynamic problems in layered media. Doklady AN SSSR. 1990. V. 310. No 2. P. 323-327 (in Russian).
5. Bouchon M. A review of the discrete wavenumber method//Pageoph. 2003, 160, 445–465.
6. Kennett B.L.N. Seismic wave propagation in stratified media. Cambridge: Cambridge University Press. 1983. 342 p.
7. Muller G.. The reflectivity method: a tutorial. J. Geophys., v. 58, pp. 153-174, 1985.
8. Panza, G.F., Romanelli, F. and Vaccari, F. Seismic wave propagation in laterally heterogeneous anelastic media: theory and applications to seismic zonation. Advances in Geophysics. 2001. V. 43. P. 1-95.
9. Pavlov V.M. A convenient technique for calculating synthetic seismograms in a layered half-space. Proceedings of the International Conference "Problems of Geocosmos" / St. Petersburg: 2002. P. 320-323.

АЛГОРИТМ РАСЧЕТА СИНТЕТИЧЕСКИХ СЕЙСМОГРАММ В СЛОИСТОМ ПОЛУПРОСТРАНСТВЕ С ПРИМЕНЕНИЕМ МАТРИЧНОГО ИМПЕДАНСА

Павлов В.М.

Камчатский филиал Геофизической службы РАН, г.Петропавловск-Камчатский

Предлагается новый метод расчета полных синтетических сейсмограмм от дипольного точечного источника в плоскопараллельной среде, состоящей из однородных упругих изотропных слоев. Следуя идее работы [2], вводится искусственная цилиндрическая граница (ИЦГ), на которой задаются определенные условия. Это позволяет получить представления для смещения и напряжения на горизонтальной плоскости в частотной области в виде рядов по дискретным волновым числам.

Неизвестные коэффициенты, входящие в представления, зависят от глубины и образуют вектор движения-напряжения, который удовлетворяет системе обыкновенных дифференциальных уравнений.

Для решения этой системы уравнений вводится матричный импеданс [3, 9] – матричная функция глубины, на которую нужно умножить вектор движения, чтобы получить вектор напряжения. Для импеданса получается самостоятельное нелинейное уравнение. С помощью импеданса строится пропагатор для вектора движения. Как для импеданса, так и для пропагатора вектора движения получаются замкнутые аналитические формулы, не содержащие экспонент с положительными показателями. На основе этих формул строится алгоритм расчета сейсмограмм, свободный от ограничений на число и толщину слоев, а также на диапазон частот, представляющих интерес. Алгоритм тестируется с помощью аналитического решения (рис. 1, 2).

Предлагаемый алгоритм является развитием метода Фатьянова [4], в основе которого лежит использование потенциалов смещений и так называемых, вспомогательных функций. В работах автора [3,9] вспомогательные функции (матричный импеданс) были введены непосредственно для векторов движения-напряжения без использования потенциалов.

Алгоритм принципиально отличается от других, существующих в настоящее время [1, 5-8] (ссылки не претендуют на полноту).

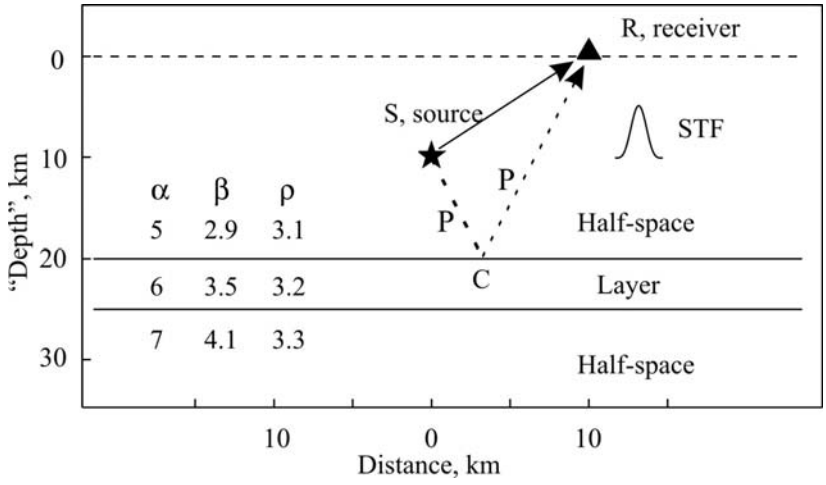


Рис. 1. Два полупространства, разде-ленные слоем мощности 5 км. Источник (И) – на глубине 10 км. Приемник (П) – на глубине 0 км и на эпицентральном расстоянии 10 км. Приведены значения скоростей и плотности. ВФИ – временная функция источника с длительностью 0.25 с. Отраженная PP-вол-на (луч ИОП) приходит в П через 6.3 с. До этого времени прямые волны такие же, как в безграничном пространстве.

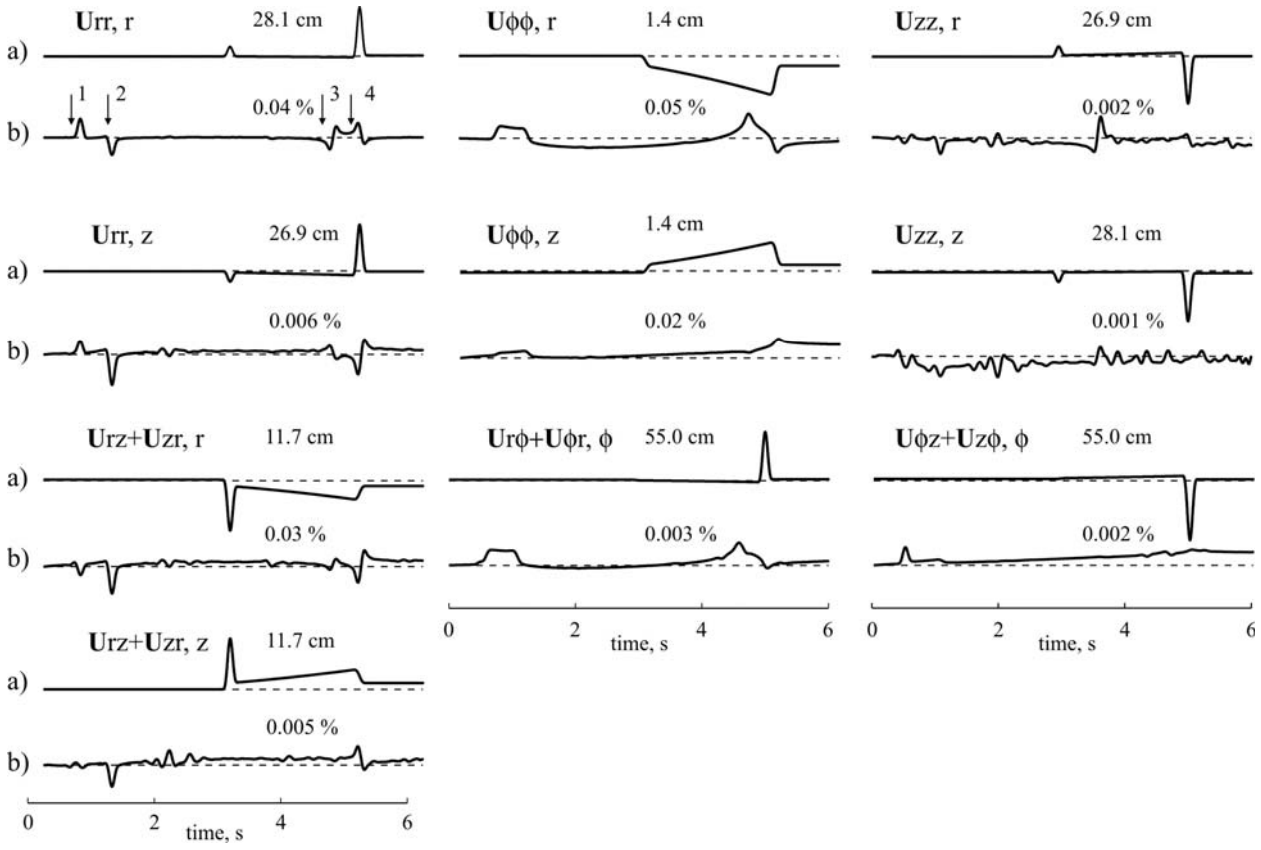


Рис. 2. Функции Грина (свернуты с ВФИ), рассчитанные по алгоритму (а) и их разности с аналитическим решением (б). **U**pq (p,q=r,φ,z) – вектор смещений, порождаемый компонентой M*pq*=M_0 (M*qp*=M*pq*, $M_0=10^{18}$ Нм). Расстояние до (ИЦГ) 86 км. Стрелками помечены импульсы, отраженные от ИЦГ. Импульсы 2, 4 сначала отразились от слоя, а затем от ИГ. Приведены максимальные (по модулю) амплитуды; для разностей – отношение к этим амплитудам в процентах.

Список литературы

1. Аки К., Ричардс П. Количественная сейсмология. Т. 1. М.: Мир. 1983. 520 с.
2. Алексеев А.С., Михайленко Б.Г. Метод расчета теоретических сейсмограмм для сложнопостроенных моделей сред // Доклады АН СССР. 1978. Т. 240. № 5. С. 1062-1065.
3. Павлов В.М. Матричный импеданс в задаче расчета синтетических сейсмограмм в слоисто-однородной изотропной упругой среде // Физика Земли. 2009. № 10. С. 14-24.
4. Фатьянов А.Г. Полуаналитический метод решения прямых динамических задач в слоистых средах // Доклады АН СССР. 1990. Т. 310. № 2. С. 323-327.
5. Bouchon M. A review of the discrete wavenumber method//Pageoph. 2003, 160, 445–465.
6. Kennett B.L.N. Seismic wave propagation in stratified media. Cambridge: Cambridge University Press. 1983. 342 p.
7. Muller G.. The reflectivity method: a tutorial. J. Geophys., v. 58, pp. 153-174, 1985.
8. Panza, G.F., Romanelli, F. and Vaccari, F. Seismic wave propagation in laterally heterogeneous anelastic media: theory and applications to seismic zonation. Advances in Geophysics. 2001. V. 43. P. 1-95.
9. Pavlov V.M. A convenient technique for calculating synthetic seismograms in a layered half-space. Proceedings of the International Conference “Problems of Geocosmos” / St. Petersburg: 2002. P. 320-323.

REGIONAL PLENTY SEISMICITY OF KAMCHATKA AND KOMANDORSKY ISLANDS ACCORDING TO THE CATALOGUE OF KB GS THE RUSSIAN ACADEMY OF SCIENCES

Nazarova Z. A.

The Kamchatka branch of Geophysical service of the Russian Academy of Sciences, 683006, Petropavlovsk-Kamchatskij, parkway Pijpa 9, nazarova_zoya@mail.ru

Kamchatka and Komandorsky Islands - area of the raised seismic activity. The difficult structure of a zone of a joint of island arches Kurile - Kamchatka and Aleutian leaves the mark on localization of regional seismicity. One of the most widespread kinds of seismicity is a plenty of earthquakes. There are they often enough and are observed on a land, in gulfs along east coast of Kamchatka and in Pacific ocean around a deep-water trench. The basic part plenty's earthquakes is dated for breaks of a deep-water trench. The nature of their origin up to the end isn't studied till now and is of interest for researchers. In the given work attempt to characterize plenty seismic conditions during the last years monitoring around Kamchatka and Komandorsky Islands is made.

РЕГИОНАЛЬНАЯ РОЕВАЯ СЕЙСМИЧНОСТЬ КАМЧАТКИ И КОМАНДОРСКИХ ОСТРОВОВ ПО ДАННЫМ КАТАЛОГА КФ ГС РАН

Назарова З.А.

Камчатский филиал Геофизической службы РАН, 683006, г. Петропавловск-Камчатский, бульвар Пийпа 9, nazarova_zoya@mail.ru

Камчатка и Командорские острова - район повышенной сейсмической активности. Сложное строение зоны сочленения островных дуг Курило - Камчатской и Алеутской накладывает свой отпечаток на локализацию региональной сейсмичности. Один из наиболее распространенных видов сейсмичности это рой землетрясений. Происходят они довольно часто и наблюдаются на суши, в заливах вдоль восточного побережья Камчатки и в Тихом океане в районе глубоководного желоба. Основная часть роев землетрясений приурочена к разломам глубоководного желоба. Природа их происхождения до сих пор до конца не изучена и представляет интерес для исследователей. В данной работе сделана попытка охарактеризовать роевую сейсмическую обстановку за последние годы мониторинга в районе Камчатки и Командорских островов.

The 20-s Regional Surface-Wave Magnitude for the Russian Far East

Olga S.Chubarova[1], Alexander A. Gusev[1, 2], Svetlana A.Vikulina[2]

[1]*Institute of Volcanology and Seismology, Far East Branch, Russian Academy of Sciences, Petropavlovsk-Kamchatsky, Russia*
[2]*Kamchatka Branch , Geophysical Service, Russian Academy of Sciences, Petropavlovsk-Kamchatsky, Russia*

A modified surface-wave magnitude scale M_s(20R) is constructed that permits one to extend the common teleseismic magnitude scale M_s(20), originally defined for epicentral distances in excess of 20°, to the regional distance range (0.7-20°) .

The data set used in this study contains digital records of 434 earthquakes of the North-Western Pacific region of 1993-2009 recorded at 12 BB seismic stations. The new scale is based on amplitudes of surface waves within a narrow frequency range 0.04-0.063 Hz (periods 16-25 s) with the central frequency 0.05 Hz = 1/20 s. The use of the wave periods close to 20 s is a standard approach for the common 20-s surface-wave magnitude. In this case, selection of this period range takes place naturally because of wave dispersion. To generalize this approach to distances shorter than 20°, we filter a BB record employing an appropriate digital bandpass filter. Data analysis have revealed that for an optimal representation of amplitude decay with distance, two separate calibration curve must be introduced, one for the marginal areas of NW Pacific and another for adjacent continental areas. The application of the new scale allows one to determine low-frequency parameters of M=3-4 earthquakes, too small for seismic moment determination in an island-arc environment. Single-station rms accuracy of determination of M_s(20R) is 0.22.

In difference with Soloviev's broad-band M_s(BB), also defined for the regional distance range, the new M_s(20R) magnitude scale provides a spectrally-definite parameter for the regional distances; it matches well to M_s(NEIC) and provide historical continuity with the classical Gutenberg's M_s scale.

EFFECTS OF THE 1971 KAMCHATSKY PENINSULA EARTHQUAKE ON NORTHERN KAMCHATSKY BAY

SeanPaul La Selle[1], Joanne Bourgeois[1], Randall J. Leveque[2]

[1]Earth & Space Sciences, Univ. of Washington. Seattle, WA, USA.
[2]Applied Mathematics, Univ. of Washington. Seattle, WA, USA.

The 1971 Kamchatsky Peninsula earthquake (Mw 7.8) triggered a tsunami that was recorded on tide gauges 70 km away in the town of Ust-Kamchatsk, as well as in Hilo, HI, but with little reported local runup. At the north end of Kamchatsky Bay (Figure 1), we have identified sandy deposits attributed to the 1971 tsunami that overtop beach ridges 8-11 meters above sea-level (Figure 1). Ust-Kamchatsk is less than five kilometers to the west of these deposits, and written records from 1971 report little tsunami damage to structures near the beach, suggesting that the tsunami height was significantly lower near the town. Runup from deposits of the 1971 tsunami have been recorded on the open coast of Kamchatsky Peninsula (Martin et al. 2008), but the data for Kamchatsky Bay are sparse. We will try to determine if the tsunami height was actually smaller in coastal Ust-Kamchatsk by cataloguing and quantifying spatial variations in deposit runup values along Kamchatsky Bay. Then, by modeling tsunami runup from a variety of earthquake sources, we will determine if a submarine canyon in Kamchatsky Bay focuses tsunami runup to the east of Ust-Kamchatsk.

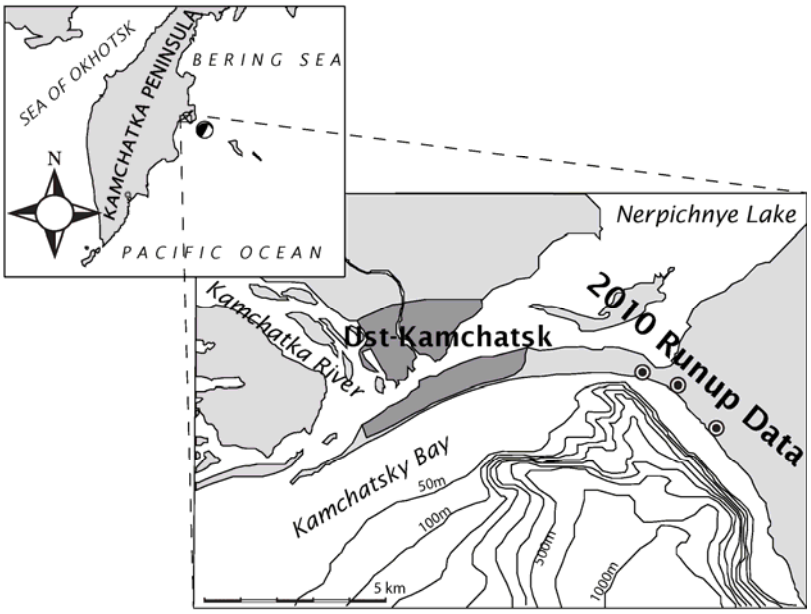


Figure 1: Map of Kamchatsky Bay. Gray areas are land. Contour lines show bathymetry, note the submarine canyon on the east side of the bay. The town of Ust-Kamchatsk is located on the west side of Dembi Spit. Three profiles measured in 2010 (circles) show where 1971 tsunami deposits were found, indicating overtopping of 8-11 m high beach ridges.

Along Kamchatsky Bay, the 1971 tsunami deposit is easily identifiable as a sand layer directly overlying a deposit of 1964 Shiveluch tephra. Ust-Kamchatsk, in the last century, has been damaged by larger tsunamis than 1971, but the lack of locally preserved marker tephra older than 1964 makes it difficult to distinguish other historical tsunami deposits from one another. Also, historical data for older earthquakes are less reliable or nonexistent. Therefore, the 1971 event is the prime candidate to model and compare to field data. However, one caveat of studying this

relatively recent event is the possibility that the deposit has been reworked by human activity in areas closer to the town.

To model tsunamis, we use GeoClaw, which models depth averaged flows with adaptive refinement (Leveque et al. 2011, online). After specifying the sea-surface deformation due to a given earthquake, the model propagates the resulting wave over bathymetry and onto land (Figure 2), where we can determine the modeled runup. We will use measured runup in the field to compare to modeled runup in order to determine if the bathymetry in Kamchatsky Bay is a large control on runup. There is a submarine canyon on the east side of the bay (Figure 1), and we would like to see how this canyon in particular influences runup. By modeling similar sized earthquakes, but with different epicenter locations, we can determine whether or not the bathymetry consistently produces higher runup to the east of Ust-Kamchatsk, and whether the specific location of the 1971 rupture causes this behavior..

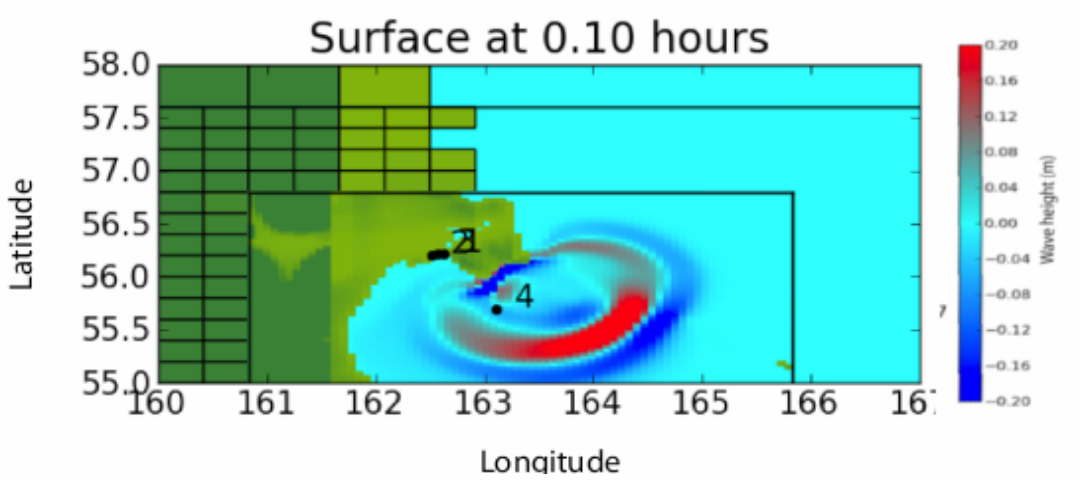


Figure 2: Preliminary model run of the 1971 tsunami in GeoClaw, showing waves propagating from the earthquake epicenter six minutes after the rupture. Earthquake source from Martin et al, 2008.

Preserved tsunami deposits have been vital in determining tsunami and earthquake recurrence intervals in Kamchatka because of the short and often incomplete written record in this region. (Pinegina, Bourgeois, 2001). A better understanding of the magnitude of the 1971 tsunami in addition to modeling tsunami runup in Ust-Kamchatsk will provide a broader picture of the tsunami hazards posed to communities in this region.

References

Leveque, R.J, Berger, M.J., George, D.G., Mandli, K. *The Geoclaw Software for Depth-Averaged Flows with Adaptive Refinement*. , 2011. Internet resource. **arXiv:1008.0455v2 [physics.geo-ph]**

Martin, M.E, J Bourgeois, H Houston, V.V Titov, R Weiss, and T.K Pinegina. "Combining Constraints from Tsunami Modeling and Sedimentology to Untangle the 1969 Ozernoi and 1971 Kamchatskii Tsunamis."*Geophysical Research Letters*. 35.1 (2008). Print.

Pinegina, T K, and J Bourgeois. "Historical and Paleo-Tsunami Deposits on Kamchatka, Russia: Long-Term Chronologies and Long-Distance Correlations." *Natural Hazards and Earth System Science*. 1.4 (2001): 177-185. Print.

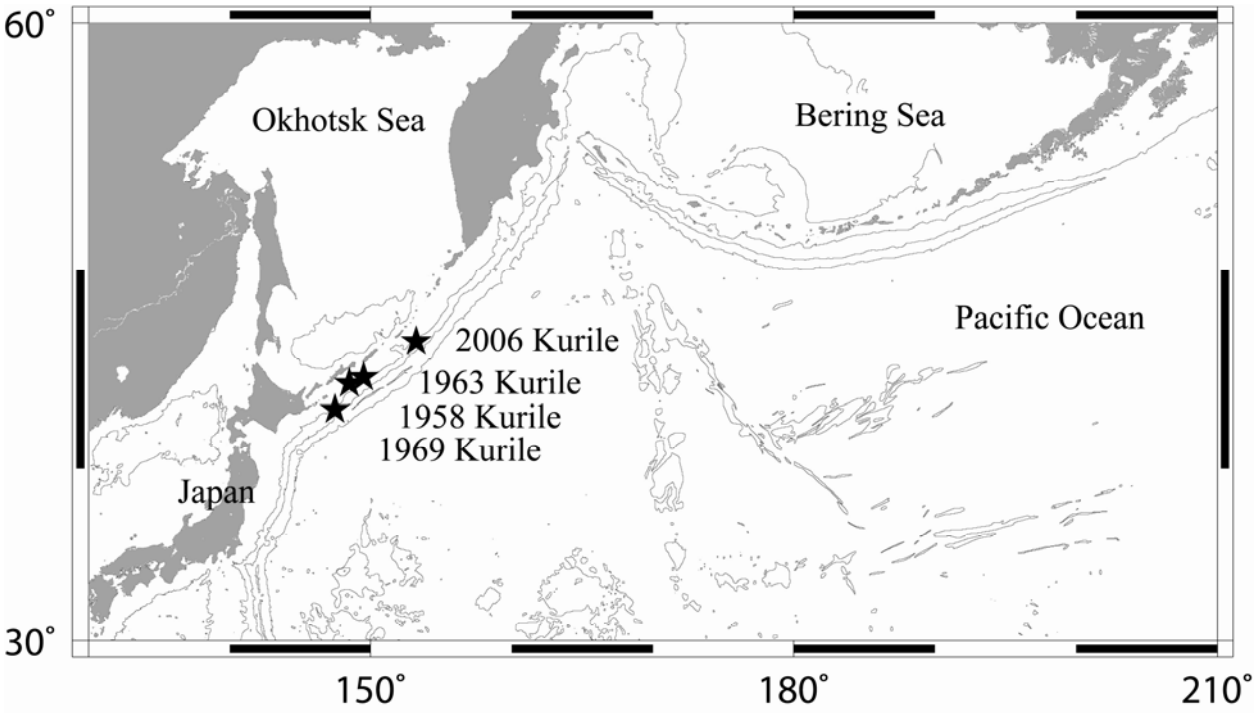
Relations of Great Kurile Earthquakes Estimated from Tsunami Waveforms

Kei Ioki and Yuichiro Tanioka

Institute of Seismology and Volcanology, Hokkaido University, Japan

The Pacific plate subducts about 8cm per year under the Kurile Islands, so many great earthquakes occurred in the Kurile subduction zone. On 13 October 1963, great Kurile earthquake (M_w 8.5, Mt 8.4) occurred off the Etorofu Island. This event was an underthrsut earthquake. The epicenter of the 1963 earthquake is located at 44.8˚N, 149.5˚E, depth = 60 km. Also the largest aftershock (Ms 7.2, Mt 7.9) occurred on 20 October 1963. This aftershock generated an unusually large tsunami relative to the size of the seismic waves. The epicenter of the 1963 aftershock is located at 44.7˚N, 150.7˚E, depth = 10 km. The 2006 Kurile earthquake occurred northeast of the 1963 Kurile earthquake. The epicenter of the 2006 earthquake is located at 46.6˚N, 153.2˚E, depth = 30 km. To examine whether seismic gap exist between 1963 and 2006 earthquakes and to understand source processes of the main shock and the largest aftershock, slip distributions of the 1963 great earthquake and the largest aftershock were estimated using tsunami waveforms recorded at tide gauges along Pacific Ocean and Okhotsk Sea coast. In the case of the main shock, using 24 subfaults of 50 km×50 km, slip amounts on each subfault were determined by the tsunami waveform inversion. The result shows that large slip amounts were found at the intermediate depth and the shallow part of the rupture area. The total seismic moment was estimated to be 2.4×10^{21} Nm (M_w 8.2) by assuming that the rigidity is 4.0×10^{10} N/m^2. The 2006 earthquake occurred just next to the 1963 earthquake and no seismic gap exists between source areas of the 1963 and 2006 earthquakes. In the case of the largest aftershock, using 14 subfaults of 50 km×50 km, slip amounts were estimated. Large slip amounts were found at the shallow plate interface near the trench. This largest aftershock is a tsunami earthquake. The seismic moment was estimated to be 1.1×10^{21} Nm (M_w 8.0) by assuming that the rigidity is 4.0×10^{10} N/m^2. On 6 November 1958, the great Etorofu earthquake (M_w 8.3) occurred southwest of the 1963 Kurile earthquake. The epicenter of the 1958 earthquake is located at 44.4˚N, 148.6˚E, depth = 80 km. This earthquake was originally defined as an interplate earthquake although the depth was slightly deep. However, the earthquake was characterized by a high stress drop, a low aftershock activity at shallow depth, large high-frequency seismic waves, a large felt area, and a relatively small aftershock area. Therefore, the 1958 great earthquake was recently defined as a slab event. In this study, dip, depth, slip amount of the earthquake were estimated using tsunami waveforms recorded at tide gauge stations along the Pacific Ocean. Strike and rake of the fault model were fixed to be 225 and 90 degrees, respectively. First step, a rupture area previously estimated from aftershocks within 3 days, 150 km×80 km, was used. The tsunami was numerically computed using interplate earthquake model (dip = 20 degree, depth = 16 km) and slab earthquake model (dip = from 20 to 60 degree every 10 degree, depth = from 27.5 km to 47.5 km every 10 km). We found that a slab earthquake model of dip = 40 degree, depth = 37.5 km best fit observed and computed tsunami waveforms. Second step, tsunami waveforms were calculated using various source models which have different rupture area at the same other parameters. However, the computed tsunami waveforms from the original rupture area, 150 km×80 km, best explained the observed tsunami waveforms. Third step, using 48 subfaults of 25 km×20 km, slip amounts were estimated by tsunami waveform inversion with the fault model decided parameters. Subfaults of large slip amounts were almost same as the rupture area of aftershock within 3 days. The seismic moment was estimated to be 1.7×10^{21} Nm (M_w 8.1) by assuming that the rigidity is 6.5×10^{10} N/m^2.

About the 1969 earthquake, the earthquake (Mw 8.2) occurred southwest of the 1958 earthquake. The epicenter of the 1969 earthquake is located at 43.2˚N, 147.5˚E, depth = 33 km. The 1969 and 1963 events were interplate earthquakes, but the 1958 event was a slab earthquake. Slip distribution of the 1969 earthquake will be estimated from tsunami waveform inversion to investigate source process of the earthquake and relations of locations of the 1969 and 1963 earthquake.



REGIONAL INFORMATIONAL-PROCESSING CENTER ”PETROPAVLOVSK” IN 2010–2011: OPERATIONAL EXPERIENCE FROM THE POINT OF REGULATIONS OF TSUNAMI WARNING SYSTEM AND SEISMIC URGENT MESSAGE SERVICE

V.N. Chebrov, D.V. Chebrov, D.A. Ototuk, S.A. Vikulina

Kamchatka branch of Geophysical survey of RAS, Petropavlovsk-Kamchatsky, Russia

Seismic observation system of Tsunami Warning System (TWS) at modern time consists of seismological network and Regional Informational-Processing Centers (RIPC). RIPC’es in parallel, in real time mode receive seismic data and estimate earthquake parameters. According to estimation results, RIPC’es may take a decisions about tsunami probability. Seismic network, deployed in the course of modernization 2006–2010 now consists of five base stations, six auxiliary ones and 16 strong ground motion observe points. Base stations represents seismic groups, that located in major population coast settlements, and consist of velocimeters and accelerometers.

According to currently in force TWS regulations, seismic subsystem (SS) of TWS must provide earthquake parameters estimation not later than defined time interval till beginning of registration on the tsunami-station. For the specific tsunami stations “Petropavlovsk” and “Yuhno-Sahalinsk” time normatives are:

- 10 minutes for epicentral distances less than 1000 km
- 20 minutes for epicentral distances 1000–2000 km
- 30 minutes for epicentral distances 2000–3000 km.

Zone of responsibility for “Yuzhno-Sahalinsk” established as 3000 km range, and for “Petropavlovsk” – 1000 km range. Regulation, discussed here was formed for TWS-configuration, than was released in 1958.

After modernization of TWS (2006–2010), many of its characteristics had changed. First of all we are talking about characteristics of communication systems, observations systems and processing tools. Key new features are network processing and triple reservation of RIPC’es. All of RIPC’es have equal and full access to seismic data. Thus, new TWS is more reliable than ever before, and provide more accurate estimations of earthquake parameters. So, there is question about changing regulations of SS TWS, and taking into account all real possible of the new system.

The main quality characteristics of SS TWS are the accuracy of earthquake parameters estimation and operation time for the potential tsunamigenic earthquakes (large enough). While developing new regulations of TWS, both theoretical and practical results should be taken into account.

During an order of two years (2008–2010) the new seismic subsystem was working in experimental operating mode. In the 2010, November TWS was released. Despite small operation experience (from the point of seismology), SS TWS has processed not only usual for this region events, but catastrophic earthquake (Tokhoku, Japan, March 11, 2011, $M_W = 9.1$). Results of processing this extraordinary event must be taken into account when developing new regulations of TWS, and planning for further development of seismological and hydrophysical subsystems of TWS. Thus, by now enough material is accumulated to estimate real capabilities of new generation SS TWS.

In this paper results of work Regional Informational-Processing Center “Petropavlovsk” in 2010–2011 discussed. Real quality of estimations earthquake parameters (accuracy and operational time) in a point of regulations of TWS and Seismic Urgent Message Service is showed. Questions of new regulations of new generation development are discussed.

РАБОТА РИОЦ ПЕТРОПАВЛОВСК В 2010–2011 ГГ. ПО РЕГЛАМЕНТАМ СПЦ И ССД

В.Н. Чебров, Д.В. Чебров, Д.А. Ототюк, С.А. Викулина

Камчатский филиал Геофизической службы РАН, Петропавловск-Камчатский

Система сейсмологических наблюдений в службе предупреждения о цунами на настоящее время состоит из сети сейсмических станций и региональных информационно-обрабатывающих центров. РИОЦ одновременно и параллельно, в реальном времени, получают данные наблюдений и производят оценки параметров очагов землетрясений и могут принимать решение о возможности цунами. Сейсмическая сеть, развернутая в рамках модернизации СПЦ 2006–2010, состоит из пяти опорных станций, шести вспомогательных, и 16 пунктов регистрации сильных движений. При этом, опорные станции представляют собой сейсмические группы, расположенные в районах крупных населенных пунктов, состоящие из велосиметров и акселерометров.

По действующим в настоящее время регламентам, СП СПЦ должна дать оценку параметров землетрясения, произошедшего в зоне ответственности, и предупреждение о возможности цунами не позднее: 10 минут с момента начала регистрации события на станциях «Петропавловск» и «Южно-Сахалинск» при удалении от них очагов до 1000 км; 20 минут – до 2000 км; 30 минут – до 3000 км. Зона ответственности для станции «Южно-Сахалинск» определена 3000 километрами, и 1000 км для станции «Петропавловск». Эти требования по времени реакции системы были сформулированы для СПЦ, действовавшей в период с 1958 года по 2006.

После ввода в эксплуатацию СП СПЦ нового поколения изменились характеристики системы наблюдений, систем связи и средств обработки. Ключевые нововведения – это переход на обработку по сети и тройное резервирование РИОЦ, все из которых обладают равными и полными правами доступа к сейсмическим данным. Таким образом, новая система обладает повышенной надежностью и может обеспечивать большую надежность, достоверность и точность оценок. Вследствие чего, возникает вопрос об изменении регламентов сейсмической службы в СПЦ и приведения их в соответствие с реальными возможностями новой системы.

Главными показателями качества работы СП СПЦ являются точность оценок параметров потенциально цунамигенных землетрясений и время реакции системы на такие события. При планировании новых регламентов должны учитываться не только теоретические обоснования, но и практические результаты.

В течение примерно двух лет (2008–2010) новая сейсмическая подсистема работала в опытном режиме, а с ноября 2010 года, после испытаний она была принята в эксплуатацию. Несмотря на то, что система работает сравнительно недавно, уже имеется опыт обработки в режиме реального времени не только сейсмичности, характерной для данного региона, но и катастрофического землетрясения (Тохоку, 11 марта 2011 г.). Данные, полученные при обработке этого неординарного события, обязательно должны быть учтены при разработке новых регламентов СПЦ и при планировании дальнейшего развития как сейсмологической, так и гидрофизической подсистем СПЦ. Таким образом, за это время накопилось достаточно материала, чтобы оценить реальные возможности СП СПЦ нового поколения по точности и своевременности оценки параметров землетрясений и надежности принятия решения о возможности о цунами для Дальневосточного региона.

В данной работе обсуждаются результаты работы Регионального информационно-обрабатывающего центра (РИОЦ) «Петропавловск» в 2010–2011 годах. Анализируется соответствие фактических показателей качества работы РИОЦ действующим регламентам СПЦ и ССД. Также полученные результаты могут быть положены в основу новой концепции регламента СП СПЦ нового поколения.

Identification and analysis of topography according to SRTM, based on application of the scale-space theory

O.V. Rybas, G.Z. Gilmanova

Russian Academy of Sciences, Far Eastern Branch, Institute of Tectonics and Geophysics named after Yu. A. Kosygin

Theory of scalable space (Witkin, 1983; Koenderink, 1984; Koenderink, van Doorn, 1987) makes it possible to: a) to provide initial information in the form, for which when zooming in detailing decreases monotonically, without creating new features and b) determine the nature of the relationship multiscale representations.

The relief is one of the key indicators of geodynamic processes in the surface layer of the earth, and reflects the geological structure of territory. Therefore, the application of the scale space theory for the identification and analysis of relief patterns, related to the solution of problems of geomorphology, tectonics and geology. Structure, identified from the initial data of different scale t, may not only differ from each other, but also be used as a complementary design, allowing to build the most complete picture of the nature of the signal.

In order to identify major structural elements and details of their geological structure of the digital elevation model - SRTM03, SRTM30_Plus (radar mode) developed a method of interpreting the source material, includes a selection of linear and dome-shaped structures with operations for calculating the modulus of the first derivative of the coordinate - modulus of the gradient topography that characterizes the state of the surface on the steepness of the slope and direction (azimuth) and the second derivative of the coordinate on the surface - the surface Laplacian of Gauss, identifying objects dome shape.

The examples indicates efficiency of the scale space theory for the allocation of relief structures, zones of different types of faults, tectonic units, the ability to more accurately determine the size of various geomorphological, tectonic and geological sites. Discharge from the distractions and masking parts of the transformed radar images helped to identify the most significant features of the major geological structure in the region, generalized projections of regional and global structures (Fig. 1).

Ample opportunity of transformed digital elevation models for the tectonic zoning, geological mapping, structural imaging, lineament analysis may find its application in all phases of regional geological studies. Particularly important to apply this kind of research in inaccessible regions.

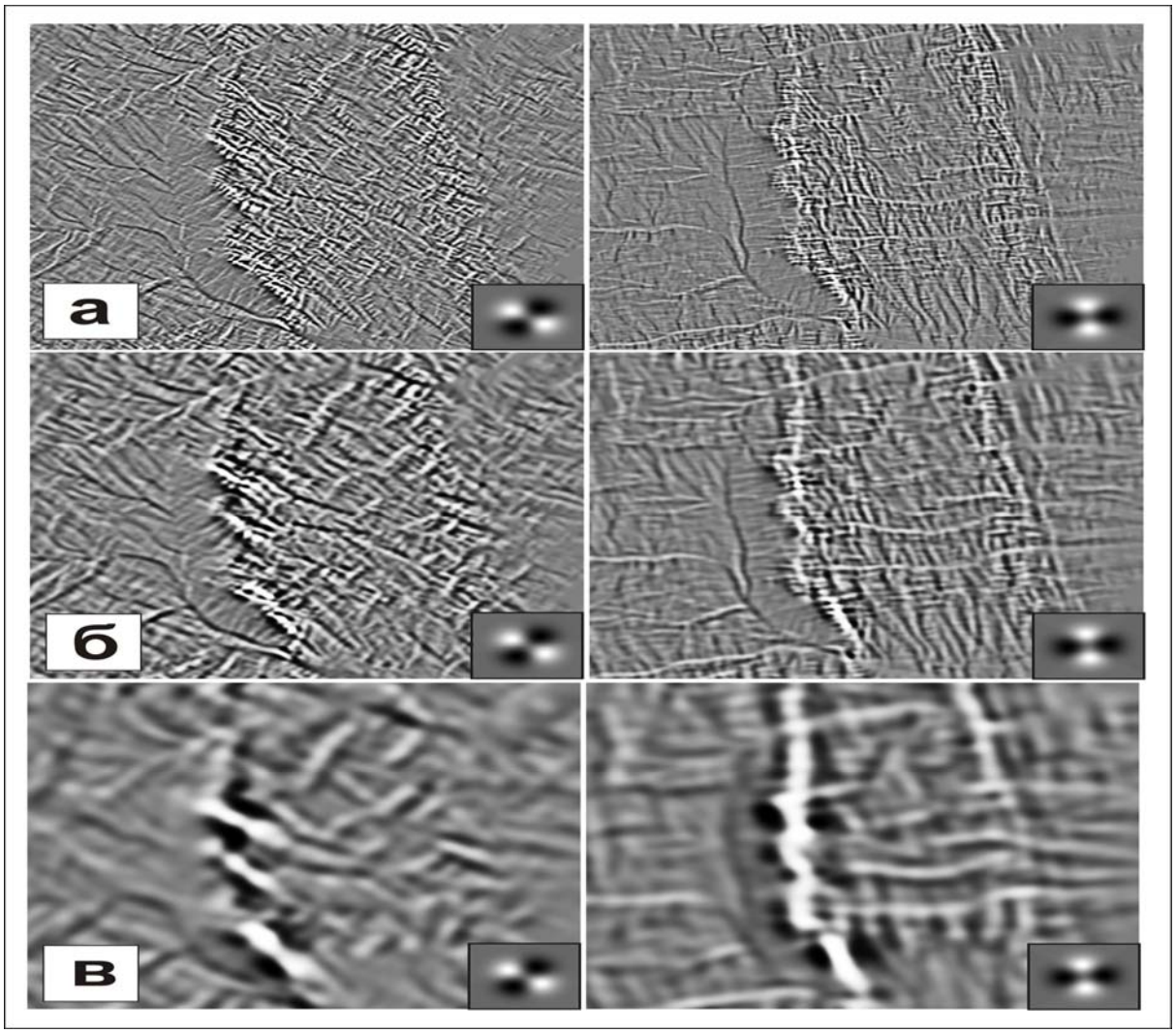


Fig. 1. Northern Sakhalin seismic zone (Neftegorsk district) where the right-lateral slip tectonics is developed. Six options Lxy at t = 1, 4, 64 (a, b, c, respectively) and φ 1 = 80 ° (260 °) (left) and φ 2 = 130 ° (310 °) (right). Every scene is accompanied by the shape of the derivative of Gaussian kernel.

References:

Koenderink J.J., van Doorn A.J. Representation of Local Geometry in the Visual System // Biol. Cyb. 1987. Vol. 55. 367- 375.

Witkin A. P. Scale-space fltering // Proc. 8th Int. Joint Conf. Art. Intell., 1983. 1019 -1022.

Young R. A., Lesperance R. M., Meyer W. W. The Gaussian Derivative model for spatial-temporal vision: I. Cortical model // Spatial Vision. 2001. Vol. 14, No. 3, 4. pp. 261-319.

Выделение и анализ структур рельефа по данным радиолокационной съемки на основе применение теории масштабируемого пространства

О.В.Рыбас, Г.З. Гильманова

Институт тектоники и геофизики им. Ю. А. Косыгина ДВО РАН, г. Хабаровск

Теория масштабируемого пространства (Witkin, 1983; Koenderink, 1984; Koenderink, van Doorn, 1987) дает возможность: а) представить исходную информацию в виде, когда при увеличении масштаба деталировка монотонно уменьшается, не создавая при этом новых особенностей; б) определить характер связи разномасштабных представлений.

Рельеф является одним из основных показателей развития геодинамических процессов, протекающих в приповерхностном слое Земли, и отражает геологическое строение территории. Поэтому применение теории масштабируемого пространства для выделения и анализа структур рельефа, связано с решением задач геоморфологии, тектоники и геологии. Структуры, выделенные из исходных данных разного масштаба t, могут не только существенно отличаться друг от друга, но быть использованы и как взаимно дополняющие конструкции, позволяющие строить максимально полную картину о характере исследуемого сигнала.

С целью выявления крупных структурных элементов и деталей их геологического строения в цифровых моделях рельефа SRTM03 и SRTM30_Plus (радарная съемка) разработана методика дешифрирования исходного материала, включающая выделение линейных и куполообразных структур посредством операций вычисления модуля первой производной по координате – модуля градиента рельефа, характеризующего состояние поверхности по крутизне и по направлению склона (азимуту), и второй производной по координате на поверхности – лапласиана поверхности Гаусса, идентифицирующего объекты куполообразной формы.

Показана эффективность применения теории масштабируемого пространства для выделения структур рельефа, зон различных типов, разрывных нарушений, тектонических блоков; возможность более точного определения размеров различных геоморфологических, тектонических и геологических объектов. Разгрузка от отвлекающих и маскирующих деталей преобразованных радарных снимков способствует выявлению наиболее существенных крупных черт геологического строения региона, генерализованных проекций региональных и глобальных структур (рис.1).

Широкие возможности преобразованных цифровых моделей рельефа при тектоническом районировании территорий, геологическом картировании, структурных построениях, линеаментном анализе могут найти свое применение на всех этапах региональных геологических исследований. Особо важно применять подобного рода исследования в трудно доступных регионах.

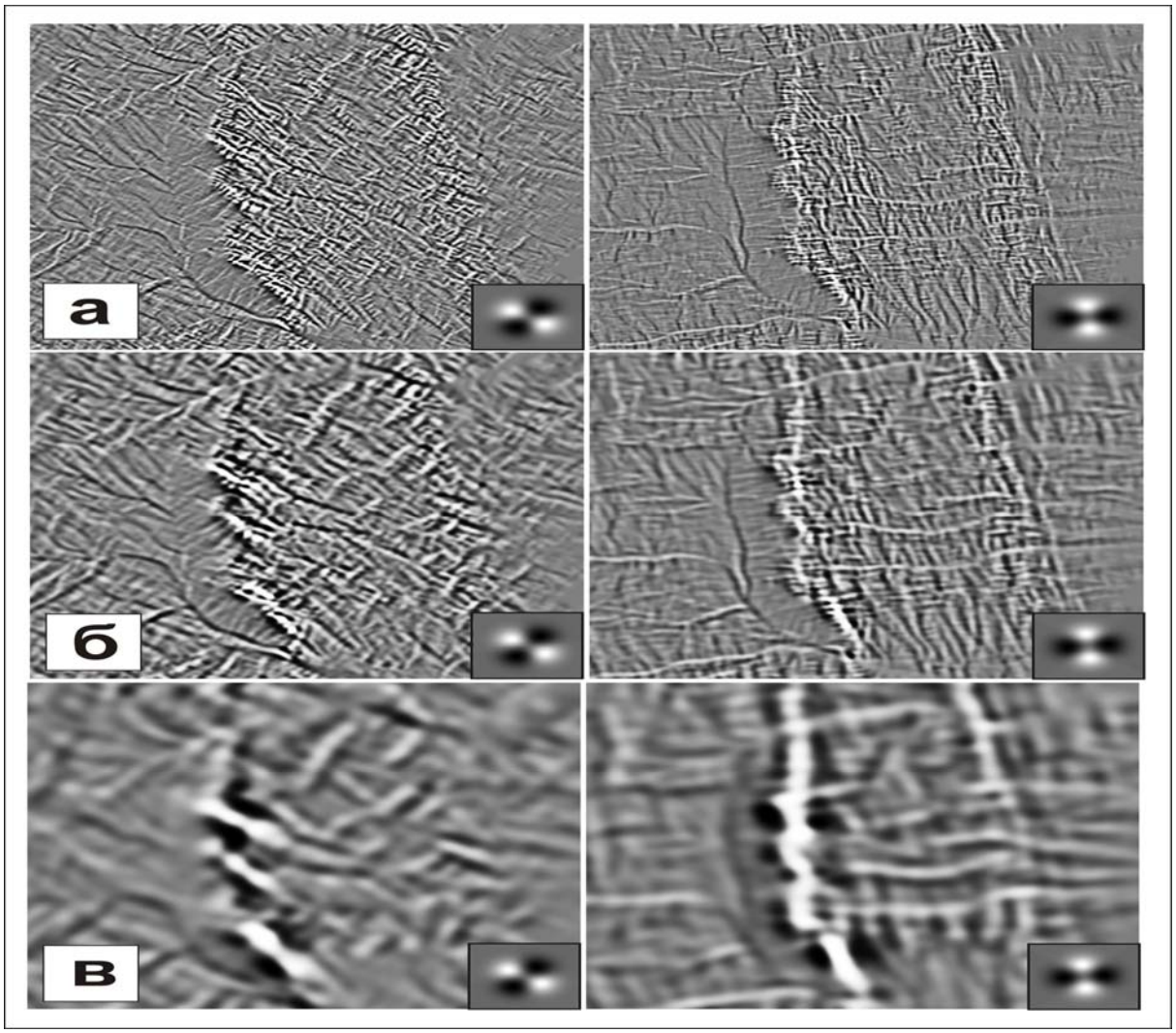


Рис. 1. Участок сейсмоактивной зоны северного Сахалина (район Нефтегорска), где развита правосторонняя сдвиговая тектоника. Шесть вариантов масштабных представлений при t=1, 4, 64 (а, б, в , соответственно) и φ_1=80°(260°) (левые) и φ_2=130°(310°) (правые). Каждая сцена сопровождается формой производной ядра Гаусса.

Список литературы:

Koenderink J.J., van Doorn A.J. Representation of Local Geometry in the Visual System // Biol. Cyb. 1987. Vol. 55. 367-375.
Witkin A. P. Scale-space fltering // Proc. 8th Int. Joint Conf. Art. Intell., 1983. 1019-1022.
Young R. A., Lesperance R. M., Meyer W. W. The Gaussian Derivative model for spatial-temporal vision: I. Cortical model // Spatial Vision. 2001. Vol. 14, No. 3,4. pp.261-319.

RECONSTRUCTING TSUNAMIGENIC EARTHQUAKES ON THE NORTHERN KAMCHATKA SUBDUCTION ZONE: THE 1997 KRONOTSKY EARTHQUAKE AND TSUNAMI AND THEIR PREDECESSORS

Joanne Bourgeois (1), Tatiana Pinegina (2), and several modelers
[1]Earth & Space Sciences, Univ. of Washington. Seattle, WA, USA jbourgeo@uw.edu
[2]Institute of Volcanology and Seismology, FED RAS, Petropavlovsk-Kamchatskiy, Russia

The northern Kamchatka segment of the Japan-Kuril-Kamchatka subduction zone has historically been characterized by more segmented behavior than southern Kamchatka (Fig. 1). Some details of these ruptures can be elucidated by examining tsunami runup records, including runup reconstructed from tsunami deposits (as in MacInnes et al., 2010). The most recent large earthquake in this region occurred on 5 December 1997, a Mw 7.8 offshore of Kronotsky Cape. The tsunami from this earthquake was recorded on tide gages at several stations in the Hawaiian Islands to be 0.15 to 0.30 m amplitude, but local tide gages at Ust-Kamchatsk and on Bering Island were not working. A limited post-tsunami survey found no more than about 2 m runup, south of Kronotsky Cape. However, this survey did not go north of Kronotsky Cape, where later-discovered tsunami-deposit evidence (and a corroborating eyewitness account) suggests that in 1997 there was local runup of 1.8 to 7.3 m at least 55 km along the coast (Fig. 2).

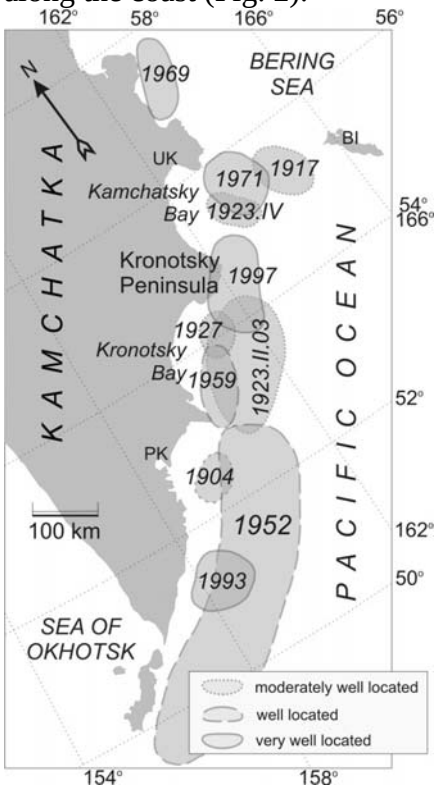


Figure 1. Interpreted rupture locations of largest 20th century earthquakes along the Kamchatka portion of the Kuril-Kamchatka subduction zone (after Gusev and Shumilina, 2004; their estimate of quality of location). PK = Petropavlovsk-Kamchatskiy; UK = Ust Kamchatsk; BI = Bering Island. This abstract suggests a revision of the source region for 1997.

Other historical earthquakes and tsunamis affecting Kamchatsky Bay (Fig. 1). The 1971 Kamchatsky earthquake and tsunami are discussed in LaSelle et al. JKASP abstract; 1917 is not well located or understood. Two local, large tsunamis hit this region in 1923. The deposit we identify as "1923" (above historical tephra $Ksht_3$, AD 1907) is larger than 1997 (Fig. 2), which in turn is larger locally than Kamchatka 1952 or Chile 1960. We tentatively interpret this deposit to be from the Mw 8.5, 4 Feb 1923 earthquake located in an overlapping region to the 5 Dec 1997 earthquake (Fig. 1), in sum farther south. The 14 April 1923 earthquake is reported to have generated high runup near Ust' Kamchatsk; tide-gage amplitude in Hilo is 0.3 m, comparable to Kronotsky 1997. Based on this far-field record, we tentatively suggest a Mw of 7.8 for this event. The record of pre-20th century earthquakes and tsunamis is spotty. Earthquakes on 17 May 1841 and 17 October 1737 originated in the region of the 1952 south Kamchatka great earthquake. There is possibly a large (earthquake and) tsunami on Bering Island on 4 November 1737. Other possibilities in northeast Kamchatka are an 1849 earthquake in the vicinity of the Komandorsky Islands, and a 1791 event which has an intriguing account of having affected the mouth of the Kamchatka River (Ust' Kamchatsk), reaching 7 km upstream.

Modeling 1997. Given the post-tsunami survey reported runup and given that the deposits surveyed in our field campaign of A.D. 2000 are from the 1997 tsunami any model must

explain relatively low runup on Krontosky Peninsula and relatively high runup to the north (Fig. 2). The smooth runup distribution and the ratio of maximum runup to distance over which the tsunami had significant runup (order of 10^{-5}) indicate this tsunami was typical of a seismogenic source rather than a landslide source. The far-field tide-gage records are also indicative of a broad rather than a point source. Higher runup north of the cape can be explained by a distributed-slip tsunami source (earthquake) with concentrated slip in the northern part of the rupture; this northern part was a seismic gap between two events in 1923. In order to explain low runup to the south, we suggest the rupture there was partly located below the peninsula.

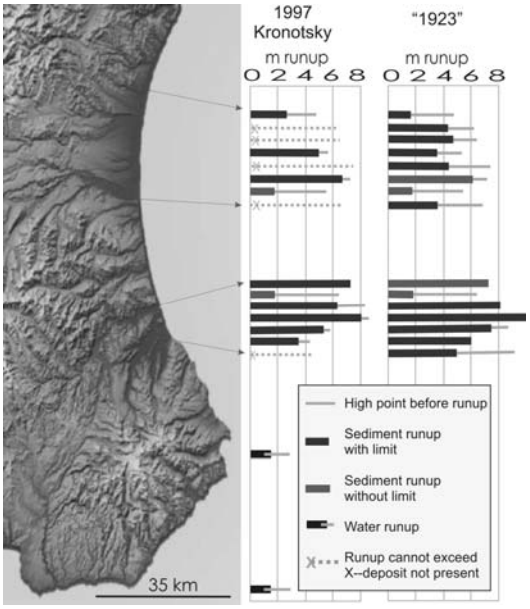


Fig. 2. Indicators of tsunami runup on and north of Kronotsky Peninsula generated by the 5 Dec 1997 and (4 Feb?) 1923 earthquakes; "water runup" indicates measurements of wrack lines in the post-tsunami survey.

Paleotsunamis between Ksht$_3$ (AD 1907) and KS$_1$ (c. AD 250). We base our analysis on the number of tsunami deposits between two distinctive marker tephra, separated by about 1700 calendar years. In any one profile, the number of deposits in this interval tends to decrease away from the coast and at higher elevations, although there is scatter in the data, likely due to preservation and identification differences. Including "1923" itself, all other pre-1997 deposits (typically 10-12) are more extensive than 1997. Most of these deposits are similar in extent and character to 1923, with 3-5 being more extensive than 1923. We do not have evidence of dramatically larger tsunamis than "1923," but the local terrain studied is not necessarily conducive to finding greater inundation, such as in Kiritappu marsh, Hokkaido. Still, the data suggest that this coast may experience a larger-than-1923 earthquake and attendant tsunami at least once every ~400 years, and tsunamis larger than 1997 at least every ~200 years. See Pinegina et al. (2003) for an analysis of Kronotsky Bay to the south.

Implications of this case study are several. The size of the tsunami based on its deposits and on a corroborating eyewitness account constrains the rupture characteristics of this earthquake. This recent historical tsunami also helps us interpret earlier historical and well as prehistorical earthquakes and tsunamis along the northern part of the Kamchatka subduction zone. Tsunamis originating from this region commonly have an impact not only locally but also on Hawaii, and in some cases even on the western coast of the Americas.

Gusev, A.A. and Shumilina, L.S., 2004. Recurrence of Kamchatka strong earthquakes on a scale of moment magnitudes: Izvestiya, Physics of the Solid Earth, v. 40(3), p. 206-215.

MacInnes, B.T. , Weiss, R., Bourgeois, J. and Pinegina, T.K., 2010**.** Slip distribution of the 1952 Kamchatka great earthquake based on near-field tsunami deposits and historical records. Bull. Seismological Society of America, v. 100(4), p. 1695-1709.

Pinegina, T.K., Bourgeois, J., Bazanova, L.I., Melekestsev, I.V., and Braitseva, O.A.,2003: A millennial-scale record of Holocene tsunamis on the Kronotsky Bay coast, Kamchatka, Russia: Quaternary Res., 59: 36-47.

Acknowledgments. Vera Ponomareva helped get us to field sites and consulted on marker tephra. Vasily Titov, Adit Gusman and Bre MacInnes have run tsunami models for 1997; Yuichiro Tanioka provided us with an early analysis by S.W. Sohn.

We dedicate this work to the memory of Sasha Storcheus.

Holocene vertical movement of the east coast of Kamchatsky Peninsula (Kamchatka) based on coastal marine terraces

Tatiana Pinegina[1], Joanne Bourgeois[2], Andrey Kozhurin[3], Ekaterina Kravchunovskaya[1]

[1] Institute of Volcanology and Seismology FEB RAS, Petropavlovsk-Kamchatsky, Russia, 683006; e-mail: tsunami@kscnet.ru
[2] Dept. of Earth & Space Sciences, University of Washington, USA, WA 98195-1310
[3] Geological Institute, Russian Academy of Sciences, Moscow, Russia, 119017

Recent geological and geomorphologic studies of aggradational Holocene coastal terraces provided new data on rates and directions of vertical movement of the coastal areas of the Kamchatsky Peninsula (Pinegina et al., 2010), deformation of which may reflect the mode of the interaction of the northwest-moving Komandorsky Island block with the Kamchatka mainland (Geist, Scholl, 1994; Gaedicke et al., 2000; Freitag et al., 2001). Based on 32 shoreline profiles and about 300 excavations we , quantify vertical movement using differential elevations of paleosurfaces dated with marker tephra layers (Pedoja et al., in prep).Variation in elevations both along single profiles and between adjacent profiles were examined (Figure 1).

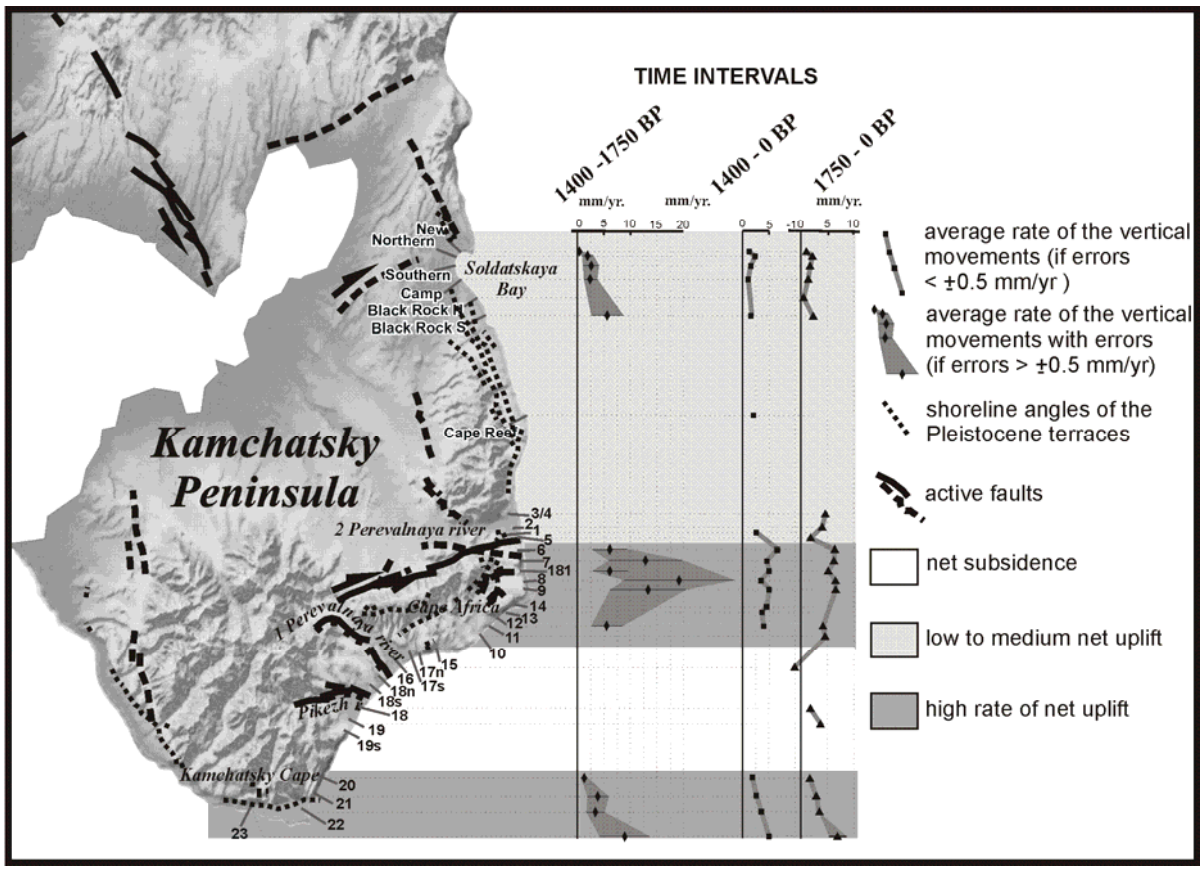


Figure 1. Average rate of Holocene vertical movements (mm/yr or m/ka) along the east coast of Kamchatsky Peninsula

Based on our data we conclude that:

1) Average rates of vertical movement of the Kamchatsky Peninsula coastal area during the last ~2000 years varied in the range between -1.04±0.07 and +6.79±1.71 mm/yr. The most intensive Holocene vertical movement took place around the Cape Africa and Cape Kamchatsky. Coasts surrounding uplifted mountainous massifs of these capes also experienced net positive vertical

movement, suggesting that Holocene deformation inherited the longer-term trends of the Pleistocene.

2) The values of average rates of vertical movement differ from one time interval to another for the same coastal localities. The highest gradients in along-coast rate variation took place during an interval about 350 years long, between ~250 and ~600 AD.

3) The analysis of our data and comparison with instrumental seismological (GCMT catalogue) and geodetic (Kirienko, Zolotarskaya, 1989) data lead us to hypothesize that coastal deformation of marine terraces was most likely coseismic. The primary structures producing earthquakes and coseismic deformation could be onshore faults and their underwater extensions, and offshore faults.

4) We found a spatial correlation between active-fault distribution (Kozhurin, 2007) and parts of the coast where parameters of vertical movement rapidly change. We infer therefore that coastal vertical movement and movement on active faults are the interrelated effects of a single process of deformation of the Kamchatsky Peninsula block.

Our data strongly suggest that since at least the late Pleistocene (Pedoja et al., in prep.) Cape Africa and Cape Kamchatsky have been experiencing uplift. We interpret these movements to be a consequence of NW-SE directed crustal shortening of the Kamchatsky Peninsula block and probably its thrusting over the Kamchatky Strait.

This work was supported by NSF (grant N ARC-0508109), RFBR (grants N 09-05-00125, 11-05-00136), & RFBR-FEBRAS (grant N 11-05-98534)

References

Freitag R., Gaedicke C., Baranov B., Tsukanov N. Collisional processes at the junction of the Aleutian-Kamchatka arcs: new evidence from fission track analysis and field observations / Terra Nova, 2001. N13. P. 433-442

Gaedicke C., Baranov B., Seliverstov N., Alexeiev D., Tsukanov N., Freitag R. Structure of an active arc-continent collision area: the Aleutian–Kamchatka junction / Tectonophysics, 2000. N 325. P. 63–85

Geist E.L., Scholl D.W. Large-scale deformation related to the collision of the Aleutian Arc with Kamchatka / Tectonics, 1994. N 13. P. 538-560

Kozhurin A.I. Active Faulting in the Kamchatsky Peninsula, Kamchatka-Aleutian Junction. In: Eichelberger J, Gordeev E, Izbekov P, Lees J (eds) Volcanism and Subduction: The Kamchatka Region. American Geophysical Union, Washington, DC, 2007. P. 263-282

Pedoja K., Authemayou C., Pinegina T., Bourgeois J., Delcaillau B., Regard V. "Arc-continent collision" of the Aleutian-Komandorsky arc into Kamchatka: insight into Quaternary tectonic segmentation through marine-terrace and drainage analysis (in prep.)

Pinegina T.K., Kravchunovskaya E.A., Lander A.V., Kozhurin A.I., Bourgeois J., Martin M.E. Holocene vertical movement of Kamchatsky Peninsula coast (Kamchatka) based on studies of marine terraces / Bulletin of Kamchatka regional association "Educational-scientific center". Earth Sciences, 2010. N 15. P. 231-247

Kirienko A.P., Zolotarskaya S.V. Some patterns of surface deformations of East Kamchatka during the period from 1966-1983 / Volcanology and Seismology, 1989. N 2. P. 80-93

Global Centroid Moment Tensor Catalog (http://www.globalcmt.org/CMTsearch.html)

THE MANIFESTATION OF STRONG SUBDUCTION EARTHQUAKES AND LOCAL GEODYNAMIC ACTIVATION IN CHANGES OF WATER LEVEL IN THE WELL E-1, KAMCHATKA

Kopylova G.N., Boldina S.V.

Kamchatka Branch, Geophysical Survey RAS, Petropavlovsk-Kamchatsky, gala@emsd.ru

Water level observations in the well E-1 (53.26 lat., 158.48 long., depth 665 м) are carried out by Kamchatka branch of Geophysical service RAS since 1987 [1]. The well is located not far (11 km) from the active volcano Koryakskiy. In changes of water level are reviled the increases and decreases during 3-6 years with amplitudes from tens cm up to 1.5 m, barometric variations and changes due to strong earthquakes. The tidal and seasonal variations are not manifested in water level changes. The well E-1 exposes in depth 625-645 m the groundwater reservoir containing fluid (water and gas) with increased compressibility [1, 2].

Two types of geodynamic effects are extracted in changes of water level: 1 - water level decreases with the accelerated velocity within one week - months before 70-80% of subduction earthquakes with M≥5 on distances up to 350 km (hydrogeodynamic precursor), 2 – the rising of water level with amplitude 1.22 m during middle 2006 to 2009 preceding and following to the swarm of earthquakes (K_S≤8.3) in area of volcano Koryakskiy and phreatic eruption [3] (fig.).

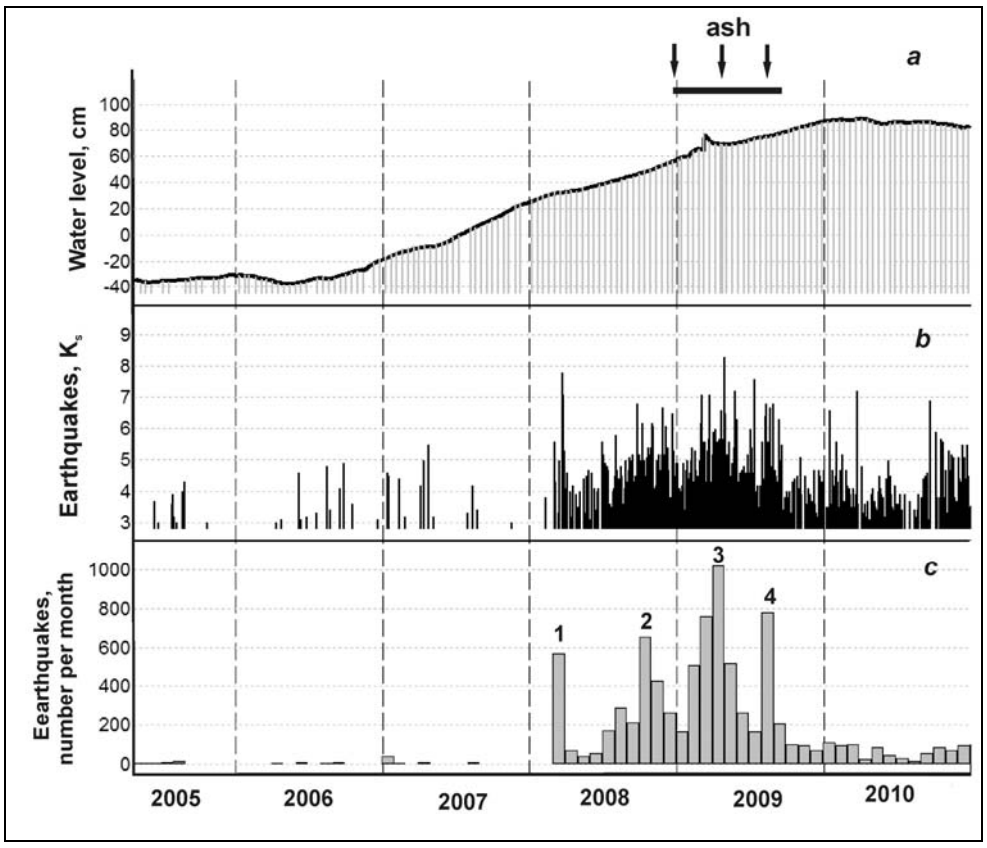


Fig. Water level changes in the well E-1 in 2005 - 2010 (*a*) in comparison with the seismicity (*b*) and the activity of volcano Koryakskiy (the time of phreatic eruption is shown by horizontal line); *c* – the amount earthquakes with K_S≥4.0 per month in area of volcano Koryakskiy (the numbers indicate the peaks of seismic activity: 1 - March 2008; 2 - October 2008; 3 - April 2009; 4 - August 2009).

The attenuation of the well's sensitivity to earthquakes preparation processes was observed during the rising of water level (fig.). It was manifested in the absence of hydrogeodynamic precursors before earthquakes with M≥5 in 2007-2009. The sensitivity of the well E-1 to earthquakes preparation processes was recovered in 2010 after the termination of water level rising. Hydrogeodynamic precursors in water level were fixed before all three seismic events with M≥5 in 2010.

The water level rising continued 3.5 years and showed the pore pressure increase in the reservoir as a result of the volumetric compression. The source of the volumetric compression was connected with preparation and development of the swarm of earthquakes and volcano Koryakskiy eruption. The increase of pore pressure was equal 12.2 kPa (0.12 bar) taking into account to the elastic parameters of reservoir and the amplitude of water level rising. The volumetric compression of the groundwater reservoir $\Delta\varepsilon = -(4.1\text{-}9.9)\cdot 10^{-6}$.

The tectonic stresses due to structure formation of the expansion zone in the earth's crust are the most probable source of the water-saturated rocks compression [3]. The continuous growth of tectonic stresses was accompanied by the activation of weak seismicity in depth 0-10 km within the extended submeridional area since March 2008 and by phreatic eruption of volcano Koryakskiy in 2009.

The long-term observations of the water level show the unique sensitivity of the well E-1 with respect to preparation processes of strong subduction earthquakes and to the geodynamic activation in the interior of the Avachinskaya volcanotectonic depression accompanied by the swarm of earthquakes and phreatic eruption of volcano. The example of this well give a demonstration of two types of the present-day geodynamic processes reflected in water level changes: 1 - preparation and realization of strong subduction earthquakes and 2 - preparation and realization of local displacements in the continental crust accompanied by seismic and volcanic activation. Such processes can «collide» at each other and cause the overlapping responses in water level changes.

Reference

1. Kopylova G.N. Variations of water level in Elizovskaya-1 well, Kamchatka due to large earthquakes: 1987-1998 Observations // Vulkanol. Seismol. 2001. № 2. P. 39–52 [in Russian].

2. Kopylova G.N. The application of water level observations in wells for searching earthquakes precursors (on the example of Kamchatka) // Geofizicheskye issledovanya. 2009. №. 2. V. 10. P. 56-68 [in Russian].

3. Seliverstov N. I. The eruption of Koryakskiy volcano at // Vestnik KRAUNTs, Nauki o Zemle. 2009. №. 1. V. 13. P. 7–9 [in Russian].

ПРОЯВЛЕНИЕ ЭФФЕКТОВ СИЛЬНЫХ СУБДУКЦИОННЫХ ЗЕМЛЕТРЯСЕНИЙ И ЛОКАЛЬНОЙ ГЕОДИНАМИЧЕСКОЙ АКТИВИЗАЦИИ В ИЗМЕНЕНИЯХ УРОВНЯ ВОДЫ В СКВАЖИНЕ Е-1, КАМЧАТКА

Копылова Г.Н., Болдина С.В.

Камчатский филиал Геофизической службы РАН, г. Петропавловск-Камчатский, gala@emsd.ru

Уровнемерные наблюдения на скважине Е-1 (53.26° с.ш., 158.48° в.д., глубина 665 м) проводятся Камчатским филиалом Геофизической службы РАН с 1987 г. [1]. Она находится в 11 км от действующего вулкана Корякский. В изменениях уровня воды проявляются повышения и понижения продолжительностью 3 - 6 лет с амплитудами от первых десятков см до 1.5 м, слабые барометрические вариации и изменения в связи с сильными землетрясениями. Приливные и сезонные изменения уровня воды не проявляются. Скважина вскрывает резервуар подземных вод в зоне затрудненного водообмена с повышенной сжимаемостью поровой воды, содержащей газовую фазу [1, 2].

В изменениях уровня воды выделены два типа геодинамических эффектов: 1 – понижения уровня с повышенной скоростью в течение недели - первых месяцев примерно перед 70-80% субдукционных землетрясений с M≥5 на расстояниях до 350 км (гидрогеодинамический предвестник); 2 - повышение уровня воды с середины 2006 по 2009 гг., предшествующее и сопутствующее рою слабых (K_S≤8.3) землетрясений в районе влк. Корякский и его фумарольной активизации [3] (рис.).

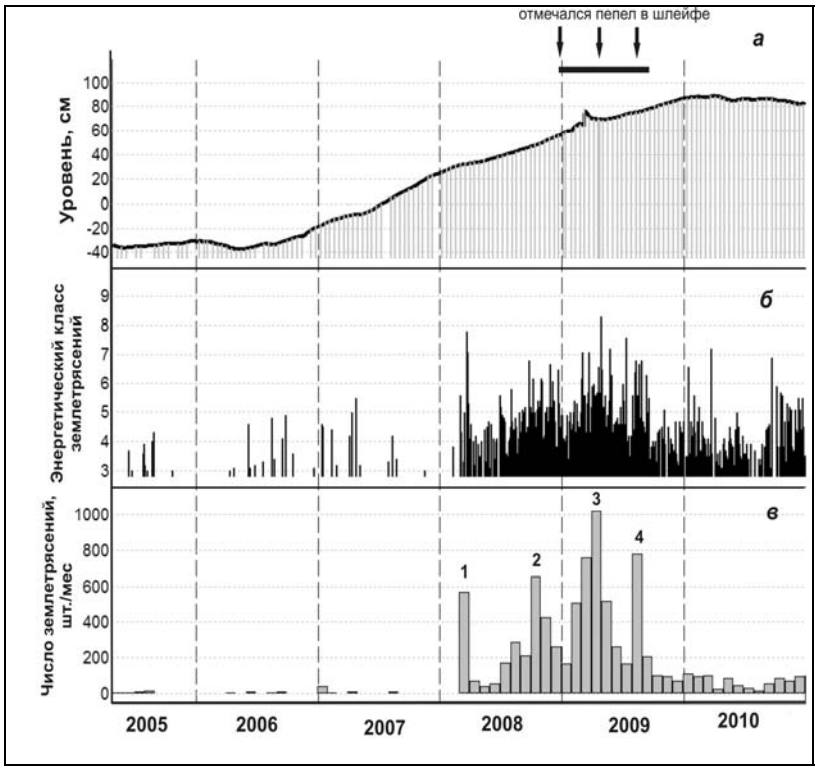


Рис. Изменение уровня воды в скважине Е-1 в 2005 – 2010 гг. (*а*) в сопоставлении с сейсмичностью (*б*) и вулканической активностью вулкана Корякский (горизонтальной линией показано время фреатического извержения); *в* – суммарное за месяц количество землетрясений с K_S≥4.0 в районе влк. Корякский (цифрами обозначены максимумы сейсмической активности: 1 – март 2008 г., 2 – октябрь 2008 г., 3 – апрель 2009 г., 4 – август 2009 г.).

Во время повышения уровня воды (рис.) наблюдалось ослабление чувствительности скважины к процессам подготовки землетрясений, возникающих в процессе поддвига Тихоокеанской океанической плиты под Охотоморскую плиту континентального типа. Это проявлялось в отсутствии гидрогеодинамического предвестника перед такими землетрясениями в 2007-2009 гг. Чувствительность скважины к процессам подготовки субдукционных землетрясений восстановилась в 2010 г. после окончания повышения уровня воды. В 2010 г. гидрогеодинамический предвестник был зафиксирован перед всеми тремя сейсмическими событиями с $M \geq 5$.

Повышение уровня воды продолжалось 3.5 года и показывало рост порового давления вследствие возникновения источника деформации объемного сжатия водовмещающих пород. Источник был связан с подготовкой и развитием роя землетрясений и извержения влк. Корякского. Амплитуда повышения уровня составила 1.22 м. С учетом упругих параметров резервуара по амплитуде повышения уровня воды рост порового давления составил 12.2 кПа или 0.12 бар. Величина деформации объемного сжатия в районе скважины составляла $\Delta\varepsilon = -(4.1 - 9.9)\cdot 10^{-6}$.

Наиболее вероятным источником сжатия водовмещающих пород являются тектонические напряжения, связанные с формированием субмеридиональной раздвиговой зоны в земной коре в районе влк. Корякский [3]. Рост тектонических напряжений с марта 2008 г. сопровождался активизацией слабой сейсмичности в пределах протяженной субмеридиональной зоны и слабым фреатическим эксплозивным извержением.

Многолетний мониторинг уровня воды показывает уникальную чувствительность гидродинамического режима скважины Е-1 по отношению к процессам подготовки сильных субдукционных землетрясений и к геодинамической активизации в недрах Авачинской вулканотектонической депрессии, сопровождающейся роем землетрясений и фреатическим извержением вулкана Корякский. На примере этой скважины показано, что, по крайней мере, два вида современных геодинамических процессов: 1 – подготовка и реализация сильных субдукционных землетрясений и 2 – локальные движения в пределах континентальной коры, сопровождающиеся сейсмической и вулканической активизацией, могут «накладываться» друг на друга и вызывать перекрывающие друг друга отклики в изменениях уровня воды.

Литература

1. Копылова Г.Н. Изменения уровня воды в скважине Елизовская-1, Камчатка, вызванные сильными землетрясениями (по данным наблюдений в 1987-1998 гг.) // Вулканология и сейсмология. 2001. № 2. С. 39-52.

2. Копылова Г.Н. Оценка информативности уровнемерных наблюдений в скважинах для поиска гидрогеодинамических предвестников землетрясений (на примере Камчатки) // Геофизические исследования. 2009. Т. 10. № 2. С. 56-68.

3. Селиверстов Н.И. Активизация вулкана Корякский на Камчатке // Вестник КРАУНЦ. Науки о Земле. 2009. № 1. Вып. 13. С. 7-9.

Significance Radiolarian data for the solution of the tectonic and paleogeographic problems on the Russian Far East

Palechek Tatiana
Geological Institute of the Russian Academy of Sciences. Moscow, Russia, tatiana@ilran.ru

The North Pacific region has the very complicate geological structure. And there are no good stratigrafic scale was compiling for that time. The important investigations in this area are determine so much geographical association and active geodynamic processes between ocean and continental margin that fix structure this marginal belt and commonality geological processes and many paleogeographic and biotic events in Mezosoic and Cenosoic time.
It is a very important in a view of modern accretion tectonic conception about geological structure of this region. According of this conception the structure of the northern part of Pacific Ocean's margin was combined by accretion alien blocks (terranes) of different geological nature to Eurasian margin. Radiolarians, as wrote japans authors in the book «Radiolarians and radiolarian terranes» [12], can show direct evidence for important of the approaches heterogeneous tectonics slides. Today there is investigation of radiolarians by modern technology and devices namely – possibility extraction radiolarians skeletons from solid rocks and the latest study of volumetric forms by scan electronic microprobe lead out radiolarians in a range top-level microfossils that using for zonal stratigraphy and correlation between different continent [4].

On some areas of Kamchatka [1-4, 6], Koryak Highland [5, 9], Taigonos Peninsula [10], Sakhalin Island [8] was shown the significance of radiolarian data for solution tectonic and paleogeographic problems.

For example, we examine area of the Anastasiya Bay area of Koryak Highland. Volcanogenic-siliceous and sedimentary-volcanogenic rocks complexes are distinguished in the Anastasiya Bay area. The age of siliceous beds in these complexes was inferred from radiolarian finds. The volcanogenic-siliceous complex was probably formed within a marginal sea basin and the sedimentary-volcanogenic complex in an island-arc and its slope settings. The data obtained allow us to reconstruct the hypothetical lateral succession of the Campanian-Maastrichtian paleogeographic settings: the continental margin – marginal sea – island arc – oceanic basin [11].

The next example, we examine area of the Omgon Range (Western Kamchatka). We extracted radiolarians from volcanogenic- chert deposits of the different blocks [2, 7]. Investigation of rock complexes in the Omgon Range demonstrated that deposits of various ages, originated from various geodynamic settings, were tectonically merged in its structure. Deposits of the Middle Jurassic volcanic complex that were formed in an oceanic and/or marginal marine environment occur as tectonic slices and blocks in the Albian-Campanian terrigenous matrix. The terrigenous complex was formed in a marginal continental environment. This allows interpreting the rock complexes of the Omgon Range as a fragment of the Cretaceous accretionary prism, which originated from the offscraping of slices and blocks of oceanic rocks and their juxtaposition with marginal continental deposits. The accretionary prism was formed along with the subduction of the Pacific paleoceanic plates under the Eurasian continental margin, which gave rise to volcanism within the Okhotsk-Chukotka belt [3].

The investigation of accretional complex from Taigonos Peninsula showed tectonic coexistence of different ages and paleoclimatic positions of slices [10]. Radiolarians extracted from cherty rocks, which consist in to sedimentary-volcanic deposits of accretionary complex of the Povorotnyi Cape (Taigonos Peninsula). The studied radiolarian assemblages are of the Middle (Bajocian-Callovian), Middle – Late (Callovian-Oxfordian) and Late Jurassic (Kimmeridgian – Tithonian) ages. Based on taxonomic composition and morphology of tests, the Bajocian – Callovian assemblage is attributed to the north tethyan type, while the Callovian-Oxfordian and Kimmeridgian-Tithonian assemblages are of the boreal affinity.

In present time radiolarians are ortostratigraphic group of the faunas and occupy a leading position in the stratigraphy of the sedimentary deposits. Recently, the precision of radiolarian analysis was grown owing to fashion methods of the extract radiolarians and usage scanning electronic microscope. Because of this, appearance of many new works on biostratigraphy of the volcanic-chert rocks from the Russian Far East have been published [1-11].

References

1. Bakhteev M.K., Palechek T.N., Tikhomirova S.R., Morozov O.A. Campanian Radiolarians from the north part of Valaginsky Ridge (Eastern Kamchatka). Stratigraphy and Geological Correlation, 2002, vol.10, No.4, pp.52-61.
2. Bogdanov N.A., Bondarenko G.E., Vishnevskaya V.S., Izvekov I.N. Middle-Upper Jurassic and Lower Cretaceous Radiolarian complexes from Omgon Ridge (Western Kamchatka). Dokl. AN Sci., 1991. vol. 321. №2. p. 344-348.
3. Bogdanov N.A., Soloviev A.V., Ledneva G.V., Palechek T.N., Lander A.V., Garver J. I.., Verzhbitsky V.E., Kurilov D.V. The structure of the Cretaceous Accretionary Prism in the Omgon Range, Western Kamchatka. Geotectonics. 2003, vol.37, no.4, p.316-327.
4. Vishnevskaya V.S. Radiolarian Biostratigraphy of the Jurassic and Cretaceous in Russia (GEOS, Moscow, 2001. 376 p.) (in Russian).
5. Geology of the south part of Koryak Upland. Moscow, Nauka, 1987, 167p.
6. Western Kamchatka: Mesozoic Geological Evolution. Ed. By Gladenkov Yu.B. and Palandzhyan S.A. Moscow, Scientific World, 2005, 224 p., 96 phototabl. (in Russian).
7. . Kazintsova L.I. , Lobov L.M. About finds of Berriasian-Valanginian Radiolarians in volcanic-cherty sediments on the Western Kamchatka. Abstracts of Meeting " Radiolarians and biostratigraphy", Sverdlovsk, 1987. pp.38-39.
8. Kazintsova L.I. Albian-Maastrikhtian Radiolarians from Western Sakhalin. In: Materials of XI Radiolarian Meeting. Spb.-M., pp.31-32.
9. Palechek T.N. Candidate's Dissertation in Geology and Mineralogy (Moscow,1997.25p.)
10. Palechek T.N., Palandzhan S.A. Jurassic Radiolarians and Age of Cherty Rocks in the Povorotnyi Cape, the Taigonos Peninsula (Northeast Russia). Stratigraphy and Geological Correlation, 2007, vol.15, No.1, pp.67-88.
11. Soloviev A.V., Palechek T.N., Palechek R.M. Tectonostratigraphy of the north part of Olutor zone (Koryak Upland, Anastasia Bay). Stratigraphy and Geological Correlation, 1998. vol. 6. №4. pp.92-105.
12. Recent Progress of Reseach on Radiolarians and Radiolarian Terranes of Japan // News of Osaka Micropaleontol. 1986. Spec. Vol. №7. MRT Newsletter, №2.

Значение данных радиоляриевого анализа при решении тектонических и палеогеографических проблем на Северо-Востоке России

Палечек Т.Н.

Геологический институт РАН, Москва, Россия, tatiana@ilran.ru

Северотихоокеанский регион является одним из наиболее сложных в геологическом отношении и в то же время остается до сих пор одним из наименее разработанных в плане стратиграфии регионов. Важность исследований в этом регионе определяется тем обстоятельством, что географическая сопряженнность и активное геодинамическое взаимодействие океана и окраины континента предопределили современный структурный план переходной области и общность различных геологических процессов и многих палеогеографических и биотических событий на протяжении мезозоя-кайнозоя.
Это чрезвычайно важно в свете современных представлений о геологическом строении региона с позиций аккреционной тектоники, согласно которым тектоническая структура северного обрамления Тихого океана сформировалась в результате причленения к активной окраине Евразии чужеродных блоков (террейнов), имевших разную геологическую природу. Радиолярии, как подчеркивают авторы японского сборника “Радиолярии и радиоляриевые террейны” [13], могут служить прямым доказательством значительного сближения разнородных тектонических пластин. В настоящее время изучение радиолярий с использованием последних достижений науки и техники, а именно – возможности выделения скелетов радиолярий из плотных пород и последующего изучения объемных форм в сканирующем электронном микроскопе, вывело их в ранг ведущих микроорганизмов, используемых для зональной стратиграфии и межконтинентальных корреляций [4].
На примере ряда районов Камчатки [1-4,6], Корякского нагорья [5,9], п-ова Тайгонос [10], Сахалина [8] показано значение данных радиоляриевого анализа при решении тектонических и палеогеографических проблем. Рассмотрим несколько примеров.
Так, в р-не бухты Анастасии (Корякское нагорье) были изучены два комплекса вулканогенно-кремнистый (окраинноморский) и осадочно-вулканогенный, сформированный в пределах островной дуги и ее склона. Возраст кремнистых отложений определялся по радиоляриям. Благодаря полученным данным для кампан-маастрихтского времени был реконструирован возможный палеолатеральный ряд: континентальный склон – впадина окраинного моря – поднятие островной дуги – впадина океанического бассейна [12].
Возраст вулканогенного комплекса в р-не хребта Омгон (Западная Камчатка) был обоснован определениями радиолярий как среднеюрский-раннемеловой [2,7]. Изучение комплексов хребта Омгон показало, что в его структуре тектонически совмещены разновозрастные отложения, сформированные в разных геодинамических обстановках. Образования среднеюрского-раннемелового вулканогенного комплекса океанического и/или окраинно-морского генезиса залегают в виде тектонических пластин и блоков в терригенном цементе альб-кампанского возраста. Терригенный комплекс накапливался в окраинно-континентальной обстановке. Все это позволило рассматривать комплексы хребта Омгон как фрагмент меловой аккреционной призмы, сформированной за счет соскабливания пластин и блоков океанической природы и совмещения их с окраинно-континентальными отложениями [3].
Благодаря впервые найденным радиоляриям кампанского возраста из кремнисто-вулканогенных отложений, слагающих разрез в береговых обрывах бухты Моховой в р-не г.Петропавловска-Камчатского, эти отложения были датированы и сопоставлены с валагинской серией Восточной Камчатки. Такая датировка для данных отложений получена впервые, ранее возраст определялся лишь предположительно как позднемеловой [11].

Таким образом, радиолярии играют важную роль при решении различных задач в районах со сложным геологическим строением.

Литература

1. Бахтеев М.К., Палечек Т.Н., Тихомирова С.Р. Кампанские радиолярии северной части Валагинского хребта (Восточная Камчатка). Стратиграфия. Геологическая корреляция. 2002. Т. 10. №4. С.52-61.
2. Богданов Н.А., Бондаренко Г.Е., Вишневская В.С., Извеков И.Н. Средне-верхнеюрские и нижнемеловые комплексы радиолярий Омгонского хребта (Западная Камчатка). Докл.Акад.Наук, 1991. т. 321. №2. С. 344-348.
3. Богданов Н.А., Соловьев А.В., Леднева Г.В., Палечек Т.Н., Ландер А.В., Гарвер Дж.И., Вержбицкий В.Е., Курилов Д.В. Строение меловой аккреционной призмы хребта Омгон (Западная Камчатка).Геотектоника. 2003. №4. С.64-76
4. Вишневская В.С. Радиоляриевая биостратиграфия юры и мела России. М.: ГЕОС, 2001, 376 с.
5. Геология юга Корякского нагорья. М., Наука, 1987, 167с.
6. Западная Камчатка: геологическое развитие в мезозое / Коллектив авторов.- М.:Научный мир, 2005.-224 с., вкл.96 с.
7. Казинцова Л.И., Лобов Л.М. О находке берриас-валанжинских радиолярий в вулканогенно-кремнистых отложениях Западной Камчатки. Тезисы докладов “Радиолярии и биостратиграфия “, Свердловск: 1987. С.38-39.
8. Казинцова Л.И. Радиолярии альба-маастрихта Западного Сахалина. В сборнике XI семинара по радиоляриям “Радиоляриология на рубеже тысячелетий: итоги и перспективы”, С-П. – М., 2000. С.31-32.
9. Палечек Т.Н. Строение и условия формирования верхнемеловых вулканогенно-кремнистых отложений Олюторского района (на основе радиоляриевого анализа). Автореф. дис. … канд. геол.-мин. наук. М.: Ин-т литосферы РАН, 1997. 25 с.
10. Палечек. Т.Н., Паланджян С.А. Юрские радиолярии и возраст кремнистых пород мыса Поворотного, полуостров Тайгонос (Северо-Восток России). Стратиграфия. Геологическая корреляция. 2007. Т. 15. № 1. С. 73-94.
11. Савельев Д.П., Палечек Т.Н., Портнягин М.В. Кампанские океанические кремнисто-вулканогенные отложения в фундаменте Восточного Камчатского вулканического пояса. Тихоокеанская геология. 2005. Т.24, №2, С.46-54.
12. Соловьев А.В., Палечек Т.Н., Палечек Р.М. Тектоностратиграфия северной части Олюторской зоны (Корякское нагорье, район бухты Анастасии). Стратиграфия. Геологическая корреляция. 1998. Т. 6. №4. С.92-105.
13. Recent Progress of Reseach on Radiolarians and Radiolarian Terranes of Japan // News of Osaka Micropaleontol. 1986. Spec. Vol. №7. MRT Newsletter, №2.

DEFORMATIONS ON THE BOUNDARY BETWEEN THE EURASIAN AND AMURIAN PLATES

S.V. Ashurkov, V.A. Sankov
Institute of the Earth's Crust SB RAS, Irkutsk, Russia

Deformation style and intensity on the lithospheric plate boundaries are determined by the kinematics of plate motion. Direct geodetic measurements of horizontal plate motions make it possible to compare theoretical and observable deformations on the interplate boundaries with the aim of verifying solutions and determining additional factors that influence structure and seismicity therein. A comparison was made between the velocity vectors computed from GPS observations and Holocene horizontal displacements along the faults [Sankov et al., 2000; Sankov et al., 2004] and stress-strain state of the geological environment along the northern boundary of the Amurian plate.

The data obtained during the measurements on the Amur-Zeya geodynamic test site and the additional data have been used to derive the horizontal velocity field that served as the basis for estimating the relative rotation of the Eurasian (EU) and Amurian (AM) plates. According to these estimates, the pole of the Amurian plate rotation relative to the Eurasian plate is located in between 58.95±0.52 North latitude and 122.29±0.73 East longitude, and an angular velocity is 0.095±0.003 deg/My [Ashurkov et al., 2011].

The Amurian plate rotation parameters have been used to determine the rates and directions of divergent motions in the various parts of the BRS and convergent motions within the Tukuringra-Dzhagdinsk seismic branch. The obtained theoretical plate motion vectors have been compared with the direction of minimum horizontal compression axes [Petit et al, 1996] and axes of seismotectonic deformation (STD) elongation [Neotectonics …, 2000] for the divergent part of the Amurian and Eurasian interplate boundary and with the orientation of maximum horizontal compression axes [Barth & Wenzel, 2010] and STD for the convergent part of it. As Figure 1 shows, the directions of theoretical displacement vectors obtained from GPS observations correlate well with those of principal stress axes along the entire boundary. The distribution of divergence rate in the Baikal rift system corresponds to the order in which the opening of basins occurred from the South Baikal and Chara that is consistent with N.A. Logatchev's concept about gradual growth of the rift system in this direction [2003]. A cardinal change in the type of motion along the plate boundary occurs nearby the Olekma River valley. V.S. Imaev and his co-authors [2000] earlier concluded that that the stress-strain state of the Earth's crust therein changed near the 121 meridian.

The work has been done under financial support of RFBR projects No. 08-05-00992, 08-05-98113; SIE SB RAS project No. 56 and DES Program project No. 7.7.

Ashurkov S.V., San'kov V.A., Miroshnichenko A.I., Lukhnev A.V., Sorokin A.P., Serov M.A., Byzov L.M. GPS geodetic constraints on the kinematics of the Amurian Plate // Russian Geology and Geophysics, 2011, v. 52, p. 239–249.

Barth A., Wenzel F. New constraints on the intraplate stress field of the Amurian plate deduced from light earthquake focal mechanisms // Tectonophysics (2009), doi:10.1016/j.tecto.2009.01.029

Imaev, V.S., Imaeva, L.P & Kozmin, B.M. (2000). – Seismotectonics of Yakutia. – GEOS, Moscow, 227 pp. (in Russian).

Logatchev, N.A History and geodynamics of the Baikal rift. // Russian Geology and Geophysics, 2000, v. 44, №5, p. 373-387.

Neotectonics, geodynamics and seismicity of the North Eurasia. (2000). – Grachev, A.F. (ed.). – UIPhE RAS, Moscow, 487 pp. (in Russian).

Petit C., Deverchere J., , Houdry F., Sankov V., Melnikova V., Delvaux D. Present-day stress field changes along the Baikal rift and tectonic implications // Tectonics, 1996, v. 15, № 6, p. 1171–1191.

Sankov V., **Deverchere J., Gaudemer Y., Houdry F., Filippov A.** Geometry and rate in the North Baikal Rift, Siberia // Tectonics, 2000. Vol. 19, № 4, P.707-722.

San'kov, V.A., Chipizubov, A.V., Lukhnev, A.V., Smekalin, O.P., Miroshnichenko, A.I., Calais, E. & Déverchère, J. Assessment of a large earthquake risk in the zone of Main Sayan Fault using GPS geodesy and paleoseismology. // Russian Geology and Geophysics, 2004, v. 45, №11, p. 1317-1324.

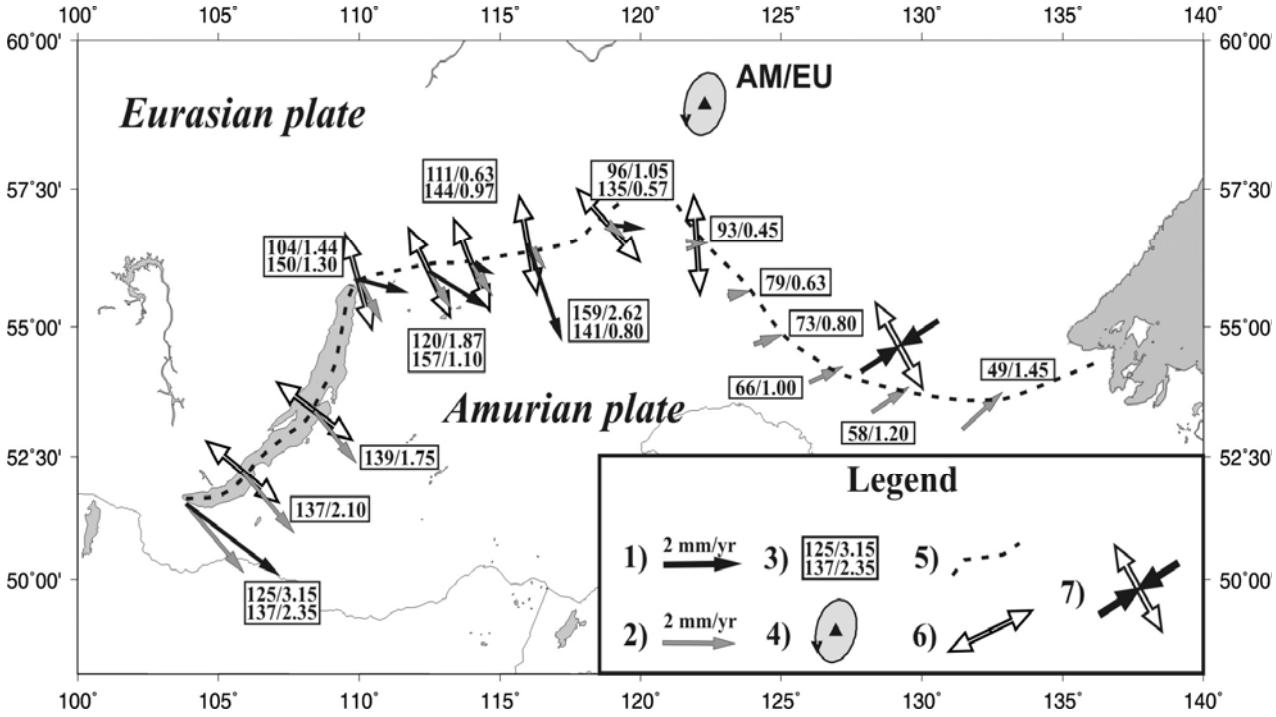


Figure 1. Divergence and convergence velocities on the boundary between the Eurasian and Amur plates.

1 – vectors of divergence from the geological data (Sankov et al., 2000, updated; Sankov et al., 2004), 2 – theoretical vectors of motions from the GPS data, 3 – azimuth/velocity mm/yr (at the top – from the geological data, at the bottom – from the GPS data), 4 – pole of rotation of the Amur plate relative to Eurasia (ellipse – pole error, arrow shows counterclockwise rotation), 5 – interplate boundary, 6 – orientation of the minimum horizontal compressive stress Sh (Petit et al, 1996), 7 – orientation of maximum (SH – black) and minimum (Sh – white) horizontal compressive stresses (Barth, Wenzel, 2009)].

ДЕФОРМАЦИИ НА МЕЖПЛИТНОЙ ГРАНИЦЕ ЕВРАЗИЙСКОЙ И АМУРСКОЙ ПЛИТ

Ашурков С.В., Саньков В.А.
Институт земной коры СО РАН, Иркутск, Россия

Стиль и интенсивность деформаций на границах литосферных плит определяет кинематика их движения. Наличие результатов прямых измерений горизонтальных смещений плит геодезическими методами дает возможность сопоставления теоретических и наблюдаемых деформаций на межплитных границах с целью верификации решений и определения дополнительных факторов, влияющих на формирование ее структуры и сейсмичности. Проведено сопоставление расчетных векторов скоростей по данным GPS измерений с голоценовыми смещениями по разломам [Sankov et al., 2000; Саньков В.А. и др., 2004] и напряженно-деформированным состоянием геологической среды, вдоль северной границы Амурской плиты

По данным измерений на Амуро-Зейском геодинамическом полигоне с привлечением дополнительных данных было получено поле скоростей горизонтальных движений пунктов. На его основе полученны параметры относительного вращения Евразийской (EU) и Амурских (AM) плит, в соответствии с которыми полюс вращения Амурской плиты относительно Евразийской расположен в районе 58.95±0.52 с.ш., 122.29±0.73 в.д., а угловая скорость составляет 0.095±0.003 град/млн. лет [Ашурков и др., 2011].

С использованием параметров вращения Амурской плиты в Евразийской системе отсчета рассчитаны скорости и направления дивергентных движений на различных участках БРС, и конвергентных в пределах Тукурингро-Джагдинской сейсмической ветви. Полученные теоретические векторы плитных движений сопоставлены с направлением осей минимального горизонтального сжатия [Petit et al, 1996] и осей удлинения сейсмотектонических деформаций (СТД) [Новейшая тектоника …, 2000] для дивергентного участка межплитной границы, а также с ориентацией осей максимального горизонтального сжатия [Barth, Wenzel, 2010] и СТД для конвергентной части границы Амурской и Евразийской плит. Как видно из рисунка 1, направления теоретических векторов смещений, полученные по результатам GPS измерений, показывают хорошее сходство с направлениями главных осей напряжений на всем протяжении границы. Распределение скорости дивергенции в Байкальской рифтовой системе соответствует очередности раскрытия впадин от Южно-Байкальской до Чарской, что соответствует концепции Н.А. Логачева [2003] о постепенном разрастании рифовой системы в этом направлении. Кардинальное изменение типа подвижки по границе плит происходит в районе долины р. Олекма. Ранее В.С. Имаев с соавторами [2000] на основании геолого-структурных и сейсмологических данных сделали вывод о смене напряженно-деформированного состояния земной коры в этом районе, вблизи 121 меридиана.

Работа выполняется при финансовой поддержке РФФИ (№№08-05-00992, 08-05-98113), МИП СО РАН №56 и Программы ОНЗ №7.7.

Ашурков С.В., Саньков В.А., Мирошниченко А.И., Лухнев А.В., Сорокин А.П., Серов М.А., Бызов Л.М. Кинематика Амурской плиты по данным GPS геодезии // Геология и геофизика, том 51, 2010, №7

Логачев Н.А. История и геодинамика Байкальского рифта // Геология и геофизика. 2003. Т. 44. С. 391- 406.

Имаев В.С., Имаева Л.П., Козьмин Б.М. Сейсмотектоника Якутии. М., ГЕОС, 2000, 227 с.

Новейшая тектоника, геодинамика и сейсмичность Северной Евразии /Отв. ред. А.Ф. Грачев. М.: ОИФЗ, 2000. 487 с.

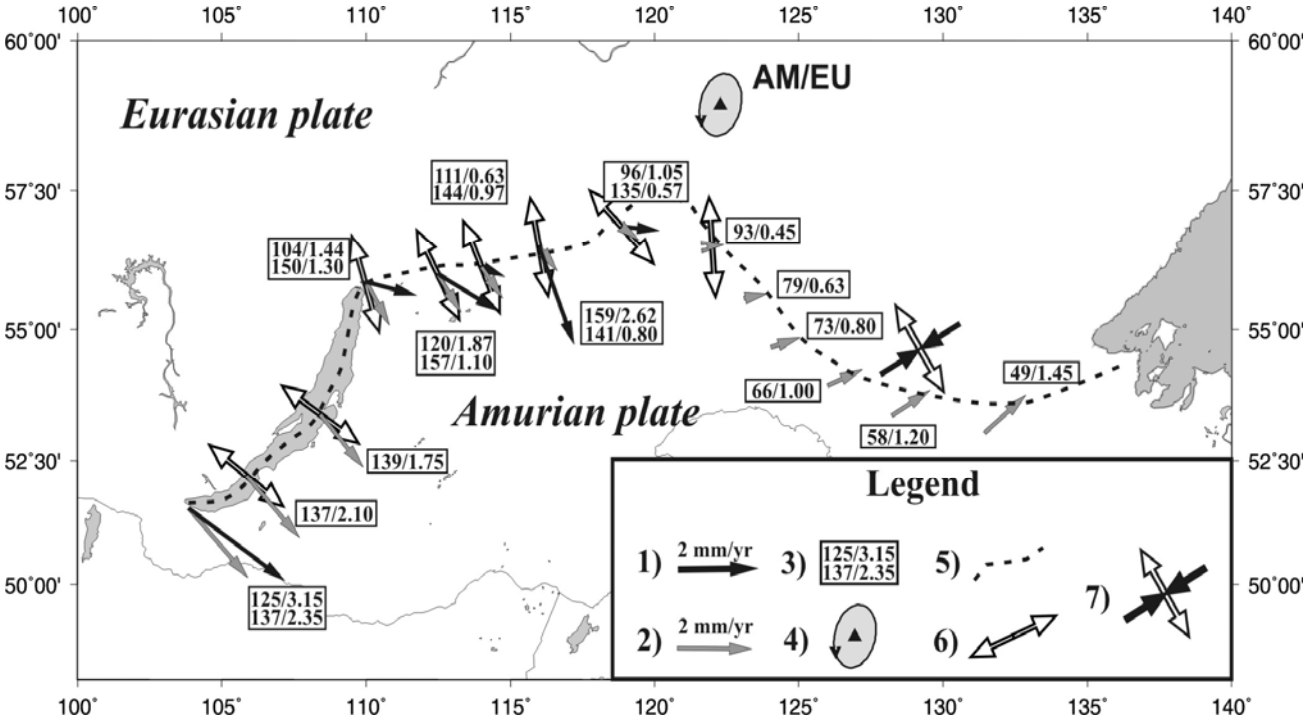
Саньков В.А., Чипизубов А.В., Лухнев А.В., Смекалин О.П., МирошниченкоА.И., Кале Э., Девершер Ж. Подход к оценке опасности сильного землетрясения в зоне Главного Саянского разлома по данным GPS-геодезии и палеосейсмологии // Геология и геофизика, 2004. №11. – С. 1369-1376

Barth A., Wenzel F. New constraints on the intraplate stress field of the Amurian plate deduced from light earthquake focal mechanisms // Tectonophysics (2009), doi:10.1016/j.tecto.2009.01.029

Petit C., Deverchere J., , Houdry F., Sankov V., Melnikova V., Delvaux D. Present-day stress field changes along the Baikal rift and tectonic implications // Tectonics, 1996, v. 15, № 6, p. 1171–1191.

Sankov V., **Deverchere J., Gaudemer Y., Houdry F., Filippov A.** Geometry and rate in the North Baikal Rift, Siberia // Tectonics, 2000. Vol. 19, № 4, P.707-722.

Рис.1. Скорости дивергенции и конвергенции на межплитной границе Евразийской и Амурской плит.



1 – векторы дивергенции по геологическим данным [Sankov et al., 2000 с изменениями; Саньков и др., 2004а], 2 – теоретические векторы движений по данным GPS измерений, 3 – азимут/скорость в мм/год (сверху – по геологическим данным, снизу – по данным GPS), 4 – полюс вращения Амурской плиты относительно Евразийской (эллипс – ошибка определения полюса, стрелка указывает на вращение против часовой стрелки), 5 – межплитная граница, 6 – ориентация минимального горизонтального сжимающего напряжения Sh [Petit et al, 1996], 7 – ориентация горизонтального максимального (SH – черные стрелки) и минимального (Sh – белые стрелки) сжимающего напряжения [Barth, Wenzel, 2010]

Relationship between the interplate quasi-static slip and the focal region of M7-class interplate earthquakes in the Hyuga-nada, SW Japan subduction zone

#Yusuke YAMASHITA[1], Hiroshi SHIMIZU[1], Kenji UEHIRA[1], and Mikio FUJII[2]

1. Institute of Seismology and Volcanology (SEVO), Kyushu University, JAPAN
2. Toyama Local Meteorological Observatory, JAPAN

Corresponding author: Y. YAMASHITA (yamac@sevo.kyushu-u.ac.jp)

Introduction

In the Hyuga-nada region, the Philippine Sea Plate subducts northwestward beneath the Eurasian Plate an approximate rate of 5–7 cm/year, and M7-class interplate earthquakes have repeatedly occurred at decade years interval. Estimating of these focal regions arenecessary for understanding the heterogeneous interplate coupling in this region. We relocate the hypocenters of the main shock and aftershocks for the major interplate earthquakes which occurred in 1931 (Mjma7.1), 1941 (Mjma7.2), 1961 (Mjma7.0), and 1970 (Mjma6.7), and compare them with the quasi-static slip rate estimated by the analysis of small repeating earthquakes.

Data and Method

We used the smoked-paper records and the Seismological Bulletin of the Japan Meteorological Agency (JMA). All hypocenters were relocated mainly using S-P time data, and also using P wave arrival time data buttheweightwas set to one fifthof the S-P time data for reducing the error caused by inaccuracies of the clock. All the main shock events were re-picked the S-P time from the smoked-paper records.We calculated the hypocenter location that minimizes the S-P time and P wave traveltime residual usingDown-hill Simplex algorism.Because these eventswere assumed the interplate earthquakes, we fixed the focal depth located on the plate boundary obtained by the ocean bottom seismological observation [Uehira *et al*. (2010)]. Theoretical S-P times were calculated by 3D ray trace with 3D velocity structure model.

Result and Discussion

Fig. 1 shows the result of the relocation of main shock (star) and the estimated focal region (ellipse) from the aftershock distribution. Main shocks were located on the low quasi-static slip area which is consistent with previous study [Yamashita *et al*. (submitted in GRL)]. Focal region of 1931 and 1961 events overlapped, and two asperities for Oct. and Dec. 1996 events were also included in the 1931 and 1961 focal regions. In addition, this region is consistent with the low quasi-static slip rate area. Theseresultindicatethat the 1996events were the “repeated ruptureof asperities”with a recurrence interval of 30 ~ 35 years.

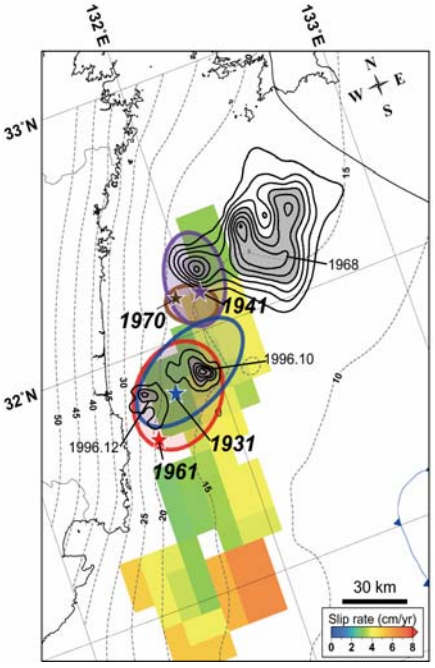


Fig.1 Distribution of the relocated main shock hypocenters (star) and estimated focal regions (ellipse).

Surface uplift and rock exhumation of morphotectonic blocks at the active fore-arc of Kamchatka, Russia

Ralf Freitag[1,#], Dorthe Pflanz[1,*], Christoph Gaedicke[2], Nikolay Tsukanov[3], Boris Baranov[3], Matthias Krbetschek[4]

[1]University Jena, Institute of Earth Sciences, Structural Geology Group, Burgweg 11, 07749 Jena, Germany

[2]Fereral Institute for Geosciences and Natural Resources, Geozentrum Hannover, Stilleweg 2, 30655 Hannover, Germany

[3]P.P. Shirshov Institute of Oceanology, 36, Nahimovski prospect, Moscow, Russia, 117997

[4]Sächsische Akademie der Wissenschaften zu Leipzig, Forschungsstelle Geochronologie Quartär, Institut für Angewandte Physik der TU Bergakademie Freiberg, Leipziger Str. 23, 09596 Freiberg, Germany

[#]now at Fereral Institute for Geosciences and Natural Resources, Geozentrum Hannover

[*]now at National Taiwan University, Dep. of Geosciences, No.1. Sec. 4th, Roosevelt Rd., Taipei 10617, Taiwan

The growth of continental crust by accretion of allochtonous terranes at the active margin of Kamchatka is documented since Mesozoic times. This growth is expressed by differential uplift and exhumation of seismotectonic and morphotectonic blocks of the accretionary wedge along the Kamchatka trench, depending on the accretion of lower plate material. The kinematics of uplift and exhumation can be grasped by analysing the deformation with structural and neotectonic techniques and quantified by thermochronological methods (fission-track dating) up to Lower Pliocene times.
Due to differential uplift of seismotectonic blocks and the interplay with sea level changes, numerous (sub-) recent marine and alluvial terraces have been formed on the Pacific side of Kamchatka. Fission-track dating of the underlying blocks and radiometric dating of the resting terraces by optical stimulated luminescence (OSL) and dating using cosmogenic nuclides, combined with sea level high stands, allows the documentation and quantification of the relative vertical movement of the seismotectonic blocks with very high resolution up to Recent times.
Results from our subproject TP1 in the framework of the integrated german-russian research project KALMAR (*K*urile-Kamchatka and *AL*eutean *MAR*ginal Sea-Island Arc Systems: Geodynamic and Climate Interaction in Space and Time, grant number BMBF 03G0640C) are the following: The mean exhumation rates along the Kamchatka margin varies from about 0.2 up to 1.1 mm/yr. The exhumation rates can be linked to morphotectonic blocks and exhumation is partially separated along discrete trench-orthogonal active faults. These active faults can be structurally mapped onshore Kamchatka and they seam to be related to pre-existing features of the incoming Pacific Plate.
First OSL-ages of the terraces resting on top of the morphotectonic blocks point to recent uplift rates varying from about 2.8 mm/yr up to about 7.5 mm/yr in specific areas during Holocene times. The OSL-ages are generally in a good agreement with the results from dating using the method of cosmogenic nuclides. A good correlation between lower plate convergence, fore-arc geometry, exhumation, elevation and age of marine and alluvial terraces is found.

Two marine expeditions, which where carried out in the framework of the KALMAR project (TP2) during summer 2009 achieved geophysical as well as geological data off Kamchatka. We combine the onshore data with the marine dataset e.g. to extend the onshore mapping of the block-separating active faults through the fore-arc to the lower plate. We might estimate the coherence between lower plate convergence (geometry, direction, velocity, physical properties) and upper plate deformation, in other words the seismical and mechanical coupling between upper and lower plate along the Kamchatka trench trough time.

The Krusenstern Fault, NW Pacific: A Reactivated Cretaceous Transform Fault?

Ralf Freitag[1*], Christoph Gaedicke[1], Nikolay Tsukanov[2], Udo Barckhausen[1], Dieter Franke[1], Ingo Heyde[1], Stefan Ladage[1], Rüdiger Lutz[1], Michael Schnabel[1]

[1] Federal Institute for Geosciences and Natural Resources (BGR), Geozentrum Hannover, Stilleweg 2, 30655 Hannover, Germany; [*]corresponding author: ralf.freitag@bgr.de

[2] P.P. Shirshov Institute of Oceanology, 36, Nahimovski prospect, Moscow, Russia, 117997

Since Lower Cretaceous times, the Pacific Plate converges against the active margin of Kamchatka where it is subducting along the Kuril-Kamchatka trench. During subduction, the upper plate is strongly deformed by shortening and exhumation. Since the Upper Cretaceous, numerous allochthonous terranes were accreted to Kamchatka as part of the Eurasian Plate. At latest Kronotsky-Shipunsky terrane, an island arc of Lower Cretaceous age accreted in the Upper Miocene about 9 Ma ago. Recently, the Meiji-Rise, the northwestern most part of the Emperor Seamount Chain approach the subduction zone. The Meiji-Rise is Upper Cretaceous in age (81-85 Ma) and is elevated about 2500 m above the surrounding seafloor. Meiji is bordered by a system of dextral strike-slip faults of the Aleutian trench in the NE and by a former transform fault in the SW: the Krusenstern Fault.

The Krusenstern Fault was crossed several times during the RV Sonne cruise SO201-1a and was mapped with geophysical methods. It comprises only minor asymmetries and vertical displacement in the SE and is covered completely by sediments. The displacement and morphological expression of the fault increase rapidly towards the NW. In profile BGR09-107, the SW shoulder of the asymmetric transform fault is already about 1000 m above the surrounding seafloor. In this profile, a relay ramp was mapped pointing to a former dextral plate movement along the fault.

Further in the NW (profile BGR09-109), the displacement increases rapidly while the rough morphology is covered by young deep sea sediments. On the northwestern most profile, the recent activity of the Krusenstern Fault is proofed by echo sounder data: The surface sediments are shifted about 35 m and from MCS it is visible that it is a deep-seated crustal fault. The Krusenstern fault is a crustal normal fault dipping towards NE, which means the NE area of the Meiji Seamount is structural lower. It is not clear from our data wether there is a strike slip component along the fault.

Because no magnetic anomalies are detectable on the oceanic crust, one can only speculate about the age of the Krusenstern Fault. The acute angle of the fault and the longitudinal shape of the Meiji seamount make a synchronous evolution unlikely. The fact, that the fault seems to be covered by another seamount south of Tenji points to a pre-Emperor age. Some authors interpret the fault as a transform fault of the mid-ocean ridge between the Pacific Plate and the Kula Plate during the Cretaceous Long Normal Superchron.

The reactivation of the Krusenstern Fault may be the result of the subduction and accretion of the Meiji seamount at the Kamchatka margin. The Meiji Seamount is elevated about 2500 m relative to the surrounding seafloor, the crust is much thicker. As the linear extension of the trench does not change, this area must subducting faster in the north of Krusenstern Fault, where the Meiji Seamount is located. The Krusenstern Fault is compensating this different vertical movement in the vicinity of the trench. The sharp bend of the magmatic arc onshore Kamchatka lies in the direct continuation of the Krusenstern Fault. For larger earthquakes, the Krusenstern Fault may act as a segment boundary.

Structure of the uppermost sedimentary layers in Kamchatka - Aleutian island arc junction area from high resolution echosound data (SO-201 Leg 1a, Leg 2 KALMAR).

N.V. Tsukanov[1], Ch. Gaedike[2], K. A. Baranov[1], K. A. Dozorova[1], R. Freitag[2].
[1]Institute of Oceanology, Russian Academy of Sciences, Moscow, e-mail: paleogeo@ocean.ru, [2] Federal Institute for Geosciences and Natural Resources (BGR), Hannover, e-mail: gaedicke@bgr.de

Geological and geophysical investigations have been carried out from board of RV "Sonne", cruises SO-201leg1a, leg 2 (Cruise Report 2009, SO-201, Leg 1a, Leg 2) from summer to autumn 2009. Study areas were located in Kamchatka and Aleutian island arcs junction area, Komandor Basin of the Bering Sea and northern Emperor Seamounts (ESM) and Emperor Trough (ET). The work was performed in the frame of the Russian-German Project KALMAR and included acoustic profiling by on-board profilograph PARASOUND P70. This report presents obtained data on structure of the upper part (up to 100 m) of the sedimentary cover in different structures of the Kamchatka continental margin, northwestern Pacific Plate and the Bering Sea. The data were recorded in PS3 and SEGY formats and were processed by R. Lutz (BGR) in REFLEXW for consequent interpretation (Cruise Report 2009, SO-201, Leg 1a).

(1) The areas away from the influence of the continental slope and seamounts is generally dominated by an acoustic faces characterized by numerous distinct, closely spaced and continuous parallel reflectors, about 2-3 m in thickness. As usual, these reflectors are conformable with the surface topography and can be traceable over tenth of kilometers. The acoustic penetration is often around 50-75 m and some times about 100 m. The draping character and the layered internal reflection pattern suggest undisturbed pelagic or hemipelagic depositional conditions. This style of acoustic reflection is dominated in the top of Shirshov Ridge and Mejia Swell, north-west Pacific plate. (2) Similar acoustic faces generally dominate in the deepest areas of Komandorsky basin of Bering Sea but thickness of internal layers is bigger (about 5-7 m). The acoustic transparencies of the observed layers showed internal homogenization and very high acoustic reflection. It is probably the result of disintegration of slope-failed masses and their transport by turbiditic or debris flow. These layers are separated from each other by continuous parallel reflectors which are about 2-3 m thick. In some places near the slope and other topographic highs the uppermost sedimentary sequence is about 7 - 10 m thick and has irregular structure and a hummocky surface. It is traceable over tens of kilometers and is characterized by lens-shaped forms of layers that are separated by layers with good stratification from others lenses. Possibly, there are shear slides. (3) The uppermost sedimentary sequence along the Shirshov Ridge is different at the West and East flank. Acoustic facies at the East flank is characterized by numerous continuous or lens-parallel reflectors, closely spaced with diffuse acoustic reflections. The thickness of these layers is 7-10 m. The visible thickness is about 50-75 m. The sediment cover is disturbed by normal folds with a vertical offset of about 5-10 m. Erosional canyons crossing this area. In this case sediment layers are lens-shaped and feather out to the side of these canyons. The Western flank of Shirshov Ridge is characterized by steeper relief with many erosional canyons and topographic highs. Diffuse reflections obtained from these areas provide little information about the uppermost sedimentary sequence. The normal faults separate Shirshov Ridge from the Komandorsky Basin. The upper part of sediment cover is about 25 - 35 m thick and contains lens-strata and, as usual, feather out in thickness (15 -25 m) to topographic highs and faults. Very often the acoustic layers are folded. (4) Massif of Volcanologist is characterized by step fault and volcanic cones relief. The sediments are less then 25-35 m in thickness and cover plain. In general, acoustic facies is characterized by numerous distinct, closely spaced lenses form layers, about several meters in thickness. They are separated by layers about 5-7 m in thickness with homogeneous internal structure. Reflectors are conformable with the basement surface topography. (5) Another type of section is typical for ESM and ET having dissected bottom relief. Maximum visible thickness of the sedimentary cover reaches 80 m. Two types of records are

distinguished; they alternate in the section and characterize different sedimentary complexes with different internal structure. The first complex is formed by lens-like sedimentary bodies with length varying from several kilometers up to several tens of kilometers. They are formed by acoustically transparent unstratified complexes. Usually, these sedimentary bodies are developed in bottom relief depressions. Their visible thickness varies from 10 m to 40 m and internal structure is conditioned by disintegration and mixing of sedimentary masses during their transportation by underwater currents and flows. The second complex is formed by well-stratified sedimentary horizons similar to those described above. Their thickness reaches 40-60 m becoming thinner in relief lows, where they are interstratified with deposits of the first complex. They are observed on ESM, on the plain between ESM and ET, on ESM flanks. Geometry and internal structure of these bodies and analysis of bottom relief justify that they were formed by debris flows. Besides, they are stratified by thin-bedded sedimentary complexes characterizing pelagic background sedimentation. (6) In the studied parts of Kamchatka continental slope (the Bering Sea, Kronotsky Bay) sediments on the echograms have a homogeneous coarsely-stratified structure. The internal structure on the echograms is characterized by chaotic structure. Considerably long frequently lens-like interlayers subdivided by thin layers with intensive reflective characteristics are distinguished. Visible thickness of the sedimentary cover is from 10-15 m to 60 m. Sedimentary unit developed in the central part of the profile and composing the scarp on the slope has different structure. Thickness of sedimentary body increases up to 40 m. The records are characterized by thin-bedded, lens-like internal structure with intensive reflectors. The sedimentary cover in depressions within Kronotsky Bay have similar structures. Characteristic features of its upper part are: absence of thin-bedded structure, presence of numerous interlayers with intensive reflection connected with their coarse composition and presence of numerous lens-like layers. These features are typical for sediments formed in conditions of active sedimentary material removal by turbiditic flows and underwater currents, which nearly completely smooth over background pelagic sedimentation.

Fulfilled study of sedimentary cover upper part structure in the investigated area shows that in general structure and composition of sedimentary cover is mainly conditioned by local bottom relief features and are formed by depositional, redistribution and/or erosional processes. Along with background sedimentation the important role belong to complexes formed by different underwater flows and currents. Authors express gratitude to scientific staff that obtained and processed the PARASOUND P70 data and crew of RV “Sonne”. The investigations were funded by BMBF, Project No. 03G0201B and Minobrnauka.

References

Seliverstov N.I. Structure offshore areas of Kamchatka and geodynamics juntiong area Kuril-Kamchatka and Aleutian island arcs. M. Nauchny Mir. 1998. 164 c.

Kurile-Kamchatka and ALeutian MARginal Sea-IslandArc Systems: Geodynamic and Climate Interaction. CRUISE REPORT, NR, 32, Sonne Cruise SO-201, Leg 1a. 2009.Yokohama. P. 105

Kurile-Kamchatka and ALeutian MARginal Sea-IslandArc Systems: Geodynamic and Climate Interaction FS Sonne Cruise Report SO 201-KALMAR Leg2

Magmatic evolution of Avachinsky volcano (Kamchatka) during the Holocene revealed from composition of tephra, their matrix glasses and melt inclusions in minerals

Krasheninnikov S.P.[1], Portnyagin M.V.[1, 2], Bazanova L.I.[3], Ponomareva V.V. [3]

1 - Vernadsky Institute of Geochemistry RAS, Russia, Moscow;
2 - Leibnitz Institute of Marine Research, Germany, Kiel;
3 - Institute of Volcanology and Seismology FEB RAS, Russia, Petropavlovsk-Kamchatsky.
E-mail: spkrasheninnikov@mail.ru

Avachinsky volcano is one of the most active volcanoes in the frontal volcanic zone of Kamchatka. Previous studies have recognized two distinct phases in the Holocene eruptive history of Avachinsky: 1) early phase of rare and voluminous andesitic eruptions (7.3-3.5 ^{14}C ka BP) and 2) later phase of frequent eruptions of basaltic andesites associated with the construction of the Young Cone (3.5 ^{14}C ka BP to the present) [1]. The change in the eruptive style was marked by the initial eruption of the Young Cone ~3.5 ^{14}C ka BP, which produced ≥3.6 km^3 of basaltic andesite tephra [2, 3]. In order to assess the chemical changes of Avachinsky magma, we have studied a representative collection of 61 samples representing 40 main Holocene eruptions from the ^{14}C-dated composite section covering the entire history of the volcano. Here we report the results of this study, obtained by chemical analysis of bulk tephra samples, microprobe investigation of matrix glasses (~600 an.) and more than 500 melt inclusions in minerals.

Both matrix glasses and melt inclusions in minerals have systematically more evolved compositions compared to their host rocks and span a large range of compositions within the fields of the low- and middle-K island-arc series. Low- and marginally middle-K rhyolitic compositions of glasses and inclusions predominate during the early Holocene. Relatively high-K melt inclusions were found in minerals from six tephra samples. The compositions of matrix glasses and inclusions change to predominantly middle-K dacitic and andesitic in the late Holocene (fig. 1). Primitive basaltic melt inclusions occur in olivine in the 600 ^{14}C yrs old tephra. Chemically contrasting glass shards and melt inclusions were found in the samples of different ages and often found in the same tephra sample. The data on matrix glasses and melt inclusions thus testify an important role of magma mixing in the origin of Avachinsky rocks that occurred along with fractional crystallization. Compositions of bulk tephra span a much narrower range of compositions compared to matrix glasses and melt inclusions and represent magmas formed by effective mixing of compositionally contrasting melts, crystallization and accumulation of phenocrysts.

The most pronounced chemical changes in the composition of bulk rocks from andesites to basaltic andesites correlate with the beginning of the later phase of activity at 3.5 ^{14}C ka BP. The data on melt inclusions and matrix glasses indicate, however, arrival of relatively K-rich mafic melts in the magma feeding system starting already at ca. 4.1 ^{14}C ka BP (fig. 1). The catastrophic eruption AV 3500 and the volcano changes at 3.5 ^{14}C ka BP were thus preceded by frequent injections of mafic K-rich magmas in the magma chamber beneath Avachinsky volcano during the previous 500-600 ^{14}C years.

On the basis of our new data, we propose that the Holocene evolution of Avachinsky volcano was driven by fractional crystallization associated with periodic injections of mafic middle-K magmas into initially low-K silicic magma reservoir, perhaps, left over after deceasing of Kozelsky volcano, whose early Holocene products are compositionally quite similar with Avacha's early phase. The injections of mafic magmas and subsequent volcanic eruptions led to exhausting of the low-K rhyolite magmas and resulted in the systematic change of magma compositions to more

mafic and K-rich over time. The most pronounced changes in the magma composition had occurred during period from 4.1 to 3.5 ^{14}C ka BP.

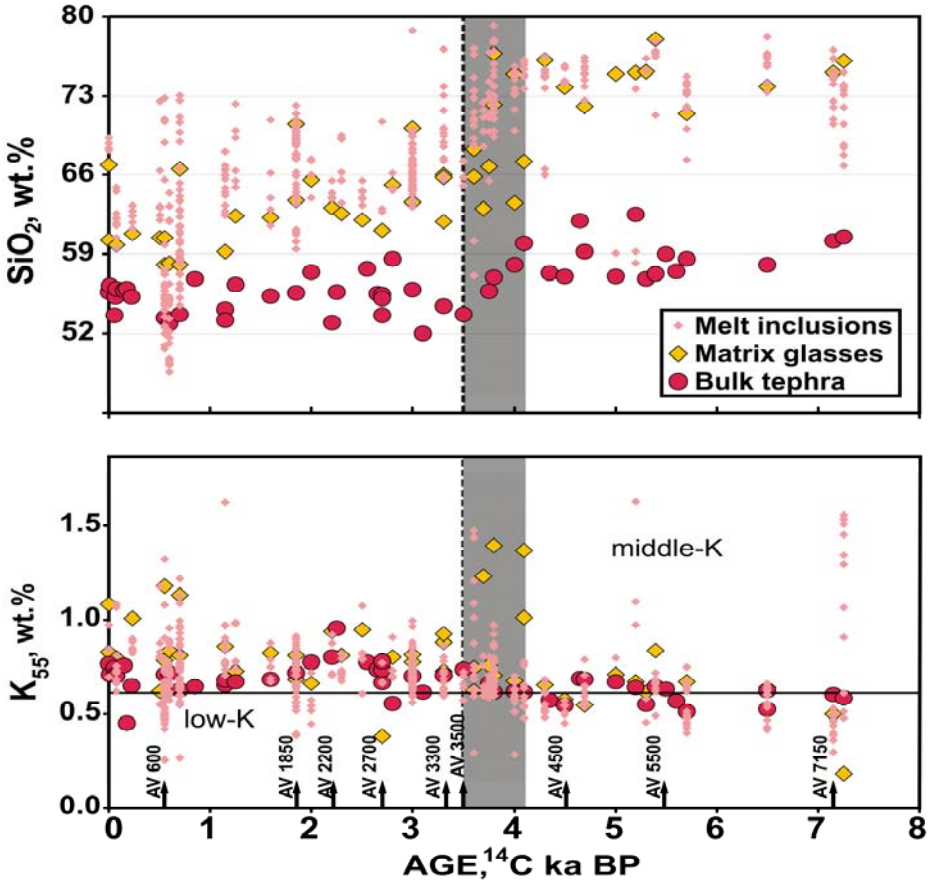


Figure 1. Variations of SiO_2 and K_{55} contents in matrix glasses, melt inclusions and bulk tephras of Avachinsky volcano during the last 8 ^{14}C ka. K_{55} is K_2O content normalized to 55 wt. % of SiO_2. Dashed line - the border dividing andesitic and basaltic andesites phases of volcanic activity; grey field – time period of frequent injections of mafic K-rich magmas in the magma chamber; black arrows – the largest Holocene eruptions of Avachinsky volcano.

References:

1. Braitseva OA, Bazanova LI, Melekestsev IV, Sulerzhitskiy LD 1998 // Volcanol Seismol 20 (1): 1-27.

2. Bazanova LI, Braitseva OA, Puzankov MYu, Sulerzhitskiy LD 2003 // Volcanol Seismol (5): 20-40.

3. Bazanova LI, Braitseva OA, Melekestsev IV, Sulerzhitskiy LD. 2004 // Volcanol Seismol (6): 3-8 [in Russian].

Магматическая эволюция Авачинского вулкана (Камчатка) в голоцене, выявленная по валовым составам тефр, составам их матричных стекол и расплавных включений в минералах

Крашенинников С.П.[1], Портнягин М.В.[1, 2], Базанова Л.И.[3], Пономарева В.В.[3]

1 – Институт геохимии и аналитической химии им. В.И. Вернадского РАН, Россия, Москва;
2 – Лейбниц Институт морских исследований, Германия, Киль;
3 – Институт вулканологии и сейсмологии ДВО РАН, Россия, Петропавловск-Камчатский.
E-mail: spkrasheninnikov@mail.ru

Авачинский вулкан является одним из наиболее активных вулканов вулканической фронтальной зоны Камчатки. Предыдущие исследования показали, что в голоценовой истории Авачинского вулкана можно выделить две главные фазы активности: 1) ранняя фаза редких, но сильных извержений андезитов (7.3-3.5 тыс. ^{14}C л.н.) и 2) поздняя фаза частых извержений андезибазальтов, связанная с образованием Молодого конуса (3.5 тыс. ^{14}C л.н. и по настоящее время) [1]. Смена характера эруптивной активности была отмечена инициальным извержением Молодого конуса ~3.5 тыс. ^{14}C л.н., которое вынесло на поверхность более 3.6 км^3 андезибазальтовой пирокластики [2, 3]. С целью изучения вариаций химического состава авачинских магм, нами была изучена представительная коллекция 61 образца тефр, представляющих 40 главных голоценовых извержений. Образцы были отобраны из датированного сводного разреза, отражающего всю историю активности вулкана. Представленные в этой работе результаты получены на основе валовых химических анализов образцов тефр, микрозондовых исследований матричных стекол (~600 ан.) и более, чем 500 расплавных включений в минералах.

Матричные стекла и расплавные включения в минералах имеют систематически более дифференцированные составы по сравнению с валовыми составами пород. Составы стекол широко варьируют и относятся к низко- и умеренно-K островодужным сериям. На протяжении раннеголоценового времени преобладали низко- и пограничные с ними умеренно-K риолитовые составы матричных стекол и расплавных включений. Расплавные включения с относительно повышенными содержаниями калия были обнаружены в минералах шести образцов пирокластики. В позднеголоценовое время составы матричных стекол и расплавных включений сменяются преимущественно умеренно-K дацитовыми и андезитовыми (Рис. 1). В оливинах из образца тефры с возрастом 600 ^{14}C л. были найдены примитивные базальтовые расплавные включения. Химически контрастные фрагменты стекол и расплавные включения были обнаружены в образцах разных возрастов, нередко в одном образце тефры. Таким образом, данные по матричным стеклам и расплавным включениям указывают на важность процессов смешения магм в формировании пород Авачинского вулкана, которое происходило совместно с фракционной кристаллизацией. Валовые составы тефр имеют более узкий спектр составов, по сравнению с матричными стеклами и расплавными включениями. Эти составы представляют магмы, образованные в результате эффективного смешения разных по составам расплавов, кристаллизации и кумуляции вкрапленников.

Наиболее ярко выраженные изменения валовых составов тефр, от андезитов к андезибазальтам, соотносятся с началом поздней фазы активности вулкана (3.5 тыс. ^{14}C л.н.). Однако, данные по расплавным включениям и матричным стеклам указывают на поступление относительно обогащенных калием основных расплавов в магмоподводящую систему уже на рубеже 4.1 тыс. ^{14}C л.н. (Рис. 1). Катастрофическое извержение АВ 3500 и резкие изменения в характере активности и составах вулканитов 3.5 тыс. ^{14}C л.н. были вызваны частыми инъекциями основных, богатых K магм в магматический очаг под Авачинским вулканом в течение предшествующих 500-600 ^{14}C лет.

На основе новых данных, мы предполагаем, что голоценовая эволюция Авачинского вулкана была вызвана процессами фракционной кристаллизации, сопровождавшимися периодическими инъекциями основных умеренно-K магм в изначально низко-K кремнекислый магматический очаг. Возможно, этот очаг был унаследован Авачинским вулканом после затухания своего предшественника - Козельского вулкана, раннеголоценовые вулканиты которого близки по составу самым первым голоценовым тефрам Авачинского вулкана. Инъекции основных магм и последующие вулканические извержения привели к истощению очага риолитовыми низко-K расплавами и, в результате, к систематическим изменениям состава магм во времени на все более основной и обогащенный калием. Наиболее ярко выраженные изменения состава магм произошли в период от 4.1 до 3.5 тыс. ^{14}C л.н.

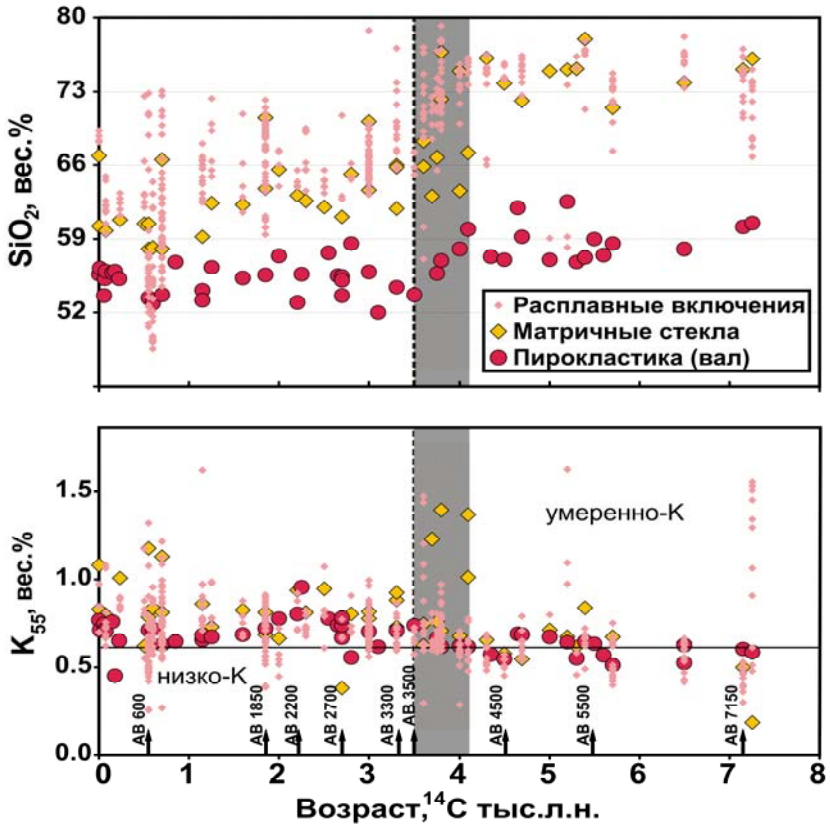


Рисунок 1. Вариации содержаний SiO_2 и K_{55} в матричных стеклах, расплавных включениях и валовых составах тефр Авачинского вулкана в последние 8 ^{14}C тыс.л. K_{55} – содержания K_2O нормализованные к 55 вес.% Si_2O. Пунктирная линия – граница, разделяющая раннюю и позднюю фазы активности; серое поле – период частых инъекций основных, богатых K магм в магматический очаг; черные стрелки – крупнейшие голоценовые извержения Авачинского вулкана.

Список литературы:

1. Брайцева О.А., Базанова Л.И., Мелекесцев И.В., Сулержицкий Л.Д. // Вулк. и сейсм. 1998 №1. с.3-24.

2. Базанова Л.И., Брайцева О.А., Пузанков М.Ю., Сулержицкий Л.Д. // Вулк. и сейсм. 2003 №5. с.20-40.

3. Базанова Л.И., Брайцева О.А., Мелекесцев И.В., Сулержицкий Л.Д. // Вулк. и сейсм. 2004 № 6. с.15-20.

U-Pb age of caldera Uxichan rocks at Sredinniy Ridge, Kamchatka – application of LA-ICP-MS to young zircon dating

Yuri A. Kostitsyn, Maria O. Anosova

V.I.Vernadsky Institsute of Geochemistry and Analytical Chemistry(GEOKHI) RAS
Kosygin str., 19, Moscow119991 Russia. kostitsyn@geokhi.ru

Uxichan volcanic center is the largest one at Kamchatka. Its complex constitution is generally ascribed to many-stage and long-lasting formation. There are many statements in literature concerning the time and duration of the volcanic center formation but they are usually based on a complex set of geological data or are simply declarative without any explanation. Age of the volcano basement is estimated as late Miocene – Pliocene [1], i.e. about 5.3 Ma according to International Stratigraphic Scale. Some researchers include pyroclastic deposits of the basement into Uxichan volcanic sequence itself. However practically all publications referred to the age of Uxichan rocks [1-3], mention long time of its formation, from at least early Pliocene up to late Pleistocene and even Holocene. Thus, it is supposed that this volcano grew during several million years.

On the other hand the associations of chemically differing magmatic rocks with the same volcanic center could imply relative short time of its formation. We have carried out this special study to resolve the chronological problem.

Several stages of the volcanic center formation are recognized [1-4]: (1) basement, formed by mid-potassium volcanic rocks, mostly pyroclastic; (2) mid- and high-potassium basalts, andesitic basalts and andesites formed stratovolcano; (3) the most productive stage – formation of the largest shield volcano which is about 50 km in diameter and is mostly made of by shoshonites, latites and ignimbrites; (4) collapse caldera with extrusion complex of high-potassium latites, dacites, trachidacites and trachirhyodacites in its central part. Finally there are many monogenic cinder cones cutting the Uxichan shield edifice.

Such poly-stages scenario of formation, complex structure and chemical diversity of volcanic rocks suggest a long time of the volcano growth.

K-Ar system studies of some Uxichan volcanic rocks were undertaken to define its age. K-Ar age of the bottom lava flows was reported as 3.6 Ma [3] (without confidence interval). Two ignimbrites from the lower part of cross-section were dated at 3.56±0.50 and 3.34±0.07 Ma by ^{40}Ar-^{39}Ar technique on plagioclase separates [5]. The last two dates do not differ from one another at the errors limits. Probably it is to be concluded that all three results date the same age, which is defined by the best figure from these cited measurements, i.e. 3.34±0.07 Ma.

Complex structure of the Uxichan volcano and its supposed long lasting evolution complicates the studies of the volcanic center history. Using classic approach one would have had to undertake sampling and isotopic dating of many individual volcanic strata and sub-volcanic bodies, that appears to be very time and labor consuming task. That is why we have used rather uncommon approach of zircon sampling – take a schlich sample from Ukrainskiy stream near its exit from the Uxichan caldera.

Single grains isotopic studies of zircon were made in laboratory of isotopic geochemistry and geochronology at GEOKHI RAS by laser ablation technique (LA-ICP-MS).

We have obtained rather unexpected result. For 88 individual grains of zircon separation a common concordant age was obtained at 3.28±0.04 Ma. The result definitely indicates that there are no cropped out rocks at the Uxichan caldera surface having another, particularly younger age. It is well probably that basaltic rocks, especially mid-K, do not contain zircon, but more acid and more alkaline rocks, such as latites, ignimbrites, brought zircon through central part of the caldera where they were extruded and effused. Particularly, collapse caldera formation followed eruption of dacites and other acid rocks containing zircon. Thus, overall interval of the volcanic center formation spans very short time that looks like a single events at 3.28±0.04 Ma. Anyways, at the

obtained confidence interval level of the geochronological study it is impossible to resolve times of initial and final stages in the Uxichan volcanic center formation.

Reference

1. Ogorodov N.V., Kozhemiaka N.N., Vazhevskaya A.A. et al. Volcanos and Quaternary volcanism of Kamchatka Sredinniy Ridge. 1972. Moscow. Nauka. 192 pp.
2. Antipin V.S., Volynets O.N., Perepelov A.B. et al. Geological relationships and geochemical evolution of calc-alkaline and sub-alkaline volcanism of Uxichan caldera (Kamchatka). // Geochemistry of magmatic rocks at modern and older active zones. 1987, Novosibirsk. Nauka. p. 73-90.
3. Perepelov A.B., Chaschin A.A. Martynov Yu.A. Central-Kamchatka zone (pliocene –holocene) // Geodynamics, magmatism and metallogeny of the Russia East. 2006. Vladivostok. Dalnauka. p. 382-398.
4. Vasilevskiy M.M., Stephanov yu.M., Wide B.I. et al. Metallogeny of the Kamchatka upper structure level and ore specialization problems. // Prognostic assessment of ore-bearing volcanic suites. 1977. Moscow. Nedra. p. 14-59.
5. Bindeman I.N., Leonov V.L., Izbekov P.E., et al., *Large-volume silicic volcanism in Kamchatka: Ar-Ar and U-Pb ages, isotopic, and geochemical characteristics of major pre-Holocene caldera-forming eruptions.* // Journal of Volcanology and Geothermal Research, 2010. 189(1-2): 57-80.

U-Pb возраст пород кальдеры Уксичан в Срединном хребте Камчатки – применение LA-ICP-MS к датированию молодых цирконов

Ю.А.Костицын, М.О.Аносова

Институт геохимии и аналитической химии им. В.И. Вернадского РАН
119991, г. Москва, ул. Косыгина, 19; kostitsyn@geokhi.ru

Вулканический центр Уксичан – крупнейший на Камчатке – интересен, прежде всего, сложностью своего строения, которая воспринималась всегда как признак многоэтапности, длительности формирования. По поводу истории развития этого вулкана в литературе можно встретить разные оценки, основанные, как правило, на комплексе геологических данных, или просто приведённые без какого-либо обоснования. Возраст фундамента оценивается позднемиоцен-плиоценовым [1], что по современной международной стратиграфической шкале отвечает ~5.3 млн. лет. Некоторые исследователи эффузивно-пирокластические отложения фундамента также относят к образованиям собственно вулкана Уксичан . Но практически во всех работах, где так или иначе упоминается возраст пород этого вулканического центра [1-3], отмечается большая длительность его формирования, от, по крайней мере, раннего плиоцена до позднего плейстоцена и даже голоцена. То есть предполагается, что длительность формирования вулкана Уксичан составляет несколько миллионов лет.

В то же время, приуроченность магматических пород разного состава к единому вулканическому центру позволяет предположить сближенность во времени их образования. Для разрешения этого противоречия мы поставили специальные геохронологические исследования.

В строении вулканического центра выделяется несколько этажей или стадий формирования [1-4]: (1) фундамент, сложенный умереннокалиевыми вулканогенными породами, преимущественно пирокластическими; (2) умеренно- и высококалиевые базальты, андезибазальты и андезиты стратовулкана; (3) самая продуктивная стадия – формирование крупнейшего щитового вулкана, занимающего площадь диаметром около 50 км и сложенного преимущественно шошонитами, латитами и игнимбритами; (4) кальдера обрушения, в центральной части которой образовался экструзивный комплекс высококалиевых латитов, дацитов, трахидацитов и трахириодацитов. Кроме того, щитовую постройку Уксичана прорывает множество наложенных более мелких моногенных конусов. Такая многостадийность и сложность строения вулканического центра, а также контрастность химического состава вулканитов, подталкивали к мысли о длительности его формирования.

Для определения возраста вулканитов Уксичана предпринимались изотопные исследования их K-Ar системы. Так, K-Ar возраст лав из нижних горизонтов разреза [3] составляет 3.6 млн. лет (погрешность, к сожалению, не указана), а возраст двух образцов игнимбритов, также из нижней части вулканической толщи, определённый ^{40}Ar-^{39}Ar методом по плагиоклазу, составил 3.56±0.50 и 3.34±0.07 млн.лет [5]. Последние две даты не различаются в пределах погрешностей. Отличается ли от них первая из трёх дат, сказать трудно, т.к. её доверительный интервал не указан, поэтому скорее всего следует принять, что все три даты указывают на один и тот же возраст, который определяется лучшим из цитированных трёх определений, т.е. 3.34±0.07 млн.лет.

Сложное строение вулканического центра и предполагаемое длительное его развитие делает задачу изучения истории его формирования довольно непростой. При классическом подходе пришлось бы опробовать и датировать множество отдельных вулканических и субвулканических тел, что было бы слишком трудоёмко. Поэтому мы применили иной, нестандартный подход: циркон для анализа был отобран шлиховым опробованием в ручье

Украинский вблизи его выхода из кальдеры. Это сделано для того, чтобы получить представительную пробу, содержащую циркон из всех породы кальдеры Уксичан. Изотопные исследования индивидуальных зёрен циркона проводились в лаборатории изотопной геохимии и геохронологии ГЕОХИ РАН методом лазерной абляции. Результат исследования оказался для нас неожиданным. По 88 индивидуальным зёрнам циркона получено единое значение возраста 3.28±0.04 млн.лет. Этот факт определённо указывает на то, что в пределах кальдеры не обнажаются породы, содержащие цирконы другого, в частности, более молодого возраста. Весьма вероятно, что базальты, особенно умеренно-калиевые их разности не содержат циркона, однако на всех этапах становления кальдеры присутствовали породы среднего и более кислого состава, латиты, игнимбриты. В частности, образование кальдеры обрушения на заключительном этапе формирования вулканического центра Уксичан сопровождалось образованием дацитов, в которых циркон присутствует. Следовательно, весь период формирования вулканического центра, за исключением, быть может, поздних моногенных шлаковых конусов, в настоящий момент выглядит как единое событие возрастом 3.28±0.04 млн.лет. Во всяком случае, на имеющемся уровне точности геохронологических исследований различить время начала и завершения формирования вулканического центра Уксичан не удаётся.

Список литературы

1. Огородов Н.В., Кожемяка Н.Н., Важеевская А.А. и др. *Вулканы и четвертичный вулканизм Срединного хребта Камчатки*. 1972, Москва: Наука. 192 С.
2. Антипин В.С., Волынец О.Н., Перепелов А.Б. и др. *Геологические соотношения и геохимическая эволюция известково-щелочного и субщелочного вулканизма кальдеры Уксичан (Камчатка)*, // *Геохимия магматических пород современных и древних активных зон*. 1987, Наука: Новосибирск. с. 73-90.
3. Перепелов А.Б., Чащин А.А., Мартынов Ю.А. *Срединно-камчатская зона (плиоцен-голоцен)*, // *Геодинамика, магматизм и металлогения Востока России*, Ханчук А.И., Editor. 2006, Дальнаука: Владивосток. с. 382-398.
4. Василевский М.М., Стефанов Ю.М., Широкий Б.И. и др. *Металлогения верхнего структурного этажа Камчатки и проблемы рудной специализации этапов тектоно-магматического развития складчатых областей*, // *Прогнозная оценка рудоносности вулканогенных формаций*. 1977, Недра: Москва. с. 14-59.
5. Bindeman I.N., Leonov V.L., Izbekov P.E., et al., *Large-volume silicic volcanism in Kamchatka: Ar-Ar and U-Pb ages, isotopic, and geochemical characteristics of major pre-Holocene caldera-forming eruptions.* // Journal of Volcanology and Geothermal Research, 2010. 189(1-2): 57-80.

Oxygen isotopes in Miocene-Quaternary volcanic rocks from Sredinny Range, Kamchatka

Anna Volynets[1,2], Gerhard Wörner[2], Rheinhold Przybilla [2]

1 Institute of volcanology and seismology FEB RAS, Petropavlovsk-Kamchatsky, Russia
2 Geowissenschaftliches Zentrum, Georg-August-Universität Göttingen, Germany

Volcanic rocks of Kamchatka have broad variations of oxygen isotope composition (Bindeman et al., 2004, 2005; Dorendorf et al., 2000; Pokrovsky and Volynets, 1999; etc.). Here we present new data on $\delta^{18}O$ in volcanic rocks from Sredinny Range (SR) of Kamchatka. We analyzed 11 samples from Quaternary rocks of Alnej volcano, Sedanka, Kekuknajsky and Right Ozernaya monogenetic lava fields, Tobeltsen and Nilgimelkin cinder cones (north SR), as well as 6 samples of Miocene-Pliocene plateau basalts of Left and Right Ozernaya rivers, Dvuh'urtochnoe plateau and Kruki Ridge. Only fresh, inclusion-free olivine grains were selected for the analyses. Composition of olivine in selected rock samples is Fo65-87 in plateau lavas and Fo60-85 in monogenetic lava samples. Measured $\delta^{18}O_{olivine}$ values vary from 5.47 to 7.78 ‰, and are substantially higher than mantle values ($\delta^{18}O_{olivine}$~5-5.5‰, Eiler, 2001). Calculated $\delta^{18}O_{melt}$=6.17-8.48 ‰ ($\delta^{18}O_{melt}$= $\delta^{18}O_{olivine}$+0.7). The observed variations cannot be connected to the fractional crystallization processes, which is confirmed by the absence of correlations with Mg# and SiO_2 content in the whole rocks. Oxygen isotope composition also does not correlate with the age of the studied rocks and with the geographic location of the volcanic edifices (from the south to the north of SR): high $\delta^{18}O$-olivines are found both in young and old rocks, in the southern and northern parts of SR.
Depending on the other geochemical characteristics of the rocks, subduction fluids (Dorendorf et al., 2000), sediment melts and/or crust material contamination (Bindeman et al., 2005) have been suggested as heavy oxygen isotope sources for the island-arc volcanic rocks. SR volcanic rocks have mantle-like $^{87}Sr/^{86}Sr$ (0.7028-0.70336, Volynets et al., 2010) and non-radiogenic lead isotope composition (for ex. $^{206}Pb/^{204}Pb$ ~ 18.2, Volynets et al., 2010). Crust or sediment contamination would be expressed in elevated Sr and Pb isotope values which should be correlated with ^{18}O enrichment (not observed). On the other hand, the mantle wedge below SR has been strongly metasomatized by the fluids during the previous subduction episode in Miocene-Pliocene, when SR represented the volcanic front of the subduction zone (Lander & Shapiro, 2007). This is confirmed by the elevated fluid-mobile elements content and variably high fluid-mobile/incompartible element ratios in all volcanic rocks from SR, both old and young. However, such fluid-mobile element enrichment is observed in many arc magmas but is not related to such elevated ^{18}O. Thus, a distinct scenario must be envisioned. We argue that ^{18}O enrichment in SR rocks may be caused by massive fluid influx from the subducting Emperor Seamount chain into the cold frontal part of the mantle wedge leading to serpentinization (with >15% H_2O). Reheating and melting of such old serpentinized mantle wedge during arc migration and back arc rifting results in heavy oxygen isotope enrichment in young volcanic rocks in the back-arc environment.
This work has been supported by DAAD A/10/08073, RFBR 10-05-01122 and RI-112/001/610

"Leading scientific schools" grants to A.V.

Bindeman I.N., Ponomareva V.V., Bailey J.C., Valley J.W. (2004) Volcanic arc of Kamchatka: a province with high- $\delta^{18}O$ magma sources and large scale $^{18}O/^{16}O$ depletion of the upper crust // Geochimica et Cosmochimica Acta 68, p. 841- 865

Bindeman I.N., Eiler J.M., Yogodzinski G.M., Tatsumi Y., Sterne C.R., Grove T.L., Portnyagin M., Hoernle K., Danyushevsky L.V. (2005) Oxygen isotope evidence for slab melting in modern and ancient subduction zones // Earth and Planetary Science Letters 235, p. 480- 496

Dorendorf F., Wiechert U., Wörner G. (2000) Hydrated sub-arc mantle: a source for the Kluchevskoy volcano, Kamchatka/Russia // Earth and Planetary Science Letters 175, 69-86.

Eiler J.M. (2001) Oxygen isotope variations in basaltic lavas and upper mantle rocks// Reviews in Mineralogy and Geochemistry 43, p. 319-364

Lander A.V., Shapiro M.N. (2007) The origin of the modern Kamchatka subduction zone // Volcanism and Subduction: the Kamchatka Region. Geophysical Monograph Series 172, p. 57-64

Pokrovsky B.G., Volynets O.N. (1999) Oxygen-isotope geochemistry in volcanic rocks of the Kurile–Kamchatka arc // Petrology 7, p. 227–251

Volynets A., Churikova T., Wörner G., Gordeychik B., Layer P. (2010) Mafic Late Miocene - Quaternary volcanic rocks in the Kamchatka back arc region: implications for subduction geometry and slab history at the Pacific-Aleutian junction // Contributions to mineralogy and petrology, 159:659–687

EARLY EOCENE STAGE OF THE MAGMATISM IN THE SREDINNIY RANGE OF KAMCHATKA

A.V. Soloviev, M.V. Luchitskaya
Geological Institute of RAS, Moscow, Russia

The Early Eocene (nearby 52±2 million years ago) migmatites and granites are widespread in the south of the Sredinniy Range of Kamchatka [1, 4, 5]. The equigranular highalumina two-mica granite with garnet and migmatites, as well as tonilites and trondhjemites with mantle features are present within Sredinny Range [4]. The composition of the Early Eocene granitoids allows us to compare them with S-type Cordilleran granite. In addition to the Early Eocene migmatites and granitoids, coeval (55-49 Ma) norite-kortlandite intrusions bearing sulphide copper-nickel mineralization are also known in the south of the Sredinniy Range of Kamchatka [2, 3, 6, 7]. This allows to distinguish the Early Eocene phase of magmatic activity in Kamchatka.

The collision of the Achaivayam-Valaginskiy ensimatic island arc with Kamchatka margin of Eurasia, which began 55-53 million years ago [1, 5], preceded the Early Eocene magmatism. During the process of collision arc complexes were overthrusted upon the deposits of the continental margin, causing their rapid subsidence, warming of the crust, migmatization and melting of granites, tonalites and trondhjemites about 52±2 million years ago, at temperatures from 645 to 815 º C. For such a rapid warming (up to 3-5 million years) an additional source of heat was needed, which, apparently, was the mantle that impacted on the base of the crust as a result of slab detachment.

Thus, the characteristics of the granitoids and data on the norite-kortlandite intrusions bearing copper-nickel mineralization, allow to suggest the involvement of mantle material in the process of the Early Eocene syncollision magmogenesis in Kamchatka.

This study was supported by the Grant of the President RF (MD-1053.2010.5) and by RFBR (Grant № 10-05-00191).

1. *Hourigan, J.K., Brandon, M.T., Soloviev, A.V., Kirmasov, A.B., Garver, J.I., Stevenson J., Reiners, P.W.* Eocene arc-continent collision and crustal consolidation in Kamchatka, Russian Far East // American Journal of Science. Vol. 309. May. 2009. p. 333-396.
2. *Konnikov E.G., Chubarov V.M., Poletaev V.A., Bukhtiyarov P.G.* New data on the structure and geochemistry of the Dukuk gabbro-norite-cortlandite massif of Kamchatka // Russian Journal of Pacific Geology. 2010. Vol. 4, № 6. pp. 470–482.
3. *Konnikov E.G., Chubarov V.M., Travin A.V., Matukov D.I., Sidorov E.G.* Formation time of the Ni-bearing norite-cortlandite association of East Asia // Geochemistry International. 2006. Vol. 44. № 5. pp. 516-521.
4. *Luchitskaya M.V., Solov'ev A.V., Hourigan J.K.* Two Stages of Granite Formation in the Sredinny Range, Kamchatka: Tectonic and Geodynamic Setting of Granitic Rocks // Geotectonics. 2008. Vol. 42. № 4. pp. 286–304.
5. *Soloviev A.V.* Investigation of the tectonic processes at the convergent settings of lithosphere plates: fission-track and structural analysis. M.: Nauka, 2008. 319 p. (In Russian).
6. *Stepanov V.A., Trukhin Yu.P.* Age of the Shanuch copper-nickel deposit in Kamchatka // Doklady Earth Sciences. 2007. T. 417. № 1. C. 1193-1194.
7. *Trukhin Yu.P., Stepanov V.A., Sidorov M.D.* The Kamchatka nickel-bearing province // Doklady Earth Sciences. 2008. T. 419. № 1. C. 214-216.

РАННЕЭОЦЕНОВЫЙ ЭТАП МАГМАТИЗМА В СРЕДИННОМ ХРЕБТЕ КАМЧАТКИ

А.В.Соловьев, М.В.Лучицкая
Геологический институт РАН, Москва 119017, Пыжевский пер., д. 7

На юге Срединного хребта Камчатки в раннем эоцене (около 52±2 млн. лет назад) широко проявлены процессы мигматизации и гранитообразования [1, 5, 8]. В пределах Малкинского поднятия присутствуют как равномернозернистые высокоглиноземистые двуслюдяные гранатсодержащие граниты и мигматиты, так и несущие мантийную метку тоналиты, трондьемиты [1]. Особенности состава раннеэоценовых гранитоидов позволяют сравнивать их с Кордильерским S-типом гранитов. Кроме раннеэоценовых мигматитов и гранитоидов на юге Срединного хребта Камчатки известны одновозрастные (55-49 млн. лет) интрузии норит-кортландитовой формации, несущие сульфидную медно-никелевую минерализацию [2, 3, 4, 6, 7]. Это позволяет выделить раннеэоценовый этап магматической активности на Камчатке.

Коллизия Ачайваям-Валагинской энсиматической островной дуги с Камчатской окраиной Евразии, начавшаяся 55–53 млн. лет назад [1, 8], предшествовала раннеэоценовому магматизму. В процессе коллизии комплексы дуги были надвинуты на отложения континентальной окраины, что вызвало их быстрое погружение, прогрев коры, мигматизацию и выплавление гранитов, тоналитов и трондьемитов 52±2 млн. лет назад при температурах от 645 до 815ºС. Для настолько быстрого прогрева (максимум 3–5 млн. лет) необходим дополнительный источник тепла, которым, по-видимому, являлась мантия, воздействовавшая на основание коры в результате отрыва слэба.

Таким образом, особенности состава гранитоидов и данные о интрузиях норит-кортландитовой формации, несущих медно-никелевое оруденение, позволяют предполагать вовлечение мантийного вещества в процесс раннеэоценового коллизионного магмогенеза на Камчатке.

Работа выполнена при финансовой поддержке Гранта Президента РФ МД-1053.2010.5 и РФФИ (грант № 10-05-00191).

1. *Лучицкая М.В., Соловьев А.В., Хоуриган Дж.К.* Два этапа формирования гранитоидов Срединного хребта Камчатки: их тектоническая и геодинамическая позиция // Геотектоника. 2008. № 4. С. 49-69.
2. *Конников Э.Г., Чубаров В.М., Полетаев В.А., Бахтияров П.Г.* Новые структурные и геохимические данные о габбро-норит-кортландитовом массиве Дукук, Камчатка // Тихоокеанская геология. 2010. Т. 29. №6. С. 13–25.
3. *Конников Э.Г., Чубаров В.М., Травин В.А., Матуков Д.И., Сидоров Е.Г.* Время проявления никеленосной норит-кортландитовой формации на востоке азиатского континента // Геохимия. 2006. № 5. С. 564-570.
4. *Сидоров Е.Г.* Платиноносность базит-гипербазитовых комплексов Корякско-Камчатского региона. Автореф. дис. … докт. геол.-минерал. наук. Петропав.-Камчат., 2009. 46 с.
5. *Соловьев А.В.* Изучение тектонических процессов в областях конвергенции литосферных плит: методы трекового датирования и структурного анализа // М.: Наука, 2008. 319 с. (Тр. ГИН РАН; Вып. 577).
6. *Степанов В.А., Трухин Ю.П.* О возрасте Шанучского медно-никелевого месторождения Камчатки // ДАН. 2007. Т. 417. № 1 С. 84-86.
7. *Трухин Ю.П., Степанов В.А., Сидоров М.Д.* Камчатская никеленосная провинция // ДАН. 2008. Т. 418. № 6. С. 802–805.
8. *Hourigan, J.K., Brandon, M.T., Soloviev, A.V., Kirmasov, A.B., Garver, J.I., Stevenson J., Reiners, P.W.* Eocene arc-continent collision and crustal consolidation in Kamchatka, Russian Far East // American Journal of Science. Vol. 309. May. 2009. p. 333-396.

HOLOCENE ERUPTIVE ACTIVITY OF THE SOUTHERNMOST KAMCHATKAN VOLCANOES

Vera Ponomareva[1], Natalia Zaretskaya[2], Leopold Sulerzhitsky[2], Oleg Dirksen[1]

[1] Institute of Volcanology and Seismology FEB RAS, Piip Blvd. 9, Petropavlovsk-Kamchatsky, 683006, Russia; email: ponomareva@kscnet.ru
[2] Geological Institute, Pyzhevsky per. 7, Moscow, 119017, Russia

Understanding of the Holocene eruptive histories is important for the long-term forecast of the volcanic activity and determining new targets for the volcano monitoring. In addition, the detailed data on the past activity of a volcano is important for the research on its magmatic evolution. In this talk we will summarize the Holocene activity of the southernmost Kamchatkan volcanoes (Zheltovsky, Iliinsky, Kurile Lake caldera, Dikii Greben', Kambalny, and Kosheleva) reconstructed based on geological and geomorphological mapping, tephrochronological studies, radiocarbon dating and bulk rock geochemical data. Our studies show that the volcanoes of this region may resume their activity in near future [1].

The largest Holocene eruption of this region (coded KO) resulted in the formation of the **Kurile Lake caldera** ~8400 cal. BP. This was one of the largest Holocene explosive eruptions globally [2, 3]. KO tephra was dispersed to the northwest. It covered most of the Kamchatka Peninsula, Okhotsk Sea and a part of the Asian mainland as far as ~1700 km away from the source. Deposits of the pyroclastic density currents filled the valleys and covered the surrounding plateaus with a thin layer of pumiceous material at a distance of ~50 km from the source. In the course of the eruption, composition of the erupted products changed from rhyolite to basaltic andesite and back to rhyolite. Soon after the KO eruption, Iliinsky and Dikii Greben' volcanoes started to form.

Iliinsky volcano was the most active one during the Holocene (Fig.1). Its most recent eruption took place in 1901 after a ~1800 yrs long repose period. During its past eruptions the volcano produced lava flows, pyroclastic density currents, scoria avalanches and fall-out deposits. Tephra was dispersed as far as 100 km from the source. Eruptive products are medium-K basalts, andesites and dacites compositionally related to the tephra of the Kurile Lake caldera-forming eruption.

Dikii Greben' volcano had three distinct and relatively short eruptive phases: ~8400, 5000 and 1500 cal BP. Each phase included formation of lava domes, pyroclastic density currents, lava flows and tephra falls. The latter were dispersed at a distances of >30 km from the volcano. The most recent eruptive phase was marked by a dome collapse and formation of a large debris avalanche [4]. The volcano is composed of medium-K andesite, dacite and rhyodacite [5] with the K contents higher than that in the Iliinsky volcano rocks.

Kambalny volcano started to form in early Holocene. About 7200 cal. BP its edifice was destroyed by a series of sector collapses. One of those resulted in the largest Holocene debris avalanche in Kamchatka [4]. Later eruptions built a new cone, which almost filled the collapse crater. About 650 cal BP a large phreatic eruption produced tephra, which covered the southwestern slope of the volcano and was dispersed at a distance of ~150 km [6]. Kambalny rocks are low-K basalts and basaltic andesites.

Zheltovsky volcano was active around 4000 cal. BP and then entered a long repose period. About 500 cal. BP the volcanic activity resumed, and in the early 1800-ies a large explosive eruption occurred, which produced basaltic bombs and lapilli. Lahars associated with both eruptions reached the Pacific coast. Zheltovsky Holocene rocks are low-K basalts and andesites.

Kosheleva volcano produced a strong explosive eruption ~7400 cal. BP. Its tephra was dispersed at a distance of more than 50 km. Later eruptions produced lava flows and a flank cinder cone. The volcano has been being virtually dormant since ~3000 cal. BP. Kosheleva Holocene rocks are high-K basalts, andesites and dacites.

All the considered volcanoes, except for Dikii Greben', produced strong (VEI=5) explosive eruptions in Holocene. Long period of volcanic quiescence in this region, which started ~1300 cal. BP, was interrupted by Kambalny eruption (~650 cal. BP) and then by eruptions from Zheltovsky and Iliinsky. These eruptions likely have opened a new active period of the southernmost Kamchatkan volcanoes.

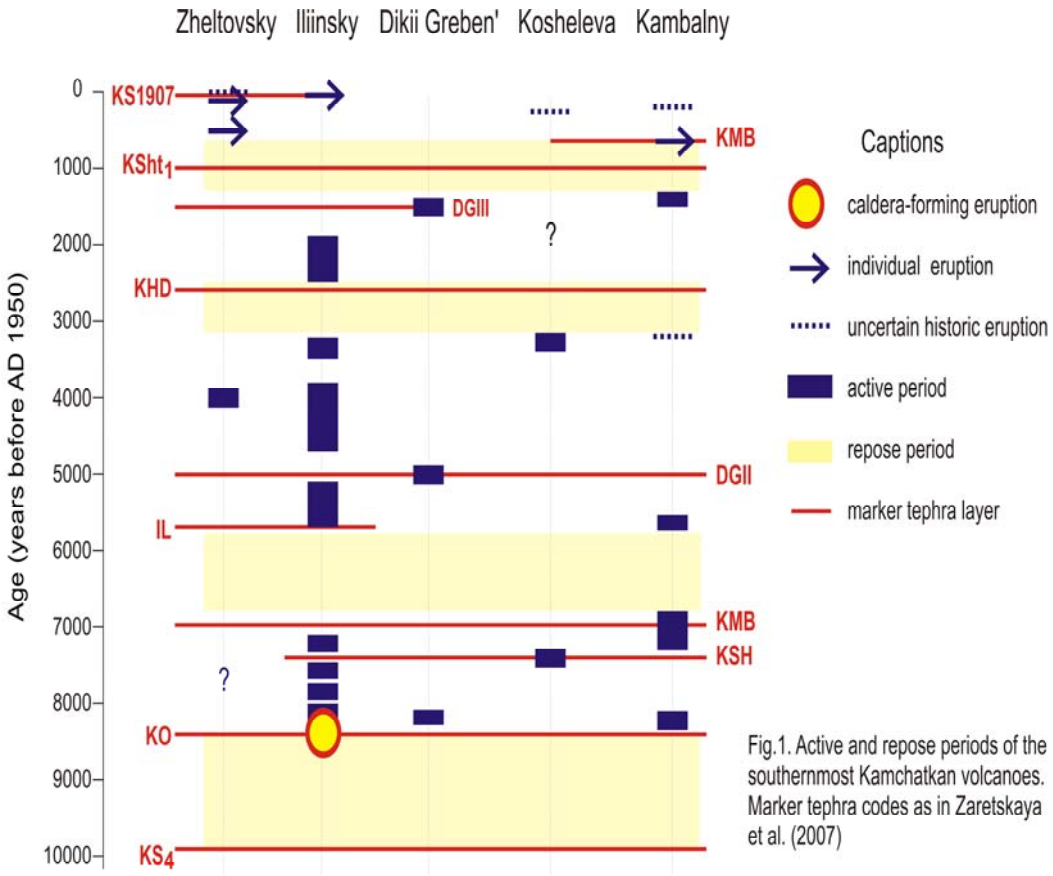


Fig.1. Active and repose periods of the southernmost Kamchatkan volcanoes. Marker tephra codes as in Zaretskaya et al. (2007)

References

1. Ponomareva et al., 2001. In: Tephras, chronology and archeology, CDERAD press: 91-100
2. Zaretskaya et al., 2001. Geochronometria, 20: 95-102
3. Ponomareva et al., 2004. J Volcanol Geotherm Res, 136: 199-222
4. Ponomareva et al., 2006. J Volcanol Geotherm Res, 158: 117-138
5. Bindeman I.N., Bailey J.C. 1994. Contrib Mineral Petrol 117: 263–278
6. Zaretskaya et al., 2007. Radiocarbon, 49/2: 1065-1078

ГОЛОЦЕНОВЫЙ РЕЖИМ АКТИВНОСТИ САМЫХ ЮЖНЫХ ВУЛКАНОВ КАМЧАТКИ

В.В.Пономарева[1], Н.Е.Зарецкая[2], Л.Д.Сулержицкий[2], О.В. Дирксен[1]

[1]Институт вулканологии и сейсмологии ДВО РАН, Петропавловск-Камчатский, 683006, бульвар Пийпа, 9, E-mail: ponomareva@kscnet.ru
[2]Геологический институт РАН, Москва, 119017, Пыжевский пер., 7

Детальные данные о режиме активности вулканов за последние тысячи лет являются основой для долгосрочного прогноза извержений и организации мониторинга текущей вулканической деятельности, а также для постановки работ по изучению эволюции составов магм. В этом докладе мы рассмотрим голоценовую активность вулканов самого юга Камчатки (Желтовский, Ильинский, кальдера Курильского озера, Дикий Гребень, Камбальный, Кошелева), восстановленную на основе геолого-геоморфоло-гического картирования, тефрохронологических исследований, радиоуглеродного датирования и изучения химического состава изверженных пород. Наши данные показывают, что вулканы района могут в скором времени возобновить свою деятельность [1].

Самое мощное голоценовое извержение данного района, приведшее к образованию **кальдеры Курильского озера (КО)** ~8400 лет назад (л.н.), вошло в первую десятку крупнейших эксплозивных голоценовых извержений мира [2, 3, 4]. Тефра выпала над большой частью Камчатки, Охотским морем и далее на северо-запад на расстоянии ~1700 км. Пирокластические потоки заполнили долины и перекрыли возвышенности тонким плащом пирокластики на расстоянии ~50 км от источника. Состав пород во время извержения менялся от риолитов к андезибазальтам и вновь к риолитам. Вскоре после извержения возникли вулканы Ильинский и Дикий Гребень.

Вулкан Ильинский был самым активным в голоцене (рис.1). Последнее его извержение произошло в 1901 г. после периода покоя длительностью ~1800 лет. При извержениях вулкана происходило образование лавовых и пирокластических потоков, шлаковых лавин и тефры. Тефра распространялась на расстояние более 100 км. Продукты вулкана представлены умеренно-калиевой базальт-андезит-дацитовой серией, родственной породам кальдерообразующего извержения КО.

Вулкан Дикий Гребень проявлял активность трижды за голоцен: ~8400, 5000 и 1500 л.н. Каждый период активности включал формирование лавовых куполов, образование пирокластических и лавовых потоков и выбросы тефры, которая распространялась на расстояние >30 км. Во время последнего извержения произошел крупный обвал купола [5]. Вулкан сложен породами умеренно-калиевой андезит-риодацитовой серии [6] с более высоким содержанием калия по сравнению с породами в.Ильинский.

Вулкан Камбальный возник в раннем голоцене. Около 7200 л.н. постройка вулкана была разрушена серией обвалов, один из которых привел к образованию самой крупной голоценовой обломочной лавины на Камчатке [5]. Последовавшие эффузивно-эксплозивные извержения построили новый конус, почти замаскировавший обвальный цирк. Около 650 л.н. произошло сильное фреатическое извержение, тефра которого плащом покрыла ЮЗ склон вулкана и распространилась как минимум на ~150 км [7]. Породы вулкана - низко-калиевые базальты и андезибазальты.

Вулкан Желтовский был активен ~4000 л.н., а затем вступил в длительный период покоя. Около 500 л.н. активность вулкана возобновилась, а в начале XVIII века произошло сильное эксплозивное извержение с выбросом базальтовых бомб и лапилли. Лахары, связанные с обоими извержениями, дошли до побережья Тихого океана. Голоценовые породы вулкана представлены низко-калиевой базальт-андезитовой серией.

Вулкан Кошелева имел сильное эксплозивное извержение ~7400 л.н. Тефра этого извержения распространилась далее чем на 50 км. За время последующих извержений произошло излияние лавовых потоков из вершинного кратера вулкана и образование побочного шлакового конуса на его склоне. Вулкан находится в состоянии относительного покоя последние 3000 лет. Продукты голоценовых извержений представлены высоко-калиевой базальт-андезит-дацитовой серией.

Итак, все рассматриваемые вулканы, кроме Дикого Гребня, имели в прошлом сильные (VEI=5) эксплозивные извержения. Длительный период покоя в данном районе, начавшийся ~1300 л.н., был прерван извержениями Камбального (650 л.н.), а затем Желтовского и Ильинского. Возможно, что эти извержения открыли новый этап в активности вулканов самого юга Камчатки.

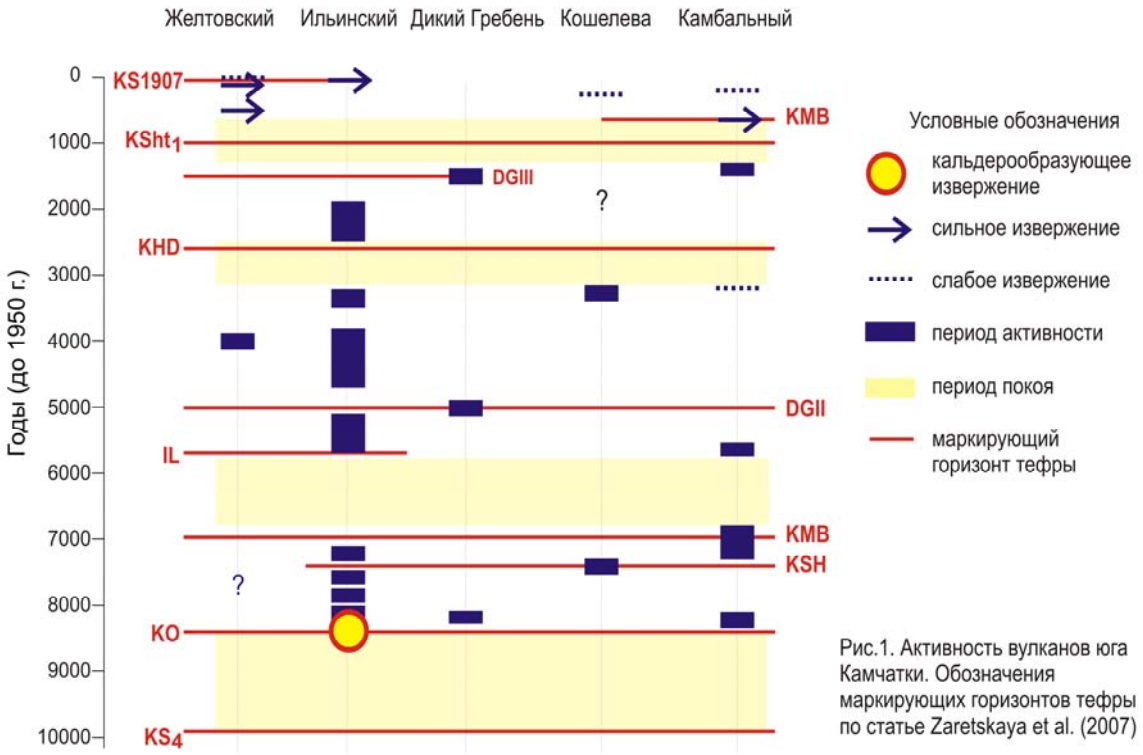


Рис.1. Активность вулканов юга Камчатки. Обозначения маркирующих горизонтов тефры по статье Zaretskaya et al. (2007)

Литература

1. Ponomareva et al., 2001. In: Tephras, chronology and archeology, CDERAD press: 91-100
2. Zaretskaya et al., 2001. Geochronometria, 20: 95-102
3. Ponomareva et al., 2004. J Volcanol Geotherm Res, 136: 199-222
4. Пономарева и др. В кн.: Экстремальные природные явления и катастрофы. М.: ИФЗ РАН, 2010. С. 219-238
5. Ponomareva et al., 2006. J Volcanol Geotherm Res, 158: 117-138
6. Bindeman I.N., Bailey J.C. 1994. Contrib Mineral Petrol 117: 263–278
7. Zaretskaya et al., 2007. Radiocarbon, 49/2: 1065-1078

Swath bathymetric investigations of the submarine Volcanologists Massif, Komandorsky Basin

Boris Baranov[1], Reinhart Werner[2], Nikolay Tsukanov[1], Karine Dozorova[1]
[1] IO RAS, P.P. Shirshov Institute of Oceanology RAS, Nakhimovsky prospekt 36, 117997 Moscow, Russia; email: bbaranov@ocean.ru
[2] IFM-GEOMAR, Leibniz-Institut für Meereswissenschaften, Gebäude Ostufer, Wischhofstrasse 1-3, 24148 Kiel, Germany

The most peculiar feature of the Komandorsky Basin (Western Bering Sea) floor is a huge volcanic massif located about 60 km to the north from the Komandorsky Islands. This structure called Volcanologists Massif was discovered in 1984 during RV Vulkanolog Cruise (Seliverstov et al., 1986). It has diameter of about 40 km and height more then 3.5 km. Up to beginning of 90-th Volcanologists Massif was investigated by different methods including single-beam echosounder mapping (Seliverstov, 1998).

For the first time the swath bathymetric investigations were conducted on this structure in autumn of 2009 during RV Sonne Cruise SO 201-2. This cruise was carried on in the frame of German-Russian project KALMAR (**K**urile-Kamchatka and **Al**eutian **M**arginal Sea – Island **Ar**c System).

Swath bathymetric surveys give us an opportunity to clarify the main structural features of the Volcanologists Massif area including its central part (Piip Volcano), Komandor Graben and Alpha Ridge. So, real idea was obtained about distribution of the normal fault scarps, which locate in western and eastern parts of the Volcanologists Massif and in the Komandor Graben. The strikes of the normal faults scarps suggest dextral strike-slip movements along the fracture zone associated with the Alpha Ridge.

In addition to many volcanic forms including flank cones, volcanic ridges and lava flows were detected in the Volcanologists Massif. The flank cones are the most peculiar features among them. 57 cones locate in Volcanologists Massif, besides about half of them (25 cones) are spaced at Piip volcano. The height of cones changes from 10 m up to 250 m and their diameters vary from 100 m up to 1,5 km. Main amount of the flank cones locates to the west from the Piip Volcano axis.

According to Nakamura (1977) the distribution of the flank cones will be elongated in the direction of the maximum horizontal compression (S_H) of the regional stress. To determine direction of the S_H we have used two parameters (Paulsen, Wilson, 2010): (1) flank cones alignments based on cone centers, and (2) flank cones alignments based on cone shapes. Two directions of the S_H were obtained, namely NW-SE and NNE-SSW (Fig. 1B, inset). First direction is weakly expressed and corresponds to direction of the maximum horizontal stress obtained on base of focal mechanism solutions (Heidbach et al., 2008). The second direction is determined by existence of feeder dikes, which trend parallel to the S_H direction and orthogonal to the minimum horizontal stress (S_h). S_h direction is roughly coincided with strikes of normal faults scarps, which are determined by regional extension existing in this part of the Komandorsky Basin.

The investigations were funded by BMBF, Germany and Minobrnauka, Russia.

References

Heidbach O, Tingay M, Barth A, Reinecker J, Kurfeß D, and Müller B (2008) The World Stress Map database release 2008 doi:10.1594/GFZ.WSM.Rel2008

Nakamura K (1977) Volcanoes as possible indicators of tectonic stress orientation – principle and proposal. Journal of Volcanology and Geothermal Research 2:1-16

Paulsen TS, Wilson TJ (2010) New criteria for systematic mapping and reliability assessment of monogenetic volcanic vent alignments and elongate volcanic vents for crustal stress analyses. Tectonophysics 482: 16–28

Seliverstov NI, Avdeiko GP, Ivanenko AN, Shkira VA, Khabunaya SA (1986) New submarine volcano in the western Aleutian Arc. Volcanology and Seismology 5: 3-16 (in Russian)

Seliverstov NI (1998) Seafloor structure offshore the Kamchatka Peninsula and geodynamics of the junction of the Kurile-Kamchatka/Aleutian islands arcs. Scientific World, Moscow: 164 (in Russian)

Geochemical evidence for subduction related origin of the Bowers and Shirshov Ridges (Bering Sea, NW Pacific)

Maren Wanke[1,2], Maxim Portnyagin[1], Reinhard Werner[1], Folkmar Hauff[1], Kaj Hoernle[1], Dieter Garbe-Schönberg[2]

[1] IFM-GEOMAR, Leibniz Institute of Marine Sciences, Wischhofstraße 1-3, 24148 Kiel, Germany
[2] Institute of Geosciences, Christian-Albrechts-University of Kiel, Ludewig-Meyn-Straße 10, 24118 Kiel, Germany

The Bowers and Shirshov Ridges (hereafter BR and SR, respectively) are two prominent submarine structures of unknown age and provenance in the Bering Sea (Fig. 1). So far only a few geochemical data exist on the composition of basement rocks from the SR (Silantyev et al. 1985) and none for the BR. Age and geochemical data are crucial to evaluate if the ridges represent remnant island arcs (Cooper et al. 1981, Scholl 2007), intra-oceanic rises, accreted onto the continental margin (Ben-Avraham & Cooper 1981), an ancient spreading center (SR: Kienle 1972) or parts of the Mesozoic Hawaiian hot-spot (Steinberger & Gaina 2007).

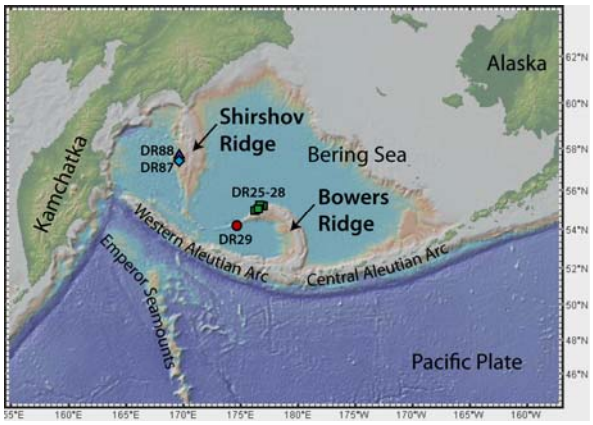


Fig. 1: Map of the study area. Each symbol indicates a dredge location (DR) on the BR (squares), the SR (triangle and diamond) or on a seamount next to the BR (circle).

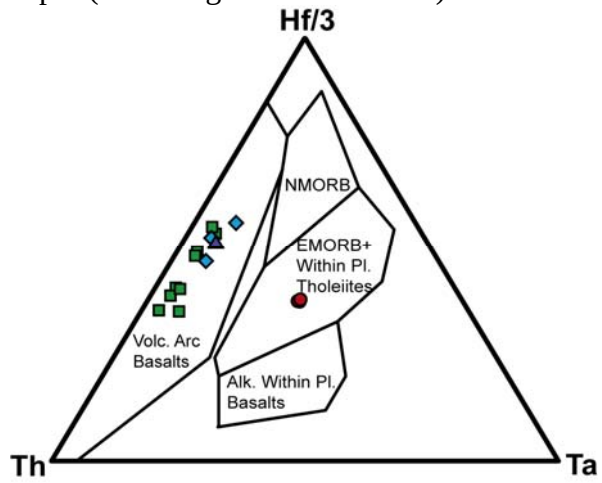


Fig. 2: Th-Hf-Ta diagram after Wood (1980) showing different tectonic settings for BR and SR and one seamount in between. Symbols refer to Fig. 1.

Here we report the first geochemical data on the composition of the basement rocks from the BR and SR, recovered during KALMAR R/V SONNE cruise 201 (Legs 1b and 2) in 2009. Fresh to moderately altered volcanic rocks were dredged from the northern slope of the BR, from seamounts on the western extension of the BR and from the western slope of the central part of the SR. We studied the petrography of the samples and carried out geochemical analyses of major and trace elements by XRF and ICPMS at ACME Lab (Vancouver, Canada) and CAU (Kiel). Sr-Nd-Pb(ds) isotopes were analyzed by TIMS at the IFM-GEOMAR (Kiel).

The rocks from the northwestern slope of the BR are clinopyroxene (cpx)-phyric basalts with minor amounts of olivine (ol) and plagioclase (plag) microphenocrysts, as well as hbl-plag-cpx-bearing basaltic andesites and trachyandesites. The rocks are strongly enriched in LREE (La_N/Yb_N = 3.2 – 8.5, N indicates normalization to primitive mantle), fluid-mobile elements (Pb, Ba, U, K) relative to NMORB and exhibit clear negative anomalies of HFSE (Nb, Ta and Ti) in primitive mantle-normalized incompatible element diagrams. The BR rocks also have a moderate adakitic signature, as indicated by elevated Sr_N/Y_N ratios (6.9 – 12.9). Hbl-cpx-plag

trachybasalts from the SR have similar major and trace element compositions (La_N/Yb_N = 2.1 – 4.9) to the BR rocks. The other magmatic series from the SR comprises massive trachyandesites, trachytes and dacites with rare phenocrysts of plag and cpx. These rocks also have island-arc type incompatible element patterns and are distinct from other rock types from the BR and SR with less LREE enriched patterns (La_N/Yb_N ~ 1.8) and a strong negative Eu anomaly (Eu/Eu* = 0.74).

The rocks from BR have relatively unradiogenic Sr and Pb isotopes ($^{87}Sr/^{86}Sr$ = 0.70296 – 0.70311, $^{206}Pb/^{204}Pb$ = 18.22 – 18.30) and radiogenic Nd ($^{143}Nd/^{144}Nd$ = 0.51312 – 0.51314) compositions, which are well within the Aleutian Arc isotope array and intermediate between typical compositions of the Central and Western Aleutian rocks (Kelemen et al. 2003). The rocks from SR have slightly more radiogenic $^{87}Sr/^{86}Sr$ (0.70338 – 0.70414) and similar $^{143}Nd/^{144}Nd$ isotope compositions to the BR rocks. Silicic SR rocks have distinctively high $^{206}Pb/^{204}Pb$ (18.46 – 18.47) ratios compared to basalts from BR and SR.

Rocks dredged from a seamount on the western extension of the BR have very distinctive petrographic and geochemical characteristics. These are ol-phyric pillow basalts with minor (less than 5%) amounts of plag and cpx. The freshest whole rocks and pillow-rim glasses have relatively smooth patterns of incompatible trace elements, akin to intraplate oceanic basalts (Fig. 2). Trace element geochemical characteristics of the seamount basalts are similar to Hawaiian tholeiites. That might suggest the preservation of the older Hawaiian seamounts in the Bering Sea. Sr-Nd-Pb isotope data and our preliminary age determinations from the U-Pb-Th systematics of the rocks do not support this hypothesis. According to our current interpretation, the intraplate-type basalts west of the Bowers Ridge most likely originated by low-degree melting of the local mantle along a transform-like ridge connecting Bowers and Shirshov Ridges.

In summary, petrography and geochemical results indicate an island-arc origin (Fig. 2) for major parts of the BR and SR. Isotope data suggest that the BR and parts of the SR could have developed as parts of the former Aleutian Arc. Our further studies will be focused on obtaining absolute age data for the studied rocks, which will allow combining the petrologic data with tectonic and geodynamic models for the NW Pacific.

References

Ben-Avraham Z, Cooper AK (1981) Early evolution of the Bering Sea by collision of oceanic rises and North Pacific subduction zones. Geol. Soc. Am. Bull. 92: 485-495

Cooper AK, Marlow MS, Ben-Avraham Z (1981) Multichannel seismic evidence bearing on the origin of Bowers Ridge, Bering Sea. Geol. Soc. Am. Bull. 92: 474-484

Kelemen PB, Yogodzinski GM, Scholl DW (2003) Along-Strike Variation in the Aleutian Island Arc: Genesis of High Mg# Andesite and Implications for Continental Crust. In: Eiler J (ed): Inside the Subduction Factory. American Geophysical Union, Monograph 138: 223-276

Kienle J (1971) Gravity and magnetic measurements over Bowers Ridge and Shirshov Ridge, Bering Sea. Journal of Geophysical Research, 76: 7138-7153

Scholl D W (2007) Viewing the tectonic evolution of the Kamchatka-Aleutian (KAT) connection with an Alaska crustal extrusion perspective. In: Eichelberger JC, Gordeev E, Izbekov P, Kasahara M, Lees J (eds): Volcanism and subduction the Kamchatka region, American Geophysical Union, Monograph 172: 3-35

Silantyev SA, Baranov BV, Kolesov GM (1985) Geochemistry and petrology of amphibolites from the Shirshov Ridge (Bering Sea). Geochimiya 12: 1694-1704

Steinberger B, Gaina C (2007) Plate-tectonic reconstructions predict part of the Hawaiian hotspot track to be preserved in the Bering Sea. Geology 35: 407-410

Wood DA (1980) The application of a Th-Hf-Ta diagram to problems of tectnomagmatic classification and to establishing the nature of crustal contamination of basaltic lavas of the British Tertiary volcanic province. Earth and Planetary Science Letters 50: 11-30

First data on geochemistry of oceanic peridotites from NW Pacific and their possible contribution to volcanism in Kamchatka and Aleutian Arc

Krasnova E[2], Portnyagin M[1,2], Silantyev S[2], Werner R[1], Hoernle K[1]
[1]Leibniz Institute of Marine Sciences, IFM-GEOMAR, Wischhofstr. 1-3, 24114 Kiel, Germany
[2]V.I.Vernadsky Institute of Geochemistry and Analytical Chemistry RAN, Kosygin St. 19, 119991 Moscow, Russia

The Stalemate Fracture Zone (FZ) is a 500 km long SE-NW trending transverse ridge between the northernmost Emperor Seamounts and the Aleutian Trench which originated by flexural uplift of Cretaceous (?) oceanic lithosphere along a transform fault at the Kula-Pacific plate boundary [1]. Sampling at the Stalemate FZ and the fossil Kula-Pacific Rift valley was carried out during the R/V SONNE cruise SO201 Leg 1b in July 2009. A broad spectrum of rocks including serpentinites (DR37), gabbro (DR7,40), dolerites (DR7) and basalts (DR38,41) were obtained. These rocks are thought to represent a complete section of oceanic lithosphere formed at the fossil Kula-Pacific Spreading Center. A study of these rocks will allow us to reconstruct the conditions of magma generation responsible for the formation of the NW Pacific oceanic crust and also to estimate the composition of subducting slab beneath the Western Aleutian Island Arc.

Strongly altered mantle rocks ranging from pyroxene-rich lherzolites and pyroxene-poor dunites were obtained at the station DR37 at the northern SVZ bend. The compositions of primary minerals (Cpx, Opx, Sp) change systematically from lherzolites to dunites. For example, spinel in lherzolites has higher Mg#, NiO, lower Cr#, Fe^{3+}# and TiO_2 (Mg#=0.65-0.68, NiO=0.26-0.34 wt%, Cr#=0.26-0.33, Fe^{3+}#=0.021-0.030, TiO_2=0.04-0.09 wt%) than spinel in dunites (Mg#=0.56-0.64, Cr#=0.38-0.43, TiO_2=0.19-0.28 wt%, NiO=0.19-0.26%, Fe^{3+}#=0.027-0.043). The variations of clinopyroxene and spinel compositions can be explained by the two-stage process [2]: 1) near fractional melting of depleted mantle to 10-12%, 2) interaction of the residual lherzolite with N-MORB-like melts to form dunites. The protolith of lherzolites and dunites dredged from the SFZ can thus represent disintegrated parts of shallow oceanic mantle variably modified by melt percolation.

Secondary alteration of the peridotites included serpentinization and also silicification of the dunites (Silantyev et al., 2011). These later processes overprinted nearly completely the primary bulk composition of the studied rocks (Fig. 1). The secondary alteration caused strong enrichment of the rocks in fluid mobile elements (U, Li, Sb, Ba) and U-shaped patterns of REE with strong negative Ce anomaly reflecting precipitation of REE from the seawater and very large water-rock ratios during alteration.

Several studies proposed an important role of subducting serpentinites as a source of fluids in subduction zones (e.g. Ruepcke et al., 2004). Judging from our results, serpentinized peridotites can represent an important type of rocks comprising fracture zones in the NW Pacific. Being subducted and dehydrated beneath the Aleutian Arc (Stalemate FZ) and Kamchatka (Krusenstern FZ), the serpentinized peridotites can be an important source of water-rich fluids enriched in Sb, Mo, U, Pb and Li. Detailed studies of active volcanoes located above subducting fracture zones (e.g., Kronotsky Volcano in Kamchatka located above the subducting Krusenstern FZ) can help identify contribution of oceanic serpentinites to island arc volcanism.

This study was financially supported by the Russian Foundation for Basic Research, project no. 09-05-00008-a, and KALMAR project.

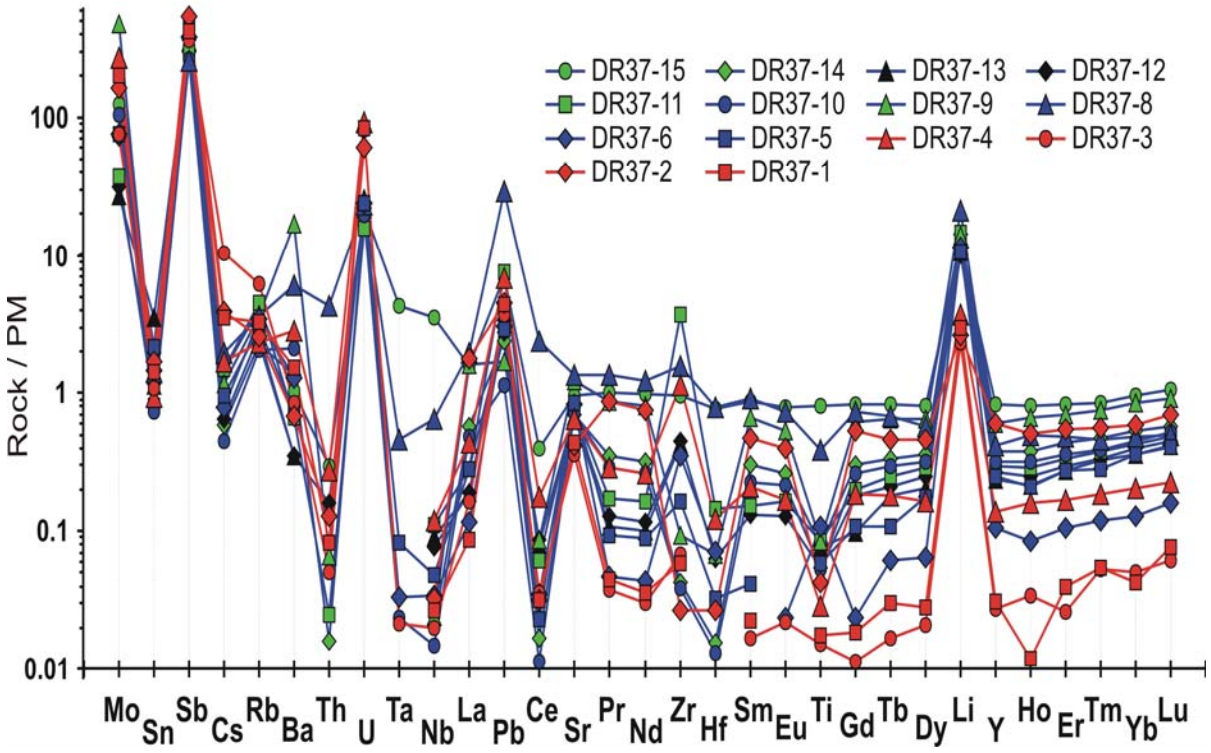


Figure. 1. Primitive mantle-normalized trace element patterns of the Stalemate FZ peridotites. The composition of primitive mantle is after [3].

References

[1] Lonsdale, P., 1988, Paleogene history of the Kula plate: Offshore evidence and onshore implications: Geological Society of America Bulletin, v. 100, p. 733-754.

[2] Kelemen, P.B., Shimizu, N., and Salters, V.J.M., 1995, Extraction of mid-ocean-ridge basalt from the upwelling mantle by focused flow of melt in dunite channels: Nature, v. 375, p. 747-753.

[3] McDonough W.F. & Sun S.-S., 1995, The composition of the Earth. Chemical Geology 120: 223-253

[4] Silantyev S., Novoselov A., Krasnova E., Portnyagin M., Hauff F., Werner R. Silisification of peridotites from Stalemate FZ (NW Pacific): Tectonic and geochemical applications. Petrology, in press.

[5] Rüpke L.H., Morgan J.P., Hort M., Connolly J.A.D., 2004, Serpentine and the subduction zone water cycle. Earth Planet. Sci. Lett. 223(1-2):17-34

Первые данные по геохимии перидотитов северо-западной части Тихого океана и их возможный вклад в вулканизм Камчатки и Алеутской островной дуги

Краснова Е [2], Портнягин М[1,2], Силантьев С[2], Вернер Р[1], Хёрнле К[1]

[1] Leibniz Institute of Marine Sciences, IFM-GEOMAR, Wischhofstr. 1-3, 24114 Киль, Германия
[2] Институт геохимии и аналитической химии им В.И. Вернадского РАН, ул. Косыгина 19, 119991 Москва, Россия

Разломная зона Стелмейт (РЗ) представляет собой поперечный хребет, простирающийся с ЮВ на СЗ на расстояние в 500 км и располагающийся между северными отрогами вулканической цепи Императорских подводных гор и Алеутским глубоководным желобом. В этой акватории Тихого океана вдоль трансформного разлома на границе плит Кула-Пацифик наблюдается поднятие к поверхности океанического дна меловой океанической литосферы [1]. Драгирование в пределах РЗ Стелмейт и палео-рифтовой долины Кула-Пацифик проводилось в течение рейса НИС SONNE SO201 Leg 1b в июне 2009 года.

Собранная в рейсе коллекция образцов представлена серпентинитами (DR37), габбро (DR7, 40), долеритами (DR 7, 40) и базальтами (DR38, 41). Данный петрографический спектр пород представляет полный разрез древней океанической литосферы канонического типа в районе спредингового центра Кула-Пацифик. Изучение имеющейся коллекции образцов позволяет реконструировать основные этапы магматической эволюции океанической коры СЗ части Тихого океана, а также, оценить вклад ее вещества в надсубдукционный магматизм Восточных Алеут.

На 37 станции в северной части разломной зоны Стелмейт были подняты практически нацело серпентинизированные лерцолиты, богатые клинопироксеном и окварцованные аподунитовы серпентиниты, обедненные клинопироксеном. Состав первичных минералов (шпинель, клинопироксен и ортопироксен) меняются систематически от лерцолитов к дунитам. Например, шпинель в лерцолитах имеет более высокие содержания Mg#, NiO, более низкие Cr#, Fe^{3+}# и TiO_2 (Mg#=0.65-0.68, NiO=0.26-0.34%, Cr#=0.26-0.33, Fe^{3+}#=0.021-0.030, TiO_2=0.04-0.09 wt%), чем шпинель в дунитах (Mg#=0.56-0.64, Cr#=0.38-0.43, TiO_2=0.19-0.28 wt%, NiO=0.19-0.26%, Fe^{3+}#=0.027-0.043.

Вариация составов клинопироксена и шпинели могут объясняться двухэтапным процессом образования перидотитов: 1) образование обедненных лерцолитов в результате 10-12% оклофракционного плавления деплетированной мантии, 2) формирование дунитов при взаимодействии лерцолитов с подобным расплавом N-MORB. Таким образом, лерцолиты и дуниты драгированные в разломной зоне Стелмейт могут представлять собой фрагменты малоглубинной океанической мантии, в различной степени модифицированной в результате взаимодействия с просачивающимися глубинными расплавами.

Низкотемпературные изменения перидотитов заключались в их серпентинизации и окварцевании дунитов [4]. Эти вторичные процессы оказали большое влияние на содержания главных и рассеянных элементов в изученных породах (рис. 1). Именно с вторичными изменениями связано обогащение пород мобильными элементами (U, Li, Sb, Ba) и U-образная форма спектров нормализованных содержаний РЗЭ с сильной отрицательной Ce аномалией, отражающая взаимодействие пород с морской водой и высокое отношение вода-порода.

В ряде работ предполагалось, что океанические серпентиниты являются важным источником флюидов в зонах субдукции (например, [5]). Судя по нашим данным, серпентинизированные перидотиты слагают крупные участки разломных зон северо-западной части Тихого океана. Будучи субдуцированными под Алеутскую островную дугу

(разломная зона Стелмейт) и Камчатку (разломная зона Крузенштерн), эти породы могут быть важным источником водного флюида обогащенного Sb, Mo, U, Pb and Li. Детальное изучение активных вулканов, расположенных над разломными зонами на субдуцирующей океанской плите (например, вулкан Кроноцкий на Камчатке, расположенный над разломной зоной Крузенштейн), может помочь при оценке вклада океанических серпентинитов в вулканизм островных дуг.

Проведенное исследование было поддержано немецко-российским проектом KALMAR и Российским Фондом Фундаментальных Исследований (грант РФФИ № 09-05-00008).

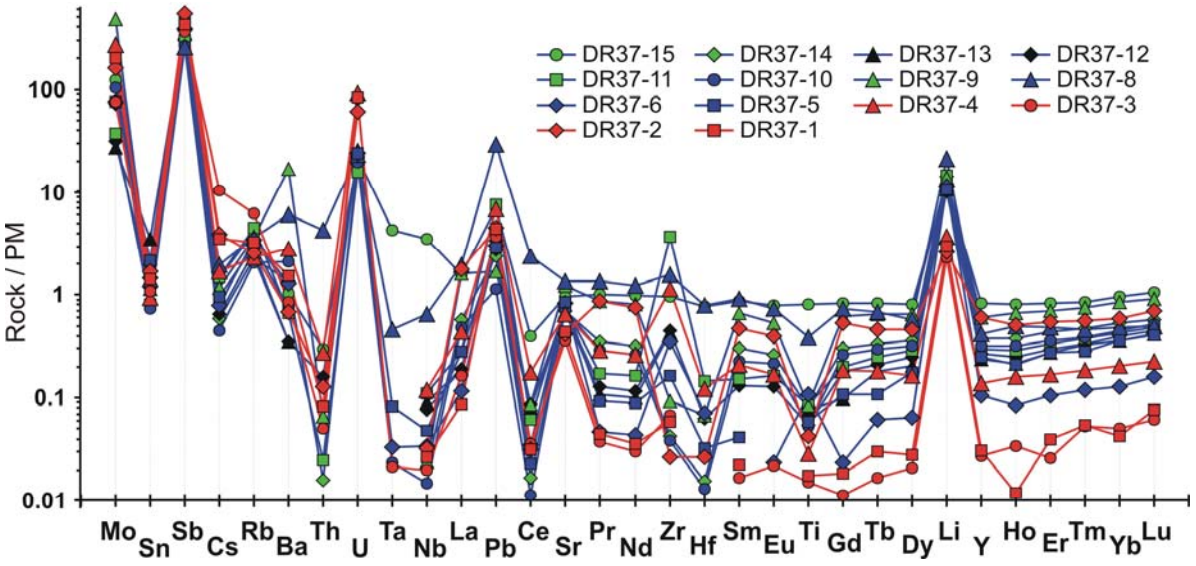


Рис. 1. Содержания рассеянных элементов в перидотитах разломной зоны Стелмейт, нормированные к составу примитивной мантии по [3].

Литература

[1] Lonsdale, P., 1988, Paleogene history of the Kula plate: Offshore evidence and onshore implications: Geological Society of America Bulletin, v. 100, p. 733-754.

[2] Kelemen, P.B., Shimizu, N., and Salters, V.J.M., 1995, Extraction of mid-ocean-ridge basalt from the upwelling mantle by focused flow of melt in dunite channels: Nature, v. 375, p. 747-753.

[3] McDonough W.F. & Sun S.-s. (1995) The composition of the Earth. Chemical Geology 120: 223-253

[4] Силантьев С., Новоселов А., Краснова Е., Портнягин М, Хауфф Ф., Вернер Р., 2011, Силификация перидотитов разлома Стэлмейт (северо-запад Тихого океана): реконструкция условий низкотемпературного выветривания и их тектоническая интерпретация, Петрология.

[5] Rüpke L.H., Morgan J.P., Hort M., Connolly JAD., 2004, Serpentine and the subduction zone water cycle. Earth Planet. Sci. Lett. 223(1-2):17-34

Estimates of Current Plate Motions around the Bering Sea and Northeast Asia Based on GPS Measurements

Jeffrey T. Freymueller, Geophysical Institute, University of Alaska Fairbanks, Fairbanks, AK 99775 USA (jeff.freymueller@gi.alaska.edu)

Grigory M. Steblov, Institute of Physics of the Earth RAS, Moscow 123995, Russia; also at Geophysical Survey RAS, Obninsk 249030, Russia (steblov@gps.gsras.ru)

Dmitry I. Frolov, Ioffe Physico-Technical Institute RAS, St. Petersburg 194021, Russia (dm.frolov@mail.ioffe.ru)

Mikhail G. Kogan, Lamont-Doherty Earth Observatory, Earth Institute at Columbia University, Palisades, NY, 10964 USA (kogan@ldeo.columbia.edu)

The location of the boundary between the North American and Eurasian plates in northeast Asia has long been subject to considerable uncertainty. The two plates diverge at spreading centers in the North Atlantic and Arctic Oceans, and converge in northeastern Asia. Because the pole of relative plate motion is located in the same area, relative plate motions are slow and deformation may be diffuse. GPS measurements made over the last decade on the Russian and American sides of the boundary show a more complex pattern of present motions. The crust of the Bering Sea and most of Alaska moves significantly relative to stable North America, making it likely that the edge of the undeforming North American plate lies well within North America. A similar pattern holds for northeast Asia. Overall, the region consists of a collage of small microplates or blocks moving relative to each other, with some of the microplate boundaries being uncertain or controversial, and some proposed microplates perhaps being regions of diffuse deformation rather than rigid plates. Here we use new and reanalyzed GPS data to reassess the proposed motion of the Bering plate and its boundaries, including a new microplate model for southern Alaska.

Marine volcanological and petrological studies with R/V SONNE in the NW Pacific and Bering Sea: SO201 KALMAR cruise results

Portnyagin M[1,2], Hoernle K[1], Werner R[1], Hauff F[1], Meicher D[1], Yogodzinski G[3], Baranov B[4], Silantiev S[2], Wanke M[1], Krasnova E[2]

[1]Leibniz Institute of Marine Sciences, IFM-GEOMAR, Wischhofstr. 1-3, 24114 Kiel, Germany; email: mportnyagin@ifm-geomar.de
[2]V.I.Vernadsky Institute of Geochemistry and Analytical Chemistry RAN, Kosygin St. 19, 119991 Moscow, Russia
[3]Department of Earth & Ocean Sciences, University of South Carolina, 701 Sumter St., EWSC617, Columbia SC 29208, USA
[4]P.P.Shirshov Institute of Oceanology, Nakhimovski Prospekt 36, 117997 Moscow, Russia
5 Institute of volcanology and seismology, Piip 9, 683006 Petropavlovsk-Kamchatsky, Russia

The research project SO201 KALMAR included bathymetric mapping of volcanic and tectonic structures and dredging of basement rocks in the NW Pacific and Bering Sea, the areas adjacent to the Kamchatka-Aleutian Arc junction. This research has been carried out within the KALMAR project and aimed at reconstructing of temporal and compositional evolution of volcanism associating with the Kamchatka-Aleutian junction. The major goals for the marine research with R/V SONNE were to collect information about the age and composition of the NW Pacific oceanic crust subducting beneath Kamchatka and Aleutian Arc, to study the extent and compositional peculiarity of young submarine volcanism along the Western Aleutian Arc and to explore the origin and evolution of submerged Bowers and Shirshov Ridges in the Bering See.

Multi-beam mapping of the ocean floor and dredging were carried out during Leg 1b (10.06.-06.07.2010) and Leg 2 (30.08.-08-10.2009) of the SO201 KALMAR expedition (Fig. 1). A total of 74 dredges were carried out. Of these deployments, 65 (or 87%) yielded rocks of clearly *in situ* magmatic or sedimentary origin. Magmatic and metamorphic basement rocks were recovered from three major working areas: (1) NW Pacific oceanic crust including northernmost Emperor Ridge Seamounts, Emperor Trough, Stalemate Fracture Zone and the Kula-Pacific Rift, (2) Volcanologists Massif and young submarine volcanoes along the Western Aleutian Arc, and (3) Shirshov and Bowers Ridges in the Bering Sea. In most areas magmatic rocks were sampled for the first time. The SO201 cruise reports providing description of the dredged samples and on-board generated bathymetric maps of the studied areas are available in English at:

http://www.ifm-geomar.de/fileadmin/ifm-geomar/fuer_alle/institut/publikationen/ifm-geomar_rep32.pdf (SO201 Leg 1b)
http://www.ifm-geomar.de/fileadmin/ifm-geomar/fuer_alle/institut/publikationen/ifm-geomar_rep35.pdf (SO201 Leg 2)

In this presentation we are going to give an overview of the KALMAR cruise results and to demonstrate first geochemical data on the dredged rock compositions. Additional information about the KALMAR marine research can be found in the presentations by Wanke et al. and Krasnova et al. (this volume).

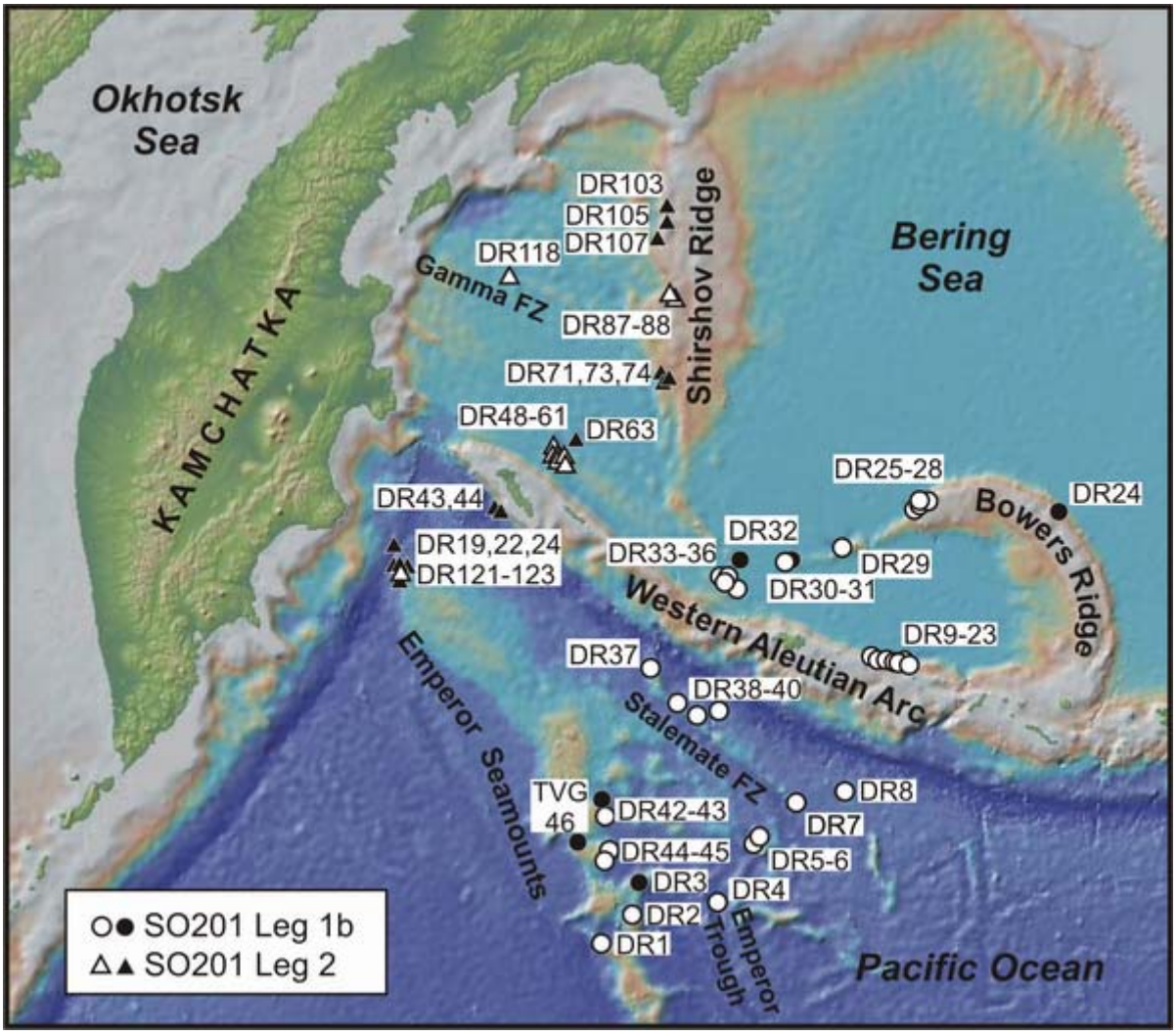


Fig. 1. Locations of dredge (DR) and TV-grab (TVG) stations during SO201 KALMAR Legs 1b and 2. White symbols denote stations where in-situ magmatic rocks were recovered, black symbols - stations with sedimentary or metamorphic rocks.

Морские вулканологические и петрологические исследования на НИС ЗОННЕ в СЗ Пацифике и Беринговом море: Результаты рейсов SO201 KALMAR

Портнягин М.[1,2], Хернле К.[1], Вернер Р.[1], Хауфф Ф.[1], Майхер Д.[1], Ягодзинский Дж.[3], Баранов Б.В.[4], Силантьев С.А.[2], Ванке М.[1], Краснова Е.А.[2], Савельев Д.П.[5]

[1] Leibniz Institute of Marine Sciences, IFM-GEOMAR, Wischhofstr. 1-3, 24114 Kiel, Germany; e-mail: mportnyagin@ifm-geomar.de
[2] Институт геохимии и аналитической химии им. В.И. Вернадского РАН, ул. Косыгина, 19, 119991 Москва, Россия
[3] Department of Earth & Ocean Sciences, University of South Carolina, 701 Sumter St., EWSC617, Columbia SC 29208, USA
[4] Институт океанологии им. П.П.Ширшова РАН, Нахимовский проспект 36, 117997 Москва, Россия
[5] Институт вулканологии и сейсмологии ДВО РАН, б-р Пиипа 9, 683006 Петропавловск-Камчатский, Россия

Проект SO201 KALMAR включал батиметрические исследования вулканических и тектонических структур и драгирование пород фундамента северо-западной Пацифики и Берингова моря, вблизи сочленения Курило-Камчатской и Алеутской островных дуг. Это исследование являлось частью проекта КАЛЬМАР, основная задача которого в области вулканологии и петрологии – это реконструкция эволюции состава вулканизма Камчатско-Алеутского сочленения во времени. Главными задачами морских работ на НИС ЗОННЕ был сбор информации о возрасте и составе океанической коры северо-западной Пацифики, субдуцирующей под Камчатку и Алеутскую островную дугу, изучение пространственного распределения и особенностей состава подводных вулканов вдоль западного сегмента Алеутской островной дуги и выяснение происхождения и эволюции подводных хребтов Ширшова и Бауэрс в Беринговом море.

Многолучевая батиметрическая съемка океанического дна и драгирование проводились в течении 2-х этапов экспедиции проекта КАЛЬМАР: SO201-1b (10.06.-06.07.2010) and SO201-2 (30.08.-08-10.2009) (Рис. 1). Всего было проведено 74 драгировки, из которых 72 (или 97%) доставили на борт судна породы морского дна, в большинстве своем (87%) представляющие коренные магматические и осадочные породы. Коренные магматические и метаморфические породы фундамента были драгированы в трех основных районах: (1) район северо-западной Пацифики, включающий наиболее северные гайоты Имперторской цепи подводных гор, Императорский трог, хребет Стелмейт и древний рифт Кула-Пасифик, (2) массив Вулканологов и молодые подводные вулканы вдоль Западно-Алеутской дуги, и (3) хребты Ширшова и Бауэрс в Беринговом море. В большинстве районов магматические породы были подняты впервые. Отчеты о рейсах SO201 проекта КАЛЬМАР, содержащие информацию о результатах драгировок и созданные во время рейса батиметрические карты изученных районов, доступны на английском языке по следующим адресам:

http://www.ifm-geomar.de/fileadmin/ifm-geomar/fuer_alle/institut/publikationen/ifm-geomar_rep32.pdf (SO201 Leg 1b)

http://www.ifm-geomar.de/fileadmin/ifm-geomar/fuer_alle/institut/publikationen/ifm-geomar_rep35.pdf (SO201 Leg 2)

В докладе будет представлен обзор основных результатов рейсов КАЛЬМАР и показаны первые результаты геохимического изучения драгированных пород. Дополнительную информацию о результатах морских исследований проекта КАЛЬМАР можно узнать из докладов Wanke et al. и Krasnova et al. (см. материалы JKASP-2011).

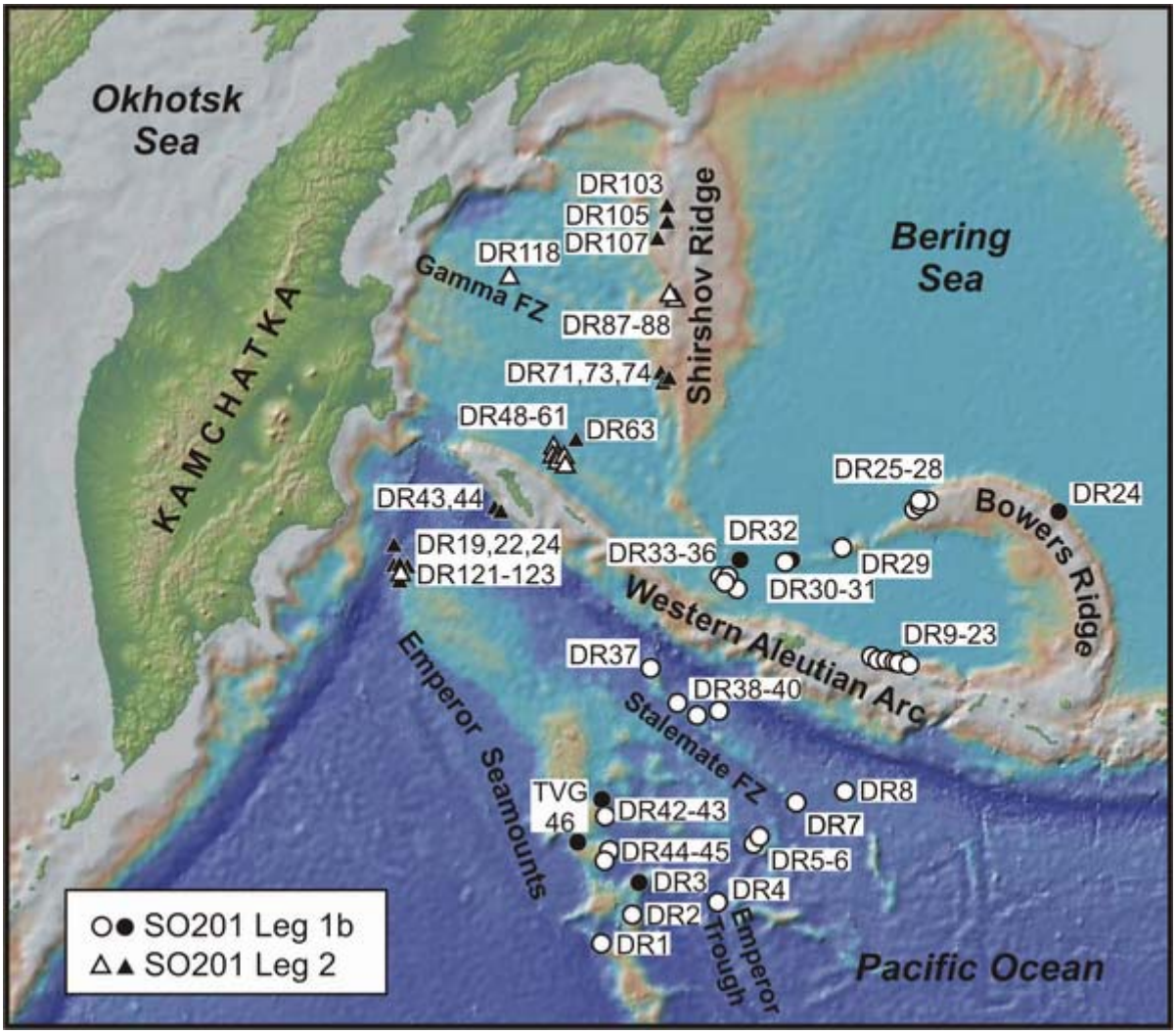


Рис. 1. Места станций драгировок (DR) и спуска TV-грейфера (TVG) во время рейсов SO201 KALMAR 1b и 2. Белые значки указывают на станции, где были подняты коренные магматические породы и мантийные перидотиты; черные значки – станции, где подняты коренные осадочные или метаморфические породы.

KALMAR – "Kurile-Kamchatka and Aleutean Marginal Sea-Island Arc Systems: Geodynamic and Climate Interaction in Space and Time" – A Russian - German Research Initiative.

C. van den Bogaard (1), C. Dullo (1), B. Baranov (2) and KALMAR Scientists
(1) Leibniz Institute of Marine Sciences, IFM-GEOMAR, Kiel, Germany, (2) P.P. Shirshov Institute of Oceanology RAS, Moscow, Russia (cbogaard@ifm-geomar.de / Phone: +494316002647)

KALMAR is a Russian-German collaborative research project focussing on the large area of the triple junction of the Kurile-Kamchatka and Aleutian Island Arc system. Since 2006 German and Russian scientists work together towards a better understanding of the processes that control the subduction and the geodynamic and climatic development in this complex climate driving region. Research in five closely coupled subprojects involve a wide range of geophysical, tectonic, volcanological and petrological approaches as well as paleo-oceanographic and climate research. The geochemical refinement of the tephrostratigraphic framework of Pleistocene and Holocene tephra in Kamchatka provided independent time markers for an exact correlation of the various climate archives from land and marine sites.

With the participation of scientists, young researchers and students from Russia, Germany and the United States we carried out several land expeditions on Kamchatka since summer 2007 as well as three geomarine cruises in the NW-Pacific and the western Bering Sea with the German research vessel SONNE in 2009. In SO201 Leg 1a (16.05. - 09.06.2009) the research concentrated on the geophysical investigation of the subducting plate, during SO201 Leg 1b (10.06. - 06.07.2009) and SO201 Leg 2 (30.08. - 08.10.2009) the research concentrated on volcanological, petrological, tectonic and paleoceanographic questions. One focus of the cruises was the study on the composition of the mantle and the oceanic crust, the seamounts and their ages. Details of these aspects of the expeditions will be shown by Portnyagin et al. (this meeting). Another focus of the cruise were paleo-oceanographic investigations on the sediments along the eastern continental slope of Kamchatka, in the Komandorsky Basin, and on the Shirshov Ridge to explore paleoclimate archives to get an insight in the subpolar water mass transfer and the oceanographic and climatic development in the subarctic NW-Pacific.

This presentation will give an overview of the work done within KALMAR; specific research focuses are given in several other presentations during this meeting.

VARIABLE FLUIDS AND MANTLE SOURCES DOCUMENTED IN THE GEOCHEMISTRY OF KAMEN VOLCANO AND THE KLUCHEVSKAYA VOLCANIC GROUP

T. G. Churikova[1, 3], B.N. Gordeychik[2], G. Wörner[3], B. V. Ivanov[1]
[1]*Instinute of Volcanology and Seismology, FED, RAS, Petropavlovsk-Kamchatskii, Russia*
[2]*Institute of Experimental Mineralogy RAS, Chernogolovka, Russia*
[3]*GZG Abteilung Geochemie, Universität Göttingen, Germany*

Kamen volcano is located in centre of the Kluchevskaya Group of Volcanoes (KGV) surrounded by active Klyuchevskoy, Bezymianny and Ploskie Sopky (Ushkovsky and Krestoivsky) volcanoes. This group of Quaternary volcanoes is dominantly of basaltic to andesitic composition and overlies an older plateau of mostly basalt–basaltic andesite lavas.

Kamen and Bezymianny volcanoes form single geochemical trends on all petrochemical diagrams suggesting a common source. Lavas of the Ploskie Sopky, Kluchevskoy and Kamen/Bezymianny form distinct trends and also differ in mineral composition and thus probably originated from different primary magmas [Churikova et al., 2010]. All rocks of the Kamen volcano as well as lavas of the neighboring volcanoes (see Figure) have typical island-arc signatures with significant but different enrichment in LILE and LREE and low HFSE.

The concentrations of HFSE and HREE in water-rich fluid are negligible [Brenan et al., 1995], and their concentrations in the rocks are determined by mantle sources. Approximating curves, drawn through HFSE and HREE for plateau basalts, Kamen and Kluchevskoy stratovolcanoes show that trace element contents are systematically decreasing in this sequence with younger ages (see Figure).

The plateau lavas with eruptive centres below Ushkovsky volcano formed at about 270 ka [Calkins, 2004]. At that time the mantle wedge was close in composition to NMORB mantle and was not as depleted by previous magmatic events as for more recent lavas. The ratios of middle to heavy REE in plateau basalts and in NMORB mantle are close to unity. The High-K series rocks from Ploskie Sopky volcano were also derived from such magmas. With time the upper mantle under KGV became more and more depleted as result of voluminous eruptions of plateau basalts.

Kamen volcano, which ended it's activity in the Late Pleistocene [Melekestsev, Braitseva, 1984] has depleted HREE compared to NMORB and formed from a more depleted upper mantle. Nb, Ta and HREE in most magnesian basalts from Kamen volcano are lower than in NMORB, the ratios $HREE_{Kamen}/HREE_{NMORB}$ are about 0,7 (see Figure). It is important that most mafic rocks from Bezymianny volcano with MgO>5% have the same degree of depletion and in fact are similar to Kamen volcano lavas in other trace element characteristics as well, which testify to the same primary magmas for both volcanoes.

Holocene and historical lavas of the Klyuchevskoy and Krestovsky volcanoes were formed from an even more depleted mantle source, which is shown by lowest Nb, Ta and HREE. $HREE_{Kluch}/HREE_{NMORB}$ varies from 0,52 to 0,55. The rocks of the monogenetic cones from the western slope of Kamen volcano have the same characteristics. Thus, the same upper mantle source, which is tapped by magmas with the same degree of melting (10-12% [Churikova et al., 2001]) is systematically depleted with time.

It was shown by melt inclusion studies in olivines across the Kamchatka arc [Churikova et al., 2007], that the fluid composition gradually changes with increasing slab depth. The fluid that dominates at the arc front carries the highest amounts of B, Cl and chalcophile elements as well as LILE F, S and LREE. The fluids released below the Central Kamchatka Depression is more enriched in S and U and show highest S/K_2O and U/Th ratios. Additionally this fluid is enriched in ^{87}Sr and ^{18}O. A third, distinct back arc fluid is observed at the Sredinny Ridge and is enriched in F, Li Be, LILE and LREE.

Lavas from KGV volcanoes have largely different fluid signatures, owing to their location all three fluids are involved in it's magma genesis. (1) the B-rich for arc fluid, which was transported it maximum distance to this depth with the still relatively cold subducted slab, (2) The

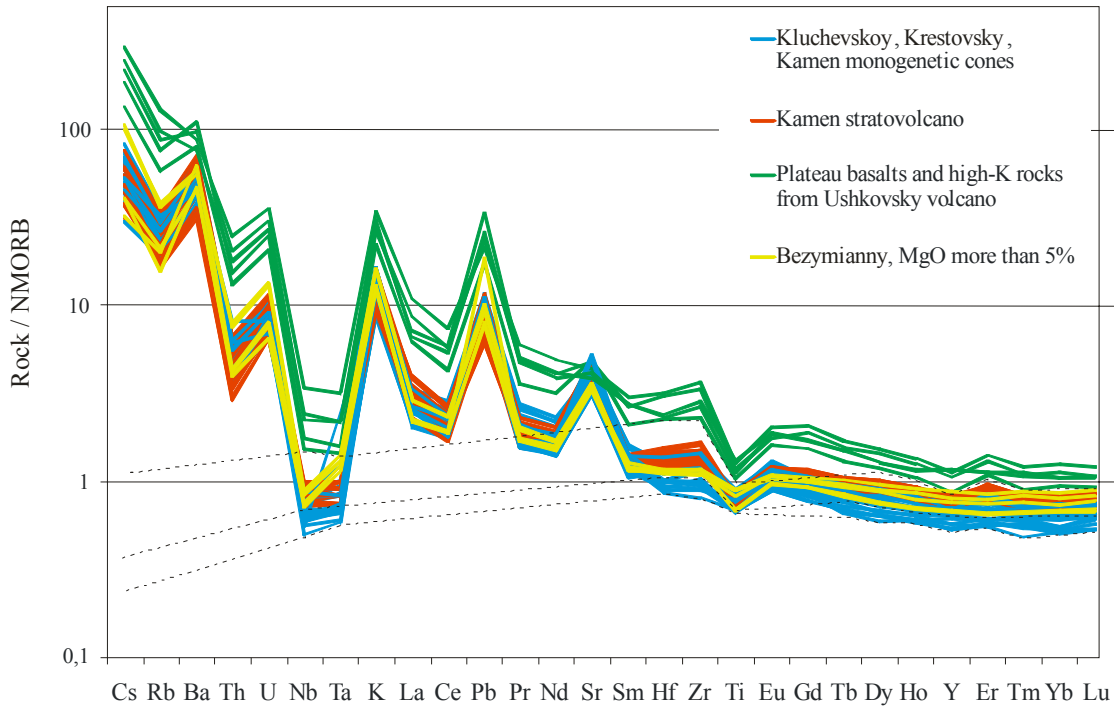
"central" fluid dominates below the KGV and (3) the influence of the back arc fluid just starts to be seen. The Cl/S ratio in Kamen melts is 2-3 times higher than in melts of Klyuchevskoy volcano. Kluchevskoy melts show good correlations of F/Yb with B/Yb, but not with Li/Yb, suggesting the influence of frontal and central fluids. Samples from Kamen volcano are enriched in all three ratios resulting in positive correlation between them and suggesting the influence of all three fluids. While Kluchevskoy volcano rocks are systematically enriched in U/Nb, Cs/Yb and Ce/Nb ratios, Kamen volcano lavas show enrichment in Li/Yb. These data imply that Kluchevskoy and Kamen volcanoes, which are situated nearby each other, show quite different fluid patterns.

Thus, trace and volatile elements distribution in rocks and melt inclusions KGV show that the fluid composition can be different even at neighboring volcanoes. The KGV appears to be a place where several fluids occur together, suggesting a large heterogeneity in the fluids that modified mantle.

Thus, the observed geochemical diversity of KGV rocks is the result of both gradual depletion with time of the mantle NMORB-type source due to the intense previous magmatic events in this area and by the addition of distinct fluids to this mantle source.

This research was supported by RFBR grant # 08-05-00600.

Brenan J.M. et al. // Geochim. Cosmochim. Acta, 1995, V 59, p. 3331-3350; *Calkins J.A.* // JKASP IV, 2004, p. 53-54; *Churikova T. et al.* // Contr. Miner. Petr., 2007, V 154, N 2, p. 217–239; *Churikova T. et al.* // EGU2010-12866-2; *Churikova T. et al.* // J. Petr., 2001, V 42, N 8, p. 1567-1593; *Melekestsev I.V, Braitseva O.A.* // Volc. Seism., 1984, V 4, p. 14-23; *Sun S., McDonough W.F.* // Spec. Publ. Vol. Geol. Soc. Lond., 1989, N 42, p. 313-345.



NMORB-normalized trace element patterns for KGV rocks. Dashed lines show the approximated patterns without the subduction component for three different in age volcanic suites. Only samples with MgO>5% are shown for Bezymianny volcano. N-MORB values are from Sun and McDonough (1989).

РАЗЛИЧНЫЕ ФЛЮИДНЫЕ И МАНТИЙНЫЕ ИСТОЧНИКИ ПО ГЕОХИМИИ ПОРОД ВУЛКАНА КАМЕНЬ И ВУЛКАНОВ КЛЮЧЕВСКОЙ ГРУППЫ

Т.Г. Чурикова[1, 3], Б.Н. Гордейчик[2], Г. Вёрнер[3], Б.В. Иванов[1]
[1]Институт вулканологии и сейсмологии ДВО РАН, Петропавловск-Камчатский, Россия
[2]Институт экспериментальной минералогии РАН, Черноголовка, Россия
[3]Центр геологических наук Гёттингенского университета, Гёттинген, Германия

Представлены геохимические исследования пород вулкана Камень, находящегося в центре Ключевской группы вулканов (КГВ), в окружении активных вулканов Ключевского, Безымянного и Плоских Сопок (Ушковский и Крестовский). Вся КГВ, в свою очередь, расположена на подстилающем базальтовом плато.

Вулканы Камень и Безымянный формируют единые тренды на всех петрохимических диаграммах, что указывает на их генетическое родство. Лавы вулканов Камень, Ключевской и Плоские Сопки формируют разнонаправленные тренды и различаются по составам породообразующих минералов, т.е. не обнаруживают прямой генетической связи [Churikova et al., 2010].

Все породы вулкана Камень, как и лавы соседних вулканов (см. рис.) имеют типичные островодужные признаки со значительным, но различным обогащением по LILE и LREE и низкими HFSE. В водном флюиде концентрации HFSE и HREE малы [Brenan et al., 1995], и их концентрации в породах определяются мантийным источником. Аппроксимирующие линии, проведенные через HFSE и HREE для пород платобазальтов, вулканов Камень и Ключевской, показывают, что содержания микроэлементов в этой последовательности закономерно понижаются с уменьшением возраста пород (см. рис.).

Породы платобазальтов, центр излияния которых находился под вулканом Ушковский, образовались около 270 тыс. л.н. [Calkins, 2004]. В то время мантийный клин, не обедненный выплавками вещества, представлял собой верхнюю мантию типа NMORB, поскольку отношения средних к тяжелым REE в породах плато и в NMORB близки к единице. Высококалиевая серия пород вулкана Плоские Сопки наследовала этот очаг мантийного источника. Вследствие объемных выплавок платобазальтов вещество верхней мантии под КГВ обеднялось.

Вулкан Камень, закончивший свою активность в позднем плейстоцене [Мелекесцев, Брайцева, 1984], сформировался на уже частично обедненном субстрате и имеет обедненную ветвь HREE. Отношения Nb, Ta и HREE в наиболее примитивных базальтах вулкана Камень к содержаниям этих элементов в NMORB составляет 0,7 (см. рис.). Важно отметить, что наиболее основные породы вулкана Безымянный с содержанием MgO>5% имеют аналогичную степень обеднения и фактически идентичны лавам вулкана Камень, что свидетельствует о едином очаге этих вулканов.

Породы голоценовых и исторических извержений вулканов Ключевской и Плоский Ближний были сформированы из еще более обедненного вещества мантии, о чем свидетельствуют наиболее низкие отношения Nb, Ta и HREE к содержаниям этих элементов в NMORB, опускающиеся до 0,52-0,55. К этой же категории относятся и породы моногенных конусов, расположенные на западном склоне вулкана Камень.

Таким образом, можно проследить, как единый мантийный источник, представляющий собой вещество верхней мантии с одинаковой степенью плавления (10-12% [Churikova et al., 2001]), систематически обедняясь с течением времени, создает магматические очаги с различной степенью обогащения.

При изучении расплавных включений в оливинах вкрест простирания Камчатской дуги [Churikova et al., 2007] было показано, что состав субдукционного флюида последовательно меняется с увеличением глубины погружения океанической плиты. На фронте дуги доминирует фронтальный флюид, в наивысшей степени обогащенный по B, Cl и халькофильным элементам, а также по LILE, F, S и LREE. Породы КГВ были доминированы центральным флюидом, обогащенным по S и U, с наивысшими S/K_2O и U/Th отношениями.

В дополнение этот флюид был необычно обогащен изотопами ^{87}Sr и ^{18}O. В Срединном хребте наблюдается задуговой флюид, сильно обогащенный как F, Li и Be, так и LILE и LREE. Положение КГВ таково, что в пределах этой группы вулканов в той или иной степени все три флюида участвуют в формировании пород – заканчивает свою работу фронтальный флюид, доминирует центральный флюид, и начинает влиять задуговой флюид. Так, Cl/S отношение в расплавах вулкана Камня в 2-3 раза выше, чем в расплавах Ключевского вулкана. В расплавах Ключевского вулкана наблюдается корреляция F/Yb и B/Yb отношений, но отсутствует корреляция с Li/Yb, что свидетельствует о влиянии фронтального и центрального флюидов. В расплавах же вулкана Камень наблюдается корреляция между всеми тремя отношениями, предполагая влияние всех трех флюидов. В то время, как породы Ключевского вулкана систематически обогащены по U/Nb, Cs/Yb и Ce/Nb отношениям, породы вулкана Камень обнаруживают более высокие Li/Yb значения. Все эти данные свидетельствуют о различном составе флюидной добавки в расплавы вулканов Камень и Ключевской.

Распределение редких и летучих элементов в породах и расплавных включениях КГВ показывает, что состав флюидной компоненты может быть различен даже на соседних вулканах. КГВ является местом, где несколько флюидов пересекаются и накладываются, образуя гетерогенность метасоматизированной флюидом мантии.

Таким образом, наблюдаемое геохимическое разнообразие пород в пределах КГВ обусловлено как постепенным обеднением мантийного источника типа NMORB ввиду больших мантийных выплавок в этом регионе, так и добавкой к мантийному источнику различных по составу флюидов.

Работа выполнена при поддержке гранта РФФИ № 08-05-00600.

Мелекесцев И.В., Брайцева О.А. // Вулк. Сейсм., 1984, № 4. с. 14-23; *Brenan et al.* // Geochim. Cosmochim. Acta, 1995, V 59, p. 3331-3350; *Calkins J.A.* // JKASP IV, 2004, p. 53-54; *Churikova T. et al.* // Contr. Miner. Petr., 2007, V 154, N 2, p. 217–239; *Churikova T. et al.* // EGU2010-12866-2; *Churikova T. et al.* // J. Petr., 2001, V 42, N 8, p. 1567-1593; *Sun S., McDonough W.F.* // Spec. Publ. Vol. Geol. Soc. Lond., 1989, N 42, p. 313-345.

ERUPTIVE HISTORY AND STRUCTURE OF YOTEI VOLCANO, SOUTHWESTERN HOKKAIDO, JAPAN

Shimpei Uesawa[1] and Mitsuhiro Nakagawa[1]
[1]Department of Natural History Sci., Graduate School of Sci., Hokkaido University.

Yotei Volcano is an active large stratovolcano located at Kril and NE Japan arc-arc junction. Although there are few pioneering geological and petrological studies of this volcano (e.g. Katsui, 1956; Kashiwabara et al., 1976), eruptive history and structure of this volcano are not revealed sufficiently. Generally, it is difficult to understand whole structure of stratovolcanoes with only geological study because of its few field occurrences. In order to reveal eruptive history and structure of Yotei Volcano, geological and petrological investigations were carried out on the Yotei Volcano and its surround area, and volcanic edifices were correlated with tephras using petrological method.

Around the foot of Yotei Volcano, 43 tephra units from Yotei Volcano interbedded in soil layers are identified (Y1 - Y43 in descending order), and four widespread tephras were also recognized. In addition, Kimobetsu pyroclastic flow deposits distributed in eastern area of Yotei Volcano and Shiribetsu-dake debris avalanche deposit distributed in southern foot of Yotei vlcano underlie Yotei tephras. Based on the thick volcanic ash soil layer indicating long dormancy among the tephra groups, Yotei tephras are distinguished into three groups: Yotei tephra group I, Yotei tephra group II and Yotei tephra group III. In particular, petrological characteristics of Yotei tephra group I is different from other groups. Yotei tephra group I is characterized in comprising porphyritic (phenocryst content = 47.2-5.8 wt. %) pumice containing hornblende and quartz whereas others are in comprising aphiric (phenocryst content = 14.5-0.3 wt. %) pumice and scoria with absence of hornblende and quartz. Additionally, Yotei tephra group II is distinct from Yotei tephra group III in whole-rock composition. Kimobetsu pyroclasitc flow deposits comprise porphyritic pumice containing hornblende and quartz and are distinct from Yotei tephras in Whole-rock composition. Moreover, nine ^{14}C ages are obtained from soils beneath Yotei tephra units (ca. 43 ka - 17.7 ka) and Fission-Track ages of pumices from Kimobetsu pyroclastic flow deposits are also obtained (ca. 50 ka) in this study. Thus, we can do chrolonogy of Yotei and Kimobetsu pyroclastic flow deposits. On the other hand, Yotei volcanic edifice can be distinguished into three groups: Yotei volcanic edifice I to III in ascending order on the basis of stratigraphic relations, degrees of preserved land forms and petrological characteristics. Additionally, Shiribetsu-dake volcanic edifices (including debris avalanche deposit) distributed in western area of Kimobetsu pyroclastic flow deposits are distinct from Yotei volcanic edifice in petrological characteristics (Fig. 1).

Based on the characteristics of whole-rock compositions, these Yotei volcanic edifice groups are conformed to Yotei tephra group I, Yotei tephra group II and Yotei tephra group III in ascending order, respectively. In addition, Kimobetsu pyroclastic flow deposits are conformed to Shiribetsu-dake volcanic edifices in whole-rock composition. As a result, Yotei Volcano can be divided into two volcanoes: Pre-Yotei Volcano and Yotei Volcano by long dormancy (>7,000). Moreover, Yotei Volcano consists of two stages separated by dormancy (~3,500) namely Early Yotei Volcano and Late Yotei Volcano. Based on the chronology of Yotei Volcano, Pre-Yotei Volcano started its activity at least from approximately 50 ka until ca. 40 ka, and Yotei volcano has been active from ca. 33 ka to present astride dormancy from ca. 17.5 ka to ca. 14 ka. Shiribetsu-dake also had been active around the same time as Pre-Yotei volcano or older period. Then, we can recognize that the activity of Yotei volcano has changed coupling with eruption rates, eruptive styles, and magma types, and that eruption rate of Early Yotei Volcano (1.5 km^3/ky) is anomaly value. These relationships indicate that magma systems beneath the volcano affect to growth process and eruptive stages of this volcano.

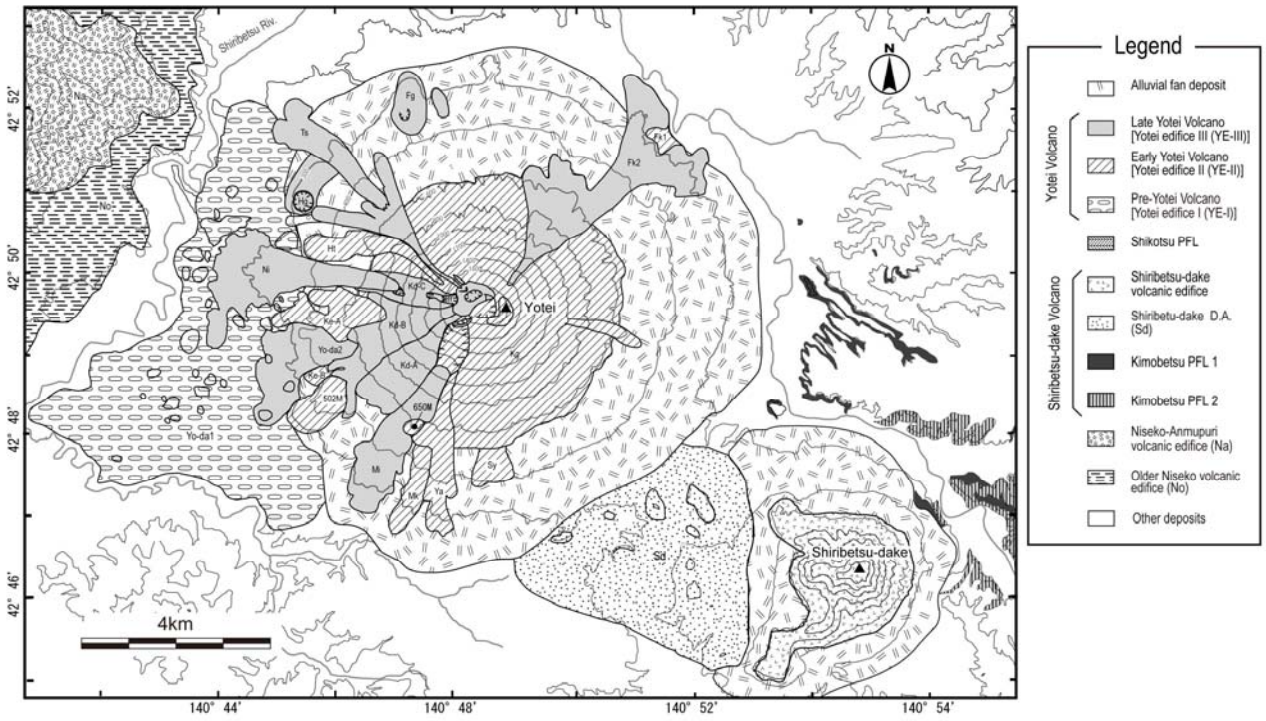


Fig. 1 Geological map of Yotei Volcano, Shiribetsu-dake Volcano and related pyroclastic flow deposits.

Impacts of powerful volcanic eruption of Sarychev Peak volcano (2009, Kuril Islands) on ecosystems

S.Yu.Grishin
Institute of Biology and Soil Science, FEB RAS, Vladivostok, Russia

Sarychev Peak volcano (Matua Island, Kurils) had erupted strongly in the middle of June 2009. As a result of the eruption the north-western half of the island turned into a volcanic desert. Field survey to analyze the damage and restore of ecosystems was held in the summer of 2010. Landscape changes were recorded also by satellite imagery.

By the beginning of the eruption the nature of the island was stayed in a phase of transition from the spring (the slopes of the volcano) to summer (foot of the volcano). During intense effusive-explosive eruption about 200 million m^3 of volcanic rocks were erupted, it were pyroclastic flow deposits mostly (estimation of volume of volcanic rocks was held together with O. Girina). The pyroclastic flows came down most intensively to the western (from the south-west to north-west) and north-eastern slopes of the volcano. Pyroclastic flow deposits have been introduced into the sea, creating a new land, protruding up to 400 m from the former shoreline. The area of thick pyroclastic deposits is about 15 km^2 (estimated from the ASTER TIR satellite images).

Pyroclastic flows are completely buried vegetation of the foothills of the volcano and pyroclastic surges charred and stripped trunks of alder, leaving on some slopes extensive tracts of dead thickets. Intense thermal and mechanical shock (repeated possibly), as well as chemical poisoning and partial burial of hot material, resulted in the death of alder thickets.

Lava flows poured out from the crater to the north-eastern and northern slopes. The north-eastern flow had finished their march at an altitude of about 220 m, and the northern flow stopped at an altitude of 430 m. The width of flows is about 100-150 m, length - about 2.1 and 2.4 km (horizontal projection), the area of effusions - 0.8 km^2. Lava buried vegetation on the slopes.

Ash fall of moderate intensity outside the cone was small: the thickness of sediment varies from 1-2 cm in the south-eastern outskirts of the island up to 3-5 cm on the flank of the volcano (altitude 600 m). Under these conditions, ash falls did not cause significant damage to vegetation. The bulk of the tephra, apparently, fell outside the island.

Lahars, born by the interaction of pyroclastic flows and vast snowfields, came down on the beds of streams. The largest of them was longer than 4 km, it passed through the gully stream by narrow (width about 50 meters), but a powerful flood, scraping off vegetation and soil along the sides of the bed. The lahar reached the runway in the south-east part of the island.

Restoration of vegetation to a state that was observed before the eruption, may take several decades on the slopes, covered by old lava flows and overlain by thin (up to a few decimeters) fresh unconsolidated sediments. The successions on new lava flows and thick pyroclastic deposits can take hundreds of years. However, it is hardly feasible in conditions of extremely high volcanic activity, since successions periodically interrupted by another eruption. Sparse vegetation at this stage of the volcano genesis appears to be can not be shaped into developed, mature vegetation.

Воздействие на экосистемы мощного извержения вулкана Пик Сарычева (2009 г., Курилы)

С.Ю.Гришин (Биолого-почвенный институт ДВО РАН, Владивосток)

В середине июня 2009 г. произошло очень сильное извержение активнейшего вулкана Курильских островов - Пик Сарычева (остров Матуа). В его результате северо-западная половина острова превратилась в вулканическую пустыню. Полевое обследование с целью анализа поражения и восстановления экосистем проведено летом 2010 г.; изменения ландшафтов фиксировались также по спутниковым снимкам.

К началу извержения природа острова находилась в фазе перехода от весны (склоны вулкана) к лету (подножия вулкана). В ходе мощного эффузивно-эксплозивного извержения которого было извергнуто около 200 млн. $м^3$ вулканитов, основную часть которых составили отложения пирокластических потоков (оценка объема вулканитов проведена совместно с О.А.Гириной). Наиболее интенсивно (по объему продуктов и длине прохождения) пирокластические потоки низвергались на западные (от юго-запада до северо-запада) и северо-восточные склоны вулкана. Отложения пирокластических потоков внедрились в море, образовав новую сушу, выступающую до 400 м от прежней береговой линии. Площадь мощных многометровых отложений составила около 15 $км^2$ (оценка по снимкам ASTER TIR).

Пирокластические потоки полностью погребли растительность подножий вулкана, а пирокластические волны обугливали и обдирали стволы ольховника, оставив на ряде склонов обширные массивы мертвых зарослей. Интенсивный (возможно неоднократный) термический и механический удар, а также химическое отравление и частичное погребение горячим материалом, привели к гибели заросли стланика.

Лавовые потоки излились из кратера на северо-восточный и северный склоны. Северо-восточный поток закончил свое продвижение на высоте около 220 м, а северный остановился на высоте 430 м. Ширина потоков около 100-150 м, длина – около 2.1 и 2.4 км (в горизонтальной проекции), площадь излияний – 0.8 $км^2$. Лава погребла растительность на склонах.

Пеплопад умеренной силы вне конуса был небольшим: мощность отложений от 1-2 см на юго-восточной окраине острова и до 3-5 см на склоне вулкана (высота 600 м). В этих условиях пеплопад не нанес существенного ущерба растительности. Основная масса тефры, по-видимому, выпала за пределами острова.

Лахары, рожденные взаимодействием пирокластических потоков и обширных снежников, сошли по склонам вулкана; крупнейший из них, длиной более 4 км, узким (ширина около 50 м), но мощным потоком прошел по распадку ручья, сметая грязевой массой стланиковую растительность по бортам русла и достиг своим конусом выноса взлетно-посадочной полосы в юго-восточной части острова.

Восстановление растительности до состояния, наблюдавшегося перед извержением, может занять нескольких десятков лет на склонах, сформированных старыми лавовыми потоками и перекрытых маломощными (доли метра) свежими рыхлыми отложениями. На новых лавовых потоках и многометровых отложениях пирокластических потоков сукцессия может длиться сотни лет. Однако это вряд ли реально в условиях крайне высокой вулканической активности, поскольку сукцессии периодически прерываются очередным извержением. Разреженная растительность на данном этапе развития вулкана, по-видимому, не сможет сформироваться в развитый, зрелый растительный покров.

Tephrostratigraphy and petrological study of Chikurachki and Fuss volcanoes, western Paramushir Island, northern Kurile Islands

Takeshi Hasegawa[a,*], Mitsuhiro Nakagawa[b], Mitsuhiro Yoshimoto[b], Yoshihiro Ishizuka[c], Wataru Hirose[d], Sho-ichi Seki[b], Vera Ponomareva[e] and Rybin Alexander[f]

[a] Ibaraki Univ., Japan, [b] Hokkaido Univ., Japan, [c] Geological Survey of Japan, [d] Geological Survey of Hokkaido, Japan, [e] IVS, Petropavlovsk-Kamchatsky, Russia, [f] IMGG, Yuzhno-Sakhalinsk, Russia

A tephrostratigraphic and petrological study of the Chikurachki (1,816 m)-Tatarinov-Lomonosov volcanic chain (CTL volcanic chain) and Fuss (1,772 m), located at the southern part of Paramushir Island in the northern Kurile Islands, was carried out to reveal the explosive eruption history during the Holocene and the temporal change of the magma systems of these active volcanoes. We described tephra successions at 54 sites and identified more than 20 major eruptive units consisting of pumice fall, scoria fall and ash fall deposits, each of which are separated by paleosol or peat layers. The source volcano of each recognized tephra layer is confirmed by correlation with proximal deposits of each eruption center with respect to petrography and whole-rock and glass chemistry. The age of each layer was determined by radiocarbon dating and the stratigraphic relationship with the dated, widespread tephra from Kamchatka according to the thickness of paleosol sandwiched between tephra layers. The Holocene activity in this region was initiated by eruptions from the Tatarinov and Lomonosov volcanoes. After the eruptions, the Fuss and Chikurachki volcanoes started their explosive activities at ca. 7.5 ka, soon after the deposition of widespread tephra from the Kurile Lake caldera in southern Kamchatka. Compared with Fuss located on the back-arc side, Chikurachki has frequent, repeated explosive and voluminous eruptions. Whole-rock compositions of the rocks of the CTL volcanic chain and Fuss are classified into medium-K and high-K groups, respectively. These suggest that magma systems beneath the CTL volcanic chain and Fuss differ from each other and have been independently constructed. The rocks of the Chikurachki volcano are basalt-basaltic andesite and have gradually changed their chemical compositions; when graphed as SiO_2-oxide diagram, these form smooth trends. This suggests that the magma system could evolve mainly by fractional crystallization. In contrast, matrix glass chemistries for Fuss pumices are distinct for each eruption and show different K_2O levels on a SiO_2-K_2O diagram. This implies that the magma system of Fuss has been frequently replaced. Both volcanoes have been active under the same subduction system. However, the Chikurachki volcano would continue eruptive activity under a stable magma system with a higher magma discharge rate, whereas Fuss may continue construction with an intermittent supply of distinct, small magma batches.

Human Responses to Prehistoric Earthquakes and Seismic Uplift on the Northeast coast of Kamchatka

Dustin Keeler

The Kamchatsky Peninsulaon the Northeastern Coast of Kamchatka was a very seismically active area in prehistory. The earthquakes caused significant land uplift that shifted the shorelines at various periods during the past 6000 years. During the 2009, 2010, and 2011 field seasons a survey for new archaeological sites was conducted along the paleoshorelines and the present coast. The sites were relatively dated in the field using known volcanic tephra layers. This paper will present the results of a regional settlement pattern analysis that examines the responses of the human inhabitants of this region to the seismic uplift and subsequent shoreline shifts in prehistory.

Main stages of formation of structure "non-volcanic" islands of the Aleutian island arc in the Pleistocene

Bulochnikova A.S.

Moscow State University, Moscow

Aleutian island arc is special, special position in the island arcs of the Pacific Ocean. The story of her research has for several centuries, but until now the degree of scrutiny of this area can be called a very weak, and the problems in the dynamics and history of the Aleutian arc are the most controversial in science. Aleutian island arc is a single submarine base, broken into several large blocks, each of which is complicated by a group of islands. Formation of all elements of the island arc occurred in the conditions of activation of tectonic, seismic, volcanic processes. However difference in these processes in time and space led to the development of that history, geology, structure, dynamics and modern topography of these islands are different. In science, there is still the problem of reconstructing the history of the territories in which the formation of a leading role is played by a set of endogenous processes. Traditionally, to identify the role of tectonics, volcanism, seismic activity in geomorphological studies used data obtained by experts related sciences (geology, geophysics, etc.). In this case, the relief of any territory are reflected even the slightest manifestation of endogenous processes. This article presents the results of a study whose purpose was to develop and test methods restore the history of this territory on the basis of geomorphological analysis.

From the concept of V. Penka [2], we know that at equal rates of uplift and denudation, the slope characterizes the slope of the velocity structure, provided that the structure rises evenly. Thus, knowing the average slope (ie the ratio of excess to half the width of the block), block slopes, if we take the slopes of the lines were determined relative rates of movement for each of the selected blocks. The duration of uplift determined by the height and speed of lifting. Such studies, though not yet have wide distribution in geomorphology, but the results of some of them have already been published [1]. Was solved a new problem - the transition from relative to absolute morfotektonic parameters, ie translation relative to an absolute time scale. This requires a time frame, as that was selected coastline. It's age was taken out of the dating of sediments foot marine terrace. Knowing the height and time determined by the rate of uplift of the reference block. To restore the spatial-temporal chain of events, we calculated the height of each block to the stratigraphic boundaries highlighted. The result has been formulated scheme of successive stages of uplift for the 36 islands of the Aleutian arc, not having in the territory of the volcanic apparatus.

Boundary of the early and middle Pleistocene taken to separate the new phase of development of the northwestern Pacific. In the early Pleistocene, most areas experienced a significant dip, accompanied by attenuation of volcanic rejuvenation of fault zones of the north-western and north-eastern directions. The only exception is the northern part of Bering Island, where there are basaltic outpourings early Pleistocene. At this time there is a low standing sea-level, cold climate.

The latest stage of development, which lasted throughout the Middle Pleistocene-Holocene, is decisive in shaping contemporary topography of the region. In the early Middle Pleistocene are activated upstream of tectonic movements along faults, prepared at the previous stage of development. On Bering Island, Mednij and Unalaska at that time begin to rise the first structures. This, above all, the blocks south of Bering Island, some areas of the Bering Sea coast of Menij, as well as the central part of Unalaska. The sea level at that time was close to the modern, so there were a few isolated areas of the island land. In the southern part of the modern Bering Island, to our knowledge, there has been a structure similar to the graben. It consists of two wings, divided into two sub-vertical faults. Each wing consists of a step width of 8-9 km, the height of the ledge about 40 meters south wing structures raised with respect to the northern 55 m, its maximum height is 102.8 m. In the northern part of Bering Island at this time there was an area of land,

currently time occupied lakes Ladyginskoe, Shenginskoe, Havanskoe, etc. In this area in the late Pliocene is an active outpouring of basalt, which led to the formation of separate arrays of type canteens, pork mountains. In present-day island of copper in the early Middle Pleistocene, there are several arrays raised to 90 m above sea level.

In the mid-Pleistocene active uplift islands continues. It includes several large islands of Andreanof group (Tanaga, Kanaga, Adak).Within the group of Commander Islands obosablivayutsya several separate sites. In the southern part of Bering Island begins actively raised portion that connects the two isolated array, as described above. For this area is characterized by high (3 mm / year) the rate of uplift, during the period he reached the mark of 70 m. In addition, in the north obosablivaetsya landmass to the north of the previously mentioned section of Pliocene effusions. It is worth noting that the boundaries of the rising blocks coincide with lithologic boundaries distribution of Paleogene sediments. Thus, the older sediments, composing the block, the sooner he began to rise. This trend is typical of other parts of the Commander's islands of the archipelago, which is probably indicative of heredity uplift. Mednij island is presented as well as at the previous stage, in the form of three isolated islands, but their height and area increased. Unalaska Island at this time is a single land mass, the outlines of which are already close to the modern.

In the second half of the Middle Pleistocene active uplift has affected all the major islands of the arc. At this time, are beginning to rise Attu, Kiska, Amlya, Kagalaska, Atka, Akutan, Akun and Tigalda. Lifting speed of these islands are different, but their structure quickly formed. Thus, by the end of the Pleistocene from the sea level beyond the structure of almost all the major islands of the arc.

History of the Late Pleistocene is closely linked to changes in sea level and global epochs of glaciation. In terms of morphostructural Islands, the following changes. In the early Late Pleistocene start up the structure of small islands. This, above all, a few islands in the east of the island group and Andreanof Rats Agathe and Delarovsky island. Ending the era of revitalization around 40,000 years ago, it was to this point, according to the calculations, all the modern Aleutian island arc somehow seemed above sea level. In Holocene uplift islands and separate units has continued.

1. Kravchynovskaya EA Determining the relative age of the movement of crustal blocks morfotektoniki methods (for example, Bering Island) / / Vestnik MGU. 2008. Ser.geogr., № 4
2. Penk W. Morphology, MA: Gos.izdat.geogr.lit-ry, 1961

Основные этапы формирования структуры «невулканических» островов Алеутской островной дуги в плейстоцене

Булочникова А.С.

МГУ им. М.В. Ломоносова, г.Москва

Алеутская островная дуга занимает особенное, принципиальное положение в системе островных дуг Тихого океана. История ее исследования насчитывает несколько веков, однако до сих пор степень изученности этой территории можно назвать крайне слабой, а вопросы динамики и истории развития Алеутской дуги являются наиболее спорными в науке. Алеутская островная дуга представляет собой единое подводное основание, разбитое на несколько крупных блоков, каждый из которых осложнен группой островов. Формирование всех элементов островной дуги происходило в условиях активизации тектонических, сейсмических, вулканических процессов. Однако дифференциация этих процессов в пространстве и времени привела к тому, что история развития, геология, структура, современная динамика и рельеф этих островов различны. В науке до сих пор существует проблема восстановления истории развития территорий, в формировании которых ведущую роль играет комплекс эндогенных процессов. Традиционно для выявления роли тектоники, вулканизма, сейсмической активности в геоморфологических исследованиях используются данные, полученных специалистами смежных наук (геологами, геофизиками и др.). При этом в рельефе любой территории находят отражение даже самые незначительные проявления эндогенных процессов. В данной статье представлены результаты исследования, целью которого была разработка и апробирование методики восстановления истории развития такой территории на базе геоморфологического анализа.

Из концепции В.Пенка [2] известно, что при равных темпах поднятия и денудации, уклон склона характеризует скорость движения структуры, при условии, что структура поднимается равномерно. Таким образом, зная средний уклон (т.е. отношение превышения к половине ширины блока) склонов блока, если принять склоны прямыми, были определены относительные темпы движения для каждого из выделенных блоков. Длительность поднятия определяется высотой и скоростью поднятия. Подобные исследования хоть и не имеют пока широкого распространения в геоморфологии, но результаты некоторых из них уже опубликованы [1]. Была решена новая задача – переход от относительных к абсолютным морфотектоническим параметрам, т.е. перевод относительной шкалы времени в абсолютную. Для этого необходим временной репер, в качестве которого была выбрана береговая линия. Ее возраст был взят из датировки отложений подошвы морской террасы. Зная высоту и время, определяем скорость поднятия эталонного блока. Для восстановления пространственно-временной цепочки событий были рассчитаны высоты каждого из блоков для границы стратиграфических выделов. В результате была составлена схема последовательных этапов поднятия для 36 островов Алеутской дуги, не имеющих на территории вулканических аппаратов.

Границей раннего и среднего плейстоцена принято отделять новейший этап развития всей северо-западной части Тихого океана. В раннем плейстоцене большинство районов испытало значительное погружение, сопровождавшееся затуханием вулканизма, омоложением разломных зон северо-западного и северо-восточного направлений. Исключением является лишь северная часть острова Беринга, где отмечаются базальтовые излияния начала плейстоцена. В это время отмечается низкое стояние уровня моря, похолодание климата.

Новейший этап развития, который продлился в течение среднего плейстоцена-голоцена, является определяющим в формировании облика современного рельефа региона. В начале среднего плейстоцена происходит активизация восходящих тектонических движений

по разломам, подготовленным на предыдущем этапе развития. На островах Беринга, Медный и Уналашка в это время начинают подниматься первые структуры. Это, прежде всего, блоки южной части острова Беринга, некоторые участки беринговоморского побережья острова Медный, а так же центральные массивы Уналашки. Уровень моря в это время был близок к современному, поэтому существовали несколько изолированных участков островной суши. В южной части современного острова Беринга, по нашим данным, наметилась структура, похожая на грабен. Она состоит из двух крыльев, разбитых на две части субвертикальными разломами. Каждое крыло состоит из ступени шириной 8-9 км, высота уступа около 40 м. Южное крыло структуры поднято относительно северного на 55 м, его максимальная высота составляет 102,8 м. В северной части острова Беринга в это время существовал участок суши, в настоящее время занятый озерами Ладыгинское, Шенгинское, Гаванское и др. На этой территории в конце плиоцена происходило активное излияние базальтов, что привело к формированию отдельных массивов типа Столовых, Свиных гор. На территории современного острова Медный в начале среднего плейстоцена существует несколько массивов, поднятых на 90 м над уровнем моря.

В середине среднего плейстоцена активное поднятие островов продолжается. В него включены уже несколько крупных островов из Андреяновской группы (Танага, Канага, Адак). В пределах группы Командорских островов обосабливаются несколько отдельных участков. В южной части острова Беринга начинает активно подниматься участок, соединяющий два изолированных массива, описанных выше. Для этого района характерна высокая (3 мм/ год) скорость поднятия, за рассматриваемый период он достиг отметки 70 м. Кроме того, на севере острова обосабливается массив суши к северу от ранее упоминавшегося участка плиоценовых излияний. Стоит отметить, что границы поднимающихся блоков совпадают с литологическими границами распространения палеогеновых отложений. Таким образом, чем древнее отложения, слагающие блок, тем раньше он начал подниматься. Такая тенденция характерна и для других частей островов Командорского архипелага, что, вероятно, свидетельствует об унаследованности поднятия. На острове Медный суша представлена так же, как и на предыдущем этапе, в виде трех изолированных островков, однако их высота и площадь увеличились. Остров Уналашка в это время представляет собой единый массив суши, очертания которого уже близки к современным.

Во второй половине среднего плейстоцена активное поднятие затронуло уже все крупные острова дуги. В это время начинают активно подниматься Атту, Киска, Амля, Кагаласка, Атка, Акутан, Акун и Тигалда. Скорости поднятия этих островов различны, но их структуры быстро формируются. Таким образом, к концу среднего плейстоцена из под уровня моря выходят структуры почти всех крупных островов дуги.

История позднего плейстоцена тесно связана с изменением уровня океана и глобальными эпохами оледенения. В морфоструктурном плане островов происходят следующие изменения. В начале позднего плейстоцена начинают подниматься структуры малых островов. Это, прежде всего, несколько островов на востоке Андреяновской группы и острова Крысий, Агату и Деларовский острова. Заканчивается эпоха активизации около 40000 лет назад, именно к этому рубежу, по данным расчетов, все современные острова Алеутской дуги так или иначе показались над уровнем моря. В голоцене поднятие островов и отдельных блоков продолжалось.

1. Кравчуновская Е.А. Определение относительного возраста движения блоков земной коры методами морфотектоники (на примере острова Беринга)// Вестник МГУ. 2008. Сер.геогр., №4
2. Пенк В. Морфологически анализ, М.:Гос.издат.геогр.лит-ры, 1961

Special features of the distal tephra interlayer forming on the bottom of the marine deep basin (the catastrophic explosion of the Baegdusan Volcano as an example)

I.V. Utkin

Pacific Oceanological Institute of FEB RAS, Vladivostok

Although the recent volcanism is of the greatest abundance in Kamchatka, Kuriles and in Japan (within the Asian East), other far-eastern regions have been in existence (and even being in immediate proximity to Russian borders), where the volcanic activity has been shown during historical time by catastrophic explosions and where the renewal of the volcanic activity is of the great probability. The south of the Far East concerns such regions, and in its limits, the Chanbaishan volcanic center stands out (with the Baegdusan Volcano).

The last catastrophic explosion has occurred here (in two stages) about one thousand years ago. Its age is estimated as 934-969 AD [Machida et al., 1981, 1983] though there are sources that transfer it for XII century [Guo et al., 2002]. Such tephra quantity has been thrown out, that it could not only cover the whole central part of the Japan Sea (with the forming of the interlayer with several cm thickness), but also could reach the Japanese archipelago and even southern Kuriles [Nakagawa, Ohba, 2003]. By the procedure accepted in Japan (it also has received the international recognition), this interlayer has given the name Tomakomai (Baegdusan-Tomakomai, B-Tm) according to the place of its first land find.

The disasterness of explosions (with their destructive influence on environments, ecological conditions and the human vital activity) demands the knowledge of the possible spatial distribution of harmful products, that is impossible without studying of the concrete eruptional properties which have left their traces in the form of interlayers.

As for the generation of last ones, only meteorological (for the air environment) and oceanographical (for the water column) conditions are responsible for this process, and they, in turn, can be reconstructed, if the spatial variability of the grain-size spectrum for the concrete interlayer is studied [Utkin, 2002]. It is known, that this spectrum sensitively reacts even to small changes of parameters for water (or air) transportation environments and for bottom relief features, but thus it is necessary to consider, that this grain-size spectrum is not uniform, and consists of separate components (dynamic populations, DP) with particles differed from each other not only on genesis, but also on physical ways of their transport and deposition (transferring in suspensions, disturbing by the wave saltation, transporting by the air, crushing at explosions). Especially many DP the water environment gives, though and in the air environment it is never observed the uniformity in the particle sedimentation [Legros, 2000]

The considered interlayer (B-Tm) is unique on the grain-size levels of studiness (325 detailed analyses on 184 stations); therefore, it ideally approaches for paleo-researches.

The author of the offered work has applied (for splitting of the whole spectrum curve into dynamic populations) the physically proved model of SFT - distribution (model of fractionation and selective transportation) which have been developed by Brown & Wohletz [1995]. This model does not demand the preliminary set of its properties. In total, it was allocated five DP with modes at

1.52, 3.83, 5.60, 7.00 and 8.76 phi units (350, 70, 20, 8 and 2 microns). For each population, the complicated spatial structure has become known. It reflects both the vorticose character of the water circulation (it is noted about ten sites of particle focuses) and bottom relief features (ash particles on rises, slopes and shelves has not been sedimented). Reflexion of properties of the air environment during the explosive event gives the general orientation of the interlayer from the southwest to the northeast in the form of the bent arch (the convex part is thus turned to the southeast), as though bending around the atmospheric cyclone location on the continent.

The interlayer material is presented by fine-dispersed trachydacitic glass of silty size [Sakhno, Utkin, 2009]. Particles >0.05 mm do not exceed 2 %. The maximum size of grains is of 0.7 mm. Pelitic contents do not exceed 35 %. A prevailing texture of particles is fluid-fibrous. In the Central Basin, tephra is almost without impurities; closer to margins there are impurities of clay and siliceous substances, and at slope feet - sandy fragmental particles. In boundaries of asedimentogenic areas (the outer shelves, tops of rises, higher slopes) the interlayer is absent. On other part of the area, the interlayer thickness is great along the axis of the greatest distribution (in the middle of the Central Basin) and at feet of slopes (of mainlands and rises). In the Japan Sea area, the interlayer occupies about 0.3 mln. km^3. The total amount of the friable tephra, supplied there, has made approximately 5.0 km^3, or 2.8 km^3 in recalculation on the solid material, at total amount of friable deposits on the mainland in 96 km^3 (with the recalculation on magma volume - 24 km^3) [Horn, Schminke, 2000; Utkin, 1989].

References

Brown W.K., Wohletz K.H. A derivation of the Weibull distribution based on physical principles and its connection to the Rosin-Rammler and the lognormal distributions // Journal of Applied Physics. 1995. Vol.78, No. 4 P. 2758-2763.

Guo Z., Liu J., Sui S., et al. The mass estimation of volatile emission during 1199-1200 AD eruption of Baitoushan volcano and its significance // Science in China, Ser.D. 2002. Vol. 45. P. 530-539.

Horn S., H.-U. Schmincke H.-U. Volatile emission during the eruption of Baitoushan Volcano (China/North Korea) ca. 969 AD // Bull Volcanol. 2000. Vol. 61. P. 537-555.

Legros F. Minimum volume of a tephra fallout deposit estimated from a single isopach // J. Volcanol. Geotherm. Res. 2000. Vol.96. P.25-32.

Machida H., Arai F. Extensive ash falls in and around the Sea of Japan. // J. Volcanol. Geotherm. Res. 1983. Vol. 18. P. 151–164.

Machida H., Arai F., Moriwaki H. Volcanic ashes transported across the Sea of Japan // Kagaku. 1981. Vol.51, No.9. P.562-569.

Nakagawa M., Ohba T. Minerals in volcanic ash. 1: Primary minerals and glass // Global Environmental Research. 2003. Vol. 6, No. 2. P. 41-51.

Sakhno V.G., Utkin I.V. Correlation of ashes of the Japan Sea bottom and tephra of the Changbaishan Volcano explosive eruptions in Late Pleistocene - Holocene // Doklady Earth Sciences. 2009. Vol. 429, No. 8. P. 1249–1255.

Utkin I.V. The accumulation and the burial of pyroclastics on the marine bottom (Japan Sea deep basins as an example) // Perioceanic sedimentogenesis. Vladivostok: Dalnauka, 1989. P. 67-79 (in Russian).

Utkin I.V. The computer statistical data processing on grain-size features of marine bottom sediments for the characterization of recent sedimentary environments // Conditions of the generation of bottom sediments and related mineral deposits within marginal seas. Vladivostok: Dalnauka, 2002. P. 96-113 (in Russian).

Особенности формирования прослоя дистальной тефры на дне морской глубоководной котловины (на примере катастрофического извержения вулкана Пектусан)

И.В. Уткин

Тихоокеанский океанологический институт ДВО РАН, Владивосток

Хотя современный вулканизм на территории Востока Азии наиболее активно проявлен на Камчатке, Курильских островах и в Японии, существуют и другие районы Дальнего Востока (и даже очень близкие к границам России), где вулканическая активность проявлена в историческое время катастрофическими извержениями и велика вероятность возобновления вулканической активности. К таким регионам относится юг Дальнего Востока, в пределах которого выделяется вулканический центр Чанбайшань с вулканом Байтоушань (Пектусан, Baegdusan).

Последняя катастрофическая эксплозия произошла здесь (в две стадии) примерно тысячу лет назад. Ее возраст оценивается как 934-969 AD [Machida et al., 1981, 1983], хотя есть источники, которые переносят его на XII век [Guo et al., 2002]. Было выброшено такое количество тефры, которое смогло не только покрыть всю центральную часть акватории Японского моря (с образованием на морском дне прослоя мощностью несколько см), но и достичь Японского архипелага и даже южных Курил [Nakagawa, Ohba, 2003]. По принятой в Японии методике, получившей и международное признание, прослой получил название Томакомаи (Baegdusan-Tomakomai, B-Tm) по месту первой сухопутной находки.

Катастрофичность эксплозий и их деструктивное влияние на окружающую среду, экологическую обстановку и жизнедеятельность человека требуют знаний о возможном пространственном распространении вредных продуктов их деятельности, что невозможно без изучения свойств конкретных извержений, оставивших свой след в виде прослоев.

Что же касается формирования последних, то за этот процесс ответственны только погодные (для воздушной среды) и океанографические (для водной толщи) условия, а они, в свою очередь, могут быть воссозданы, если известна пространственная изменчивость гранулометрического спектра конкретного прослоя [Уткин, 2002]. Известно, что гранспектр чувствительно реагирует даже на мелкие изменения океанографических параметров водной (или, при воздушном переносе, воздушной) среды и особенностей рельефа местности, но при этом надо учитывать, что гранулометрический спектр (отражающий свойства среды) не един, а состоит из отдельных компонентов (динамических популяций, ДП), частицы каждого из которых отличаются друг от друга не только по генезису, но и по физическому способу их попадания в осадок (перенесение во взвеси, взмучивание волновой сальтацией, воздушный перенос, дробление при эксплозиях). Особенно много ДП дает водная среда, хотя и в воздушной среде никогда не наблюдается однородности в осаждении частиц спектра [Legros, 2000].

Изучаемый прослой (B-Tm) уникален по своей гранулометрической изученности (325 подробных анализов на 184 точках), поэтому идеально подходит для палео-исследований.

Автор предлагаемой работы применил для разбиения спектра на динамические популяции физически обоснованную модель SFT- распределения (дробления и селекции), которое разработали Brown & Wohletz [1995]. Модель не требует предварительного задания своих свойств. Всего выделилось пять ДП с модами в 1.52, 3.83, 5.60, 7.00 и 8.76 phi (350, 70, 20, 8 и 2 мкм). Для каждой популяции выявилась сложная пространственная структура, отражающая как вихреобразный характер циркуляции водной массы (отмечено около десятка участков концентрирования частиц), так и особенности донного рельефа (частицы пепла на возвышенностях, склонах и шельфах не осаждались). Отражением свойств воздушной среды во время события является общая направленность прослоя с юго-запада на северо-восток в виде изогнутой дуги (выпуклая часть при этом обращена к юго-востоку).

Материал прослоя представлен тонкодисперсным стеклом трахидацитового состава мелкоалевритовой размерности [Сахно, Уткин, 2009]. Более крупные частицы не превышают 2%. Максимальный размер зерен 0.7 мм. Содержание пелита не превышает 35%. Преобладающая текстура частиц - флюидально-волокнистая. В Центральной котловине тефра почти лишена примесей, ближе к ее окраинам появляется примесь глинистого и кремнистого вещества, а у подножий склонов - песчаные обломочные частицы. В пределах аседиментогенных областей (внешний шельф, вершины возвышенностей) прослой отсутствует. На остальной части территории мощность прослоя велика вдоль оси наибольшего распространения (по середине Центральной котловины) и у подножий склонов (материка и возвышенностей).В Японском море прослой занимает примерно 0.3 млн. км^3. Общий объем рыхлой тефры, поступивший туда, составил примерно 5.0 км^3, или 2.8 км^3 в пересчете на твердый материал, при общем объеме рыхлых отложений на суше 96 км^3 и пересчете на магму - 24 км^3 [Horn, Schminke, 2000; Уткин, 1989].

Литература

Brown W.K., Wohletz K.H. A derivation of the Weibull distribution based on physical principles and its connection to the Rosin-Rammler and the lognormal distributions // Journal of Applied Physics. 1995. Vol.78, No. 4 P. 2758-2763.

Guo Z., Liu J., Sui S., et al. The mass estimation of volatile emission during 1199-1200 AD eruption of Baitoushan volcano and its significance // Science in China, Ser.D. 2002. Vol. 45. P. 530-539.

Horn S.,´ H.-U. Schmincke H.-U. Volatile emission during the eruption of Baitoushan Volcano (China/North Korea) ca. 969 AD // Bull Volcanol. 2000. Vol. 61. P. 537-555.

Legros F. Minimum volume of a tephra fallout deposit estimated from a single isopach // J. Volcanol. Geotherm. Res. 2000. Vol.96. P.25-32.

Machida H., Arai F. Extensive ash falls in and around the Sea of Japan. // J. Volcanol. Geotherm. Res. 1983. Vol. 18. P. 151–164.

Machida H., Arai F., Moriwaki H. Volcanic ashes transported across the Sea of Japan // Kagaku. 1981. Vol.51, No.9. P.562-569.

Nakagawa M., Ohba T. Minerals in volcanic ash. 1: Primary minerals and glass // Global Environmental Research. 2003. Vol. 6, No. 2. P. 41-51.

Сахно В.Г., Уткин И.В. Пеплы вулкана Чанбайшань в осадках Японского моря: идентификация по микро- и редкоземельным элементам и определения возраста их извержений // ДАН. 2009. Т.428, №5. С. 641-647.

Уткин И.В. Седиментация и захоронение пирокластики на дне (на примере глубоководных котловин Японского моря) // Периокеанический седиментогенез. Владивосток: Дальнаука, 1989. С. 67-79.

Уткин И.В. Компьютерная статистическая обработка данных по гранулометрии морских донных осадков для характеристики обстановок современного осадкообразования // Условия образования донных осадков и связанных с ними полезных ископаемых в окраинных морях. Владивосток: Дальнаука, 2002. С. 96-113.

Multiscale studies of Subduction zones based on seismic tomography

Ivan Koulakov
Institute of Petroleum Geology and Geophysics, SBRAS, Novosibirsk
Email: KoulakovIY@ipgg.nsc.ru

In the talk I present an overview of main our results on studying deep structure beneath subduction zones using various tomographic schemes. Shape of subducting slab is studied with the use of regional tomographic scheme which is based on global seismological datasets, mainly on the ISC catalogue. As an example of regional study, I present the model of P and S velocity anomalies in the mantle beneath the Kurile-Kamchatka and Aleutian arcs (Koulakov et al., 2011a). These results show that the slab beneath the Kurile-Kamchatka ark varies its thickness and dipping angle (Figure 1). Beneath the southern Kuriles, the slab appears to be coupled and it can indicate to the eastward shift of the Subduction location. In addition, tomographic images of slabs beneath Sunda, Isu-Bonin and Marianna subduction zones are shown in the talk.

Structure of the upper part of the subduction complexes (down to ~100 depth and with the lateral size of first hundreds km) is studied based on local seismicity data recorded by local seismic stations. In the talk I shortly discuss the tomographic results corresponding to different subduction zones, such as:

1. Central Java, Merapi volcano (Koulakov et al., 2009a, Figure 2A). Based on anisotropic version of the local earthquake tomography code we revealed the paths of fluid and melt migration from the lab up to the volcanic arc. In the area of the Merapi volcano we found a low-velocity anomaly, unprecedented on its size and intensity, which apparently contains the material feeding the volcanoes of Central Java.
2. Toba Caldera, Sumatra (Koulakov et al., 2009b, Figure 2B). The obtained seismic model clearly reveals the locations of magma chambers beneath the active volcanoes of the arc. Vertical low-velocity anomaly links the seismicity cluster at 100 depth with the Toba Caldera.
3. Costa-Rica, Nicaragua (Rabbel et al., 2011). Based on results of anisotropic tomography we can propose the possibility of trench-parallel flow in the mantle wedge which is also supported by geochemical observations.
4. Central Andes. In tomography results we can clearly observe low-velocities beneath the volcanic arc which appear to be linked with two seismicity clusters in the slab at 100 and 200 km depth.

To illustrate small-scale tomographic studies of subduction zones, Ipresent one example with results of studying the accretion wedge structure at the Chilean margin along the marine DSS profile (Koulakov et al., 2011b). In the tomographic images, we can clearly see a low-velocity layer which marks the subduction channel composed of strongly fractured rocks with high water content.

References:

Koulakov I., T. Yudistira, B.-G. Luehr, and Wandono, 2009, *P*, *S* velocity and *VP*/*VS* ratio beneath the Toba caldera complex (Northern Sumatra) from local earthquake tomography, *Geophys. J. Int.*, 177, p. 1121-1139

Koulakov, I., A. Jakovlev, and B. G. Luehr (2009), Anisotropic structure beneath central Java from local earthquake tomography, Geochem. Geophys. Geosyst., 10, Q02011

KoulakovI.Yu., N.L. Dobretsov, N.A. Bushenkova , A.V. Yakovlev, (2011a). Slab shape in subduction zones beneath the Kurile–Kamchatka and Aleutian arcsbased on regional tomography results, Russian Geology and Geophysics 52, 650–667

Koulakov I., H.Kopp, and T. Stupina, (2011b), Finding a realistic velocity distribution based on iterating forward modeling and tomographic inversion, G.J.Int., 186, 349–358.

Rabbel, W., I. Koulakov, A. N. Dinc, and A. Jakovlev (2011), Arc-parallel shear deformation and escape flow in the mantle wedge of the Central America subduction zone: Evidence from P wave anisotropy, Geochem. Geophys. Geosyst., 12, Q05S31

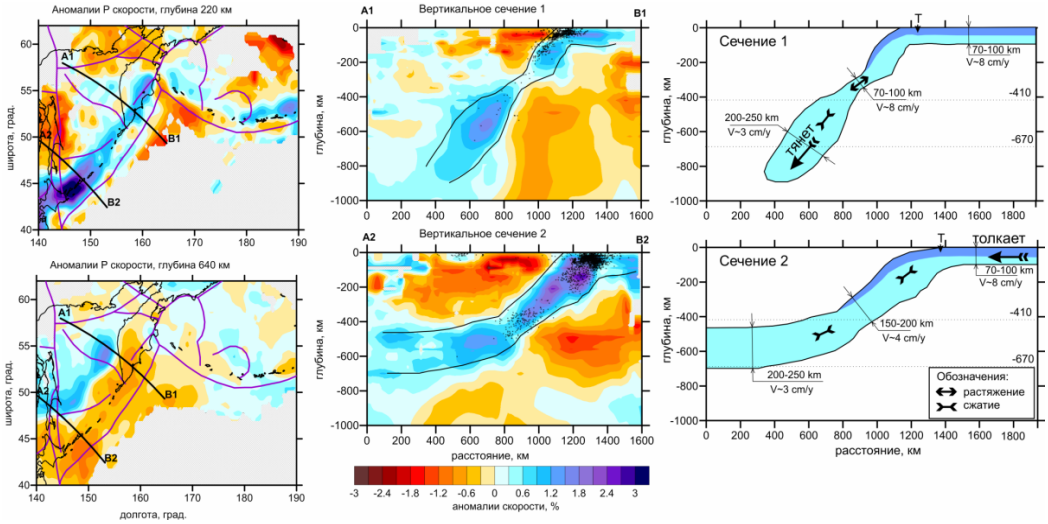


Figure1. Result of regional inversion for the Kurile-Kamchatka arc in horizontal and vertical sections (left and central columns). Right column depict force balance sin corresponding sections according to our interpretation.

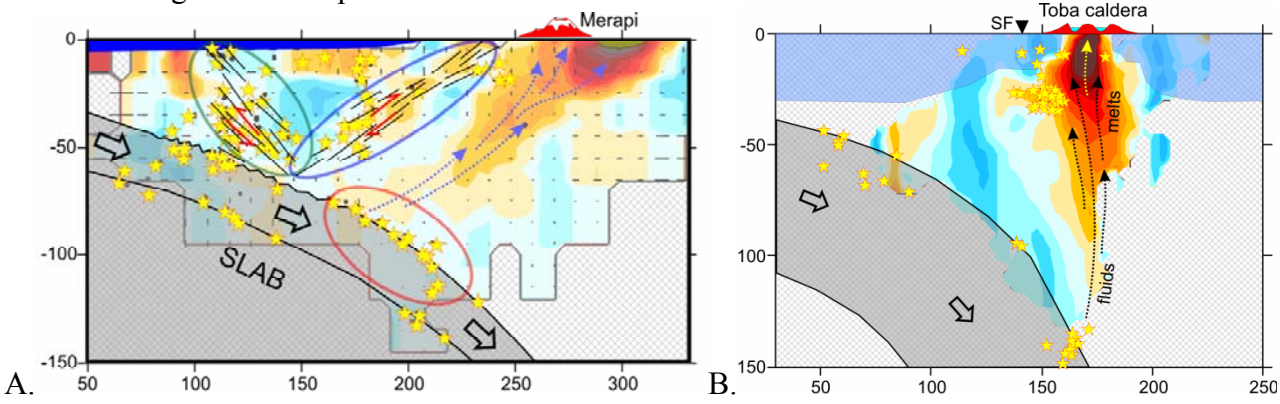


Figure2. Results of tomographic inversion in two Subduction zones: A.) Merapi (Cental Java) and B.) Toba Caldera (Sumatra). Arrow smark possible path soffluidand melt migrations, yellow stars depict location of the seismicity.

Active faulting in the Kamchatsky Peninsula as evidence for the Kamchatka-Aleutian collision

Andrey Kozhurin[1], Tatiana Pinegina[2]
[1] Geological Institute RAS, Moscow, Russia, kozhurin@ginras.ru
[2] Institute of Volcanology and Seismology FEB RAS, Petropavlovsk-Kamchatsky, Russia, tsunami@kscnet.ru

The western Aleutians (the Komadorsky Islands block, KIB) are commonly thought to be driven northwest by the subducting Pacific plate to collide with Kamchatka in the area of the Kamchatsky Peninsula. Geist and Scholl (1994) placed the collisional contact east of the Kamchatsky Peninsula, at the foot of its underwater slope. Gaedicke et all (2000), Freitag et al (2001) and Baranov et al (2010) interpreted some of active faults of the SE of the peninsula to be onshore extensions of the western Aleutians longitudinal faults, that is, placed the collisional contact within the SE of the Kamchatsky Peninsula, combining the SE portion of the peninsula into one rigid block with KIB. Kozhurin (2007) left the contact in the bottom in the west of the Kamchatsky Straight, and based on a simple model of several longitudinal blocks of western Aleutians moving northwest with rates decreasing south let the peninsula block move freely, probably rotating clock-wise.

There are two major active faults in the peninsula: major, in a sense, that they cut off the Kamchatsky Peninsula from the Kamchatka mainland thus making the peninsula to be a real separate block (faults 1 and 2 in Fig.). The fault 1 stretches N-S along the foot of the Kumroch Range steeper E-facing slope (north of ~56.45°N). Trenching and GPR data demonstrate altogether thrust movements on the shallow W-dipping fault plane. The WNW fault 2 starts from the northern termination of the fault 1 and reaches the Bering Sea shoreline, then most likely extending into the underwater Pokaty Canyon. The dominating component of slip along the fault 2 is right-lateral occurring on the likely shallow N-dipping plane. The two faults form a structural combination that strongly suggests active northwestward motion of the Peninsula block and its thrusting under the Kumroch Range, and therefore much westerly location of the main collisional contact between the Aleutians and the Kamchatka mainland. Other active faults of the peninsula manifest just the internal deformation of the peninsula block. Whether some of them are direct extensions of the western Aleutians longitudinal faults is still unclear. The kinematics of these faults (purely right-lateral for the fault 3, and mostly normal for the faults 4 and 5) does not favor the model that they are.

Thus active faulting in the Kamchatky Peninsula reflects collision of the western Aleutians with Kamchatka, but collision soft, when one of the colliding counterparts (western Aleutians) is not a single block but a set of several, which are able to move to some degree independently from each other.

This work was supported by RFBR (grants N 09-05-00125, 11-05-00136), RFBR-FEBRAS (grant N 11-05-98534)

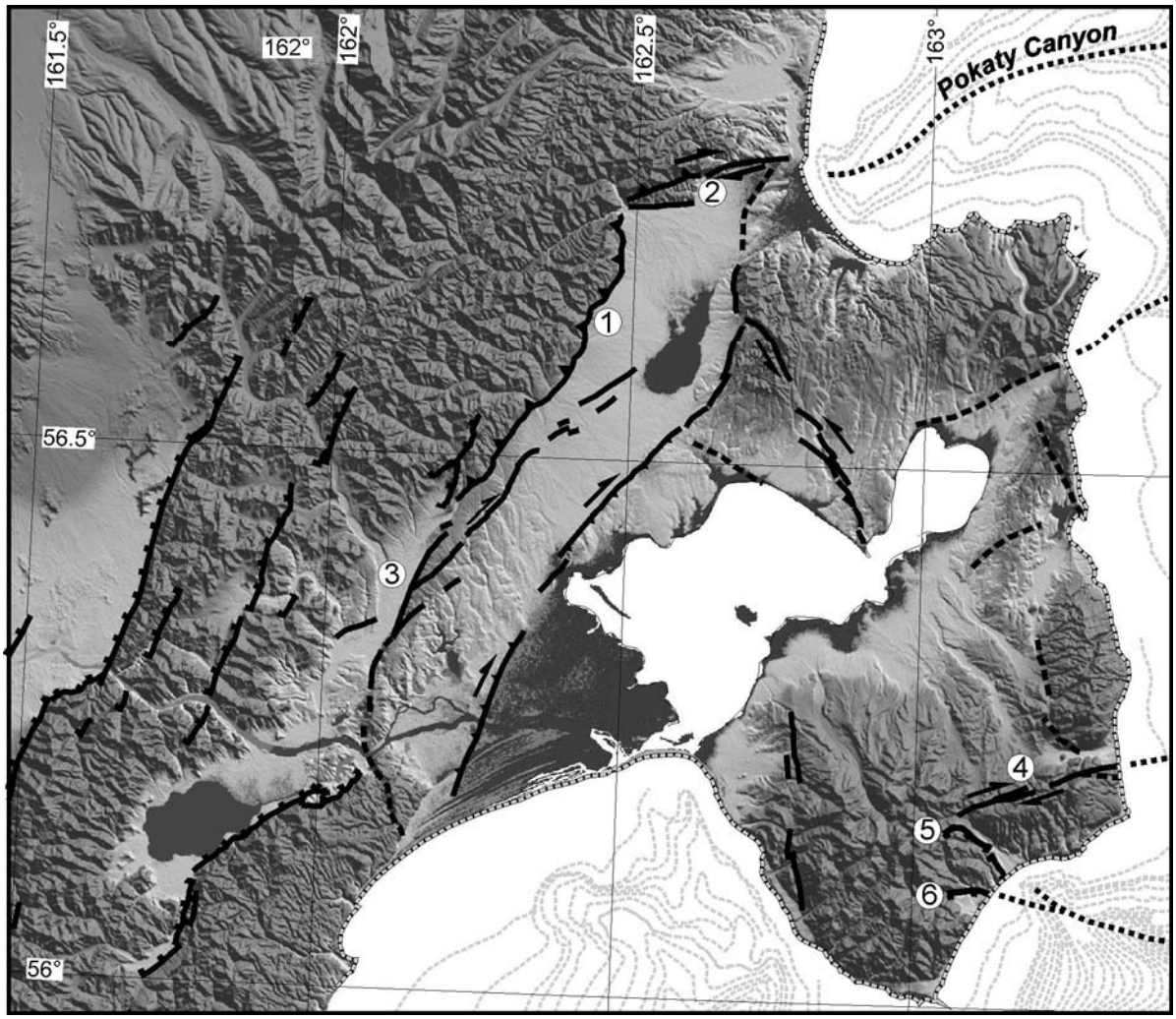


Figure Caption

Active faults in the Kamchatsky Peninsula, Kamchatka. Solid lines are for proved faults, dashed lines are for inferred faults. Arrows, ticks and teeth indicate strike-slip, normal and reverse/thrust components of movements. Dotted lines indicate probable position of underwater extensions of onshore faults. Numbers in circles are faults described in text.

References

Baranov B, Gaedicke C, Freitag R, Dozorova K (2010) Active faults of south-eastern Kamchatsky Peninsula and Komandorsky shear zone. Bulletin of Kamchatka regional association "Educational-scientific center". Earth Sciences 16: 66-77 (in Russian)

Freitag R, Gaedicke C, Baranov B, Tsukanov N (2001) Collisional processes at the junction of the Aleutian-Kamchatka arcs: new evidence from fission track analysis and field observations. Terra Nova 13: 433-442

Gaedicke C, Baranov B, Seliverstov N, Alexeiev D, Tsukanov N, Freitag R (2000) Structure of an active arc-continent collision area: the Aleutian–Kamchatka junction. Tectonophysics 325: 63–85

Geist EL, Scholl DW (1994) Large-scale deformation related to the collision of the Aleutian Arc with Kamchatka. Tectonics 13: 538-560.

Kozhurin AI (2007) Active Faulting in the Kamchatsky Peninsula, Kamchatka-Aleutian Junction. In: Eichelberger J, Gordeev E, Izbekov P, Lees J (eds) Volcanism and Subduction: The Kamchatka Region. American Geophysical Union, Washington, DC: 263-282

Активная разломная тектоника полуострова Камчатский как проявление Камчатско-Алеутской коллизии

Кожурин А.И.[1], Пинегина Т.П.[2]
[1]Геологический институт РАН, Москва, kozhurin@ginras.ru
[2]Институт вулканологии и сейсмологии ДВО РАН, Петропавловск-Камчатский, Россия, tsunami@kscnet.ru

В существующих моделях западная часть Алеутской островной дуги (Командорский блок, КБ), влекомая Тихоокеанской плитой, сталкивается с Камчатской островной дугой в районе полуострова Камчатский. При этом основной коллизионный контакт помещается или в подножье восточного подводного склона полуострова (Geist, Scholl, 1994), или же в пределах его юго-восточной части (Gaedicke et all, 2000; Freitag et al, 2001; Баранов и др., 2010). Вторая модель подразумевает, что юго-восточная часть полуострова Камчатский составляет единый блок с Командорской частью Алеут. В то же время, возможным представляется и относительно свободное перемещение блока полуострова, возможно, с компонентой его вращения по часовой стрелке, вызываемое неравномерным давлением на него со стороны продольных блоков западных Алеут, перемещающихся на СЗ со скоростью, возрастающей к югу (Kozhurin, 2007).

Среди активных разломов полуострова основными являются два (№№ 1 и 2 на рис.). Они отделяют полуостров от собственно Камчатки и, таким образом, превращают его в отдельный блок, который может перемещаться до какой-то степени независимо от своего окружения. Разлом № 1 протягивается в подножье восточного склона хр. Кумроч (севернее р. Камчатка). Данные тренчинга и георадарного профилирования свидетельствуют о надвиговой кинематике разлома и западном (под хребет) падении его плоскости. Разлом № 2 восток-северо-восточного простирания начинается у северного окончания разлома № 1 и протягивается до побережья Берингова моря и, очевидно, продолжатся в каньон Покатый. Доминирующими по нему являются правосторонние движения по, возможно, пологой падающей к северу плоскости. Два разлома образуют структурное сочетание, предполагающее активное перемещения блока полуострова примерно в СЗ направлении, его пододвигание под поднятие хр. Кумроч и, таким образом, гораздо более западное положение основного коллизионного контакта между двумя дугами. Остальные активные разломы полуострова представляют, очевидно, результат и проявление внутренней деформации блока полуострова. Являются ли те из них, что достигают береговой линии и подножья континентального склона, непосредственным наземным продолжением подводных разломов западных Алеут, до сих пор не ясно, однако имеющиеся данные об их кинематике (преобладающие правосдвиговые движения по разлому № 3 и преимущественно сбросовые по разломам №№ 4 и 5) такой модели противоречат.

Таким образом, активная разломная тектоника полуострова Камчатский представляет эффект коллизионного взаимодействия Алеутской и Камчатской островных дуг. При этом западные Алеуты, включая полуостров Камчатский, движутся не как единый жесткий блок, а состоят из нескольких относительно мелких блоков, способных перемещаться относительно друг друга («мягкая» коллизия).

Работа выполнена при финансовой поддержке грантов РФФИ № 09-05-00125, 11-05-00136, РФФИ-ДВО № 11-05-98534

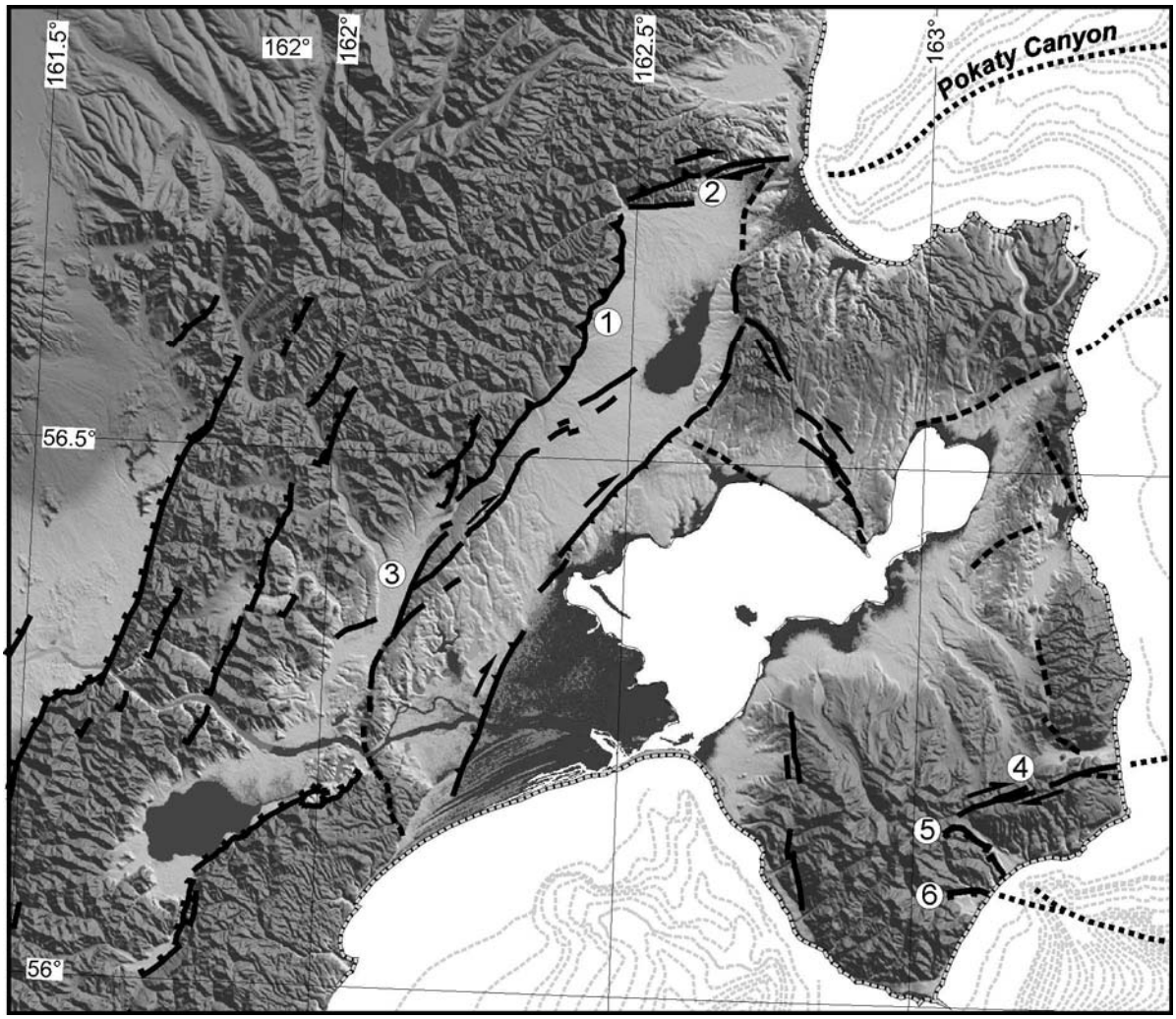


Рис. Активные разломы полуострова Камчатский, Камчатка. Сплошные линии – доказанные разломы, пунктирные – предполагаемые. Стрелки, берг-штрихи и треугольники означают направление движений по разломам – сдвиговых, сбросовых и надвиго-взбросовых, соответственно. Точечными линиями показаны возможные продолжения разломов под водой. Цифры в кружках – разломы, описываемые в тексте.

References

Baranov B, Gaedicke C, Freitag R, Dozorova K (2010) Active faults of south-eastern Kamchatsky Peninsula and Komandorsky shear zone. Bulletin of Kamchatka regional association "Educational-scientific center". Earth Sciences 16: 66-77 (in Russian)

Freitag R, Gaedicke C, Baranov B, Tsukanov N (2001) Collisional processes at the junction of the Aleutian-Kamchatka arcs: new evidence from fission track analysis and field observations. Terra Nova 13: 433-442

Gaedicke C, Baranov B, Seliverstov N, Alexeiev D, Tsukanov N, Freitag R (2000) Structure of an active arc-continent collision area: the Aleutian–Kamchatka junction. Tectonophysics 325: 63–85

Geist EL, Scholl DW (1994) Large-scale deformation related to the collision of the Aleutian Arc with Kamchatka. Tectonics 13: 538-560.

Kozhurin AI (2007) Active Faulting in the Kamchatsky Peninsula, Kamchatka-Aleutian Junction. In: Eichelberger J, Gordeev E, Izbekov P, Lees J (eds) Volcanism and Subduction: The Kamchatka Region. American Geophysical Union, Washington, DC: 263-282

Slow Slip Events and Nonvolcanic tremor in the Mexican Subduction Zone

V. Kostoglodov[1], A. Husker[1], N.M. Shapiro[2], M. Campillo[3], N. Cotte[3], A. Walpersdorf[3]

[1]Instituto de Geofísica, UNAM, México, [2]IPGP, Paris, France, [3]LGIT, Grenoble, France

Last decade was remarkably fruitful in discovering new seismotectonic phenomena: Slow Slip Events (SSE) and Nonvolcanic Tremor (NVT) in different active plate boundaries, particularly in subduction zones. Pioneering studies of SSE (*Dragert et al*., 2001) and NVT (*Obara*, 2002) awaken a concentrated quest in seismology and geodesy for the SSE and NVT detection and localization technique (*Schwartz and Rokosky,* 2007), space-time distribution and relation between SSE and NVT, physical explanation of the both and their importance for the earthquake hazard mitigation (e.g., *Beroza and Ide,* 2009).

Several large SSE (1998, 2001-2002, 2006, 2009-2010) of the equivalent seismic magnitude Mw~7.5 have been detected and studied in the Mexican subduction zone using GPS records (Figure 1). Since 2005, when continuous seismic data became available the NVT studies started in Mexico, a strong modulation of the tremor activity by the SSE was determined (*Payero et al.,* 2008, *Kostoglodov et al.,* 2010).

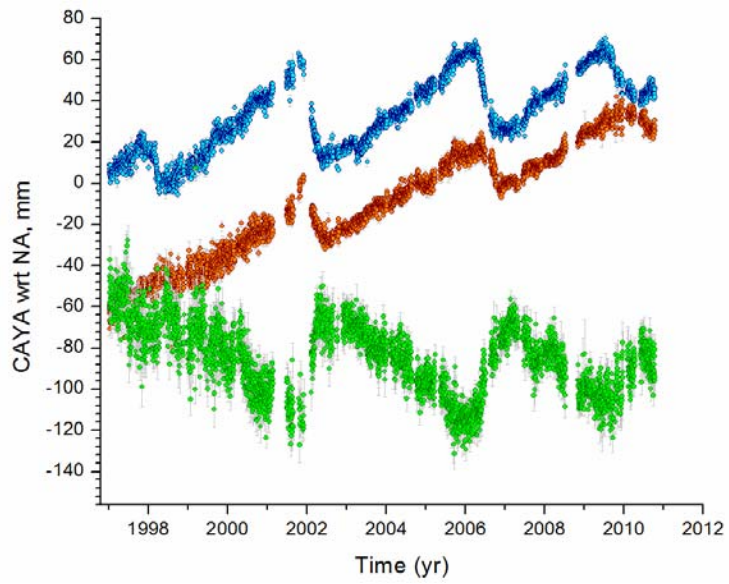


Figure 1. Time series (with respect to the fixed North America) at the Cayaco permanent GPS station, located on the Pacific coast of Mexico, ~60 km NW from Acapulco City. Several large anomalous surface displacements can be observed, which correspond to the 1998, 2001-2002, 2006, and 2009-2010 SSE. Upper curve is NS component, EW component is in the middle, and the bottom curve is the vertical component. Secular compression occurs in the direction of the plate convergence, and the long-term subsidence of the coast is about 2 mm/vr.

Detailed analysis of the NVT epicenters distribution (2005-2007, MASE project) and modeling of the 2006 SSE in Mexico show that the NVT bursts with a duration of a few weeks occur periodically every 3-4 months without clear GPS indication of large concurrent slow events. These NVT were localized over the plate interface in a band of 170-240 km from the trench, further than the SSE dislocation area (80-170 km). Then the 2006 SSE excited several repeated strong episodes of tremor which extended trenchward and partly populated downdip portion of the SSE zone (Figure 2).

We observed also a fixed spot along the plate interface, ~210 km from the trench, over which the tremor occurs almost continuously. This “sweet spot” of NVT surprisingly well coincides

with the maximum of modeled metamorphic dehydration of the subducted oceanic plate crust (*Manea et al.,* 2004).

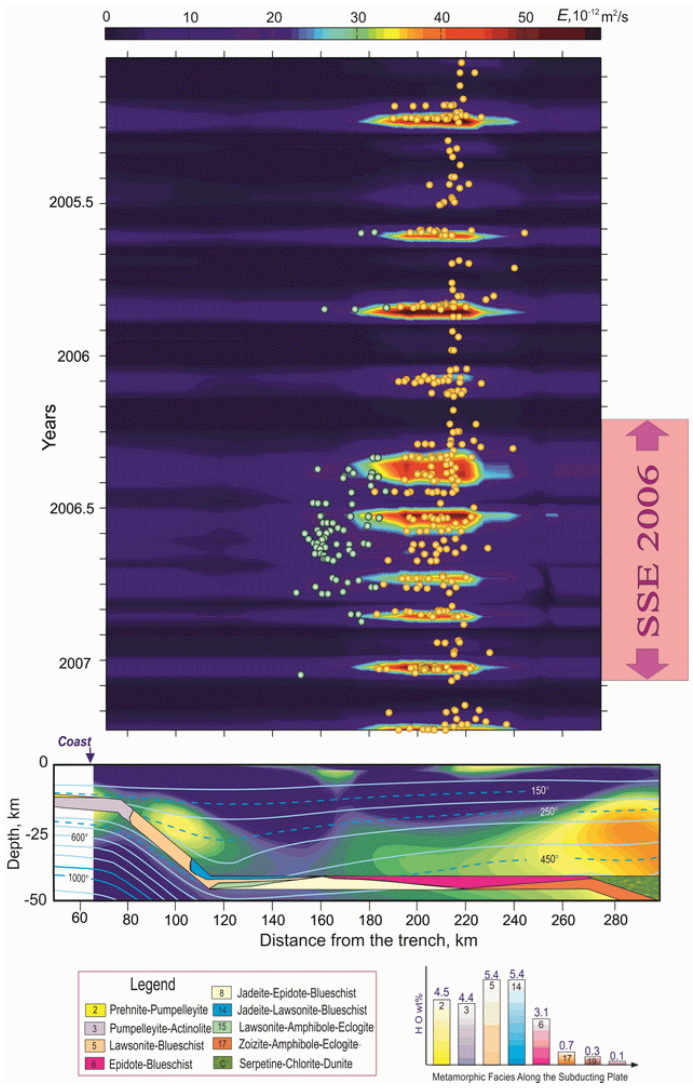


Figure 2. The NVT energy and epicenter locations. In the top panel the background color is the NVT seismic energy measured at the surface. The dots are the epicenters of the NVT from the inversion. The green dots are the trenchward, updip, low energy epicenters. The y-axis is the time and the x-axis is distance from the trench. The cross-section of the crust and slab in the lower panel (profile MASE) aligns with distance from the trench (x-axis) in order to demonstrate the details from the phase transitions in the slab [*Manea et al.*, 2004] and the conductivity measured in the crust [*Jödicke et al.*, 2006]. Blue in the background image of cross-section represents high resistivity and low conductivity, and red is the opposite. Temperature contours from *Manea et al.* [2004] are also shown in the cross-section. The legend at the bottom details the metamorphic phase transitions as noted in the different colors within the slab in the cross-section. The numbers listed within the bars in the bar graph note the phase transition in the legend. Numbers above the bars are the maximum wt per cent H_2O, which can be released by the metamorphic dehydration.

References

Beroza, G. C., and S. Ide (2009), Deep Tremors and Slow Quakes, *Science*, *324*(5930), 1025-1026.

Dragert, H., K. Wang, and T. S. James (2001), A Silent Slip Event on the Deeper Cascadia Subduction Interface, *Science*, *292*(5521), 1525-1528.

Jödicke, H., A. Jording, et al. (2006). "Fluid release from the subducted Cocos plate and partial melting of the crust deduced from magnetotelluric studies in southern Mexico: Implications for the generation of volcanism and subduction dynamics." J. Geophys. Res. **111**.

Kostoglodov, V., A. Husker, et al. (2010). "The 2006 slow slip event and nonvolcanic tremor in the Mexican subduction zone." Geophys. Res. Lett. **37**(24): L24301.

Manea, V. C., M. Manea, V. Kostoglodov, C. A. Currie, G. Sewell (2004), Thermal structure, coupling and metamorphism in the Mexican subduction zone beneath Guerrero *Geophys J Int*, *158*(2), 775-784.

Obara, K. (2002), Nonvolcanic Deep Tremor Associated with Subduction in Southwest Japan, *Science*, *296*(5573), 1679-1681.

Payero, J. S., V. Kostoglodov, et al. (2008). "Nonvolcanic tremor observed in the Mexican subduction zone." Geophysical Research Letters **35**(7).

Schwartz, S. Y., and J. M. Rokosky (2007), Slow slip events and seismic tremor at circum-Pacific subduction zones, *Rev. Geophys.*, *45*.

Study on Deep-Focus Earthquakes beneath North-Western Margin of East Sea

Geunyoung Kim

Earthquake Research Center,

Korea Institute of Geoscience and Mineral Resources, Daejeon, Republic of Korea

Body waves recorded at broadband seismic stations in Korea, China and Russia are analyzed to study 5 deep focus earthquakes include February 18, 2010 M_w 6.9 deep-focus earthquake beneath North-western margin of East Sea and 4 nearby located mid-size events. All of the analyzed earthquakes have focal-depths deeper than 550 km and magnitudes ranging from 4.3 to 6.9. These events are relocated using double difference hypocenter location algorithm (hypoDD). Also, focal mechanisms are estimated using first motions and relative amplitudes of *P* and *S* arrivals.

He isotopes and geodynamics of the Mexican Pacific coast

Yuri Taran and Vladimir Kostoglodov

Institute of Geophysics, UNAM, Mexico

Theoretically, the subduction of the oceanic plate with a cold surface beneath the continental plate should result in a low terrestrial heat flow in the coastal area adjacent to the trench. Nevertheless, many hot and warm springs are known in this zone distributed more o less uniformly from the Tehauntepec isthmus at south (~16°N) to Punta Mita at north (~21°N). Two oceanic plates are subducting beneath the continental North America Plate along the Mexican Pacific coast: Cocos Plate south of Colima graben (~19°N) and a young Rivera Plate to the north of Colima graben. The trench is situated ~ 60 km from the shore line which is close comparing with other continental margins. Chemical and isotopic composition of waters, helium, carbon and nitrogen isotopes in bubbling gases were obtained for 29 groups of thermal springs between 16°N and 21°N, in a ~30 km-wide zone along the coast. Their temperature and salinity ranges are 35-90°C and 100-20,000 ppm, respectively. The observed $^3He/^4He$ ratios were 0.16Ra to 4.5Ra (where $Ra=1.4x10^{-6}$, the air ratio) indicating that some springs discharge gas with a high contribution of mantle helium while the others contain helium of the crustal origin. High $^3He/^4He$ ratios were measured in springs located close to Colima graben, the apparent surface border between Rivera and Cocos plates and also within the Puerto-Vallarta (Rio Ameca) graben at the northernmost part of the coastal forearc zone. The permeability of these areas to the mantle He is interpreted as a margin effect at the northern part of the subduction zone and as a "slab window" in the vicinity and to the south of Colima graben; a discontinuity between subducting plates.

The nitrogen isotopic composition is in a good positive correlation with the N_2/Ar ratios. The highest $\delta^{15}N$ of 4-5‰ were measured for gases with N_2/Ar >300, indicating a presence of non-atmospheric nitrogen of sedimentary origin. These high values are associated with the high-salinity springs which probably connected with the accreted to the continental slope organic-rich sedimentary material.

The geographic distribution of $^3He/^4He$ ratios were used for the first-order estimation of distribution of the heat flow within the studied area. We suggest that for the thermal modeling of the forearc heat flow, the heterogeneity of the heat sources (slab margins and slab discontinuities) should be taken into account. The $^3He/^4He$ distribution can help to constrain the geometry of zones permeable for the mantle heat and volatiles.

Mechanism of the Intraplate Earthquakes in and around the Korean Peninsula

Myung-Soon Jun

Earthquake Research Center, Korea Institute of Geoscience and Mineral Resources, Daejeon, Korea

Abstract

Earthquakes in and the around the Korean Peninsula are rather small in size with infrequent occurrence and show diffuse geographic distribution. The occurrence of earthquakes in this region does not correlated with any known specific surface geologic features.

In Korea, instrumental earthquake recording has started since 1905 however, Korea has 2000-year long history with more than 2000 documents which include not only earthquake information but also many other natural phenomena. Fig. 1, shows the historical seismicity for 2000 years and instrumental seismicity since the 20 century.

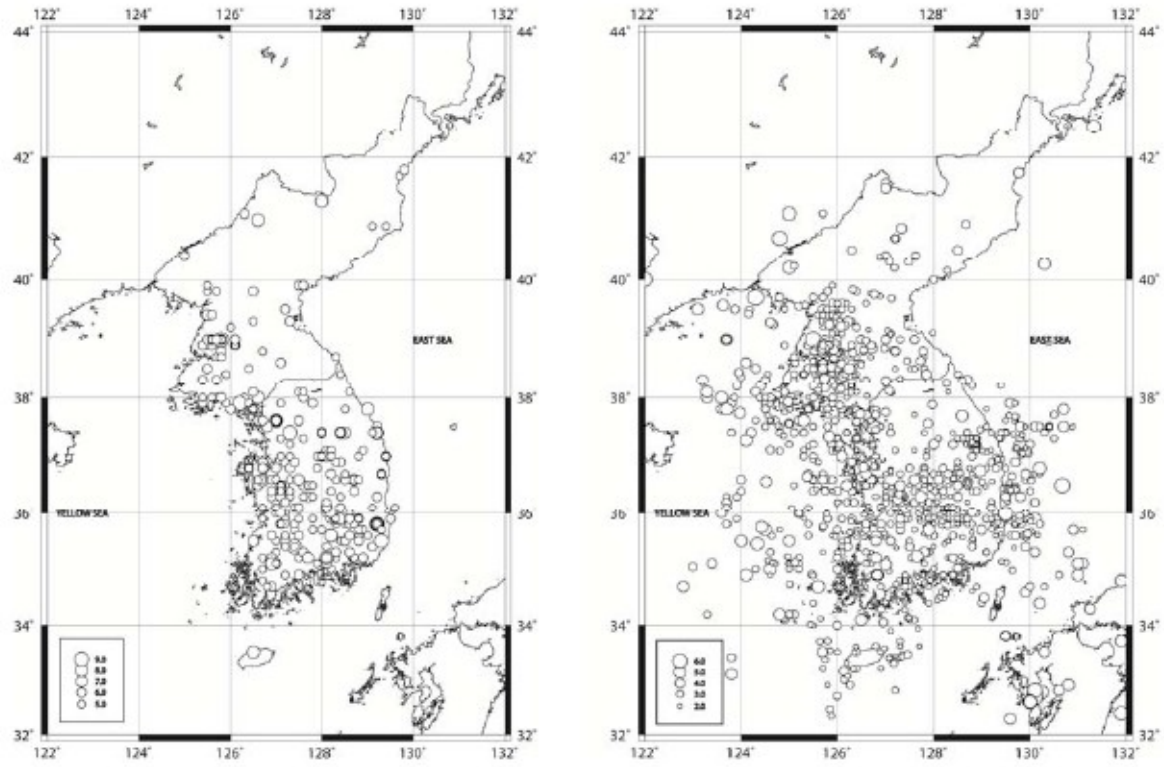


Fig. 1. Historical Seismicity(left) and instrumental seismicity(right) in the Korean Peninsula

The focal mechanism of 19 (M>4.5) shallow intraplate earthquakes in and around the Korean Peninsula since 1936 were analyzed(Fig. 2). Considering the low seismicity in the region, these studied shallow earthquakes may representative for the epicentral region and characterize the state of stress of the earth crust. The majority of earthquake source

mechanism in this region show predominant strike-slip faulting on steeply dipping nodal planes together with small amount of thrust components. In the Korean Peninsula, six earthquakes show predominant strike slip faulting and one event from the western central part of Korea show normal faulting. In the Yellow Sea, three earthquakes show strike slip faulting and two events show thrust faulting. Along the eastern coast of the Korean Peninsula, from the East Sea (Sea of Japan), four earthquakes show strike slip faulting and two events show thrust faulting.

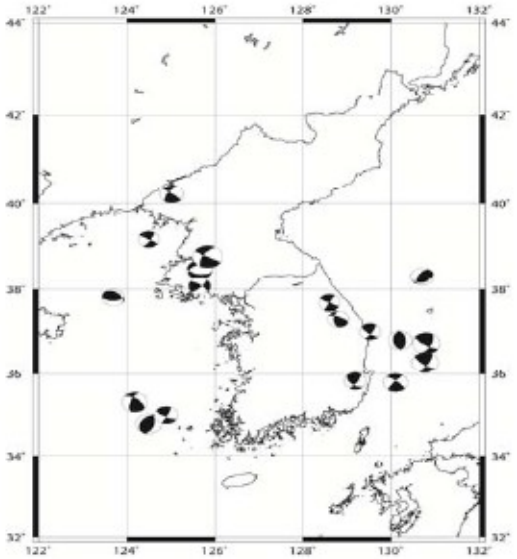


Fig. 2. Epicentral distribution of 19 studied earthquakes and their simplified mechanisms

The seismogenic zone indicated by the deduced focal depths of earthquakes from the Yellow Sea, the Korean Peninsula and the western part of the East Sea are very shallow and restricted to the upper 10km of the crust. While focal depth from the southwestern part of the East Sea show larger than 20km. Since the depth of crust in this region is about half of the typical continental crust (about 15km) and probably being oceanic crust, these events from the SW of the East Sea might occur in the upper most mantle.

We compared the earthquake source parameters in the region with other shallow (h<60km) focus earthquakes in neighboring regions, i.e. in northeastern China, southwestern part of Japan and the eastern part of the East Sea, which are also part of the Eurasian plate(Fig. 3). We compared data which source mechanisms are obtained by centroid moment tensor inversion from USGS since 1976.

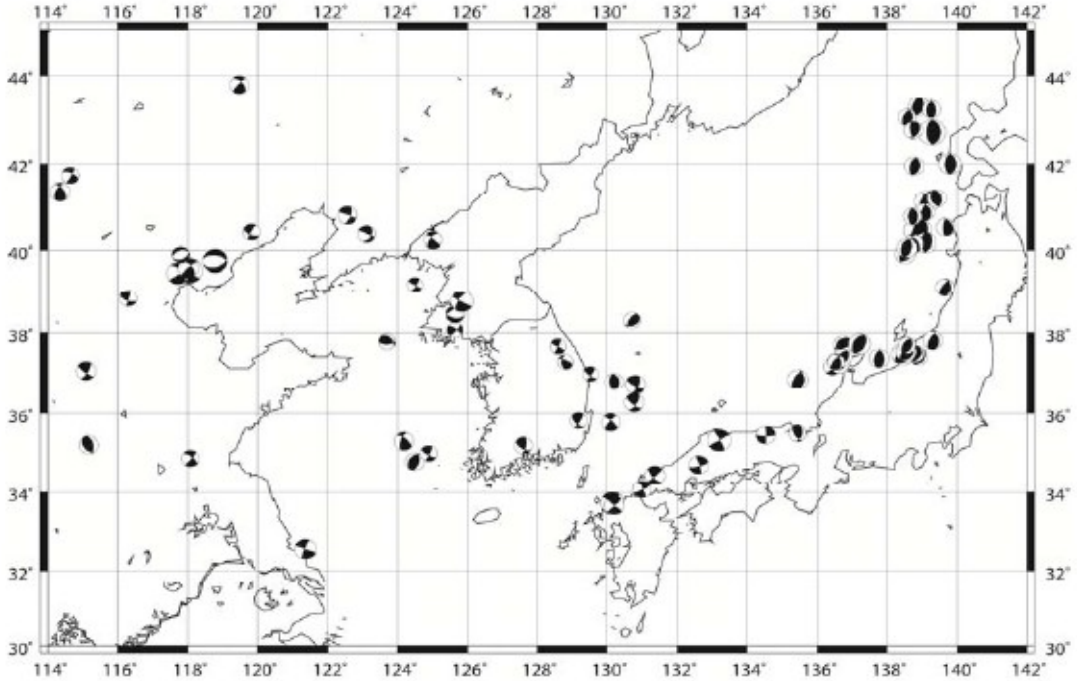


Fig. 3. Comparison of earthquake mechanisms from the Korean Peninsula and neighboring regions.

Two major differences are evident from the pattern of earthquake mechanisms. The first difference is the faulting style. Thrust faulting is dominant in the eastern part of the East Sea, while strike slip faulting dominates around the Korean Peninsula, southwestern part of Japan and in northeastern China. The other major difference is the direction of P-axes. Around the Korean Peninsula, the trend of P-axes shows almost horizontal in ENE - WSW direction. In NW China and SW Japan, the P-axes trend ENE - WSW direction which are similar to that observed around the Korean Peninsula. By contrast, ESE - WNW trending P-axes with almost vertical T-axes are dominant in the eastern part of the East Sea. This stress pattern departs considerably from the Korean Peninsula but is consistent with the relative motion of the Pacific plate against Eurasian plate along the Japan Trench. One possible explanation for the difference in the P-axis direction around the Korean Peninsula with the eastern part of the East Sea is that the collision of Indian plate gives appreciable effect to the stress field to the extent large enough to control the seismicity in and around the Korean Peninsula, NE China and SW Japan.

Island-arc magma sources and island-arc volcanism evolution.

Plechov P.Yu.

Geological department of Moscow State University
pavel@web.ru

New petrologic and geodynamic model for island arc systems is proposed to satisfactory explain of space and spatial variations of island arc volcanic series. The main idea of the model is step-by-step involving of additional sources of melting to magma generation processes during evolution of the island arc system. Each stage of the island arc evolution is characterized by the specific set of volcanic series.

Primitive island arcs are defined by one main source of magma. Magma generated by fluid induced melting of the mantle wedge above subducted slab. As a result, Hi-Mg and Low-K basalts are predominant volcanic rocks in primitive island arcs. It has clear island arc geochemical signature which produced by fluid-mobile influx from the slab.

The thickness of the island arc crust is growing up during island arc evolution and magmas could be more evolved with island arc crust growth. This crust is consists of volcanogenic material, which usually altered to greenschists. Global scale of such low-grade metamorphism is proved by occurrence of wide distributed few-million years old island arc volcanic rocks, which mostly metamorphized. These greenschists could be easily transformed to amphibolites in lower parts of island arc crust. Thus, after several million years primitive island arc became a developed island arc with crust which consists of rocks metamorfized in greenschists and amphibolite facies.

Large volume of silica-rich and intermediate volcanic rocks is common for developed island arc. It may be explained by additional new area of magma generation inside the crust [Tamura,Tatsumi,2002; Dufek, Bergantz,2005]. Partial melting of greenschists produce silica-rich melts [Montel,Vielzeuf,1997], amphibolites could produce silica-rich melts at the low pressure [Johannes,Holtz,1996; Nakajima, Arima,1998; Lupulesku, Watson,1999] or could be “granitized” [Selbekk et al.,2002]. Experiments [Rapp,Watson,1995; Gardien et al.,2000] and calculations [Kimura et al.,2002] shows that partial melting of amphibolites in water-saturated conditions and at 8-10 kbar of the pressure (it’s corresponds to lower parts of developed island arcs) could produce andesibasalts or even basalts (at high degree of the partial melting). It’s important, that amphibole is a restite phase at these conditions. If we assume that the lower crust amphibolites are formed from high-Mg basalts of previous stage, it leads to producing of less magnesian melts than high-Mg basalts of primitive island arcs. Amphibole-bearing restite could preserve significant amount of LREE, Nb, Ti and K. As a result of melting of the island arc lower crust we can expect magmas which are well corresponding to low-K tholeitic island arc series of volcanic fronts of developed island arcs.

I suppose that magmas could emanate simultaneously from several levels of the island arc system: 1) high-Mg low-K basalts could be generated by fluid-induced melting of the mantle wedge; 2) low-K andesibasalts and basalts are from amphibolite melting at the lower crust conditions; 3) silica-rich magmas could be formed by melting of island arc upper crust metamorphic rocks. All these magmas could mixing each other in transitional magma chambers and then erupt in the same volcanic center with hybrid rocks forming. Such scheme is a very confusing factor for clear determination of volcanic series for a lot of island arc volcanoes.

Mature island arcs (like Japan or Kamchatka) are developing after jump of a subduction zone toward to ocean. Such jumps are very common for most of known island arcs and responsible for two-chain structure of island arcs. Volcanic front starts to form again after such jump following the scenario which described above, whereas former volcanic front shifts to backarc settings and could suffer farther evolution. Fluid induced melting is impossible at this stage and could be only as relics. At the moment the island arc crust under forming volcanic front is consist of metavolcanic rocks in upper part and restites of melting in lower part of the crust. As was concerned above, melting at lower crust settings could leads to amphibole enrichment in restites and after dehydratation will form pyroxenites or amphibole-bearing pyroxenites. P.Kelemen and coauthors [Kelemen et al., 2003] demonstrated occurrence of pyroxenites in lower part of the palaeoarc Talkeetna (Alaska) and shows with mass-balance that significant amount of pyroxenites were delaminated. If these pyroxenites were formed as restites after producing of low-K volcanic front magmas, it means that its composition will be complementary with low-K magmas, i.e. pyroxenites will be enriched in K, Ti, Nb, LREE in comparison with primary amphibolites, which formed after primitive island arc basalts. [Jull,Kelemen, 2001] demonstrated that pyroxenitic lower crust is gravitational unstable and has higher density than undergoing mantle. It’s relatively clear that time of an extinction of the former volcanic front

(ceasing of fluid and melt inflow to island arc crust) is ideal for delamination of main part of pyroxenites in the lower part of island arc crust. Sinking of delaminated blocks leads to magma generation due to both partial melting of the pyroxenites and disturb of the mantle. According this model the new source of the magma will form in the area of former volcanic front due to delamination and dehydratation of delaminated blocks of pyroxenites and amphibole-bearing pyroxenites of lower part of a island arc system. These magmas should be enriched in LREE, Nb, Ti, K in comparison with «typical» island arc calc-alkaline magmas. Such geochemical signature is typical for subalkaline volcanic rocks, which erupts in former volcanic fronts. Sometimes heat flow could be enough for new act of upper crust melting after delamination and new magma influx. It could lead to silica-rich magmas appearance inside areas of subalkaline volcanism.

According suggested petrologic and geodynamic model of island arc evolution we can determine several stages: 1) primitive island arc with dominated fluid induced mantle melting; 2) developed island arc with combination of fluid-induced mantle melting and island arc crust melting; 3) mature island arc with former volcanic front and melting of delaminating blocks under this one. Assuming the model, the geochemical zoning of synchronous volcanism across mature (two or more chains) island arc system could be explained by several zones with different sets of magma sources due to evolution of island arc system and jumps of volcanic front position.

References:

1 Dufek J., Bergantz G. W. Lower crustal magma genesis and preservation: a stochastic framework for the evaluation of basalt–crust interaction // J. Petr., 2005, V. 46(11), p. 2167-2195.
2 Gardien V., Thompson A.B., Ulmer P. Melting of biotite + plagioclase + quartz gneisses: the role of H2O in the stability of amphibole // J. Petr., 2000, V. 41, p. 651–666.
3 Johannes W., Holtz F. Petrogenesis and Experimental petrology of granitic rocks // Heidelberg: Springer, 1996, 355 p.
4 Jull M., Kelemen P. B. (2001) On the conditions for lower crustal convective instability // J. Geophys. Res., 2001, V. 106, p. 6423–6446.
5 Kelemen P.B., Hanghoj K., Greene A.R. One view of the geochemistry of subduction-related magamatic arcs, with emphasis on primitive andesite and lower crust // In: Treatise on Geochemistry. Oxford: Elsevier–Pergamon, 2003, p. 593–659.
6 Kimura J., Johida T., Iizumi S. Origin of Low-K intermediate lavas at Nekoma volcano, NE Honshu arc, Japan: Geochemical constraints for lower-crustal melts // J.Petr., 2002, V. 48, № 4, p. 631-661
7 Lupulescu A., Watson E.B. Low melt fraction connectivity of granitic and tonalitic melts in a mafic crustal rock at 800 C and 1 GPa // Contrib Mineral Petrol, 1999, V. 134, p. 202-216.
8 Montel J.M., Vielzeuf D. Partial melting of metagreywackes. Part II: compositions of minerals and melts // Contrib Mineral Petrol., 1997, V. 128, p.176-196.
9 Nakajima K., Arima M. Melting experiments on hydrous low-K tholeiite: implications for the genesis of tonalitic crust in the Izu–Bonin–Mariana arc // Island Arc, 1998, V. 7, p. 359–373.
10 Rapp E.P., Watson E.B. Dehydratation melting of metabasalt at 8-32 kbar: implications for continental growth and crustal-mantle recycling // J. Petr., 1995, V. 36, p. 891-931.
11 Tamura Y., Tatsumi Y. Remelting of an andesitic crust as a possible origin for rhyolitic magma in oceanic arcs; an example from the Izu-Bonin Arc // J. Petr., 2002, V. 43(6), p.1029-1047.
12 Selbekk R.S., Bray C., Spooner E.T.C. Formation of tonalite in island arcs by seawater-induced anatexis of mafic rocks; evidence from the Lyngen Magmatic Complex, North Norwegian Caledonides // Chem. Geol., 2002, V. 182, p. 69–84.

Источники островодужных магм и эволюция островодужного вулканизма.

П.Ю.Плечов

Геологический факультет Московского Государственного Университета имени М.В.Ломоносова
pavel@web.ru

Предлагается для обсуждения геодинамическая модель развития островодужной системы, которая удовлетворительно объясняет специфику проявления различных островодужных магматических серий, связывая изменение характера вулканизма в различных зонах островной дуги с вовлечением дополнительных источников магмогенерации по мере эволюции островодужной системы. Выделяется несколько стадий развития островодужной системы, каждая из которых характеризуется собственной формацией вулканических пород.

На стадии примитивной островной дуги доминирует один источник магмогенерации, связанный с плавлением мантийного клина под воздействием флюида, отделяющегося от субдуцированной океанической плиты. При этом образуются магнезиальные низкокалиевые базальты, с ярко выраженной островодужной геохимической спецификой за счет привнесения легкомобильных компонентов флюидом из субдуцированной плиты.

По мере эволюции островной дуги постепенно увеличивается мощность островодужной коры, что приводит к возможности дифференциации магм при их подъеме. Островодужная кора примитивных островных дуг сложена преимущественно вулканогенным материалом, который легко подвергается метаморфизму фации зеленых сланцев. Глобальный масштаб низкотемпературного метаморфизма островодужных вулканитов демонстрируется тем, что практически все вулканические породы островных дуг старше нескольких млн. лет частично или полностью метаморфизованы. По мере формирования островодужной коры и накоплению вулканитов, нижние части коры подвергаются метаморфизму амфиболитовой фации, т.е. островодужная кора в момент перехода от стадии примитивной островной дуги к стадии развитой островной дуги, сложена не базальтами, а метаморфизованными в зеленосланцевой и амфиболитовой фациях породами.

Характерный для стадии развитой островной дуги большой объем кислых вулканитов и андезитов объясняется появлением новой области магмогенерации за счет частичного плавления островодужной коры [Tamura,Tatsumi,2002; Dufek, Bergantz,2005]. При частичном плавлении зеленых сланцев образуются кислые расплавы [Montel,Vielzeuf,1997]. При частичном плавлении амфиболитов при низких давлениях также образуются кислые расплавы [Johannes,Holtz,1996; Nakajima, Arima,1998; Lupulesku, Watson,1999] или амфиболиты подвергаются гранитизации [Selbekk et al.,2002]. Эксперименты [Rapp,Watson,1995; Gardien et al.,2000] и численное моделирование [Kimura et al.,2002] показали, что в водонасыщенной системе при давлениях 8-10 кбар, соответствующих низам островодужной коры развитых островных дуг возможно плавление амфиболитов с образованием андезибазальтовых и даже базальтовых (при больших степенях плавления) расплавов. При этом, амфибол остается в рестите от плавления. Если, в качестве субстрата выступают амфиболиты, которые по химическому составу соответствуют магнезиальным базальтам примитивных островных дуг то, образующиеся расплавы будут существенно менее магнезиальны, чем исходный субстрат. Кроме этого, наличие амфибола в рестите связывает существенную часть легких REE, Nb, Ti и калия. Таким образом, при плавлении вещества примитивных островных дуг в условиях низов мощной островодужной коры появляются магмы, обладающие всеми специфическими чертами низкокалиевых серий вулканических фронтов развитых островных дуг.

В развитых островодужных системах вполне вероятны случаи, когда магмогенерация происходит одновременно на нескольких уровнях: 1) в мантии, за счет привнесенного флюида продолжают образовываться магнезиальные низкокалиевые базальты 2) в нижних частях островодужной коры происходит плавление амфиболитов с образованием низкокалиевых магм 3) в средних и верхних частях островодужной коры происходит генерация кислых магм. Поднимающиеся магмы из различных источников могут взаимодействовать друг с другом на уровне промежуточных очагов и изливаться в одних и тех вулканических центрах, образуя гибридные породы. Поэтому, четкое разделение вулканитов по типам магмогенерации возможно не для любых вулканических центров.

Переход от стадии развитой островной дуги к зрелой островной дуге связывается со смещением зоны субдукции по направлению к океану. Такое смещение характерно для подавляющего большинства известных островных дуг и обуславливает их двучленное строение. Фронтальная дуга начинает формироваться по сценарию, описанному выше, тогда как бывший вулканический фронт, оказавшийся в тыловой зоне, претерпевает дальнейшую эволюцию. На этой стадии вулканическая деятельность, связанная с привносом флюида из субдуцированной плиты в мантию, практически прекращается и может носить только реликтовый характер. Строение коры этой зоны островодужной системы характеризуется дифференцированными частично метаморфизованными вулканитами в верхних структурных ярусах и породами, оставшимися от частичного плавления островодужной коры в нижних структурных ярусах. Как было рассмотрено выше, плавление в условиях низов островодужной коры может приводить к накоплению амфибола в рестите, что при условии

частичной дегидратации и дальнейшего метаморфизма приводит к образованию пироксенитов, или амфиболовых пироксенитов. [Kelemen et al., 2003] показали на основе масс-баланса островодужной системы и детально изученных разрезов палеодуги Талкитна (Аляска), что для низов островодужной коры характерно присутствие пироксенитов. Если эти пироксениты образовались как реститы при генерации низкокалиевых серий вулканического фронта, то они по составу должны быть комплементарны этим сериям - обогащены калием, титаном, ниобием и легкими REE по сравнению с первоначальными амфиболитами, отвечавшими по составу островодужным базальтам примитивных островных дуг. [Jull,Kelemen, 2001] показали, что в условиях нижней части островодужной коры пироксениты будут тяжелее, чем подстилающая их мантия при достижении некоторой критической мощности островодужной коры, что приводит к их гравитационной нестабильности. Можно предположить, что стадия отмирающего вулканического фронта, на которой островодужная кора перестает подпитываться мантийными расплавами и флюидопотоками, является идеальной для создания условий, при которых происходит деламинация (по Kelemen et al.,2003) основной части пироксенитов нижней части островодужной коры. При этом, погружение блоков пироксенитов и амфиболовых пироксенитов в мантию должно вызывать формирование расплавов как за счет частичного плавления этих пироксенитов, так и за счет возмущений в мантии возникающих вследствие этого погружения. Таким образом, исходя из предложенной модели, в тыловой зоне островных дуг после перерыва в вулканической активности начинает формироваться новая область магмогенерации, связанная с деламинацией и дегидратацией пироксенитов и амфиболовых пироксенитов нижней части островодужной коры. Исходя из состава пироксенитов, рассмотренного выше, расплавы должны быть обогащены легкими REE, Nb, Ti, калием по сравнению с низкокалиевыми «типично островодужными» сериями. Такая геохимическая специфика как раз и характерна для субщелочных вулканитов, появляющихся на зрелой стадии развития островодужной системы. Вполне возможно, что теплового потока, создаваемого процессами деламинации и поднимающимися магмами, на некоторой стадии окажется достаточно, чтобы вызвать дополнительное плавление в средних и верхних частях островодужной коры, что может проявиться в появлении кислых магм. При локализации и гибридизации расплавов из разных зон магмогенерации эти кислые вулканиты также могут иметь субщелочную или даже щелочную специфику.

Таким образом, по мере эволюции дуги и развития зрелой островодужной системы к доминирующему на стадии примитивной островной дуги плавлению мантийного источника добавляются коровые источники магмогенерации. Специфика вулканических серий развитых островных дуг преимущественно определяется плавлением пород корового субстрата, таких как амфиболиты и амфиболовые пироксениты. Вследствие общей эволюции островодужной системы и последовательному смещению вулканического фронта навстречу субдуцирующей плите на зрелых островных дугах может возникать характерная геохимическая зональность синхронного вулканизма в пределах нескольких различных по условиям магмогенерации зон.

Литература:

1. Dufek J., Bergantz G. W. Lower crustal magma genesis and preservation: a stochastic framework for the evaluation of basalt–crust interaction // J. Petr., 2005, V. 46(11), p. 2167-2195.
2. Gardien V., Thompson A.B., Ulmer P. Melting of biotite + plagioclase + quartz gneisses: the role of H2O in the stability of amphibole // J. Petr., 2000, V. 41, p. 651–666.
3. Johannes W., Holtz F. Petrogenesis and Experimental petrology of granitic rocks // Heidelberg: Springer, 1996, 355 p.
4. Jull M., Kelemen P. B. (2001) On the conditions for lower crustal convective instability // J. Geophys. Res., 2001, V. 106, p. 6423–6446.
5. Kelemen P.B., Hanghoj K., Greene A.R. One view of the geochemistry of subduction-related magamatic arcs, with emphasis on primitive andesite and lower crust // In: Treatise on Geochemistry. Oxford: Elsevier–Pergamon, 2003, p. 593–659.
6. Kimura J., Johida T., Iizumi S. Origin of Low-K intermediate lavas at Nekoma volcano, NE Honshu arc, Japan: Geochemical constraints for lower-crustal melts // J.Petr., 2002, V. 48, № 4, p. 631-661
7. Lupulescu A., Watson E.B. Low melt fraction connectivity of granitic and tonalitic melts in a mafic crustal rock at 800 C and 1 GPa // Contrib Mineral Petrol, 1999, V. 134, p. 202-216.
8. Montel J.M., Vielzeuf D. Partial melting of metagreywackes. Part II: compositions of minerals and melts // Contrib Mineral Petrol., 1997, V. 128, p.176-196.
9. Nakajima K., Arima M. Melting experiments on hydrous low-K tholeiite: implications for the genesis of tonalitic crust in the Izu–Bonin–Mariana arc // Island Arc, 1998, V. 7, p. 359–373.
10. Rapp E.P., Watson E.B. Dehydratation melting of metabasalt at 8-32 kbar: implications for continental growth and crustal-mantle recycling // J. Petr., 1995, V. 36, p. 891-931.
11. Tamura Y., Tatsumi Y. Remelting of an andesitic crust as a possible origin for rhyolitic magma in oceanic arcs; an example from the Izu-Bonin Arc // J. Petr., 2002, V. 43(6), p.1029-1047.
12. Selbekk R.S., Bray C., Spooner E.T.C. Formation of tonalite in island arcs by seawater-induced anatexis of mafic rocks; evidence from the Lyngen Magmatic Complex, North Norwegian Caledonides // Chem. Geol., 2002, V. 182, p. 69–84.

Geodynamic conditions for adakites and intraplate lavas genesis in subduction zone of Eastern Kamchatka

G.P. Avdeiko [1], O.V. Kuvikas[1], A.A. Palueva [1]
[1] Institute of Volcanology and Seismology FEB RAS, Petropavlovsk-Kamchatski, *683006;*
e-mail: gavdeiko@kscnet.ru

Subduction system of Eastern Kamchatka includes various types of rocks, e.g. typical calc-alkaline (CA) rocks of island arc type, alkaline basalts with intraplate geochemical properties (NEB), and high magnesium andesites and andakites. There are two types of adakites and NEB distribution – they may occur within the same area (positions 1, 3-5, fig. 1) or may occupy different zones. Volcanic rocks of NEB type and adakites show fragmented distribution being typical rocks for initial stage of subduction. They occur only within the segment where subduction zone "jumps" to the modern position [1]. Age and chemistry data show evolution from intraplate alkaline and transitional basalts (7-12 MA) through rocks with adakite properties (3-8 MA) to modern CA rocks [5].

Formation of NEB and adakites depends on geodynamic evolution of Kamchatka (fig. 2). In late Oligocene-Miocene, a subduction zone under the Sredinny Ridge with its volcanic arc was located about 200 km far from its recent position. In late Miocene the subduction zone "jumped" to its recent location causing formation of a segment in the volcanic arc of Eastern Kamchtka (fig. 1, 2a). On the initial stage of subduction process a front part of a new slab suffered melting caused by heat from hot asthenosphere (fig. 2b). Additional heating of both the Pacific plate and the asthenosphere was caused probably by a flexure forming and volcanism related to the flexure forming of the Pacific plate before its approach to the subduction zone (see model in [4]). In the asthenosphere, mantle diapir or a plume of "andersonian" type were forming in the same zone of interaction illustrated at the model in [3]. Low decompression melting of diapir caused its upwelling, while low partial melting influenced composition of melt of NEB. Formation of NEB and adakites followed probably the same scenario at Mount Saint Helens [2], in Zamboanga volcanic arc, the Philippines [7], at Daisen и Sambe volcanoes [6], and within the Valovayam River in Kamchatka (position1, fig. 1). The same mechanism is responsible for distribution of NEB and adakites in transform faults in Kamchatsky Mys peninsula and in the southern part of Central Kamchatka Depression (positions 2, 3 and 5, fig. 5), where "jump" of the subduction zone caused slab windows. This is the very place where slab edges interact with hot asthenosphere.

This hypothesis describes how NEB and adakites from island arcs are located in the zone of subduction "jump" and gives explanations for short-term formation of these rocks, and low volume of erupted material.

References:

1. Avdeiko et al., 2007: AGU Monograph 172, 41-60.
2. *Defant, Drummond, 1993***:** Geology 21: 547-550.
3. *Faccenna et al, 2010:* EPSL 299 (1-2): 54-68.
4. *Hirano et al, 2006:* Science 313: 1426-1428.
5. *Hoernle et al.,2009:* GCA 73(13).
6. *Morris, 1995:* Geology 23 (5): 395–398.
7. *Sajona et al, 1996:* J. Petrology37 (3): 693-726.

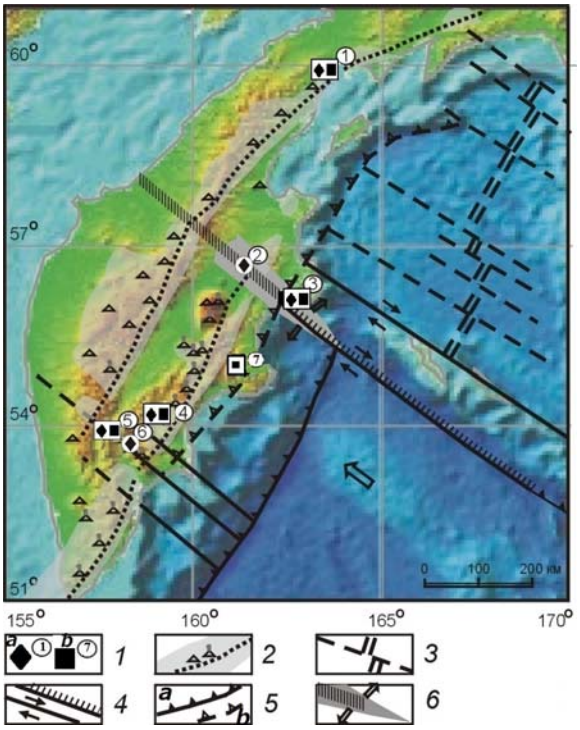


Fig.1. Tectonic position of Kamchatka NEB and adakites .
1 – Adakites locations (a), intraplate lavas (b); *2* – volcanic belts, volcano and volcanic front; *3* – paleo-rifts and transform faults, 4 - trenches (a) and paleo-trenches (b); 5 –faults; *6* – slab window.

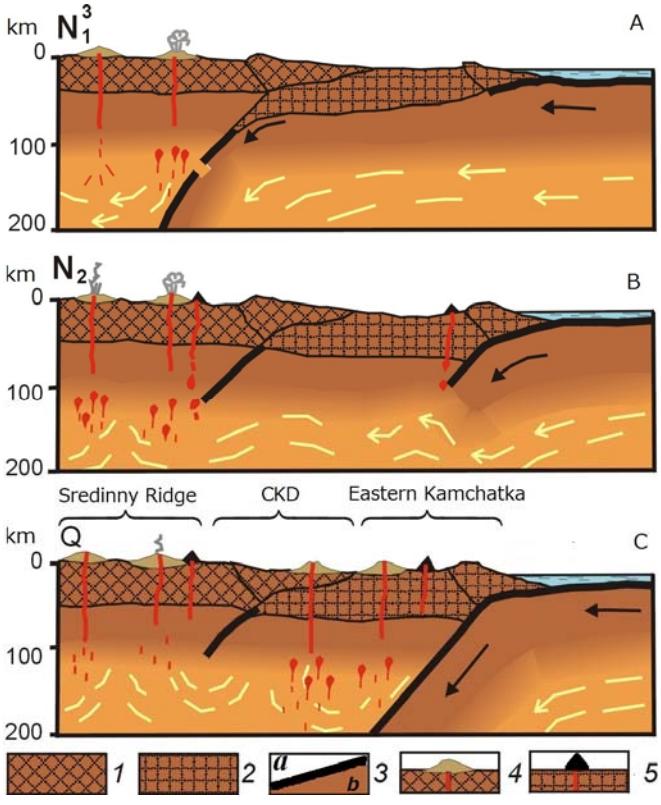


Fig. 2 The model of the Miocene-Quaternary geodynamic evolution and Kamchatka volcanism.
1 – the continental crust; 2 – Kronotskaya paleoarc continental crust; 3 – the oceanic crust (a) and the lithosphere (b), the arrows show the Pacific plate direction; 4 – volcanoes; 5 – NEB and adakite formations .

Геодинамические условия образования адакитов и внутриплитных лав в зоне субдукции Восточной Камчатки

Г.П. Авдейко [1], О.В. Кувикас[1], А.А. Палуева [1]
[1] *Институт вулканологии и сейсмологии ДВО РАН, Петропавловск-Камчатский, 683006;* e-mail: gavdeiko@kscnet.ru

В пределах субдукционной системы Восточной Камчатки, наряду с обычными известково-щелочными (ИЩ) породами островодужного типа, встречаются щелочные базальты с внутриплитными геохимическими характеристиками (NEB), высокомагнезиальные андезиты и адакиты (рис. 1). Имеются случаи совместного (позиции 1, 3-5 на рис. 1) и раздельного нахождения NEB и адакитов. Вулканические породы NEB типа и адакиты распространены фрагментарно и встречаются только в том сегменте, в котором произошел перескок зоны субдукции на современное положение [1]. Они характерны для раннего этапа субдукции. По возрастным характеристикам намечается эволюционный ряд от щелочных внутриплитных и переходных базальтов (7-12 млн. лет) через породы с адакитовыми характеристиками (3-8 млн. лет) до современных известково-щелочных пород [5].

Формирование NEB и адакитов определяется геодинамической эволюцией Камчатки (рис.2). В позднем олигоцене-миоцене существовала зона субдукции под Срединный хребет, располагавшаяся примерно в 200 км от ее современного положения, и соответствующая ей вулканическая дуга. В конце миоцена произошел «перескок» субдукции на современное положение и начал формироваться сегмент вулканической дуги Восточной Камчатки (рис. 1 и 2а). На начальном этапе субдукции происходило плавление головной части вновь сформированного слэба на контакте с горячей астеносферой (рис 2б). Дополнительный разогрев Тихоокеанской плиты и астеносферы, вероятно, был связан с флексурообразованием и вулканизмом Тихоокеанской плиты по модели [4] еще до подхода ее к зоне субдукции. В астеносфере на этом же контакте происходило формирование мантийного диапира или плюма типа «andersonian» по модели [3]. В результате апвеллинга диапира происходило его декомпрессионное плавление, а расплав NEB типа обусловлен низкой степени парциального плавления. По такому же сценарию, по-видимому, происходило образование NEB и адакитов на вулкане Сент Хеленс [2], в вулканической дуге Zamboanga, Филиппины [7], на вулканах Daisen и Sambe [6], в районе р. Валоваям на Камчатке (позиция 1 на рис. 1). Аналогичным образом объясняется приуроченность NEB и адакитов к трансформным разломам на полуострове Камчатский мыс и на юге Срединной Камчатской Депрессии (позиции 2. 3. и 5 на рис. 1), где в период «перескока» зоны субдукции открывались субдукционные окна (slab windows). Здесь также наблюдается контакт краев слэба с горячей астеносферой.

Рассмотренная гипотеза объясняет и приуроченность редких в островных дугах NEB и адакитов и к зоне «перескока субдукции, и кратковременность, и малый объём их проявления.

Список литературы

8. Avdeiko et al., 2007: AGU Monograph 172, 41-60.
9. *Defant, Drummond,1993:*Geology 21: 547-550.
10. *Faccenna et al,2010:* Earth and Planetary Science Letters 299 (1-2): 54-68.
11. *Hirano et al,2006:* Science 313: 1426-1428.
12. *Hoernle et al.,2009:* GCA 73(13).
13. *Morris, 1995:* Geology 23 (5): 395–398.
14. *Sajona et al,1996:* Journal of petrology37 (3): 693-726.

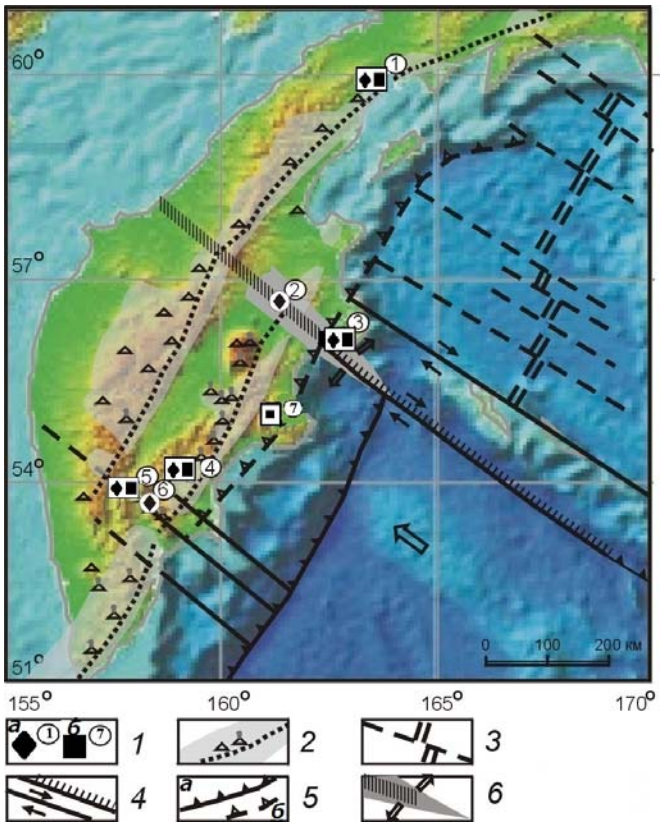


Рис.1.Тектоническое положение адакитов и NEB Камчатки.
1 – Местоположение адакитов (а), внутриплитных лав (б) *2* – вулканические пояса, вулканы, и вулканический фронт; *3* – палеорифты и трансформные разломы; *4* – желоба (а) и палеожелоба (б); *5* – разрывные нарушения; *6* – субдукционное окно.

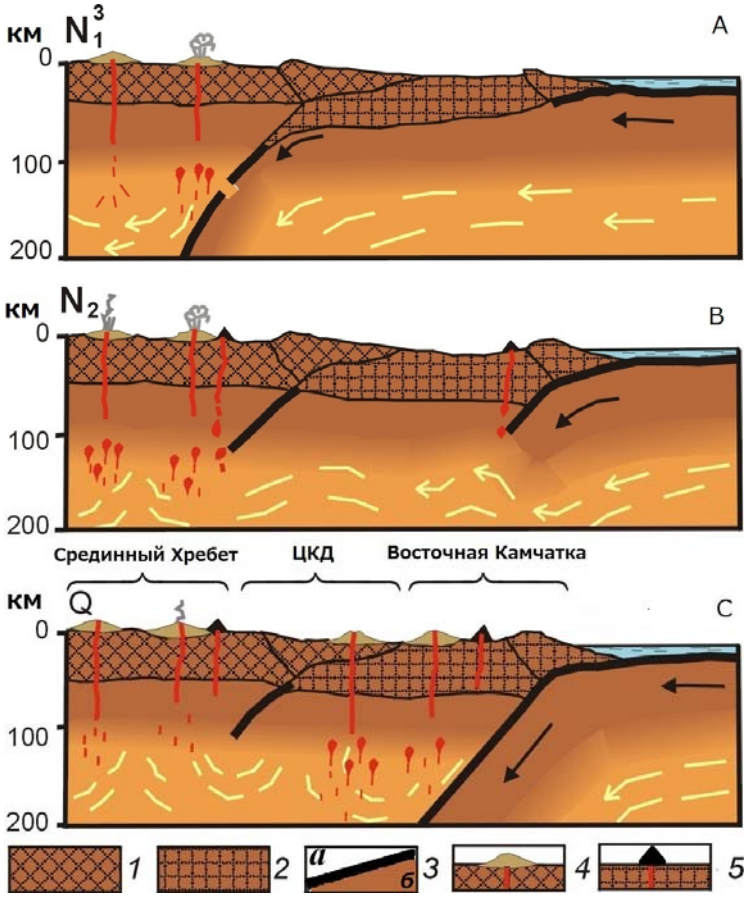


Рис. 2. Модель миоцен-четвертичной геодинамической эволюции и вулканизма Камчатки
1 – континентальная кора; 2 – континентальная кора Кроноцкой палеодуги 3 – океаническая кора (*а*) и литосфера (*б*) со стрелками направления движения Тихоокеанской плиты; 4 – вулканы; 5 – NEB и адакитовые постройки.

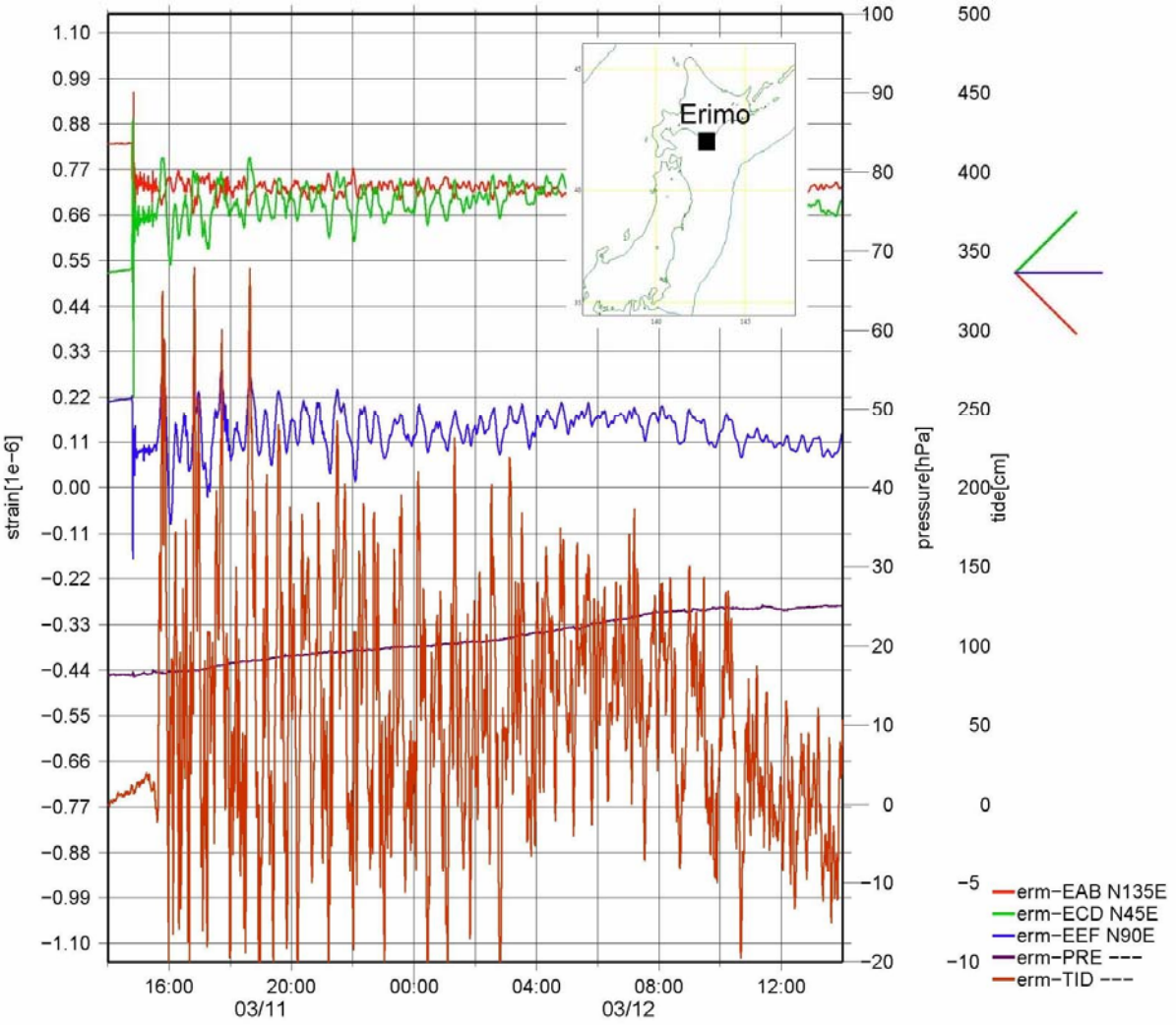
The 2011 Tohoku earthquake tsunami recorded by strain and tilt sensors at Erimo, Hokkaido, Japan

Akinari Shinjo and Hiroaki Takahashi
Institute of Seismology and Volcanology, Hokkaido University, Sapporo, Japan
a-shinjo0915@mail.sci.hokudai.ac.jp, hiroaki@mail.sci.hokudai.ac.jp

The 2011 M 9.0 Tohoku-oki earthquake generated catastrophic huge tsunami. Inhabitable areas along Pacific coast from Tohoku and Kanto regions were devastated by it. Real-time tsunami information from tide gauge stations should primary play important role for disaster operation. Unfortunately, functions of important tide stations were interrupted or destroyed by several severe troubles. Blackout due to strong ground motion was one of factors for failures. Backup battery system can solve this. Satellite communication also contributes to be keeping data transfer system.

Though tide gage or mareograph are the instruments to measure sea water level change, detector must be installed nearby sea. Sensors by bobber or ultrasonic technique have limit of maxim height itself, can not observe 30m height tsunami in principle. These conditions are not appropriate for hazardous tsunami observation. Destructive tsunami may destroy all functions of tidal stations, and in fact, we saw disappearing tide gage stations without traces by tsunami attack. Tsunami height information from Japan Meteorological Agency was devoid of data from most destroyed area. This data loss was crucial for disaster operation. This experience asks for another stable measurement system of gigantic tsunami. GPS-buoy system on sea is one of suitable techniques for hazardous tsunami observation.

Tsunami propagation generate loading on crust, hence, strain and tilt changes should be induced. We operate strain and tilt measurements with ultrasonic tsunami height sensor at Erimo, Hokkaido, Japan. Distance from mareograph to tunnel with crustal deformation sensors is 985m. Direct sea level measurement by ultrasonic sensor allows us to neglect effects of phase shift and nonlinear behavior due to sea-to-well conduit. Clear tilt and strain changes due to tsunami arriving were recorded. Maximum tsunami height by mareograph was 300cm. Observed coherent strain and tilt changes were 3*10-6 and 0.2*10-6, respectively. These values exceed minimum sensitivity considerably. Strain and tilt changes due to possible 60m height tsunami are much lesser than mechanical threshold of sensors. Tilt was more sensitive than strain, may reflect one-half loading. These facts clearly indicate strain and tiltmeters are available as tsunami sensor without height limitation.




```
start :2011/03/11 14:00:00
end   :2011/03/12 14:00:00
origin:// ,
Lat. N,  Lon. E,
Dep.  km Mj:
strike: dip: rake: score:
```

Earthquakes and tsunamis as sources of natural-technological disasters: the example of March 11, 2011 Tohoku events in Japan

Petrova Elena
Faculty of Geography, Lomonosov Moscow State University, Russia, epgeo@mail.ru

In recent years, the number and severity of natural-technological accidents and disasters are increasing all over the world. The term "natural-technological disaster" (Natech) applies to technological accidents and disasters triggered by any natural process or phenomenon. Their growth is accounted for, on the one hand, by observed increasing in frequency and intensity of various natural hazards, and on the other hand, by much more complicated structure of modern territorial and production complexes situated in zones of natural risk, as well as by increasing advancement of economic activities into the areas prone to natural hazards. Natural-technological disasters caused by earthquakes and devastating tsunamis have the most serious impact. A distinctive feature of these events is their synergistic nature, as a disaster spawns a secondary disaster that increases the impact on the technosphere, resulting in simultaneous occurrences of numerous technospheric accidents. Usually it is very difficult to deal with the consequences of such natural-technological disasters, because one has to cope not only with the primary aftermaths of the natural disaster, but also with the secondary effects of a number of technological accidents, which can be much more serious. These consequences are the more severe the higher are the population density and concentration of industrial facilities and infrastructure (especially hazardous objects, such as nuclear power plants, oil refineries and chemical plants, oil, gas, and gasoline piplines) in disaster-affected areas. However, all rapid reaction forces and resources tend to be aimed primarily at fighting the elements, which limits the capability to eliminate secondary technological impacts, especially in situations when transport facilities and necessary infrastructure are destroyed, and economic ties are broken.

One of the most large-scaled natural-technological disasters occurred on March 11, 2011 in Japan, as a result of a massive 9.0-magnitude earthquake off the northeast coast of Honshu Island, that caused a more than 30-meter tsunami. This disaster was yet another tragic confirmation of the vulnerability of modern techno-sphere and society, even such a highly developed one, as the Japanese, to the impact of natural hazards. The greatest number of fatalities and losses was caused by the tsunami, that struck the Miyagi, Iwate, Fukushima, Chiba, and Ibaraki prefectures. According to estimates made by the Japanese authorities, more than 25 thousand people died or are missing (including more than 22 thousand people as the tsunami victims). The infrastructure in the north-east of the country is damaged to a considerable extent (more than 130 thousand houses have been completely or partially destroyed, another 265 thousand homes were seriously damaged, thousands of miles of communications, roads and railways, more than 70 bridges were destroyed). With a total damage exceeded $300 billion, this disaster is the most destructive on record. The 2011 Tohoku earthquake and tsunami caused a number of technological accidents, including accidents at "Fukushima-1" and "Onagava" nuclear power plants, explosions and fires at refineries in Chiba, and at a petrochemical plant in Sendai, a number of other fires, railway, water, road, and other accidents. 148 lives have been lost in fires, 260 houses have been destroyed by fires (earthquake-report.com/2011).

The most serious consequence of the 2011 Tohoku earthquake and tsunami was a series of accidents at "Fukushima-1" nuclear power plant, which resulted in several leaks of radioactive substances into the atmosphere and the ocean. The accident was initially assigned to the 5-th, and later to the highest 7-th level of danger on 7-point International Nuclear Event Scale (INES). Right after the accident people (about 77 thousand) were evacuated from the 20-kilometer zone around the power plant, and the presence of people in the exclusion zone was prohibited. Later the evacuation area was extended to 60 kilometers.

The disaster had an impact on economic development not only in Japan but also in other countries. Many Japanese companies have suffered significant losses. The NPP “Hamaoka” situated in the Shizuoka Prefecture (200 km from Tokyo) with a predicted high probability of massive earthquake, was stopped. However, Japan, as well as Russia, does not intend to completely abandon nuclear power. Meanwhile some other countries declared a revision of their atomic energy programs. For example, the German government announced the decision to stop the operation of all the country's nuclear power plants by 2022.

Hopefully the lessons of the Japanese disaster will contribute to the increasing of safety of nuclear power plants and other high-risk facilities in our country. One of the main lessons of this tragedy lies in the fact that while placing, constructing and operating such facilities, it is necessary to consider carefully the potential impacts, including natural hazards.

Землетрясения и цунами как источники природно-техногенных катастроф: на примере события 11 марта 2011 г. в Японии

Петрова Е.Г.
Географический ф-т МГУ им. М.В. Ломоносова, Москва, epgeo@mail.ru

В последние годы в мире в целом отмечается нарастание числа и тяжести природно-техногенных аварий и катастроф. Под природно-техногенными понимаются аварии и катастрофы в техногенной сфере, спровоцированные какими-либо природными процессами или явлениями. Их рост объясняется, с одной стороны, наблюдающимся увеличением повторяемости и интенсивности проявления различных неблагоприятных и опасных природных процессов и явлений, а с другой стороны, значительно усложнившимся составом современных территориально-производственных комплексов, попадающих в зону природного риска, а также все большим продвижением экономической деятельности в районы, подверженные опасным природным воздействиям. Наиболее тяжелыми последствиями характеризуются природно-техногенные катастрофы, вызываемые землетрясениями и цунами разрушительной силы. Отличительной особенностью таких событий является их синергетический характер, когда воздействие на техносферу одного стихийного бедствия усиливается воздействием вызванного им другого стихийного бедствия, провоцируя одновременное возникновение многочисленных техносферных аварий. Ликвидация последствий подобных природно-техногенных катастроф обычно бывает сильно затруднена, поскольку приходится одновременно справляться не только с первичными последствиями самого стихийного бедствия, но и с вторичными последствиями целого ряда техногенных аварий, которые могут быть гораздо более серьезными. Последствия эти тем более тяжелы, чем выше плотность населения и концентрация промышленных и инфраструктурных объектов (особенно, объектов повышенной опасности, таких как АЭС, нефтеперерабатывающие и химические предприятия, нефте-, газо- и продуктопроводы) в затрагиваемых бедствием районах. При этом все силы и средства быстрого реагирования, как правило, бывают направлены, прежде всего, на борьбу со стихией, что ограничивает возможности ликвидации вторичных техногенных последствий, особенно в условиях, когда транспортные коммуникации и необходимая инфраструктура могут оказаться разрушенными, а экономические связи нарушаются.

Одна из крупнейших природно-техногенных катастроф произошла 11 марта 2011 г. в Японии в результате 9-ти балльного землетрясения у северо-восточного побережья острова Хонсю, вызвавшего более чем 30-тиметровые волны цунами. Эта катастрофа явилась очередным трагическим подтверждением уязвимости современной техносферы и общества, даже такого высокоразвитого, как японское, к воздействию природных опасностей. Наибольшее количество жертв и разрушений было вызвано цунами, основной удар которых пришелся на префектуры Мияги, Иватэ, Фукусима, Чиба и Ибараки. По оценкам японских властей, более 25 тыс. человек погибли или считаются пропавшими без вести (в том числе, более 22 тыс. человек – жертвы цунами). Значительно повреждена инфраструктура на северо-востоке страны (более 130 тыс. домов разрушены полностью или частично, еще 265 тыс. домов получили различные повреждения; уничтожены тысячи километров коммуникаций, автомобильных и железных дорог, разрушено более 70 мостов). По суммарному объему нанесенного ущерба, который превысил 300 млрд. долларов, это стихийное бедствие стало самым разрушительным за всю историю наблюдений. Землетрясение и цунами спровоцировали целый ряд техногенных аварий, в том числе аварии на АЭС «Фукусима-1» и «Онагава», взрывы и пожары на НПЗ в Чибе и на нефтехимическом предприятии в Сендае, множество других пожаров, железнодорожных катастроф, водных, автомобильных и других аварий. От пожаров погибло 148 человек, разрушено 260 домов (earthquake-report.com/2011).

Самым серьезным последствием события 11 марта 2011 г. стала серия аварий на АЭС «Фукусима-1», в результате которых произошло несколько утечек радиоактивных веществ в атмосферу и в океан. Аварии сначала был присвоен 5-й, а позднее – высший 7-й уровень опасности по 7-ми-балльной международной шкале ядерных событий (INES). Сразу после аварии было эвакуировано население из 20-ти-километровой зоны вокруг АЭС (около 77 тыс. человек), введен запрет на нахождение людей в зоне отчуждения; впоследствии зона эвакуации была расширена до 60-ти километров.

Катастрофа оказала воздействие на развитие экономики не только в самой Японии, но и в других странах. Многие японские компании понесли значительные убытки. Была остановлена АЭС «Хамаока» в префектуре Сидзуока (в 200 км от Токио), где по прогнозам, велика вероятность сильного землетрясения. Вместе с тем, Япония, как и Россия, не намерена полностью отказываться от развития атомной энергетики. В то время как некоторые другие страны заявили о пересмотре своих атомно-энергетических программ. Правительство Германии объявило, например, о решении прекратить эксплуатацию всех АЭС страны к 2022 году.

Остается надеяться, что уроки японской катастрофы послужат повышению безопасности АЭС и других повышенно опасных объектов в нашей стране. Один из основных уроков этой трагедии заключается в том, что при размещении, строительстве и эксплуатации таких объектов необходимо учитывать потенциально возможные воздействия на них, в том числе и природные.

Co- and post-seismic deformation of the 2011 off Pacific coast of Tohoku earthquake, Japan

Mako Ohzono[1], Yusaku Ohta[2], Takeshi Iinuma[2], and Satoshi Miura[3]

1. *Institute of Seismology and Volcanology, Graduate School of Science, Hokkaido University, Sapporo, Japan*
2. *Research Center for Prediction Earthquakes and Volcanic Eruptions, Graduate School of Science, Tohoku University, Sendai, Japan*
3. *Earthquake Research Institute, University of Tokyo, Tokyo, Japan*

The 11 March 2011 off the Pacific coast of Tohoku earthquake (M9.0, hereafter 2011 Tohoku earthquake) occurred at the subduction zone of Japan Trench, which is a plate boundary between the Pacific plate and the Okhotsk (or North American) plate. This huge earthquake generated a large tsunami, which caused a devastating disaster including the loss of more than 12,200 lives up to April 7. The Geospatial Information Authority of Japan (GSI) established GEONET, a nation wide GPS network composed of more than 1,300 stations (e.g. Hatanaka, 2003). There are, however, not so many GEONET sites near the coastline and some small offshore islands because of the area's accessibility problem. Since 1994, Tohoku University (TU) established new continuous GPS stations in Tohoku region to complement GEONET and improve detectability of the interplate slip expected during the predicted Miyagi-oki earthquake (Miura et al., 2004, 2006).

In order to investigate the co- and post-seismic crustal deformation, we estimated daily coordinates at 741 GPS sites, which include TU, GSI, Japan Nuclear Energy Safety Organization (JNES), National Astronomical Observatory (NAO), and International GNSS Service (IGS). We used Bernese GPS Software version 5.0 (Dach *et al.*, 2007) with precise ephemerides and earth rotation parameters distributed by IGS. Coordinates are referred to the ITRF2008 (Altamimi *et al.*, 2011) by constraining daily coordinate of four IGS sites (aira, daej, khaj, and yssk).

During the co-seismic displacement, two nearest GPS sites from the epicenter (knk, and en3, Kinkasan and Enoshima islands) recorded 5.6m of horizontal displacement directing ESE, and 1.2m of subsidence. It is the largest value among whole onshore GPS sites including GEONET site. Co-seismic horizontal displacement shows E~ESE directing in whole Tohoku region. On the other hand, significant subsidence appears along the Pacific coast. The simple rectangular fault model on the plate interface approximately explains observed co-seismic displacement field. For more detail, Iinuma *et al.* (2011) estimated variable slip distribution using same GPS data set, and its principal slip region is consistent with location of our estimated fault.

Post-seismic deformation is also revealed at extended region in and around Tohoku region. As of middle of May 2011 (two months after the mainshock), daily coordinate time series are well fitted with logarithmic function, assuming frictional afterslip (e.g., Morone et al., 1991). It is thought that afterslip is dominant in the early post-seismic period rather than viscoelastic relaxation. Thus this fitted logarithmic pattern is reasonable to explain the coordinate time evolution. The post-seismic deformation caused by such a huge earthquake, however, will expect during the several decades. In addition, effect of viscoelastic relaxation will be significant in later period (e.g., 1964 Alaska earthquake, discussed in Suito *and* Freymueller, 2009). It is important to continue monitoring post-seismic deformation by dense GPS network and estimate its mechanism, as a future works.

The imaging a lava dome density structure in Unzen with cosmic-ray muons

Seigo Miyamoto (3), Nicola D'Ambrosio (1), Giovanni De Lellis (5,6), Mitsuhiro Nakamura (4), Toshiyuki Nakano (4), Pasquale Noli (5,6), Hiroshi Shimizu (2), Paolo Strolin (5,6), Cristiano Bozza (7), Hiromichi Taketa (3), and Hiroyuki K.M. Tanaka (3)

(1) Ist Nazl Fis Nucl, Gran Sasso, I-67010 Laquila, Italy , (2) Kyushu Univ, Inst Seismol & Volcanol, Nagasaki 8550843,Japan, (3) Univ Tokyo, Earthquake Res Inst, Bunkyo Ku, Tokyo 1130032, Japan (miyamoto@eri.u-tokyo.ac.jp), (4) Nagoya Univ, Nagoya, Aichi 4648602, Japan , (5) Ist Nazl Fis Nucl, Naples, Italy, (6) Univ Naples Federico 2, Dipartimento Sci Fis, I-80126 Naples, Italy, (7) Salerno Univ, Italy

It is significant for the growth model of lava dome which has viscous magma to investigate the density structure in it. The first observation of the imaging a inner density structure in lava dome with cosmic-ray muons was performed by Tanaka et al. (2007) in Showa-shinzan, Japan. The result indicates that the growth model advanced by I. Yokoyama in 2002 is most compatible. The imaging analysis of Unzen lava dome with cosmic-ray muons is going on. The lastest lava dome in Mt. Unzen was formed in the eruption from January 1991 to early 1995 and the activity was calmed down in 1995. The formation of the lava dome in Unzen can be divided into two characteristic growth period, exogenous and endogenous. The exogenous dominant period is from January in 1991 to late 1993, the endogenous dominant period is from the end of 1993 to early 1995. Nakada et al (1995) observed that the surface of the lava dome was moving from the in endogenous period in Unzen. They proposed a growth model in the endogenous period in Unzen, which is based on their observation and the model includes "peel" structure. According to the dome growth model by Nakada et al, the current density structure in the lava dome should be the following:

1. The ellipsoidal massive part is in the center of lava dome.
2. The talus spread around the massive ellipsoidal.

In the talus region, there are a lot of air gaps, which makes the clear contrast in the image of density with muon-radiography. The muon detector, nuclear emulsion films which has high position resolution and 0.85m^2 effective area, was installed in Unzen from early December 2010 to the end of March. Now the analysis of nuclear emulsion is going on. We will report the preliminary result of the imaging Unzen lava dome.

Sensitivity study of eruption source parameters in numerical models for volcanic ash transport and deposition

K. B. Moiseenko [(1)], N. A. Malik [(2)]

[(1)] Obukhov Institute of Atmospheric Physics RAS, Moscow, konst.dvina@mail.ru
[(2)] Institute of Volcanology and Seismology FEB RAS,
Petropavlovsk-Kamchatsky, malik@kscnet.ru

Ash clouds due to volcanic eruptions are one of the major natural hazards affecting human activity. During volcanic eruptions, volcanic ash transport and dispersion models are commonly used in order to forecast ash propagation through the atmosphere downwind over hours to days to assess potential hazards to aircraft and human health. To predict correctly the ash cloud's propagation, these models require various source parameters to describe initial distribution of gaseous and aerosol compounds in the atmosphere in the vicinity of eruption. Unfortunately, the definition of key source parameters in particular events is not a trivial task due to lack of information on eruption cloud height, particle size distribution, start and end time of the eruption as well as its intensity. In this study, we use Hybrid Particle and Concentration Trasport (HYPACT) model which is a part of Regional Atmospheric Modeling System (RAMS6.0) to study sensitivity of eruption source parameters for volcanic ash transport prediction.

The results of numerical calculations for ash propagation are compared against the sample measurements conducted immediately after explosive eruption events on Bezymianny Volcano (Kamchatka) on 24 December 2006 and 17 December 2009, Karymsky on 21 April 2007, and Kizimen on 13 January 2011. It follows from the both model simulations and measurement data that the different assumptions on vertical mass distribution in the eruptive column can result in dramatically different ashfall patterns for the particles whose size ranges from 5 – 250 μm. The general notion is that the light particles (up to 50 – 70 μm) are distributed rather uniformly in the eruptive column, whereas for the larger particles there is a tendency for the eruptions of moderate intensity to accumulate in the first 3 – 4 km above the vent. Such non-uniformity is a result of complex interplay between two opposite factors: upwind convective transport and downward sedimentation due to gravity force. Volcanic particles aggregation in the event on Bezymianny 2006 seems to have dramatic effect on ash deposition resulting in enhanced deposited density values in the vicinity of the volcano. We use the inverse procedure based on least squares approach to restore total volume of erupted ash from computed and observed loadings. The obtained values for the eruption rates are in a good agreement with those obtained independently basing on observed terminal heights of eruption columns. This may serve as indication of good model performance in its ability to predict ash cloud transport and dispersion, as well as to restore total amounts of erupted tephra with use of the inverse modeling approach.

As example, estimations for source mass discharge rate based on plume height have been conducted for eruption event on Bezymianny Volcano (Kamchatka) on 24 December 2006 are considered briefly. The maximum height H of volcanic column was about 10 – 13 km based on visual inspection and satellite images of the volcanic plume. The atmospheric sounding at Kljuchi shows a tropopause at 8.8 km (280 mbar), so the terminal height of the volcanic column was well above the tropopause level. Invoking the relation between the

source mass discharge rate Q [kg/s] feeding volcanic column and maximum height (Carazzo et al., 2008, J. Geophys. Res. 113, B9) for the mid-latitude lapse rates,

$$Q = a H^4, \qquad (1)$$

where a=74 kg/s/km^4 (H<12 km), and time duration of the event 50 min, we obtained the value of 2.12 Mt as a rough estimate for the upper limit of total amount of ash particles emitted. Basing on best-fit arguments (see Figure 1), the total amount of ash particles (with the diameter less then 1 mm) emitted was about 1.75 Mt which is consistent with the above estimate (2.1 Mt) with use of Eq.(1).

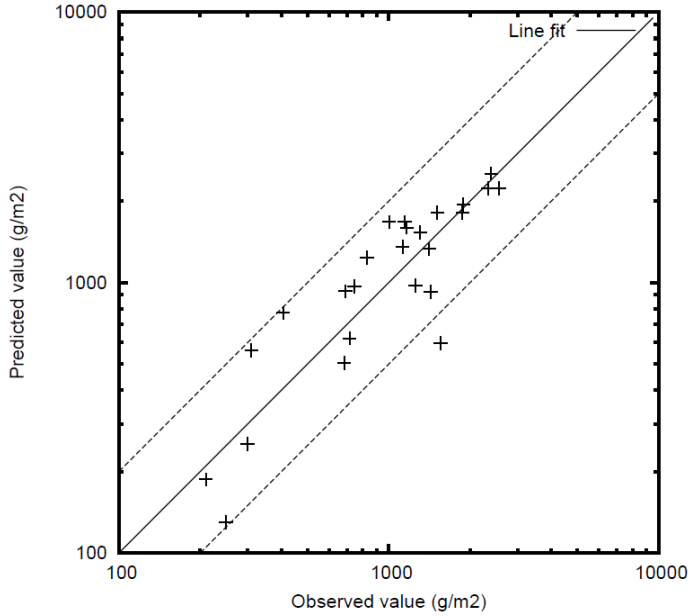


Figure 1. Comparison between computed and observed ground ash loadings based on the ash samplings around Volcano Bezymiannii after the explosive eruption event on 24 Dec 2006. Dashed lines indicate over- and under-estimations of ½ and 2 times the observed values.

The phreatic explosion consequences in Golovnina Caldera (Kunashir, Kurile Islands)

D. N. Kozlov

Institute of Marine Geology and Geophysics, FEB RAS Yuzhno-Sakhalinsk, Russia

The Golovnina Caldera is situated in the southern part of Kunashir Island. It is the highly truncated cone with the diameter about 10 km, and caldera diameter is about 4 km. Two extrusive domes of andesite-dacite composition are in the center of caldera. According to radiocarbon dating the giant explosions forming caldera were more than once 30-40 thousand years ago. The last phase of activation is connected with phreatic explosion as a result of which the crater Kipiashchii with the diameter 350 m formed. Now the volcano shows the regularly solfataric activity in submarine and coastal parts of the Goriachee and Kipiashchee lakes. The temperature of the solfataras is about 101°C (Marchinin, 1959; Fedorchenko, 1962). During large eruptions Golovnin volcano is dangerous for the settlements Dubovoe, Golovnino, Ivanovskoe, Alehino (the distance from Golovnon volcano up to 15 km).

The products of crater Kipiashchii phreatic explosion were studied for the creation of volcanic zonation maps of the southern part of Kunashir.

The crater of Kipiashchee lake cuts to lake deposits and the southern part of extrusive dome. The lake water is acid, sulphate-chloride with the mineralization 1.5 g/l and pH 3.32. The water temperature in the area of term outflow is not higher then 80-100єC , the surface temperature in other parts of lake is 30-60º C. The high of the crater upper rim is 195 m above the sea level , the crater depth is 30 m, the depth from water line is 24 m , the lake square is 66000 m². The sulphur content in the rocks near solfataric vents is up to 30-40%. The sulphur reserves are 40-45 thousand tons . Kipiashchee lake is connected with Goriachee lake by narrow channel. The formation of explosion funnel on data of different researchers has happened about 640-680 (Fazlullin, Batoyan, 1989) to 1000 years ago (Raszhigaeva, Ganzey, 2006).

We made an attempt to reconstruct the phreatic explosion in Kipiashchii crater. For the geographical allocation of the points with the use of GPS receiver we made a plan on the covering of the territory that is situated on the distance 2-3 km from Kipiashchee lake. In these points the descriptions of soil sections layers, their thickness measurings and other lithological special features were done. The sections near the explosion center are studied in more details. The samples selection, the description of the parameters of occurrence and other characteristics (inclusions, galls, irregularity of distribution, the samples selection for the radiocarbon dating) were done here.

As a result of the works done in the caldera of Golovnin volcano the information about the character of phreatic explosion deposits was collected. The thickness of the layer changes from 2-2,5 m on the lake shore up to 50-60 cm on the distance 500 m; on the distance 1500 the thickness of the layer is 20-30 cm; on the distance 2000-2500 m the thickness of the layer is 2-5 cm. The average diameter of the fragmental material is 8-12 cm on the distance 1000m and 3-5 cm on the distance 2000 m from the lake. On the lake shore the ballistic blocks with the diameter from 0.5-1.5 m are. The volume of material outburst was calculated on the base of this area mapping. This volume is 0.00241 км³, that corresponds with the volume of the funnel which is equal 0.00245 км³. The direction of the outburst material maximum is the south-west. The data systematization and their study allow to make the maps of isopachytes and isopleths of the phreatic explosion products. (Kozlov, Belousov, 2007; Kozlov, Belousov, 2006; Kozlov, Zharkov 2009).Received material will allow to work out the dynamical model of this nature process and to appreciate the dangerous of this wide spread natural phenomena .

Последствия фреатического взрыва в кальдере Головнина (Кунашир, Курильские о-ва)

Д. Н. Козлов
Институт морской геологии и геофизики ДВО РАН, г. Южно-Сахалинск, Россия.

Кальдера Головнина находится в южной части острова Кунашир. Представляет собой сильно усеченный конус с диаметром основания около 10 км, с кальдерой около 4 км в поперечнике. В центре кальдеры находятся два экструзивных купола андезито-дацитового состава. По данным радиоуглеродного датирования гигантские кальдерообразующие взрывы происходили неоднократно 30-40 тыс. лет назад. Последний этап активизации связан с фреатическим взрывом, в результате, которого образовался кратер Кипящий, диаметром около 350 м. В настоящее время, вулкан проявляет постоянную сольфатарную деятельность в подводной и прибрежной частях озер Кипящее и Горячее. Температура сольфатар не превышает 101°С. (Мархинин, 1959; Федорченко, 1962). При сильных извержениях вулкан Головнина представляет опасность для населенных пунктов Дубовое, Головнина, Ивановское, Алехино (удаление от вулкана Головнина до 15 км).

Для создания карт вулканического районирования южной части острова Кунашир нами были изучены продукты фреатического извержения кратера Кипящего.

Кратер озера Кипящего врезан в озерные отложения и южную часть Центрального экструзивного купола. Вода озера кислая, сульфатно-хлоридная с общей минерализацией 1,5 г\л и pH 3,32. Температура воды в районе разгрузки термальных вод не превышает 80-100°С, температура водной поверхности в других частях озера варьируется от 30 до 60°С. Высота верхней кромки кратера 195 м. над уровнем моря, общая глубина кратера 30м, глубина от уреза воды 24м, площадь озера 66000 м². Содержание серы в породах, находящихся вблизи сольфатарных выходов, доходит до 30-40 %. Общие запасы серы оцениваются в 40-45 тыс. тонн. Узким каналом оз. Кипящее соединено с оз. Горячим. Образование воронки взрыва, по оценкам разных исследователей, произошло от 640-680 л.н. (Фазлуллин, Батоян, 1989) до 1000 л.н. (Разжигаева, Ганзей, 2006).

Нами предпринята попытка реконструкции фреатического взрыва кратера Кипящего. Для географической привязки точек с помощью GPS приемника был составлен план по покрытию территории, находящейся на удалении 2-3 км от озера Кипящего. В этих точках проводилось описание слоев почвенных разрезов, измерение их мощности и других литологических особенностей. Более детально изучались разрезы в непосредственной близости от центра взрыва. Здесь проводился отбор образцов, описание параметров залегания и других характеристик (включения, линзы, неравномерность распределения, отбор проб для радиоуглеродного датирования).

В результате работ, проведенных в кальдере вулкана Головнина, собрана информация о характере отложений фреатического взрыва. Мощность слоя варьирует от 2-2,5м по берегам озера; до 50-60см на удалении 500 метров; на расстоянии 1500м мощность слоя 20-30 см; 2-5 сантиметровый слой распространяется на дистанции 2000-2500м. Средний диаметр обломочного материала составляет 8-12см на удалении 1000м и 3-5см на расстоянии 2000м от озера. На берегу озера встречаются баллистические блоки диаметром от 0,5 до 1,5 м. На основании проведенного площадного картирования был вычислен объем выброшенного материала, который составил 0.00241 км³, что довольно хорошо сходится с объемом воронки озера, который равен 0.00245 км³. Направление максимального разноса обломочного материала – юго-запад. Систематизация данных и их обработка позволила составить карты изопахит и изоплет продуктов фреатического взрыва.(Козлов, Белоусов, 2007; Kozlov, Belousov, 2006; Козлов, Жарков 2009). Полученный материал позволит разработать динамическую модель этого природного процесса и оценить степень опасности этого широко распространенного природного явления.

Solfataric and hydrothermal activity of volcanoes of Kunashir Island (Southern Kuriles, Russia)

Zharkov R.V.
Institute of Marine Geology and Geophysics FEB RAS

In Kunashir Island four active volcanoes are, three of which are on solfataric-hydrothermal stage of activity: volcanoes Golovnin (547 м), Mendeleev (889 м) and Ruruy (1485 м).

Modern solfataric-hydrothermal activity of Golovnina volcano (southern part of island) is shown as outputs solfataric gases and a hydroterm inside of caldera and on the foot of a volcano on the Okhotsk Sea coast. Inside caldera there are young extrusive andesite-dacite domes, six solfataric fields and two lakes, formed, basically, due to thermal waters. At coast, at northern foot of the volcano, hydrothermal outputs form Northern-Alekhinskiy and Southern-Alekhinskiy groups of thermal springs, the formation of these thermal waters is connected with Vneshniy extrusive dome (Zotov et al., 1988). For volcanoes-calderas to which Golovnin volcano concerns another features of distribution of hydroterm types are characteristic, than for stratovolcanoes. In the center of caldera of Golovnin volcano there are two extrusive domes, on their periphery as of hydrothermal-phreatic eruptions the lakes and solfataric fields formed. On solfataric fields there are outputs of gases with temperature up to 101 °C and outputs of acid, carbonic, sulphatic hydroterms with difficult cation structure. It is remarkable, that on coast of Kipyashchee Lake acid, carbonic, sulphatic thermal springs and subneutral, carbonic, sulphatic-hydrocarbonaceous calcite-sodium thermal springs adjoin. On periphery of the volcano, in the area of Vneshniy extrusive dome, mainly, acid, carbonic, sulphatic-chloride sodium-calcite Alekhinskiy thermal springs with temperature up to 55 °C discharge. The basic part of Southern-Alekhinskiy groups of thermal springs and outputs of steam with temperature up to 110 °C is located on the narrow beaches. Outside the Vneshniy dome subneutral, hydrocarbonaceous-sulphatic calcite-sodium terms with temperature up to 53 °C discharge. Isotope composition of hydrogen, oxygen, argon, helium and neon of thermal springs of Golovnin volcano (Baskov, Surikov, 1989; Cheshko, 1994; Chudaev, 2003) also corresponds to local meteoric waters.

Mendeleev volcano (the central part of island) is a stratovolcano, on the top of which extrusive dome of dacite composition is. Along annular fractures on periphery of extrusive dome the explosion funnels were formed, which now represent extinct and active solfataric fields (Abdurakhmanov et al., 2004). Outputs solfataric gases are concentrated on four active solfataric fields of a volcano: South-Eastern, Eastern, North-Eastern, North-Western. In valleys of the rivers and streams, originating from solfataric fields and from slopes of a volcano the groups of thermal springs of a various chemical composition are located. Thermal springs are located in the riverhead of Chetverikova Stream, Lechebnyy Stream, in the valley of Kislyy Stream, in the riverhead Lesnaya River, in the top and bottom current of Doktorskiy Stream, in the bottom current of Valentiny Stream, Tret'yakova Stream and Zmeinyy Stream, and also on the coast of Pacific Ocean in the area of cape Goryachiy. For hydrothermal systems of stratovolcanoes, such as Mendeleev volcano, are revealed the certain regularity of change of chemical and gas composition of thermal waters with height, depending on the distance from the center of a volcano to his periphery.

This regularity was allocated by many researchers (Markhinin, Stratula, 1977; Dunichev, 1983; Chudaev, Chudaeva, 2004 and many others), it proves by our data. On solfataric fields and in head of streams, besides the solfataric gases with temperature 100-108 °C, acid, carbonic, sulphatic sodium-calcite-magnesian hydroterms with raised maintenance Al^{3+}, Fe^{2+}, H^{+} and a mineralization up to 1 g/l are. Below, in the valleys of streams, acid hydroterms of chloride-sulphatic sodium structure with a mineralization 2-4 g/l (the thermal springs of Low group of Kislyy Stream and Doktorskiy Stream) is situated. At foot of the volcano the outputs of subneutral thermal springs mainly chloride sodium composition, with a mineralization from 0.6 g/l up to 15 g/l (Mouth group of Kislyy Stream, Stolbovskie springs, Tret'yakovskie thermal springs and hydrothermal outputs of the Goryachiy Plyazh) are located. Isotope composition of hydrogen, oxygen, argon, helium and neon in hydroterms of the

volcano Mendeleev (Baskov, Surikov, 1989; Cheshko, 1994; Chudaev, 2003; Chudaev, Chudaeva, 2004) corresponds to local meteoric waters that are explained by their prevailing participation in formation of hydroterms.

On Ruruy volcano (northern part of island) thermal and solfataric activity is concentrated on the western slope on the area about 1.5 км^2, solfataric fields and thermal springs form Neskuchenskaya group of thermal springs. The temperature of waters of thermal springs of Neskuchenskaya group varies from 40 °C in valleys of streams up to 90-100 °C on solfataric fields and on sea coast. On a chemical composition the waters of thermal springs investigated by us can be divided into three groups having different anion structure: sulphatic, sulphatic-hydrocarbonaceous, hydrocarbonaceous-sulphatic. The group of sulphatic thermal waters includes acid thermal springs of solfataric fields, neutral and alkalescent sulphatic-hydrocarbonaceous thermal springs are located below on the slope and on a sea coast. On a first sea terrace hydrocarbonaceous-sulphatic thermal springs is situated. Cations structure of thermal springs, irrespective of values pH, temperatures and heights of an output is practically equal. The isotope structure of hydrogen and oxygen of thermal waters (Cheshko, 1994) is practically identical to meteoric waters. It shows that in a feed of thermal waters, mainly, participate waters of an atmospheric origin which are heated up on depth and then rise to a surface.

Thus, high solfataric-hydrothermal activity is characteristic for volcanoes of Kunashir Island. Here practically all types of thermal waters known in the region of active volcanism locate. On different morphologenetic types of volcanoes (“difficult” stratovolcanoes Ruruy and Mendeleev, Golovnina Caldera) special regularities of change of hydrochemical types of thermal waters from the center to periphery of volcanoes are observed.

Gravity change with crustal deformation observed at Tokachi-dake volcano, Hokkaido, Japan

Noritoshi Okazaki[1] and Hiroaki Takahashi[2]
[1]Geological Survey of Hokkaido, Hokkaido Local Government, Sapporo, Japan
[2]Institute of Seismology and Volcanology, Hokkaido University, Sapporo, Japan

Tokachi-dake volcano, located at central Hokkaido with 2077m height, is one of active volcanoes in Kuril-Japan trench junction, and erupted in 1926, 1962 and 1988-89. Anomalous activation in geothermal activity and seismicity prior to above three eruptions had been observed. Re-activation in geothermal activity near active craters had stated and increased from 1995 to 2000, but its activity gradually decreased till 2006. Localized crustal deformation, however, has been detected by GPS in 2007 and accelerated in 2008 to 2009. It has still continued in 2011.

Repeating GPS observation network in and near active crater was constructed in 1998. This network is designed to observable both crustal deformation by GPS and gravity change by gravity meter. Data from simultaneous observation enable us to distinguish the source of deformation, deeper magmatic or shallow geothermal. We started GPS and gravity hybrid observation in 1998 by SCINTREX CG-3M gravity meter. More than one time measurements at a bench mark has been done to reduce measurement errors during a round-trip observation. Gravity meter has changed to SCINTREC CG-5 till 2010.

Figure indicated gravity changes since 1998. Reference benchmark is located at 3.4km northwest from active crater. No significant gravity changes were observed from reference to 3km distant. Gravity difference less than 0.2mGal in there indicated no gravity change during a decade. On the other hand, clear gravity decreasing with 0.12-0.14mGal, which indicating uplifting, was appeared at near crater benchmarks. GPS observation also indicated 0.3m uplifting at same benchmarks, and its free-air correction with 0.3086mGal/m give 0.1mGal reduction of gravity. These facts strongly implied gravity change was due to localized uplifting of ground surface, not due to magmatic activity.

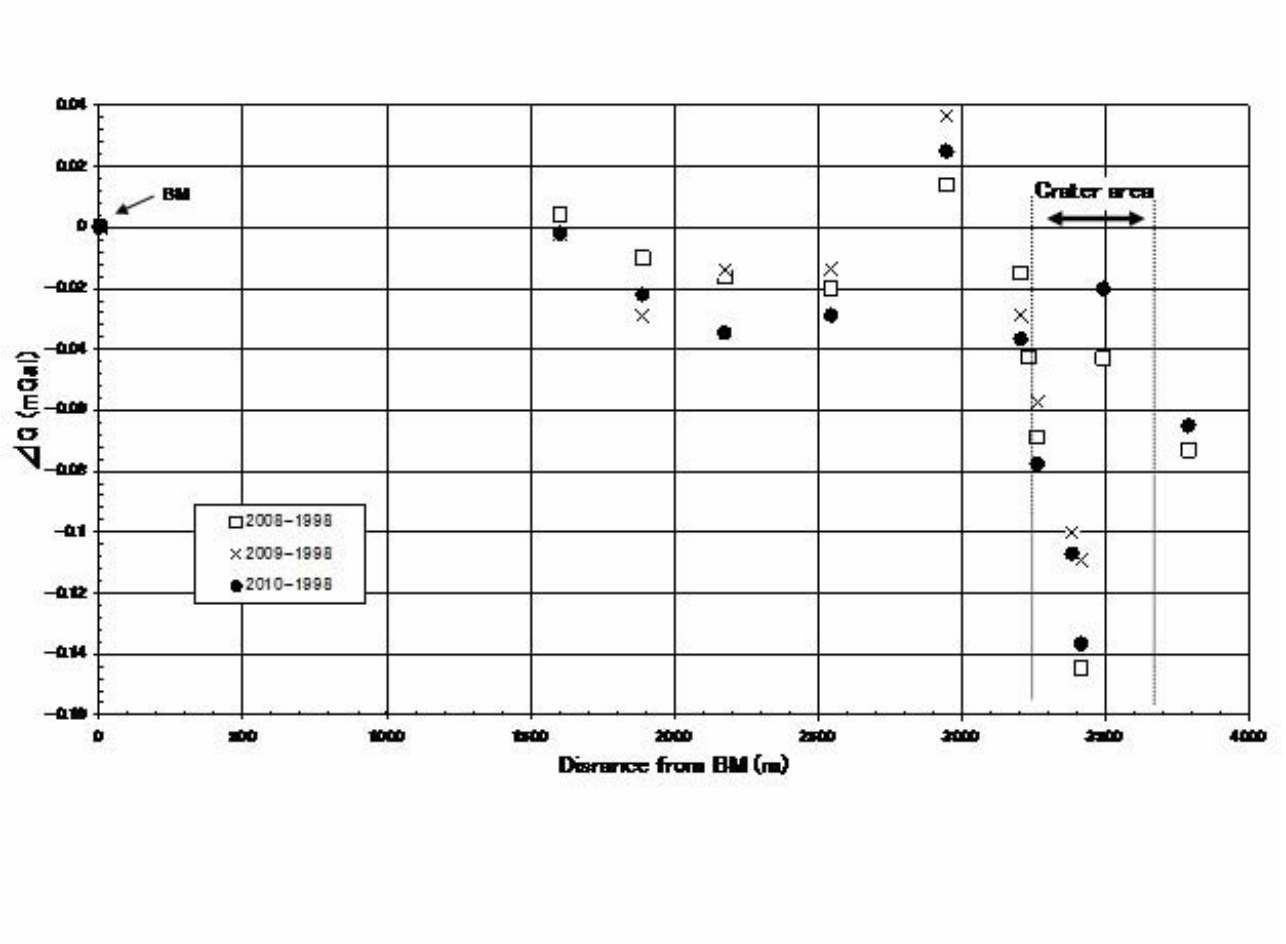


Figure caption. Gravity changes at Tokachi-dake volcano since 1998. Reference benchmark is situated 3.4km northwest of active crater. Clear gravity decreasings were observed at bench marks in crater area.

Features of dynamics of ice files on active volcanoes, Kamchatka

Muravyev Y.D.[1], Muravyev A.Y.[2], Osipova G.B.[2]

[1)] Institute of Volcanology and Seismology FED RAS, Petropavlovsk-Kamchatsky
[2)] Institute of Geography RAS, Moscow

The most part of glaciers of Kamchatka is placed on volcanic massifs, and on many of them signs of dynamic instability are well expressed. So around Kljuchevskoy volcanic massif of such glaciers at least 10. These are glaciers Bilchenok, Bogdanovicha, Ermana, Schmidta, Sopochny, etc. Peculiarities of dynamics of these glaciers basically are connected with their reaction to effects of seismic preparation, and also eruptive and seismic activity during eruptions.
As a result of eruptions there is an accumulation of a pyroclastic material on a surface of glaciers, there is a water significant amount on contact of ice to a bed, seismic activity amplifies that, despite adverse modern environmental conditions, causes advancing of glaciers.

So, during time of paroxismal eruption of the Kljuchevskoy volcano in 1944-45 about 250-300 million м^3 mixes of ice and erupted material in the form of a landslide have descended in area of accumulation of Erman Glacier. As a result this glacier continuously advances, having promoted by now more than on 4 km. During strong eruption of the Kljuchevskoy volcano in 1978 the advancing of the Schmidt Glacier has begun. It proceeded till 1987 when eruption has destroyed an average part of glacial tongue. Now the new advance of this glacier connected with topmost eruptions of the Kljuchevskoy volcano 2005-2010 is observed
There are also other examples of the glacial advances, which triggered by eruptions of volcanoes. The advancing of a Cheremoshny glacier has begun during Big fissure eruption of Tolbachik volcano in 1975/76
After eruption of the Avachinsky volcano in 1991 the Halaktyrsky glacier on a southern slope of volcanic construction advances to this day. The Kozelsky glacier, which tongue has been blocked by a thick layer (1,5-2m) of the superficial moraine consisting of products of eruptions of the Avachinsky volcano in 1945 is advancing.

The researches of evolution of the Bilchenok glacier – the largest surging glacier in Russia - are of particular interest. it's area of accumulation is located in a caldera of Ushkovsky volcano in Kljuchevskoy volcanic massif. The maximum position its tongue reached in the end of 19 centuries. After the period of degradation activization and advancement of glacier were fixed in 1949. The powerful surge of a glacier has occurred in 1959/60 when the front of its tongue has considerably advanced and has gone down in birch wood. The following surge of a glacier has occurred in 1980-83. Its scales were less considerable, and the volume of the transferred weight was in 3,5 times less, than at previous. During research of peculiarities of this surge its coincidence on time with strengthening of seismic actvity in vicinities of Ushkovsky volcano and evidences of volcanic activity at its top has been noted.
Now there is a next motion of this glacier. Under the available data glacier its tongue again has reached the maximum position.
Researches have shown that large advances of the Bilchenok glacier are preceded by less considerable ones, leading to increase of deterrant "stopper" in a trailer part of a glacier and to accumulation of additional pressure on an overlying site. Thus, duple character of "big surging cycle" of Bilchenok glacier irrespective of the reasons causing it is possible.

Особенности динамики ледяных массивов на действующих вулканах, Камчатка

Муравьев Я.Д.[1], Муравьев А.Я.[2], Осипова Г.Б[2].

1 – Институт вулканологии и сейсмологии ДВО РАН
2 – Институт географии РАН

Большая часть ледников Камчатки приурочена к вулканическим массивам, и на многих из них хорошо выражены признаки динамической нестабильности. Так в районе Ключевской группы вулканов таких ледников по крайней мере 10. Это ледники Бильченок, Богдановича, Эрмана, Шмидта, Сопочный, Влодавца и др. Особенности динамики этих ледников в основном связаны с их реакцией на эффекты сейсмической подготовки извержений, а также эруптивной и сейсмической активности во время самих извержений.

В результате вулканической активности происходит аккумуляция пирокластического материала на поверхности ледников, появляется значительное количество воды на контакте льда с ложем, усиливается интенсивность вулканических землетрясений, что, несмотря на неблагоприятные современные климатические условия, вызывает наступление языков ледников и стационирование их на белее низких высотах. Так, во время пароксимального извержения Ключевского вулкана в 1944-45 гг. около 250-300 млн $м^3$ смеси льда и изверженного материала в виде вулкано-гляциального оползня сошли в область питания ледника Эрмана. В результате этот ледник непрерывно наступает, продвинувшись к настоящему времени более чем на 4 км.

Имеются и другие примеры ледниковых подвижек, триггером которых являлись извержения вулканов. Подвижка ледника Черемошный на вулкане Толбачик началась во время Большого трещинного Толбачинского извержения 1975/76 гг. После извержения Авачинского вулкана в январе 1991 г. по сей день наступает Халактырский ледник, залегающий на южном склоне вулканической постройки. Наступает ледник Козельский, язык которого был перекрыт толстым слоем (1,2-2м) поверхностной морены, состоящей из шлаков извержения Авачинского вулкана в феврале1945 г.

Особый интерес представляют исследование эволюции крупнейшего в России пульсирующего ледника Бильченок, область питания которого расположена в кальдере вулкана Ушковский в Ключевской группе вулканов. Максимального положения его язык достигал в конце 19 века. Вслед за периодом отступания активизация и продвижение ледника отмечены в 1949 г. Мощная подвижка ледника произошла в 1959/60 г., когда фронт его языка продвинулся на 3 км и спустился в березовый лес. Следующая подвижка ледника произошла в 1982/84 гг. Ее масштабы были менее значительны, а объем перенесенной массы был в 3,5 раза меньше, чем в 1959/60. При исследовании особенностей этой подвижки было отмечено ее совпадение по времени с усилением сейсмической деятельности под Ушковским вулканом и термальной активности в его вершинных кратерах. В настоящее время происходит очередная подвижка этого ледника.

Главным источником опасности для территорий окружающих действующий вулкан являются наводнения и лахары, образующиеся при взаимодействии раскаленных продуктов извержения со снегом и льдом на его склонах.

Исследования показали, что крупным подвижкам ледника Бильченок предшествуют менее значительные подвижки, приводящие к образованию пробок в концевой части ледника и к накоплению дополнительных напряжений на вышележащих участках. Таким образом, возможен «двухтактный» характер пульсационного цикла ледника Бильченок независимо от вызывающих его причин.

Dynamics of the glaciers of the Kluchevskoy group of volcanoes: remote sensing data

Melnikov D.V., Muravjev Y.D.
Institute of Volcanology and Seismology FEB RAS, Petropavlovsk-Kamchatsky, Russia

Glaciers on volcanoes from Kluchevskoy group are strongly influenced by active volcanism. The increase of the volcanic activity leads to the changes in the glaciers' regime. About 30 glaciers, covering the area of 225.2 km^2, lay on volcanoes from the Kluchevskoy group. We can monitor the dynamic of glaciers' movements using the remote sensing methods.

Two types of satellite data are used in this work. Multi-spectral images (TERRA ASTER, Landsat, EO-1 ALI) were used for the visual control of changes in glaciers contours during the period from 2005 until 2011. We performed the correlation between activation of volcanoes, products of their eruptions (ash, pyroclastic flows, lava flows) and the shape of glaciers.

The second type of the data is satellite interferometry on a base of ALOS PALSAR data for the period from 2007 until 2010. Radar remote sensing methods represent the optimal solution for the research of the dynamic processes covering the large remote areas, difficult to access for the field works. Here we present the estimates of velocities of the Sredny, Erman and apical glaciers of Kluchevskoy volcano. The activity of glaciers at Kluchevskoy group of volcanoes is high; we defined their morphometric parameters and the distribution limits. We suppose that the activity of some glaciers is directly connected to the intensive eruptions of Kluchevskoy volcano.

Lahar danger of Kliuchevskoy volcano massif (Kamchatka)

Ludmila Kuksina[1], Elena Klimenko[1], Yaroslav Muravyev[2]

[1] Lomonosov Moscow State University, Moscow, Russian Federation

(ludmilakuksina@gmail.com)

[2] Institute of Volcanology and Seismology, Petropavlovsk-Kamchatsky, Russian Federation

(ya.muravyev@bk.ru)

Among the processes that accompany volcanic eruptions in Kamchatka, lahars (volcanic mudflows) are the most dangerous events for utility structures and local population. Population aggregates, surrounding Kliuchevskoy volcano massif, are situated far away from volcanoes (for example Kliuchi settlement is in 30 km from Kliuchevskoy volcano). Thereby they can't be damaged by pyroclastic or lava flows and scorching clouds because their action radius doesn't surpass 25 km. On the other hand lahars, which are even formed during slight eruptions, can cover a distance of 30 km and more.

In Kamchatka lahars are formed as the result of intensive snow and ice melting caused by solid discharges of scorching material. Movement of these flows, saturated with volcanic ash, slag and blocks of lava, occurs with velocity about 60 km in hour. They can lead to extensive damage and victims. That's why the estimation of probable lahars volume is necessary for population protection. In modern conditions we could make calculations with adequate accuracy and efficiency relying on GIS technologies (fig. 1).

Laharing is usually connected with the valleys of "dry" rivers draining slopes and foots of active volcanoes. The main subject of this research is rivers of Kliuchevskoy volcano massif, where lahars had ever occurred, and those ones, which are considered to be potentially dangerous of lahars. Therefore, the objective is to reveal the features of lahar flow formation as well as their danger estimation for the territories surrounding active volcanoes. The work is based on the results of field works, published works and cartographic and remote sensing materials.

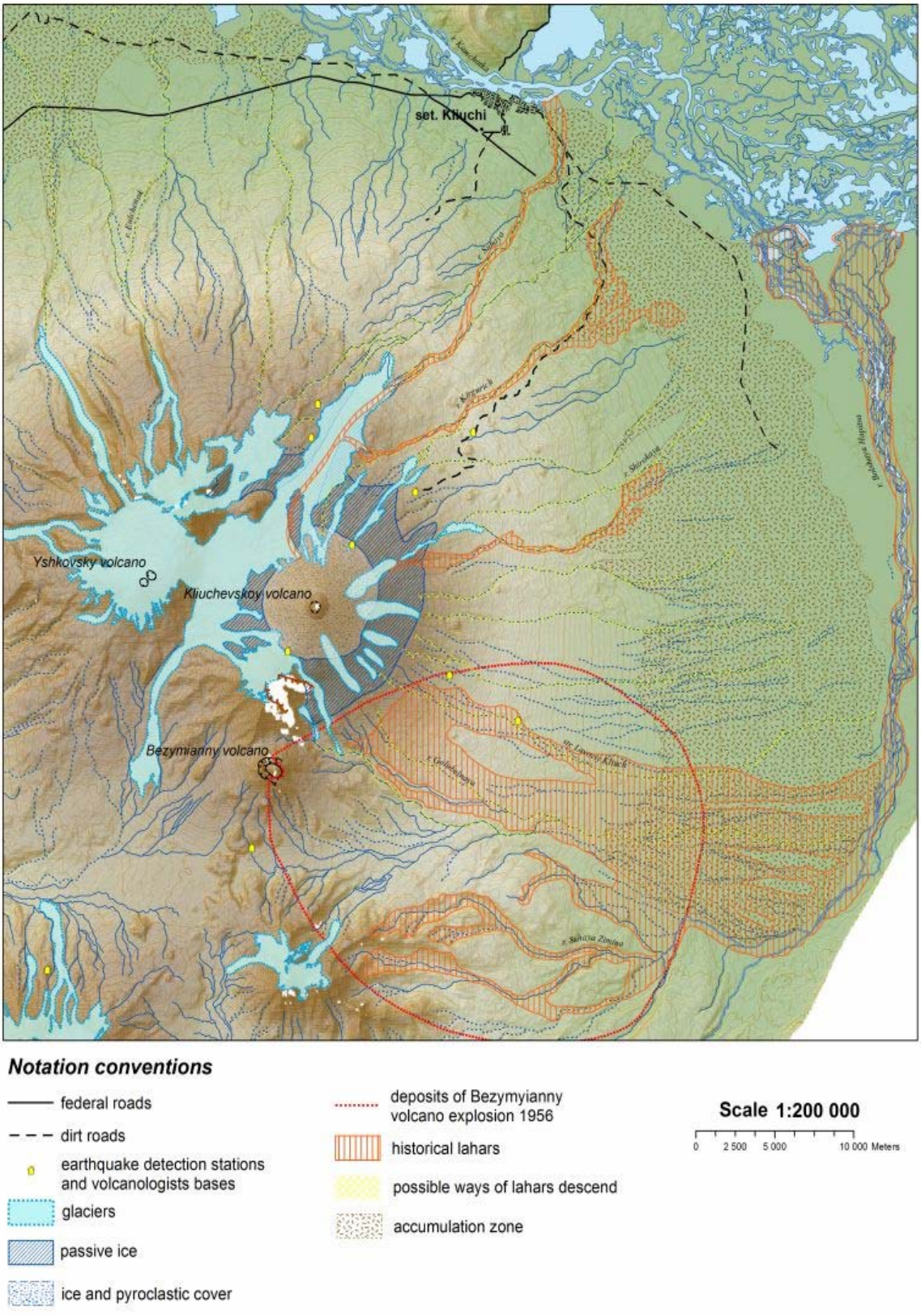


Fig. 1. Lahars of Kliuchevskoy volcano massif

Reflexion of development of volcanic activity of Klyuchevskoi volcanoes group in dynamics of *P-waves* velocity field (Under the seismological data**)**

L.B.Slavina[1], N.B.Pivovarova[1], S.L.Senyukov[2]
[1] Institution of physicists of the Earth of the Russian Academy of Sciences, Moscow, slavina@ifz.ru
[2] Kamchatka branch of Geophysical service of the Russian Academy of Sciences, Petropavlovsk-Kamchatsky

The Klyuchevskoy group of volcanoes (KVG) is the most powerful active group located in the north of Kamchatka and includes such active volcanoes as Klyuchevskoy, Krestovsky, Ushkovsky, Bezymianny, and Plosky Tolbachik. In the north Sheveluch volcano also belongs to this group. Now volcanoes of Klyuchevskoy group are in an activization stage, and it gives an urgency of carrying out of researches of features of dynamics of a structure of this group. In the given work the results of calculations of P-waves (V_P) velocity field in the area of Kljuchevskoy group according to volcanic earthquakes registered by the network of telemetric stations in the investigated area are presented. Calculations of the velocity field were carried out on the basis of results of processing of the weak volcanic earthquakes parameters registered in KF GS of the Russian Academy of Sciences during the period since 2005 to 2009.

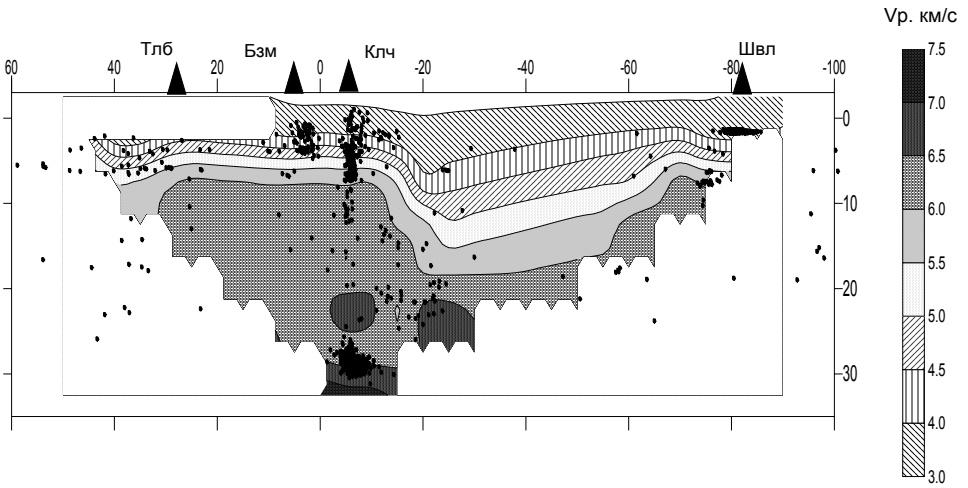
The principle of convertibility of wave fields is put in a basis of a design procedure of velocities *of P-waves* in the three-dimensional environment, namely the travel time of a seismic wave from point M_i (source) to point S_j (receiver) is equal to the travel time of this wave from point S_j to point M_i. Use of this principle allows considering set of travel times of a seismic wave from reasonably weak earthquakes to some seismic station, as a travel time of a reversible wave from this seismic station to chosen, closely located hypocenters of earthquakes.

As the initial information for considered algorithm serve: the system of seismic stations located in plane Z=0, co-ordinates of the hypocenters of earthquakes M_i (X_i, Y_i, Z_i), the travel time of a seismic wave from i-th focus to j-i stations - t_{ij}. Under this information three-dimensional distribution of speed V (X, Y, Z) in the areas occupied with the foci of earthquakes is defined. The technique developed by the authors [*Pivovarova, Slavina, 1981*] has allowed to restore velocity n the field of concentration of the volcanic earthquakes foci and to track its change in time and on depth. Calculations were carried out on the time periods characterizing various conditions of the activity of volcanoes according to the monitoring of volcanic activity, carried out in KF GS of the Russian Academy of Sciences.

Any of the methods applied before, including DSS, owing to methodical features did not allow tracking change of speeds in time and their communication with the process of volcanic activization.

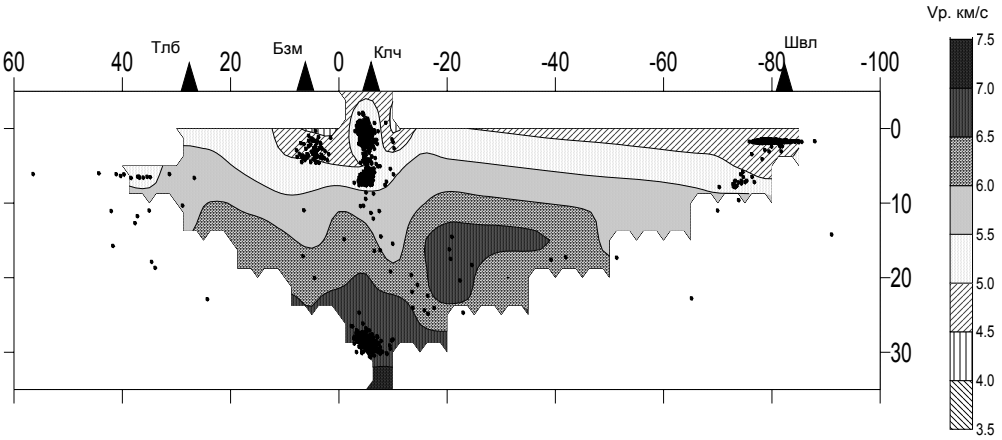
Carrying out the analysis of calculations of velocity cuts in plane XZ, it was possible to allocate characteristic features of the velocity field inherent in various conditions of volcanoes. So, during the periods of a quiet condition of volcanoes when earthquakes are localized on depths Z> 25-30 km, on borders of crust and mantle it is possible to observe restless behavior of the velocity isolines, lifting of high-speed horizons with V_P~6.5-7.0 km/s upwards with formation of separate ledges, in the direction of volcanic constructions. These values of velocity characterize so-called [*Fedotov, 2010*] crust-mantle mix. Lifting of magmas from deeper horizons of mantle upwards. During the periods of activity of volcanoes when earthquakes tend lifting upwards, in area of intermediate depths and in constructions of volcanoes, we see alignment of high-velocity borders, as though calm of a high-velocity field.

Two high-speed cuts, characterizing the various periods of volcanic activization are presented lower. The cut is constructed for the interval of time after central-type eruption in the spring of 2007: 01.12.2007-01.06.2008.



The velocity field is characterized by equal enough and quiet behavior of isolines. The isoline of 6.0 km/s velocity under volcanoes Klyuchevskoy and Bezymianny is fixed on depth of 8-10 km, at X =-20 the km step-like immersing to depth of 18-20 km is observed, with the subsequent lifting in the direction of Sheveluch volcano.

The following cut is constructed for the interval of 01.06-01.10.2008



Character of the velocity has changed, perturbations in the form of ledges of isoline V_P=6.0 km/s under the Klyuchevskoy volcano, and also an abnormal stain with values V_P=6.5-7.0 km/s on depths of 15-20 km northeast of the Klyuchevskoy volcano are observed.

Pivovarova N.B., Slavina L.B., design procedure and research of stability of three-dimensional fields of speeds of longitudinal waves (on an example of Kamchatka)//Izv. AH the USSR, Sulfurs. Physics of the Earth, 1981, №12, C.19-27.

Slavina L.B., Pivovarova N.B., Levin V. I. Use of the seismological data for studying of a high-speed structure of an active volcanic zone// Volcanology and Seismology, 2005. № 2. With. 45-56.

Slavina L.B., Pivovarova N.B., Garagash I.A., Levin V. I. Three-dimensional high-speed model of environment and a field of pressure of area of the Karymski volcanic center//Physics of the Earth, 2004, №7. C.13-24.

Fedotov S.A., Zharinov N.A., Gontovaja L.I.Magmatic feeding system of Klyuchevskoy group of volcanoes (Kamchatka) by data about its eruptions, earthquakes and deep structure.//Volcanology and seismology. 2010. № 1. With. 3-35.

Slavina L.B., Pivovarova N.B. Three-dimensional velocity model of focal zones and refinement of hypocenter parameters//Phys. of the Earth and Planet. Inter., 1992.V.75.p. 77-88

Отражение процесса развития вулканической активности Ключевской группы вулканов в динамике поля скорости *P*-волн (по сейсмологическим данным)

Л.Б. Славина[1], Н.Б. Пивоварова[1], С.Л. Сенюков[2]
[1]Институт физики Земли РАН, г. Москва, slavina@ifz.ru
[2] Камчатский филиал Геофизической службы РАН, г. Петропавловск-Камчатский

Ключевская группа вулканов (КГВ) является наиболее мощной действующей группой, расположенной на севере Камчатки и включает такие действующие вулканы как Ключевской, Крестовский, Ушковский, Безымянный и Плоский Толбачик. На севере к этой группе относится также вулкан Шивелуч. В настоящее время вулканы Ключевской группы находятся в стадии активизации, и это придает актуальность проведения исследований особенностей динамики строения этой группы. В данной работе представлены результаты расчетов поля скорости Р-волн (V_P) в области Ключевской группы по данным вулканических землетрясений, зарегистрированных сетью телеметрических станций в исследуемом районе. Расчеты поля скорости проводились на основании результатов обработки параметров слабых вулканических землетрясений, зарегистрированных в КФ ГС РАН в период с 2005 г. по 2009 г.

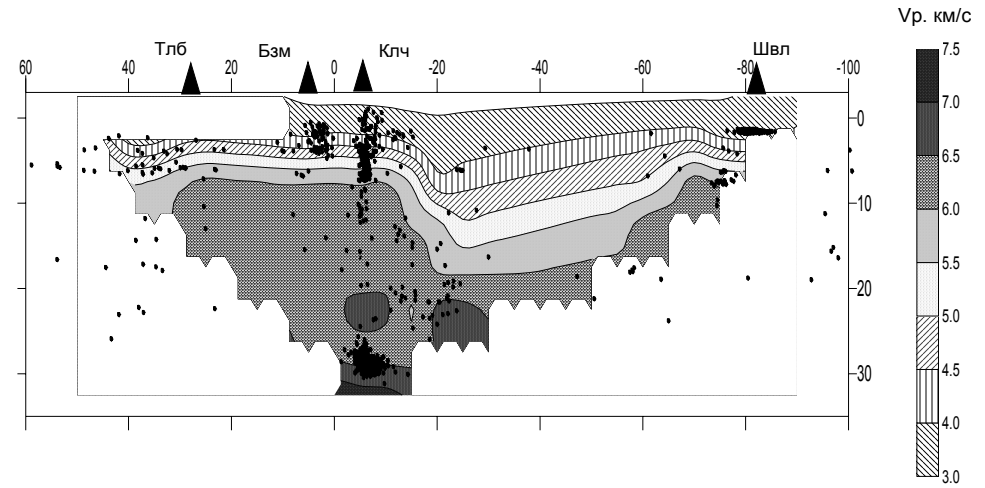
В основу методики расчета скоростей *P*-волн в трехмерной среде положен принцип обратимости волновых полей, а именно − время распространения сейсмической волны из точки M_i (источника) до точки S_j (приемника) равно времени распространения этой волны от точки S_j до точки M_i. Использование этого принципа позволяет рассматривать множество времен пробега сейсмической волны от достаточно слабых землетрясений до некоторой сейсмической станции, как времена пробега обратимой волны от этой сейсмической станции до выбранных, близкорасположенных гипоцентров землетрясений.

Исходной информацией для рассматриваемого алгоритма служат: система сейсмических станций, расположенная в плоскости Z=0, координаты гипоцентров землетрясений $M_i(X_i, Y_i, Z_i)$, времена пробега сейсмической волны от i-го очага до j-й станции – t_{ij}. По этой информации определяется трехмерное распределение скорости $V(X, Y, Z)$ в областях, занимаемых очагами землетрясений. Разработанная авторами методика [*Пивоварова, Славина, 1981*] позволила восстановить скорость в области концентрации очагов вулканических землетрясений и проследить за изменением ее во времени и по глубине. Расчеты проводились по временным периодам, характеризующим различное состояние активности вулканов по данным мониторинга вулканической активности, осуществляемых в КФ ГС РАН.

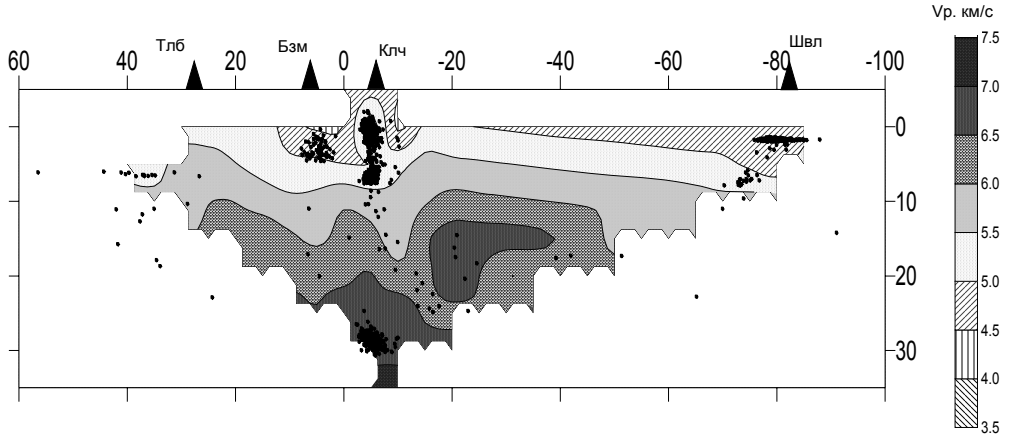
Ни один из применявшихся ранее методов, включая ГСЗ, в силу методических особенностей не позволял проследить за изменением скоростей во времени и их связи с процессом вулканической активизации.

Проводя анализ расчетов скоростных разрезов в плоскости XZ, удалось выделить характерные особенности поля скорости, присущие различным состояниям вулканов. Так, в периоды спокойного состояния вулканов, когда землетрясения локализуются на глубинах Z>25-30 км, на границах коры и мантии можно наблюдать неспокойное поведение изолиний скорости, подъем вверх высокоскоростных горизонтов с V_P~6.5-7.0 км/с с образованием отдельных выступов, в направлении вулканических построек. Эти значения скорости характеризуют так называемую [*Федотов, 2010*] коромантийную смесь. Подъем магм из более глубоких горизонтов мантии вверх. В периоды активности вулканов, когда землетрясения имеют тенденцию подъема вверх, в область промежуточных глубин и в постройку вулканов, мы видим выравнивание скоростных границ, как бы успокоение скоростного поля.

Ниже приведены два скоростных разреза, характеризующих различные периоды вулканической активизации. Разрез построен для интервала времени после вершинного извержения весной 2007 г. - 01.12.2007-01.06.2008 гг.



Поле скорости характеризуется достаточно ровным и спокойным поведением изолиний. Изолиния скорости 6.0 км/с под вулканами Ключевской и Безымянный фиксируется на глубине 8-10 км, при X=-20 км наблюдается ступенеобразное погружение до глубины 18-20 км, с последующим подъемом в направлении вулкана Шивелуч. Следующий разрез построен для интервала 01.06-01.10.2008 г.



Характер поля скорости изменился, наблюдаются возмущения в виде выступов изолинии V_P=6.0 км/с под Ключевским вулканом, а также аномальное пятно со значениями V_P=6.5-7.0 км/с на глубинах 15-20 км северо-восточнее Ключевского вулкана.

Пивоварова Н.Б., Славина Л.Б., Методика расчета и исследование устойчивости трехмерных полей скоростей продольных волн(на примере Камчатки)// Изв. АН СССР,Сер. Физика Земли,1981,№12,С.19-27.

Славина Л.Б., Пивоварова Н.Б., Левина В.И. Использование сейсмологических данных для изучения скоростного строения активной вулканической зоны // Вулканология и Сейсмология, 2005. № 2. С. 45-56.

Славина Л.Б., Пивоварова Н.Б., Гарагаш И.А.,Левина В.И. Трехмерная скоростная модель среды и поле напряжений района Карымского вулканического центра //Физика Земли,2004, №7. С.13-24.

Федотов С.А., Жаринов Н.А., Гонтовая Л.И. Магматическая питающая система Ключевской группы вулканов (Камчатка) по данным об ее извержениях, землетрясениях и глубинном строении.// Вулканология и сейсмология. 2010. № 1. С. 3-35.

Slavina L.B., Pivovarova N.B. Three-dimensional velocity model of focal zones and refinement of hypocenter parameters//Phys. of the Earth and Planet. Inter., 1992.V.75.p. 77-88

S.A. Khubunaya, L.I. Gontovaya, S.V. Moskalyova
Institute of Volcanology and Seismology FEB RAS
A.V. Sobolev, V.G. Batanova
V.I. Vernadsky Institute of Geochemistry and Analytical Chemistry SB RAS
D.V. Kuzmin, O.B. Kuzmina
V.S. Sobolev Institute of Geology and Mineralogy RAS

About the peripheral magma chamber of the Klyuchevskoi Volcano

From September 7 till October 2, 1994, there was a powerful apical eruption of the Klyuchevskoi Volcano. The most significant characteristics of this eruption are the absence of the abyssal seismic preparation before it's beginning and the powerful Plinian stage at the end of the eruption. The composition of the volcanic products was greatly differentiated. The eruption began with the ejecting of the scoria lapilli of the andesite-basalts (SiO2=55-56%) and it ended with the effusion of the pyroclastic flows of the basalts (SiO2=52-53%). Such extent of differentiation within single apical eruption of the Klyuchevskoi Volcano is reported for the first time.

The natural quenched glasses of the melt inclusions in the olivines of the scoria lappilli also show highly differentiated composition: from high-aluminous basalts to andesites. The concentrations of the volatiles (S and Cl) in the inclusions drastically diminish with the increase of SiO_2.

Massive study of the basalts and andesite-basalts of the initial and final stages of the 1994 eruption revealed significant differences in composition of their phenocrysts. The lavas and scoriae of the initial stage are typical high-aluminous andesite-basalts characteristic for all the apical eruptions of the volcano with low-magnesium clinopyroxenes and olivines (Fo79-65), with inclusions of the titanomagnetites. The blocks and fragments of the lavas of the pyroclastic flows of the final stage of the eruption as well as the described high-aluminous andesite-basalts contain homeogeneous inclusions of the plagioclase and magnetite accumulative rocks and high-magnesium phenocrysts of pyroxenes and olivines (Fo 91-85) with the inclusions of chromium spinel.

Reported here results suggest that there can be a layered magma chamber under the cone of the volcano. In the beginning of the eruption the magma came through from the upper apical part of the chamber. In the final, Plinian phase of the eruption the magma from the lower part of the peripheral intermediate chamber was taken as a result of a powerful explosion.

The reported data on the existence of a magma chamber under the cone of the Klyuchevskoi Volcano conform to the results of seismological and gravimetric structure studies. Accordingly, in the velocity model constructed with the seismic tomography method under the Klyuchevskoi group of volcanoes, a down warping of the foundation with the low values of Vp and Vs in the depths interval of 0-7 km has been discovered. The anomaly of Vp within the limits of this zone may reach 15%. The obtained seismic data do not contradict the possibility of the presence of a peripheral chamber within the limits of the discovered area.

As a result of the gravitational modeling carried out on the Klyuchevskoi Volcano under its cone in the 90s at the depth of 0-5 km a zone of low density (2,5 g/cm3) has been marked out that can also be connected to the peripheral magma chamber with the diameter of about 10 km.

Seismological study on precursors of the small phreatic eruptions at Meakan-dake volcano in 2006 and 2008

Hiroshi AOYAMA[1)] and Masashi OGISO[2),*)]

1) Institute of Seismology and Volcanology, Graduate School of Science, Hokkaido University, N10W8, Kita-ku, Sapporo, Hokkaido, 060-0810, JAPAN

2) Sapporo District Meteorological Observatory, Japan Meteorological Agency, N2W18, Chuo-ku, Sapporo, Hokkaido, 060-0002, JAPAN

*) Now at Osaka District Meteorological Observatory, Japan Meteorological Agency,4-1-76, Otemae, Chuo-ku, Osaka, Osaka, 540-0008, JAPAN

Meakan-dake volcano is an andesitic stratovolcano at an elevation of 1,498 meters; it stands on the southwestern rim of Akan Caldera in eastern Hokkaido. The documented eruptions since 1957 have all been phreatic explosions that occurred at the Pon-machineshiri summit crater (Figure 1). In the past quarter century, the volcano has produced five phreatic explosions in 1988, 1996, 1998, 2006 and 2008. Although it's not always true that volcanic earthquake swarms are accompanied by eruptive activities, the 2006 and 2008 eruptions had several evident seismic swarms and tremors months in advance. The eruption in 2006 was the first one that was observed by a broadband seismometer in Meakan-dake volcano.

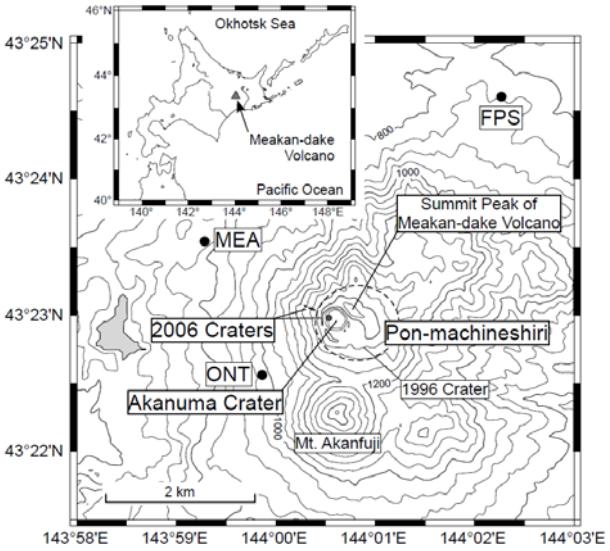


Figure 1. Contour map of Meakan-dake volcano showing location of seismic station (black circle). Contours represent 50-m elevation intervals. Dark and light gray spots are crater areas made by the 2006 and 1996 explosions, respectively. Inset shows location of Meakan-dake volcano.

The eruption on March 21, 2006 was associated with two precursory seismic swarms, the first one continued for about five days from February 18 to 22, comprising more than 1250 earthquakes. About 20 days later, on March 11, the second swarm began. Then, the seismicity increased once again one day prior to the phreatic explosion on March 21. The first swarm comprised small earthquakes and two volcanic tremors. The volcanic tremors occurred at around 0552, February 19, and at 0550, February 20. The

largest earthquake during this swarm overlapped with the first tremor, and soon after the first tremor, the number of earthquakes began to decrease.

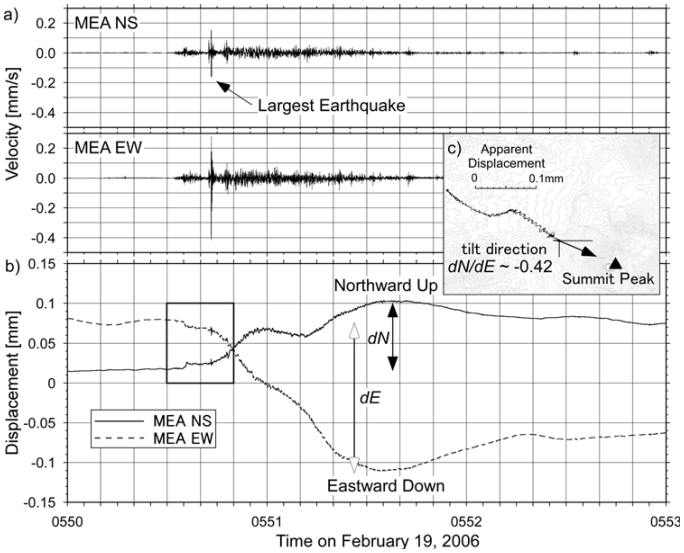


Figure 2. (a) Horizontal ground velocity at MEA. (b) Displacement traces obtained by simple integration. (c) Maximum downward tilt direction estimated from displacement traces.

An anomalous very-long period signal (VLP signal) was found in the seismic trace of the first tremor recorded at station MEA. The signal was masked by a short-period motion in the original velocity waveform, but a considerable DC step of about 0.21 mm appeared in displacement trace, especially prominent in the horizontal components (Figure 2). Such step in the displacement trace of the horizontal components can be attributed to an inclination of a seismometer due to tilt change. Aoyama and Oshima [2008] theoretically obtained the conversion factor from apparent displacement to tilt change for CMG-40T seismometer as 4.48 μrad/mm and confirmed the value and tilt response of CMG-40T by a laboratory experiment. Since the observed waveform can be regarded as the sum of translational motion and rotational motion, they estimated a time function of volumetric change under the isotropic source assumption. After the 2006 eruption, ISV, Hokkaido University installed two additional CMG-40T seismometers in Meakandake volcano area.

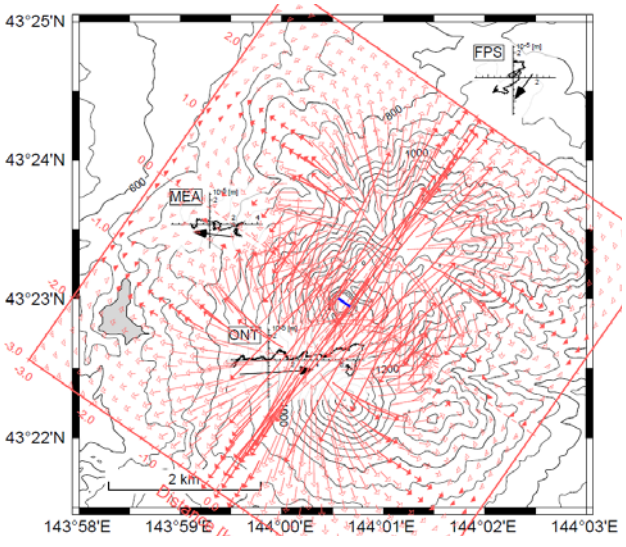


Figure 3. Down-dipping directions of the three seismic stations estimated from apparent displacement traces. Red arrows are theoretically expected spatial distribution of down dipping tilt change at the ground surface due to opening of a vertical crack beneath Akanuma crater. Amount of dike opening is arbitrary.

The eruption on November 18, 2008 was also preceded by three seismic swarms; the first one began on September 26 and continued for about 5 days and the second one observed in late October. Increase in seismicity began again since No-

vember 5 and the third swarm lasted more than 10 days till the eruption on November 18. Several volcanic tremors have also been observed during the precursory stages over about two months. The biggest tremor occurred on September 26, which only consisted of short period components, was large in amplitude but short in duration. On the other hand, a long sustaining tremor occurred at around 0053, November 16, contained strange VLP component that suggests tilt changes. The VLP signal was commonly recorded at three broad-band seismic stations; one of them, station MEA, indicates subsidence of the mountain side similar to the tilt motion of the 2006 precursor, and the remaining two conversely suggest uplift of the summit area. Such variation of the observed tilt motions may be explained by a non-isotropic source having azimuthal dependence on the surface deformation. Spatial pattern of the tilt change is modestly explained by the expansion of a vertical dike striking in the NW – SE direction located under the summit Akanuma crater. Although we still have only two examples, these two activities revealed that the broad-band seismometer is very effective for monitoring of tilt change associated with the volcanic activities.

Both tilt changes coincident with volcanic tremor in 2006 and 2008 preceded the phreatic eruption. A possible mechanism that caused the tilt change may be migration and/or phase change of volcanic fluid under the ground. For the 2008 eruption, source location of the volcanic tremor occurred on November 16 was investigated by the grid search method using high-frequency seismic signal amplitude (e.g., Battaglia and Aki, 2003; Kumagai et al., 2010). Centroid of the estimated source location is almost 1km away southward from the summit crater. This result may be inconsistent to the location of the vertical dike assumed to be a source of the tilt change that is located just beneath the summit crater. Future monitoring and researches will elucidate this inconsistency.

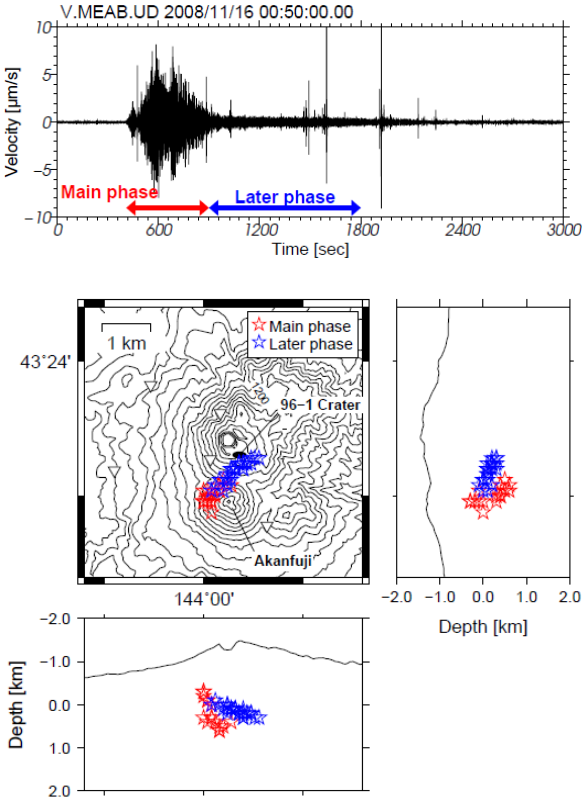


Figure 4. Velocity waveform of the volcanick tremor on Novemver 16, 2008 and its source location estimated from amplitude distribution.

ERUPSTION OF EBEKO VOLCANO AT 2009-2010 (PARAMUSHIR ISLAND, THE KURILES)

Kotenko T., Kotenko L., Sandimirova E., Shapar´ V., Timofeeva I.

Institute of Volcanology and Seismology, Far East Branch Russian Academy of Sciences, Petropavlovsk-Kamchatsky, 683006, Russia e-mail: kotenko@sakhalin.ru

Keywords: *a volcano, eruption, fumaroles, phreatic, resurgent ash*

Ebeko volcano is one of the most active ones in the Northern Kuril Islands. It is characterized periodically repeating phreatic-magmatic and phreatic eruptions along with strengthened fumarolic activity with single ash plumes happening (for example 1998). The previous historical eruptions of a volcano Ebeko are fixed in 1793, 1833-1834, 1859, 1934-35, 1963, 1965, 1967-1971, 1987-1991. The summit of Ebeko volcano has three adjoining craters with diameters 250-300 m each. Heat efflux and discharge of hydrothermal within the crater area take place on solfataric and fumarolic fields and on other heated sites on an area of > 1 km^2 .

Per 2005 the capacity of fumaroles in an Active funnel of Northern crater has increased, there there was a acid thermal lake. Also was formed new powerful fumarolic field Iyulsky ("Of July"), the temperatures of gases on which have increased within three months from 100°C up to 500°C (Kotenko et al., 2007). The geochemical harbingers of preparing eruption of a volcano were fixed: increase of ratio S/Cl, S/C, H_2S/SO_2, H_2O/CO_2 in fumarolic gases, in February, 2008 replaced by fall. The contents of gases of group of sulfur (SO_2, H_2S), HCl, N_2, Ar, H_2 on a background of growth of temperature of fumarolic gases also has increased. The given harbingers of eruptions are established for many of andesite volcanos, including for a volcano Ebeko (Menyailov et al., 1985, Menyailov et al., 1988, Fazlullin et al., 1998).

In 2009 began new eruptive cycle of a volcano Ebeko (Kotenko et al., 2010). A series of eruptions was located in an Active funnel of Northern crater. The first eruption last from January 29 till June 18, 2009. The character of eruption consist in the constant expiration of a gas-ash mix on height up to 300-1000 м above a crater and periodic ash explosions. The frequency of ejections was from 3 up to 15 events per day, height - 0.5 - 3.7 kms. The volcano produced phreatic event erupting resurgent ash. Total volume of the erupted materials comprised about 19 thousand of тons. By results of chemical and mineralogical analysis the ashes is on structure daziandesite and dazite.

After ending eruption of 2009 the volcano was in a condition high of fumarolic activity. The thermal capacity only of fumarolic jets made on the average 250 MW at background in the intereruptive period ~30 MW. In 2010 there were two eruptions of a volcano Ebeko - April 28 and July 2. Both eruptions were explosive short-term with small quantity of the cast out material (1.2 and 95 т accordingly). First - is probable on April 28, directly was not observed because of bad weather, is established on a layer of ashes around of a crater. The thefra was postponed in radius no more than 300 м from eruptive funnel. The second eruption has taken place on July 2, it proceeded 1 hour 27 mines. Height of ashes column made 700 м, length of 6 kms. The extending loop was focused on east. All eruptive material represents resurgent ashes. The basic fraction has the size less than 0.063 mm. The ashes is on structure daziandesite. Thus, both eruptions are phreatic. The volcanic earthquakes 4 type (on classification by Tokarev) were observed within 21.5 hours before the second eruption. Eruption of July 2 were anticipated by growth of the relations of sulfur to chlorine and sulfur to carbon in structure of volcanic gases.

After ending eruptions the chemical structure of fumarolic gases has come nearer to intereruptive period. The total issue of fumarolic gases still exceeds usual background issue of gases basically at the expense of a thermal flow from eruptive funnel and makes 80-110 MW.

This work was done with financial support from Russian Foundation for Fundamental Research (project 09-05-00022a) and Bureau of Far East Department of Russian Academy of Sciences (FED RAS) (project 09-III-A-08-418).

REFERENCES

Kotenko T.A., Kotenko L.V., Shapar V.N. Activation of Ebeko volcano in 2005-2006 (the Paramushir Island, North Kuril Islands) // Vulcanologiya i seismologiya. № 5. (2007) P. 3-13.
Kotenko T.A., Kotenko L.V., Sandimirova E.I., Shapar´ V.N., Timofeeva I.F. Eruption of Ebeko volcano from January through June 2009 (the Paramushir Island, the Kuriles) // Bulletin of Kamchatka regional association «Educational-scientific center». Earth sciences. № 1. (2010). P. 56-68.
Menyailov I.A., Nikitina L.P., Shapar V.N. Results of geochemical Monitoring of the activity of Ebeko volcano (Kuril Islands) used for eruption prediction // Journal of Geodynamics. N 3. (1985) P. 259-274.
Menyailov I.A., Ovsyannikov A.A., Shirokov V.A. Eruption of Ebeko volcano in October - December 1987 // Vulcanologiya i seismologiya. № 3. (1988). P. 105-108.
Fazlullin S.M., Timofeeva I. F., Kotenko L.V., Shapar V.N. Experience of tracking behind a condition of Ebeko volcano (Kuril islands) // Materials of the Russian -Japanese field seminar " Education of minerals and ore in volcano-hydrothermal systems of island arches: from model to operation ". Petropavlovsk-Kamchatsky. (1998). P. 252-255.

ИЗВЕРЖЕНИЯ ВУЛКАНА ЭБЕКО В 2009-2010 ГГ. (О. ПАРАМУШИР, КУРИЛЫ)

Котенко Т., Котенко Л., Сандимирова Е., Шапарь В., Тимофеева И.

Институт Вулканологии и Сейсмологии ДВО РАН, Петропавловск-Камчатский, 683006, Россия

Ключевые слова: вулкан, извержение, фумаролы, фреатический, резургентный пепел.

Вулкан Эбеко является одним из наиболее активных действующих вулканов Северных Курильских островов. Для него характерны периодически повторяющиеся фреато-магматические и фреатические извержения и активизация фумарольной деятельности с единичными выбросами пепла (например в 1998 г.). Предыдущие исторические извержения вулкана Эбеко зафиксированы в 1793 г., 1833-1834 гг., 1859 г., 1934-35 гг., 1963 г., 1965 г., 1967-1971 г., 1987-1991 гг. Вершина вулкана Эбеко представляет собой цепочку из трех сросшихся кратеров диаметром 250-300 м каждый. Вынос тепла и разгрузка гидротерм в пределах кратерной зоны происходит на сольфатарных и фумарольных полях и прогретых участках на площади ≥ 1 км^2.

В 2005 г. усилилась фумарольная деятельность в Активной воронке Северного кратера, там возникло термальное кислое озеро. Также образовалось новое мощное фумарольное поле Июльское, температуры газов на котором возросли в течение трех месяцев от 100°С до 500°С (Котенко и др., 2007). Были зафиксированы геохимические предвестники готовящегося извержения вулкана: увеличение соотношений S/Cl, S/C, H_2S/SO_2, H_2O/CO_2 в фумарольных газах, в феврале 2008 г. сменившееся падением. Также увеличилось содержание газов группы серы (SO_2, H_2S), HCl, N_2 , Ar, H_2 на фоне роста температуры фумарольных газов. Данные предвестники извержений установлены для многих андезитовых вулканов, в том числе и для вулкана Эбеко (Menyailov et al., 1985, Меняйлов и др., 1988, Фазлуллин и др., 1998).

В 2009 г. начался новый эруптивный цикл вулкана Эбеко (Котенко и др., 2010). Серия извержений была локализована в Активной воронке Северного кратера. Первое извержение длилось с 29 января по 18 июня 2009 г. Характер извержения заключался в постоянном истечении газо-пепловой смеси на высоту до 300-1000 м над кратером и периодическом усилении активности, выражающемся в резком увеличении в струе содержания пепла и увеличении ее дебита. Частота пепловых выбросов составляла от 3 до 15 событий в сутки, высота - 0,5 – 3,7 км. Извержение было фреатическим, изверженные продукты представлены резургентными пеплами. Объем вынесенного материала ~ 19 тыс. т. По химическому и минеральному составу свежевыпавшая тефра относится к дациандезитам, наиболее кислая разность – к дацитам

После завершения извержения 2009 г. вулкан находился в состоянии высокой фумарольной активности. Тепловая мощность только фумарольных струй составляла в среднем 250 МВт при фоновой в межэруптивный период ~30 МВт. В 2010 г. произошли два извержения вулкана Эбеко - 28 апреля и 2 июля. Оба извержения были эксплозивными кратковременными с небольшим количеством изверженного материала (1,2 и 95 т соответственно). Первое – вероятно 28 апреля, непосредственно не наблюдалось из-за плохой погоды, установлено по пепловым отложениям в прикратерной зоне. Тефра отложилась в радиусе не более 300 м от эруптивного жерла. Второе извержение произошло 2 июля, заключалось в одиночном пепловом выбросе, длившемся 1 ч 27 мин. Высота пеплового столба достигала 700 м, длина 6 км. Расширяющийся шлейф был ориентирован на восток. Весь изверженный материал представляет собой резургентный пепел. Основная фракция имеет размер менее 0,063 мм. По химическому и минеральному составу тефра относится к дациандезитам. Таким образом, оба извержения являются фреатическими.

Вулканические землетрясения 4 типа по классификации Токарева наблюдались в течение 21,5 ч перед вторым извержением. Извержение 2 июля предварялись ростом отношений серы к хлору и серы к углероду в составе вулканических газов.

После окончания извержений химический состав фумарольных газов приблизился к межэруптивному. Суммарная эмиссия фумарольных газов все еще превышает обычную фоновую эмиссию газов в основном за счет теплового потока эруптивного жерла и составляет 80-110 МВт.

Работа выполнена при финансовой поддержке Президиума ДВО РАН, проект 09-III-A-08-418, Российского фонда фундаментальных исследований, проект 09-05-00022а.

Ссылки

Котенко Т.А., Котенко Л.В., Шапарь В.Н. Активизация вулкана Эбеко в 2005-2006 гг. (остров Парамушир, Северные Курильские острова) // Вулканология и сейсмология. 2007. № 5. С. 1-11.

Котенко Т.А., Котенко Л.В, Сандимирова Е. И., Шапарь В.Н., Тимофеева И. Ф. Извержение вулкана Эбеко в январе-июне 2009 г. (остров Парамушир, Курильские острова) // Вестник КРАУНЦ. Серия «Науки о Земле». 2010. №1. Вып. 15. С. 56-68.

Меняйлов И.А., Овсянников А.А., Широков В.А. Извержение вулкана Эбеко в октябре - декабре 1987г. // Вулканология и сейсмология. 1988. № 3. С. 105-108.

Фазлуллин С.М., Тимофеева И.Ф., Котенко Л.В. и др. Опыт слежения за состоянием вулкана Эбеко (Курильские острова) // Материалы Российско-японского полевого семинара «Минерало - рудообразование в вулкано - гидротермальных системах островных дуг: от модели к эксплуатации». Петропавловск-Камчатский. 1998. С. 252-255.

Menyailov I.A., Nikitina L.P., Shapar V.N. Results of geochemical Monitoring of the activity of Ebeko volcano (Kuril Islands) used for eruption prediction // Journal of Geodynamics. N 3. (1985) P. 259-274.

Quaternary eruptive history of Sarychev Peak volcano, Matua Island, Kuril Islands

A.V. Degterev[1], A.V. Rybin[1], I.V. Melekescev[2], N.G. Razjigaeva[3]

[1]Institute of Marine Geology and Geophysics FEB RAS
[2]Institute of volcanology and seismology FEB RAS
[3]Pacific Institute of Geography FEB RAS

Eruptive history of Quaternary volcanoes of the Kurile Island Arc including active and potentially active are now studied poorly. The researches on reconstruction of Pleistocene-Holocene volcanism were done only in southern (Kunashir, Iturup) and northern (Paramushir, Onekotan) parts of the arc. So, the Central Kurile Islands is a real "white spot"- remote and almost inaccessible region.

Strong explosive-effusive eruption of Sarychev Peak volcano (fig. 1) in June 2009 initiated the beginning of special geology-volcanological works directed to detailed reconstruction of eruptive history of this volcano (Levin at el. 2010).

Sarychev Peak volcano (coordinates 48°05′24.49″ N. and 153°12′08.18″ E; absolute height 1446 m) represents intercalderal stratovolcano with summit crater (fig. 1). The volcano is located in caldera (D=3.5-4 km) of ancient (probably Pleistocene age) volcano Matua formed north-western part of the island (the Central Kurile Islands) (Gorshkov 1967; Laverov at el. 2005). Sarychev Peak volcano is one of the active volcanoes of the Kurile Arc; it is fixed not less than 10 its eruptions: in 1760th, 1878-1879, 1923, 1928, 1930, 1946, 1954, 1960, 1976, 2009 years. (Andreev at el., 1978; 1967; Levin at el. 2010; Shilov, 1962; Rybin et al., 2011).

The works on study of eruptive history of Sarychev Peak volcano included the complex of geologo- and geomorphologic–volcanological researches under the leading role of tephrachronology (Thorainsson, 1944; Braitseva at el., 1978). During the field works 9 sections of soil-pyroclastic covers were studied, which were made at different distance (4-7 km) from eruptive center, 3 of them were the fullest and by the time of sedimentation corresponded with late Pleistocene- early Holocene. Every section was described in detailes and sampled (by layers)

On the base of conducted investigations 3 main stages in eruptive history of Sarychev Peak volcano were detected:

Caldera-forming stage (late Pleistocene-early Holocene). Caldera-forming eruption of Matua volcano with formation of caldera which size was 3,5×4 km, and massive outburst of andesite pyroclastic;

Andesite stage (nearly all Holocene). Eruptive centers were located in the bounds of formed caldera. During this stage about 30 eruptions of different power were established, among them catastrophic eruptions were. The products of the eruptions are represented by the horizons of pumiceous andesites of light-yellow color.

Andesite-basalt stage (500-600 y.a.). During this stage modern Sarychev Peak stratovolcano was formed (I.V. Melekestsev was the first who suggested this). The activity of the volcano was mainly explosive and explosive-effusive. The eruptions were accompanied by numerous pyroclastic flows, thick covers of which are now seen in shore cliffs of the island. Tephra of Andesite-basalt stage is the thick layer of scoria having bi-structure. The low part of the section is formed by the layer of brown scoria (м=0.1-0.3 m), upper (0.5-1.2 m) is of black, dark brown of multiple stratified scoria.

Besides in soil-pyroclastic cover of Matua the layers of transit tephra were found – the ashes of caldera-forming eruption of Ushishir volcano (~1900-2000 y.a.) and strong eruptive event in Medvezh'ya caldera (Iturup Isl.) (~2100 л.н.) (Razjigaev at el., 2011 (in publishing); Nakagawa et al., 2008). In the Middle Holocene part of the section the ash of one of caldera-forming eruptions of Zavaritsky volcano is (Simushir Isl.)

The work is supported by Grants RFFR (№ 10-05-00797, № 09-05-00003) and FEB RAS (№ 11-III-B-08-015).

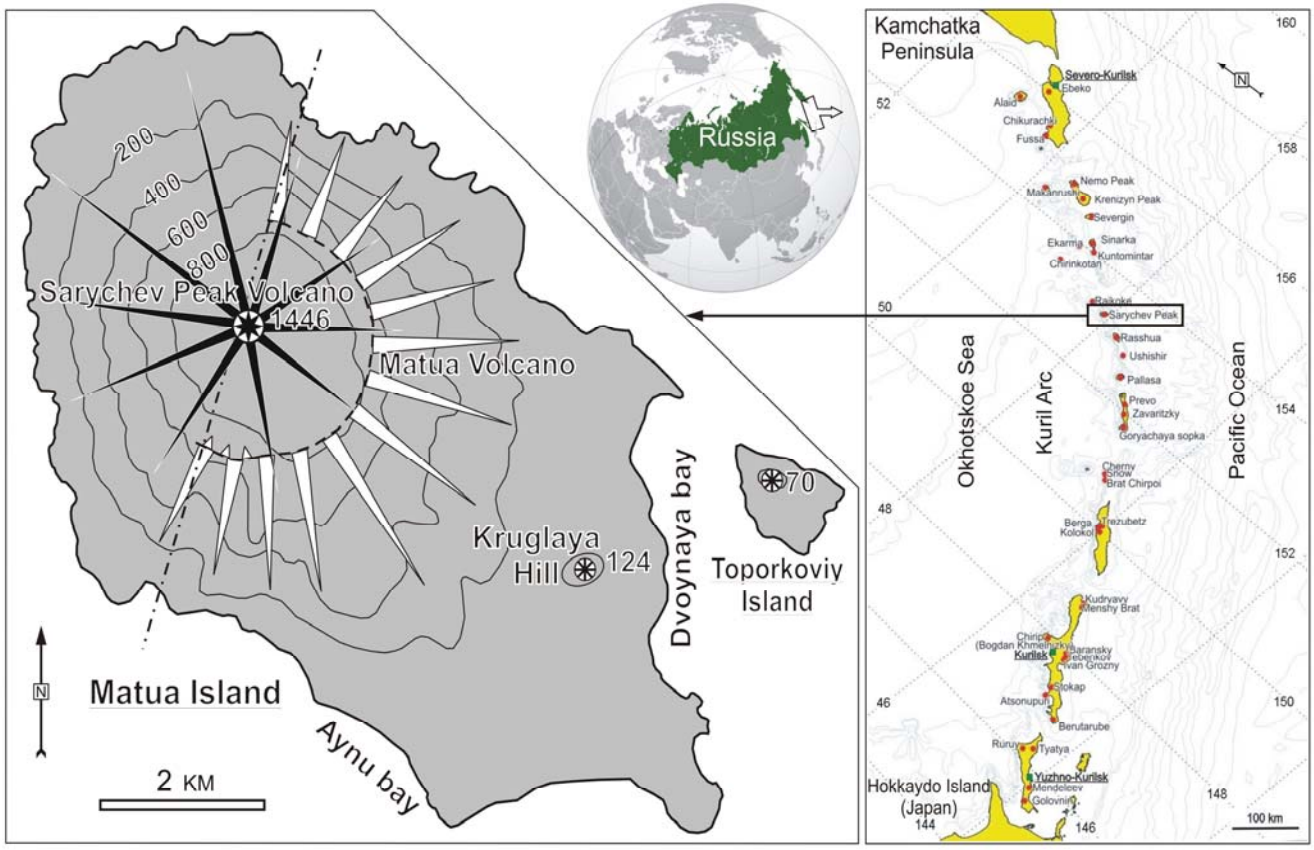


Fig. 1. Geological scheme of Sarychev Peak volcano, stroke shows the line of fault picked out by G.S.Gorshkov (1967). The map of the Kurile Islands is on the additional map.

2010-2011 Eruptive activity of Shinmoedake Volcano, Kyushu, Japan

Koji Kato[1], Shin'ichi Matsusue[2], Hiroshi Yamauchi[1]
[1]Fukuoka Volcano Observation and Information Center, JMA,
[2]Kagoshima Local Meteorological Observatory, JMA

Introduction

Shinmoedake volcano is one of the members of Kirishimayama volcanoes group, located in Kyushu, southwestern Japan. Major eruptions occurred in 1716 – 1717, fall out deposits, pyroclastic flows and mudflows were widely dispersed around the volcano. Recently, small phreatic eruption occurred in 1959 and 1991. After Shinmoedake volcano repeated phreatic eruption on August, 2008 and during March – July 2010, started magmatic eruptions from 19 January, 2011, after 300 years dormancy.

Fukuoka Volcano Observation and Information Center, JMA and Kagoshima Local Meteorological Observatory, JMA monitor Shinmoedake volcano for 24 hours a day. Based on an analyzed result of monitoring, a volcanic warning is released. In this presentation, we report about 2010 - 2011eruptive activity of Shinmoedake volcano with the observational data manly by the JMA.

2010-2011 eruptive activity

The first precursory eruption, occurred at August 2008, was phreatic one, which produced tephra of 0.2 million ton (Geshi et al., 2010). The next eruption occurred on 30 March 2010 and small ones happened successively on 17 April, 27 May, 27 and 28 June, 5 and 10 July. The inflation of magma chamber around several kilometers NW of Shinmoedake volcano had been observed by GPS network since December 2010. On 19 January, a small phreatomagmatic eruption occurred. On 26 January morning, a small phreatomagmatic eruption occurred again. At 14:49, eruptive activity moved into the sub-plinian eruptions and ash plumes rose to a maximum altitude of 3,000m above the crater. On 26 January at 18:00, JMA raised the volcanic alert level from 2 to 3, transitioning the volcano into a period of possible high activity (Target area had changed from the area around the crater to the non-residential areas near the crater). Sub-plinian eruption continued on 27 January, and deposited about 10 million m3 (DRE) of tephra (Nakada et al.,2011). On 28 January, a lava which a diameter of several 10 meters was appeared on the crater floor (Nakada et al., 2011), and the lava in the crater had grown 500 meters in diameter on 30 January (Ando et al,. 2011).

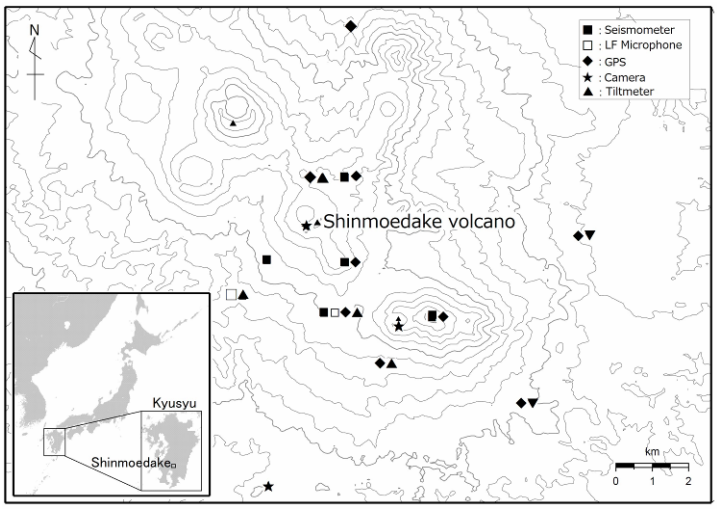


Fig.1 Volcanic observation at Shinmoedake volcano.



Fig.2 Sub-plinian eruption on 27 January.

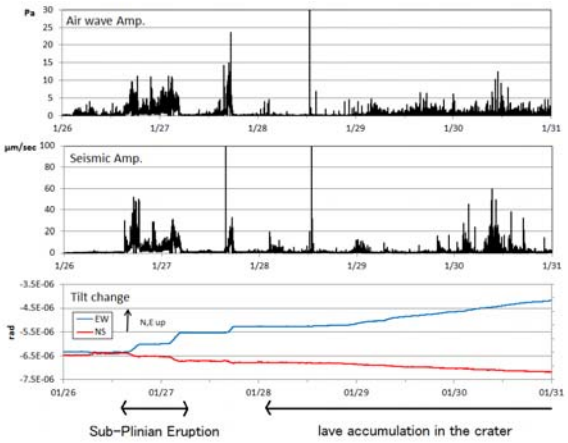


Fig.3 Air wave, seismic Amp. and tilt change.

On 31 January at 01:35, The target alert area was enlarged from 2km to 3km radius from the crater (Volcanic alert level was still 3) , taking into account the danger of pyroclastic flow. Finally, the lava in the crater grew up to about 600m (about 10 million m3) in diameter by 2 February.

Accompanying sub-plinian eruptions and lava effusion, deflation of magma chamber around several kilometers NW of Shinmoedake was observed by GPS measurements and tiltmeter. The volume of inflation before the 2011 eruptions (20 million m3) is roughly equal to that of magma erupted during 26-31 January.

Vulcanian eruption occurred on 1st February at 07:54. Ballistic bombs reached 3.2km distant from the crater and windows glasses were broken by strong air wave. On 1st February at 11:20, the target alert area was enlarged from 3km to 4km radius from the crater (Volcanic alert level was still 3), taking into account the danger of ballistics. After that, eruptions including volcanian ones intermittently occurred.

Preceding these eruptions, tilt changes and increase of volcanic earthquakes were observed before several hours to 2days of eruptions. Tilt changes and increase of volcanic earthquakes indicate that magma ascent from magma chamber to Shinmoedake volcano intermittently.

Though the sulfur-dioxide fluxes were 11,000-12,000 ton/day on January, it decreased more than an order of magnitude to several hundred ton/day after the middle of February.

On March, volcanic activity have become lower compared to the peak activity from January to the beginning of February although intermittent eruptions have occurred and GPS measurements detected that the supply of magma to deeper magma chamber around several kilometers NW of Shinmoedake has continued since the beginning of February. On 22 March at 17:00, the target alert area was reduced from 4 km to a 3 km radius from the crater (Volcanic alert level was still 3).

IVS FEB RAS GEOPORTAL AS A SINGLE POINT OF ACCESS TO VOLCANOLOGICAL AND SEISMOLOGICAL DATA

Romanova I.M.

Institute of Volcanology and Seismology FEB RAS, Piip Blvd. 9, Petropavlovsk-Kamchatsky, 683006, Russia; e-mail: roman@kscnet.ru

Geoportal as a peripheral node of Spatial Data Infrastructure (SDI) of Russian Academy of Sciences was created in the Institute of Volcanology and Seismology (IVS) FEB RAS in 2010 and has been developing since that time. IVS FEB RAS Geoportal promotes systematization and integration of a wide range of scientific information, accumulated in the Institute over many years of research. It provides a single point of access to the distributed volcanological and seismological data (http://geoportal.kscnet.ru).

Architecture of the Geoportal is being developing on the base of free open source software (GeoNetwork, GeoServer, etc.) that is distributed under the GPL license (GNU General Public License), as recommended by the OGC (Open Geospatial Consortium).

Currently, the Geoportal provides access to the following information resources: «Volcanoes of the Kuril-Kamchatka Island Arc» (VOKKIA) Information System, «Active volcanoes of Kamchatka and Northern Kuriles» catalogue, «Holocene Kamchatka Volcanoes» catalogue, «Late Cenozoic Pacific Submarine Volcanoes» database, archives of Kamchatkan Volcanic Eruption Response Team (KVERT), «Earthquakes of the Northern Group of Kamchatka Volcanoes 1973-1996» database etc.

The Geoportal includes a Web Map Server for publication of layers of spatial data (http://geoportal.kscnet.ru/geoserver/) and spatial data Visualization Services for displaying raster and vector data layers and creating thematic maps (http://geoportal.kscnet.ru/intermap/).

The Geoportal contains also a Metadata Management System and a Metadata Catalogue for data search (http://geoportal.kscnet.ru/geonetwork/). Metadata in the Catalogue correspond to the international standards, which provide the interoperability with other Metadata Catalogues in the Internet. The Catalogue contains descriptions of information volcanological and seismological resources: databases, datasets, publications, geoinformation systems (GIS), maps, photos, video content etc.

The Metadata Management System provides an ability for integration with other Metadata Catalogues through a mechanism of metadata harvesting. The harvesting allows to copy metadata from remote sources, while the data available for download, remain at remote nodes. The system allows also to provide the metadata from the Catalogue of IVS to other Metadata Catalogue Services in the Internet.

At the beginning of June 2011 IVS Metadata Catalogue contains descriptions of more than 1,000 information resources. 107 metadata records describe resources of IVS FEB RAS. The rest of the records were obtained using metadata harvesting from remote sources. They describe volcanological and seismological resources in research institutes, centers, geological surveys of USA, Canada, France, Peru, Colombia and other countries.

IVS FEB RAS Geoportal can provide the integration of information space of IVS in the global science information space.

ГЕОПОРТАЛ ИВиС ДВО РАН КАК ЕДИНАЯ ТОЧКА ДОСТУПА К ВУЛКАНОЛОГИЧЕСКИМ И СЕЙСМОЛОГИЧЕСКИМ ДАННЫМ

Романова И.М.

Институт вулканологии и сейсмологии ДВО РАН, г. Петропавловск-Камчатский,
e-mail: roman@kscnet.ru

С 2010 г. в Институте вулканологии и сейсмологии (ИВиС) ДВО РАН создается геопортал − периферийный узел инфраструктуры пространственных данных (ИПД) Российской академии наук. Геопортал ИВиС ДВО РАН способствует систематизации и интеграции широкого комплекса научной информации, накопленной в институте за многие годы исследований, предоставляет единую точку доступа к распределенным вулканологическим и сейсмологическим данным (http://geoportal.kscnet.ru).

Архитектура Геопортала ИВиС ДВО РАН разработана на базе свободных программных продуктов с открытым исходным кодом (GeoNetwork, GeoServer и др.), распространяемых по лицензии GPL (GNU General Public License), что соответствует рекомендациям OGC (Open Geospatial Consortium).

В настоящее время Геопортал предоставляет доступ к следующим информационным ресурсам: Информационной системе «Вулканы Курило-Камчатской островной дуги» («Volcanoes of the Kuril-Kamchatka Island Arc», VOKKIA), Каталогу «Активные вулканы Камчатки и Северных Курил», Каталогу «Голоценовые вулканы Камчатки», Базе данных «Позднекайнозойские подводные вулканы Тихого океана», Архивам Группы реагирования на вулканические извержения (Kamchatka Volcanic Eruption Response Team, KVERT), Базе данных «Землетрясения района Северной группы вулканов Камчатки 1973-1996 гг.» и др.

Геопортал включает картографический сервер для публикации слоев пространственных данных, а также сервисы для визуализации растровых и векторных слоев данных и создания тематических карт (http://geoportal.kscnet.ru/intermap/).

Кроме того, Геопортал содержит систему управления метаданными и Каталог метаданных для поиска данных (http://geoportal.kscnet.ru/geonetwork/). Метаданные в каталоге соответствуют международным стандартам, что обеспечивает свойство интероперабельности с другими каталогами метаданных в сети Интернет. Каталог содержит описания информационных ресурсов вулканологической и сейсмологической тематики: баз данных, наборов данных, геоинформационных систем, карт, фотографий, видеофильмов, спутниковых снимков, публикаций и др.

Система управления метаданными предоставляет возможность интеграции с другими каталогами метаданных через механизм сбора метаданных (harvesting). Механизм harvesting обеспечивает копирование метаданных из удаленных источников, при этом данные, доступные для загрузки, остаются на удаленных узлах.
В то же время система позволяет предоставлять метаданные из Каталога ИВиС ДВО РАН в другие службы каталогов сети Интернет.

На начало июня 2011 г. Каталог содержит описания более 1000 информационных ресурсов, из которых 104 записи метаданных описывают ресурсы ИВиС ДВО РАН. Остальные записи получены в процессе сбора метаданных из удаленных источников и описывают вулканологические и сейсмологические ресурсы научных институтов, центров и геологических служб США, Канады, Франции, Перу, Колумбии и др. стран.

Геопортал ИВиС ДВО РАН обеспечит интеграцию информационного пространства ИВиС в глобальное информационное научное пространство.

KAMCHATKAN VOLCANIC ERUPTION RESPONSE TEAM (KVERT) PROJECT IN 2009-2011

Olga A. Girina[1] and Christina A. Neal[2]
[1]*Institute of Volcanology and Seismology FED RAS, Russia*
[2]*US Geological Survey, Alaska Science Center, Alaska Volcano Observatory USGS, USA*

Since its founding, the Kamchatkan Volcanic Eruption Response Team (KVERT) has been a collaborative project of scientists from the Institute of Volcanology and Seismology, the Kamchatka Branch of Geophysical Surveys, and the Alaska Volcano Observatory (IVS, KB GS and AVO).

The purpose of KVERT is to reduce the risk of costly, damaging, and possibly deadly encounters of aircraft with volcanic ash clouds. To reduce this risk, KVERT collects all possible volcanic information and issues eruption alerts to aviation and other emergency officials.

KVERT was founded by Institute of Volcanic Geology and Geochemistry FED RAS in 1993 (in 2004, IVGG merged with the Institute of Volcanology to become IVS). KVERT analyzes volcano monitoring data (seismic, satellite, visual and video, and pilot reports), assigns the Aviation Color Code, and issues reports on eruptive activity and unrest at Kamchatkan (since 1993) and Northern Kurile (since 2003) volcanoes.

KVERT receives seismic monitoring data from KB GS (the Laboratory for Seismic and Volcanic Activity). KB GS maintains telemetered seismic stations to investigate 11 of the most active volcanoes in Kamchatka. Data are received around the clock and analysts evaluate data each day for every volcano to determine the number and type of seismic events at these monitored volcanoes.

Satellite data are provided from several sources to KVERT. AVO conducts satellite analysis of the Kuriles, Kamchatka, and Alaska as part of it daily monitoring and sends the interpretation to KVERT staff. KVERT interprets MODIS and MTSAT images and processes AVHRR data to look for evidence of volcanic ash and thermal anomalies. KVERT obtains visual volcanic information from volcanologist's field trips, web-cameras that monitor Klyuchevskoy (established in 2000), Sheveluch (2002), Bezymianny (2003), Koryaksky (2009) and Gorely (2011) volcanoes, and pilots.

KVERT staff work closely with staff of AVO, AMC (Airport Meteorological Center) at Yelizovo Airport and the Tokyo Volcanic Ash Advisory Center (VAAC), the Anchorage VAAC, and the Washington VAAC to release timely eruption warnings. Urgent information is sent by email to government agencies, aviation services, and scientists (>300 users) located throughout the North Pacific region. KVERT staff also notify AMC and other emergency agencies in Kamchatka by telephone. KVERT Information Releases are formal written notifications that are sent by email to these same users to announce Aviation Color Code changes and significant changes in activity. These statements are posted on the KVERT and the AVO web site. AVO sends KVERT Information Releases by facsimile to more than 60 US government and domestic and international air carriers.

During the period of April 2009-May 2011, eruptions of 6 of Kamchatkan volcanoes were potentially dangerous for aviation: three significant events occurred at Bezymianny (2009, 2010 and 2011), one protracted eruption at Klyuchevskoy (from 2009 till 2010), three short events at Koryaksky (2009) and an ongoing ash eruption at Kizimen (2010-2011). Eruptions of Karymsky and Sheveluch volcanoes have continued essentially uninterrupted throughout the period 2009-2011 and have also posed a hazard to aviation intermittently.

Volcano Monitoring and Warning System in Hokkaido, Japan

Tomoyuki Matsumura
Volcanic Observations and Information Center,
Sapporo District Meteorological Observatory,
Japan Meteorological Agency

In order to mitigate volcanic disasters, Sapporo Volcanic Observations and Information Center(VOIC) has responsibility for conducting constant watch for volcanic activities in Hokkaido and issuing Volcanic Warnings and Volcanic Forecasts.

In recent years, our volcanic observation networks for nine volcanoes have been improved. These volcanoes are supposed that the possibility of eruption within 100 years is high. For example, in Mt.Tokachidake, various types of equipments (seismometers, tiltmeters, infrasonic microphones and GPSs) were additionally installed. Using these improved networks, nine volcanoes in Hokkaido have been under constant watch by Sapporo VOIC.

We began issuing Volcanic Warnings and Volcanic Forecasts from Dec. 1st, 2007 to mitigate volcanic disasters. These are issued in relation to expected volcanic disasters, and detail the target areas and explanation of precaution.

We also began issuing Volcanic Alert Levels with Volcanic Warnings and Volcanic Forecasts. Volcanic Alert Levels are classified into five levels in terms of the target areas and action to be taken. They are described with action summary keywords: "Evacuate", "Prepare to evacuate", "Do not approach the volcano", "Do not approach the crater", and "Normal". These descriptions enable residents and climbers to take quick and appropriate action against disasters. Volcanic Alert Levels have been applied to five most active volcanoes in Hokkaido by Sapporo VOIC.

In this presentation, we will introduce about the observation networks in Hokkaido, current Volcanic Alert Levels applied to five volcanoes, and recent volcanic activities.(i.e. minor eruptions at Mt. Meakandake in 2008, thermal and crustal activities in Mt. Tarumae and Mt. Tokachidake.)

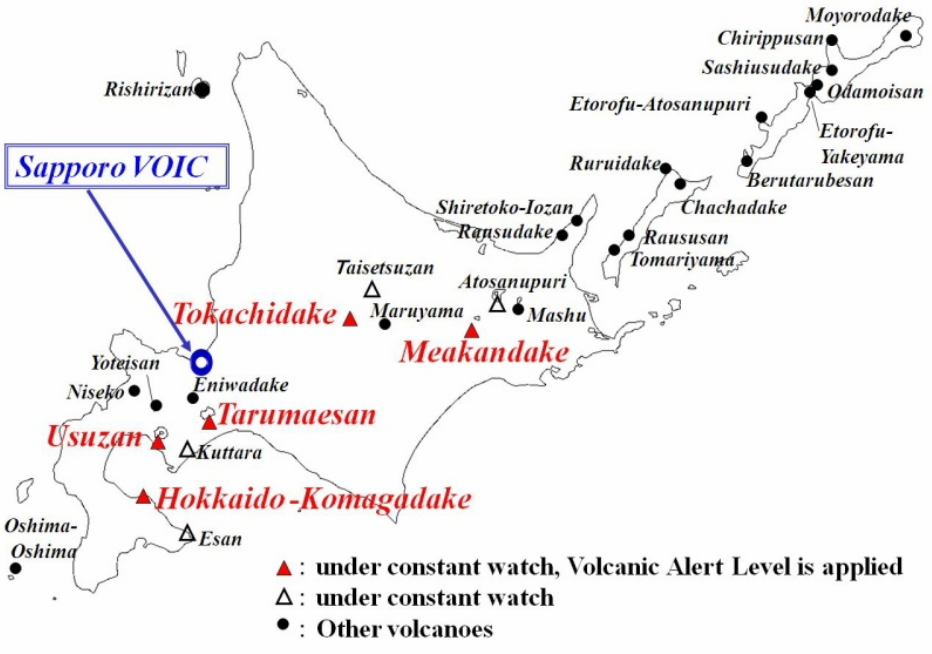


Fig1. Distribution of active volcanoes in Hokkaido.



Fig2. Minor eruption at Mt.Meakandake in Nov. 2008.
(Courtesy of Hokkaido Government.)



Fig3. Weak-glows on high-sensitive camera in Mt. Tarumae in 2011.
Changes in thermal activities have been observed in recent years.

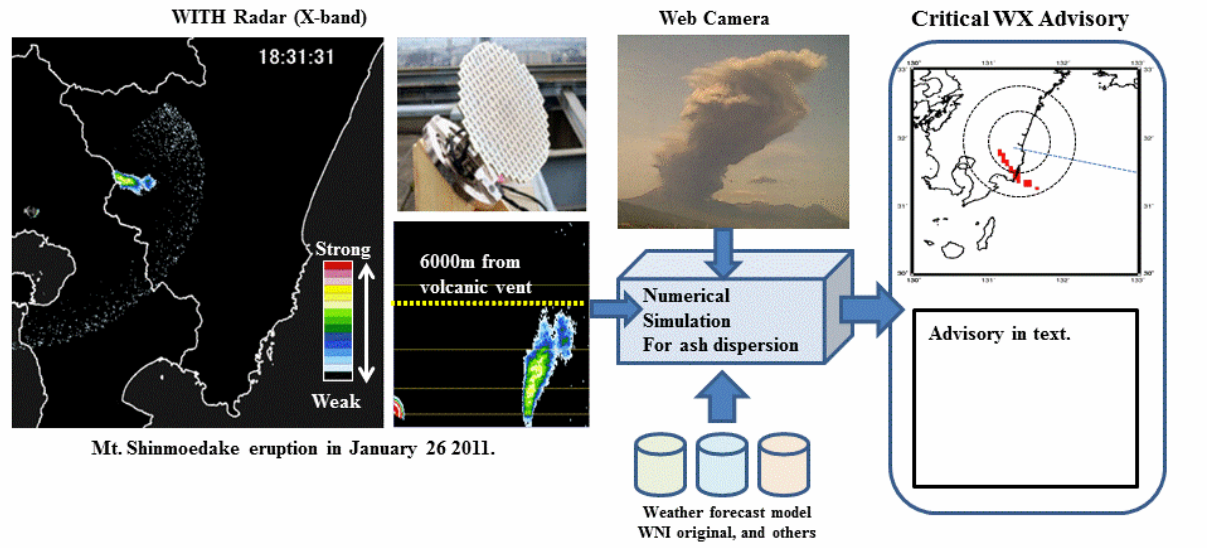
Volcanic Ash Advisory for Transportation

NaokoTaki, Marco Magnani, HiroharuSuyama
WeathernewsInc.,Chiba, Japan.

On April 2010, a series of eruptions from Eyjafjallajökull in the south of Iceland had an enormous impact on the European air traffic industry, and increased the needs and demands for accurate ash concentration forecasts and risk aversion information from the major airlines. From that moment Weathernews Inc. started the VAAT (Volcanic Ash Advisory for Transportation) project to support the needs of the transportation industry.

The VAAT project captured volcanic ash plume using WITH Radar (X-band Radar) in the recent Mt. Shinmoedake eruption in Japan. We estimate that the Radar captured lapilli more than 3mm in diameter. From that Radar return we were able to detect the eruption and to determine the height and the spread of the plume. Now, we are simulating the concentration of ash, monitoring the diffusion of ash using satellite imagery, and estimating the volume of the plume from web cameras.

Additionally, in the spring of this year, we began to develop a new system with the University of Oklahoma which is capable of real-time monitoring of airborne volcanic ash (the concentration more than 4mg/m^3). The VAAT project will try to estimate stereoscopic ash concentration through the means of new technology and innovation including this new Radar and LIDAR (Laser radar). This presentation demonstrates both the results so far and the focus of future work.



FEATURES OF ASHES FROM THE 2009 KORYAKSKY VOLCANO ERUPTION.

Anikin L.P., Vergasova L.P., Maximov A.P., Ovsiannikov A.A., Chubarov V.M.

Institute of Volcanology and Seismology FED RAS (Petropavlovsk-Kamchatsky)

maximov@kscnet.ru

In order to study nature and mechanism that caused the last unrest of Koryaksky Volcano the authors analyzed chemical, mineralogical and granulometric compositions of ashes from the 2009 eruption. Bulk chemical composition of ashes corresponds to medium-potassic calk-alcaline andesites. Remarkable feature of the composition is high sulfur content (1.8 – 2.85 wt.%). The ashes are very fine-dispersed: fraction with < 0,063 mm dominates while particles larger than 0.5 mm are very rare.

Minerals of these ashes can be divided into 3 main groups: (1) the rock-forming minerals of basic and intermediated igneous rocks (plagioclase, orto- and clinopyroxenes, olivine, magnetite and also volcanic glass), (2) accessory minerals (sphen, rutile, zircon, corund, garnet, pyrite, ilmenite, spinel, muassanit, apatite, pyrrhotite), (3) minerals that may have hydrothermal genesis (gypsum, barite, pyrite, sulfur, quartz, cristobalite, amorphous silica, silica phases with low sum of microprobe analyses, sulphides of ferrum, potassic feldspar). In addition, there are numerous light gray porous grains of pumice appearance. Particles of colourless acid glass with spherulitic structure described in ashes from the Koryaksky 1957 eruption were not revealed.

Granulometric and mineralogical characteristics of ashes denote their complex, hydrothermal - resurgent origin. Absence in ashes of fresh glass particles, presence of hydrothermal minerals and visual observations suggest that this eruption is not related directly to magmatic process and refers to hydrothermal-fracture type.

VOLUMETRIC CHANGES OF BEZYMIANNY VOLCANO

Dvigalo V.N., Ushakov S., Svirid I.Yu., Shevchenko A.V. and Izbekov P.E.

Institute of Volcanology and Seismology, Piip Bvd, Petropavlovsk-Kamchatsky, Russia
Alaska Volcano Observatory, Geophysical Institute, UAF, 903 Koyukuk, Fairbanks, Alaska

Bezymianny Volcano, Kamchatka erupted explosively on March 30, 1956 after ca. 1000 period of quiescence. The collapse of the eastern flank of the volcano followed by a directed blast and 4-hour-long explosive activity excavated a 1.3x2.5 km horse-shoe crater open to the East. The eruption continued through extrusive activity, which by the end of the 1956 formed a 300-m-tall dome in the middle of the crater. The extrusive dome growth accompanied by frequent partial collapses and block-and-ash flows dominated through mid 70s, when short vigorous explosions from central vent followed by effusions of viscous lava flows gradually became the prevailed eruption mechanisms.

The volumetric changes of the Bezymianny dome have been measured by routine aerial surveys and stereophotogrammetry since 1956. In early 90s the observations has been interrupted due to the lack of funding. Support from the PIRE-Kamchatka project allowed us to resume Bezymianny dome aerial surveys and make three consecutive measurements on June 31, 2006, September 5, 2009, and July 24, 2010. The acquired data was used to generate high resolution digital elevation models of the dome area and to determine morphological and volumetric changes in response to the most recent eruptive activity.

Our observations indicate that by 2005-2006 a new crater formed at the summit of the dome. This crater served as a vent for each of seven explosive-effusive events that occurred during 2006-2010. Volumetric changes due to extrusive activity between early 90s and 2006 and during 2006-2010 have been minimal and only occurred in the crater area. At present the dome is entirely covered by lava flows and pyroclastic flow deposits erupted from the central vent. The average annual increase of the dome volume for the 2006-2010 period was 6.8×10^6 cubic meters. Pyroclastic deposits filled the area between the dome and the 1956 crater rim, elevated the flow of the 1956 crater, and reduced the height of the rim above the floor to 26 and 24 meters in northern and southern sectors, correspondingly. As of July 2010, the height of the dome was 2951 meters, which is still 134 meters lower than the pre-1956 height of Bezymianny.

It appears that at the end of 70s the volume of the dome became high enough to suppress significantly both endogeneous and exogeneous dome growth. Concurrently, the erupted magmas become progressively less silicic, hotter, and likely less viscous. As the result, the eruptive behavior changed and Bezymianny Volcano continued rebuilding its edifice through explosive and effusive eruptions from the central vent, as normal stratovolcanoes do.

Whole-Rock Geochemistry, Geothermometry, and Computer-Based Modal Analysis of the 1956-Present Eruptive Products of Bezymianny Volcano, Kamchatka, Russia

Jill S. Shipman[1], Maxim G. Gavrilenko[2], and Pavel E. Izbekov[1]

[1]Alaska Volcano Observatory/Geophysical Institute, University of Alaska Fairbanks, Fairbanks, AK. USA
[2]Active Volcanism Laboratory, Institute of Volcanology and Seismology, Petropavlovsk-Kamchatsky, Russia

Complementary data sets from major element whole-rock geochemical analyses, geothermometry, and mineral modal analyses are used to characterize the evolution of magma in the Bezymianny system. Bezymianny Volcano is an ideal laboratory for studies into magmatic evolution at volcanoes which have experienced edifice collapse. A comprehensive sample repository representing over 50 years of volcanic activity provides the unique ability to investigate the factors which sustain its ongoing eruptive activity.

Whole-rock geochemical analyses show a progressive trend toward more mafic compositions with 61.0 wt. % SiO_2 in 1956 to 56.6 wt. % SiO_2 in 2010. Major element trends are consistent with linear two-component magma mixing. Co-existing Fe-Ti oxides and two-pyroxene geothermometry calibrations show crystallization temperatures for the 1956 eruption range between 900°C and 950°C (accuracy of ±30°C). >From 1956 to 2007, a general warming trend is observed with an increase to 1050°C ± 30°C.

We developed a computer-based modal analysis technique for the rapid quantification of large data sets. We use image processing, ENVI®, software to analyze high resolution petrographic thin section imagery acquired in both plane and cross polar light. Steps required include: 1) color training of desired mineral phases; 2) supervised classification based on a maximum likelihood algorithm; and 3) post-classification output of modal abundance. This technique demonstrates a low residual error when compared with manual point count analyses and the product can be used for feature extraction and crystal size distribution analysis. The modal analysis results are summarized in Figure 1.

Bezymianny's correlated chemical and temperature trend can be interpreted as reflecting mafic recharge subsequent to the initial collapse-blast-plinian sequence. Furthermore, (1) an increase in crystallization temperatures; (2) temporal changes in modal abundances; and (3) a transition in the character of effusive eruptions from dome growth to summit lava flow morphology all suggest a mafic source entering the system is responsible for fueling its highly regular and ongoing activity.

Petrology of mafic enclaves in andesites of October 2007 eruption of Bezymianny volcano (Kamchatka)

Vesta O. Davydova[1], Vasily D. Shcherbakov[1], Pavel Yu. Plechov[1], Pavel E. Izbekov[2]
[1]Geological department of Lomonosov Moscow State University, Moscow, Russia
[2]Geophysical Institute, University of Alaska, Fairbanks, Alaska, USA

The October 2007 eruption products of Bezymianny volcano contain mafic enclaves of rounded shape, 5 to 40 cm in diameter. Enclaves are composed of plagioclase, low- and high-Ca pyroxene and glass. Increasing of crystal and bubbles size toward the center of enclave, large sieve core plagioclase phenocrysts, elongated and skeletal crystals in groundmass are inherent to all found enclaves, which suggests that they formed as a result of injection of hotter magma into magma reservoir. Olivine (Fo_{76-78}) and high-Al hornblende (up to 14 wt.% Al_2O_3) phenocrysts surrounded by reaction rims are common in enclaves. A few enclaves contain harzburgite xenolites of mantle origin (Shcherbakov, Plechov 2010). Enclaves are basaltic andesites in composition (~54 wt.% SiO_2) and which is slightly less evolved than host rocks (~56 wt.% SiO_2).

Coexisting pairs of low- and high-Ca pyroxenes gives the temperature of enclave goundmass crystallization in range 940-1010°C, which is a little higher than crystallization temperature of phenocrysts assemblage of host andesites (Shcherbakov et al. 2011). Presence of high-Al hornblende and sieve-textured plagioclases attributed to large scale decompression melting (Nelson, Montana, 1992) argue for deep origin of the enclaves. Based on recently developed thermobarometer (Ridolfi et al. 2010) pressure of hornblende crystallization is 630±70 MPa, which correspond to depth of ~20 km.

Based on petrological observation we suggest that Bezymianny magma system contains at least two crustal magma chambers at different depth. The shallow magma chamber (77-87 MPa) is periodically supplied with slightly less evolved magma from beneath. Due to small compositional and thermal contrast between host and intruding magma interaction between them results only into oscillatory zoning of phenocrysts in host magma due to thermal fluctuations (Shcherbakov et al. 2011) and fast crystallization (quenching) of enclaves resulting in strong normal zoning and skeletal shape of crystals. Large compositional diversity of rock-forming minerals common for andesitic volcanoes is not observed due to close mineral compositions in host andesite and enclaves.

Magma intruding into shallow magma chamber likely originated at large depth (630±70 MPa) and experienced large scale ascent before injecting into shallow chamber, which is recorded in large sieve-textured plagioclases. Low Mg# of pyroxenes argue for relatively evolved bulk composition of the deep magma chamber (e.g. basaltic andesites), however olivine xenocrysts and mantle xenoliths of mantle harzburgites found in the enclaves suggest influx of more primitive magmas.

THE 1955-2010 PERIOD OF ERUPTIVE ACTIVITY AT BEZYMIANNY VOLCANO, KAMCHATKA: STORY IN ROCKS

Pavel Izbekov[1] and PIRE team[2]

[1] Alaska Volcano Observatory, Geophysical Institute, University of Alaska Fairbanks
[2] http://gps.alaska.edu/PIRE/index.html

Bezymianny volcano in Kamchatka has been in a state of nearly continuous eruptive activity for more than five decades. It started in late 1955 after ca. 1000 years of quiescence. A moderate explosive and extrusive eruption from the central vent of the volcano abruptly escalated on March 30, 1956, when a sudden collapse of the eastern flank of the volcano triggered an energetic directed blast followed by four hours of paroxysmal explosive eruption. The eruption destroyed summit of the volcano and formed a 1.3-km-wide horseshoe crater breached to the east. Within weeks the volcano started rebuilding its edifice through extrusion of the dome in the middle of the crater, intermittent dome collapses, and associated block-and-ash flows. By mid 70s, as the volume of the dome increased, the dome-building extrusive activity became complemented by short explosive events with pyroclastic flows and surges followed by effusions of lava flows. In late 90s the explosive eruptions became remarkably regular with 1-2 events per year.

The erupted Bezymianny magmas were remarkably homogeneous both texturally and compositionally. Their composition changed gradually from 60.9 wt. % SiO_2 in 1956 to 56.8 wt. % SiO_2 in 2010. The composition of exceptionally rare mafic enclaves from the products of the 1997 and 2007 eruptions overlapped with the composition of recent Kliuchevskoy magmas. The MgO-SiO_2 binary diagram shows that MgO content increased linearly from 1956 to ca. 1973 along the mixing line connecting points corresponding to the 1956 andesite and the high-Mg, Kliuchevskoy-type basalt. In ca. 1973 the linear trend changed the slope and followed a mixing line between 1973 magma and low-Mg Kliuchevskoy-type basalt. The same kink in trend is observed in a variety of other elements (Turner et al., this volume). The 2009 and 2010 magmas of Bezymianny contained light-colored enclaves of vesicular amphibole-bearing andesites, which composition mimicked the composition of magmas erupted in 1989 and during 1997-2003.

The change in whole-rock composition correlated with changes in magma temperature and mineral assemblage. Based on ilmenite-magnetite and two-pyroxene geothermometry the pre-eruptive temperature of Bezymianny magmas increased from 950°C in 1956 to 1050°C in 2006 (Shipman et al., this volume). Amphibole, abundant in 1956 magma, gradually disappeared by mid 60s and most recently occurred only as resorbed cores in OPx-CPx-Pl aggregates. Its composition changed from 8-10 wt. % Al_2O_3 in 1956 to 13-15 wt. % Al_2O_3 in 2010. The modal proportion and size of clinopyroxene crystals gradually increased; its composition became more Mg-rich. This correlated with increase of Mg content in orthopyroxenes. Despite conspicuous changes in whole rock composition and temperature, the range of compositional variations of plagioclase remained nearly the same. It is remarkable that plagioclase composition returned repeatedly to 48-50 mol. % An throughout the entire period of eruptive activity. The compositional plateaus in the oscillatory zoned plagioclases preceding the outermost dissolution boundaries in the 1956 magma compositionally resembled those in the most recent eruptive products.

Although the new data from a trace element study of plagioclases, ion microprobe study of melt inclusions, and phase equilibria experiments may slightly modify our interpretation, the observed compositional trends are generally consistent with continuous input(s) of Kliuchevskoy-like basalts to the magma system of Bezymianny volcano.

Evaluating the uncertainties of the estimated vertical velocities of Bezymianny GPS network

R.M.S. Fernandes(1,2), J. Freymueller(3), M.S. Bos(4), Ronni Grapenthin(3)

(1) University of Beira Interior, Instituto D. Luíz, Covilhã, Portugal
(2) Delft University of Technology, Delft, The Netherlands
(3) University of Alaska, Fairbanks, Alaska, USA
(4) CIIMAR, Porto, Portugal

The Bezymianny GPS network has been installed in 2006 in order to monitor this volcano that has suffered several eruptions in the last 50 years. The GPS network consisted of 10 permanent sites distributed around the volcano edifice. However, due to the extreme difficult conditions, two of the stations acquired very few days of observations and most of other eight also contain large periods with no observations – mainly caused by power failures.
In this study, we start by focus on the sensitivity of the vertical estimations to different processing parameters. We have processed the entire dataset acquired until the summer of 2010 (4 years for most stations) using the GIPSY-OASIS software package. We analyze the time-series obtained using state-of-art mapping functions (GMF and VMF1) at different elevation angles in order to investigate how much the selection of the mapping function together with the cut-off angle can affect the estimated trend and associated uncertainties. This provides us upper limits on the variation of the vertical velocities in function of the used models.
In addition, we compute more realistic trend errors for the vertical motions by taking into account the temporal correlations that exists within the data. The necessity of using something more realistic than a white noise model in the least-squares solution of the GPS derived motion is obvious when different parts of the time-series produce rates that are significantly more diverging than one should expect from the formal errors. We use here an algorithm based on the Maximum Likelihood Estimation method that takes into account the existence of significant number of gaps in the time-series without destroying the symmetric structure of the matrices involved. The use of temporal correlations between the associated uncertainties of the time-series is mainly based on the fact that we are concentrated on a small spatial network.

DEFORMATIONS IN BEZYMIANNY VOLCANO AREA ACCORDING TO GPS AND INSAR DATA

Sergey Serovetnikov [1], Nikolay Titkov [1], Dmitry Melnikov[2] , Sergey Senyukov[1], Ronny Grapenthin.[3] (sssu@emsd.ru)

[1] Kamchatka Branch Geophysical Service, Petropavlovsk-Kamchatsky, Russia.
[2] Science Institute of Volcanology and Seismology FEB RAS (IVS)
[3] Alaska Volcano Observatory,Geophysical Institute,Univ.of Alaska Fairbanks,USA.

GPS network configuration in Bezymianny volcano area, allows registering surface deformations caused by the volcano activity. Within 6 years are registered the movements from 7 strong volcano eruptions.

The analysis of received data has shown a possible dependence of Bezymianny volcano activity from activity of Klyuchevskoy volcano, and Bezymianny volcano has the subordinated value in the given system.GPS data are shown the basic deformations are localized in volcano dome area and have significant reduction of amplitude outside the 1956 caldera.

For technical reasons GPS network cannot be spread to volcano dome and the deformations above a pressure source can be estimated only indirectly.

The Interferometer (InSAR) data are allowed to receive the information about surface deformations in investigated area. Unfortunately, the exact quantitative estimation of deformations by a satellite interferometric method is complicated in view of time uncorrelation. However, a series of interferometric pairs for the period from June till September, 2007 (data ALOS PALSAR) has allowed receiving relative deformations for a Bezymianny volcano dome and surrounding area.

Association of GPS/InSAR results allows to specify the deformation processes during preparation of eruption and to simulate a source of pressure under the Bezymianny volcano dome.

Use the modern representations about deep structure on the seismic data and surface deformation data, allows receiving the fullest picture of development of volcanic processes of Bezymianny volcano.

ДЕФОРМАЦИИ В РАЙОНЕ ВУЛКАНА БЕЗЫМЯННЫЙ ПО ДАННЫМ GPS И INSAR МОНИТОРИНГА

Сероветников С.С.[1] , Титков Н.Н.[1], Сенюков С.Л.[1], Мельников Д.В.[2], Grapenthin R.[3] (sssu@emsd.ru)

[1] Камчатский филиал Геофизической службы РАН, г. Петропавловск-Камчатский.
[2] Институт Вулканологии и Сейсмологии ДВО РАН, г. Петропавловск-Камчатский.
[3] Alaska Volcano Observatory,Geophysical Institute,Univ.of Alaska Fairbanks,USA.

Конфигурация сети GPS станций в районе вулкана Безымянный позволяет проводить мониторинг деформаций поверхности вызванных активностью вулкана. В течение 6 лет непрерывного мониторинга зарегистрированы движения, вызванные 7 сильными извержениями вулкана.

Анализ полученных данных показал возможную зависимость активности вулкана Безымянный от активности близкорасположенного вулкана Ключевская сопка, причем вулкан Безымянный имеет подчиненное значение в данной системе. Так же данные показывают, что основные деформации, предваряющие извержение локализованы в районе купола вулкана и имеют резкое сокращение амплитуды вне кальдеры 1956 г.

По техническим причинам сеть GPS станций не может быть распространена на купол вулкана и деформационная картина над источником давления может оцениваться лишь косвенно.

Данные интерферометрии InSAR позволяют получать информацию о деформациях поверхности исследуемого района. К сожалению, точная количественная оценка деформаций с помощью метода спутниковой интерферометрии затруднена ввиду временной декорреляции. Однако, серия интерферометрических пар за период с июня по сентябрь 2007 года (данные ALOS PALSAR) позволила получить картину относительных деформаций для купола вулкана Безымянный и окружающего района.

Объединение результатов GPS и InSAR мониторинга позволяет значительно уточнить представления о деформационных процессах происходящих в исследуемом районе во время подготовки извержения, а так же смоделировать источник давления под куполом вулкана Безымянный.

Использование современных представлений о глубинной структуре района на основе сейсмических данных и данных о деформации поверхности позволяет получить наиболее полную картину развития вулканических процессов вулкана Безымянный.

Surface deformation of Bezymianny volcano, Kamchatka, recorded by GPS: The eruptions from 2005-2010 and long-term, long-wavelength subsidence.

Ronni Grapenthin[1], Jeffrey T. Freymueller[1], Sergey Serovetnikov[2]
[1]Geophysical Institute / Alaska Volcano Observatory, Univ. of Alaska Fairbanks, AK, USA.
[2]Kamchatkan Branch of Geophysical Service of RAS, Petropavlovsk-Kamchatskiy, Russia.

Bezymianny Volcano in Kamchatka reactivated after a roughly 1000 year hiatus in 1956 with an eruption that culminated into a directed blast removing about 0.6 km^3 of material from the edifice. Today eruptive activity occurs roughly every 6 months with a violent explosion lasting for 2 – 20 minutes that creates lava flows and pyroclastic flows.

In 2005 the volcano was instrumented with an array of 6 campaign and 8 continuous GPS stations, none of which are telemetered. The campaign sites have been measured during annual summer field work during which we also recovered data of the continuous sites. The first eruption recorded by a partial continuous GPS network was the December 24, 2006, event. Between then and the last data recovery in the summer of 2010 six additional eruptions occurred.

We analyze the data in the International Terrestrial Reference Frame (ITRF) using the GIPSY/OASIS software and find a relatively uniform network wide subsidence of about 7-9 mm/yr for the observation period from 2005 to 2010. This could be induced by continuous depressurization of a deeply seated magma reservoir, likely beneath Kluichevskoy volcano to the North of Bezymianny. Other possible sources could be a regional surface loading effect, or a combination of loading and volcanic signal. Surface load effects could be induced by the new dome growing inside Bezymianny's horseshoe shaped crater and other material emplaced during the regular eruptions. Loading effects due to Kliuchevskoy, the tallest mountain in Asia, should also be taken into consideration.

Preliminary analysis of pre-eruptive displacements shows little to no inflationary signal in the near field prior to the explosive events, which suggests either a very deep or a very shallow magma source. We invert the GPS time series for a variety of deformation sources including magmatic source models and surface loads to infer a detailed interpretation of the volcanic system and its evolution during over time. By employing a kinematic GPS processing strategy we are able to investigate short-term co-eruptive deformation dynamics.

Seismic Trends in Recent Bezymianny Eruptions

Michael West
University of Alaska Fairbanks, Fairbanks, AK, USA
mewest@alaska.edu

A digital broadband seismic network recorded seismic activity at Bezymianny from 2006 to 2010. This instrumentation complimented the analog monitoring network operated by the Kamchatka Branch of Geophysical Services (KBGS) by providing seismic records within a few kilometers of the summit that recorded on scale during the height of explosive eruptions and captured the very low frequency component of the ground motion. This network was in place for nine significant explosive episodes. These eruptions included short explosions of juvenile material, dome collapses and periods of sustained eruption lasting hours.

In the past two decades, Bezymianny has settled into a relatively stable eruption pattern with sub-Plinian eruptions occurring on a roughly semi-annual basis. This pattern suggests a steady state process in which each eruption returns the volcano to a similar state. After several months of quiescence, the thresholds for explosion are again exceeded and a short-lived but relatively powerful (VEI 2-3) eruption ensues. The key objective in explaining recent activity is to determine the feature(s) that are controlling this relatively unusual quasi-periodic activity. One option is that the eruption consistency reflects a very steady flux of homogeneous magma into the crustal reservoir several kilometers below the summit. Pressure builds in this reservoir until it is sufficient to ream out the conduit and erupt explosively. A second explanation holds that the lava dome that has reoccupied the crater following the catastrophic 1956 eruption is currently acting as a control gate for eruptions. This “cap” provides a constant lithospheric load and a consistent barrier in temperature, density and mechanical properties. Because the dome has changed little in the past decade it has provided a consistent threshold to overcome for eruption. These two models can be characterized, albeit oversimplified, as “bottom-driven” and “top-driven” eruption models. A critical distinction between the two models is whether eruptions are being fed from a deep source (below kilometers of conduit) or a shallow source (just under dome).

Clues to the validity of either model can be found in the eruption seismic records. In this talk we present evidence for and against these models based on eruption energies and durations, earthquake locations, precursory seismic activity, multiplet earthquakes and very long period (VLP) eruption seismicity.

Characterization and interpretation of volcanic activity at Bezymianny volcano from 2007 through 2010: A volcanic-gas perspective

Taryn Lopez[1], Sergey Ushakov[2], Pavel Izbekov[1], Cindy Werner[3], Cathy Cahill[1] and Simon Carn[4]
[1]University of Alaska Fairbanks Geophysical Institute
[2]Institute of Volcanology and Seismology FEB RAS
[3]United States Geological Survey Volcano Emissions Project
[4]Michigan Technological University

Volcanic gas measurements at Bezymianny volcano, Kamchatka, Russia, from 2007– 2010 are used herein to (1) infer the relative depth or degassing state of a source magma according to solubility differences among gas species, (2) distinguish between open and plugged conduit systems through changes in sulfur dioxide (SO_2) emission rates, and (3) estimate the first-order total eruptive mass of magma through estimates of total eruptive SO_2. To characterize and interpret recent activity at Bezymianny, we measured volcanic gas composition from fumarole samples, calculated SO_2 emission rates from scanning FLYSPEC ultraviolet (UV) spectrometer measurements, and derived eruptive SO_2 masses from Ozone Monitoring System (OMI) satellite data. During the study period, five explosive eruptions occurred at Bezymianny: May 2007, October/November 2007, August 2008, December 2009, and May/June 2010. Preliminary results are shown in the table below (note that samples marked by the asterisks were collected six weeks after the May 31, 2010 eruption).

We interpret the low ratios of CO_2/H_2O and SO_2/HCl observed in the August 2007 fumarole samples to indicate degassing of a shallow, largely degassed magma source, and the high total emission rates to suggest an open conduit system. If the system remained open, the October 2007 eruption may have been triggered by a partial lava dome collapse, which decreased pressure on the magmatic system at depth, prompted magma ascent, and culminated in an explosive eruption. Using the OMI SO_2 eruptive mass and the method by Blake (2003), the mass of eruptive magma was ~1.5 $x10^6$ tonnes for this eruption. In contrast, the high ratios of CO_2/H_2O and SO_2/HCl observed in the July 2009 fumarole samples may indicate degassing of a fresh and/or deep magma source and low total emission rates suggest a partially sealed conduit. Thus, we propose that the December 2009 eruption may have been the result of overpressure in the conduit due to confined degassing of a fresh, ascending magma. An alternate hypothesis is that hydrothermal or meteoric water preferentially scrubbed the highly water-soluble gases and decreased the overall emission rates. No SO_2 was detected by OMI for this event due to poor signal-to-noise for high latitude, winter conditions. Incomplete datasets in 2008 and 2010 prevent us from proposing eruption mechanisms for those events. In 2008, no gas composition data were acquired and the observed SO_2 emission rates were not significantly different from 2007 and 2009 emissions. Additionally, SO_2 from Bezymianny eruptions in 2008 was not conclusively detected by OMI due to a contemporaneous eruption of Kasatochi volcano, Alaska. Derived eruptive SO_2 masses from OMI for the 2007 and 2010 eruptions were strikingly similar, suggesting that these eruptions had similar eruption masses. This study suggests that combined measurements of volcanic gas composition, SO_2 emission rates, and eruptive SO_2 masses can be used to elucidate volcanic behavior and help characterize eruptive activity. Notably, the October 2007 and December 2009 eruptions of Bezymianny may have been triggered by partial dome collapse and intrusion of new magma combined with conduit sealing, respectively; multidisciplinary datasets could be used to test these hypotheses.

Year	CO_2/H_2O	SO_2/HCl	SO_2 Emission Rate (t/d)	Total Emission Rate (t/d)	OMI Eruptive SO_2 Mass (t)	Magma Eruptive Mass (t)
2007	0.02	0.42	278 +/-130	~33,900	~4,900	~$1.5*10^6$
2008	NA	NA	140 +/- 95	NA	NA	NA
2009	0.34	23.61	97 +/- 50	~800	NA	NA
2010	0.02*	6.03*	NA	NA	~4,900	~$1.5*10^6$

MAGMA SYSTEM RESPONSE TO VOLCANO EDIFICE COLLAPSE: RESULTS OF THE 2005-2011 NSF-PIRE PROJECT AT BEZYMIANNY VOLCANO, KAMCHATKA

Pavel Izbekov[1] and PIRE team[2]

[1] Alaska Volcano Observatory, Geophysical Institute, University of Alaska Fairbanks
[2] http://gps.alaska.edu/PIRE/index.html

Bezymianny volcano has been the main target of the 5-year multi-disciplinary international project investigating the unloading effect of edifice collapse on active magma system. The eruption of Bezymianny in 1956 started with the same sequence of events as the eruption of Mount St. Helens in 1980, i.e. flank collapse – directed blast – explosive activity – extrusive dome growth. Unlike Mount St. Helens, its Russian twin has remained active and continued re-building its edifice through extrusive activity punctuated by vigorous explosions one-two times a year.



Bezymianny, Kamen', and Kliuchevskoy volcanoes in July 2010 during the most recent field campaign

We use Bezymianny as a natural laboratory to investigate magma system response to edifice collapse. We have acquired seismic and deformation data sets, as well as comprehensive suites of geochemical data to characterize ongoing eruptive activity at Bezymianny. The collected data sets are being used to predict what Mount St Helens will do in the future. Of equal importance is the introduction of American graduate students to international science. We have made the research truly collaborative, with American students working directly with their Russian peers and Russian senior scientists. Each student in the project is responsible for a particular facet of the research. In most cases we have planned these research activities to dovetail with a student's existing thesis work. In several cases, the PIRE project has allowed students to apply tools developed for their primary thesis work to another volcano. This equally benefits our project and the thesis work of our students.

Our project involves 42 students (25 from US universities) and 17 faculty (6 from the US); all have some in-hand data that they have collected from Bezymianny volcano. Their levels of participation vary widely, but their cumulative contributions are impressive. Eight students from the 2006 and 2007 campaigns have already successfully defended their Ph.D. degrees and four have earned their Masters. The results of the project have been presented at special sessions dedicated to our project at the 2009 JKASP meeting in Fairbanks, AK, and at the 2010 Fall AGU meeting in San Francisco. The current list of project publications includes 10 papers in peer-reviewed journals, 11 dissertations, and 68 abstracts. There are several manuscripts in review and 16 in preparation for submission to the special issue of the Journal of Volcanology and Geothermal Research dedicated to this project. This talk serves merely as an introduction to 14 more talks presenting the results of the NSF-PIRE project at the 2011 JKASP meeting.

1977-2010 ACTIVITY OF BEZYMIANNY VOLCANO

Olga A. Girina
Institute of Volcanology and Seismology FEB RAS, Petropavlovsk-Kamchatsky, Russia,
girina@kscnet.ru

Bezymianny volcano is one of the most active volcanoes of Kamchatka, Russia. Volcanic activity of Bezymianny started in October 1955 from moderate explosive eruptions, which lasted for about half a year. On March 30 the climactic eruption occurred: catastrophic directed blast and strong Plinian activity. A growth of the lava dome Novy into the explosive crater continues from 1956 till present.

39 strong explosive eruptions of this volcano occurred in 1977-2010. Ash plumes rose up to 15 km (49,200 ft.) ASL and drifted about 1,500 km mainly to the eastern and western directions from the volcano. Always as result of these explosive eruptions there were formed tephra and pyroclastic flows deposits; and an effusion of lava flows on the lava dome occurred after explosive phases of these eruptions. Pyroclastic flows deposits were accumulating in the valleys on the south-eastern flank of the volcano. The run-out of the flows deposits varied from 3-4 till 13 km. The volume of pyroclastic deposits of eruptions varied from 0.001 till 0.05 cubic km. Lava flows effused mainly on the eastern, northern and southern slopes of the lava dome. The run-out of the lava flows varied from 0.1 till 1.2 km.

Crustal displacements of East Asia caused by the Tohoku earthquake of March 11, 2011, Mw =9.0

N.V. Shestakov[1,2], Hiroaki Takahashi[3], Mako Ohzono[3], V.G. Bykov[4], M.D. Gerasimenko[1], A.S. Prytkov[5], V.A. Bormotov[4], M.N. Luneva[4], A.G. Kolomiets[1], G.N. Gerasimov[1], N.F. Vasilenko[5], Jeongho Baek[6,7], Pil-Ho Park[7], A.A. Sorokin[8], V.F. Bakhtiarov[9], N.N. Titkov[9], S.S. Serovetnikov[9]

[1] – Institute of Applied Mathematics, FEB RAS, Vladivostok, Russia

[2] – Kwangwoon University, Seoul, South Korea

[3] – Institute of Seismology and Volcanology, Graduate School of Science, Hokkaido University, Sapporo, Japan

[4] – Institute of Tectonics and Geophysics, FEB RAS, Khabarovsk, Russia

[5] – Institute of Marine Geology and Geophysics, FEB RAS, Yuzhno-Sakhalinsk, Russia

[6] – Korea Astronomy and Space Science Institute, Daejeon, South Korea

[7] – University of Science and Technology, Daejeon, South Korea

[8] – Data processing center, FEB RAS, Khabarovsk, Russia

[9] – Kamchatkan Branch of Geophysical Survey of RAS, Petropavlovsk-Kamchatsky, Russia

The Great Tohoku earthquake Mw = 9.0 occurred at 5:46 UTC on March 11, 2011 near the northeastern coast of Honshu Island, Japan. It was one of the largest seismic events occurred during the last 100 years. The destructive tsunami generated by the earthquake was observed along the Pacific coast of Japan and detected in a broad area around Japan.

The epicenter of the 2011 Tohoku earthquake was located on the subducting active plate boundary between the Pacific and North American or Eurasian plates depending on the assumed plate boundary configuration. A series of large fore- and aftershocks preceded and have still been succeeding the mainshock. More than 60 these events had magnitudes greater or equal to 6.0.

Long-period stress accumulation in this region is caused by the Pacific plate subduction beneath the Japan Island Arc with relative velocity 91-92 mm/yr with respect to Eurasia or 83 mm/yr with respect to North American plate.

According to the numerous seismic and geodetic observations the 2011 Great Tohoku earthquake displays the thrust faulting mechanism with the maximum slip value varying from 10 to more than 50 m. The estimated rupture length is ranging from 300 to 500 km according to the different fault models.

In contrast to the Sumatra-Andaman region, this seismic event occurred near the highly populated region almost uniformly covered by dense geodetic, seismic and other type geophysical networks. That is why a lot of invaluable measurement information becomes available from the

nearest to the earthquake epicenter zone. This information is intensively analyzing now.

The 2011 Tohoku earthquake caused large co- and postseismic crustal displacements and deformations over the Japanese Islands. The eastward horizontal coseismic displacements and subsidence greater than 4.0 m and -0.6 m were observed, respectively, in the area closest to the epicenter by the GPS Earth Observation Network (GEONET) operated by the Geospatial Information Authority of Japan (GSI). Almost all the other areas of Japan exhibit significant crustal deformations ranging from one centimeter to a few decimeters (see figure). The intense eastward postseismic horizontal displacements have still been continuing in Northern Honshu. Their maximum value had reached 50 cm by May 1, 2011.

The most intense coseismic deformations outside of the Japanese Islands (up to 4-5 cm) had occurred in the area striking westward from the epicenter and covering the southern of continental part of the Russian Far East, territories of South and North Korea and North East China. Notable coseismic deformations ranging from several millimeters to 1.5 cm approximately were also observed in the adjacent continental regions (see figure).

Almost all detected offset vectors are oriented approximately toward the epicenter. This result speaks either in favor of a single-segment rupture of a relatively short length striking approximately along the Japan Trench and located eastward from Northern Honshu or the existence of a compact area near the epicenter characterized by a very intense slip with respect to other rupture segments. Therefore, the 2011 Tohoku earthquake should be characterized by far large maximum slip value as compared to the Great Sumatra-Andaman multi-segment event.

A size of the region displaying measurable coseismic deformations coused by the 2011 Tohoku earthquake is smaller with respect to the area affected by the Great Sumatra-Andaman quake for which 5-10 mm coseismic jumps were detected at stations located more than 3,000 km away from the earthquake epicenter

It is interesting that among three processed continuous GPS stations distributed over Sakhalin Island not a single observation site detected notable coseismic offset. However in contrast to Sakhalin, Kunashir Island exhibits almost northward coseismic offset with a magnitude of about 10 mm. This point to the proximity of the area to the nodal plane of the rupture and imposes constrains on its northern extension.

A simple preliminary rectangular fault model with a uniform slip was developed based on GPS-detected far-field coseismic displacements under the homogenous elastic half-space assumption. A single-segment rupture of 200×96 km^2 with oblique slip of about 22.9 m, characterized by the seismic moment of $1.32\cdot10^{22}$ Nm (Mw=8.7) was obtained from GPS data inversion. Our model in general describes well both far- and near-field coseismic deformations and approximately constrains the major slip area. However, the Kanto region and the area located near the southern edge of the fault plane surface projection show significant disagreement with our

coseismic displacement estimates. This fact can be explained by a relatively low slip resolution of our model and rupture length underestimation. The far-field data are sensitive to the most intense slip only. Therefore, we cannot resolve for the southern part of the rupture characterized by far less slip values. Nevertheless, our simple model demonstrates a possibility of fast preliminary source parameter determination of a large earthquake using a sparse regional GPS network. This result is very important for the tsunami early warning system development.

GPS stations in the south of the Russian Far East, North East China and the Korean Peninsula exhibit the postseismic displacements along with coseismic deformations. The maximum magnitudes of postseismic offset detected at some of the network stations already exceeded 25% of appropriate coseismic offset value and have still been continuing. The character of postseismic deformations tell in favor of afterslip nature of the observed postseismic signals.

The significant part of our observation GPS network is performing the high-sampling rate (1-Hz) data recording. A number of good waveforms of the long-period surface waves were obtained from these systems. These data provide us a possibility to study various characteristics of the low-frequency wave propagation, viscoelastic and rheological properties of the earth's crust between the Japanese Islands and the continent, etc.

Движения земной коры Восточной Азии, вызванные землетрясением Тохоку 11 марта 2011г., Mw =9.0

Н.В. Шестаков[1,2], Хироаки Такахаши[3], Мако Охзоно[3], В.Г. Быков[4], М.Д. Герасименко[1], А.С. Прытков[5], В.А. Бормотов[4], М.Н. Лунева[4], А.Г. Коломиец[1], Г.Н. Герасимов[1], Н.Ф. Василенко[5], Джеонгхо Баек[6,7], Пил-Хо Парк[7], А.А. Сорокин[8], В.Ф. Бахтияров[9], Н.Н. Титков[9], С.С. Сероветников[9]

[1] – Институт прикладной математики ДВО РАН, г. Владивосток, Россия

[2] – Университет Кванун, г. Сеул, Республика Корея

[3] – Институт сейсмологии и вулканологии Хокайдского университета, г. Саппоро, Япония

[4] – Институт тектоники и геофизики ДВО РАН, г. Хабаровск, Россия

[5] – Институт морской геологии и геофизики ДВО РАН, г. Южно-Сахалинск

[6] – Корейский институт астрономии и космических исследований, г. Дайджон, Республика Корея

[7] – Университет науки и технологий, г. Дайджон, Республика Корея

[8] – Вычислительный центр ДВО РАН, г. Хабаровск

[9] – Камчатский филиал геофизической службы РАН, г. Петропавловск-Камчатский, Россия

11 марта 2011г. в 05:46UTC у тихоокеанского побережья о. Хонсю произошло одно из сильнейших за последние 100 лет землетрясений с магнитудой Mw = 9.0 (землетрясение Тохоку), породившее катастрофическое цунами, вызвавшее большие разрушения на восточном побережье Японских островов. Очаг сейсмического события находился вблизи конвергентной границы, вдоль которой Тихоокеанская плита погружается (субдуцирует) под Северо-Американскую или Евразийскую плиту, в зависимости от принятой конфигурации их границ. Землетрясению Тохоку предшествовала серия сильных форшоковых сейсмических толчков, а после основного события последовала серия многочисленных афтершоков, 62 из которых имели магнитуду $Mw \geq 6.0$ и которые продолжаются до сих пор.

Накоплению напряжений в данном районе способствует быстрое относительное движение Тихоокеанской плиты, происходящее со скоростью около 80мм/год. Согласно многочисленным сейсмологическим и геодезическим определениям механизм очага землетрясения – пологий взброс-меганадвиг со стороны Тохоку. Амплитуда смещений в очаговой области по разным оценкам достигает 30-50 м, а длина сейсморазрыва около 400 км.

В отличие от Суматра-Андаманского землетрясения 2004 г., данное сейсмическое событие произошло вблизи густонаселенной территории, полностью покрытой плотными сетями сейсмологических, геодезических и иных типов геофизических наблюдений, что позволило получить значительный объем разнообразной измерительной информации в

ближней к эпицентру зоне, интенсивный анализ которой сейчас продолжается.

Землетрясение Тохоку вызвало значительные смещения и деформации земной коры. По данным японской национальной GPS-сети GEONET ближайшие к эпицентру районы Японии испытали косейсмические смещения к востоку и юго-востоку, а также опускание. Максимальная величина горизонтальной и вертикальной подвижки составила 4,4 м и -0,75 метров, соответственно. В последующие после землетрясения дни наблюдались значительные постсейсмические смещения, максимальная величина которых, по данным Японского агентства геопространственных данных (GSI), к 12 мая достигла 53 см.

Горизонтальные косейсмические смещения земной коры, варьирующие от нескольких миллиметров до нескольких сантиметров, также были зарегистрированы и в удаленной от эпицентра зоне – на юге Дальнего Востока РФ, на территории Восточного Китая и всем Корейском полуострове. Наиболее интенсивные подвижки до 4-5 см произошли на юге Приморского края и Корейском полуострове, а также расположенных к востоку от него островах. Все векторы смещений ориентированы в направлении эпицентра землетрясения, что указывает на относительно небольшие размеры сейсморазрыва, который, однако, характеризуется значительно большей максимальной величиной смещения в очаге по сравнению с Суматро-Андаманским землетрясением. На это указывают также и меньшие размеры области измеримых GPS-методами косейсмических смещений (более 1мм), размеры которой не превосходят по нашим оценкам 2500-2900км к западу от эпицентра. Интересно отметить, что ни одна из трех GPS станций, расположенных на о. Сахалин (г. Южно-Сахалинск, Углегорск, Оха) не зарегистрировала сколько-нибудь значительных косейсмических-смещений, в отличие от станции KUNA (о. Кунашир), демонстрирующей подвижку к северу с амплитудой около 10 мм, что объясняется ее расположением вблизи нодальной плоскости сейсморазрыва.

Путем инверсии оценок косейсмических смещений GPS пунктов дальней зоны была построена предварительная модель очага землетрясения Тохоку в виде одной плоскости разрыва размерами 200×96 км^2 и равномерным смещением по ней, равным 22.9 м. Полученный сейсмический момент $M_0 = 1.3 \cdot 10^{22}$ Нм соответствует моментной магнитуде Mw = 8.7, что несколько меньше соответствующего ее значения по сейсмологическим данным. Построенная простая модель вполне удовлетворительно объясняет косейсмические горизонтальные смещения в дальней и ближней зоне, за исключением района Канто и небольшой области южнее г. Сендай, демонстрирующей значительно большие смещения чем предсказывает наша модель. Этот эффект, а также занижение магнитуды, по-видимому, связаны с достаточно низкой разрешающей способностью нашей модели, которая не позволяет учесть влияние южной части сейсмического разрыва, смещения в которой значительно меньше чем по северному участку, на котором реализовались основные

подвижки в очаге. Именно этот участок наиболее интенсивных смещений, наиболее вероятно, фиксируется нашей моделью. Тем не менее, полученный результат показывает, что на базе редкой региональной GPS сети можно оперативно и с достаточно высокой точностью оценить параметры очага удаленного землетрясения, в том числе характер и величину смещения по разрыву, сейсмический момент и моментную магнитуду, что имеет важное значение для организации работы службы раннего предупреждения о цунами.

Данные GPS станций, расположенные на юге Приморья, северо-востоке Китая и в Южной Корее, также зарегистрировали и продолжают регистрировать заметные постсейсмические смещения величина, которых для отдельных пунктов (VLAD, Владивосток) достигла 25% от косейсмической подвижки. Характер этих смещений указывает на продолжающийся афтерслип в плоскости сейсморазрыва.

Поскольку, в настоящее время, значительная часть пунктов GPS-наблюдений осуществляет регистрацию спутниковых сигналов с интервалом 1 сек (1Гц), удалось получить большое количество записей поверхностных колебаний, дающих обширный материал для изучения характеристик и особенностей распространения низкочастотных волн, а так же реализации косейсмических смещений, порожденных землетрясением Тохоку.

Эти и другие полученные результаты будут представлены в докладе.

Death Rate of Tsunami Disaster of 2011 East Japan Supergiant Earthquake

KIMATA Fumiaki, Makoto TAKAHASHI and Shigeyoshi TANAKA*
Graduate School of Environmental Studies, Nagoya University, 464-7801 Japan
kimata@seis.nagoya-u.ac.jp

There are many tsunami disaster histories in the Pacific Coast of East Japan, such as 1896 M8.5 Meiji-Sanriku and 1933 M8.1 Showa-Sanriku tsunamis. In the Meiji-Sanriku Tsunami, tsunami earthquake occurred and people felt small shaking and they had no ideas of tsunami attack. Over 26,000 people were killed by 10- 15 m height tsunami. There was death rates over 30% were reported in three counties of Iwate prefecture.

On March 11, 2011, a mega-thrust earthquake was occurred in the subduction zone of Japan Trench. Japan Metrological Agency (JMA) issued the tsunami warming in five minutes after the shaking. In the Pacific Coast area, high breakwaters over 10 m or 15 m height were built after the 1960 Chile Earthquake Tsunami. Tsunami drills are renewed every year, and the last one was done on March 3, 2011.

However we lost over 23,000 peoples by tsunami attack on March 11. It is no chance to investigate the death rate of tsunami disaster until now. We estimated the rates from the population of the area of tsunami attack, and dead and missing persons. The rates suggest over 10% in four local cities and towns. It is sure that some neighborhood association lost over 30% population by the tsunami. It is high rate than that of death by earthquakes.

Before the March 11 Tsunami, it is pointed out low proportion of people evacuated under the JMA warming and no evacuation issue from the local governments in Japan. Additionally JMA underestimated the earthquake magnitude and tsunami height of the March 11 event. It is clear that we could not save the human lives with only the early tsunami warming system.

Simulation of tsunami and long-period ground motions during the M9.0 2011 Tohoku-oki earthquake

Anatoly Petukhin , Kunikazu Yoshida, Ken Miyakoshi

Geo-Research Institute, Japan

On March 11, 2001, M9.0 earthquake has occurred east off the Pacific coast of Tohoku, as a result of thrust faulting on the interface of plate boundary between the Pacific and North American plates. This earthquake generated tsunami of 30-40m high and strong ground motions up to 1000gal and more. This is one of the best geophysically-recorded great earthquakes and due to this numerous source models were generated using teleseismic, GPS, strong ground motion and tsunami data. The question we addressing here is the possibility of evenly good simulation of observed ground motions and tsunami using the same source model.

Here we used rupture process of the 2011 Tohoku earthquake inverted by the multi-time window linear waveform inversion method using the long-period (20-200s) strong-ground motion data (Yoshida et al., 2011). A single planar fault model of 470 km in strike and 130 km in dip is assumed. The rupture velocity inferred to be slower than 2.5 km/s at early stage of the rupture process. The inverted slip distribution shows a large elongated asperity (large slip area) with a maximum slip of 47 m which is located on the shallower part of the fault plane, slightly north of epicenter (Figure 1). Area of the moment rate large amplitudes, which is responsible for generation of short period ground motions, is shifted to deeper part of the source and have tendency to scatter in a few strong motion generation areas. This is consistent with the empirical Green’s function simulation results of Irikura and Kurahashi (2011).

We simulated tsunami using fully nonlinear Bousinessq type model of Watts et al. (2003), and source model of Yoshida et al. (2011) and compared it with observation data and with results of simulation using other source models. Simulation results fit observed tsunami waves in the off-shore area (Figure 2), and inundation data on the coast of the Miyagi and Fukushima prefectures (Figure 3). On the coast of Iwate prefecture, north of asperity, simulated amplitudes are smaller than observed ones. Possible reason of the underestimated simulated amplitudes is a small resolution of used bathymetry data for this area.

Source modeling using ground motions with periods shorter than 20s is troublesome, because we need to calculate large volume of the 3-D Green’s functions, instead of a simple 1-D case, which is valid for periods 20s and more. In order to check if the long period source model can explain ground motions at shorter periods, we simulated waves for periods 5s and more using 3-D velocity model compiled from the J-SHIS deep sedimentary structure model, subduction plate model, Conrad and Moho model of Katsumata (2010).

Acknowlegements. We used the seismic waveform data of the F-net, K-NET, and KiK-net networks, tsunami waveform data of the Nationwide Ocean Wave Information network for Ports and Harbours (NOWPHAS), and tsunami field observations of Building Research Institute. Deep sedimentary structure model is developed by NIED.

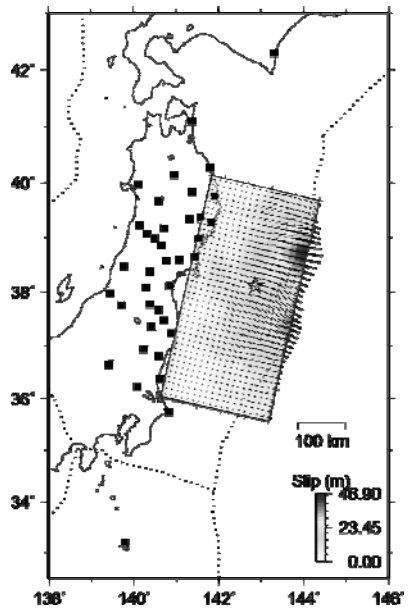


Figure 1. Slip distribution of the source model. Points – hard rock sites used for source inversion.

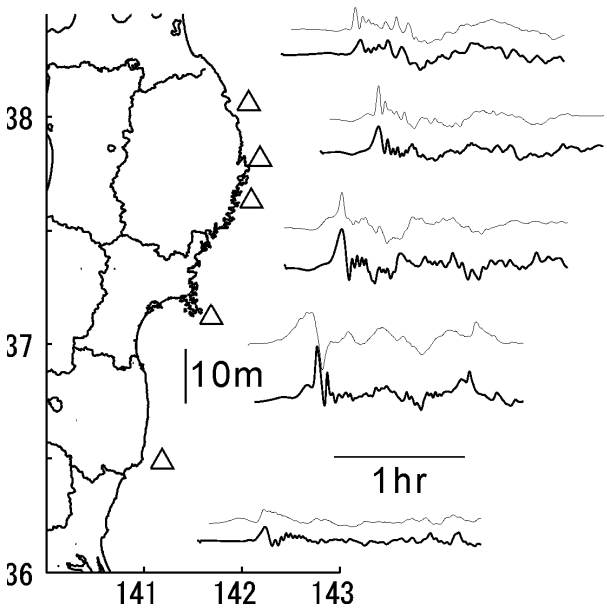


Figure 2. Comparison of observed (upper wave) and simulated (lower wave) tsunami waveforms for off-shore GPS tsunami meters (triangles).

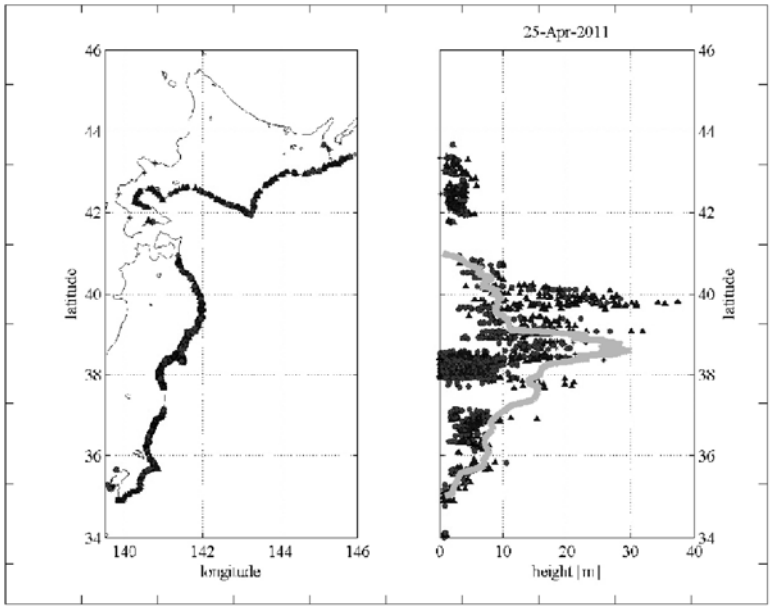
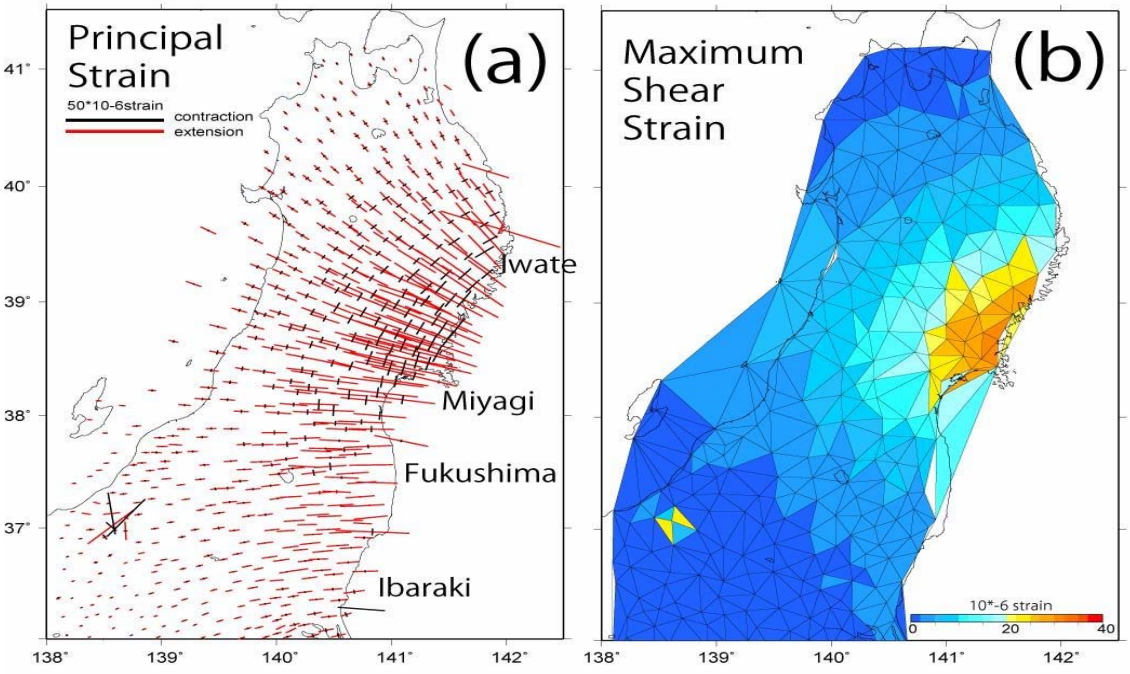


Figure 3. Comparison of observed (points) and simulated (line) maximum amplitudes of tsunami.

Static strain and stress changes in eastern Japan due to the 2011 Tohoku earthquake, Japan, as derived from GPS data

Hiroaki Takahashi
Institute of Seismology and Volcanology, Hokkaido University, Sapporo, Japan
hiroaki@mail.sci.hokudai.ac.jp

The 2011 M 9.0 Tohoku-oki earthquake induced regional crustal deformation not only on the Japanese Islands but also northeastern Asia. Strain release due to mainshock faulting should cause strain redistribution in overriding plates. The dense GPS network in Japan enables us to calculate coseismic strain and stress changes from observed data. Strain is a more objective indicator than displacement because no reference frame is required. The coseismic strain field clearly indicates island-scale strain redistribution. Huge extensional strain changes were concentrated in southern Iwate and northern Miyagi regions with maximum value 45*10-6, which might correspond with approximately 250-500 years of strain accumulation. This implies relatively large strain accumulation and releasing off these regions. Small strain decay in northernmost Niigata-Kobe tectonic zone and anomalous coulomb failure stress change in Mt. Fuji region were observed. Triggered earthquakes occurring above regions might be associated with these anomalies, and/or these non-uniform crustal deformations may reflect crustal heterogeneity.



THE ERUPTION OF EKARMA VOLCANO IN 2010

Rybin A.V., [1] Degterev A.V., [1] Chibisova M.V., [1] Neroda A.S., [2] Melekestsev I.V., [3] Izbekov P.E., [4] Chashchin S.A., [5] Koroteev I.G.[1]

[1]*Institute of Marine Geology and Geophysics FEB RAS, Yuzhno-Sakhalinsk, Russia*
[2]*Il'ichev Pacific Oceanology Institute FEB RAS, Vladivostok, Russia*
[3]*Institute of volcanology and seismology FEB RAS, Petropavlovsk-Kamchatsky, Russia*
[4]*Geophysical Institute of Alaska University Фэрбенкс, Fairbanks, USA*
[5]*Far East Geological Institute FEB RAS, Vladivostok, Russia*

Ekarma Island is located in the northern group of the Kurile Islands between Chirinkotan and Shiashkotan Islands. Ekarma volcano occupies the western half of the island (48° 57'N; 153° 56'E). Its height is 1171 m. It is a single stratovolcano formed by numerous lava flows with lengths up to 3 km. All the eruptions occurred from summit crater, the last of them is represented by vigorous flow of fan-like form erupted to western direction.

According to Gorshkov data the only great eruption occurred in 1767-1769, which formed the modern view of the volcano. (Gorshkov, 1967). In May24 1980 the information about series of the explosions, lasted during an hour, was received from passing ship, the black eruptive column rose on the height more than 1 km (Ivanov at.el. 1981). This is the only mention about the activity of the volcano during such long period.

The analysis of satellite images during the period from 2000 till 2008 also showed the absence of the manifestations of volcano activity and only since June 2009 weak fumarolic activity is fixed on the southern slope of the volcano.

The information about the behavior of the eruption was receive from A.S. Neroda, scientific worker of Il'ichev Pacific Oceanology Institute FEB RAS, which with the group of the researchers on the investigation of the Kurile population of eared seals was in Skala Dolgaya Island (The group of Lovushki Islands) (42 km to the south-west of Ekarma Island) from May, 28 till July, 11. They observed two episode of the activity of the volcano in June, 16 and 30, which were accompanied with ash emission. On the southern slope of the volcano three isolated sites with intensive steam-gas activity were formed on the heights 720, 820 and 1160 meters.

The study of the volcano was conducted after the eruption in August, 24 1910. The surroundings of the volcano were covered with light-grey ash. On the southern and northern slopes the descending of the lahars were found. Ash collected on the summit part of the volcano (thickness up to 5 sm) granulometrically related to aleuropelite: the fraction lesser than 0.05 mm is 73.9 %, the share of other fractions does not usually exceed 3-4 % and it is predominantly presented by angular particles of effusive rocks, in lesser degree by the fragments of the crystals of plagioclase, pyroxene, rarer olivine and also their growths. Besides that in great number changed rocks are met: pyrite, sulfur, gypsum, manifested the resurgent character of pyroclastic. Also the view of the particles shows thos – the considerable part of the fragments is covered with hydroxide of ferrum. The preliminary volume of the erupted material is $2*10^5$ м^3.

The eruption influenced to the ecosystem of the island. On the height 250-300 m the plants with the signs of damage were met, on the height about 550 m the most part of the plant was desiccated, larger bushes (alder, willow) also had the obvious signs of influence of volcanic agents.

At present time steam-gas activity is only on the central and upper fumarolic sites of the volcano.

ИЗВЕРЖЕНИЕ ВУЛКАНА ЭКАРМА В 2010 ГОДУ

Рыбин А.В[1]., Дегтерев А.В[1]., Чибисова М.В[1]., Нерода А.С[2]., Мелекесцев И.В[3]., Избеков П.Э[4]., Чащин С.А[5]., Коротеев И.Г[1].

[1]*Институт морской геологии и геофизики ДВО РАН, Южно-Сахалинск, Россия*

[2]*Тихоокеанский океанологический институт им. В.И. Ильичева ДВО РАН, Владивосток, Россия*

[3]*Институт вулканологии и сейсмологии ДВО РАН, Петропавловск-Камчатский, Россия*

[4]*Геофизический институт при университете штата Аляска, Фэрбенкс, США*

[5]*Дальневосточный геологический институт, Владивосток, Россия*

Остров Экарма находится в северной группе Курильских островов и расположен между островами Чиринкотан и Шиашкотан. Вулкан Экарма занимает западную половину острова (48° 57'N; 153° 56'E). Высота 1171 м. Это одиночный стратовулкан сформированный многочисленными лавовыми потоками длиной до 3 км. Все извержения происходили из вершинного кратера, последнее из них представлено вязким потоком веерообразной формы излившимся в западном направлении.

По данным Г.С.Горшкова единственное сильное извержение произошло в 1767-1769 годах, которое и сформировало современный облик вулкана. (Горшков, 1967)24 мая 1980г. с проходящего судна было получено сообщение о серии взрывов, происходивших в течение часа, черный эруптивный столб поднимался на высоту более 1 км (Иванов и др., 1981). Это единственное упоминание об активности вулкана за столь долгий период.

Анализ космических снимков в период с 2000 по 2008 годы, также показал, отсутствие признаков активности вулкана и только начиная с июня 2009 года на южном склоне вулкана фиксируется слабая фумарольная активность.

Информация о ходе извержения поступила от А.С. Нероды, научного сотрудника Тихоокеанского океанологического института им. В.И.Ильичева ДВО РАН, который в составе группы исследователей по изучению Курильской популяции сивуча находился на острове Скала Долгая (группа островов Ловушки) (42 км юго-западнее острова Экарма) с 28 мая по 11 июля. Ими наблюдалось два эпизода активизации вулкана 16 и 30 июня, сопровождавшиеся выбросом пепла. На южном склоне вулкана образовались три изолированные площадки на высотах 720, 820 и 1160 метров с интенсивной парогазовой деятельностью.

Обследование вулкана было проведено после извержения 24 августа 2010 года. Окрестности вулкана были покрыты светло- серым пеплом. На южном и северном склонах обнаружены сходы лахар. Пепел, отобранный с вершинной части вулкана (мощность до 5 см), в гранулометрическом отношении соответствует алевропелиту: фракция менее 0.05 мм составляет 73.9 %, доля остальных фракций обычно не превышает 3-4 % и представлен преимущественно угловатыми частицами эффузивных пород, в меньшей степени обломками кристаллов плагиоклаза, пироксена, реже оливина, а также их сростками. Кроме того, в большом количестве встречаются измененные породы: пирит, сера, гипс, свидетельствующие о резургентном характере пирокластики. На это же указывает и облик частиц - значительная часть обломков покрыта налетом гидроокислов железа. Ориентировочный объем изверженного материала составляет $2*10^5$ $м^3$.

Извержение оказало некоторое воздействие на экосистему острова. С высоты 250-300 м начали встречаться растения с признаками поражения, далее, на высоте около 550 м, большинство растений было иссушено, более крупные кустарники (ива, ольха) также имели явные следы воздействия (засохшие листья и пр.) вулканических агентов.

В настоящее время парогазовая активность сохранилась только на средней и верхней фумарольных площадках вулкана.

THE VOLCANIC ERUPTIONS OF KAMCHATKA: ONE DECADE OF NASA SATELLITE OBSERVATIONS

Michael Ramsey[1], Rick Wessels[2], Jonathan Dehn[3], Kenneth Duda[4], Adam Carter[5] and Shellie Rose[6]

[1] *Department of Geology and Planetary Science, Univ. of Pittsburgh, Pittsburgh, PA, USA.*
[2] *Alaska Volcano Observatory, USGS Alaska Science Center, Anchorage, AK, USA.*
[3] *Geophysical Institute/Alaska Volcano Observatory, Univ. of Alaska, Fairbanks, AK, USA.*
[4] *EROS Data Center, Sioux Falls, SD, USA.*
[5] *Exxon Mobile Corporation, Houston, TX, USA.*
[6] *United States Army Corps of Engineers, Alexandria, VA, USA.*

For the past eleven years, the joint US-Japanese Advanced Spaceborne Thermal Emission and Reflection Radiometer (ASTER) instrument has been acquiring image-based data of volcanic eruptions in the Northern Pacific region. There have been more ASTER observations of Kamchatka volcanoes than any other location on the globe. The ASTER sensor has three distinct wavelength regions (visible/near infrared (VNIR), short wave infrared (SWIR) and thermal infrared (TIR)) and three spatial resolutions (15, 30 and 90 m/pixel). The data have proven extremely valuable for volcanological studies due the broad wavelength range, high spatial resolution, thermal infrared observations at night, and the ability to create digital elevation models (DEMs). At higher latitudes, the temporal resolution improves from the nominal 16 day repeat time to better than 7 days, which can then be further improved with off-nadir pointing and novel approaches such as integration with the data from other satellite sensors.

Early ASTER observations of the numerous eruptions in Kamchatka spurred interest in using the sensor for volcano monitoring in the north Pacific. These data gave rise to a now seven year long program of rapid response scheduling and imaging of volcanic activity throughout the Aleutian, Kamchatka and Kurile arcs. This program was designed to automate the ability of the ASTER instrument for targeted observations and expedited processing. The urgent request protocol (URP) is one of the unique characteristics of ASTER, which provides a limited number of emergency observations, typically at a much-improved temporal resolution and quicker processing time. The system has been combined with the operational monitoring carried out by the Alaska Volcano Observatory (AVO), which relies on high temporal/low spatial resolution (4-6 hours/1.1-km) AVHRR data to detect thermal anomalies and plumes. The integrated ASTER URP program has resulted in a much improved observational frequency (e.g., daily over three day periods) and the data being made available within 2-4 hours after it is acquired.

Automated hot spot alarms from the AVHRR data (assuming the volcanic activity is strong enough to be detected) trigger ASTER acquisitions using the "rapid response" mode. Specifically for Kamchatka, the URP Program has resulted in more than 700 additional ASTER images of the most thermally-active volcanoes (e.g., Shiveluch, Kliuchevskoi, Karymsky Bezymianny and Kizimen). The program is now averaging one new ASTER image over the Kamchatka Peninsula approximately every three days, with 48% of the total archive focused on Shiveluch due to its long-lived persistent activity. These data have produced valuable quantitative information on the small-scale activity and larger eruptions.

Numerous eruptions have been observed in Kamchatka, which have displayed varying volcanic styles. The high spatial resolution and moderate spectral resolution (particularly of the ASTER TIR system) has been ideal for deriving the composition, vesicularity, and emplacement rates of active domes and flows. The entire ASTER archive was queried and two specific examples are presented here. Bezymianny is characterized by a summit lava dome and overlapping pyroclastic flow (PF) deposits to the southeast. Three explosive eruptions (24 December 2006, 11

May 2007, and 14 October 2007) generated pyroclastic flows dominated by juvenile material primarily due to column collapse. Following this, a gravitational lava dome collapse event generated block and ash flow on 5 November 2007. ASTER data acquired over this time period detected three periods of increased thermal activity that coincided with each eruption. For two of these periods, the thermal output increased significantly just prior to the eruption (Figure 1). These data provide information on an actively changing explosive volcanic system and specifically documents changes over recently-emplaced and cooling PF deposits.

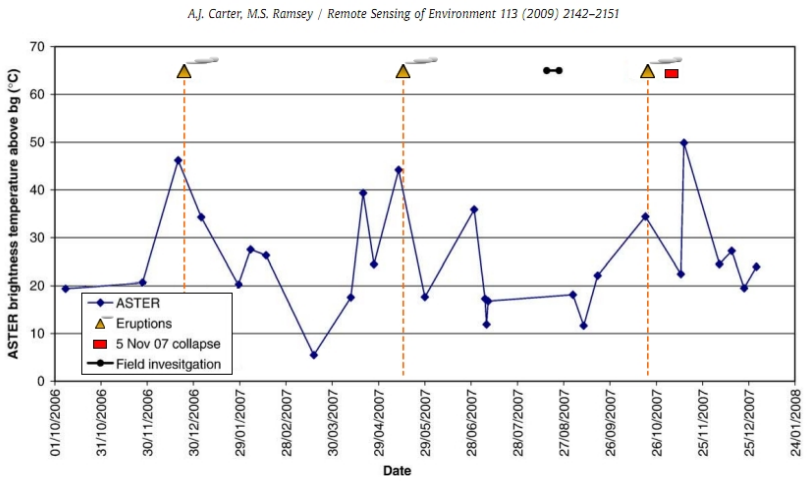


Figure 1. *ASTER TIR-derived pixel-integrated max brightness temperature over the Bezymianny lava dome from Oct. 2006 to Dec. 2007. Significantly elevated temperatures were noted around the times of the Dec. 2006 and May 2007 eruptions. However, only slightly-elevated temperatures were detected prior to the Oct. 2007 eruption, which may have been caused by thin clouds obscuring the dome. ASTER temperatures are accurate to within 2°C, which provides an error margin on the data.*

Shiveluch Volcano is one of the largest and most vigorous andesitic volcanoes in Kamchatka. The volcano has been in a long period of heightened activity during the years from 2004-2010. ASTER TIR data were collected during both day- and night-time satellite overpasses prior to and following the large eruption of 27 Feb 2005 and the dome growth that followed. During a field campaign six months later, the summit crater was overflown by helicopter and an actively-extruding silicic lava dome was imaged. The airborne and spaceborne TIR data were compared to long distance ground-based photography of the dome in order to calculate the extrusion rates. This highly active period at Shiveluch provided a unique base from which to extend previous models of silicic lava dome growth and subsequent collapse.

In summary, the ASTER rapid response program in Kamchatka and Alaska has resulted in hundreds of new ASTER scenes. The ongoing research/operational program is a collaboration between NASA, the USGS, AVO, IVS/KVERT, the University of Pittsburgh (UP) and the University of Alaska – Fairbanks (UAF) and has proven to be highly successful. This work has recently been funded by NASA for another three years. The focus on the North Pacific will continue and a new goal has been added to expand the system globally using detections from the MODIS sensors. The program should improve the frequency of ASTER data for active eruptions worldwide and provide a template for future sensors and sensor web integration.

THE ERUPTION OF KIZIMEN VOLCANO DURING 2010-2011 ACCORDING TO SEISMIC DATA

V. T. Garbuzova, O.V. Sobolevskaya
The Kamchatka Branch of Geophysical Survey of Russian Academy of Sciences, Petropavlovsk-Kamchatsky, Russia, 683006. garb@emsd.ru, sva06@emsd.ru

In this paper the seismicity of Kizimen volcano during 2010-2011 was investigate. The preparation of the volcano's explosive eruptions possibly has begun in July, 2009 and continued till December 2010r. The quantity of earthquakes and the increasing of events energy class (Ks) was gradually observed.

In 2010 r high level of seismicity around volcano has remained and even has considerably grown. The characteristic seismic signals which usually accompany such volcanic processes, as explosions and a pyroclatic flows began to registered near volcano. Weak volcanic tremor was record during 08.12.10 till the end of the year.

The staff of seismic and volcanic activity research laboratory had been made the official forecast on the base of the seismic information analysis during the investigated period, which was passed to main organizations interested in it. This successful forecast of the explosive eruption was made without any experience about this volcano eruption seismic data. It was made due to accumulated experience on Kamchatkan volcanoes monitoring and different data about volcanoes of the world.

Further, till the end of the year, seismic activity, in the form of a considerable quantity of weak local shallow earthquakes and weak volcanic tremor. The volcanic activity with ash emissions continued to observe.

The quantity of earthquakes and the events energy class (Ks) in February and March, 2011 were decrease, but it was not a decreasing of volcanic activity.

ИЗВЕРЖЕНИЕ ВУЛКАНА КИЗИМЕН В 2010-2011 ГГ. ПО СЕЙСМИЧЕСКИМ ДАННЫМ.

В.Т. Гарбузова, О.В. Соболевская
Камчатский филиал Геофизической службы Российской Академии наук, Петропавловск-Камчатский, Россия. garb@emsd.ru, sva06@emsd.ru
683006, г. Петропавловск-Камчатский, бульвар Пийпа 9.

В работе была исследована сейсмичность вулкана Кизимен за период 2010-2011 гг. Подготовка эксплозивного извержения вулкана Кизимен вероятно началась еще в июле 2009 г. и продолжалась до декабря 2010г. Постепенно нарастало количество землетрясений I-III типов, а так же наблюдалось увеличение энергетического класса событий.

В 2010 г высокий уровень сейсмичности в районе вулкана сохранился и даже значительно вырос. Помимо землетрясений с разных глубин, на вулкане стали регистрироваться характерные сейсмические сигналы, которые обычно сопровождают такие вулканические процессы, как взрывы газа и сход пирокластических потоков. В период с 08.12.10 и до конца года регистрировалось слабое вулканическое дрожание.

На основании анализа сейсмической информации в течение исследуемого периода, сотрудниками лаборатории ИСВА был сделан официальный прогноз, который был передан в КФ РЭС и участникам международного проекта KVERT. Успешный прогноз сильного эксплозивного извержения вулкана Кизимен был сделан сотрудниками лаборатории ИСВА при отсутствии опыта регистрации извержений этого вулкана по сейсмическим данным, благодаря накопленному опыту по слежению за Камчатскими вулканами и с привлечением литературных данных о подобных вулканах мира.

В дальнейшем, до конца года, продолжала наблюдаться сейсмическая активность, в виде большого количества слабых локальных поверхностных землетрясений и слабого вулканического дрожания, и вулканическая активность, в виде пепловых выбросов. В феврале-марте 2011 г. энергия землетрясений и их количество несколько снизились, но это не было снижением вулканической активности. В мае значительно увеличилось количество мощных поверхностных событий и амплитуда вулканического дрожания, что возможно свидетельствует о подготовке к пароксизмальной стадии извержения.

EXPERIMENTAL MODELING OF PERIODICITIES IN THE DYNAMICS OF LAVA FOUNTAINING

Ozerov A. Yu.
Institute of Volcanology and Seismology, Far East Branch, Russian Academy of Sciences, Petropavlovsk-Kamchatsky, Russia, ozerov@ozerov.ru

Periodic fountaining of incandescent volcanic bombs is one of the most grandiose processes on the Earth. Fountaining episodes begin sharply, without preliminary seismic preparation. Glowing bombs in the form of a fan or a vertical stream are thrown out to the height of 50 – 500 m depending on the character of the volcano and intensity of the eruption. During low intensity fountaining about 10 - 100 tons/s of volcanic bombs are ejected to the surface, during average – 100 - 1 000 tons/s, and during strong – over 1 000 tons/s.

Volcanic bombs are formed of liquid basalt magma as a result of bursting of gas bubbles formed in the melt during magma's ascent to the surface. Mass exsolution of magmatic bubbles from the melt leads to fountaining of incandescent bombs.

Since 1983 we have been conducting volcanological and geophysical (volcanic tremor) studying of incandescent fountains at Klyuchevskoy volcano. Analysis of continuously registered geophysical data (volcanic tremor), processed by means of statistical analysis, allowed us for the first time to identify steady periodicities in the dynamics of fountaining which are manifested in a wide time range: from tens of minutes – to tens of hours [*Ozerov and Konov,* 1988]. During studying of eruptions in 1984, 1993 and 2007 it has been established that at steady increase of magma discharge in the volcanic crater three regimes of fountaining are sequentially manifested: steady low-intensity, periodic and steady high-intensity. Two intervals of change of the regime (ICR) – ICR-1 of "entry" to the periodic regime and ICR-2 of "exit" from it have been identified [*Ozerov et al.,* 2007]. The obtained results laid the basis for laboratory experiments.

Analysis of descriptions of eruptions and seismograms at other basalt volcanoes of the world has allowed to establish periodic fountaining at the following volcanoes: Tolbachik (Kamchatka), Etna (Sicily), Kilauea (Hawaii), Niragongo (Africa), Karkar (Papua New Guinea); in literature only 1 description of periodicity in the dynamics of fountaining can be found for an underwater volcano NW Rota-1 in the Mariana Trench [*Chadwick et al.,* 2008].

Fountaining of incandescent bombs is poorly studied in Volcanology. Attempts to involve known gas-liquid regimes in vertical conduits - bubbly, slug, annular and disperse - have not offered an unambiguous explanation of the reasons of this phenomenon. Therefore to study this phenomenon the author undertook laboratory experiments since 2003.

Our goal was to reveal the reasons of periodicities in the dynamics of fountaining of incandescent bombs at basalt volcanoes. Experimental studies included studying of behavior of gas bubbles during their barbotage in vertical pipes through model liquids of various densities with subsequent comparison of the obtained data to real volcanic events. For these studies a Complex Apparatus for Modeling Basaltic Eruptions – CAMBE in a "barbotage column» version has been designed.

While constructing the complex apparatus we did our best to consider the parameters of real feeding magma systems. Klyuchevskoy volcano (Kamchatka) has been accepted as a basis – a typical basaltic volcano. The complex apparatus consists of two systems – modeling and registrating.

The modeling system represents a transparent, vertically positioned plastic hose with the height of 15 700 mm and internal diameter of 18 mm. The bottom end of the hose is plugged with a stopper through which a hollow needle is entered. The top part of the hose is opened; it enters an aquarium that receives the arriving model liquid. The hose simulates a feeding channel of a volcano, and an aquarium - a volcano crater. In the experiments liquid and gas are used. For modeling liquid we used a 35 % glycerin in water solution. As a barbotage gas we used usual compressed air

supplied from a gas cylinder. The majority of experiments have been conducted with the bubbles of one size that relates to the internal diameter of the hose as ~ 1:20 which excludes a possibility of locking the internal section of the hose with a large bubble.

In the course of experiments, a new earlier unknown morphologically steady gas-hydrodynamic structure - an open bubbly cluster has been identified. It represents a volume of liquid with high concentration of bubbles, separated with a liquid containing no free gas phase from above and from below. A set of open bubbly clusters (following one another at a fixed distance), divided by liquid without bubbles, represents a periodic regime of open clusters. This regime is the key one in the course of periodic fountaining of incandescent bombs in the volcanic crater.

Origination of cluster regime leads to essential redistribution of bubbles in the barbotage column which at the surface results in intensive splatter of the liquid due to bursting of cluster bubbles. In the intervals between arrival of clusters the liquid surface remains quiet. Thus, steady periodic fountaining of the liquid is realized. These data allow us to assume that during volcanic eruption similar process takes place, when bursting of cluster bubbles at the crater in liquid magma produces lava fountaining, and elastic basalt bombs are thrown out.

Additional information was obtained through acoustic studies on CAMBE on the change of pressure of the sound wave generated by bursting of bubbles on the surface of the model liquid. Results of acoustic studies are comparable with the data of volcanic tremor during eruptions at Klyuchevskoy in 1984, 1993 and 2008. Comparison of natural and experimental plots shows their big similarity in consecutive realization of three regimes (accordingly, in the pair natural process – experiment: uniform low-intensity – uniform low debit, periodic in both processes, uniform high-intensity – uniform high debit). Two intervals of change of the regime (ICR) have been identified, both during volcanic eruptions and in the experiments: ICR-1 "entry" in a periodic regime and ICR-2 "exit" from it. The obtained data justified the experimental results on CAMBE with reference to the mechanism of the processes occurring in the feeding conduit of Klyuchevskoy volcano.

Based on the conducted experiments and natural studies a new model of gas-hydrodynamic movement of magma melt in the conduit of a basalt volcano is offered. Realization of various regimes of the two-phase magma melt flow on the surface is responsible for variety of explosive phenomena in the volcanic crater. Depending on the manifestation of the type of the regime basaltic volcanoes can display various types of explosive activity: 1 – steady low debit regime – steady ash emission with a small amount of volcanic bombs, 2 – periodic regime – energetic periodic fountaining of incandescent bombs, and 3 – steady high debit regime – intensive long monotonous “work” of fountains of volcanic bombs.

References:

Chadwick W.W., Cashman K.V., Embley R.W., Matsumoto H., Dziak R.P., de Ronde C.E.J., Lau T. K., Deardorff N.D., Merle S.G. Direct video and hydrophone observations of submarine explosive eruptions at NW Rota-1 volcano, Mariana arc. J. Geophys. Res. 2008. V. 113, B08S10, P. 1–23.

Ozerov A.Yu., Firstov P.P., Gavrilov V.A. Periodicities in the dynamics of eruptions of Klyuchevskoy volcano, Kamchatka // Volcanism and Subduction: The Kamchatka Region. Geophysical Monograph Series. 2007. V. 172. P. 283–291.

Ozerov A.Yu., Konov A.S. Regularities the dynamics of Klyuchevskoy volcano eruption // Proceeding Kagoshima International Conference of Volcanoes. Japan. 1988. P. 63–65.

ЭКСПЕРИМЕНТАЛЬНОЕ МОДЕЛИРОВАНИЕ ПЕРИОДИЧНОСТЕЙ В ДИНАМИКЕ ЛАВОВЫХ ФОНТАНОВ

Озеров А.Ю.
Institute of Volcanology and Seismology, Far East Branch, Russian Academy of Sciences, Petropavlovsk-Kamchatsky, Russia, ozerov@ozerov.ru

Периодическое фонтанирование раскаленных бомб - один из наиболее грандиозных процессов на Земле. Эпизоды фонтанирования начинаются резко, без предварительной сейсмической подготовки. Светящиеся бомбы в виде веера или вертикальной струи могут выбрасываться на высоту, которая в зависимости от характера вулкана и интенсивности извержения, изменяется в интервале 50-500 м. При фонтанировании слабой интенсивности на поверхность Земли поступает - 10 - 100 тонн/с вулканических бомб, при средней – 100 - 1 000 тонн/с, при сильной – свыше 1 000 тонн/с.

Вулканические бомбы образуются из жидкой базальтовой магмы за счет лопающихся газовых пузырей, образующихся в расплаве при подъеме к поверхности. Массовое выделение магматических пузырей из расплава приводит к фонтанированию раскаленных бомб.

С 1983 года нами проводились вулканологические и геофизические (вулканическое дрожание) изучение раскаленных фонтанов на Ключевском вулкане. На основе анализа непрерывно регистрируемых геофизических данных (вулканическое дрожание), обработанных с помощью методов статистического анализа, впервые в динамике фонтанирования установлены устойчивые периодичности, которые проявляются в широком временном диапазоне: десятки минут – десятки часов [*Ozerov and Konov,* 1988]. При исследовании извержений 1984, 1993 и 2007 гг. было установлено, что при равномерном повышении расхода магмы в кратере вулкана последовательно проявляются три режима фонтанирования: равномерный низкоинтенсивный, периодический и равномерный высокоинтенсивный. Были определены две области смены режима – ОСР-1 «входа» в периодический режим и ОСР-2 «выхода» из него [*Ozerov et al.,* 2007]. Полученные результаты были положены в основу лабораторных экспериментов.

Анализ описаний извержений и сейсмограмм на других базальтовых вулканах мира позволил установить периодическое фонтанирование на вулканах: Толбачинском (Камчатка), Этна (Сицилия), Килауэа (Гавайи), Нирагонго (Конго, Африка), Каркар (Папуа Новая Гвинея), в литературе известно единственное описание периодичности в динамике фонтанирования для подводного вулкана NW Rota-1 в Марианской впадине [*Chadwick et al.,* 2008].

Процесс фонтанирования раскаленных бомб является одним из слабоизученных в вулканологии. Попытки привлечь известные газожидкостные режимы в вертикальных каналах: пузырьковый, снарядный, кольцевой и дисперсный не дали однозначного объяснения причин этого явления. Поэтому для изучения этого феномена автором с 2003 года проводились лабораторные эксперименты.

Задачей исследований было предусмотрено выявление причин периодичностей в динамике фонтанирования раскаленных бомб на базальтовых вулканах. Экспериментальные исследования включали изучение поведения газовых пузырьков при их барботировании сквозь модельные жидкости разной плотности в вертикальных трубах с последующим сопоставлением полученных данных с реальными вулканическими событиями. Для этих исследований был сконструирован Комплекс Аппаратуры Моделирования Базальтовых Извержений – КАМБИ в варианте «барботажная колонна».

При создании установки мы стремились максимально учесть соотношения параметров реальных питающих магматических систем. За основу принят вулкан Ключевской (Камчатка) – типичный представитель базальтовых вулканов. Установка состоит из двух систем - моделирующей и регистрирующей.

Моделирующая система представляет собой прозрачную вертикально расположенную пластиковую трубку высотой – 15 700 мм, внутренний диаметр 18 мм. Нижний торец трубки герметизирован пробкой, сквозь которую в трубку введена полая игла. Верхняя часть трубки открыта и введена в аквариум, созданный для приема поступающей модельной жидкости. Трубка имитирует питающий канал вулкана, а аквариум - кратер вулкана. В работе используется жидкость и газ. В качестве модельной жидкости применяется 35% раствор глицерина в воде. В качестве барботирующего газа применяется обычный воздух,

поступающий под давлением из газового баллона. Основной массив экспериментов был проведен с пузырьками одного размера при отношении диаметра пузырька к внутреннему диаметру трубки примерно 1:20, что исключает возможность запирания внутреннего сечения трубки крупным пузырьком.

В процессе экспериментальных исследований выявлена новая, ранее неизвестная морфологически устойчивая газогидродинамическая структура – открытый пузырьковый кластер. Он представляет собой объем жидкости с высокой концентрацией пузырьков, сверху и снизу ограниченный жидкостью, не содержащей свободной газовой фазы. Совокупность открытых пузырьковых кластеров (следующих друг за другом на фиксированном расстоянии), разделенных между собой слоем жидкости без пузырьков, представляет периодический режим открытых кластеров. Этот режим – определяющий в процессе периодического фонтанирования раскаленных бомб в кратере вулкана.

Возникновение кластерного режима приводит к существенному перераспределению пузырьков в барботажной колонне, которое на поверхности жидкости приводит к интенсивному разбрызгиванию жидкости за счет лопающихся пузырьков кластера. В промежутках между поступлением кластеров поверхность жидкости остается в спокойном состоянии. Таким образом, реализуется устойчивое периодическое фонтанирование жидкости. Эти данные позволяют полагать, что во время извержения на вулкане наблюдается аналогичный процесс, когда из жидкой магмы в кратере за счет лопающихся пузырьков кластера происходит фонтанирование лавы, и вылетают пластичные базальтовые бомбы.

Дополнительную информацию дало акустическое исследование на КАМБИ по изменению давления звуковой волны, генерируемой лопающимися пузырьками на поверхности модельной жидкости. Результаты акустических исследований сопоставлены с данными вулканического дрожания при извержениях Ключевского вулкана 1984, 1993 и 2008 гг. Сравнение природного и модельного графиков демонстрирует большое их сходство в последовательной реализации трех режимов (соответственно в паре природный процесс – эксперимент: равномерный низкоинтерсивный – равномерный низкодебитный, периодический в обоих процессах, равномерный высокоинтенсивный – равномерный высокодебитный). При этом выявлены две области смены режима (ОСР) как при извержениях вулкана, так и в экспериментальных исследованиях: ОСР-1 «входа» в периодический режим и ОСР-2 «выхода» из него. Полученные данные подтвердили справедливость приложения результатов экспериментальных исследований на КАМБИ применительно к механизму процессов, происходящих в подводящем канале Ключевского вулкана.

На основе проведенных экспериментальных и натурных исследований предложена новая модель газогидродинамического движения магматического расплава в подводящем канале базальтового вулкана. Реализация на поверхности различных режимов течения двухфазного магматического расплава ответственна за многообразие эксплозивных явлений в кратере вулкана. В зависимости от проявления типа режима на базальтовых вулканах могут проявляться различные типы эксплозивной деятельности: 1 –равномерный низкодебитный режим – равномерная пепловая эмиссия с небольшим количеством вулканических бомб, 2 – периодический режим – энергичное периодическое фонтанирование раскаленных бомб, 3 – равномерный высокодебитный режим – интенсивная продолжительная монотонная «работа» фонтанов раскаленных бомб.

References:

Chadwick W.W., Cashman K.V., Embley R.W., Matsumoto H., Dziak R.P., de Ronde C.E.J., Lau T. K., Deardorff N.D., Merle S.G. Direct video and hydrophone observations of submarine explosive eruptions at NW Rota-1 volcano, Mariana arc. J. Geophys. Res. 2008. V. 113, B08S10, P. 1–23.

Ozerov A.Yu., Firstov P.P., Gavrilov V.A. Periodicities in the dynamics of eruptions of Klyuchevskoy volcano, Kamchatka // Volcanism and Subduction: The Kamchatka Region. Geophysical Monograph Series. 2007. V. 172. P. 283–291.

Ozerov A.Yu., Konov A.S. Regularities the dynamics of the Klyuchevskoy volcano eruption // Proceeding Kagoshima International Conference of Volcanoes. Japan. 1988. P. 63–65.

Understanding the relation between pre-eruptive bubble size distribution and observed ash particle sizes: Prospects for prediction of volcanic ash hazards

Alex Proussevitch[1], Gopal Mulukutla[1], Kim Genareau[2], and Dork Sahagian[2]

[1] Complex Systems Research Center, University of New Hampshire, USA.
[2] Earth & Environmental Sciences, Lehigh University, USA.

Recent advances in measuring pre-eruptive bubble size distributions (BSDs) from ash particle surface morphology now make it possible to calibrate ash fragmentation models for prediction of pyroclastic characteristics of concern to human health and infrastructure. The same magma bodies can generate various eruption products ranging from course bombs to fine ash, with a wide range of fractionation between these end members that in turn depends on the pre-eruptive bubble size distributions.

We have examined (a) distal ash fall deposits from the 1980 Mount St. Helens (MSH) lateral blast, and (b) the basaltic sub-plinian 1974 eruption of Fuego (Guatemala) using stereo-scanning electron microscopy (SSEM) to obtain pre-eruptive bubble size distributions (BSDs). The analysis routine involved (i) building of digital elevation models of single ash grains from SSEM stereo-pair images (using MeX software), and (ii) calculation of individual vesicle volumes using the BubbleMaker software package developed by the authors. We found two separate and independent ash particle populations within the examined samples: (1) Simple ash particles that contain no bubbles within their interiors, but are parts of the walls of individual bubbles; and (2) larger, compound ash particles that contain multiple bubble imprints on their surfaces as well as additional complete bubbles within their interiors. In the case of MSH eruption BSDs of the two ash types do not vary with distance from the vent, but compound ash particles did not travel beyond a distance of ~300 km from the source where primarily simple ash fragments are observed. These simple fragments are about four orders of magnitude smaller (by volume) than the bubble sizes observed on their surfaces, suggesting that bubble fragmentation leads to the generation of multiple simple ash fragments per nucleated bubble. Although the volume represented by simple ash particles is a minor fraction of the total erupted mass, their number density is quite high and exceeds those for compound ashes.

In order to assess fragmentation efficiency we have devised a method to produce spatial models of bubble textures that match inferred BSDs of pre-fragmentation magma in the eruption column based on conditions of 1-stage bubble nucleation and random nuclear spacing, with either of two bubble growth schemes- (1) unconfined growth in the absence of neighboring bubbles, and (2) limited growth in a melt volume shared with neighboring bubbles. These scenarios lead to different BSDs, thus controlling fragmentation thresholds and patterns. BSD leads to the thickness distribution of bubble walls and plateau borders, so we can predict the size distribution of ash particles formed by rupture of thinnest inter-bubble films, as well as the fraction of compound fragments or clasts derived from parcels of magmatic foam containing thicker walls. As such it is possible to determine the magmatic conditions that lead to eruptions with a high fraction of fine ash of concern to volcanic hazards and respiratory heath.

MONITORING OF VOLCANIC ACTIVITY IN THE KURILE ISLANDS BY SVERT GROUP (SAKHALIN VOLCANIC ERUPTIONS RESPONSE TEAM)

Rybin A.V., Chibisova M.V.
Institute of Marine Geology and Geophysics FEB RAS, Yuzhno-Sakhalinsk, Russia

In 2003 for the organization of the monitoring of active volcanoes of the Kurile Islands SVERT (Sakhalin volcanic eruptions response team) was created on the base IMGG together with Sakhalin Branch of Geophysical Survey RAS and FSI NPP "Rosgeolfond" under the support of Alaska Volcanological Observatory (AVO, University of Alaska, Fairbanks). Its zone of responsibility includes the territory from Kunashir Island to Onekotan Island. The observations of the volcanoes of northern group of the islands (Paramushir and Atlasova), according to the mutual agreement, Kamchatka volcanic eruptions response team (KVERT) conducts. The main directions of SVERT activity connected with collecting and analysis of all accessible information about active volcanoes and creating every-day informational reports on this base. Data of high-orbital meteorological satellites TERRA (spectrumradiometer MODIS), NOAA (spectrumradiometer AVHRR) and MTSAT are the basement for every-day monitoring. The materials obtained during this period show that on the base of the methods of distance satellite sounding (DSS) it is possible to fix even small changes of the state of the volcanoes of the Kurile Islands.

During the period of observations all the events, connected with the activity of volcanoes, were monitored. In June 2009 the strong eruption of Sarychev Peak occurred, the forerunners of it were fixed 23 hours before the beginning of the eruptive activity. During the period of eruption from 11 till 19 of June more than 23 volcanic explosions occurred, eruptive clouds rose up to the height of 8-16 km, and in some cases up to 21 km. The plume of volcanic ash stretched to the west and north-west up to 1.5 thousand km, to the east and south-east more than 3 thousand km. The eruption didn't present the considerable hazard for population because of great distance from the settlements. The ash clouds presented the most danger, complicated the situation for airlines passed along the Kurile Islands. The information about probable eruption and the dynamics of the spreading of ash clouds were represented to all interested organizations.

In 2009 IMGG FEB RAS began to create the system of video-observations of active volcanoes of the Southern Kurile Islands. During the first stage IP-videocamera Trendnet TV-IP201W was placed on seismic station of settlement Yuzhno-Sakhalinsk at the distance 11 km from Mendeleev volcano. For the transmission in Internet the standard devices of the provider with aligned routing are used. The materials of the observations are now available on the servers http://www.imgg.ru and http://webcam.sakh.com/?webcam=mendeleev&lang=ru. In future we are planning to install the web-cameras for the observation of Tyatya volcano (Kunashir Isl.), Ivan Grozny and Baransky volcanoes (Iturup Isl.)

МОНИТОРИНГ ВУЛКАНИЧЕСКОЙ АКТИВНОСТИ НА КУРИЛЬСКИХ ОСТРОВАХ ГРУППОЙ SVERT (САХАЛИНСКАЯ ГРУППА РЕАГИРОВАНИЯ НА ВУЛКАНИЧЕСКИЕ ИЗВЕРЖЕНИЯ).

Рыбин А.В., Чибисова М.В.
Институт морской геологии и геофизики ДВО РАН, Южно-Сахалинск, Россия

В 2003 г. для организации мониторинга активных вулканов Курильских островов на базе ИМГиГ ДВО РАН совместно с Сахалинским филиалом геофизической службы РАН и ФГУ НПП «Росгеолфонд» при поддержке Аляскинской вулканологической обсерватории (AVO, University of Alaska, Fairbanks) была создана группа SVERT (Sakhalin volcanic eruptions response team) Сахалинская группа оперативного реагирования на вулканические извержения. Зона ответственности включает территорию от о-ва Кунашир до о-ва Онекотан. Наблюдения за вулканами северной группы островов (Парамушир и Атласова) по взаимной договоренности проводит камчатская группа оперативного реагирования на вулканические извержения (KVERT). Основные направления деятельности группы SVERT связаны со сбором и анализом всей доступной информации по активным вулканам и созданием на этой базе ежедневных информационных отчетов. Основой для ежедневного мониторинга служат данные высокоорбитальных метеорологических спутников TERRA (спектрорадиометр MODIS), NOAA (спектрорадиометр AVHRR) и MTSAT. Материалы, полученные за этот период, показывают, что на основе методов дистанционного спутникового зондирования (ДСЗ) возможна фиксация даже незначительных изменений в состоянии вулканов Курильских островов.

За период наблюдений были отслежены все события, связанные с активизацией вулканов. В июне 2009 года произошло сильное извержение вулкана Пик Сарычева, предвестники которого были зафиксированы за 23 часа до начала эруптивной деятельности. В период извержения с 11 по 19 июня произошло более 23 вулканических взрывов, эруптивные тучи поднимались на высоту до 8-16 км, а в ряде случаев и до 21 км. Шлейф вулканического пепла протягивался на запад и северо-запад на 1.5 тыс. км, на восток и юго-восток более чем на 3 тыс. км. Извержение не представляло существенной угрозы для населения в силу значительной удаленности населенных пунктов. Наибольшую опасность представляли пепловые облака, осложнявшие ситуацию для авиалиний, проходящих вдоль Курильских островов. Информация о готовящемся извержении и динамике распространения пепловых облаков представлялась всем заинтересованным организациям.

В 2009 году ИМГиГ ДВО РАН начал создавать систему видеонаблюдений за активными вулканами Южных Курил. На первом этапе IP-видеокамера Trendnet TV-IP201W установлена на сейсмостанции пос. Южно-Курильск на расстоянии 11км от влк. Менделеева. Для передачи по сети Интернет используется стандартное оборудование провайдера с настроенной маршрутизацией. Материалы наблюдений в настоящее время доступны на серверах http://www.imgg.ru и http://webcam.sakh.com/?webcam=mendeleev&lang=ru. В будущем планируется установить вебкамеры для наблюдений за вулканами Тятя (о-в Кунашир), Иван Грозный и Баранского (о-в Итуруп).

KVERT PROJECT: DANGER FOR AVIATION DURING ERUPTIONS OF KAMCHATKAN VOLCANOES IN 2009-2010

O. Girina, A. Manevich, D. Melnikov, S. Ushakov, A. Nuzhdaev, O. Konovalova, Y. Demyanchuk
Institute of Volcanology and Seismology FEB RAS, KVERT, Petropavlovsk-Kamchatsky, Russia,
girina@kscnet.ru

The Kamchatkan Volcanic Eruption Response Team (KVERT) is a collaborative project of scientists from the Institute of Volcanology and Seismology, the Kamchatka Branch of Geophysical Surveys, and the Alaska Volcano Observatory. The purpose of KVERT is to reduce the risk of costly, damaging, and possibly deadly encounters of aircraft with volcanic ash clouds. To reduce this risk KVERT collects all possible volcanic information and issues eruption alerts to aviation and other emergency officials. There are 30 active volcanoes in Kamchatka and 4 of them continuously active. In 2009-2010 six strong explosive eruptions of Klyuchevskoy, Sheveluch, Bezymianny, Kizimen, Karymsky and Koryaksky took place. In addition, higher fumarolic activity of Gorely volcano was observed in 2010.

Sheveluch: a Aviation Color Code (ACC) was mainly Orange owing to continuous of lava dome growth and moderate or strong explosive activity of the volcano. It was Red on 26-28 April, 2009; 10 September, 2009; and 27-29 October, 2010; because in these days explosions produced ashes up to 10-15 km above see level (ASL). Strong paroxysmal explosive eruption of the volcano occurred on October 27, 2010. Ash plumes rose ~ 12 km ASL and extended about 2500 km to the east from the volcano. A pyroclastic flow deposits area was 20 km^2.
Klyuchevskoy: ACC was Orange on 1-28 January, 2009; Yellow - on 29 January – 10 June, 2009; Green on 11 June - 31 July, 2009. And after that: Yellow on 01 August - 07 October, 2009; Orange on 08 October, 2009 - 21 October, 2010; Red on 22-29 October, 2010; Orange on 30 October – 16 December, 2010; Yellow on 17-31 December, 2010. Explosive-effusive eruptions of the volcano occurred from October 2008 till January 2009, and from August 2009 till November 2010. Paroxysmal phase of last eruption was on October 22-27, 2010: ash plumes rose up to 8-9 km ASL and extended > 2300 km to the east from the volcano. Five lava flows effused from the terminal crater down different flanks of the volcano.
Bezymianny: ACC was Yellow on 01 January – 15 December, 2009; Red on 16 December, 2009; Orange on 17-20 December, 2009; Yellow on 21 December, 2009 - 06 February, 2010; Orange on 07-10 February, 2010; Yellow on 11 December - 23 May, 2010; Orange on 24-30 May, 2010; Red on 31 May, 2010; Orange on 01-02 June, 2010; Yellow on 03 June - 31 December 2010. During of paroxysmal phases of the eruptions ash plumes rose ~10 km ASL and extended from the volcano ~ 400 km to the west on 16 December, 2009; and ~250 km to the west and later 160 km to the north-east and > 600 km to the south on 31 May, 2010.
Kizimen volcano woke up after repose in beginning November 2010 (previous eruption was 1928-1929). ACC was Green on 01 January - 29 July, 2009; Yellow on 30 July - 30 August, 2009; Green on 31 July - 09 October, 2009; Yellow on 10 October - 11 November, 2009; Green on 12 November, 2009 – 24 November, 2010. And after that in 2010: Yellow on 25 November – 09 December; Orange on 10-11 December; Red on 12 December; Orange on 13-26 December; Red on 27-28 December; Orange on 29-31 December. Strong explosive events began to registering from 09 December, 2010. On December 12, 2010, ash plumes rose up to 10 km ASL and extended > 500 km from the volcano. During the eruption ash falls were noted in the different areas of Petropavlovsk-Kamchatsky, Yelizovo, Paratunka and the others. Eruption of the volcano continued in January-May 2011.

Karymsky: ACC was mainly Orange owing to moderate and strong explosive activity of the volcano. ACC was in 2009: Orange on 01 January - 23 April; Yellow on 24 April - 30 August; Green on 31 August - 20 September; Yellow on 21-23 September; Orange on 24 September - 31 December. In 2010 it was: Orange on 01 January - 24 February; Yellow on 25 February - 28 March; Orange on 29 March - 31 December. The very strong explosive events were registered at the volcano on June 11, 2010: ash plumes extended about 196 km to the east from the volcano.

Koryaksky volcano woke up in December 2008 (previous eruption was 1956-1957). In 2009 ACC was Orange on 01-06 January; Yellow on 07 January - 02 March; Orange on 03 March - 27 April; Yellow on 28 April - 16 August; Orange on 17 August - 02 September; Yellow on 03 September – 04 November; Green on 05 November – 31 December. During the intensification of the volcano in 2008-2009, there were three periods when gas-steam plumes contained ash, and the volcano represented a danger to aviation: 23-28 December, 2008; 4 March - 18 April, 2009, and 13-27 August, 2009. The most activity of the volcano was in March-April, 2009: the greatest height of ash-gas-steam plumes was 5.5 km a.s.l. and length - about 680 km.

Gorely. Strong fumarolic activity of the volcano began to noting from June 2010. A new vent on the wall of Gorely active crater was discovered on June 17. A temperature of magmatic gas was of 800-900^{0}C. ACC was Green in 2009 and 01 January - 23 June 2009; Yellow on 24 June - 31 December, 2010.

Volcanic Ash Advisory for Transportation:
(implement of volcanoes monitoring systems of active explosive volcanoes to increase the reliability of ash plume dispersion modeling and ash concentration charts).

Marco Magnani, Naoko Taki, Hiroaru Suyama.
(*Weathernews Inc.,Chiba, Japan)*

On April 2010, a series of eruptions from Eyjafjallajökull in the south of Iceland had an enormous impact on the European air traffic industry, and increased the needs and demands for accurate ash concentration forecasts and risk aversion information from the major airlines. From that moment Weathernews Inc. started the VAAT (Volcanic Ash Advisory for Transportation) project to support the needs of the transportation industry.

Our project uses a new, non-standard approach to increase the precision of our models, so that we can determine the ash concentration in the volcanic plumes, as well the ash dispersion patterns with high level of precision. So far most of the research institutions, weather agencies, etc based their modeling on satellites images and web cameras, when available, but now Weathernews has been using new methods of monitoring, having developed for example the "WITH RADAR" (X-band radar), which is capable of scanning the ash cloud every 6 seconds and to monitor the volcanic ash even on night time, 24 hours a day. The "WITH RADAR" was already employed with success this year during the Shinmoedake eruption in Kyushu Island.

Furthermore we are planning to extend more the installation of web cameras, especially in countries where the infrastructures are not developed enough, but with a large number of active explosive volcanoes, as for example Indonesia, Philippine and Kamchatka.

In conclusion Weathernews wants to base as much as possible the modeling on direct monitoring of the volcanoes, in order to increase the ash plumes dispersion forecast precision and to provide reliable ash concentration charts, which are fundamental information for the aviation operators. In order to achieve these goals Weathernews is implementing the traditional monitoring systems and at the same time developing new non standard monitoring systems, such the "WITH RADAR".

Monitoring precursory unrest and the 2009 eruption of Redoubt Volcano, AK by high-resolution satellite and airborne thermal infrared imaging

Rick Wessels[1], R. Greg Vaughan[2], Matt Patrick[3] and Michelle Coombs[1]

[1]Alaska Volcano Observatory, U.S. Geological Survey, Anchorage, AK, USA
[2] Astrogeology Science Center, U.S. Geological Survey, Flagstaff, AZ, USA
[3]Hawaiian Volcano Observatory, U.S. Geological Survey, Hawai'i National Park, HI, USA

We use a combination of satellite and airborne high-resolution visible/near-infrared and thermal infrared (TIR) image data to detect and measure changes at Redoubt Volcano before, during, and after the 2008-2009 unrest and eruption. The high-resolution TIR remote sensing response initially focused on detecting and monitoring changes in possible thermal areas and other surface features to assess the extent of unrest and the likelihood and timing of an eruption. As the eruption commenced, the TIR response changed to measuring and monitoring eruptive products and surveying edifice for any new features. During the effusion of lava domes and flows, the TIR data readily identify areas of active lava and gas effusion as well as providing a means to measure dimensions, assess flow structures and textures.

Advanced Spaceborne Thermal Emission and Reflection Radiometer (ASTER) TIR images show that the permanently ice-covered stratovolcano began to develop persistent weak thermal anomalies in areas of ice-melt holes and crevasses in the ice-filled summit crater in late 2008 until mid-March 2009. On 23 January 2009, mudflows began to sporadically discharge from below the summit fumaroles down the Drift Glacier and into the Drift River as the level of seismicity and gas emissions rose significantly. A phreatic explosion on 15 March was followed one week later (23 March-4 April) by a series of at least 19 magmatic explosive events that produced high-altitude ash clouds and large lahars. Two (or three) lava domes extruded and were destroyed between 23 March and 4 April. After 4 April, the eruption extruded a large lava dome that continued to grow until at least late June 2009.

Satellite TIR data from the ASTER, Landsat 5 TM and Landsat 7 ETM+ imaged the summit over 250 times from September 2007 through May 2011. ASTER has five TIR bands at 90-m resolution while Landsat 5 TM and 7 ETM+ have one broadband TIR band at 120-m and 60-m resolution respectively. A survey of ASTER nighttime TIR data detected no obvious thermal features on the upper flanks or at the summit of Redoubt from 2000 to late 2007. A weak thermal feature first appears in ASTER TIR nighttime data from 2007. These initial weak thermal anomalies, midway down Drift Glacier, were possibly caused by small outbreaks of melt water flowing from the summit above. By October 2008, low temperature summit thermal features began to appear in ASTER TIR and persisted through the first explosions on 15 and 23 March 2009. Though clouds and ash plumes obscured the summit during most of the explosive phase, frequent satellite TIR data acquired during the post-April 4 effusive phase of the eruption show persistently high thermal emission from the growing dome and the hot talus on the slope below. The variations in thermal emissions paralleled the measured variations in lava effusion rates. The hot areas persist after the eruption ceased around 1 July and continued until at least December 2009 (Fig. 1).

Airborne Forward-Looking Infrared (FLIR) images from 14 field missions flown between November 2008 and August 2010 provide higher resolution details of the thermal features. Pre-eruption FLIR surveys in November 2008 and February 2009 documented two warm summit areas and a waterfall on the north flank below the summit crater. Areas of warm exposed rock expanded as temperatures gradually increased. While the summit was mostly covered in thick clouds and ash plumes for most of the explosive phase of the eruption, a 31 March FLIR survey captured partial glimpses of the lava dome beneath the ash plume. FLIR surveys after 4 April document the gradual growth and cooling of the final lava dome. The most recent FLIR data from August 2010 show that fumaroles along the southeast flank of the cooling dome still had temperatures over 300°C.

Beyond temperatures, the high-resolution TIR data were used to monitor changes in the lava dome textures and measure the dimensions of the growing final dome. Retrospective analysis of archived high-resolution satellite TIR data detected subtle, small-scale changes in surface thermal activity more than 16 months before the 2009 eruption of Redoubt Volcano. While a few of the infrequent individual ASTER TIR scenes were able to detect these subtle temperature anomalies, robust detection and identification of early thermal precursors at active volcanoes requires new high resolution multispectral TIR satellite sensors with frequent, at least daily, night and day acquisitions.

Recent seismicity and crustal deformation around Mt. Fuji

Yuhki Kohno, Hideki Ueda, Eisuke Fujita, Toshikazu Tanada, Tomofumi Kozono, Masashi Nagai, Tetsuya Jitsufuchi, Taku Ozawa, Motoo Ukawa
National Research Institute for Earth Science and Disaster Prevention, Japan.

Mt. Fuji is located on the middle of Honshu, Japan, and is about 100 km south-west of Tokyo. This volcano is also situated on the triple junction where the Philippine Sea Plate, the Okhotsk Plate and the Amurian Plate meet. The last eruption (Hoei eruption) occurred in 1707, and the total volume of this eruption was estimated about 0.7 km^3. National Research Institute for Earth Science and Disaster Prevention (NIED) has started monitoring of Mt. Fuji in 1980s and installed borehole seismometers, tiltmeters, GPS, and broadband seismometers at 6 stations around Mt. Fuji since 1990's. We have found that low frequency earthquakes are occurring at the depth from 10 to 20 km beneath of the edifice, where the magma reservoir is estimated from the result of seismic tomography. The activity of low frequency earthquakes became rather high in 2000 and the higher activities have not been observed since then. On the other hand, non-low-frequency (volcano-tectonic) earthquakes also often occur around the volcano. The number of VT earthquakes beneath south flank of Mt. Fuji has been increased since 2008. The crustal deformation data had not indicated volcanic deformation so far.

There was the M_{JMA}6.4 earthquake beneath south flank of Mt. Fuji, at the depth of 15 km, on March 15, 2011, where the seismicity had increased since 2008 as noted above. From the inversion of co-seismic crustal deformation data obtained by GPS (GEONET and NIED) and tiltmeters (NIED), we got a proper fault model as almost vertical, running NNE-SSW and the dimension of 6km x 6km, almost same extent with the distribution area of aftershocks. These aftershocks are tectonic earthquakes and have occurred until now but its numbers are decreasing.

It had been feared that Mt. Fuji may erupt followed by this big earthquake because of stimulation to the subsurface magma reservoir, however non-increasing number of the low frequency earthquakes and volcanic-tremor have been observed by our observation network. Moreover a result of simulation which calculates the effect of stress to the magma reservoir induced our speculation that the big earthquake affect slightly into the magma chamber. We also should keep monitoring of Mt Fuji carefully.

Variable feeding regimes of the Kljuchevskoy group volcanoes (Kamchatka, Russia) derived from time-dependent seismic tomography

Ivan Koulakov, Evgeniy I. Gordeev, Nikolay L. Dobretsov, Valery A. Vernikovsky, Sergey Senyukov, Andrey Jakovlev, and Kayrly Jaxybulatov

We present the results of time-dependent local earthquake tomography for the Kljuchevskoy group of volcanoes in Kamchatka. We consider the time period from 2001 to 2008, which covers several stages of activity for Kljuchevskoy and Bezymianny volcanoes. During the entire period, we robustly observe a mantle channel below 25 km depth with anomalously high Vp/Vs values (up to 2.2), which is interpreted to be the main feeding source of the volcanoes of the group. In the crust, we derived complex structure that varies over the observation time. During the preeruptive period, we detected two levels of magma sources: one in the middle crust and one just below Kljuchevskoy volcano. In 2005, a year of powerful eruptions of Kljuchevskoy and Bezymianny volcanoes, we observe a general increase in Vp/Vs throughout the crust. In the relaxation period following the eruption, the Vp/Vs values are generally low, and no anomalous zones in the crust are observed. We propose that very rapid variations in Vp/Vs are most likely due to abrupt changes in stress and deformation regime, which cause fracturing and the active transport of fluids. This causes positive feedback, and the excessive stresses in the crust lead to volcanic eruptions.

THE MAGMATIC FEEDING SYSTEM OF THE KLYUCHEVSKAYA GROUP OF VOLCANOES (KAMCHATKA), ITS DEEP STRUCTURE, PROPERTIES AND ACTIVITY. THE GEOPHYSICAL MODEL.

Sergei Fedotov[1,2], Nicolay Zharinov[1], Larissa Gontovaya[1]

(1)-Institute of Volcanology and Seismology, Far East Division,
Russian Academy of Sciences, Petropavlovsk-Kamchatskiy, Russia 683006
(2)-Schmidt Institute of Physics of the Earth, Russian Academy of Sciences, Moscow, Russia 123995 karetn@list.ru, fedotov@kscnet.ru , nzhar@kscnet.ru

The Klyuchevskaya Group of Volcanoes (KGV) is the most powerful volcanic center of island arcs and subduction zones of the world. Several significant results derived since the 1960s have been reported, emerging from the study of magma sources, eruptions, earthquakes, deformations and deep structure of KGV [Fedotov, et al., 2010(1); Fedotov, et al., 2010(2)].

The first evidence for the magma chamber of Klyuchevskoi Volcano has been published by G.S.Gorshkov in 1956 [Gorshkov, 1956]. He studied attenuation of shear waves from Japanese earthquakes and found that the probable magma chamber is in the upper mantle beneath the volcano at a depth of about 60 km.

In later decades an anomalous, nearly vertical column-like zone 2 km in diameter extending from 50 km depth was identified by geophysical methods. An andesite magma chamber was found at a depth of 10-20 km beneath the Bezymyannyi Volcano; this chamber is connected with the magma conduit of the basaltic Klyuchevskoi Volcano.

Fundamental scientific results were derived from comprehensive studies of the Great Tolbachik fissure eruption [GTFE]. It occurred between July 6, 1975 and December 10, 1976. On seismological data, rise of deep basalts occurred within 10 days before eruption from depth of 10-20 km. From the top of caldera Ploskii Tolbachik 0.35 км^3 megaplagiophyre basalts of the previous eruptions sank down into magmatic feeding system. In the feeding magmatic chambers and channels there was a mixture of two types of basalts. By calculations, the volume of that part of magmatic feeding system KGV from which there was an outflow of magmas during GTFE is estimated by size (1.6-4.0)10^3 км^3. During of eruption stops crust earthquakes appear under most parts of KGV. It showed that under all KGV there was a system of the interconnected magmatic chambers.

Subsidences of the earth surface after eruptions are noted also on the volcano Bezymmyannyi. According to the leveling executed in 1978 and 1987 along a profile, laid at distance 5 km from volcano subsidence of the earth surface to 50 mm was noted. On these data the centre of magmatic pressure under the volcano Bezymmyannyi was on the depth 9.5 km.

The repeated leveling survey executed on a radial profile located on the NE slope of the Klyuchevskoi volcano also marked sign-variable vertical displacements: rise before preparation of eruptions and putting down of the earth surface after the summit eruptions.

Estimations of the sizes of the intermediate and peripheral chambers of the Kljuchevskoi volcano were received at processing of geodetic data about vertical displacement on slopes and the volcano foot in 1982-2010. It was accepted, that deformations on a surface were created by changes of effective pressure in two chambers, the intermediate and peripheral ones which depths are equal 25 and 3 km. Average volumes of the intermediate and peripheral magmatic chambers have appeared equal 156.2 and 30.7 км^3, the volume of intermediate chamber is approximately in 5 times more then peripheral one.

Seismotomography methods are applied for studying of a structure and properties of the earth crust and the mantle, the magmatic chambers and magmatic feeding systems of volcanoes under KGV. Received seismotomography data confirm that the deep source of substance and energy of

magma formation is located at the top border of a seismofocal zone or plate. The area enriched by melts stretches upwards to the earth crust through the asthenosphere. On level-by-level maps and vertical sections of seismic velocity anomalies for the depths of 0-40 km, the probable arrangement of the magmatic chambers of active volcanoes, possible zones of magma movement and the solidified chambers in the earth crust under KGV are visible. There are intensive anomalies under all KGV. The low velocities are observed on depths of 25-35 and 0-10 km under the Kljuchevskoi volcano.

The geophysical model of modern magmatic feeding system of KGV is constructed [Fedotov, etc., 2010(1); Fedotov et al., 2010(2)].

1. Depths about 160 km under KGV, the upper part of a plunging Pacific plate.
An energy source and fluids necessary for magma origin are here.

2. Depths of 160-40 km, the asthenosphere. A partial melting, formation of picritic magmas, gravitational convection, and rise of diapires and asthenosphere magmatic columns occur here.

3. Depths of 40-25 km, the crust-mantle layers. The excess pressure of ultramafic magmas should be maximum. Here at a base of the lithosphere intrusions and main accumulation of magmas occur, first of all, in the intermediate chamber of the Klyuchevskoi volcano where it is accompanied by many small long-period earthquakes.

4. Depths of 25-5 km, earth crust. The rise of magmas to the Klyuchevskoi volcano, to other volcanoes and differentiation of magmas, the crust magmatic chambers of the andesite volcano Bezymmyannyi and of the basaltic volcano Ploskii Tolbachik are here. These main active volcanoes of KGV located in its average part are stretched along the axis of volcanic belt of Kamchatka. On depths of 35-5 km under all KGV is located a big complex system of the connected magmatic chambers which total volume can exceed 1900 км^3.

5. Depths of 5-0 km, the upper part of the crust and the volcano edifices over them. The formation of magmas and the accumulation of magmas of summit and adventive eruptions of the Klyuchevskoi volcano, intrusion over numerous dikes and sills from its feeding channel occur here. Volume of the peripheral magmatic chambers of KGV volcanoes is 10 times less than intermediate ones. Under summit caldera of the volcano Ploskii Tolbachik is found its peripheral chamber, volume 50 км^3.

References.

Gorshkov G.S. On the Depth of the Magma Chamber beneath Klyuchevskoi Volcano, *Dokl. AN SSSR,* 1956, *vol*.106, no. 4, pp. 703-705.

Fedotov S.A., Zharinov N.A., Gontovaya L.I..Magmatic feeding System of Klyuchevskaya Group of Volcanoes, Kamchatka, by Data about Its Eruptions, Earthquakes, Deformations and a Deep Structure//Volcanology and Seismology. 2010. No.1.pp. 3-35.

S. A. Fedotov, N. A. Zharinov and L I. Gontovaya. The Magmatic System of the Klyuchevskaya Group of Volcanoes Inferred from Data on Its Eruptions, Earthquakes, Deformation, and Deep Structure//Journal of Volcanology and Seismology. 2010, vol. 4, no.1, pp.1-33.

МАГМАТИЧЕСКАЯ ПИТАЮЩАЯ СИСТЕМА КЛЮЧЕВСКОЙ ГРУППЫ ВУЛКАНОВ (КАМЧАТКА), ЕЕ СТРОЕНИЕ, СВОЙСТВА И ДЕЯТЕЛЬНОСТЬ. ГЕОФИЗИЧЕСКАЯ МОДЕЛЬ.

С.А. Федотов, Н.А. Жаринов, Л.И. Гонтовая

Институт вулканологии и сейсмологии ДВО РАН, Петропавловск-Камчатский, karetn@list.ru, fedotov@kscnet.ru, nzhar@kscnet.ru

Ключевская группа вулканов (КГВ), находящаяся на Камчатке в северной части Курило-Камчатского вулканического пояса, является одним из наиболее мощных вулканических центров мира. Приводится ряд показательных результатов, полученных с 1960-х годов при изучении источников магм, извержений, землетрясений, деформаций и глубинного строения КГВ [Федотов и др., 2010; Fedotov et al., 2010].

Первые данные о магматическом очаге Ключевского вулкана были опубликованы Г.С. Горшковым в 1956 г.[Горшков, 1956]. Он нашел по данным об экранировании поперечных волн японских землетрясений, что этот очаг находится в верхней мантии на глубине около 60 км.

В последующие десятилетия геофизическими методами под Ключевским вулканом была выделена аномальная, почти вертикальная столбообразная зона поперечником 2 км, поднимающаяся с глубины 50 км. Под вулканом Безымянный на глубине 10-20 км обнаружен андезитовый магматический очаг, соединяющийся с магмоводом базальтового Ключевского вулкана.

Важнейшие сведения были получены при всесторонних исследованиях Большого трещинного Толбачинского извержения (БТТИ), которое происходило с 06.07.1975 до 10.12.1976 г. По сейсмологическим данным, подъем глубинных базальтов происходил в течение 10 дней перед извержением с глубины 10-20 км. Из вершинной кальдеры Плоского Толбачика опустилось в магматическую питающую систему 0.35 км^3 мегаплагиофировых базальтов предыдущих извержений. В питающих магматических очагах и каналах происходило смешение двух типов базальтов. По расчетам, объем той части магматической питающей системы КГВ, из которой происходил отток магм во время БТТИ, оценивается величиной (1.6-4.0) 10^3 км^3. При остановках извержения начинались коровые землетрясения под большей частью КГВ. Это указывало на то, что под всей КГВ находится система взаимосвязанных магматических очагов.

Проседания земной поверхности после извержений отмечены также на вулкане Безымянный. По данным нивелировок, выполненных в 1978 и 1987 гг. вдоль трассы, проложенной в 5 км по касательной к вулкану, отмечены опускания земной поверхности до 50 мм. По этим данным центр магматического давления под вулканом Безымянный находился на глубине 9.5 км.

Многократные повторные наблюдения, выполненные на радиальном к вулкану профиле на СВ склоне вулкана Ключевской, также отмечают знакопеременные вертикальные смещения: подъемы перед подготовкой извержений и опускания земной поверхности после прекращения извержений.

Оценки размеров промежуточного и периферического очагов Ключевского вулкана получены при обработке геодезических данных о вертикальных смещениях на склонах и подножье вулкана в 1982-2010 гг. Было принято, что деформации на поверхности создаются изменениями эффективного давления в двух центрах, промежуточном и периферическом очагах, глубины которых равны 25 и 3 км. Средние величины объемов промежуточного и периферического магматических очагов оказались равными 156.2 и 30.7 км^3, промежуточный очаг по объему примерно в 5 раз больше периферического.

Для изучения строения и свойств земной коры и мантии, магматических очагов и магматических питающих систем вулканов под КГВ применяются методы сейсмотомографии. Полученные сейсмотомографические данные подтверждают, что глубинный источник вещества и энергии магмообразования находится у верхней границы сейсмофокального слоя, откуда вверх к земной коре сквозь астеносферу протягивается область, обогащенная расплавами. На послойных картах и вертикальных разрезах аномалий скоростей для глубин 0-40 км видно вероятное расположение магматических очагов действующих вулканов, возможных зон перетекания магм и застывших очагов в земной коре под КГВ. Интенсивные аномалии имеются под всей КГВ. Пониженные скорости наблюдаются на глубинах 25-35 и 0-10 км под Ключевским вулканом.

Построена геофизическая модель современной магматической питающей системы КГВ [Федотов и др., 2010; Fedotov et al., 2010].

1. Глубины около 160 км под КГВ, верхняя часть погружающейся Тихоокеанской плиты. Здесь находится источник энергии и летучих, необходимых для зарождения магм.

2. Глубины 160-40 км, астеносфера. Здесь происходят частичное плавление, формирование пикритовых магм, гравитационная конвекция, подъем диапиров и астеносферных магматических колонн.

3. Глубины 40-25 км, коромантийные слои. Избыточное давление мантийных магм должно быть максимальным. Здесь у подошвы литосферы происходят внедрение интрузий и основное накопление магм, в первую очередь, в промежуточном очаге Ключевского вулкана, оно сопровождается множеством слабых длиннопериодных землетрясений.

4. Глубины 25-5 км, земная кора. Здесь происходят подъем магм к Ключевскому вулкану, к другим вулканам и дифференциация магм, находятся коровые магматические очаги андезитового вулкана Безымянный и базальтового вулкана Плоский Толбачик. Эти главные действующие вулканы КГВ, расположенные в ее средней части, протягиваются по разлому вдоль вулканического пояса Камчатки. На глубинах 35-5 км под всей КГВ находится большая сложная система связанных магматических очагов, общий объем которых может превышать 1900 км^3.

5. Глубины 5-0 км, верхние слои коры и постройки вулканов над ними. Здесь происходит формирование магм и накопление магм вершинных и побочных извержений Ключевского вулкана, внедрение из его питающего канала многочисленных даек и силлов. Объем периферических магматических очагов вулканов КГВ на порядок меньше, чем промежуточных. Под вершинной кальдерой вулкана Плоский Толбачик находится его периферический очаг объемом 50 км^3.

Литература.

Горшков Г.С. О глубине магматического очага Ключевского вулкана // Докл. АН СССР. 1956. Т.106.№4. С. 703-705.

Федотов С.А., Жаринов Н.А., Гонтовая Л.И. Магматическая питающая система Ключевской группы вулканов, Камчатка, по данным об ее извержениях, землетрясениях, деформациях и глубинном строении // Вулканология и сейсмология. 2010. №1. С. 3-35.

S. A. Fedotov, N. A. Zharinov and L. I. Gontovaya. The Magmatic System of the Klyuchevskaya Group of Volcanoes Inferred from Data on Its Eruptions, Earthquakes, Deformation, and Deep Structure// Journal of Volcanology and Seismology. 2010, Vol.4, №1, pp.1-33.